ISBN 978-82-326-3568-9 (printed ver.)
ISBN 978-82-326-3569-6 (electronic ver.)
ISSN 1503-8181

NTNU
Norwegian University of
Science and Technology

Jimita Toraskar

Doctoral thesis

Doctoral theses at NTNU, 2018:390

NTNU
Norwegian University of Science and Technology
Thesis for the Degree of
Philosophiae Doctor
Faculty of Medicine and Health Sciences
Department of Clinical and Molecular Medicine

NTNU

Doctoral theses at NTNU, 2018:390

Jimita Toraskar

Nephronectin in breast cancer progression and metastasis

NTNU
Norwegian University of
Science and Technology

Jimita Toraskar

Nephronectin in breast cancer progression and metastasis

Thesis for the Degree of Philosophiae Doctor

Trondheim, December 2018

Norwegian University of Science and Technology
Faculty of Medicine and Health Sciences
Department of Clinical and Molecular Medicine

NTNU
Norwegian University of
Science and Technology

NTNU
Norwegian University of Science and Technology

Thesis for the Degree of Philosophiae Doctor

Faculty of Medicine and Health Sciences
Department of Clinical and Molecular Medicine

ISBN 978-82-326-3568-9 (printed ver.)
ISBN 978-82-326-3569-6 (electronic ver.)
ISSN 1503-8181

Doctoral theses at NTNU, 2018:390

Printed by NTNU Grafisk senter

Nephronectin i brystkreftutvikling og metastaser

Brystkreft i seg selv er vanligivs ikke dødelig for pasientene som får det, men dersom sykdommen får anledning til å spre seg (metastasere) til andre organer kan utkomme bli alvorlig. Kreftsvulster kan virke kaotiske med en blanding av mange celletyper omgitt av en kompleks matrix av extracellulære proteiner som legger til rette for at kreftcellene kan vokse. Faktisk er det slik at kreftsvulster som vokser på mange måter kan ligne utviklingen av organer som foregår på fosterstadiet. Nephronectin (NPNT) er et protein som vanligvis kun uttrykkes i organer som er under utvikling, og normalt ikke uttrykt i for eksempel normalt brystvev. Arbeidet i denne avhandlingen avdekker at NPNT kan spille en rolle for utvikling og metastasering av brystkreft. Resultatene våre viser at i et materiale med kreftprøver fra 842 pasienter var NPNT uttrykt i 596 av pasientene. Videre har vi vist at et vesikulær/granulært uttrykk av NPNT i mindre enn 10% av kreftcellene i svulstene var korrelert med dårlig prognose. Dette granulære mønsteret fikk oss til å spekulere i at NPNT muligens er involvert i kommunikasjon via vesikler. Extracellulære vesikler fra kreftceller er kjent for å bidra i intercellulær kommunikasjon både lokalt i svulsten og systemisk i hele kroppen. Slike vesikler skilt ut fra kreftsvulster er gjerne pakket med ulike onkogene molekyler som kan påvirke kreftutviklingen og spredning til andre organer. Resultatene våre viser at NPNT er ett av proteinene som finnes i extracellulære vesikler fra brystkreftceller, og vi har funnet en ny trunkert form av proteinet som er oppkonsentrert i disse vesiklene. Videre har vi vist at den totale proteinsammensetningen i extracellulære vesikler endrer seg når cellene uttrykker høyt nivå av NPNT.

Brystkreft sprer seg vanligvis til bein, lever, lunge og hjerne. Normalt er det utfordrende for celler fra et organ å overleve og vokse i et annet organ med et annet mikromiljø enn det opprinnelige. Denne avhandlingen beskriver de onkogene egenskapene til NPNT og hvordan NPNT bidrar til å fremme kreftutvikling. Vi har funnet at NPNT fremmer viabilitet, adhesjon og tilknytningsuavhengig cellevekst via proteinets integrin-bindingsmotiver. Disse onkogene egenskapene til NPNT-proteinet gjør kreftcellene bedre i stand til å metastasere til for eksempel lunger. Ulike ligander kan aktivere ulike intracellulære signalveier, til tross for binding til samme reseptor. Derfor er det viktig å undersøke hvilke signalveier som påvirkes av ulike ligander i ulike celletyper. Resultatene våre viser at NPNT induserer fosforylering av p38 via integrin interaksjonssetet som forsterker bindingen av NPNT til reseptoren og at dette fremmer viablitet i 66cl4 celler. På bakgrunn av dette foreslås det at målrettet blokkering av begge integrininteraksjonssetene kan være en mulig strategi for å blokkere de kreftfremmende egenskapene til NPNT.

Table of Contents

Acknowledgements

This work was performed at the Department of Clinical and Molecular Medicine at the Faculty of Medicine and Health Sciences, Norwegian University of Science and Technology (NTNU) during the years 2015-2018. I am grateful for the financial support from Central Norway Regional Health Authority.

First of all, I wish to express my sincere and humble gratitude to my main supervisor Tonje S. Steigedal for nurturing my skills and strengths. These four years were filled with challenges but together we overcame them all. Thank you for always having my back and keeping me focused. Everything that I have learnt under your supervision has made my life more meaningful.

I would especially like to acknowledge the support of our collaborators at the University of Tromsø- Gunbjørg Svineng and Synnøve Magnussen for their helpful comments, great support and timely advice. I am also indebted to my co-supervisor Geir Bjørkøy for numerous ideas and fostering my curiosity in science. I thank my co-supervisor Steinar Lundgren for recruiting me in this project at NTNU. I would like to express thanks to all the members of the 'Gastroenterology and Inflammation group' for a great and welcoming work environment. Thank you Liv Thommesen, for precise proof-reading of this thesis. I would also like to thank my co-authors for their contributions and clever discussions. All the technical advices received from Anne Kristensen, Bjørn Munkvold, Berit Doseth, Bjørnar Sporsheim and Kjartan Egeberg are really appreciated. I value the skills learnt at Hector Peinado's lab in Spain, which has been fundamental for this project. Thank you Åsmund Flobak, for encouraging me to participate in 'Forsker Grand Prix'.

Adjusting in Norway would have been difficult without the friendship and support of Nina, Bernt and Lena. I really appreciate your kind-heartedness and the warmth that you have provided me at home in Trondheim. The unspoken rule of 'love thy neighbors' stands true when I think of my helpful neighbors, Cristina, Jose, Petra and Iris. A special mention of my wonderful friends who always showed me warmth and support- Smita, Ulrike, Joana, Arpit, Shareq, Kath, Babsi, Neeruja, Evelina, Akshay, Nayan, Paritosh, Avni, Darshi, Rithika, Ali, Pooja, Pranav, Ram, Divya and Rahul. Thank you guys for the life-long memories we have created.

Delighted to have cousins like, Niti, Toral, Sunny and Mainak who have kept me sane during tough times. It is nice to have a best friend that I can always count on, Sohil, you have been my pillar of support. Fortunate to have a friend like Sumit, who can literally fly oceans for me. I thank my friend Molly, who has turned me into an assertive go-getter. I am indebted to my friend Olga, for changing my perspective towards life.

My deepest gratitude to my mother, Nita for giving me the best upbringing and such a wonderful life. I am also grateful to my aunt, Kalpana for teaching me a fun and enthusiastic way of living. I am glad to have a well-wisher in Hansa kaki. Also, thankful to the lessons learnt from my art teacher Geeta Mathuria who has been my idol since childhood. Words are not enough to recognize my grandparent's unconditional love and countless sacrifices. I love my grandma for filling my life with so much positivity. My grandfather would have been the happiest person to see me reach this far.

I miss you dada!

Thank you for all your love and support!

Trondheim, September 2018

Jimita Toraskar

List of papers

This thesis is based on the following papers:

I. T.S. Steigedal, **J. Toraskar**, R.P. Redvers, M. Valla, S.N. Magnussen, A.M. Bofin, S. Opdahl, S. Lundgren, B.L. Eckhardt, J.M. Lamar, J. Doherty, R.O. Hynes, R.L. Anderson, G. Svineng, Nephronectin is Correlated with Poor Prognosis in Breast Cancer and Promotes Metastasis via its Integrin-Binding Motifs, Neoplasia (New York, N.Y.), 20 (2018) 387-400.

II. **J.Toraskar**, S.N.Magnussen, K.Chawla, G.Svineng, T.S.Steigedal, Nephronectin mediates p38 MAPK-induced cell viability via its integrin binding enhancer motif, Published in FEBS Open Bio (2018).

III. **J.Toraskar**, S.N.Magnussen, L.Hagen, A.Sharma, L.Hoang, G.Bjørkøy, G.Svineng, T.S.Steigedal, A novel truncated form of Nephronectin is present in exosomes from 66cl4-cells
Under review in Journal of Proteome Research.

Abbreviations

AIA	Alanine-Isoleucine-Alanine
ALIX	Apoptotic linked gene-2 interacting protein X
BAD	Bcl-2-associated death promoter protein
BafA1	Bafilomycin A1
BCL-2	Apoptosis regulator identified in B cell lymphoma 2
BMDC	Bone marrow derived cells
CHMP4B	Charged Multivesicular Body Protein 4B
CK5	Cytokeratin 5
CTCs	Circulating tumor cells
DTC	Disseminated tumor cells
ECM	Extracellular matrix
EGF	Epidermal growth factor
EGFL6	EGF-like protein 6
EGFR	EGF receptor
EIE	Glutamic acid-Isoleucine-Glutamic acid
ER	Estrogen receptor
ERK	Extracellular signal regulated kinases
EV	Empty vector
FAK	Focal adhesion kinase
GAPDH	Glyceraldehyde-3-Phosphate Dehydrogenase
GM130	Golgi matrix protein 130 kD ortholog
HEPES	4-(2-hydroxyethyl)-1-piperazineethanesulfonic acid
HER-2	Human epidermal growth factor receptor 2
HES	Hematoxylin eosin saffron
ILVs	Intraluminal vesicles
IPA	Ingenuity pathway analysis
JNK	Jun N-terminal kinase
KRAS	Oncogene first identified in kirsten rat sarcoma virus
MAM	Meprin, A-5 protein, and receptor protein-tyrosine phosphatase mu
MAPK	Mitogen activated protein kinase

MAP2K	MAPK kinase
MAP3K	MAPK kinase kinase
MKNK1	MAP kinase-interacting serine/threonine-protein kinase 1
MMPs	Matrix metalloproteinases
MMTV-PyMT	Mouse mammary tumor virus-polyomavirus middle T-antigen
MV	Microvesicles
MVB	Multivesicular bodies
NPNT	Nephronectin
PCR	Polymerase chain reaction
PI3K	Phosphatidylinositol 3-kinase
POEM	Preosteoblast EGF-like repeat protein with MAM motif
PR	Progesterone receptor
PTI	Protein transport inhibitor
PTMs	Post translational modifications
RAD51	DNA repair protein RAD51 homolog 1
RGD	Arginine-Glycine-Aspartic acid
RGE	Arginine-Glycine-Glutamic acid
rmNPNT	Recombinant mouse NPNT
RPPA	Reverse phase protein array
RT-qPCR	Quantitative reverse transcription PCR
sEVs	Small extracellular vesicles
shNPNT	Knockdown of NPNT using a short-hair pin RNAs
SRC	Proto-oncogene tyrosine-protein kinase Src
TME	Tumor microenvironment

Abstract

Breast cancer is life threatening due to its ability to spread and invade other tissues. The best approach in solving a problem of this sort is to be able to reason backwards. Tumors appear chaotic as they are composed of multiple abnormal cell types and a complex matrix of proteins that cushions the tumor cells extracellularly. In fact, some characteristics of tumor development resemble those seen in developing organs. Nephronectin (NPNT) is identified in several developing organs, but it is absent in normal healthy breast tissue. However for breast cancer progression and metastasis, NPNT appears to play a significant role, as elaborated in this thesis. Our results show that 596 out of 842 breast cancer cases stain positive for NPNT and the cytoplasmic granular staining pattern in less than 10% of the tumor cells correlates with poor prognosis. This granular staining pattern could indicate the involvement of vesicular communication. Extracellular vesicles derived from tumor cells facilitate intercellular communication both locally and systemically in the body. These vesicles are packed with oncogenic traits that can influence cancer progression, and metastasis. As per our investigation, NPNT is one the signaling molecules packed in the extracellular vesicles derived from breast cancer cells. Interestingly, the truncated form of NPNT was concentrated in these vesicles. We further show that the protein of small extracellular vesicles is altered upon NPNT expression in 66cl4 mouse breast cancer cells.

Breast cancer cells mainly spread to bones, liver, lungs and brain. It is challenging for the cancer cells to survive and adapt to a distant tissue microenvironment which is different compared to the primary tumor. In this thesis we highlight several oncogenic properties which are enhanced in presence of NPNT. We found that NPNT promotes viability, adhesion and anchorage-independent growth via its integrin-binding motifs. These oncogenic properties bestowed on tumor cells by NPNT enables them to colonize the lungs more efficiently. Different ligands can activate different intracellular signaling pathways, although binding to the same receptor. Therefore, it is important to investigate and document key signaling molecules triggered by different ligands in specific cell types. Our results indicate that NPNT induces phosphorylation of p38 MAPK via its enhancer motif to promote viability in 66cl4 cells. Therefore, we suggest that targeting both the enhancer and the RGD motif simultaneously would be more effective in rendering NPNT protein inactive.

Introduction

Breast cancer is the most common form of cancer in women. Understanding the molecular mechanisms governing breast cancer progression and metastasis is vital for improving the patient outcomes. The steps in cancer progression are comparable to that of a chronic wound. The abnormal proliferation of tumor cells may disrupt the tissue homeostasis leading to increase in acidosis and hypoxia [1]. These changes activates wound repair mechanisms in the host tissue such as increasing vascularization to supply nutrients/remove waste, recruiting bone marrow derived cells (BMDCs) and leukocytes similar to an inflammatory response at the site of growing tumor. An aberrant reactive microenvironment is created by this abnormal mix of cells, surrounding the primary tumor (reviewed in [2, 3]). Several extracellular matrix (ECM) proteins in the microenvironment are deregulated in cancer progression and metastasis (reviewed in [4-6]). Though preparing a comprehensive list of ECM proteins is not straight forward [7, 8], array screens have enabled identification of ECM genes which have often been upregulated in tumor and metastases [9-12].

Nephronectin (NPNT) is a secreted ECM molecule [13-15]. In highly metastatic mouse mammary tumors, the expression of NPNT has been found to increase 30- to 80-fold facilitating the cells to metastasize; whereas metastasis to lung, spine, and kidney was significantly reduced upon NPNT knockdown [9]. Higher levels of NPNT have also been reported in metastatic breast cancer cells compared to non-metastatic cells in a different syngeneic mouse model of breast cancer [16]. Furthermore, NPNT orthologue (LOC255743) has been detected in libraries derived from two patients with invasive ductal breast carcinoma, one patient with metastatic gastric cancer, and one patient with a grade III brain astrocytoma [9]. These preliminary findings were enticing and called for characterization of NPNT's role in breast cancer. Using mouse models and patient samples, we have investigated the role of NPNT in breast cancer progression and metastasis. We have also utilized cell lines which can be genetically manipulated to study the specific molecular functions of NPNT.

Metastatic breast cancer

Breast cancer has the ability to invade surrounding normal tissue, but can also spread regionally (to nearby lymph nodes) and to distant organs of the body, known as metastasis. Staging of breast cancer patients is based on the TNM system, where the combination of information about the primary tumor (T), the regional lymph nodes (N) and distant metastasis (M) is used to determine the stage of breast cancer progression (0, I, II, III, IV) [17]/(Fig 1). Metastatic breast cancer (stage IV), accounts for 90% of the mortality [18, 19]. Metastatic cancer cells are often different than cells in the primary tumor, both in genetic composition and behavior, thus extremely difficult to treat [20].

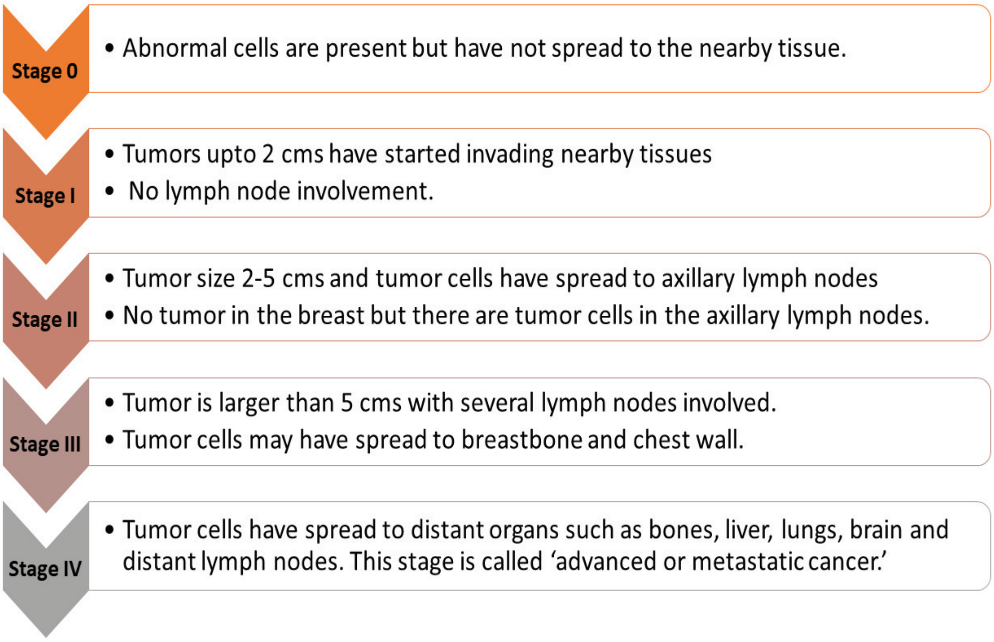

***Figure 1**: The stages of breast cancer progression (modified from [21]).*

There are seven basic steps involved in establishment of a metastatic tumor [22, 23]/(Fig 2):

1) *Invasion and infiltration of surrounding normal host tissue by primary tumor cells*. The population of cells in primary tumor may vary genetically and phenotypically. Most human tumor cells migrate collectively as opposed to most cells *in vivo* or *in vitro* where the tumor cells migrate individually [24].

2) *Intravasation* is the release of neoplastic cells into the blood stream or lymphatic vessels. This step could be active or passive depending on the tumor type, surrounding tissue microenvironment and vasculature [25]. The contribution of epithelial mesenchymal transition for intravasation of tumor cells remains elusive [26].

3) *Transport and survival of tumor cells in the circulation* is challenging. Tumor cells that have entered the circulation are called circulating tumor cells (CTCs). Some CTCs adapt and device mechanisms to survive the harsh conditions in the circulation [23]. Platelets and CTCs can form a bolus, to protect CTCs from stress during transit [27].

4) *Arrest of CTCs in the microvessels of the target organ (or lymph node).* Either the arrested CTCs start growing that lead to the rupture of the microvessel or proceeds to the next step in metastasis, extravasation [23]. In addition to the geometry of the microvessel, the haemodynamic flow also regulates metastatic spread [28].

5) *Extravasation* is the exit of CTCs from the microvessels to the target tissue. The fraction of CTCs that enter the distant sites is called disseminated tumor cells (DTCs) [29]. The microenvironment at the secondary site is very different compared to the primary tumors. This makes extravasation a distinct step which is likely more difficult than intravasation [30, 31].

6) *Initial colonization of tumor cells and formation of micro-metastasis within the target tissue*. Successful extravasation of DTCs is not enough for formation of micro-metastasis [32]. Certain DTCs may remain dormant (G0-G1 arrest) unless aided by growth stimuli [33]. The microenvironment at the secondary site is harsh and several systemic signals are needed to prepare the secondary site for arrival of tumor cells [34, 35]. Secondary tumor is formed upon successful interaction of the DTCs with the microenvironment at the secondary site.

7) *Angiogenesis and formation of macrometastasis*. Angiogenesis is triggered at the secondary tumor by increased hypoxia, acidic tumor microenvironment, mechanical stress, infiltration of inflammatory cells and other angiogenic regulators [36, 37]. Tumor vasculature is different than the normal one [36, 38]. The blood flow is disordered, resulting in lower therapeutic effectiveness and metastasis of metastases.

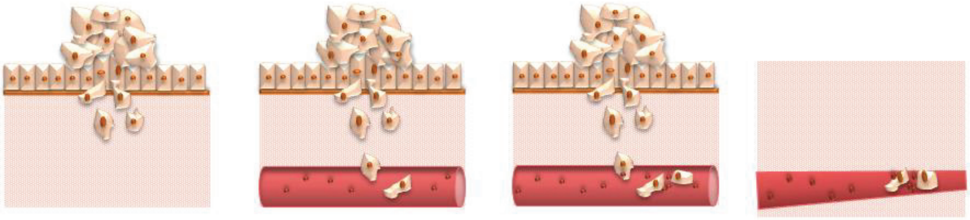

Invasion of neighboring tissue

Intravasation

Struggle for survival in bloodstream

Tumor cells arrest in narrow microvessels

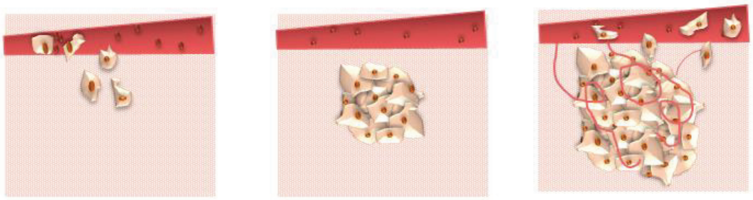

Extravasation

Formation of micro-metastases

Angiogenesis and metastasis of metastases

Fig 2: *Different steps of cancer progression and metastasis (modified from [39]). Primary tumor cells can invade the neighboring tissue, enter the blood vessels (intravasation) and circulate in the vascular system. Some of the CTCs adhere to blood vessel walls and are able to extravasate. In presence of appropriate signals, the DTCs migrate and colonize into the local tissue. Cells of the secondary tumor can further metastasize to other organs (metastasis of metastases).*

Organotropic metastasis

The tendency of different primary tumors to metastasize to distinct organs is known as “organotropic metastasis”. This is a non-random process regulated by subtypes of breast cancer, host organ microenvironment, and cancer cells-target tissue interactions. In case of breast cancer, tumor cells have a propensity to metastasize to bones, liver, lungs and brain and distant lymph nodes [40, 41]. To explain the metastatic patterns two hypotheses have been put forward [41, 42].

- In 1889, Stephen Paget suggested the seed-and-soil theory [43]. According to this hypothesis, the metastasis formation depends on the intrinsic properties of cancer cells (seed), and the ability of cancer cells to interact with host cells and/or other microenvironmental factors present within the target organs (soil)[44].
- In 1928, James Ewing, challenged the seed-and soil-theory with an alternative hypothesis [45], where he advocated that the circulation patterns solely determines which organs are likely to host CTCs upon mechanical arrest in the capillary network [46]. However, ‘mechanical arrest’ may not fully explain the organ-specific patterns of metastases that are observed in most human cancers [44, 47].

Both the theories mentioned above are not mutually exclusive [48]. In 1976, Isaiah Fidler was the first to demonstrate that, both mechanical processes and molecular characteristics of tumor cells and their interactions with the target tissues are important in metastatic organotropism [49]. For many years, researchers have focused on understanding the molecular determinants that play critical roles in the organ-specific metastasis [50-52]. But even today, metastatic organotropism remains one of the cancer’s greatest mysteries. Understanding of organotropic metastasis is essential for better biomarker-based prediction and prognosis, development of innovative therapeutic strategy, and improvement of patient outcomes.

Mouse models of metastasis

The similarities and differences between mice and humans have to be carefully considered in cancer research [53]. Genetic differences between mice and humans can give rise to proteins with different properties. Therefore, molecules which are carcinogenic in mice may not have significant role in humans cancers or vice-versa [54]. Most tumors in mice are of mesenchymal origin whereas human tumors are of epithelial origin [55, 56]. In spite of these differences, research on mice has greatly contributed to our knowledge of cancer progression, immune system and regulation of signaling molecules. The main mouse models for studying metastatic cancer are classified as follows:

Experimental models of metastasis

In this method, the early steps of the metastasis are avoided by either introducing tumor cells directly into the blood circulation (colonization) or injection of cells directly into specific organs (tropism) [3]. When the tumor cells are directly injected in blood, the site of inoculation would influence the metastasis pattern. For example, when the cells are introduced via the tail vein, lungs are predominantly colonized; whereas liver is colonized when the cells are injected directly into the spleen or portal vein [3]. The advantage of this model is shorter incubation time for metastasis development and a greater likelihood of generating metastases in organs that may otherwise be difficult to target.

Spontaneous models of metastasis

Spontaneous models are more desirable, as metastases arises from a transplantable or transgenic primary tumor in the mouse. Injection of tumor cells directly into mammary glands (orthotopic injection) has the advantage of generating physiologically relevant “primary tumors” that may lead to spontaneous metastases in different distant sites, such as the lung [57]. Transgenic mouse models can develop *de novo* tumors in a natural microenvironment and have been shown to display better genetic heterogeneity than experimental models [58]. Though the latest research tools cannot completely match the complexity of metastasis, *in vivo* models have broadened our understanding of the problem, as summarized and argued in table 1.

Table 1: *Strengths and weaknesses of mouse models of metastasis [3, 59].*

Type of model	Strengths	Weaknesses
Experimental metastasis *(E.g. lateral tail vein injection results primarily in lung metastases[60])*	• Rapid & reproducible • Site specific development of metastases • Good metastatic seeding in the target organ • Applicable to many cell lines • Immuno-competent host if allograft • Low cost	• No primary tumor • Mouse microenvironment • Immunocompromised host if xenograft • Only models late stages of the metastatic disease • Injection of cells may inflict inflammation or wounding.
Spontaneous metastasis (Orthotopic) *(E.g. 4T1 mouse mammary cells orthotopically injected [61])*	• Mimics human cancer progression • Models several stages of metastatic cascade • Immuno-competent host if allograft • Low cost	• Mouse microenvironment • Tumor initiation cannot be assessed • Asynchronous metastatic development • Removal of primary tumor to allow development of metastases applicable only on certain types such as breast, prostate, pancreas.
Spontaneous metastasis (Transgenic) *(E.g. MMTV-PyMT mouse model [62])*	• Tumor is initiated by host mammary epithelial cells • Spontaneous tumors mimicking human disease and heterogeneity • Models all stages of metastatic cascade	• Mouse microenvironment • Low incidence of metastatic spread • Extensive breeding programs required (cost and time) • Strain-dependent effects

4T1 mouse mammary tumor model

The progression of cancer is attributed to acquired genetic instability in tumor cells, upon being subjected to a variety of external pressures such as host-defense mechanisms and growth-control regulators. Tumor cells which can adapt to these external pressures emerge as clonal variants that are more aggressive with better metastatic capability [63]. To reflect the genetic instability during cancer progression, isolated tumor cells are induced with mutagens and subjected to drug-based selection.

Several tumor subpopulations, termed 66, 67, 168, were isolated from a single mammary tumor in BALB/c mouse [64]. Later, subpopulation 410 was derived from a metastatic nodule in the lung of a BALB/c mouse carrying the subcutaneous implant of the tenth *in vivo* passage of the parent tumor [65]. Through mutagen treatment, the 66 cell line was made thioguanine and ouabain resistant and termed 66cl4 [66]. The rate of mutation have been shown to increase when both thioguanine and ouabain are used [63]. The 168FARN cell line is a diamino-purine-, 2-fluoroadenine resistant variant of 168 transfected with a plasmid containing the neomycin resistance gene [61, 67]. The 67NR cell line is geneticin resistant variant of 67 line transfected with plasmid containing the neomycin resistance gene The number of neomycin expressing clones that survive geneticin selection indicates gene transfer efficiency [61]. Through mutagen treatment, the 410 cell line was made thioguanine- and ouabain resistant and the variant was termed 4TO7 [67, 68]. The 4T1 cell line is a thioguanine-resistant variant of 410 without mutagen treatment [61]. We have collectively termed these syngeneic tumor lines (67NR, 66cl4, 168FARN, 4T1 and 4TO7) as ‘the 4T1 model’ [9]/(Fig 3). These breast cancer cell lines are immuno-compatible and can be injected back into a BALB/c mice having a functional immune system.

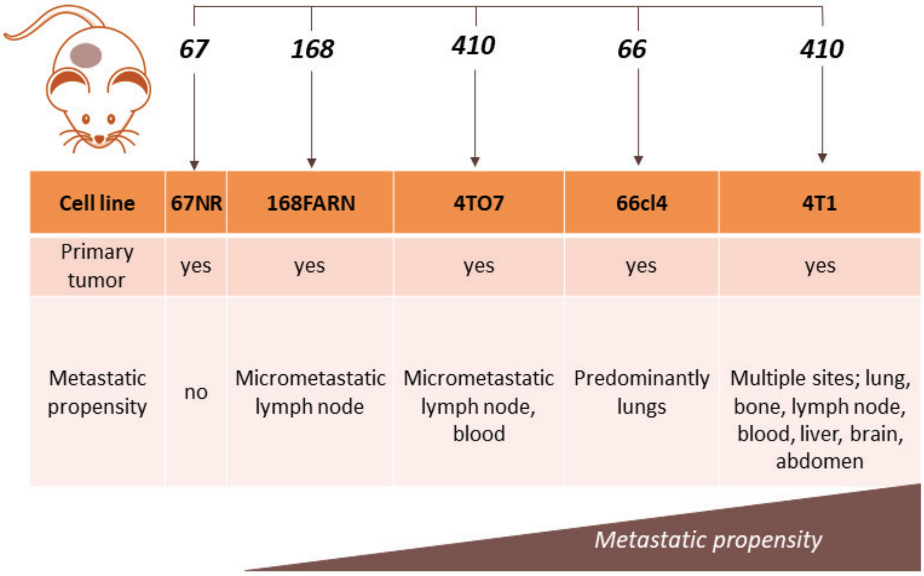

Cell line	67NR	168FARN	4TO7	66cl4	4T1
Primary tumor	yes	yes	yes	yes	yes
Metastatic propensity	no	Micrometastatic lymph node	Micrometastatic lymph node, blood	Predominantly lungs	Multiple sites; lung, bone, lymph node, blood, liver, brain, abdomen

Fig 3: *Sub-populations of cell lines derived from single spontaneous tumor in BALB/c mouse.*

'The 4T1 model' has been used to study both tumor- and host-derived factors involved in spontaneous metastasis [9, 61, 69, 70] These tumor models display features of both luminal and basal-like cancers, mimicking human breast cancer [71]. The cells from 4T1 primary tumor spontaneously metastasizes to different organs such as lungs and liver; whereas the cells from 66cl4 primary tumor predominantly metastasizes to the lungs. The cell lines 67NR, 168FARN, and 4TO7 are highly tumorigenic but very rarely metastasize spontaneously. It has been observed that non-metastatic subpopulations may metastasize in the presence of some metastatic subpopulations [72]. The 4T1 cells appear very epithelial but are highly metastatic, while the 66cl4 cells, which have undergone epithelial to mesenchymal transition (EMT), are less metastatic [73]. This indicates that tumor cells can spontaneously metastasize *in vivo*, with or without exhibiting hallmarks of EMT (*in vitro*). Most tumor cells that enter the bloodstream do not develop into metastatic nodules [74]. The cells isolated from spontaneous metastases may be more metastatic than the original parent tumor [75]. Therefore, characterization of both genetically stable metastatic and non-metastatic sublines is suggested [76].

Extracellular matrix in cancer

The cancer hallmarks are defined as, ‘the acquired evolutionary-advantageous characteristics that complementarily promote transformation of phenotypically normal cells into malignant ones, and promote progression of malignant cells while exploiting the host tissue’ [77]. In the year 2000, Hanahan and Weinberg recognized six major hallmarks acquired by cancer cells including unlimited multiplication, evasion from growth suppressors, promoting invasion and metastasis, resisting apoptosis, stimulating angiogenesis, and maintaining proliferative signaling [78]. A decade later the review was updated with emerging hallmarks including, elimination of cell energy limitation, evading immune destruction, genome instability and mutation, and tumor enhanced inflammation [22]. However, more recently the tumor microenvironment (TME) is also recognized as a hallmark of cancer [77, 79].

The TME comprises cellular and non-cellular components such as the ECM, stromal cells, immune cells, endothelial cells, BMDCs, pericytes, adipocytes, tumor vasculature and lymphatics [80]. The ECM is composed of over 300 different proteins, including glycoproteins, proteoglycans, and polysaccharides with different biomechanical and biochemical properties; that regulate tissue homeostasis, organ development and disease state [81, 82]. Interactions between the ECM and tumor cells facilitates tumor cell transformation, tissue invasion and metastasis (reviewed in [4, 83]). Changes in the ECM composition have also been shown to suppress tumor cell survival and metastatic growth [84, 85]. It is now acknowledged that the ECM can impact all the other hallmarks of cancer [86]/(Fig 4). The classification of primary breast carcinomas based on its ECM composition has been reported to have implications for clinical outcome [87]. Several ECM-proteomic studies using breast cancer patient samples and murine mammary tumors have reported novel ECM proteins in cancer progression and have identified their prognostic value [86, 88-90].

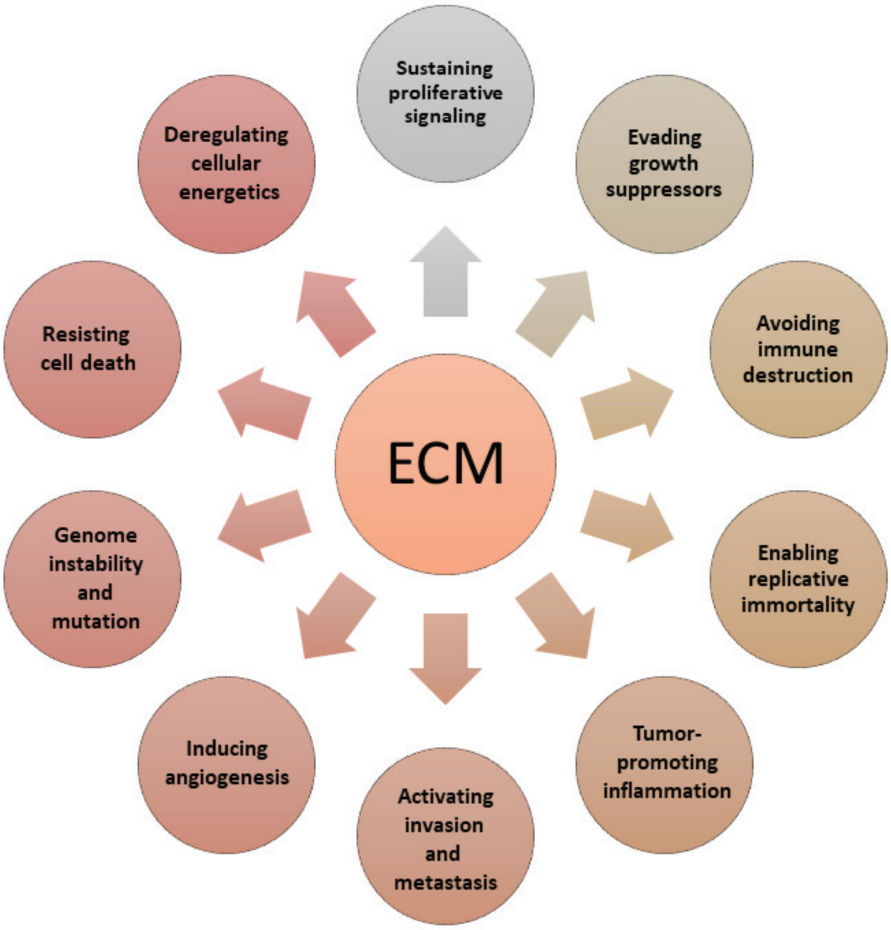

Fig 4: *Biochemical and biophysical properties of ECM can impact all hallmarks of cancer [86].*

Nephronectin (NPNT)

In 2001, Brandenberger and colleagues discovered a novel ECM protein involved in the development of kidneys and named the protein Nephronectin (Nephron: functional unit of the kidney; Nectin: cellular adhesion molecules) [13]. In the same year, Moumira and colleagues discovered the same protein with functions related to osteoblast differentiation and named it POEM (preosteoblast epidermal growth factor-like repeat protein with meprin, A-5 protein, and receptor protein-tyrosine phosphatase mu) [91].

Nephronectin structure

Human NPNT located at the chromosomal position 4q25 is involved in organization of the extracellular matrix [98]. Two transcript variants of NPNT have been reported, NPNTa (565 amino acids /61.9 kDa) and NPNTb (582 amino acids /64.0 kDa), which are particularly rich in proline and glycine [92]. Human NPNT is homologous to mouse NPNT (sharing 88 % amino acid identity) and ECM protein EGFL6 [92]. NPNT contains five EGF-like repeats, a mucin region containing an RGD sequence and a MAM domain [13]/(Fig 5). An additional integrin-binding enhancer motif (LFEIFEIER) has also been found in the mucin region [93]. The mucin region is predicted to be heavily glycosylated [13].

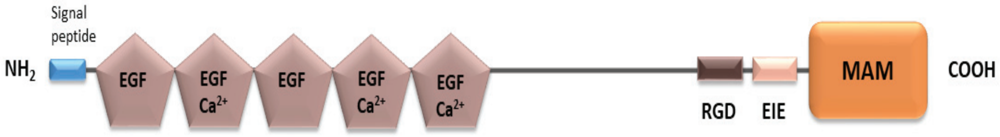

***Fig 5**: Structure of Nephronectin.*

EGF-like repeats

Epidermal growth factor-like repeats are well conserved and are found in the extracellular proteins including fibrillin-1, Notch-3, Jagged 1, factor IX and low-density lipoprotein receptor [13, 92, 94]. Some EGF-like repeats have been shown to bind calcium, which helps the protein to maintain elongated structures and project EGF like repeats from the cell surface for protein-protein interactions [95]. Disrupting calcium binding to EGF-like repeats have been reported in pathological conditions [96]. The EGF-like repeats of NPNT (between amino acids 57-250) have been shown to interact with chondroitin sulphate, another ECM protein [97]. NPNT has been shown to activate EGF receptor via EGF-like repeats [98].

RGD and LFEIFEIER sequences

The RGD sequence facilitates cell adhesion and was first discovered in fibronectin by Pierschbacher and Ruoslahti [99]. Later, several other adhesion proteins were reported to harbor RGD sequence including, vitronectin, fibrinogen, trombospondin, laminin, tenascin, osteopontin and von willebrand factor [100]. The RGD sequence of NPNT has been reported to facilitate spreading and adhesion of cardiomyocytes [101]. RGD containing proteins have also been reported to bind and interact with integrins using alternative integrin binding sequences (reviewed in [100]). In case of NPNT, both the RGD sequence and the LFEIFEIER-motif, facilitates interactions with the integrin, where the EIE-motif enhances the binding [93, 102]. NPNT contains an RGD *and LFEIFEIER* sequence at amino acids 382-384 and 395-403 respectively [13].

MAM domain

The meprin, A-5 protein, and receptor protein-tyrosine phosphatase mu (MAM) domain between amino acids 417–561 is the least conserved part of NPNT [13]. The MAM domain of NPNT facilitates interaction with heparin and heparin sulphate proteoglycans such as agrin and perlecan in the basement membranes [97]. Removal of MAM domain from the recombinant protein has been shown to facilitate release of NPNT into the culture medium [91]. This indicates that MAM domain is most likely responsible for initial cell surface binding.

Integrins

Cells interact with the ECM via several cell surface receptors, such as integrins, discoidin domain receptors, cell surface proteoglycans and hyaluronan receptor CD44, syndecans and Rhamm [5, 103]. Integrins, as the name suggests are vital for integrating the extracellular- to the intracellular environment. These Ca^{2+}/Mg^{2+} dependent transmembrane receptors are expressed in all nucleated cells and are important players in development, immune response and homeostasis [104]. Alterations in integrin expression patterns and levels in distinct cell types at different stages of cancer can regulate how it progresses (reviewed in [105-107]). As of today, 24 distinct integrin heterodimers are known in humans. Heterodimer combinations are formed by noncovalent bonding between one of the 18 alpha and 8 beta subunits. The heterodimers have overlapping ligand specificities and can thus compensate for the loss of a family member [108-110]/(Fig 6).

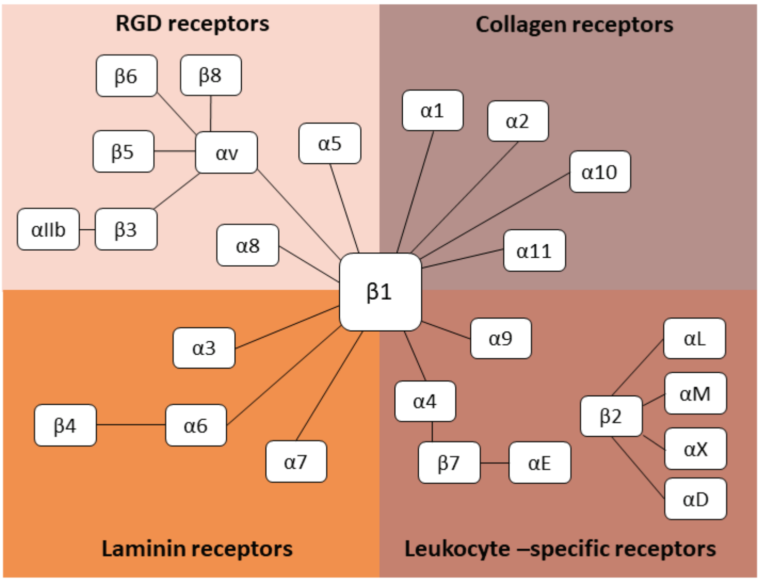

Fig 6*: Categories of integrins according to their ligand binding specificity (laminin-, collagen-, RGD binding integrins) and integrins which are specific to leukocytes (modified from [108]).*

Integrin α8β1

The integrin heterodimers containing β1 subunit constitutes the largest integrin subfamily, where β1 subunit can form heterodimers with one of the 12 different α subunits [111]. Integrin α8β1 is a member of the RGD-dependent subfamily of integrins, where the α8 subunit binds exclusively to the β1 subunit [108, 112]. The α8 subunit is distributed in vascular / visceral smooth muscle, kidney mesangial cells, alveolar walls of lungs, mesenchymal cells and in developing organs such as gut, gonads and the nephrogenic cord [112, 113]. Ligands of integrin α8β1 include fibronectin [114], vitronectin [115], tenascin-C [116], tenascin-W [117], osteopontin [118], the latency-associated peptide of transforming growth factor-β1 [119] and NPNT [13]. Brandenberger and colleagues used a soluble α8β1 heterodimer fused to alkaline phosphatase, and found that it bound to NPNT. They also showed that NPNT co-immunoprecipitates with α8β1 from kidney extracts [13]. The localization of NPNT in kidneys was found to be consistent with the α8β1 expression, where knockout mice of both NPNT and α8 subunit resulted in underdeveloped kidneys (renal agenesis) [14]. This underlines the fact that NPNT is a ligand for the α8β1 integrin. Several other integrins (αVβ3, αVβ5, αVβ6, and α4β7) could bind to NPNT, but not as strongly as α8β1 [13].

Although the RGD motif (on the ligand) is the main binding site for the β integrin subunit , there are usually other flanking motifs that will aid ligand-integrin interactions via the α subunit [120]. Sato and colleagues identified an additional motif within the mucin region of NPNT where the α8β1 integrin could bind, the LFEIFEIER motif [93]. The RGD and EIE motif function synergistically, increasing binding of α8β1 to NPNT.

Integrin signaling

Integrin signals are generated by different types of cellular stimuli such as ligand binding and/or physical changes in the surrounding environment. Integrin receptors are different from other cell surface receptors, where integrins do not have any kinase activity of their own. When activated, integrin receptors aggregate into clusters and signals are generated upon conformational changes of/in the receptor (Fig. 7). Mere clustering of integrins can also generate signals [121]. Interactions of the same ligand with different integrin heterodimers can trigger distinct signaling events in the cell [109]. Therefore it has been shown by several studies that integrin receptors can have both positive and negative effects on cancer progression, depending on the type and stage of the cancer [122-124].

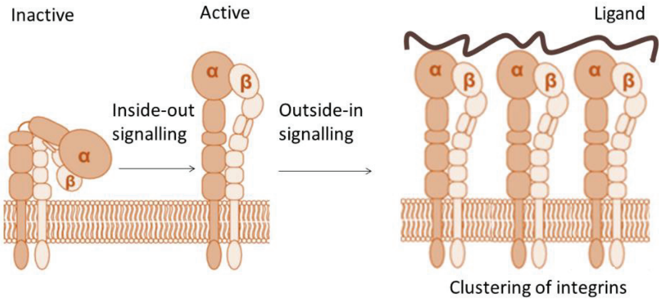

Fig 7: *Conformational changes in the extracellular domains of integrin needed for activation.*

Inside-out signaling: Intracellular signals act on the cytoplasmic domain of the integrin, resulting in straightening of the extracellular domain of the receptor. The change in conformation confers the receptor with good ligand binding capacity. Structurally active integrins on the cell surface anchors the cells to the surrounding environment [108, 125].

Outside-in signaling: Upon integrin-activation the extracellular domain of the integrin binds with the ligand and a signal is transferred into the cell by recruitment of cytoplasmic proteins, thus triggering a variety of signaling pathways including MAPK/ERK pathway, the FAK/SRC pathway, and the PI3K/AKT pathway [108, 126, 127]. Engagement of integrins by ECM ligands can increase the activity of receptor tyrosine kinases such as EGFR and their downstream intracellular mediators (reviewed in [128-130]).

Inside-in signaling: Endocytosis and recycling of integrins is tightly regulated in normal cells [131]. Aberrant changes in the ratio of receptors between the cell surface and the endosomal pool is common in cancer [132, 133]. Active integrins and ECM ligands have been found in endosomes in cancer cells [134, 135]. Furthermore, it has been shown that endosome-localized active integrins can activate FAK signaling and contribute to cancer-related processes [136, 137].

Extracellular vesicles

Over 50 years ago, Peter Wolf first reported ‘particulate material’ derived from platelets [138]. Today we define these particles as extracellular vesicles. Many other types of cells, including fibroblasts, endothelial cells, epithelial cells, neuronal cells, immune cells, as well as cancer cells actively secrete extracellular vesicles [139, 140]; which can be detected in bodily fluids such as blood, bile, fluid in bronchoalveolar lavage, breast milk, lacrimal, saliva, synovial, seminal, ascites, urine and in faeces [141-143]. Extracellular vesicles have been categorized on the basis of size and their mechanisms of release: exosomes (30-100 nm), microvesicles (100-1000 nm), apoptotic bodies (50 nm to 2 µm) and oncosomes (1-10 µm) [144]. The term “exosomes” was coined by Johnstone in 1989 [145]. In research many refer to the pellet obtained after 100,000×g ultracentrifugation as exosomes. Although this pellet is enriched in exosomes, it might also contain small microvesicles as well as protein aggregates [146]. There is evidence suggesting that more than one exosome subtype exists in cell cultures and samples of bodily fluids [147-149]. Exosomes can be further classified into large exosome vesicles (90-120 nm), small exosome vesicles (60-80 nm), or non-membranous nanoparticles (also called exomeres, ~35 nm) [149]. Therefore, it has been suggested that the pellet obtained after 100,000×g ultracentrifugation should be referred to as small extracellular vesicles (sEVs) [150].

Biogenesis and Uptake

The biogenesis of microvesicles is distinct from exosomes. Microvesicles (100-1000 nm) are formed by outward blebbing and fission of the plasma membrane, releasing these vesicles into the extracellular space [151]/(Fig. 8). The lipid composition of the plasma membrane and the organization of the peripheral cytoskeleton influences the formation of microvesicles [152]. Exosomes (30-100 nm) originate within the endosomal system, via the inward budding of the plasma membrane to form a membrane bound vacuole (early endosome). These early endosomes mature into late endosomes/multi-vesicular bodies (MVBs). The membrane of the MVBs then buds inward and pinches off to form intraluminal vesicles (ILVs), which are then released into the extracellular space upon fusion of MVB with the plasma membrane [153] / (Fig. 8). Extracellular vesicles can interact with recipient cells in several ways such as, fusion of vesicles with the target cell membrane, receptor-ligand interactions, phagocytosis, clathrin-mediated endocytosis, caveolin-mediated endocytosis, lipid raft-mediated endocytosis and macro-pinocytosis [154, 155].

Exosome Regulation

Exosomes can either promote or suppress cancer progression, where molecules carried by exosomes play a significant role [156-159]. As of today, the exosome database lists 9769 proteins, 3408 mRNAs and 2838 miRNAs; several of which are key players in cancer progression and metastasis [160]. It is becoming increasingly apparent that tumor derived exosomes contain specific sets of proteins, reflecting their cells of origin [161-164]. Similar to several other biological processes, release of exosomes is regulated by negative feedback mechanism such that the presence of certain number of exosomes in the extracellular space can hinder further release of exosomes from the same cells [165]. Though the research on exosomes is increasing exponentially, the mechanisms that control exosome formation, packaging, and trafficking are not yet completely understood (reviewed in [166-168]).

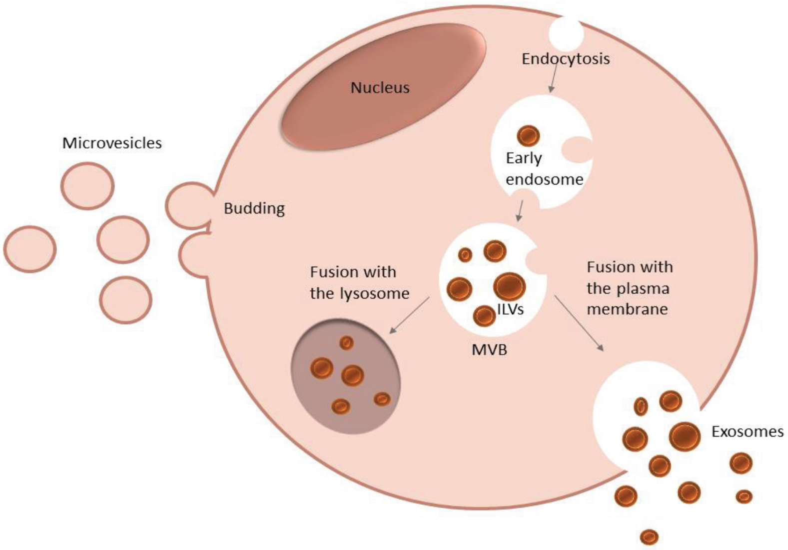

Fig 8*: Biogenesis of microvesicles and exosomes. Illustration shows that microvesicles are formed upon budding of the plasma membrane. The invagination of the endosomal membrane generates intraluminal vesicles (ILVs). Matured endosomes or multi-vesicular bodies (MVBs) store ILVs. MVBs can fuse either with lysosomes for degradation or fuse with the plasma membrane to release ILVs, which are then termed as exosomes.*

Pre-metastatic and metastatic niche

The concept of organ-specific metastasis is well-established both experimentally and clinically [42]. To further complicate the matter, the primary tumor releases enzymatic and non-enzymatic factors into the circulation that can modify the microenvironment at distant organs to create a hospitable niche for the DTCs before their arrival. In absence of a pre-metastatic niche, the DTCs may be cleared by immune cells or undergo apoptosis. Even if the DTCs manage to survive and colonize distant organs, they remain in a dormant state until further activation is initiated by metastatic growth promoting signals. In one of the first reports describing the changes in the pre-metastatic phase, it has been shown that MMP9 expression was elevated in the pre-metastatic lung by a distant primary tumor [169]. The term 'pre-metastatic niche' was coined later when it was found that tumor derived media alone is capable of inducing migration of BMDCs into specific organs [170, 171]. Several systemic mediators from primary tumors such as growth factors, cytokines, chemokines, ECM-remodeling enzymes and extracellular vesicles, can contribute to the formation of the pre-metastatic niche [172-174]. The formation of a pre-metastatic niche is initiated by modulation of vascular permeability followed by alteration of local resident cells such as fibroblasts, and then non-resident cells, such as BDMCs are recruited [170, 175, 176]. The steps in formation of a pre-metastatic niche may differ with the type of cancer [157, 177, 178].

The role of exosomes in formation of a pre-metastatic niche was first identified when melanoma derived exosomes were found to accumulate in sentinel lymph nodes, whereas control vesicles distributed evenly to regional and distant nodes [179]. Exosomes from lung-tropic breast cancer cells have been shown to promote metastatic spread of bone-tropic cancer cells into lungs [173]. Breast cancer derived exosomes have been shown to modulate behavior of BMDCs affecting the pre-metastatic niche [180-183]. These findings imply that exosomes are crucial in formation of a pre-metastatic niche and also important drivers of organotropic metastasis. Specific targeting of aberrant changes in the pre-metastatic niche has been reported to reduce metastasis in preclinical models [170, 184, 185]. Therefore, it is important to further investigate the similarities and differences between metastatic and pre-metastatic niches, in order to develop new therapeutic possibilities.

Molecular subtypes of breast cancer

A surrogate marker is defined as “a laboratory measurement that is used as a direct measure of how a patient feels, functions, or survives and is expected to predict the effect of the therapy” [186, 187]. A biomarker is a potential surrogate marker. Several surrogate markers are prognostic and predictive markers, which are used routinely in the clinic. A prognostic marker is defined as a clinical or biological characteristic that provides prognostic information in an untreated individual; whereas a predictive marker provides information about the expected effect of the treatment [188]. Common surrogate markers such as, the estrogen receptor (ER), progesterone receptor (PR), human epidermal growth factor receptor 2 (HER2) and proliferation marker Ki67 are used routinely in clinic to classify molecular subtype of breast cancer [189]. Subtyping of breast cancer directs the choice of therapy. ER positive, PR positive breast cancer cases respond better to hormone therapy than ER positive, PR negative cases [190]. Amplification/overexpression of HER2 is associated with poor prognosis [191].

It has been shown that using five biomarkers (ER, PR, HER2, EGFR, CK5/6) to identify basal-like breast cancer was superior to use of only three traditional surrogate markers (ER, PR, HER2) [192]/(Table 2). The proliferation marker Ki67 can identify a subset of Luminal B patients that can benefit from the addition of adjuvant chemotherapy to hormone therapy [193, 194]. Overexpression of epidermal growth factor receptor (EGFR) in epithelial tumors has been linked to more aggressive growth and poor prognosis [195]. It has been proposed that basal-like cells originate from luminal cells [196]. Therefore, use of cytokeratin 5 (CK5) would enable identification of myoepithelial and basal cells [197]. Both CK5 and EGFR are not assessed routinely in breast cancer but are of interest in research. In addition to use of surrogate markers in clinic, breast tissue can be analyzed for 50 signature genes (called PAM50 or Prosigna) to estimate the risk of relapse [198]. Though luminal A type patients are associated with relatively good prognosis, several patients experience relapse indicating the heterogeneity within the group [199].

Table 2: *Classification of breast cancers into molecular subtype [200].*

Molecular subtype	**Definition**
Luminal A	ER and/or PR+, HER2-, Ki67<15%
Luminal B (HER2-)	ER and/or PR+, HER2-, Ki67≥15%
Luminal B (HER2+)	ER and/or PR+, HER2+
HER2 type	ER-, PR-, HER2+
Basal	ER-, PR-, HER2+, CK5+ and/or EGFR+
5 negative	ER-, PR-, HER2-, CK5-, EGFR-

Tumor heterogeneity

Inter-tumor heterogeneity (variation among cancer patients) and intra-tumor heterogeneity (variation within a tumor) are characteristics of malignancy [201, 202]/(Table 3). The heterogeneity across the tumor makes the molecular classification difficult and misguides the choice of therapy. Therefore, understanding the molecular and cellular mechanisms of tumor heterogeneity is indispensable for better diagnosis, prognosis, and therapy of breast cancer.

Table 3: *Origin and extent of tumor heterogeneity*

Heterogeneity	**Mechanism**
Morphology	The morphology of tumor cells varies in areas of tumor (spatial), or as a tumor progresses over time (temporal) [203]. E.g., Histological classification of heterogeneous tumor is difficult [204].
Tumor micro-environment	The TME varies greatly between and within each breast cancer patient determining cancer progression and the response to therapy [205]. E.g., Tumor stiffness correspond with cancer progression[206].
Protein expression & Protein levels	The shape, size, quantity and function of a protein may vary across the tumor. E.g., Prpgesterone has been shown to generate two isoforms. The ratio of PR-B to PR-A determines the prognostic impact [207].
Cell plasticity	Cancer stem cells are characterized with remarkable plasticity. E.g., Re-expression of defined markers have induced fibroblasts to pluripotent stem cells [208].
Genetic (Clonal)	Cancer cells acquire genetic aberrations to survive changes in tissue environment and therapy. E.g., Breast cancer patients of a molecular subtype having identical treatment have different clinical outcomes [209].
Non-Genetic (Epigenetic)	Epigenetic abnormalities evolve as the cancer progresses. E.g., ER status affects epigenetic differences [210].
Stochastic	Not all genetically similar cells in a tumor are doing the same thing at any given time. E.g., All tumor cells do not display mitosis at same time [202].

Aims of this study

The interactions between tumor cells and the TME is an important feature of cancer progression, and the ECM plays a major role in these processes (reviewed in [22, 78]). A deeper understanding of the ECM of tumors and metastasis is crucial for translational research to improve survival for cancer patients. In a previous study of genes involved in the metastatic processes, increased NPNT expression was correlated with increased metastatic propensity in primary tumors of mouse mammary tumor lines [9]. NPNT was found to be upregulated in invasive vs non-invasive breast tumors [16] and to promote metastasis in a xenograft based breast cancer model [9]. However, little is known about the mechanism of action and NPNT distribution in human breast cancer. Therefore, the general objective of this thesis was (therefore) to characterize the role of NPNT in breast cancer primary tumors and metastases.

The specific aims of the thesis were to:

1. Investigate the expression pattern and distribution of NPNT in a large cohort of breast cancer patients with respect to tumor classification, clinical history and survival data.

2. Characterize the function of NPNT in various mouse mammary tumor model systems of primary tumors and metastases.

3. Describe the molecular mechanisms of the metastasis-promoting function of NPNT.
   (*in vitro and in vivo* with altered expression of NPNT)

Summary of papers

I. Nephronectin is Correlated with Poor Prognosis in Breast Cancer and Promotes Metastasis via its Integrin-Binding Motifs

In this study, we provide a comprehensive analysis of the expression pattern and distribution of NPNT in breast tumor tissue from 842 patients by immunohistochemical staining of tissue microarrays from a historic cohort. Though NPNT is widely described as an ECM protein [13-15], our findings from mouse and human tumor tissues show intracellular NPNT staining in primary tumors with both diffuse and granular staining in the cytoplasm. We found that when a granular cytoplasmic staining was observed in less than 10 % of tumor cells, this was associated with decreased survival. We suggest that granular cytoplasmic staining may represent NPNT-positive multi-vesicular bodies. We found that NPNT promotes adhesion and anchorage-independent growth via its integrin-binding motifs, and that enforced NPNT-expression in breast cancer cells promotes colonization of the lungs. It is evident that NPNT is involved in promoting breast cancer progression, warranting further investigation into NPNT as a potential prognostic marker and a possible target for therapy in NPNT-positive breast cancer patients.

II. Nephronectin mediates p38 MAPK-induced cell viability via its integrin binding enhancer motif.

The aim of this study was to investigate the biological function of NPNT in the 66cl4 cell line. We used RPPA to analyze NPNT-triggered intracellular signaling in the 66cl4 mouse breast cancer cell line with stable NPNT expression in addition to exogenously added recombinant NPNT. The results showed that the integrin binding enhancer motif is important for the cellular effects upon NPNT interaction with its receptors, including phosphorylation of p38 mitogen activated protein kinase. Furthermore, analysis using prediction tools suggests involvement of NPNT in promoting cell viability. Taken together, these results demonstrate a role for NPNT and its integrin binding motifs, in particular the EIE-enhancer motif, in the induction of p38 MAPK signaling and cell viability. Based on the current findings, we therefore suggest that dual targeting of the RGD and EIE-enhancer motif could prove to be more efficient for cancers with high NPNT levels.

III. A novel truncated form of Nephronectin is present in exosomes from 66cl4-cells

In this study, we identified three different forms of NPNT (at 80, 60 and 20 kDa respectively). The glycosylation pattern of NPNT reveals that the native 60 kDa NPNT protein is less glycosylated compared to the 80 kDa NPNT. The 80 kDa NPNT has both N-glycosylation and O-glycosylation with a sialic acid cap, whereas 60 kDa NPNT is only N-glycosylated. We also identified a truncated form of NPNT at 20 kDa, which is concentrated in the sEVs and that matrix metalloproteinase could be one of the factors involved in cleavage of NPNT. In addition to NPNT, several other proteins are differentially expressed in the cargo of the sEVs derived from mouse breast cancer cells expressing NPNT.

Discussion

Despite huge research efforts, we still do not have a complete understanding of how tumors develop and spread to distant organs. The significance of NPNT in breast cancer was well identified previously [9, 16]. In the three papers presented here, we further explore the prognostic value of NPNT; elucidate several molecular and cellular functions of NPNT and its integrin binding motifs involved in promoting breast cancer. The results discussed in this thesis will provide new knowledge about NPNT as a potential target for therapy and improves our understanding of the role of NPNT in breast cancer progression and metastasis.

Expression and distribution of NPNT

Brandenberger and colleagues reported NPNT protein expression in several types of tissues in mouse embryo such as in the lens of eye, the ear epithelia, the choroid plexus, Rathke's pouch, basal lamina of the lip, skin epithelium, basal lamina of the lung, stomach, esophagus, taste buds of the tongue. Additionally, weak protein expression was found in developing pancreas and the lobe of the ear [13]. Mouse NPNT has also been reported in piloerection [211]. Similar results from Morimura and colleagues show that NPNT mRNA was expressed in developing renal tubules, thyroid and parathyroid glands, developing bone, tooth germ, brain, inner ear, skeletal muscle, smooth muscle (except for the vascular system), and the basal cell layer of the skin in a developing mouse embryo [91]. Downregulation of NPNT mRNA in decidua basalis is associated with preclampsia in pregnant women [212]. The human protein atlas shows the expression of NPNT protein across different organs using immunohistochemistry (www.proteinatlas.org) [213]. Many of the cell processes essential for embryonic development are also central for cancer progression [214, 215]. Normal human breast is reported to be negative for NPNT protein (Fig 9). However, our results in **paper I** shows that breast cancer cases stain positive for NPNT.

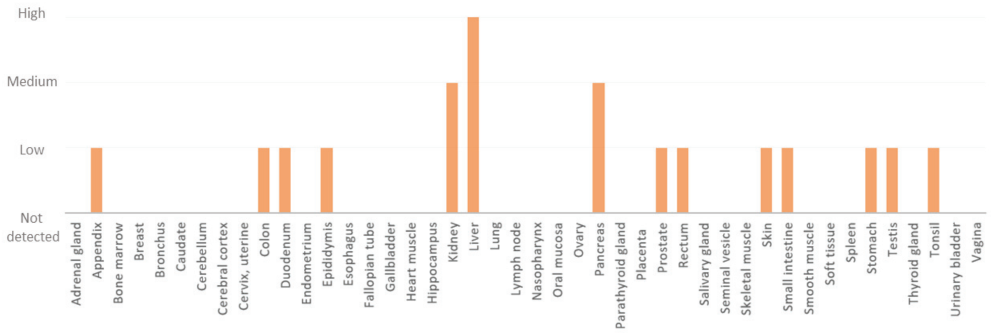

Data from Human protein atlas

Fig 9: *NPNT protein expression in different human organs.*

Our findings in **paper I** are based on a historic cohort of 1393 women, who were diagnosed with breast cancer between January 1st 1961 and December 31st 2008 in Nørd Trøndelag county in Norway [200]. The treatment of the patients in this cohort was often restricted to surgery, which allowed us to follow the near-natural course of the disease after surgery. Patients were followed until death from breast cancer or from other causes or until December 31, 2010. Out of 1393 cases, formalin-fixed paraffin-embedded tissue was available for 909 cases [200]. We considered only 842 out of 909 cases due to technical challenges. In **paper I**, we report four different intracellular staining patterns seen across 842 cases:

1) Nuclear staining (45.7% cases)
2) Diffuse positive cytoplasmic staining (50.4% cases)
3) Scattered single cells with strong cytoplasmic staining (15.3% cases)
4) Granular cytoplasmic staining (13.8% cases)

Results in **paper I** show that NPNT protein localization in our samples was tumor cell-specific with strong intracellular staining and limited staining in the extra-tumoral stromal tissue. We substantiate our findings in human cancers with the IHC analyses of the MMTV-PyMT tissues **(paper I)** where we saw similar NPNT staining patterns to those in human breast cancers, suggesting that this might be a suitable model for further studies. Although the primary site of action of ECM proteins is extracellular, table 4 mentions several ECM proteins which have identified intracellularly.

***Table 4**: List of ECM proteins identified to have an intracellular localization [7].*

Intracellular localization	ECM protein	Reference
Nucleus	• Adipocyte enhancer-binding protein-1 • Decorin • Prolargin • Biglycan • Dentin Matrix Protein-1	[216] [217] [218] [219] [220]
Cytoplasm	• Laminin • Fibromodulin • Lumican	[221] [222] [223]
Endoplasmic Reticulum	• Thrombospondin-4 and 5 • Opticin • Insulin-like growth factor binding protein-3	[224] [225] [226]

The growing evidence for intracellular roles raises many basic questions about how ECM proteins can be routed to the cytosol or nucleus. A few possibilities are listed here [7]:

1. Alternative translation initiation within mRNA transcript, could result in omission of secretory signal peptide. E.g. Alternative translation of osteopontin generates biologically active intracellular isoforms in dendritic cells [227].
2. Alternative splicing of mRNA. E.g. A new splice variant of fibulin was identified which does not encode the N-terminal sequence and therefore was trapped intracellularly [228].
3. Autophagic recycling of cytoplasmic components is increased in breast cancer cells experiencing starvation and/or hypoxia. E.g. Insulin-like growth factor binding protein 3 is recycled to promote survival of starved breast cancer cells. [226].
4. Some proteins can escape the endo/lysosomal system. E.g. Internalized EGF/EGFR complexes may leave the endosomes and enter the nucleus via nuclear pores [229].

5. Despite the presence of a secretory signal peptide, ECM proteins containing a nuclear localization sequence are destined to localize in the nucleus. E.g. The nuclear localization sequence of SLRP biglycan enables the protein to enter the nuclei of cultured cells [219].
6. Misfolded proteins in the endoplasmic reticulum are transported to the cytosol for degradation by proteasomes [230] E.g. Cholera toxin rapidly refolds upon retro-translocation and avoids cytosolic degradation [231].
7. Many ECM proteins are secreted constitutively, for others secretion is regulated according to physiological conditions. E.g. von Willebrand factor has both extra- and intra-cellular roles to accomplish in its life cycle [232].
8. ECM turnover is influenced by extracellular proteases, cellular uptake of ECM proteins, or their proteolysed fragments for intracellular degradation. E.g. MMPs control the quantity of ECM [233].
9. Cancer cells can undergo cell-cell fusion events or cell-in-cell invasion which might also result in cytoplasmic mislocalization of ECM proteins [234, 235].
10. Immunohistochemistry alone is not sufficient to determine intracellular localization. The credibility of our results in **paper I** is based on validated antibodies and immunofluorescence based co-localization with established intracellular markers. However, further investigation using mouse gene knockout or transgenic models is required to understand the specific roles of intracellular ECM proteins such as NPNT.

Intracellular localization of ECM proteins is an under-researched topic. Further research is needed to identify the pathways that lead to cytoplasmic or nuclear localization and determine the functional roles of intracellular ECM proteins in cancer cells.

Breast cancer lung metastasis

The molecular subtype of breast cancer, different gene signatures and signaling pathways of metastatic tumor cells regulate organotropic metastasis [236]. Compared to other subtypes, triple negative, basal and luminal B subtypes of breast cancer are more aggressive and show higher levels of lung specific metastasis (Fig. 10). Usually, lung metastases display little or no symptoms until the lungs are massively supplanted by metastatic tumor masses. Therefore, lung metastasis is a serious problem in breast cancer patients.

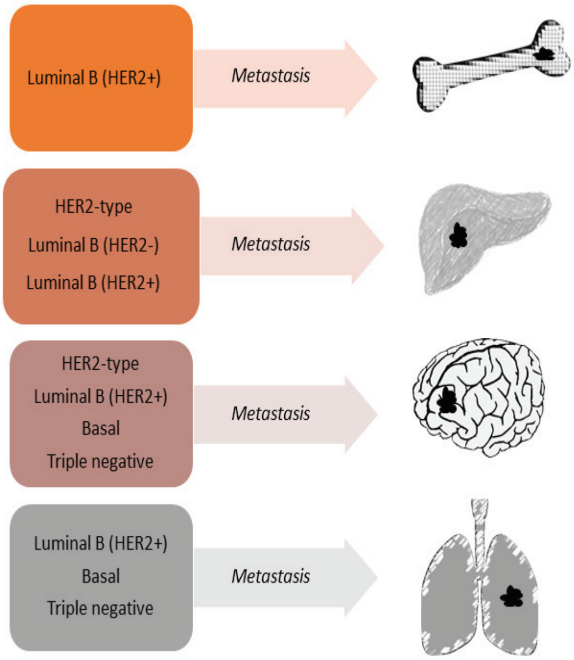

Fig 10*: Breast cancer subtypes regulate organotropic metastatses [237].*

The ECM of the lung metastases is more similar to the ECM of the primary breast tumor rather than the lung ECM [86]. Several lung metastasis signature genes are associated with poor survival [237-239]. Eckhardt et al. have previously shown that reduced NPNT expression in the highly metastatic 4T1.2 cells caused a significant reduction in metastatic tumor burden in lungs, kidneys and spine [9]. Our data in **paper I**, demonstrates that the enhanced expression of NPNT in low-metastatic 66cl4 cells does not increase spontaneous metastasis, whereas in experimental metastasis assays NPNT overexpression promotes the capability of tumor cells to seed and grow in the lungs in an integrin-dependent manner. This suggests that NPNT might be more important at the secondary site and not in the process of leaving the primary tumor. Once the cancer cells enter the blood flow, they are carried to the capillary beds of the lungs. Cancer cells have a diameter five-times larger than that of pulmonary capillaries, so they can be physically trapped in the narrowing blood vessels [240, 241]. In addition, specific surface adhesion molecules on tumor cells mediate the adhesion of cancer cells to the lung vascular endothelium. **Paper I** shows that 66cl4 cells with enhanced expression of wild-type NPNT adhered better to the culture plates than 66Cl4-EV cells. It would further be interesting to note that the 66cl4-EV cells showed a dose-dependent increase in adhesion to plates coated with rmNPNT, and this adhesion was reduced in the presence of a RGD-blocking peptide, demonstrating the involvement of RGD-binding integrins. It has been shown that the main receptor for NPNT is integrin α8β1 [13, 91]. It also appears that RGD sequence of NPNT is more important in binding to α8β1, whereas the EIE motif is more important for intracellular signaling events [93, 102]. NPNT might also interact with other receptors, for example, integrin αVβ3, on the lung endothelium in the metastatic cascade [242]. Adhesion proteins such as NPNT need to be investigated further in lung-tropic metastasis research. It would be interesting to study whether neutralizing peptides against NPNT and/or blocking the NPNT-interacting receptors would inhibit breast cancer lung metastasis.

After adhesion and extravasation into the lung parenchyma, the next challenge for metastatic cancer cells is survival and adaptation to a new microenvironment. This adaptation includes dodging the apoptotic signals in the new microenvironment [23]. Most intravenously injected cancer cells that lodge in the lung die within 2 days [243] mainly because lungs have a leukocyte-rich microenvironment [244]. Our results in **paper II** demonstrate that NPNT and its integrin binding motifs, in particular the EIE-enhancer motif, increases the ability of 66cl4 cells to survive in sparse growth conditions **(paper II)**. *In vitro* assays in **paper I** indicate that NPNT is involved in anchorage-independent growth, which could indicate that NPNT is beneficial in colony formation at the secondary site. Enforced expression of NPNT in 66cl4 cells increased both the number of metastatic lesions in lungs and the size of the colonies. These findings from **paper I and II** indicate that the expression of NPNT in breast cancer cells promotes adherence, viability and colonization in the lungs, thereby facilitating several steps in the metastatic cascade.

Signaling for survival

Resisting cell death is one of the hallmarks of cancer [22, 78]. **Paper II** shows how NPNT overexpression in breast cancer cells can avert cell death in sparse growth conditions as mimicked by serum starving cells. The signaling components of the mitogen-activated protein kinases (MAPKs) convert the extracellular stimuli into a range of cellular responses such as, proliferation, differentiation, survival and migration [245-247]. There are three major groups of MAPKs in mammals [248]: the Jun N-terminal kinase (JNK), p38 MAPK and the extracellular signal regulated protein kinases (ERK), which are also often deregulated in cancers [249]. MAPKs are evolutionarily conserved enzymes, where the activation of MAPK requires dual phosphorylation on the Threonine-X-Tyrosine motif by MAP2K kinases, which is in turn phosphorylated and activated by a MAP3K [250, 251]. Generally, activation of ERK1/2 has been linked to cell survival, whereas JNK and p38 MAPK are linked to induction of apoptosis [252]. However, this is an oversimplification of the MAPK cascade and non-canonical roles of MAPK are coming into more focus nowadays [253].

Results in **paper II** show that NPNT induced phosphorylation of p38 MAPK increases cell viability of breast cancer cell lines such as 66cl4 and 4T1. NPNT induced phosphorylation of ERK and p38 MAPK has been shown to regulate angiogenesis in endothelial cells [254]. The expression or activity of p38 MAPK is often altered in various cancers, including follicular lymphoma [255], lung [256], thyroid [257], glioma [258], head and neck squamous cell carcinomas [259], and as well as breast carcinomas [260]. The pleiotropy of p38 MAPK, inducing cell survival or cell death depends on the cell type, disease stage and type of the stimulus [261-263]. Several potential scenarios listed below discusses the conditions under which p38 MAPK activation promotes cell survival instead of cell death:

- The activation of p38 MAPK has been shown to mediate anti-apoptotic inflammatory signals, such as the cytokine interleukin-6, which is critical for survival during inflammation [264].
- Cells might undergo apoptosis only if the p38 MAPK activation is exceedingly strong [252]. If p38 MAPK signaling levels are just enough to induce growth arrest without apoptosis [265], it helps cancer cells to adapt, survive and further acquire drug resistance [266].

- The p38 MAPK signal levels can mediate cell survival instead of cell death by controlling the autophagy regulators [267], such as the anti-apoptotic (Bcl-2) and pro-apoptotic (Bad) proteins [268].
- Activated p38 MAPK has been shown to inactivate glycogen synthase kinase 3β. This further results in the accumulation β catenin [269], which is known to regulate the expression of other survival genes promoting genes, such as c-myc [270].
- The signaling levels of p38 MAPK have been associated with the G2/M checkpoint, which induces cell cycle arrest and facilitates DNA repair [271].

There are four genes that encode p38 MAPKs: MAPK14 (p38α), MAPK11 (p38β), MAPK12 (p38γ) and MAPK13 (p38δ) [272]. The p38α levels are high in most cell types and it is better characterized than other p38 MAPKs [272, 273] . Most of the published literature on p38 MAPKs refers to p38α (reviewed in [253, 262]). **Paper II** identifies the role of p38 MAPK phosphorylation in NPNT expressing cell lines. The phosphorylation p38 MAPK may regulate: (A) *Transcription factors* such as p53, activating transcription factor 2 (ATF2), Ets transcription factor (ELK1), myocyte-specific enhancer factor 2 (MEF2) and CCAAT-enhancer-binding proteins (C/EBPβ). (B) *Protein kinases* such as MAPK-activated kinase 2 (MK2), mitogen- and stress-activated protein kinase 1 (MSK1), MAPK-interacting serine/threonine kinase 1 (MNK1) and MNK2 [273, 274]/(Fig. 11). In continuation to results in **paper II**, it would be interesting to further investigate the specific role of different p38 isoforms and transcription factors regulated in NPNT induced p38 MAPK pathway.

The involvement of p38 MAPK in NPNT induced intracellular signaling was confirmed using BIRB 796 as shown in **paper II**. BIRB 796 (Doramapimod), a p38 inhibitor was first synthesized in 2002 [275]. BIRB 796 has an IC50 for p38α = 38 nM, for p38β = 65 nM, for p38γ = 200 nM, and for p38δ = 520 nM [276]. Thus the potency of BIRB 796 increases with the period of pre-incubation with the inhibitor [277]. The selectivity and specificity of BIRB 796 is well studied at different concentrations. A complete kinase profiling of this inhibitor can be found at MRC PPU [278]. At a concentration of 1µM, BIRB 796 is able to completely inhibit p38α, p38β and the activity of p38γ and p38δ is less than 50 %. However, at higher concentrations (10µM), BIRB 796 can even inhibit all p38 MAPK isoforms *in vitro* and *in vivo*, with little effect on other kinases [279]. BIRB 796 enhances efficacy of chemotherapeutic agents in multiple myeloma [280], in oral epidermoid carcinoma cells [281], and in cervical cancer [282]. It is also used in inflammation research [283, 284]. Very few p38 MAPK inhibitors have progressed beyond phase I clinical trials, owing to side effects, such as liver toxicity [285, 286]. Alternative strategies, such as targeting kinases higher in the signaling cascade or using less selective compounds, might be more successful.

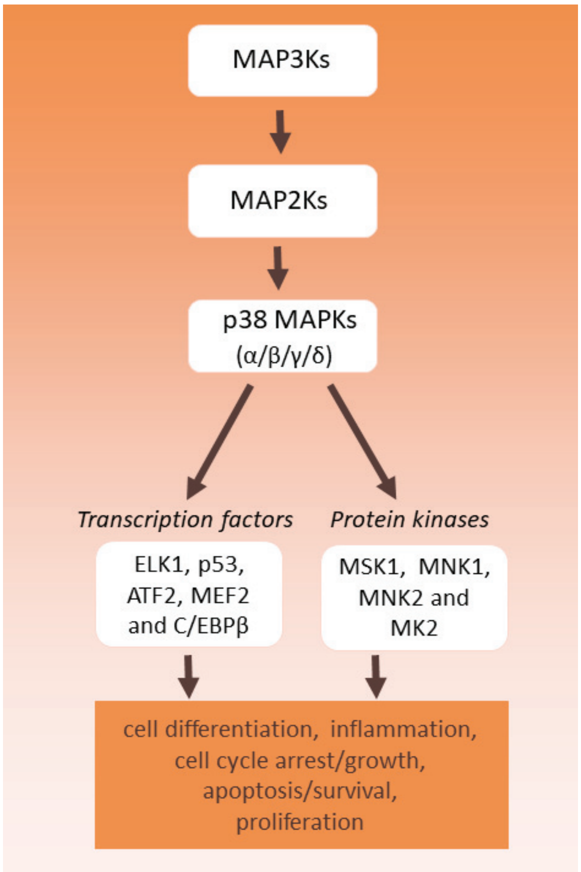

Fig 11*: The p38 MAPK signaling pathway. Different stimulus/receptors can activate MAP3Ks, which phosphorylate and activate MAP2Ks, which in turn lead to activation of p38 MAPKs through dual phosphorylation at Tyr and Thr. Activate p38 MAPK can phosphorylate protein kinases or transcription factors, which lead to the control of many cellular responses.*

NPNT-positive extracellular vesicles

Vesicular communication between the cells and their microenvironment is crucial for both normal and pathological physiology [287]. The lipid bilayer-membrane of extracellular vesicles provides a protective shield for the vulnerable biological signaling molecules, allowing them to reach distant sites. The role of cancer derived extracellular vesicles in cancer progression and metastasis is becoming increasingly recognized (reviewed in [287, 288]). NPNT has been detected previously in isolated exosomes from human ductal saliva and colorectal cancer cells [289, 290]. In **paper I**, we reported the presence of NPNT in microvesicles and exosomes derived from 66cl4 cells overexpressing NPNT and that the localization of NPNT protein in these vesicles is not integrin-dependent. Recently, NPNT has also been reported in isolated exosomes derived from 4T1 cells [291]. In **paper I,** the fraction of vesicles isolated after spinning at 100,000 x g for 70 mins, has been referred to as exosomes. However, in **paper III** we acknowledge the variation in the size distribution of vesicles present in the pellet isolated after spinning at 100,000 x g for 70 mins and is referred as small extracellular vesicles.

In **paper I**, we suggest that NPNT may be used as a prognostic marker for breast cancer, where patients with 1-10% of tumor cells showing granular staining had a poorer prognosis than those with no granular staining or more than 10% of granular-positive tumor cells. It is also important to note that our findings come from the tissue samples drawn for the periphery of each tumor. Results could also vary depending on the distribution of tumor cells and the region from where the tissue sample is drawn. In **paper I**, we report a nonlinear U-shaped correlation between granular cytoplasmic staining of NPNT and survival. Similar correlation pattern has been reported previously for various tumor markers in glioma [292], prostate [293, 294], colorectal [295, 296], and pancreatic cancer [297, 298] and breast cancer [299, 300]. Though the explanation for this phenomenon is unclear in most cases; differences in study design, specific cancer site, limited statistical power and variability in laboratory measurements may be contributing factors to these discrepancies. The race of the study population also has an impact on the distribution of molecular subtypes and breast cancer mortality [301-303]. In our cohort, majority of the cases were Luminal A subtype. So, it is not surprising that the association between the presence of any NPNT granular staining and prognosis was strongest for the Luminal A subtype. Therefore, large studies in several other cohorts are needed to confirm these findings. Granular NPNT staining pattern has also been shown previously in mouse tibias, however authors have not specifically commented on the biological relevance of this staining pattern [254]. The IHC images in **paper I** suggest that these granules seen inside the tumor cells could be MVBs, which are large, >250 nm diameter organelles that contain smaller, 50-80 nm diameter ILVs [304]. Immunofluorescence staining of 66cl4-NPNT lung metastases and MMTV-PyMT tumor tissues shown in **paper I** confirm the co-localization of NPNT with CHMP4B (a marker for charged multi-vesicular bodies). The functional role of NPNT-positive extracellular vesicles in mouse models of metastasis remains to be investigated. Tumor cells secrete more extracellular vesicles compared to normal cells [305, 306]. It has been reported that cancer cell lines with upregulated MAPK signaling pathway, secrete higher number of exosomes [307]. In continuation with our results in **paper II**, it will be interesting to investigate if inhibition of p38 MAPK in NPNT overexpressing 66cl4 cells will alter the number of exosomes released.

Extracellular vesicles such as exosomes contain bioactive proteins, sugars, lipids, metabolites and nucleic acids [140, 308]. Several databases provide information about the molecular composition of exosomes [309, 310]. In addition, it is well known that the cargo content of the exosomes reflects the origin and the status of the cell at the time of exosome generation [311]. To some degree, the cargo content of extracellular vesicles can be influenced by different cellular conditions and/or treatments [146]. Results in **paper III** show that the protein cargo of sEVs is altered, upon NPNT expression in 66cl4 cells. This cargo content of sEVs could be a reflection of the key signaling molecules induced by NPNT overexpression in 66cl4 cells, which are eventually picked up by the dynamic membrane of MVBs and finally incorporated into ILVs. Several tumor-promoting proteins are differentially packed in sEVs derived from 66cl4-NPNT cells compared to sEVs derived from 66cl4-EV cells as reported in **paper III**. Several other studies have shown to advocate the concept of alterations in sEVs cargo, upon changes in cellular conditions [290, 312, 313]. Indeed, the source of exosomes defines their function in cancer progression and metastasis. Our work is primarily based on extracellular vesicles isolated from mouse breast cancer cell lines. It will be interesting to see if we can extrapolate these findings in vesicles isolated from human breast cancer cell lines.

Post-translational modifications of NPNT

Protein regulation takes place at transcriptional, translational and post-translational levels. Post-translational modifications (PTMs) of proteins is often used as a ‘biochemical footprint’ to reflect upon the physiological processes [314]. Therefore, the PTMs associated with a protein are vital for developing optimal biomarkers.

Glycosylation

Glycosylation is a frequent PTM, where the enzymatic process produces glycosidic linkages of saccharides to other saccharides, lipids or proteins [315]. The N-linked glycosylation and O-linked glycosylation are the two most common mechanisms by which sugars are linked to proteins. In N-linked glycosylation, glycans bind to the amino group of the asparagine in the endoplasmic reticulum [316]. In O-linked glycosylation, monosaccharides bind to the hydroxyl group of serine or threonine in the Golgi apparatus [317]. Sialic acids are typically found to be terminating branches of N- and O-glycans [318]. Aberrant glycosylation in cancer is a well-documented topic [319]. Changes in the glycosylation patterns of the cell surface and the secreted glycoproteins occur during all the steps of cancer progression to regulate cell-matrix interactions, tumor proliferation, invasion, immune modulation, metastasis and angiogenesis [315, 320]. The expression of glycosylation related genes has been found different in normal breast tissue compared to that in breast carcinomas [321]. Further, it has been shown that the expression of glycosylation related genes differ in PAM 50 intrinsic subtypes of breast cancer [322].

Different PTMs such as glycosylation are also crucial for sorting of proteins into exosomes and/or microvesicles [323, 324]. In **paper III**, we showed that the heavily glycosylated 80 kDa NPNT, having both N- and sialylated O-glycosylation is recruited into exosomes, while the 60 kDa NPNT having only N-glycan is not detected in either exosomes or microvesicles. Cancer cells often have high levels of sialylated glycans [325], which are also associated with malignancy and poor prognosis in patients [326-328]. N-glycans are known to modulate the adhesion and growth of tumor cells in early stages of tumor progression, whereas O-glycans can confer resistance to oxidative stress during late stages of tumor growth [329, 330]. Breast cancer patients with high CTC counts were also reported to have high glycan levels than those with low CTC counts, implying a role of glycosylation in breast cancer metastasis [331, 332]. However, the specific role of glycans associated with NPNT remains to be investigated.

Proteolytic processing

For cancer progression, the balance between synthesis and degradation of ECM needs to be disrupted. Proteolytic factors such as matrix metalloproteinases (MMP) play a crucial role of remodeling the ECM in cancer progression and metastasis [333, 334]. MMPs can act both intracellularly and extracellularly to generate biologically active fragments [333, 335, 336]. In **paper III**, we have reported that the 20 kDa NPNT is a cleaved form of NPNT and that this cleavage is mediated at least in part by MMPs. Whether this truncated form of NPNT is biologically active remains to be investigated. On similar lines, truncated proteins such as heparanse-cleaved heparan sulphate have been reported to influence the composition and biogenesis of the extracellular vesicles [337, 338]. In **paper I**, we have shown that overexpression of NPNT in 66cl4 cells, increases the ability of cells to colonize the lungs. However, the human protein atlas (www.proteinatlas.org) shows that normal lungs have a high NPNT protein expression (Fig. 7) [339]. It could be speculated that the difference between the mechanism of the endogenous NPNT in a healthy lung and tumor cell derived NPNT could be credited to the PTMs and truncated NPNT. Further research is needed to identify whether cleaved NPNT and its PTMs has a physiological consequence on breast cancer biology.

NPNT in cancer research

Eckhardt and colleagues, were the first to identify NPNT as a tumor oncogene in metastatic breast cancer cell lines [9]. Kuphal and colleagues tested the NPNT levels in malignant melanoma and it has been shown through RT-qPCR analysis that NPNT expression was lost or reduced in malignant melanoma cell lines compared to normal melanocytes [340]. Ban and colleagues reported in 2012 that NPNT expression significantly increased in papillary thyroid carcinoma patients [341]. They have used several techniques including proteomics, IHC and RT-PCR to validate NPNT as a characteristic marker for papillary thyroid carcinoma. Åkerström and colleagues have reported that NPNT is regulated in aldosterone-producing adenomas with different somatic mutations [342]. Later in 2017, Teo and colleagues identified that NPNT expression was also upregulated in adrenocortical carcinoma. They further went on to show that NPNT confers pro-adhesive properties in aldosterone-producing adenoma cells; whereas NPNT in adrenocortical carcinoma cells acts as an anti-adhesive [343]. These studies performed over the years suggest that the expression of NPNT and its role varies across cancer types (Fig. 12).

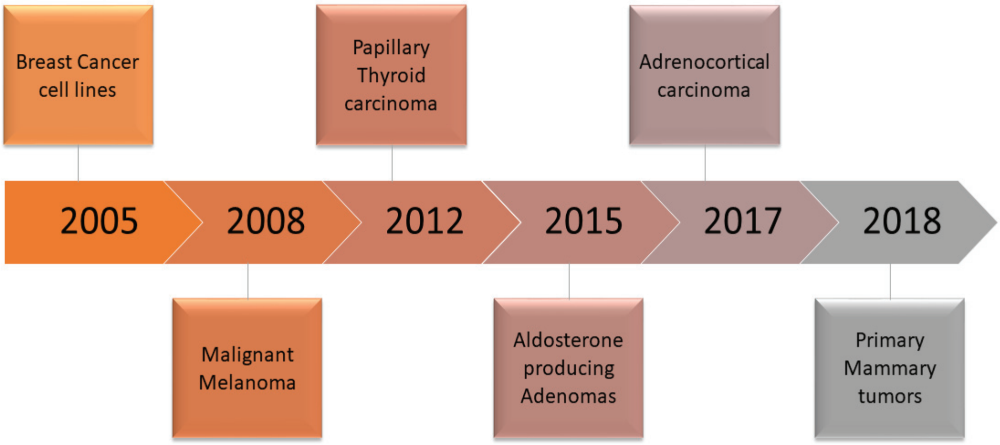

***Fig 12**: Timeline of key discoveries in NPNT-related cancer research.*

In 2018, two contradicting reports were published that discuss the role of NPNT in primary mammary tumors and metastatic organs such as lungs [344, 345]. On one hand, Dilmac and colleagues have reported that the expression of NPNT in lungs and liver is lost when breast cancer cells metastasize in these organs [344]. On the other hand, our results in **paper I** show that overexpression of NPNT in breast cancer cells promote lung colonization. The biology of mouse mammary gland changes with time and this would have an impact on the research question [346, 347]. In **paper I**, we have used mice which are in the middle of the puberty (approx.6 weeks) as opposed to the experimental setup by Dilmac et al. [344], where they have used mice after puberty (approx. 10-12 weeks). Results reported by Dilmac et al. are based on tumors which are barely palpable (1-2 mm in diameter) [344]. Instead of measuring tumor size with calipers, our findings in **paper I** are based on relative tumor burden, where we measured the level of genomic DNA from mCherry positive 66cl4 cell line variants. Another weakness in the findings of Dilmac et al. is that different numbers of cells were injected for different cell lines in the animal groups [344].

All these studies performed over the years indicate that NPNT has cancer type-specific role. Exploring the intricacies of novel proteins like NPNT in cancer type-specific landscapes could may be help us understand why some cancer cells respond to therapy and others do not.

Targeting NPNT in breast cancer

Development of a therapy starts with identification of a gene/protein within a sample of the primary tumor, whose expression correlates with patient survival (correlative studies). The effect of protein overexpression or ablation on metastatic potential should be tested in preclinical animal models (causative studies). In **paper I,** we have reported that the granular NPNT-expression in less than 10% of tumor cells correlates with poor patient survival. Further, we utilized experimental metastasis assay and MMTV-PyMT mouse model to confirm that overexpression of NPNT in tumor cells confers additional metastatic potential **(paper I)**. Investigation of the pathways triggered by overexpression of candidate proteins (target identification) forms the basis of drug development. High-throughput screens can help to identify promising compounds (Lead identification), followed by optimization where the compound is modified to improve the activity. Lastly, clinical trials are vital in establishing safety and efficacy of the treatment.

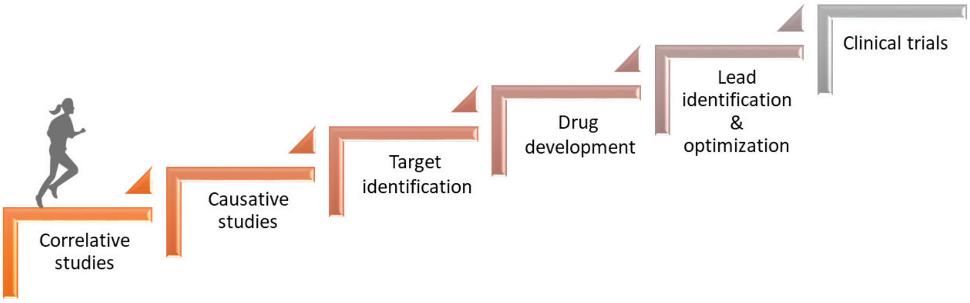

Fig 13: *The process of developing targeted therapies (summarized in [3]).*

Results in **paper I, II and III** explores possible routes of targeting NPNT in breast cancer:

Integrin inhibition has been capable of sensitizing breast cancer cells to radiotherapy, according to preclinical and *in vitro* studies [348, 349]. However, selective integrin inhibitors like cilengitide and abituzumab have failed in clinical trials [350-353]. These inhibitors block the ability of integrins to bind with RGD motif of the ECM proteins. Our fundamental results in **paper I and II** suggest that dual targeting of RGD and EIE motif could completely disrupt ligand receptor interaction and might lead to better outcomes. There are several other factors to consider when targeting integrin inhibition such as, tumor cells can evade therapy by switching between integrin heterodimers [354] and integrins in cancer cells have been shown to signal for survival irrespective of presence of the ligand [355]. Therefore, targeting downstream signaling molecules in integrin pathway seems more plausible.

p38 MAPK inhibitors are mostly based on ATP competition, where p38 MAPK is not able to bind ATP, hindering further phosphorylation of downstream targets. ATP competitors might cross-react with other kinases or non-kinase cellular proteins [356]. Therefore, out of 20 inhibitors that progressed to clinical trials, only three compounds (BIRB796, SCIO469 and VX702) entered Phase II trials (reviewed in [357-359]). In **paper II,** we utilize BIRB796 to substantiate the involvement of p38 MAPK in NPNT induced signaling. BIRB796 has also been withdrawn from trials now. It is not surprising that inhibition of p38 MAPK leads to adverse reactions, since p38 MAPK signaling is involved in many cellular processes. An alternative option is to inhibit the upstream kinases of p38 MAPK, because they have no known substrates other than the p38 MAPK isoforms.

Glycosylation mediated strategy is also one of the opportunities for cancer therapy [360, 361]. As compared to normal cells, tumor cells often display high expression levels of overall sialylation, truncated glycans, N-linked glycans and glycosphingolipids [315]. Though it remains to be investigated if glycosylation pattern of NPNT has a biological significance, we have detected that NPNT expressed by breast cancer cells has high sialyation **(paper III)**. Glycosylation is involved in protein folding, cell–cell interactions, protection of proteins from enzymatic degradation and in signal transduction pathways (reviewed in [360, 362, 363]). Therefore, glycosylation mediated strategy might have off-target effects and requires detailed investigation [364].

MMP inhibitors have failed in the past due to two main reason; firstly, broad spectrum MMP inhibitors were used in clinical trials and secondly, MMPs involved in early stages of cancer might be different from the advanced stage [334]. The catalytic activity of MMPs degrades the ECM and results in the production of ECM-derived and non-ECM bioactive fragments. MMPs process proteins to reveal its functional fragment so that proteins can interact with cells [365]. Biological significance of the cleaved ECM proteins (matrikines and matricryptins) is well reviewed [366, 367]. In **paper III**, we report MMP mediated cleavage of NPNT, where the truncated form is concentrated in extracellular vesicles. Specific MMPs that are responsible for cleavage of NPNT remain to be identified.

Extracellular vesicles such as exosomes can be explored therapeutically as they lack A/B blood group antigens and are biocompatible [368]. Therefore, exosomes released by cancer cell lines are often used to search of biomarkers for a specific cancer type [369]. In **paper I**, we reported NPNT-positive vesicles as a marker for poor prognosis in breast cancer. Exosome secretion in cancer cells is considerably higher than that of normal cells [370, 371]. Blocking release of tumor derived exosomes may reduce drug resistance and cancer progression, but it might also weaken the beneficial effect of exosomes from non-malignant cells [167]. In **paper III**, we identified several tumor promoting molecules in NPNT-positive sEVs. The specific role of NPNT-positive sEVs in breast cancer progression and metastasis needs to be investigated further using *in vivo* models.

Future perspectives

Not all *in situ* tumors become invasive [372]. Therefore, identifying and understanding the drivers of metastatic disease would have a major impact on the survival of cancer patients. Advances in MS technology coupled with the genomic information, allows identification and quantification of the novel proteins present during cancer progression and metastasis [82]. This methodology was applied to transgenic mouse mammary tumor model MMTV-PyMT to identify key ECM players in cancer progression and metastasis. In affirmation with the findings in this thesis, the MS data was promising and identified several ECM proteins including NPNT; whose expression seemed to be linked to tumor grade (unpublished results). We have used a large cohort of breast cancer patients, which contributes to our understanding of NPNT distribution and breast cancer heterogeneity. Although we report different staining patterns for NPNT in 70% of the patients in this cohort, the clinical significance of single positive cells or possible function of NPNT in the nucleus remains to be elucidated. Verifying NPNT expression and distribution in other cohorts would give us better insights.

For tumors with high NPNT, p38 MAPK appears as a potential target. However, it is essential to first uncover other downstream mediators and transcription factors involved in NPNT responsive signaling pathways. NPNT and its integrin binding motifs, is crucial for adhesion, survival and anchorage independent growth of tumor cells. Therefore, further studies should focus on targeting both the RGD and EIE-enhancer motif in cancers with high NPNT levels. We have used several different mouse models and *in vitro* experiments, however our models only mimic the human microenvironment. We did not include studies on human NPNT, which will have to be investigated in future studies.

Extracellular vesicles are immunologically inert [373] and therefore hold great potential for clinical application. Several proteins identified in NPNT-positive sEVs isolated from 66cl4-NPNT cells give an insight into the nature and severity of the disease. The potential of NPNT containing exosomes as a biomarker needs to be examined in patient samples like blood and urine.

Conclusions

Cancer progression is influenced by reciprocal interaction of tumor cells with the ECM proteins. Localization of NPNT extracellularly as well as intracellularly suggests that this protein has multiple functions in breast cancer. The results in this thesis highlight the role of NPNT in promoting adhesion, cell viability, anchorage independent growth and lung colonization. Our data indicates that p38 MAPK is an important mediator of NPNT-induced survival signaling. We uniquely identify the prognostic value of NPNT using a large cohort of breast cancer patients. We discuss post-translational modifications of NPNT (glycosylation and proteolytic processing) and further show that truncated NPNT is concentrated in the sEVs. Finally, several cancer-promoting molecules identified in NPNT-positive sEVs underline the importance of vesicular communication in cancer progression and metastasis. Overall, we propose that our findings adds several layers of information to our understanding of NPNT's role in breast cancer. These results will contribute to future design of research, prognosis and potential new treatment strategies.

References

[1] I.J. Fidler, S.J. Kim, R.R. Langley, The role of the organ microenvironment in the biology and therapy of cancer metastasis, Journal of cellular biochemistry, 101 (2007) 927-936.

[2] L.A. Liotta, E.C. Kohn, The microenvironment of the tumour-host interface, Nature, 411 (2001) 375-379.

[3] B.L. Eckhardt, P.A. Francis, B.S. Parker, R.L. Anderson, Strategies for the discovery and development of therapies for metastatic breast cancer, Nature reviews. Drug discovery, 11 (2012) 479-497.

[4] P. Lu, V.M. Weaver, Z. Werb, The extracellular matrix: a dynamic niche in cancer progression, The Journal of cell biology, 196 (2012) 395-406.

[5] M.K. Jena, J. Janjanam, Role of extracellular matrix in breast cancer development: a brief update, F1000Research, 7 (2018) 274.

[6] S. Maman, I.P. Witz, A history of exploring cancer in context, Nature reviews. Cancer, 18 (2018) 359-376.

[7] A.L. Hellewell, J.C. Adams, Insider trading: Extracellular matrix proteins and their non-canonical intracellular roles, BioEssays : news and reviews in molecular, cellular and developmental biology, 38 (2016) 77-88.

[8] S. Ozbek, P.G. Balasubramanian, R. Chiquet-Ehrismann, R.P. Tucker, J.C. Adams, The evolution of extracellular matrix, Molecular biology of the cell, 21 (2010) 4300-4305.

[9] B.L. Eckhardt, B.S. Parker, R.K. van Laar, C.M. Restall, A.L. Natoli, M.D. Tavaria, K.L. Stanley, E.K. Sloan, J.M. Moseley, R.L. Anderson, Genomic analysis of a spontaneous model of breast cancer metastasis to bone reveals a role for the extracellular matrix, Mol Cancer Res, 3 (2005) 1-13.

[10] S. Ramaswamy, K.N. Ross, E.S. Lander, T.R. Golub, A molecular signature of metastasis in primary solid tumors, Nature genetics, 33 (2003) 49-54.

[11] E.A. Clark, T.R. Golub, E.S. Lander, R.O. Hynes, Genomic analysis of metastasis reveals an essential role for RhoC, Nature, 406 (2000) 532-535.

[12] W. Wang, J.B. Wyckoff, V.C. Frohlich, Y. Oleynikov, S. Huttelmaier, J. Zavadil, L. Cermak, E.P. Bottinger, R.H. Singer, J.G. White, J.E. Segall, J.S. Condeelis, Single cell behavior in metastatic primary mammary tumors correlated with gene expression patterns revealed by molecular profiling, Cancer research, 62 (2002) 6278-6288.

[13] R. Brandenberger, A. Schmidt, J. Linton, D. Wang, C. Backus, S. Denda, U. Muller, L.F. Reichardt, Identification and characterization of a novel extracellular matrix protein nephronectin that is associated with integrin alpha8beta1 in the embryonic kidney, The Journal of cell biology, 154 (2001) 447-458.

[14] J.M. Linton, G.R. Martin, L.F. Reichardt, The ECM protein nephronectin promotes kidney development via integrin alpha8beta1-mediated stimulation of Gdnf expression, Development (Cambridge, England), 134 (2007) 2501-2509.

[15] S. Kahai, S.C. Lee, D.Y. Lee, J. Yang, M. Li, C.H. Wang, Z. Jiang, Y. Zhang, C. Peng, B.B. Yang, MicroRNA miR-378 regulates nephronectin expression modulating osteoblast differentiation by targeting GalNT-7, PloS one, 4 (2009) e7535.

[16] A.D. Borowsky, R. Namba, L.J. Young, K.W. Hunter, J.G. Hodgson, C.G. Tepper, E.T. McGoldrick, W.J. Muller, R.D. Cardiff, J.P. Gregg, Syngeneic mouse mammary carcinoma cell lines: two closely related cell lines with divergent metastatic behavior, Clinical & experimental metastasis, 22 (2005) 47-59.

[17] M.B. Amin, F.L. Greene, S.B. Edge, C.C. Compton, J.E. Gershenwald, R.K. Brookland, L. Meyer, D.M. Gress, D.R. Byrd, D.P. Winchester, The Eighth Edition AJCC Cancer Staging Manual: Continuing to build a bridge from a population-based to a more "personalized" approach to cancer staging, CA: a cancer journal for clinicians, 67 (2017) 93-99.

[18] C.L. Chaffer, R.A. Weinberg, A perspective on cancer cell metastasis, Science (New York, N.Y.), 331 (2011) 1559-1564.

[19] R.L. Siegel, K.D. Miller, A. Jemal, Cancer Statistics, 2017, CA: a cancer journal for clinicians, 67 (2017) 7-30.

[20] T. Kuukasjarvi, R. Karhu, M. Tanner, M. Kahkonen, A. Schaffer, N. Nupponen, S. Pennanen, A. Kallioniemi, O.P. Kallioniemi, J. Isola, Genetic heterogeneity and clonal evolution underlying development of asynchronous metastasis in human breast cancer, Cancer research, 57 (1997) 1597-1604.

[21] M.S. Donepudi, K. Kondapalli, S.J. Amos, P. Venkanteshan, Breast cancer statistics and markers, Journal of cancer research and therapeutics, 10 (2014) 506-511.

[22] D. Hanahan, R.A. Weinberg, Hallmarks of cancer: the next generation, Cell, 144 (2011) 646-674.

[23] J. Massague, A.C. Obenauf, Metastatic colonization by circulating tumour cells, Nature, 529 (2016) 298-306.

[24] A.G. Clark, D.M. Vignjevic, Modes of cancer cell invasion and the role of the microenvironment, Current opinion in cell biology, 36 (2015) 13-22.

[25] M. Bockhorn, R.K. Jain, L.L. Munn, Active versus passive mechanisms in metastasis: do cancer cells crawl into vessels, or are they pushed?, The Lancet. Oncology, 8 (2007) 444-448.

[26] T. Tsuji, S. Ibaragi, G.F. Hu, Epithelial-mesenchymal transition and cell cooperativity in metastasis, Cancer research, 69 (2009) 7135-7139.

[27] O.J. McCarty, S.A. Mousa, P.F. Bray, K. Konstantopoulos, Immobilized platelets support human colon carcinoma cell tethering, rolling, and firm adhesion under dynamic flow conditions, Blood, 96 (2000) 1789-1797.

[28] G. Follain, N. Osmani, A.S. Azevedo, G. Allio, L. Mercier, M.A. Karreman, G. Solecki, M.J. Garcia Leòn, O. Lefebvre, N. Fekonja, C. Hille, V. Chabannes, G. Dollé, T. Metivet, F.D. Hovsepian, C. Prudhomme, A. Pichot, N. Paul, R. Carapito, S. Bahram, B. Ruthensteiner, A. Kemmling, S. Siemonsen, T. Schneider, J. Fiehler, M. Glatzel, F. Winkler, Y. Schwab, K. Pantel, S. Harlepp, J.G. Goetz, Hemodynamic Forces Tune the Arrest, Adhesion, and Extravasation of Circulating Tumor Cells, Developmental cell, 45 (2018) 33-52.e12.

[29] A. Dasgupta, A.R. Lim, C.M. Ghajar, Circulating and disseminated tumor cells: harbingers or initiators of metastasis?, Molecular oncology, 11 (2017) 40-61.

[30] N. Reymond, B.B. d'Agua, A.J. Ridley, Crossing the endothelial barrier during metastasis, Nature reviews. Cancer, 13 (2013) 858-870.

[31] D. Stegner, S. Dutting, B. Nieswandt, Mechanistic explanation for platelet contribution to cancer metastasis, Thrombosis research, 133 Suppl 2 (2014) S149-157.

[32] I.C. MacDonald, A.C. Groom, A.F. Chambers, Cancer spread and micrometastasis development: quantitative approaches for in vivo models, BioEssays : news and reviews in molecular, cellular and developmental biology, 24 (2002) 885-893.

[33] X.L. Gao, M. Zhang, Y.L. Tang, X.H. Liang, Cancer cell dormancy: mechanisms and implications of cancer recurrence and metastasis, OncoTargets and therapy, 10 (2017) 5219-5228.

[34] B. Psaila, R.N. Kaplan, E.R. Port, D. Lyden, Priming the 'soil' for breast cancer metastasis: the pre-metastatic niche, Breast disease, 26 (2006) 65-74.

[35] H. Peinado, S. Lavotshkin, D. Lyden, The secreted factors responsible for pre-metastatic niche formation: old sayings and new thoughts, Seminars in cancer biology, 21 (2011) 139-146.

[36] P. Carmeliet, R.K. Jain, Angiogenesis in cancer and other diseases, Nature, 407 (2000) 249-257.

[37] P. Fraisl, M. Mazzone, T. Schmidt, P. Carmeliet, Regulation of angiogenesis by oxygen and metabolism, Developmental cell, 16 (2009) 167-179.

[38] K. Hida, N. Maishi, C. Torii, Y. Hida, Tumor angiogenesis--characteristics of tumor endothelial cells, International journal of clinical oncology, 21 (2016) 206-212.

[39] D. Wirtz, K. Konstantopoulos, P.C. Searson, The physics of cancer: the role of physical interactions and mechanical forces in metastasis, Nature Reviews Cancer, 11 (2011) 512.

[40] X. Lu, Y. Kang, Organotropism of breast cancer metastasis, Journal of mammary gland biology and neoplasia, 12 (2007) 153-162.

[41] M. Yousefi, R. Nosrati, A. Salmaninejad, S. Dehghani, A. Shahryari, A. Saberi, Organ-specific metastasis of breast cancer: molecular and cellular mechanisms underlying lung metastasis, Cell Oncol (Dordr), 41 (2018) 123-140.

[42] I.J. Fidler, The pathogenesis of cancer metastasis: the 'seed and soil' hypothesis revisited, Nature reviews. Cancer, 3 (2003) 453-458.

[43] S. Paget, The distribution of secondary growths in cancer of the breast. 1889, Cancer metastasis reviews, 8 (1989) 98-101.

[44] A.C. Obenauf, J. Massague, Surviving at a distance: organ specific metastasis, Trends in cancer, 1 (2015) 76-91.

[45] J. Ewing, Neoplastic Diseases: A Treatise on Tumours. , BJS, 16 (1928) 174-175.

[46] K.R. Hess, G.R. Varadhachary, S.H. Taylor, W. Wei, M.N. Raber, R. Lenzi, J.L. Abbruzzese, Metastatic patterns in adenocarcinoma, Cancer, 106 (2006) 1624-1633.

[47] J. Budczies, M. von Winterfeld, F. Klauschen, M. Bockmayr, J.K. Lennerz, C. Denkert, T. Wolf, A. Warth, M. Dietel, I. Anagnostopoulos, W. Weichert, D. Wittschieber, A. Stenzinger, The landscape of metastatic progression patterns across major human cancers, Oncotarget, 6 (2015) 570-583.

[48] G. Lorusso, C. Ruegg, New insights into the mechanisms of organ-specific breast cancer metastasis, Seminars in cancer biology, 22 (2012) 226-233.

[49] I.J. Fidler, G.L. Nicolson, Organ selectivity for implantation survival and growth of B16 melanoma variant tumor lines, Journal of the National Cancer Institute, 57 (1976) 1199-1202.

[50] P.D. Bos, X.H. Zhang, C. Nadal, W. Shu, R.R. Gomis, D.X. Nguyen, A.J. Minn, M.J. van de Vijver, W.L. Gerald, J.A. Foekens, J. Massague, Genes that mediate breast cancer metastasis to the brain, Nature, 459 (2009) 1005-1009.

[51] M. Korpal, B.J. Ell, F.M. Buffa, T. Ibrahim, M.A. Blanco, T. Celia-Terrassa, L. Mercatali, Z. Khan, H. Goodarzi, Y. Hua, Y. Wei, G. Hu, B.A. Garcia, J. Ragoussis, D. Amadori, A.L. Harris, Y. Kang, Direct targeting of Sec23a by miR-200s influences cancer cell secretome and promotes metastatic colonization, Nature medicine, 17 (2011) 1101-1108.

[52] A. Naba, K.R. Clauser, C.A. Whittaker, S.A. Carr, K.K. Tanabe, R.O. Hynes, Extracellular matrix signatures of human primary metastatic colon cancers and their metastases to liver, BMC cancer, 14 (2014) 518.

[53] P. Pound, M.B. Bracken, Is animal research sufficiently evidence based to be a cornerstone of biomedical research?, BMJ (Clinical research ed.), 348 (2014) g3387.

[54] R.L. Perlman, Mouse models of human disease: An evolutionary perspective, Evolution, medicine, and public health, 2016 (2016) 170-176.

[55] W.C. Hahn, R.A. Weinberg, Modelling the molecular circuitry of cancer, Nature reviews. Cancer, 2 (2002) 331-341.

[56] A. Rangarajan, R.A. Weinberg, Opinion: Comparative biology of mouse versus human cells: modelling human cancer in mice, Nature reviews. Cancer, 3 (2003) 952-959.

[57] D.R. Welch, Technical considerations for studying cancer metastasis in vivo, Clinical & experimental metastasis, 15 (1997) 272-306.

[58] K. Kersten, K.E. de Visser, M.H. van Miltenburg, J. Jonkers, Genetically engineered mouse models in oncology research and cancer medicine, EMBO molecular medicine, 9 (2017) 137-153.

[59] L. Gomez-Cuadrado, N. Tracey, R. Ma, B. Qian, V.G. Brunton, Mouse models of metastasis: progress and prospects, Disease models & mechanisms, 10 (2017) 1061-1074.

[60] A.J. Minn, G.P. Gupta, P.M. Siegel, P.D. Bos, W. Shu, D.D. Giri, A. Viale, A.B. Olshen, W.L. Gerald, J. Massague, Genes that mediate breast cancer metastasis to lung, Nature, 436 (2005) 518-524.

[61] C.J. Aslakson, F.R. Miller, Selective events in the metastatic process defined by analysis of the sequential dissemination of subpopulations of a mouse mammary tumor, Cancer research, 52 (1992) 1399-1405.

[62] C.T. Guy, M.A. Webster, M. Schaller, T.J. Parsons, R.D. Cardiff, W.J. Muller, Expression of the neu protooncogene in the mammary epithelium of transgenic mice induces metastatic disease,

Proceedings of the National Academy of Sciences of the United States of America, 89 (1992) 10578-10582.
[63] G.V. Sherbet, M.S. Lakshmi, 2 - Clonal evolution of the metastatic phenotype, in: G.V. Sherbet, M.S. Lakshmi (Eds.) The Genetics of Cancer, Academic Press, London, 1997, pp. 4-22.
[64] D.L. Dexter, H.M. Kowalski, B.A. Blazar, Z. Fligiel, R. Vogel, G.H. Heppner, Heterogeneity of tumor cells from a single mouse mammary tumor, Cancer research, 38 (1978) 3174-3181.
[65] G.H. Heppner, D.L. Dexter, T. DeNucci, F.R. Miller, P. Calabresi, Heterogeneity in drug sensitivity among tumor cell subpopulations of a single mammary tumor, Cancer research, 38 (1978) 3758-3763.
[66] B.E. Miller, L.D. Roi, L.M. Howard, F.R. Miller, Quantitative selectivity of contact-mediated intercellular communication in a metastatic mouse mammary tumor line, Cancer research, 43 (1983) 4102-4107.
[67] B.E. Miller, D. McInerney, D. Jackson, F.R. Miller, Metabolic cooperation between mouse mammary tumor subpopulations in three-dimensional collagen gel cultures, Cancer research, 46 (1986) 89-93.
[68] B.E. Miller, F.R. Miller, D.J. Wilburn, G.H. Heppner, Analysis of tumour cell composition in tumours composed of paired mixtures of mammary tumour cell lines, Br J Cancer, 56 (1987) 561-569.
[69] C.J. Aslakson, J.W. Rak, B.E. Miller, F.R. Miller, Differential influence of organ site on three subpopulations of a single mouse mammary tumor at two distinct steps in metastasis, International journal of cancer, 47 (1991) 466-472.
[70] M. Lelekakis, J.M. Moseley, T.J. Martin, D. Hards, E. Williams, P. Ho, D. Lowen, J. Javni, F.R. Miller, J. Slavin, R.L. Anderson, A novel orthotopic model of breast cancer metastasis to bone, Clinical & experimental metastasis, 17 (1999) 163-170.
[71] C.N. Johnstone, Y.E. Smith, Y. Cao, A.D. Burrows, R.S. Cross, X. Ling, R.P. Redvers, J.P. Doherty, B.L. Eckhardt, A.L. Natoli, C.M. Restall, E. Lucas, H.B. Pearson, S. Deb, K.L. Britt, A. Rizzitelli, J. Li, J.H. Harmey, N. Pouliot, R.L. Anderson, Functional and molecular characterisation of EO771.LMB tumours, a new C57BL/6-mouse-derived model of spontaneously metastatic mammary cancer, Disease models & mechanisms, 8 (2015) 237-251.
[72] F.R. Miller, Tumor subpopulation interactions in metastasis, Invasion & metastasis, 3 (1983) 234-242.
[73] Y. Lou, O. Preobrazhenska, U. auf dem Keller, M. Sutcliffe, L. Barclay, P.C. McDonald, C. Roskelley, C.M. Overall, S. Dedhar, Epithelial-mesenchymal transition (EMT) is not sufficient for spontaneous murine breast cancer metastasis, Developmental dynamics : an official publication of the American Association of Anatomists, 237 (2008) 2755-2768.
[74] L. Weiss, Metastatic inefficiency, Advances in cancer research, 54 (1990) 159-211.
[75] J.E. Talmadge, I.J. Fidler, Cancer metastasis is selective or random depending on the parent tumour population, Nature, 297 (1982) 593-594.
[76] F.R. Miller, B.E. Miller, G.H. Heppner, Characterization of metastatic heterogeneity among subpopulations of a single mouse mammary tumor: heterogeneity in phenotypic stability, Invasion & metastasis, 3 (1983) 22-31.
[77] Y.A. Fouad, C. Aanei, Revisiting the hallmarks of cancer, American journal of cancer research, 7 (2017) 1016-1036.
[78] D. Hanahan, R.A. Weinberg, The hallmarks of cancer, Cell, 100 (2000) 57-70.
[79] J.G. Goetz, Tumor microenvironment indoctrination: an emerging hallmark of cancer, Cell adhesion & migration, 6 (2012) 190-192.
[80] M. Wang, J. Zhao, L. Zhang, F. Wei, Y. Lian, Y. Wu, Z. Gong, S. Zhang, J. Zhou, K. Cao, X. Li, W. Xiong, G. Li, Z. Zeng, C. Guo, Role of tumor microenvironment in tumorigenesis, Journal of Cancer, 8 (2017) 761-773.
[81] R.O. Hynes, A. Naba, Overview of the matrisome--an inventory of extracellular matrix constituents and functions, Cold Spring Harbor perspectives in biology, 4 (2012) a004903.

[82] A. Naba, K.R. Clauser, S. Hoersch, H. Liu, S.A. Carr, R.O. Hynes, The matrisome: in silico definition and in vivo characterization by proteomics of normal and tumor extracellular matrices, Molecular & cellular proteomics : MCP, 11 (2012) M111.014647.

[83] A.M. Hoye, J.T. Erler, Structural ECM components in the premetastatic and metastatic niche, American journal of physiology. Cell physiology, 310 (2016) C955-967.

[84] R. Catena, N. Bhattacharya, T. El Rayes, S. Wang, H. Choi, D. Gao, S. Ryu, N. Joshi, D. Bielenberg, S.B. Lee, S.A. Haukaas, K. Gravdal, O.J. Halvorsen, L.A. Akslen, R.S. Watnick, V. Mittal, Bone marrow-derived Gr1+ cells can generate a metastasis-resistant microenvironment via induced secretion of thrombospondin-1, Cancer discovery, 3 (2013) 578-589.

[85] Z. Granot, E. Henke, E.A. Comen, T.A. King, L. Norton, R. Benezra, Tumor entrained neutrophils inhibit seeding in the premetastatic lung, Cancer cell, 20 (2011) 300-314.

[86] A.M. Socovich, A. Naba, The cancer matrisome: From comprehensive characterization to biomarker discovery, Seminars in cell & developmental biology, (2018).

[87] A. Bergamaschi, E. Tagliabue, T. Sorlie, B. Naume, T. Triulzi, R. Orlandi, H.G. Russnes, J.M. Nesland, R. Tammi, P. Auvinen, V.M. Kosma, S. Menard, A.L. Borresen-Dale, Extracellular matrix signature identifies breast cancer subgroups with different clinical outcome, The Journal of pathology, 214 (2008) 357-367.

[88] A. Naba, O.M.T. Pearce, A. Del Rosario, D. Ma, H. Ding, V. Rajeeve, P.R. Cutillas, F.R. Balkwill, R.O. Hynes, Characterization of the Extracellular Matrix of Normal and Diseased Tissues Using Proteomics, Journal of proteome research, 16 (2017) 3083-3091.

[89] A.E. Mayorca-Guiliani, C.D. Madsen, T.R. Cox, E.R. Horton, F.A. Venning, J.T. Erler, ISDoT: in situ decellularization of tissues for high-resolution imaging and proteomic analysis of native extracellular matrix, Nature medicine, 23 (2017) 890-898.

[90] A. Naba, K.R. Clauser, J.M. Lamar, S.A. Carr, R.O. Hynes, Extracellular matrix signatures of human mammary carcinoma identify novel metastasis promoters, eLife, 3 (2014) e01308.

[91] N. Morimura, Y. Tezuka, N. Watanabe, M. Yasuda, S. Miyatani, N. Hozumi, K. Tezuka Ki, Molecular cloning of POEM: a novel adhesion molecule that interacts with alpha8beta1 integrin, The Journal of biological chemistry, 276 (2001) 42172-42181.

[92] J.T. Huang, V. Lee, Identification and characterization of a novel human nephronectin gene in silico, International journal of molecular medicine, 15 (2005) 719-724.

[93] Y. Sato, T. Uemura, K. Morimitsu, R. Sato-Nishiuchi, R. Manabe, J. Takagi, M. Yamada, K. Sekiguchi, Molecular basis of the recognition of nephronectin by integrin alpha8beta1, The Journal of biological chemistry, 284 (2009) 14524-14536.

[94] C.G. Davis, The many faces of epidermal growth factor repeats, The New biologist, 2 (1990) 410-419.

[95] J. Periz, A.C. Gill, V. Knott, P.A. Handford, F.M. Tomley, Calcium binding activity of the epidermal growth factor-like domains of the apicomplexan microneme protein EtMIC4, Molecular and biochemical parasitology, 143 (2005) 192-199.

[96] J.C. Aster, W.B. Simms, Z. Zavala-Ruiz, V. Patriub, C.L. North, S.C. Blacklow, The folding and structural integrity of the first LIN-12 module of human Notch1 are calcium-dependent, Biochemistry, 38 (1999) 4736-4742.

[97] Y. Sato, C. Shimono, S. Li, I. Nakano, N. Norioka, N. Sugiura, K. Kimata, M. Yamada, K. Sekiguchi, Nephronectin binds to heparan sulfate proteoglycans via its MAM domain, Matrix biology : journal of the International Society for Matrix Biology, 32 (2013) 188-195.

[98] C. Arai, K. Yoshizaki, K. Miyazaki, K. Saito, A. Yamada, X. Han, K. Funada, E. Fukumoto, N. Haruyama, T. Iwamoto, I. Takahashi, S. Fukumoto, Nephronectin plays critical roles in Sox2 expression and proliferation in dental epithelial stem cells via EGF-like repeat domains, Sci Rep, 7 (2017) 45181.

[99] M.D. Pierschbacher, E. Ruoslahti, Variants of the cell recognition site of fibronectin that retain attachment-promoting activity, Proceedings of the National Academy of Sciences of the United States of America, 81 (1984) 5985-5988.

[100] E. Ruoslahti, RGD and other recognition sequences for integrins, Annual review of cell and developmental biology, 12 (1996) 697-715.
[101] C. Patra, F. Ricciardi, F.B. Engel, The functional properties of nephronectin: an adhesion molecule for cardiac tissue engineering, Biomaterials, 33 (2012) 4327-4335.
[102] J. Sanchez-Cortes, M. Mrksich, Using self-assembled monolayers to understand alpha8beta1-mediated cell adhesion to RGD and FEI motifs in nephronectin, ACS chemical biology, 6 (2011) 1078-1086.
[103] A.D. Theocharis, S.S. Skandalis, C. Gialeli, N.K. Karamanos, Extracellular matrix structure, Advanced drug delivery reviews, 97 (2016) 4-27.
[104] F.G. Giancotti, E. Ruoslahti, Integrin signaling, Science (New York, N.Y.), 285 (1999) 1028-1032.
[105] S. Raab-Westphal, J.F. Marshall, S.L. Goodman, Integrins as Therapeutic Targets: Successes and Cancers, Cancers, 9 (2017).
[106] M.A. Glukhova, C.H. Streuli, How integrins control breast biology, Current opinion in cell biology, 25 (2013) 633-641.
[107] L. Seguin, J.S. Desgrosellier, S.M. Weis, D.A. Cheresh, Integrins and cancer: regulators of cancer stemness, metastasis, and drug resistance, Trends in cell biology, 25 (2015) 234-240.
[108] R.O. Hynes, Integrins: bidirectional, allosteric signaling machines, Cell, 110 (2002) 673-687.
[109] H. Hamidi, J. Ivaska, Every step of the way: integrins in cancer progression and metastasis, Nature reviews. Cancer, (2018).
[110] J.D. Humphries, A. Byron, M.J. Humphries, Integrin ligands at a glance, Journal of cell science, 119 (2006) 3901-3903.
[111] M. Barczyk, S. Carracedo, D. Gullberg, Integrins, Cell and tissue research, 339 (2010) 269-280.
[112] L.M. Schnapp, J.M. Breuss, D.M. Ramos, D. Sheppard, R. Pytela, Sequence and tissue distribution of the human integrin alpha 8 subunit: a beta 1-associated alpha subunit expressed in smooth muscle cells, Journal of cell science, 108 (Pt 2) (1995) 537-544.
[113] U. Muller, D. Wang, S. Denda, J.J. Meneses, R.A. Pedersen, L.F. Reichardt, Integrin alpha8beta1 is critically important for epithelial-mesenchymal interactions during kidney morphogenesis, Cell, 88 (1997) 603-613.
[114] U. Muller, B. Bossy, K. Venstrom, L.F. Reichardt, Integrin alpha 8 beta 1 promotes attachment, cell spreading, and neurite outgrowth on fibronectin, Molecular biology of the cell, 6 (1995) 433-448.
[115] L.M. Schnapp, N. Hatch, D.M. Ramos, I.V. Klimanskaya, D. Sheppard, R. Pytela, The human integrin alpha 8 beta 1 functions as a receptor for tenascin, fibronectin, and vitronectin, The Journal of biological chemistry, 270 (1995) 23196-23202.
[116] B. Varnum-Finney, K. Venstrom, U. Muller, R. Kypta, C. Backus, M. Chiquet, L.F. Reichardt, The integrin receptor alpha 8 beta 1 mediates interactions of embryonic chick motor and sensory neurons with tenascin-C, Neuron, 14 (1995) 1213-1222.
[117] A. Scherberich, R.P. Tucker, E. Samandari, M. Brown-Luedi, D. Martin, R. Chiquet-Ehrismann, Murine tenascin-W: a novel mammalian tenascin expressed in kidney and at sites of bone and smooth muscle development, Journal of cell science, 117 (2004) 571-581.
[118] S. Denda, L.F. Reichardt, U. Muller, Identification of osteopontin as a novel ligand for the integrin alpha8 beta1 and potential roles for this integrin-ligand interaction in kidney morphogenesis, Molecular biology of the cell, 9 (1998) 1425-1435.
[119] M. Lu, J.S. Munger, M. Steadele, C. Busald, M. Tellier, L.M. Schnapp, Integrin alpha8beta1 mediates adhesion to LAP-TGFbeta1, Journal of cell science, 115 (2002) 4641-4648.
[120] J. Takagi, Structural basis for ligand recognition by RGD (Arg-Gly-Asp)-dependent integrins, Biochemical Society transactions, 32 (2004) 403-406.
[121] S. Miyamoto, H. Teramoto, O.A. Coso, J.S. Gutkind, P.D. Burbelo, S.K. Akiyama, K.M. Yamada, Integrin function: molecular hierarchies of cytoskeletal and signaling molecules, The Journal of cell biology, 131 (1995) 791-805.

[122] R.K. Gupta, S. Johansson, beta1 integrins restrict the growth of foci and spheroids, Histochemistry and cell biology, 138 (2012) 881-894.

[123] A. Kren, V. Baeriswyl, F. Lehembre, C. Wunderlin, K. Strittmatter, H. Antoniadis, R. Fassler, U. Cavallaro, G. Christofori, Increased tumor cell dissemination and cellular senescence in the absence of beta1-integrin function, The EMBO journal, 26 (2007) 2832-2842.

[124] T. Shibue, R.A. Weinberg, Integrin beta1-focal adhesion kinase signaling directs the proliferation of metastatic cancer cells disseminated in the lungs, Proceedings of the National Academy of Sciences of the United States of America, 106 (2009) 10290-10295.

[125] J.A. Askari, P.A. Buckley, A.P. Mould, M.J. Humphries, Linking integrin conformation to function, Journal of cell science, 122 (2009) 165-170.

[126] K.R. Legate, R. Fassler, Mechanisms that regulate adaptor binding to beta-integrin cytoplasmic tails, Journal of cell science, 122 (2009) 187-198.

[127] W. Longmate, C.M. DiPersio, Beyond adhesion: emerging roles for integrins in control of the tumor microenvironment, F1000Research, 6 (2017) 1612.

[128] P.M. Comoglio, C. Boccaccio, L. Trusolino, Interactions between growth factor receptors and adhesion molecules: breaking the rules, Current opinion in cell biology, 15 (2003) 565-571.

[129] C.K. Miranti, J.S. Brugge, Sensing the environment: a historical perspective on integrin signal transduction, Nature cell biology, 4 (2002) E83-90.

[130] M.A. Schwartz, M.H. Ginsberg, Networks and crosstalk: integrin signalling spreads, Nature cell biology, 4 (2002) E65-68.

[131] S.M. Frisch, K. Vuori, E. Ruoslahti, P.Y. Chan-Hui, Control of adhesion-dependent cell survival by focal adhesion kinase, The Journal of cell biology, 134 (1996) 793-799.

[132] N.R. Paul, G. Jacquemet, P.T. Caswell, Endocytic Trafficking of Integrins in Cell Migration, Current biology : CB, 25 (2015) R1092-1105.

[133] N. De Franceschi, H. Hamidi, J. Alanko, P. Sahgal, J. Ivaska, Integrin traffic - the update, Journal of cell science, 128 (2015) 839-852.

[134] P.T. Caswell, S. Vadrevu, J.C. Norman, Integrins: masters and slaves of endocytic transport, Nature reviews. Molecular cell biology, 10 (2009) 843-853.

[135] T. Pellinen, A. Arjonen, K. Vuoriluoto, K. Kallio, J.A. Fransen, J. Ivaska, Small GTPase Rab21 regulates cell adhesion and controls endosomal traffic of beta1-integrins, The Journal of cell biology, 173 (2006) 767-780.

[136] J. Alanko, A. Mai, G. Jacquemet, K. Schauer, R. Kaukonen, M. Saari, B. Goud, J. Ivaska, Integrin endosomal signalling suppresses anoikis, Nature cell biology, 17 (2015) 1412-1421.

[137] G.P. Nader, E.J. Ezratty, G.G. Gundersen, FAK, talin and PIPKIgamma regulate endocytosed integrin activation to polarize focal adhesion assembly, Nature cell biology, 18 (2016) 491-503.

[138] P. Wolf, The nature and significance of platelet products in human plasma, British journal of haematology, 13 (1967) 269-288.

[139] J. Kowal, M. Tkach, C. Thery, Biogenesis and secretion of exosomes, Current opinion in cell biology, 29 (2014) 116-125.

[140] Y.L. Tai, K.C. Chen, J.T. Hsieh, T.L. Shen, Exosomes in cancer development and clinical applications, Cancer science, (2018).

[141] K.W. Witwer, E.I. Buzas, L.T. Bemis, A. Bora, C. Lasser, J. Lotvall, E.N. Nolte-'t Hoen, M.G. Piper, S. Sivaraman, J. Skog, C. Thery, M.H. Wauben, F. Hochberg, Standardization of sample collection, isolation and analysis methods in extracellular vesicle research, Journal of extracellular vesicles, 2 (2013).

[142] D. Ha, N. Yang, V. Nadithe, Exosomes as therapeutic drug carriers and delivery vehicles across biological membranes: current perspectives and future challenges, Acta pharmaceutica Sinica. B, 6 (2016) 287-296.

[143] R. Xu, A. Rai, M. Chen, W. Suwakulsiri, D.W. Greening, R.J. Simpson, Extracellular vesicles in cancer - implications for future improvements in cancer care, Nature reviews. Clinical oncology, (2018).

[144] International society for extracellular vesicles www.isev.org.

[145] R.M. Johnstone, A. Bianchini, K. Teng, Reticulocyte maturation and exosome release: transferrin receptor containing exosomes shows multiple plasma membrane functions, Blood, 74 (1989) 1844-1851.

[146] N.P. Hessvik, A. Llorente, Current knowledge on exosome biogenesis and release, Cellular and molecular life sciences : CMLS, 75 (2018) 193-208.

[147] B.J. Tauro, D.W. Greening, R.A. Mathias, S. Mathivanan, H. Ji, R.J. Simpson, Two distinct populations of exosomes are released from LIM1863 colon carcinoma cell-derived organoids, Molecular & cellular proteomics : MCP, 12 (2013) 587-598.

[148] E. Willms, H.J. Johansson, I. Mager, Y. Lee, K.E. Blomberg, M. Sadik, A. Alaarg, C.I. Smith, J. Lehtio, S. El Andaloussi, M.J. Wood, P. Vader, Cells release subpopulations of exosomes with distinct molecular and biological properties, Sci Rep, 6 (2016) 22519.

[149] H. Zhang, D. Freitas, H.S. Kim, K. Fabijanic, Z. Li, H. Chen, M.T. Mark, H. Molina, A.B. Martin, L. Bojmar, J. Fang, S. Rampersaud, A. Hoshino, I. Matei, C.M. Kenific, M. Nakajima, A.P. Mutvei, P. Sansone, W. Buehring, H. Wang, J.P. Jimenez, L. Cohen-Gould, N. Paknejad, M. Brendel, K. Manova-Todorova, A. Magalhaes, J.A. Ferreira, H. Osorio, A.M. Silva, A. Massey, J.R. Cubillos-Ruiz, G. Galletti, P. Giannakakou, A.M. Cuervo, J. Blenis, R. Schwartz, M.S. Brady, H. Peinado, J. Bromberg, H. Matsui, C.A. Reis, D. Lyden, Identification of distinct nanoparticles and subsets of extracellular vesicles by asymmetric flow field-flow fractionation, Nature cell biology, 20 (2018) 332-343.

[150] J. Kowal, G. Arras, M. Colombo, M. Jouve, J.P. Morath, B. Primdal-Bengtson, F. Dingli, D. Loew, M. Tkach, C. Thery, Proteomic comparison defines novel markers to characterize heterogeneous populations of extracellular vesicle subtypes, Proceedings of the National Academy of Sciences of the United States of America, 113 (2016) E968-977.

[151] C. D'Souza-Schorey, J.W. Clancy, Tumor-derived microvesicles: shedding light on novel microenvironment modulators and prospective cancer biomarkers, Genes & development, 26 (2012) 1287-1299.

[152] C. D'Souza-Schorey, J.S. Schorey, Regulation and mechanisms of extracellular vesicle biogenesis and secretion, Essays in biochemistry, 62 (2018) 125-133.

[153] R. Palmulli, G. van Niel, To be or not to be... secreted as exosomes, a balance finely tuned by the mechanisms of biogenesis, Essays in biochemistry, 62 (2018) 177-191.

[154] L.A. Mulcahy, R.C. Pink, D.R. Carter, Routes and mechanisms of extracellular vesicle uptake, Journal of extracellular vesicles, 3 (2014).

[155] K.J. Svensson, H.C. Christianson, A. Wittrup, E. Bourseau-Guilmain, E. Lindqvist, L.M. Svensson, M. Morgelin, M. Belting, Exosome uptake depends on ERK1/2-heat shock protein 27 signaling and lipid Raft-mediated endocytosis negatively regulated by caveolin-1, The Journal of biological chemistry, 288 (2013) 17713-17724.

[156] S.A. Melo, H. Sugimoto, J.T. O'Connell, N. Kato, A. Villanueva, A. Vidal, L. Qiu, E. Vitkin, L.T. Perelman, C.A. Melo, A. Lucci, C. Ivan, G.A. Calin, R. Kalluri, Cancer exosomes perform cell-independent microRNA biogenesis and promote tumorigenesis, Cancer cell, 26 (2014) 707-721.

[157] B. Costa-Silva, N.M. Aiello, A.J. Ocean, S. Singh, H. Zhang, B.K. Thakur, A. Becker, A. Hoshino, M.T. Mark, H. Molina, J. Xiang, T. Zhang, T.M. Theilen, G. Garcia-Santos, C. Williams, Y. Ararso, Y. Huang, G. Rodrigues, T.L. Shen, K.J. Labori, I.M. Lothe, E.H. Kure, J. Hernandez, A. Doussot, S.H. Ebbesen, P.M. Grandgenett, M.A. Hollingsworth, M. Jain, K. Mallya, S.K. Batra, W.R. Jarnagin, R.E. Schwartz, I. Matei, H. Peinado, B.Z. Stanger, J. Bromberg, D. Lyden, Pancreatic cancer exosomes initiate pre-metastatic niche formation in the liver, Nature cell biology, 17 (2015) 816-826.

[158] E. Vulpis, F. Cecere, R. Molfetta, A. Soriani, C. Fionda, G. Peruzzi, G. Caracciolo, S. Palchetti, L. Masuelli, L. Simonelli, U. D'Oro, M.P. Abruzzese, M.T. Petrucci, M.R. Ricciardi, R. Paolini, M. Cippitelli, A. Santoni, A. Zingoni, Genotoxic stress modulates the release of exosomes from multiple myeloma cells capable of activating NK cell cytokine production: Role of HSP70/TLR2/NF-kB axis, Oncoimmunology, 6 (2017) e1279372.

[159] F. Menay, L. Herschlik, J. De Toro, F. Cocozza, R. Tsacalian, M.J. Gravisaco, M.P. Di Sciullo, A. Vendrell, C.I. Waldner, C. Mongini, Exosomes Isolated from Ascites of T-Cell Lymphoma-Bearing Mice Expressing Surface CD24 and HSP-90 Induce a Tumor-Specific Immune Response, Frontiers in immunology, 8 (2017) 286.

[160] Exocarta database, www.exocarta.org.

[161] G. Palazzolo, N.N. Albanese, D.I.C. G, D. Gygax, M.L. Vittorelli, I. Pucci-Minafra, Proteomic analysis of exosome-like vesicles derived from breast cancer cells, Anticancer research, 32 (2012) 847-860.

[162] M.P. Bard, J.P. Hegmans, A. Hemmes, T.M. Luider, R. Willemsen, L.A. Severijnen, J.P. van Meerbeeck, S.A. Burgers, H.C. Hoogsteden, B.N. Lambrecht, Proteomic analysis of exosomes isolated from human malignant pleural effusions, American journal of respiratory cell and molecular biology, 31 (2004) 114-121.

[163] J.P. Hegmans, M.P. Bard, A. Hemmes, T.M. Luider, M.J. Kleijmeer, J.B. Prins, L. Zitvogel, S.A. Burgers, H.C. Hoogsteden, B.N. Lambrecht, Proteomic analysis of exosomes secreted by human mesothelioma cells, The American journal of pathology, 164 (2004) 1807-1815.

[164] S. Mathivanan, J.W. Lim, B.J. Tauro, H. Ji, R.L. Moritz, R.J. Simpson, Proteomics analysis of A33 immunoaffinity-purified exosomes released from the human colon tumor cell line LIM1215 reveals a tissue-specific protein signature, Molecular & cellular proteomics : MCP, 9 (2010) 197-208.

[165] A. Riches, E. Campbell, E. Borger, S. Powis, Regulation of exosome release from mammary epithelial and breast cancer cells - a new regulatory pathway, European journal of cancer (Oxford, England : 1990), 50 (2014) 1025-1034.

[166] S. Jiang, C. Hu, P. Liu, M. Lu, Tumor-derived exosomes in cancer metastasis risk diagnosis and metastasis therapy, Clinical & translational oncology : official publication of the Federation of Spanish Oncology Societies and of the National Cancer Institute of Mexico, (2018).

[167] M. Moloudizargari, M.H. Asghari, M. Abdollahi, Modifying exosome release in cancer therapy: How can it help?, Pharmacological research, 134 (2018) 246-256.

[168] V. Sundararajan, F.H. Sarkar, T.S. Ramasamy, The versatile role of exosomes in cancer progression: diagnostic and therapeutic implications, Cell Oncol (Dordr), 41 (2018) 223-252.

[169] S. Hiratsuka, K. Nakamura, S. Iwai, M. Murakami, T. Itoh, H. Kijima, J.M. Shipley, R.M. Senior, M. Shibuya, MMP9 induction by vascular endothelial growth factor receptor-1 is involved in lung-specific metastasis, Cancer cell, 2 (2002) 289-300.

[170] R.N. Kaplan, R.D. Riba, S. Zacharoulis, A.H. Bramley, L. Vincent, C. Costa, D.D. MacDonald, D.K. Jin, K. Shido, S.A. Kerns, Z. Zhu, D. Hicklin, Y. Wu, J.L. Port, N. Altorki, E.R. Port, D. Ruggero, S.V. Shmelkov, K.K. Jensen, S. Rafii, D. Lyden, VEGFR1-positive haematopoietic bone marrow progenitors initiate the pre-metastatic niche, Nature, 438 (2005) 820-827.

[171] J. Sceneay, M.T. Chow, A. Chen, H.M. Halse, C.S. Wong, D.M. Andrews, E.K. Sloan, B.S. Parker, D.D. Bowtell, M.J. Smyth, A. Moller, Primary tumor hypoxia recruits CD11b+/Ly6Cmed/Ly6G+ immune suppressor cells and compromises NK cell cytotoxicity in the premetastatic niche, Cancer research, 72 (2012) 3906-3911.

[172] S.S. McAllister, R.A. Weinberg, Tumor-host interactions: a far-reaching relationship, Journal of clinical oncology : official journal of the American Society of Clinical Oncology, 28 (2010) 4022-4028.

[173] A. Hoshino, B. Costa-Silva, T.L. Shen, G. Rodrigues, A. Hashimoto, M. Tesic Mark, H. Molina, S. Kohsaka, A. Di Giannatale, S. Ceder, S. Singh, C. Williams, N. Soplop, K. Uryu, L. Pharmer, T. King, L. Bojmar, A.E. Davies, Y. Ararso, T. Zhang, H. Zhang, J. Hernandez, J.M. Weiss, V.D. Dumont-Cole, K. Kramer, L.H. Wexler, A. Narendran, G.K. Schwartz, J.H. Healey, P. Sandstrom, K.J. Labori, E.H. Kure, P.M. Grandgenett, M.A. Hollingsworth, M. de Sousa, S. Kaur, M. Jain, K. Mallya, S.K. Batra, W.R. Jarnagin, M.S. Brady, O. Fodstad, V. Muller, K. Pantel, A.J. Minn, M.J. Bissell, B.A. Garcia, Y. Kang, V.K. Rajasekhar, C.M. Ghajar, I. Matei, H. Peinado, J. Bromberg, D. Lyden, Tumour exosome integrins determine organotropic metastasis, Nature, 527 (2015) 329-335.

[174] C. Coghlin, G.I. Murray, Current and emerging concepts in tumour metastasis, The Journal of pathology, 222 (2010) 1-15.

[175] H.W. van Deventer, Q.P. Wu, D.T. Bergstralh, B.K. Davis, B.P. O'Connor, J.P. Ting, J.S. Serody, C-C chemokine receptor 5 on pulmonary fibrocytes facilitates migration and promotes metastasis via matrix metalloproteinase 9, The American journal of pathology, 173 (2008) 253-264.

[176] M. Rinderknecht, M. Detmar, Tumor lymphangiogenesis and melanoma metastasis, Journal of cellular physiology, 216 (2008) 347-354.

[177] H. Saji, M. Koike, T. Yamori, S. Saji, M. Seiki, K. Matsushima, M. Toi, Significant correlation of monocyte chemoattractant protein-1 expression with neovascularization and progression of breast carcinoma, Cancer, 92 (2001) 1085-1091.

[178] H. Peinado, M. Aleckovic, S. Lavotshkin, I. Matei, B. Costa-Silva, G. Moreno-Bueno, M. Hergueta-Redondo, C. Williams, G. Garcia-Santos, C. Ghajar, A. Nitadori-Hoshino, C. Hoffman, K. Badal, B.A. Garcia, M.K. Callahan, J. Yuan, V.R. Martins, J. Skog, R.N. Kaplan, M.S. Brady, J.D. Wolchok, P.B. Chapman, Y. Kang, J. Bromberg, D. Lyden, Melanoma exosomes educate bone marrow progenitor cells toward a pro-metastatic phenotype through MET, Nature medicine, 18 (2012) 883-891.

[179] J.L. Hood, R.S. San, S.A. Wickline, Exosomes released by melanoma cells prepare sentinel lymph nodes for tumor metastasis, Cancer research, 71 (2011) 3792-3801.

[180] S. Yu, C. Liu, K. Su, J. Wang, Y. Liu, L. Zhang, C. Li, Y. Cong, R. Kimberly, W.E. Grizzle, C. Falkson, H.G. Zhang, Tumor exosomes inhibit differentiation of bone marrow dendritic cells, Journal of immunology (Baltimore, Md. : 1950), 178 (2007) 6867-6875.

[181] X. Xiang, A. Poliakov, C. Liu, Y. Liu, Z.B. Deng, J. Wang, Z. Cheng, S.V. Shah, G.J. Wang, L. Zhang, W.E. Grizzle, J. Mobley, H.G. Zhang, Induction of myeloid-derived suppressor cells by tumor exosomes, International journal of cancer, 124 (2009) 2621-2633.

[182] Y. Liu, X. Xiang, X. Zhuang, S. Zhang, C. Liu, Z. Cheng, S. Michalek, W. Grizzle, H.G. Zhang, Contribution of MyD88 to the tumor exosome-mediated induction of myeloid derived suppressor cells, The American journal of pathology, 176 (2010) 2490-2499.

[183] F. Chalmin, S. Ladoire, G. Mignot, J. Vincent, M. Bruchard, J.P. Remy-Martin, W. Boireau, A. Rouleau, B. Simon, D. Lanneau, A. De Thonel, G. Multhoff, A. Hamman, F. Martin, B. Chauffert, E. Solary, L. Zitvogel, C. Garrido, B. Ryffel, C. Borg, L. Apetoh, C. Rebe, F. Ghiringhelli, Membrane-associated Hsp72 from tumor-derived exosomes mediates STAT3-dependent immunosuppressive function of mouse and human myeloid-derived suppressor cells, The Journal of clinical investigation, 120 (2010) 457-471.

[184] T.R. Cox, R.M.H. Rumney, E.M. Schoof, L. Perryman, A.M. Hoye, A. Agrawal, D. Bird, N.A. Latif, H. Forrest, H.R. Evans, I.D. Huggins, G. Lang, R. Linding, A. Gartland, J.T. Erler, The hypoxic cancer secretome induces pre-metastatic bone lesions through lysyl oxidase, Nature, 522 (2015) 106-110.

[185] S. Hiratsuka, A. Watanabe, Y. Sakurai, S. Akashi-Takamura, S. Ishibashi, K. Miyake, M. Shibuya, S. Akira, H. Aburatani, Y. Maru, The S100A8-serum amyloid A3-TLR4 paracrine cascade establishes a pre-metastatic phase, Nature cell biology, 10 (2008) 1349-1355.

[186] R. Temple, Are surrogate markers adequate to assess cardiovascular disease drugs?, Jama, 282 (1999) 790-795.

[187] R. Katz, Biomarkers and surrogate markers: an FDA perspective, NeuroRx : the journal of the American Society for Experimental NeuroTherapeutics, 1 (2004) 189-195.

[188] A. Italiano, Prognostic or predictive? It's time to get back to definitions!, Journal of clinical oncology : official journal of the American Society of Clinical Oncology, 29 (2011) 4718; author reply 4718-4719.

[189] A.S. Coates, E.P. Winer, A. Goldhirsch, R.D. Gelber, M. Gnant, M. Piccart-Gebhart, B. Thurlimann, H.J. Senn, Tailoring therapies--improving the management of early breast cancer: St Gallen International Expert Consensus on the Primary Therapy of Early Breast Cancer 2015, Annals of oncology : official journal of the European Society for Medical Oncology, 26 (2015) 1533-1546.

[190] G. Arpino, H. Weiss, A.V. Lee, R. Schiff, S. De Placido, C.K. Osborne, R.M. Elledge, Estrogen receptor-positive, progesterone receptor-negative breast cancer: association with growth factor

receptor expression and tamoxifen resistance, Journal of the National Cancer Institute, 97 (2005) 1254-1261.

[191] D.J. Slamon, G.M. Clark, S.G. Wong, W.J. Levin, A. Ullrich, W.L. McGuire, Human breast cancer: correlation of relapse and survival with amplification of the HER-2/neu oncogene, Science (New York, N.Y.), 235 (1987) 177-182.

[192] M.C. Cheang, D. Voduc, C. Bajdik, S. Leung, S. McKinney, S.K. Chia, C.M. Perou, T.O. Nielsen, Basal-like breast cancer defined by five biomarkers has superior prognostic value than triple-negative phenotype, Clinical cancer research : an official journal of the American Association for Cancer Research, 14 (2008) 1368-1376.

[193] C. Criscitiello, D. Disalvatore, M. De Laurentiis, L. Gelao, L. Fumagalli, M. Locatelli, V. Bagnardi, N. Rotmensz, A. Esposito, I. Minchella, S. De Placido, M. Santangelo, G. Viale, A. Goldhirsch, G. Curigliano, High Ki-67 score is indicative of a greater benefit from adjuvant chemotherapy when added to endocrine therapy in luminal B HER2 negative and node-positive breast cancer, Breast (Edinburgh, Scotland), 23 (2014) 69-75.

[194] B. Ács, V. Zámbó, L. Vízkeleti, A.M. Szász, L. Madaras, G. Szentmártoni, T. Tőkés, B.Á. Molnár, I.A. Molnár, S. Vári-Kakas, J. Kulka, A.-M. Tőkés, Ki-67 as a controversial predictive and prognostic marker in breast cancer patients treated with neoadjuvant chemotherapy, Diagnostic Pathology, 12 (2017) 20.

[195] F. Tas, E. Bilgin, S. Karabulut, D. Duranyildiz, Clinical significance of serum epidermal growth factor receptor (EGFR) levels in patients with breast cancer, Cytokine, 71 (2015) 66-70.

[196] E. Lim, F. Vaillant, D. Wu, N.C. Forrest, B. Pal, A.H. Hart, M.L. Asselin-Labat, D.E. Gyorki, T. Ward, A. Partanen, F. Feleppa, L.I. Huschtscha, H.J. Thorne, S.B. Fox, M. Yan, J.D. French, M.A. Brown, G.K. Smyth, J.E. Visvader, G.J. Lindeman, Aberrant luminal progenitors as the candidate target population for basal tumor development in BRCA1 mutation carriers, Nature medicine, 15 (2009) 907-913.

[197] R. Bhargava, S. Beriwal, K. McManus, D.J. Dabbs, CK5 is more sensitive than CK5/6 in identifying the "basal-like" phenotype of breast carcinoma, American journal of clinical pathology, 130 (2008) 724-730.

[198] H.O. Ohnstad, E. Borgen, R.S. Falk, T.G. Lien, M. Aaserud, M.A.T. Sveli, J.A. Kyte, V.N. Kristensen, G.A. Geitvik, E. Schlichting, E.A. Wist, T. Sorlie, H.G. Russnes, B. Naume, Prognostic value of PAM50 and risk of recurrence score in patients with early-stage breast cancer with long-term follow-up, Breast cancer research : BCR, 19 (2017) 120.

[199] B. Naume, X. Zhao, M. Synnestvedt, E. Borgen, H.G. Russnes, O.C. Lingjaerde, M. Stromberg, G. Wiedswang, G. Kvalheim, R. Karesen, J.M. Nesland, A.L. Borresen-Dale, T. Sorlie, Presence of bone marrow micrometastasis is associated with different recurrence risk within molecular subtypes of breast cancer, Molecular oncology, 1 (2007) 160-171.

[200] M.J. Engstrom, S. Opdahl, A.I. Hagen, P.R. Romundstad, L.A. Akslen, O.A. Haugen, L.J. Vatten, A.M. Bofin, Molecular subtypes, histopathological grade and survival in a historic cohort of breast cancer patients, Breast cancer research and treatment, 140 (2013) 463-473.

[201] G. Turashvili, E. Brogi, Tumor Heterogeneity in Breast Cancer, Front Med (Lausanne), 4 (2017) 227.

[202] S. Badve, Y. Gokmen-Polar, Tumor Heterogeneity in Breast Cancer, Advances in anatomic pathology, 22 (2015) 294-302.

[203] R.E. Ellsworth, H.L. Blackburn, C.D. Shriver, P. Soon-Shiong, D.L. Ellsworth, Molecular heterogeneity in breast cancer: State of the science and implications for patient care, Seminars in cell & developmental biology, 64 (2017) 65-72.

[204] E.H. Allott, J. Geradts, X. Sun, S.M. Cohen, G.R. Zirpoli, T. Khoury, W. Bshara, M. Chen, M.E. Sherman, J.R. Palmer, C.B. Ambrosone, A.F. Olshan, M.A. Troester, Intratumoral heterogeneity as a source of discordance in breast cancer biomarker classification, Breast cancer research : BCR, 18 (2016) 68.

[205] M.J. Bissell, W.C. Hines, Why don't we get more cancer? A proposed role of the microenvironment in restraining cancer progression, Nature medicine, 17 (2011) 320-329.

[206] J. Fenner, A.C. Stacer, F. Winterroth, T.D. Johnson, K.E. Luker, G.D. Luker, Macroscopic Stiffness of Breast Tumors Predicts Metastasis, Scientific Reports, 4 (2014) 5512.

[207] A.M. Bamberger, K. Milde-Langosch, H.M. Schulte, T. Loning, Progesterone receptor isoforms, PR-B and PR-A, in breast cancer: correlations with clinicopathologic tumor parameters and expression of AP-1 factors, Hormone research, 54 (2000) 32-37.

[208] K. Takahashi, K. Tanabe, M. Ohnuki, M. Narita, T. Ichisaka, K. Tomoda, S. Yamanaka, Induction of pluripotent stem cells from adult human fibroblasts by defined factors, Cell, 131 (2007) 861-872.

[209] C. Davies, J. Godwin, R. Gray, M. Clarke, D. Cutter, S. Darby, P. McGale, H.C. Pan, C. Taylor, Y.C. Wang, M. Dowsett, J. Ingle, R. Peto, Relevance of breast cancer hormone receptors and other factors to the efficacy of adjuvant tamoxifen: patient-level meta-analysis of randomised trials, Lancet (London, England), 378 (2011) 771-784.

[210] E. Sunami, M. Shinozaki, M.S. Sim, S.L. Nguyen, A.T. Vu, A.E. Giuliano, D.S. Hoon, Estrogen receptor and HER2/neu status affect epigenetic differences of tumor-related genes in primary breast tumors, Breast cancer research : BCR, 10 (2008) R46.

[211] H. Fujiwara, M. Ferreira, G. Donati, D.K. Marciano, J.M. Linton, Y. Sato, A. Hartner, K. Sekiguchi, L.F. Reichardt, F.M. Watt, The basement membrane of hair follicle stem cells is a muscle cell niche, Cell, 144 (2011) 577-589.

[212] M. Loset, S.B. Mundal, M.P. Johnson, M.H. Fenstad, K.A. Freed, I.A. Lian, I.P. Eide, L. Bjorge, J. Blangero, E.K. Moses, R. Austgulen, A transcriptional profile of the decidua in preeclampsia, American journal of obstetrics and gynecology, 204 (2011) 84.e81-27.

[213] M. Uhlen, E. Bjorling, C. Agaton, C.A. Szigyarto, B. Amini, E. Andersen, A.C. Andersson, P. Angelidou, A. Asplund, C. Asplund, L. Berglund, K. Bergstrom, H. Brumer, D. Cerjan, M. Ekstrom, A. Elobeid, C. Eriksson, L. Fagerberg, R. Falk, J. Fall, M. Forsberg, M.G. Bjorklund, K. Gumbel, A. Halimi, I. Hallin, C. Hamsten, M. Hansson, M. Hedhammar, G. Hercules, C. Kampf, K. Larsson, M. Lindskog, W. Lodewyckx, J. Lund, J. Lundeberg, K. Magnusson, E. Malm, P. Nilsson, J. Odling, P. Oksvold, I. Olsson, E. Oster, J. Ottosson, L. Paavilainen, A. Persson, R. Rimini, J. Rockberg, M. Runeson, A. Sivertsson, A. Skollermo, J. Steen, M. Stenvall, F. Sterky, S. Stromberg, M. Sundberg, H. Tegel, S. Tourle, E. Wahlund, A. Walden, J. Wan, H. Wernerus, J. Westberg, K. Wester, U. Wrethagen, L.L. Xu, S. Hober, F. Ponten, A human protein atlas for normal and cancer tissues based on antibody proteomics, Molecular & cellular proteomics : MCP, 4 (2005) 1920-1932.

[214] M. Egeblad, E.S. Nakasone, Z. Werb, Tumors as organs: complex tissues that interface with the entire organism, Developmental cell, 18 (2010) 884-901.

[215] K. Xie, J.L. Abbruzzese, Developmental biology informs cancer: the emerging role of the hedgehog signaling pathway in upper gastrointestinal cancers, Cancer cell, 4 (2003) 245-247.

[216] H.S. Ro, S.W. Kim, D. Wu, C. Webber, T.E. Nicholson, Gene structure and expression of the mouse adipocyte enhancer-binding protein, Gene, 280 (2001) 123-133.

[217] N. Dil, A.G. Banerjee, A role for aberrantly expressed nuclear localized decorin in migration and invasion of dysplastic and malignant oral epithelial cells, Head & neck oncology, 3 (2011) 44.

[218] N. Rucci, A. Rufo, M. Alamanou, M. Capulli, A. Del Fattore, E. Ahrman, D. Capece, V. Iansante, F. Zazzeroni, E. Alesse, D. Heinegard, A. Teti, The glycosaminoglycan-binding domain of PRELP acts as a cell type-specific NF-kappaB inhibitor that impairs osteoclastogenesis, The Journal of cell biology, 187 (2009) 669-683.

[219] Y. Liang, M. Haring, P.J. Roughley, R.K. Margolis, R.U. Margolis, Glypican and biglycan in the nuclei of neurons and glioma cells: presence of functional nuclear localization signals and dynamic changes in glypican during the cell cycle, The Journal of cell biology, 139 (1997) 851-864.

[220] K. Narayanan, A. Ramachandran, J. Hao, G. He, K.W. Park, M. Cho, A. George, Dual functional roles of dentin matrix protein 1. Implications in biomineralization and gene transcription by activation of intracellular Ca2+ store, The Journal of biological chemistry, 278 (2003) 17500-17508.

[221] M. Ii, H. Yamamoto, H. Taniguchi, Y. Adachi, M. Nakazawa, H. Ohashi, T. Tanuma, Y. Sukawa, H. Suzuki, S. Sasaki, K. Imai, Y. Shinomura, Co-expression of laminin beta3 and gamma2 chains and epigenetic inactivation of laminin alpha3 chain in gastric cancer, International journal of oncology, 39 (2011) 593-599.

[222] C. Velez-Delvalle, M. Marsch-Moreno, F. Castro-Munozledo, Y.J. Bolivar-Flores, W. Kuri-Harcuch, Fibromodulin gene is expressed in human epidermal keratinocytes in culture and in human epidermis in vivo, Biochemical and biophysical research communications, 371 (2008) 420-424.

[223] Y. Matsuda, T. Yamamoto, M. Kudo, K. Kawahara, M. Kawamoto, Y. Nakajima, K. Koizumi, N. Nakazawa, T. Ishiwata, Z. Naito, Expression and roles of lumican in lung adenocarcinoma and squamous cell carcinoma, International journal of oncology, 33 (2008) 1177-1185.

[224] J.M. Lynch, M. Maillet, D. Vanhoutte, A. Schloemer, M.A. Sargent, N.S. Blair, K.A. Lynch, T. Okada, B.J. Aronow, H. Osinska, R. Prywes, J.N. Lorenz, K. Mori, J. Lawler, J. Robbins, J.D. Molkentin, A thrombospondin-dependent pathway for a protective ER stress response, Cell, 149 (2012) 1257-1268.

[225] J. Monfort, G. Tardif, P. Roughley, P. Reboul, C. Boileau, P.N. Bishop, J.P. Pelletier, J. Martel-Pelletier, Identification of opticin, a member of the small leucine-rich repeat proteoglycan family, in human articular tissues: a novel target for MMP-13 in osteoarthritis, Osteoarthritis and cartilage, 16 (2008) 749-755.

[226] S. Grkovic, V.C. O'Reilly, S. Han, M. Hong, R.C. Baxter, S.M. Firth, IGFBP-3 binds GRP78, stimulates autophagy and promotes the survival of breast cancer cells exposed to adverse microenvironments, Oncogene, 32 (2013) 2412-2420.

[227] M.L. Shinohara, H.J. Kim, J.H. Kim, V.A. Garcia, H. Cantor, Alternative translation of osteopontin generates intracellular and secreted isoforms that mediate distinct biological activities in dendritic cells, Proceedings of the National Academy of Sciences of the United States of America, 105 (2008) 7235-7239.

[228] W.O. Twal, S.M. Hammad, S.L. Guffy, W.S. Argraves, A novel intracellular fibulin-1D variant binds to the cytoplasmic domain of integrin beta 1 subunit, Matrix biology : journal of the International Society for Matrix Biology, 43 (2015) 97-108.

[229] Y.N. Wang, H. Yamaguchi, L. Huo, Y. Du, H.J. Lee, H.H. Lee, H. Wang, J.M. Hsu, M.C. Hung, The translocon Sec61beta localized in the inner nuclear membrane transports membrane-embedded EGF receptor to the nucleus, The Journal of biological chemistry, 285 (2010) 38720-38729.

[230] B. Tsai, Y. Ye, T.A. Rapoport, Retro-translocation of proteins from the endoplasmic reticulum into the cytosol, Nature reviews. Molecular cell biology, 3 (2002) 246-255.

[231] C. Rodighiero, B. Tsai, T.A. Rapoport, W.I. Lencer, Role of ubiquitination in retro-translocation of cholera toxin and escape of cytosolic degradation, EMBO reports, 3 (2002) 1222-1227.

[232] P.J. Lenting, O.D. Christophe, C.V. Denis, von Willebrand factor biosynthesis, secretion, and clearance: connecting the far ends, Blood, 125 (2015) 2019-2028.

[233] S.S. Apte, W.C. Parks, Metalloproteinases: A parade of functions in matrix biology and an outlook for the future, Matrix biology : journal of the International Society for Matrix Biology, 44-46 (2015) 1-6.

[234] A.E. Powell, E.C. Anderson, P.S. Davies, A.D. Silk, C. Pelz, S. Impey, M.H. Wong, Fusion between Intestinal epithelial cells and macrophages in a cancer context results in nuclear reprogramming, Cancer research, 71 (2011) 1497-1505.

[235] P.S. Aguilar, M.K. Baylies, A. Fleissner, L. Helming, N. Inoue, B. Podbilewicz, H. Wang, M. Wong, Genetic basis of cell-cell fusion mechanisms, Trends in genetics : TIG, 29 (2013) 427-437.

[236] M. Smid, Y. Wang, Y. Zhang, A.M. Sieuwerts, J. Yu, J.G. Klijn, J.A. Foekens, J.W. Martens, Subtypes of breast cancer show preferential site of relapse, Cancer research, 68 (2008) 3108-3114.

[237] W. Chen, A.D. Hoffmann, H. Liu, X. Liu, Organotropism: new insights into molecular mechanisms of breast cancer metastasis, NPJ Precis Oncol, 2 (2018) 4.

[238] M.A. Blanco, Y. Kang, Signaling pathways in breast cancer metastasis - novel insights from functional genomics, Breast cancer research : BCR, 13 (2011) 206.

[239] A.J. Minn, G.P. Gupta, D. Padua, P. Bos, D.X. Nguyen, D. Nuyten, B. Kreike, Y. Zhang, Y. Wang, H. Ishwaran, J.A. Foekens, M. van de Vijver, J. Massague, Lung metastasis genes couple breast tumor size and metastatic spread, Proceedings of the National Academy of Sciences of the United States of America, 104 (2007) 6740-6745.

[240] R.R. Langley, I.J. Fidler, The seed and soil hypothesis revisited--the role of tumor-stroma interactions in metastasis to different organs, International journal of cancer, 128 (2011) 2527-2535.

[241] U.H. Weidle, F. Birzele, G. Kollmorgen, R. Ruger, Molecular Basis of Lung Tropism of Metastasis, Cancer genomics & proteomics, 13 (2016) 129-139.

[242] E.K. Sloan, N. Pouliot, K.L. Stanley, J. Chia, J.M. Moseley, D.K. Hards, R.L. Anderson, Tumor-specific expression of alphavbeta3 integrin promotes spontaneous metastasis of breast cancer to bone, Breast cancer research : BCR, 8 (2006) R20.

[243] C.W. Wong, A. Lee, L. Shientag, J. Yu, Y. Dong, G. Kao, A.B. Al-Mehdi, E.J. Bernhard, R.J. Muschel, Apoptosis: an early event in metastatic inefficiency, Cancer research, 61 (2001) 333-338.

[244] K.J. Luzzi, I.C. MacDonald, E.E. Schmidt, N. Kerkvliet, V.L. Morris, A.F. Chambers, A.C. Groom, Multistep nature of metastatic inefficiency: dormancy of solitary cells after successful extravasation and limited survival of early micrometastases, The American journal of pathology, 153 (1998) 865-873.

[245] A.R. Nebreda, A. Porras, p38 MAP kinases: beyond the stress response, Trends in biochemical sciences, 25 (2000) 257-260.

[246] J.M. Kyriakis, J. Avruch, Mammalian mitogen-activated protein kinase signal transduction pathways activated by stress and inflammation, Physiological reviews, 81 (2001) 807-869.

[247] A. Cuadrado, A.R. Nebreda, Mechanisms and functions of p38 MAPK signalling, The Biochemical journal, 429 (2010) 403-417.

[248] N.J. Kennedy, R.J. Davis, Chapter 164 - Mammalian MAP Kinases, in: R.A. Bradshaw, E.A. Dennis (Eds.) Handbook of Cell Signaling (Second Edition), Academic Press, San Diego, 2010, pp. 1315-1328.

[249] J.S. Sebolt-Leopold, R. Herrera, Targeting the mitogen-activated protein kinase cascade to treat cancer, Nature reviews. Cancer, 4 (2004) 937-947.

[250] H.J. Schaeffer, M.J. Weber, Mitogen-activated protein kinases: specific messages from ubiquitous messengers, Molecular and cellular biology, 19 (1999) 2435-2444.

[251] L. Chang, M. Karin, Mammalian MAP kinase signalling cascades, Nature, 410 (2001) 37-40.

[252] Z. Xia, M. Dickens, J. Raingeaud, R.J. Davis, M.E. Greenberg, Opposing effects of ERK and JNK-p38 MAP kinases on apoptosis, Science (New York, N.Y.), 270 (1995) 1326-1331.

[253] T.M. Thornton, M. Rincon, Non-classical p38 map kinase functions: cell cycle checkpoints and survival, International journal of biological sciences, 5 (2009) 44-51.

[254] V. Kuek, Z. Yang, S.M. Chim, S. Zhu, H. Xu, S.T. Chow, J. Tickner, V. Rosen, W. Erber, X. Li, A. Qin, Y. Qian, J. Xu, NPNT is Expressed by Osteoblasts and Mediates Angiogenesis via the Activation of Extracellular Signal-regulated Kinase, Sci Rep, 6 (2016) 36210.

[255] K.S. Elenitoba-Johnson, S.D. Jenson, R.T. Abbott, R.A. Palais, S.D. Bohling, Z. Lin, S. Tripp, P.J. Shami, L.Y. Wang, R.W. Coupland, R. Buckstein, B. Perez-Ordonez, S.L. Perkins, I.D. Dube, M.S. Lim, Involvement of multiple signaling pathways in follicular lymphoma transformation: p38-mitogen-activated protein kinase as a target for therapy, Proceedings of the National Academy of Sciences of the United States of America, 100 (2003) 7259-7264.

[256] A.K. Greenberg, S. Basu, J. Hu, T.A. Yie, K.M. Tchou-Wong, W.N. Rom, T.C. Lee, Selective p38 activation in human non-small cell lung cancer, American journal of respiratory cell and molecular biology, 26 (2002) 558-564.

[257] M. Pomerance, J. Quillard, F. Chantoux, J. Young, J.P. Blondeau, High-level expression, activation, and subcellular localization of p38-MAP kinase in thyroid neoplasms, The Journal of pathology, 209 (2006) 298-306.

[258] T. Demuth, L.B. Reavie, J.L. Rennert, M. Nakada, S. Nakada, D.B. Hoelzinger, C.E. Beaudry, A.N. Henrichs, E.M. Anderson, M.E. Berens, MAP-ing glioma invasion: mitogen-activated protein kinase kinase 3 and p38 drive glioma invasion and progression and predict patient survival, Molecular cancer therapeutics, 6 (2007) 1212-1222.

[259] M.R. Junttila, R. Ala-Aho, T. Jokilehto, J. Peltonen, M. Kallajoki, R. Grenman, P. Jaakkola, J. Westermarck, V.M. Kahari, p38alpha and p38delta mitogen-activated protein kinase isoforms regulate invasion and growth of head and neck squamous carcinoma cells, Oncogene, 26 (2007) 5267-5279.

[260] F.J. Esteva, A.A. Sahin, T.L. Smith, Y. Yang, L. Pusztai, R. Nahta, T.A. Buchholz, A.U. Buzdar, G.N. Hortobagyi, S.S. Bacus, Prognostic significance of phosphorylated P38 mitogen-activated protein kinase and HER-2 expression in lymph node-positive breast carcinoma, Cancer, 100 (2004) 499-506.

[261] H.K. Koul, M. Pal, S. Koul, Role of p38 MAP Kinase Signal Transduction in Solid Tumors, Genes & cancer, 4 (2013) 342-359.

[262] E.F. Wagner, A.R. Nebreda, Signal integration by JNK and p38 MAPK pathways in cancer development, Nature reviews. Cancer, 9 (2009) 537-549.

[263] I. Corre, F. Paris, J. Huot, The p38 pathway, a major pleiotropic cascade that transduces stress and metastatic signals in endothelial cells, Oncotarget, 8 (2017) 55684-55714.

[264] H. Kankaanranta, P.M. De Souza, P.J. Barnes, M. Salmon, M.A. Giembycz, M.A. Lindsay, SB 203580, an inhibitor of p38 mitogen-activated protein kinase, enhances constitutive apoptosis of cytokine-deprived human eosinophils, The Journal of pharmacology and experimental therapeutics, 290 (1999) 621-628.

[265] J.A. Aguirre-Ghiso, Y. Estrada, D. Liu, L. Ossowski, ERK(MAPK) activity as a determinant of tumor growth and dormancy; regulation by p38(SAPK), Cancer research, 63 (2003) 1684-1695.

[266] J.A. Aguirre-Ghiso, Models, mechanisms and clinical evidence for cancer dormancy, Nature reviews. Cancer, 7 (2007) 834-846.

[267] F. Comes, A. Matrone, P. Lastella, B. Nico, F.C. Susca, R. Bagnulo, G. Ingravallo, S. Modica, G. Lo Sasso, A. Moschetta, G. Guanti, C. Simone, A novel cell type-specific role of p38alpha in the control of autophagy and cell death in colorectal cancer cells, Cell death and differentiation, 14 (2007) 693-702.

[268] K. Takeda, I. Naguro, H. Nishitoh, A. Matsuzawa, H. Ichijo, Apoptosis signaling kinases: from stress response to health outcomes, Antioxidants & redox signaling, 15 (2011) 719-761.

[269] C. Liu, Y. Li, M. Semenov, C. Han, G.H. Baeg, Y. Tan, Z. Zhang, X. Lin, X. He, Control of beta-catenin phosphorylation/degradation by a dual-kinase mechanism, Cell, 108 (2002) 837-847.

[270] T.C. He, A.B. Sparks, C. Rago, H. Hermeking, L. Zawel, L.T. da Costa, P.J. Morin, B. Vogelstein, K.W. Kinzler, Identification of c-MYC as a target of the APC pathway, Science (New York, N.Y.), 281 (1998) 1509-1512.

[271] H.C. Reinhardt, A.S. Aslanian, J.A. Lees, M.B. Yaffe, p53-deficient cells rely on ATM- and ATR-mediated checkpoint signaling through the p38MAPK/MK2 pathway for survival after DNA damage, Cancer cell, 11 (2007) 175-189.

[272] A. Cuenda, S. Rousseau, p38 MAP-kinases pathway regulation, function and role in human diseases, Biochimica et biophysica acta, 1773 (2007) 1358-1375.

[273] K. Ono, J. Han, The p38 signal transduction pathway: activation and function, Cellular signalling, 12 (2000) 1-13.

[274] R.B. Clarke, Steroid receptors and proliferation in the human breast, Steroids, 68 (2003) 789-794.

[275] J. Regan, S. Breitfelder, P. Cirillo, T. Gilmore, A.G. Graham, E. Hickey, B. Klaus, J. Madwed, M. Moriak, N. Moss, C. Pargellis, S. Pav, A. Proto, A. Swinamer, L. Tong, C. Torcellini, Pyrazole urea-based inhibitors of p38 MAP kinase: from lead compound to clinical candidate, Journal of medicinal chemistry, 45 (2002) 2994-3008.

[276] J. Cicenas, E. Zalyte, A. Rimkus, D. Dapkus, R. Noreika, S. Urbonavicius, JNK, p38, ERK, and SGK1 Inhibitors in Cancer, Cancers, 10 (2017).

[277] J. Bain, L. Plater, M. Elliott, N. Shpiro, C.J. Hastie, H. McLauchlan, I. Klevernic, J.S. Arthur, D.R. Alessi, P. Cohen, The selectivity of protein kinase inhibitors: a further update, The Biochemical journal, 408 (2007) 297-315.

[278] MRC PPU International Centre for Kinase Profiling, http://www.kinase-screen.mrc.ac.uk/screening-compounds/341038?order=field_results_inhibition&sort=asc.

[279] Y. Kuma, G. Sabio, J. Bain, N. Shpiro, R. Marquez, A. Cuenda, BIRB796 inhibits all p38 MAPK isoforms in vitro and in vivo, The Journal of biological chemistry, 280 (2005) 19472-19479.

[280] H. Yasui, T. Hideshima, H. Ikeda, J. Jin, E.M. Ocio, T. Kiziltepe, Y. Okawa, S. Vallet, K. Podar, K. Ishitsuka, P.G. Richardson, C. Pargellis, N. Moss, N. Raje, K.C. Anderson, BIRB 796 enhances cytotoxicity triggered by bortezomib, heat shock protein (Hsp) 90 inhibitor, and dexamethasone via inhibition of p38 mitogen-activated protein kinase/Hsp27 pathway in multiple myeloma cell lines and inhibits paracrine tumour growth, British journal of haematology, 136 (2007) 414-423.

[281] D. He, X.Q. Zhao, X.G. Chen, Y. Fang, S. Singh, T.T. Talele, H.J. Qiu, Y.J. Liang, X.K. Wang, G.Q. Zhang, Z.S. Chen, L.W. Fu, BIRB796, the inhibitor of p38 mitogen-activated protein kinase, enhances the efficacy of chemotherapeutic agents in ABCB1 overexpression cells, PloS one, 8 (2013) e54181.

[282] X. Jin, Q. Mo, Y. Zhang, Y. Gao, Y. Wu, J. Li, X. Hao, D. Ma, Q. Gao, P. Chen, The p38 MAPK inhibitor BIRB796 enhances the antitumor effects of VX680 in cervical cancer, Cancer biology & therapy, 17 (2016) 566-576.

[283] S. Ryoo, J. Choi, J. Kim, S. Bae, J. Hong, S. Jo, S. Kim, Y. Lee, BIRB 796 has Distinctive Anti-inflammatory Effects on Different Cell Types, Immune network, 13 (2013) 283-288.

[284] S. Schreiber, B. Feagan, G. D'Haens, J.F. Colombel, K. Geboes, M. Yurcov, V. Isakov, O. Golovenko, C.N. Bernstein, D. Ludwig, T. Winter, U. Meier, C. Yong, J. Steffgen, Oral p38 mitogen-activated protein kinase inhibition with BIRB 796 for active Crohn's disease: a randomized, double-blind, placebo-controlled trial, Clinical gastroenterology and hepatology : the official clinical practice journal of the American Gastroenterological Association, 4 (2006) 325-334.

[285] D.M. Dambach, Potential adverse effects associated with inhibition of p38alpha/beta MAP kinases, Current topics in medicinal chemistry, 5 (2005) 929-939.

[286] D. Hammaker, G.S. Firestein, "Go upstream, young man": lessons learned from the p38 saga, Annals of the rheumatic diseases, 69 Suppl 1 (2010) i77-82.

[287] J. Maia, S. Caja, M.C. Strano Moraes, N. Couto, B. Costa-Silva, Exosome-Based Cell-Cell Communication in the Tumor Microenvironment, Frontiers in cell and developmental biology, 6 (2018) 18.

[288] N. Couto, S. Caja, J. Maia, M.C. Strano Moraes, B. Costa-Silva, Exosomes as emerging players in cancer biology, Biochimie, (2018).

[289] M. Gonzalez-Begne, B. Lu, X. Han, F.K. Hagen, A.R. Hand, J.E. Melvin, J.R. Yates, Proteomic analysis of human parotid gland exosomes by multidimensional protein identification technology (MudPIT), Journal of proteome research, 8 (2009) 1304-1314.

[290] M. Demory Beckler, J.N. Higginbotham, J.L. Franklin, A.J. Ham, P.J. Halvey, I.E. Imasuen, C. Whitwell, M. Li, D.C. Liebler, R.J. Coffey, Proteomic analysis of exosomes from mutant KRAS colon cancer cells identifies intercellular transfer of mutant KRAS, Molecular & cellular proteomics : MCP, 12 (2013) 343-355.

[291] L. Gangoda, M. Liem, C.S. Ang, S. Keerthikumar, C.G. Adda, B.S. Parker, S. Mathivanan, Proteomic Profiling of Exosomes Secreted by Breast Cancer Cells with Varying Metastatic Potential, Proteomics, 17 (2017).

[292] S. Wang, Y. Chen, F. Qu, S. He, X. Huang, H. Jiang, T. Jin, S. Wan, J. Xing, Association between leukocyte telomere length and glioma risk: a case-control study, Neuro-oncology, 16 (2014) 505-512.

[293] G. Sandblom, S. Ladjevardi, H. Garmo, E. Varenhorst, The impact of prostate-specific antigen level at diagnosis on the relative survival of 28,531 men with localized carcinoma of the prostate, Cancer, 112 (2008) 813-819.

[294] A. Salonia, F. Abdollah, U. Capitanio, N. Suardi, A. Briganti, A. Gallina, R. Colombo, M. Ferrari, G. Castagna, P. Rigatti, F. Montorsi, Serum sex steroids depict a nonlinear u-shaped association with high-risk prostate cancer at radical prostatectomy, Clinical cancer research : an official journal of the American Association for Cancer Research, 18 (2012) 3648-3657.

[295] Y. Cui, Q. Cai, S. Qu, W.H. Chow, W. Wen, Y.B. Xiang, J. Wu, N. Rothman, G. Yang, X.O. Shu, Y.T. Gao, W. Zheng, Association of leukocyte telomere length with colorectal cancer risk: nested case-control findings from the Shanghai Women's Health Study, Cancer epidemiology, biomarkers & prevention : a publication of the American Association for Cancer Research, cosponsored by the American Society of Preventive Oncology, 21 (2012) 1807-1813.

[296] K. Aleksandrova, S.C. Chuang, H. Boeing, H. Zuo, G.S. Tell, T. Pischon, M. Jenab, B. Bueno-de-Mesquita, S.E. Vollset, O. Midttun, P.M. Ueland, V. Fedirko, M. Johansson, E. Weiderpass, G. Severi, A. Racine, M.C. Boutron-Ruault, R. Kaaks, T. Kuhn, A. Tjonneland, K. Overvad, J.R. Quiros, P. Jakszyn, M.J. Sanchez, M. Dorronsoro, M.D. Chirlaque, E. Ardanaz, K.T. Khaw, N.J. Wareham, R.C. Travis, A. Trichopoulou, P. Lagiou, D. Trichopoulos, D. Palli, S. Sieri, R. Tumino, S. Panico, A.M. May, R. Palmqvist, I. Ljuslinder, S.Y. Kong, H. Freisling, M.J. Gunter, Y. Lu, A.J. Cross, E. Riboli, P. Vineis, A prospective study of the immune system activation biomarker neopterin and colorectal cancer risk, Journal of the National Cancer Institute, 107 (2015).

[297] H.G. Skinner, R.E. Gangnon, K. Litzelman, R.A. Johnson, S.T. Chari, G.M. Petersen, L.A. Boardman, Telomere length and pancreatic cancer: a case-control study, Cancer epidemiology, biomarkers & prevention : a publication of the American Association for Cancer Research, cosponsored by the American Society of Preventive Oncology, 21 (2012) 2095-2100.

[298] S.C. Chuang, R. Stolzenberg-Solomon, P.M. Ueland, S.E. Vollset, O. Midttun, A. Olsen, A. Tjonneland, K. Overvad, M.C. Boutron-Ruault, S. Morois, F. Clavel-Chapelon, B. Teucher, R. Kaaks, C. Weikert, H. Boeing, A. Trichopoulou, V. Benetou, A. Naska, M. Jenab, N. Slimani, I. Romieu, D.S. Michaud, D. Palli, S. Sieri, S. Panico, C. Sacerdote, R. Tumino, G. Skeie, E.J. Duell, L. Rodriguez, E. Molina-Montes, J.M. Huerta, N. Larranaga, A.B. Gurrea, D. Johansen, J. Manjer, W. Ye, M. Sund, P.H. Peeters, S. Jeurnink, N. Wareham, K.T. Khaw, F. Crowe, E. Riboli, B. Bueno-de-Mesquita, P. Vineis, A U-shaped relationship between plasma folate and pancreatic cancer risk in the European Prospective Investigation into Cancer and Nutrition, European journal of cancer (Oxford, England : 1990), 47 (2011) 1808-1816.

[299] S. Qu, W. Wen, X.O. Shu, W.H. Chow, Y.B. Xiang, J. Wu, B.T. Ji, N. Rothman, G. Yang, Q. Cai, Y.T. Gao, W. Zheng, Association of leukocyte telomere length with breast cancer risk: nested case-control findings from the Shanghai Women's Health Study, American journal of epidemiology, 177 (2013) 617-624.

[300] R. Duchnowska, J. Sperinde, B. Czartoryska-Arlukowicz, P. Mysliwiec, J. Winslow, B. Radecka, C. Petropoulos, R. Demlova, M. Orlikowska, A. Kowalczyk, I. Lang, B. Ziolkowska, S. Debska-Szmich, M. Merdalska, A. Grela-Wojewoda, A. Zawrocki, W. Biernat, W. Huang, J. Jassem, Predictive value of quantitative HER2, HER3 and p95HER2 levels in HER2-positive advanced breast cancer patients treated with lapatinib following progression on trastuzumab, Oncotarget, 8 (2017) 104149-104159.

[301] A.M. Noone, K.A. Cronin, S.F. Altekruse, N. Howlader, D.R. Lewis, V.I. Petkov, L. Penberthy, Cancer Incidence and Survival Trends by Subtype Using Data from the Surveillance Epidemiology and End Results Program, 1992-2013, Cancer epidemiology, biomarkers & prevention : a publication of the American Association for Cancer Research, cosponsored by the American Society of Preventive Oncology, 26 (2017) 632-641.

[302] L. Tao, L. Chu, L.I. Wang, L. Moy, M. Brammer, C. Song, M. Green, A.W. Kurian, S.L. Gomez, C.A. Clarke, Occurrence and outcome of de novo metastatic breast cancer by subtype in a large, diverse population, Cancer causes & control : CCC, 27 (2016) 1127-1138.

[303] L. Tao, S.L. Gomez, T.H. Keegan, A.W. Kurian, C.A. Clarke, Breast Cancer Mortality in African-American and Non-Hispanic White Women by Molecular Subtype and Stage at Diagnosis: A Population-Based Study, Cancer epidemiology, biomarkers & prevention : a publication of the American Association for Cancer Research, cosponsored by the American Society of Preventive Oncology, 24 (2015) 1039-1045.

[304] A.L. Altick, L.M. Baryshnikova, T.Q. Vu, C.S. von Bartheld, Quantitative analysis of multivesicular bodies (MVBs) in the hypoglossal nerve: evidence that neurotrophic factors do not use MVBs for retrograde axonal transport, The Journal of comparative neurology, 514 (2009) 641-657.

[305] M. Logozzi, A. De Milito, L. Lugini, M. Borghi, L. Calabro, M. Spada, M. Perdicchio, M.L. Marino, C. Federici, E. Iessi, D. Brambilla, G. Venturi, F. Lozupone, M. Santinami, V. Huber, M. Maio, L. Rivoltini, S. Fais, High levels of exosomes expressing CD63 and caveolin-1 in plasma of melanoma patients, PloS one, 4 (2009) e5219.

[306] P. Kharaziha, S. Ceder, Q. Li, T. Panaretakis, Tumor cell-derived exosomes: a message in a bottle, Biochimica et biophysica acta, 1826 (2012) 103-111.

[307] K. Agarwal, M. Saji, S.M. Lazaroff, A.F. Palmer, M.D. Ringel, M.E. Paulaitis, Analysis of exosome release as a cellular response to MAPK pathway inhibition, Langmuir : the ACS journal of surfaces and colloids, 31 (2015) 5440-5448.

[308] G. Raposo, W. Stoorvogel, Extracellular vesicles: exosomes, microvesicles, and friends, The Journal of cell biology, 200 (2013) 373-383.

[309] H. Kalra, R.J. Simpson, H. Ji, E. Aikawa, P. Altevogt, P. Askenase, V.C. Bond, F.E. Borras, X. Breakefield, V. Budnik, E. Buzas, G. Camussi, A. Clayton, E. Cocucci, J.M. Falcon-Perez, S. Gabrielsson, Y.S. Gho, D. Gupta, H.C. Harsha, A. Hendrix, A.F. Hill, J.M. Inal, G. Jenster, E.M. Kramer-Albers, S.K. Lim, A. Llorente, J. Lotvall, A. Marcilla, L. Mincheva-Nilsson, I. Nazarenko, R. Nieuwland, E.N. Nolte-'t Hoen, A. Pandey, T. Patel, M.G. Piper, S. Pluchino, T.S. Prasad, L. Rajendran, G. Raposo, M. Record, G.E. Reid, F. Sanchez-Madrid, R.M. Schiffelers, P. Siljander, A. Stensballe, W. Stoorvogel, D. Taylor, C. Thery, H. Valadi, B.W. van Balkom, J. Vazquez, M. Vidal, M.H. Wauben, M. Yanez-Mo, M. Zoeller, S. Mathivanan, Vesiclepedia: a compendium for extracellular vesicles with continuous community annotation, PLoS biology, 10 (2012) e1001450.

[310] D.K. Kim, B. Kang, O.Y. Kim, D.S. Choi, J. Lee, S.R. Kim, G. Go, Y.J. Yoon, J.H. Kim, S.C. Jang, K.S. Park, E.J. Choi, K.P. Kim, D.M. Desiderio, Y.K. Kim, J. Lotvall, D. Hwang, Y.S. Gho, EVpedia: an integrated database of high-throughput data for systemic analyses of extracellular vesicles, Journal of extracellular vesicles, 2 (2013).

[311] R. Kalluri, The biology and function of exosomes in cancer, The Journal of clinical investigation, 126 (2016) 1208-1215.

[312] M. Amorim, G. Fernandes, P. Oliveira, D. Martins-de-Souza, E. Dias-Neto, D. Nunes, The overexpression of a single oncogene (ERBB2/HER2) alters the proteomic landscape of extracellular vesicles, Proteomics, 14 (2014) 1472-1479.

[313] I. Nazarenko, S. Rana, A. Baumann, J. McAlear, A. Hellwig, M. Trendelenburg, G. Lochnit, K.T. Preissner, M. Zoller, Cell surface tetraspanin Tspan8 contributes to molecular pathways of exosome-induced endothelial cell activation, Cancer research, 70 (2010) 1668-1678.

[314] D.J. Leeming, A.C. Bay-Jensen, E. Vassiliadis, M.R. Larsen, K. Henriksen, M.A. Karsdal, Post-translational modifications of the extracellular matrix are key events in cancer progression: opportunities for biochemical marker development, Biomarkers : biochemical indicators of exposure, response, and susceptibility to chemicals, 16 (2011) 193-205.

[315] S.S. Pinho, C.A. Reis, Glycosylation in cancer: mechanisms and clinical implications, Nature reviews. Cancer, 15 (2015) 540-555.

[316] F. Schwarz, M. Aebi, Mechanisms and principles of N-linked protein glycosylation, Current opinion in structural biology, 21 (2011) 576-582.

[317] M.R. Kudelka, T. Ju, J. Heimburg-Molinaro, R.D. Cummings, Simple sugars to complex disease--mucin-type O-glycans in cancer, Advances in cancer research, 126 (2015) 53-135.

[318] T. Miyagi, T. Wada, K. Yamaguchi, K. Hata, Sialidase and malignancy: a minireview, Glycoconjugate journal, 20 (2004) 189-198.

[319] J. Munkley, D.J. Elliott, Hallmarks of glycosylation in cancer, Oncotarget, 7 (2016) 35478-35489.

[320] M.M. Fuster, J.D. Esko, The sweet and sour of cancer: glycans as novel therapeutic targets, Nature reviews. Cancer, 5 (2005) 526-542.

[321] I.O. Potapenko, V.D. Haakensen, T. Luders, A. Helland, I. Bukholm, T. Sorlie, V.N. Kristensen, O.C. Lingjaerde, A.L. Borresen-Dale, Glycan gene expression signatures in normal and malignant breast tissue; possible role in diagnosis and progression, Molecular oncology, 4 (2010) 98-118.

[322] T. Sorlie, C.M. Perou, R. Tibshirani, T. Aas, S. Geisler, H. Johnsen, T. Hastie, M.B. Eisen, M. van de Rijn, S.S. Jeffrey, T. Thorsen, H. Quist, J.C. Matese, P.O. Brown, D. Botstein, P.E. Lonning, A.L. Borresen-Dale, Gene expression patterns of breast carcinomas distinguish tumor subclasses with clinical implications, Proceedings of the National Academy of Sciences of the United States of America, 98 (2001) 10869-10874.

[323] K. Menck, C. Scharf, A. Bleckmann, L. Dyck, U. Rost, D. Wenzel, V.M. Dhople, L. Siam, T. Pukrop, C. Binder, F. Klemm, Tumor-derived microvesicles mediate human breast cancer invasion through differentially glycosylated EMMPRIN, Journal of molecular cell biology, 7 (2015) 143-153.

[324] O. Moreno-Gonzalo, C. Villarroya-Beltri, F. Sanchez-Madrid, Post-translational modifications of exosomal proteins, Frontiers in immunology, 5 (2014) 383.

[325] S. Hakomori, Glycosylation defining cancer malignancy: new wine in an old bottle, Proceedings of the National Academy of Sciences of the United States of America, 99 (2002) 10231-10233.

[326] M. Amado, F. Carneiro, M. Seixas, H. Clausen, M. Sobrinho-Simoes, Dimeric sialyl-Le(x) expression in gastric carcinoma correlates with venous invasion and poor outcome, Gastroenterology, 114 (1998) 462-470.

[327] T. Nakagoe, T. Sawai, T. Tsuji, M. Jibiki, M. Ohbatake, A. Nanashima, H. Yamaguchi, N. Kurosaki, T. Yasutake, H. Ayabe, Y. Tagawa, Difference in prognostic value between sialyl Lewis(a) and sialyl lewis(x) antigens in blood samples obtained from the drainage veins of the colorectal tumors, Cancer letters, 159 (2000) 159-168.

[328] T. Nakagoe, T. Sawai, T. Tsuji, M.A. Jibiki, A. Nanashima, H. Yamaguchi, T. Yasutake, H. Ayabe, K. Arisawa, H. Ishikawa, Difference in prognostic value between sialyl Lewis(a) and sialyl Lewis(x) antigen levels in the preoperative serum of gastric cancer patients, Journal of clinical gastroenterology, 34 (2002) 408-415.

[329] K.S. Lau, J.W. Dennis, N-Glycans in cancer progression, Glycobiology, 18 (2008) 750-760.

[330] W. Yi, P.M. Clark, D.E. Mason, M.C. Keenan, C. Hill, W.A. Goddard, 3rd, E.C. Peters, E.M. Driggers, L.C. Hsieh-Wilson, Phosphofructokinase 1 glycosylation regulates cell growth and metabolism, Science (New York, N.Y.), 337 (2012) 975-980.

[331] A.C. Kolbl, U. Andergassen, U. Jeschke, The Role of Glycosylation in Breast Cancer Metastasis and Cancer Control, Frontiers in oncology, 5 (2015) 219.

[332] R. Saldova, J.M. Reuben, U.M. Abd Hamid, P.M. Rudd, M. Cristofanilli, Levels of specific serum N-glycans identify breast cancer patients with higher circulating tumor cell counts, Annals of oncology : official journal of the European Society for Medical Oncology, 22 (2011) 1113-1119.

[333] J.D. Mott, Z. Werb, Regulation of matrix biology by matrix metalloproteinases, Current opinion in cell biology, 16 (2004) 558-564.

[334] A. Winer, S. Adams, P. Mignatti, Matrix Metalloproteinase Inhibitors in Cancer Therapy: Turning Past Failures Into Future Successes, Molecular cancer therapeutics, 17 (2018) 1147-1155.

[335] B. Cauwe, G. Opdenakker, Intracellular substrate cleavage: a novel dimension in the biochemistry, biology and pathology of matrix metalloproteinases, Critical reviews in biochemistry and molecular biology, 45 (2010) 351-423.

[336] E.A. Garbett, M.W.R. Reed, N.J. Brown, Proteolysis in human breast and colorectal cancer, British Journal Of Cancer, 81 (1999) 287.

[337] B. Roucourt, S. Meeussen, J. Bao, P. Zimmermann, G. David, Heparanase activates the syndecan-syntenin-ALIX exosome pathway, Cell research, 25 (2015) 412-428.

[338] C.A. Thompson, A. Purushothaman, V.C. Ramani, I. Vlodavsky, R.D. Sanderson, Heparanase regulates secretion, composition, and function of tumor cell-derived exosomes, The Journal of biological chemistry, 288 (2013) 10093-10099.

[339] M. Uhlen, L. Fagerberg, B.M. Hallstrom, C. Lindskog, P. Oksvold, A. Mardinoglu, A. Sivertsson, C. Kampf, E. Sjostedt, A. Asplund, I. Olsson, K. Edlund, E. Lundberg, S. Navani, C.A. Szigyarto, J. Odeberg, D. Djureinovic, J.O. Takanen, S. Hober, T. Alm, P.H. Edqvist, H. Berling, H. Tegel, J. Mulder, J. Rockberg, P. Nilsson, J.M. Schwenk, M. Hamsten, K. von Feilitzen, M. Forsberg, L. Persson, F. Johansson, M. Zwahlen, G. von Heijne, J. Nielsen, F. Ponten, Proteomics. Tissue-based map of the human proteome, Science (New York, N.Y.), 347 (2015) 1260419.

[340] S. Kuphal, S. Wallner, A.K. Bosserhoff, Loss of nephronectin promotes tumor progression in malignant melanoma, Cancer science, 99 (2008) 229-233.

[341] Y. Ban, G. Yamamoto, M. Takada, S. Hayashi, Y. Ban, K. Shimizu, H. Akasu, T. Igarashi, Y. Bando, T. Tachikawa, T. Hirano, Proteomic profiling of thyroid papillary carcinoma, Journal of thyroid research, 2012 (2012) 815079.

[342] T. Akerstrom, H.S. Willenberg, K. Cupisti, J. Ip, S. Backman, A. Moser, R. Maharjan, B. Robinson, K.A. Iwen, H. Dralle, D.V. C, M. Backdahl, J. Botling, P. Stalberg, G. Westin, M.K. Walz, H. Lehnert, S. Sidhu, J. Zedenius, P. Bjorklund, P. Hellman, Novel somatic mutations and distinct molecular signature in aldosterone-producing adenomas, Endocrine-related cancer, 22 (2015) 735-744.

[343] A.E. Teo, S. Garg, T.I. Johnson, W. Zhao, J. Zhou, C.E. Gomez-Sanchez, M. Gurnell, M.J. Brown, Physiological and Pathological Roles in Human Adrenal of the Glomeruli-Defining Matrix Protein NPNT (Nephronectin), Hypertension (Dallas, Tex. : 1979), 69 (2017) 1207-1216.

[344] S. Dilmac, N. Erin, N. Demir, G. Tanriover, Nephronectin is Decreased in Metastatic Breast Carcinoma and Related to Metastatic Organs, Pathology oncology research : POR, 24 (2018) 679-688.

[345] T.S. Steigedal, J. Toraskar, R.P. Redvers, M. Valla, S.N. Magnussen, A.M. Bofin, S. Opdahl, S. Lundgren, B.L. Eckhardt, J.M. Lamar, J. Doherty, R.O. Hynes, R.L. Anderson, G. Svineng, Nephronectin is Correlated with Poor Prognosis in Breast Cancer and Promotes Metastasis via its Integrin-Binding Motifs, Neoplasia (New York, N.Y.), 20 (2018) 387-400.

[346] M.D. Sternlicht, Key stages in mammary gland development: the cues that regulate ductal branching morphogenesis, Breast cancer research : BCR, 8 (2006) 201.

[347] I. Plante, M.K. Stewart, D.W. Laird, Evaluation of mammary gland development and function in mouse models, Journal of visualized experiments : JoVE, (2011).

[348] T. Hu, R. Zhou, Y. Zhao, G. Wu, Integrin alpha6/Akt/Erk signaling is essential for human breast cancer resistance to radiotherapy, Sci Rep, 6 (2016) 33376.

[349] C.C. Park, H.J. Zhang, E.S. Yao, C.J. Park, M.J. Bissell, Beta1 integrin inhibition dramatically enhances radiotherapy efficacy in human breast cancer xenografts, Cancer research, 68 (2008) 4398-4405.

[350] W.P. Mason, End of the road: confounding results of the CORE trial terminate the arduous journey of cilengitide for glioblastoma, Neuro-oncology, 17 (2015) 634-635.

[351] L.B. Nabors, K.L. Fink, T. Mikkelsen, D. Grujicic, R. Tarnawski, D.H. Nam, M. Mazurkiewicz, M. Salacz, L. Ashby, V. Zagonel, R. Depenni, J.R. Perry, C. Hicking, M. Picard, M.E. Hegi, B. Lhermitte, D.A. Reardon, Two cilengitide regimens in combination with standard treatment for patients with newly diagnosed glioblastoma and unmethylated MGMT gene promoter: results of the open-label, controlled, randomized phase II CORE study, Neuro-oncology, 17 (2015) 708-717.

[352] E. Elez, I. Kocakova, T. Hohler, U.M. Martens, C. Bokemeyer, E. Van Cutsem, B. Melichar, M. Smakal, T. Csoszi, E. Topuzov, R. Orlova, S. Tjulandin, F. Rivera, J. Straub, R. Bruns, S. Quaratino, J. Tabernero, Abituzumab combined with cetuximab plus irinotecan versus cetuximab plus irinotecan alone for patients with KRAS wild-type metastatic colorectal cancer: the randomised phase I/II POSEIDON trial, Annals of oncology : official journal of the European Society for Medical Oncology, 26 (2015) 132-140.

[353] R. Stupp, M.E. Hegi, T. Gorlia, S.C. Erridge, J. Perry, Y.K. Hong, K.D. Aldape, B. Lhermitte, T. Pietsch, D. Grujicic, J.P. Steinbach, W. Wick, R. Tarnawski, D.H. Nam, P. Hau, A. Weyerbrock, M.J. Taphoorn, C.C. Shen, N. Rao, L. Thurzo, U. Herrlinger, T. Gupta, R.D. Kortmann, K. Adamska, C. McBain, A.A. Brandes, J.C. Tonn, O. Schnell, T. Wiegel, C.Y. Kim, L.B. Nabors, D.A. Reardon, M.J. van den Bent, C. Hicking, A. Markivskyy, M. Picard, M. Weller, Cilengitide combined with standard treatment for patients with newly diagnosed glioblastoma with methylated MGMT promoter (CENTRIC EORTC 26071-22072 study): a multicentre, randomised, open-label, phase 3 trial, The Lancet. Oncology, 15 (2014) 1100-1108.

[354] J.G. Parvani, A.J. Galliher-Beckley, B.J. Schiemann, W.P. Schiemann, Targeted inactivation of beta1 integrin induces beta3 integrin switching, which drives breast cancer metastasis by TGF-beta, Molecular biology of the cell, 24 (2013) 3449-3459.

[355] R. Barrow-McGee, N. Kishi, C. Joffre, L. Ménard, A. Hervieu, B.A. Bakhouche, A.J. Noval, A. Mai, C. Guzmán, L. Robbez-Masson, X. Iturrioz, J. Hulit, C.H. Brennan, I.R. Hart, P.J. Parker, J. Ivaska, S. Kermorgant, Beta 1-integrin–c-Met cooperation reveals an inside-in survival signalling on autophagy-related endomembranes, Nature Communications, 7 (2016) 11942.

[356] J. Zhang, B. Shen, A. Lin, Novel strategies for inhibition of the p38 MAPK pathway, Trends in pharmacological sciences, 28 (2007) 286-295.

[357] M.R. Lee, C. Dominguez, MAP kinase p38 inhibitors: clinical results and an intimate look at their interactions with p38alpha protein, Current medicinal chemistry, 12 (2005) 2979-2994.

[358] D.M. Goldstein, T. Gabriel, Pathway to the clinic: inhibition of P38 MAP kinase. A review of ten chemotypes selected for development, Current topics in medicinal chemistry, 5 (2005) 1017-1029.

[359] S.T. Wrobleski, A.M. Doweyko, Structural comparison of p38 inhibitor-protein complexes: a review of recent p38 inhibitors having unique binding interactions, Current topics in medicinal chemistry, 5 (2005) 1005-1016.

[360] S.V. Moradi, W.M. Hussein, P. Varamini, P. Simerska, I. Toth, Glycosylation, an effective synthetic strategy to improve the bioavailability of therapeutic peptides, Chemical science, 7 (2016) 2492-2500.

[361] T. Kieber-Emmons, L. Hutchins, P. Emanuel, A. Pennisi, E. Siegel, F. Jousheghany, B. Karbassi, I. Makhoul, Abstract P6-10-06: Inducing immune responses to tumor associated carbohydrate antigens by a carbohydrate mimetic peptide vaccine: Clinical experience in phase I and phase II trials, Cancer research, 77 (2017) P6-10-06-P16-10-06.

[362] A. Markiv, N.D. Rambaruth, M.V. Dwek, Beyond the genome and proteome: targeting protein modifications in cancer, Current opinion in pharmacology, 12 (2012) 408-413.

[363] L. Cai, Z. Gu, J. Zhong, D. Wen, G. Chen, L. He, J. Wu, Z. Gu, Advances in glycosylation-mediated cancer-targeted drug delivery, Drug discovery today, 23 (2018) 1126-1138.

[364] W. Yu, N. Zhang, C. Li, Saccharide modified pharmaceutical nanocarriers for targeted drug and gene delivery, Current pharmaceutical design, 15 (2009) 3826-3836.

[365] A. Alaseem, K. Alhazzani, P. Dondapati, S. Alobid, A. Bishayee, A. Rathinavelu, Matrix Metalloproteinases: A challenging paradigm of cancer management, Seminars in cancer biology, (2017).

[366] S. Ricard-Blum, R. Salza, Matricryptins and matrikines: biologically active fragments of the extracellular matrix, Experimental dermatology, 23 (2014) 457-463.

[367] S. Ricard-Blum, S.D. Vallet, Matricryptins Network with Matricellular Receptors at the Surface of Endothelial and Tumor Cells, Frontiers in pharmacology, 7 (2016) 11.

[368] B.S. Batista, W.S. Eng, K.T. Pilobello, K.D. Hendricks-Munoz, L.K. Mahal, Identification of a conserved glycan signature for microvesicles, Journal of proteome research, 10 (2011) 4624-4633.

[369] S. Fais, L. O'Driscoll, F.E. Borras, E. Buzas, G. Camussi, F. Cappello, J. Carvalho, A. Cordeiro da Silva, H. Del Portillo, S. El Andaloussi, T. Ficko Trcek, R. Furlan, A. Hendrix, I. Gursel, V. Kralj-Iglic, B. Kaeffer, M. Kosanovic, M.E. Lekka, G. Lipps, M. Logozzi, A. Marcilla, M. Sammar, A. Llorente, I. Nazarenko, C. Oliveira, G. Pocsfalvi, L. Rajendran, G. Raposo, E. Rohde, P. Siljander, G. van Niel,

M.H. Vasconcelos, M. Yanez-Mo, M.L. Yliperttula, N. Zarovni, A.B. Zavec, B. Giebel, Evidence-Based Clinical Use of Nanoscale Extracellular Vesicles in Nanomedicine, ACS nano, 10 (2016) 3886-3899.

[370] N. Kosaka, Y. Yoshioka, N. Tominaga, K. Hagiwara, T. Katsuda, T. Ochiya, Dark side of the exosome: the role of the exosome in cancer metastasis and targeting the exosome as a strategy for cancer therapy, Future oncology (London, England), 10 (2014) 671-681.

[371] F.M. Khan, E. Saleh, H. Alawadhi, R. Harati, W.H. Zimmermann, R. El-Awady, Inhibition of exosome release by ketotifen enhances sensitivity of cancer cells to doxorubicin, Cancer biology & therapy, 19 (2018) 25-33.

[372] H.G. Welch, W.C. Black, Using autopsy series to estimate the disease "reservoir" for ductal carcinoma in situ of the breast: how much more breast cancer can we find?, Annals of internal medicine, 127 (1997) 1023-1028.

[373] S. El Andaloussi, S. Lakhal, I. Mager, M.J. Wood, Exosomes for targeted siRNA delivery across biological barriers, Advanced drug delivery reviews, 65 (2013) 391-397.

Paper I

NEOPLASIA
www.neoplasia.com

Volume 20 Number 4 April 2018 pp. 387–400 387

Nephronectin is Correlated with Poor Prognosis in Breast Cancer and Promotes Metastasis via its Integrin-Binding Motifs

Tonje S. Steigedal[*,†,‡,§], Jimita Toraskar[*,§], Richard P. Redvers[†,¶], Marit Valla[*,#], Synnøve N. Magnussen[**], Anna M. Bofin[*], Signe Opdahl[#], Steinar Lundgren[*,††], Bedrich L. Eckhardt[‡‡,§§,¶¶], John M. Lamar[‡,##], Judy Doherty[†], Richard O. Hynes[‡,*], Robin L. Anderson[†,¶,†††,1] and Gunbjørg Svineng[**,1]**

[*]Department of Clinical and Molecular Medicine, Faculty of Medicine and Health Sciences, Norwegian University of Science and Technology (NTNU), Trondheim, Norway; [†]Peter MacCallum Cancer Centre, East Melbourne, Victoria, Australia; [‡]David H Koch Institute for Integrative Cancer Research, Massachusetts Institute of Technology, Cambridge, MA, United States; [§]Central Norway Regional Health Authority, Stjørdal, Norway; [¶]Olivia Newton-John Cancer Research Institute, Heidelberg, Victoria, Australia; [#]Department of Public Health and Nursing, Faculty of Medicine and Health Sciences, NTNU, Trondheim, Norway; [**]Department of Medical Biology, Faculty of Health Sciences, UiT - The Arctic University of Norway, Tromsø, Norway; [††]Cancer Clinic, St. Olav's Hospital, Trondheim University Hospital, Trondheim, Norway; [‡‡]Morgan Welch Inflammatory Breast Cancer Research Program and Clinic, The University of Texas at MD Anderson Cancer Centre, Houston, TX, USA; [§§]Section of Translational Breast Cancer Research, The University of Texas at MD Anderson Cancer Centre, Houston, TX, USA; [¶¶]Department of Breast Medical Oncology, The University of Texas at MD Anderson Cancer Centre, Houston, TX 77030, USA; [##]Department of Molecular and Cellular Physiology, Albany Medical College, Albany, NY, USA; [***]Howard Hughes Medical Institute, Massachusetts Institute of Technology, Cambridge, MA, United States; [†††]School of Cancer Medicine, La Trobe University, Bundoora, Victoria, Australia

Abstract

Most cancer patients with solid tumors who succumb to their illness die of metastatic disease. While early detection and improved treatment have led to reduced mortality, even for those with metastatic cancer, some patients still respond poorly to treatment. Understanding the mechanisms of metastasis is important to improve prognostication, to stratify patients for treatment, and to identify new targets for therapy. We have shown previously that expression of nephronectin (NPNT) is correlated with metastatic propensity in breast cancer cell lines. In the present study, we provide a comprehensive analysis of the expression pattern and distribution of NPNT in breast cancer tissue from 842 patients by immunohistochemical staining of tissue microarrays from a historic cohort. Several patterns of NPNT staining were observed. An association between granular cytoplasmic

Address all correspondence to: Tonje S. Steigedal, Department of Clinical and Molecular Medicine, Faculty of Medicine and Health Sciences, NTNU, Postbox 8905, N-7491 Trondheim, Norway. E-mail: Tonje.S.Steigedal@ntnu.no

[1] These authors contributed equally to the work.

Received 28 November 2017; Revised 17 February 2018; Accepted 19 February 2018

1476-5586
https://doi.org/10.1016/j.neo.2018.02.008

staining (in <10% of tumor cells) and poor prognosis was found. We suggest that granular cytoplasmic staining may represent NPNT-positive exosomes. We found that NPNT promotes adhesion and anchorage-independent growth via its integrin-binding and enhancer motifs and that enforced expression in breast tumor cells promotes their colonization of the lungs. We propose that NPNT may be a novel prognostic marker in a subgroup of breast cancer patients.

Neoplasia (2018) 20, 387–400

Introduction

Metastasis is the major cause of death for patients with solid tumors who succumb to their disease [1]. Breast cancer metastases usually develop in multiple organs including lymph nodes, bone, lung, liver, and brain [2]. Understanding the molecular mechanisms by which breast tumors metastasize is integral to improving outcome for patients with advanced disease. However, the metastatic process and the selective preference of tumor cells for certain tissues is complex and dependent on various factors including vascular patterns, adhesion factors, and tumor cell interactions with the stroma at the metastatic site [3].

Human breast cancer is heterogeneous and is divided into subgroups that vary in gene expression profiles, phenotype, aggressiveness, metastatic propensity, and response to treatment [4–6]. A comprehensive effort with screening programs, development of new chemotherapeutic and endocrine regimens, and implementation of targeted agents has contributed to reduced breast cancer mortality [4]. Stratification of patients into optimal treatment regimens is therefore of increasing importance. The four original molecular subtypes of breast cancer (Luminal, HER2-enriched, basal-like, and normal-like) [5,6] have subsequently been divided into additional subtypes that are likely to be of clinical relevance [4,7].

Nephronectin (NPNT), also known as POEM (Preosteoblast Epidermal Growth Factor (EGF)-like repeat protein with MAM domain,) was initially identified as a gene involved in embryonic development of endocrine organs via interactions with the integrin α8β1 receptor [8–10]. Structurally, NPNT has five EGF-like domains, a MAM (meprin, A5 protein and receptor protein tyrosine phosphatase) domain, and an RGD (Arg-Gly-Asp) integrin-binding motif and is generally proposed to be a secreted glycoprotein [8,10]. It is secreted by bulge stem cells in hair follicles and induces differentiation of arrector pili muscle cells [11,12]. NPNT also functions in differentiation of atrioventricular cells and in promotion of vascularization [13,14].

Few reports exist about the role of NPNT in tumor progression and metastasis. In a previous study of genes involved in metastatic processes, we analyzed primary tumors of mouse mammary tumor lines exhibiting various degrees of metastatic capacity and found a correlation between increased *Npnt* expression levels and metastatic propensity [15]. We went on to show that knockdown of NPNT in the highly metastatic 4T1.2 mammary tumor caused a significant reduction of metastasis to lung, spine, and kidney [15]. In addition, Borowsky et al. reported higher levels of NPNT in metastatic mammary tumor cells compared to nonmetastatic cells in a different syngeneic mouse model of breast cancer, supporting a putative role of NPNT as a metastasis-promoting factor [16].

This study reports the first large-scale analysis of NPNT protein expression in human breast cancer. By immunohistochemistry (IHC), we found several different staining patterns for NPNT. Granular cytoplasmic staining was associated with poor prognosis and may be consistent with tumor cell–derived extracellular vesicles. Using preclinical models, we show the necessity of the NPNT integrin-binding site in the metastatic process. Our functional data demonstrate that the disruption of the integrin-binding site within NPNT can modulate the propensity of metastatic breast cancer cells to adhere to and colonize the lung. Collectively, our data identify a functional role for NPNT during metastasis and describe its expression and possible prognostic role in a large cohort of breast cancer patients.

Materials and Methods

Patients

The study population has been described previously in detail [17]. Briefly, of a total of 1393 new cases of breast cancer occurring between 1961 and 2008, 909 cases were available for subtyping using IHC and *in situ* hybridization (ISH) markers as surrogates for gene expression analyses, and 886 of these were assembled in tissue microarrays (TMAs). Patients were followed until death from breast cancer or from other causes, as registered by the Cause of Death Registry, or until December 31, 2010. Only cases in TMAs were included in the present study, and 842 cases were suitable for analysis. Two subtypes, 5 negative phenotype and basal-like phenotype described in Engstrom et al., were merged into triple negative in the current analysis [17]. The study was performed in accordance with the approval granted by the Regional Committee for Medical and Health Research Ethics (REK Midt-Norge, ref. no.:836/2009), and dispensation from the requirement of patient consent was granted.

Immunostaining (IHC and IF)

The patient samples were fixed in formalin, but details of the preanalytical conditions are unknown as these samples were collected over several decades. From TMAs, 4-μm–thick sections were cut and mounted on Superfrost+ glass slides, dried overnight at 37°C, and stored in the freezer at −20°C. Before IHC, slides were heated for 2 hours at 60°C and pretreated in a PT Link Pre-Treatment Module for Tissue Specimens (Dako Denmark A/S, 2600 Glostrup, DK) with buffer (High pH Target Retrieval Solution K8004) for 20 minutes at 97°C. Immunostaining for NPNT (Atlas Antibodies/Sigma Cat.: HPA003711, Lot No.: D97165, dilution 1:100) was done in a DakoCytomationAutostainer Plus (Dako) at 4°C overnight. Dako REAL EnVision Detection System with Peroxidase/DAB+, Rabbit/Mouse, code K5007, was used for visualization. The following controls were used: a negative control (omitting the primary antibody), rabbit IgG isotype control, and a positive control (normal kidney). Sections from validation and optimization of the anti-NPNT antibody (Atlas Antibodies/Sigma) on human tissues are shown in Supplementary Figure S1. The figure shows that the optimal dilution of the antibody was 1:100 in the human samples.

All mouse tissues subjected to immunostaining analyses were fixed in 10% buffered formalin for about 24 hours and embedded in paraffin following standard procedures. Tissue blocks were sectioned at 4 μm and rehydrated through Neo-clear and ethanol series. Antigen retrieval was performed in 10 mM EDTA (pH 9) by 15-minute boiling in a microwave oven. Primary antibodies; anti-human NPNT (Atlas Antibodies/Sigma, Cat.: HPA003711, Lot No.: D97165, dilution 1:150), anti-mouse NPNT (Abnova, Cat.: PAB8467, Lot No.: TG 100309, dilution 1:150), anti-V5 (CST, Cat.: 13202S, Lot No.: 2, dilution 1:150), anti-collagen V (Abcam, Cat.: ab7046, Lot No.: GR222605-7, dilution 1:200), anti-Fibronectin (Abcam, Cat.: ab2413, Lot No.: GR250744-3, dilution 1:200), and Rabbit IgG Isotype control (BD Biosciences, Cat.: 610822, Lot No.: 7069938). All antibodies were incubated at 4°C overnight. Secondary antibodies were used according to manufacturer's recommendations (Dako EnVision, Glostrup, Denmark). IF detection was performed using anti-CHMP4B (Atlas Antibodies/Sigma, Cat.: HPA051751, Lot No.: R67106, dilution 1:300, anti-V5 (CST, Cat.: 13202S, Lot No.: 2, dilution 1:150) and secondary antibodies; Goat anti-Mouse IgG (H+L) Highly Cross-Adsorbed Secondary Antibody, Alexa Fluor Plus 647, (Thermo Fisher Scientific, Cat.: A32728, Lot No.: RJ243424, dilution 1:1000) and Goat anti-Rabbit IgG (H+L) Highly Cross-Adsorbed Secondary Antibody, Alexa Fluor Plus 488 (Thermo Fisher Scientific, Cat.: A32731, Lot No.: RJ243417, dilution 1:1000). Validation of specificity of the anti-human NPNT (Atlas Antibodies/Sigma and anti-mouse NPNT (Abnova) antibodies on MMTV-PyMT mouse tissues is shown in Supplementary Figure S2.

Scoring, Reporting, and Classification of the Human Patient Samples

All TMA slides were digitized for review as described previously after both hematoxylin-eosin-saffron (HES) and IHC staining [17]. Each case was assessed by two researchers independently (by T.S.S. and A.M.B. or M.V.), one of whom (A.M.B. and M.V.) was a pathologist. Discrepant results were discussed, and consensus was reached. For diffuse cytoplasmic staining, a staining index was calculated by multiplying staining intensity by the proportion of stained cells. Staining intensity was recorded as follows: 0 (no staining), 1 (weak), 2 (moderate), and 3 (strong). The proportion of stained cells was scored as 0 (<1%), 1 (1-<10%), 2 (≥10-<50%), and 3 (≥50%). A staining index of 0-2 was interpreted as negative; 3-9, as positive. For granular cytoplasmic staining, any staining was interpreted as positive, and the proportion of stained cells was recorded as <1%, 1-<10%, ≥10-<50%, and ≥50%. The presence of scattered, strongly cytoplasmic stained tumor cells was recorded. Nuclear staining in ≥1% of tumor cells was interpreted as positive.

MMTV-PyMT Transgenic Animals

Breast tumor tissues and lungs from MMTV-PyMT animals (The Jackson Laboratory, ME, USA) were collected to represent different tumor stages and used for IHC and ISH analysis, in addition to isolation of primary cells. IHC-stained samples were assessed (by T.S.S. and J.T.) using the same scoring system as for the human samples. Mice were housed Comparative Medicine Core Facility at NTNU, and the studies were approved by The Norwegian Food Safety Authority (FOTS number 3683) and conducted in accordance with the institutional animal ethics guidelines.

Cell Culture

The mouse cell lines 67NR, 168FARN, 66cl4, 4TO7, and 4T1 were kindly provided by Dr. Fred Miller (Wayne State University, Detroit, MI) and have been described previously [18]. These cells, and the 4T1-shNPNT cells, were cultured in DMEM (Gibco, Invitrogen, Carlsbad, CA) supplemented with 10% fetal calf serum (FCS, Bovogen, VIC, Australia) and 1% (v/v) penicillin-streptomycin. 66cl4-cells with stable expression of mCherry were made as described previously [19] and cultured in α-MEM containing 5-10% FCS and 1% (v/v) penicillin-streptomycin. Cell lines are routinely tested for mycoplasma infection. In addition, a comprehensive screening for viral and bacterial pathogenic contamination was performed at Laboratorio Dynamimed, Madrid, prior to the animal experiments. Additional information about the 66cl4-NPNT and 4T1-shNPNT is described in supplementary material.

Tumor Growth and In Vivo Lung Colonization Assay

Female BALB/c mice (6-8 weeks old, Walter and Eliza Hall Institute, Melbourne, Australia, or from Taconic M&B, Skensved, Denmark) were anesthetized and injected either orthotopically into the mammary gland (1×10^5 cells) or intravenously into the tail vein (5×10^5 cells) with various mCherry-expressing 66cl4-cell line variants as described previously [15]. Mice bearing mammary tumors were culled after 35 days. Relative tumor burden (RTB) was measured based on the level of genomic DNA for mCherry compared to that of vimentin [20]. Primary tumors were collected and subjected to IHC analyses. Following intravenous injection, mice were monitored daily and sacrificed after 3 weeks. Lungs were collected and subjected to RTB, IHC, and IF analyses. Representative left lung lobes from the lung colonization assay were imaged using the EVOS FL Auto Cell Imaging System. Each image was created using a stitch of several images to cover the entire lung lobe. Mice were housed either in the Peter MacCallum Animal Care Facility or in the Comparative Medicine Core Facility at NTNU, and all animal studies were approved by either the Peter MacCallum Animal Ethics Committee (AEEC project number E411) or The Norwegian Food Safety Authority (FOTS number 4551) and conducted in accordance with the institutional animal ethics guidelines.

Isolation of Epithelial Cells

Primary epithelial cells were isolated from FVB wild-type and MMTV-PyMT transgenic mice [21]. Normal and tumor mammary tissues were minced in 5 ml DMEM/F12 (Gibco) with 2% FCS (Invitrogen), 10 mM HEPES, 10 ng/ml epidermal growth factor, 10 μg/ml insulin, 10 mg/ml BSA, 2 mM glutamine, 50 U/ml penicillin, 50 μg/ml streptomycin sulfate, and 1.5 mg/ml collagenase type IA-S (Sigma) for 3 hours at 37°C with gentle rotation. Cells were spun at 1600 rpm for 4 minutes and resuspended in trypsin prior to a second spin at 1400 rpm and resuspension in fresh medium without collagenase. Cells were incubated at 37°C with 5% CO_2 for about 2-3 weeks.

Quantitative Real-Time PCR (qRT-PCR)

Total RNA was isolated using the RNeasy kit (Qiagen, Germantown, MD) and cDNA synthesized using the First-Strand cDNA Synthesis Kit (Promega, Madison, WI). qRT-PCRs were performed using Bio-Rad SYBR Green Supermix (Bio-Rad, Hercules, CA) according to the manufacturer's instructions and analyzed using Bio-Rad Software. NPNT expression was normalized to Cdc40 and Csnk2a2 (geNormPLUS, Southampton, United Kingdom).

Table 1. Patient and Tumor Characteristics, and Risk of Death from Breast Cancer According to NPNT Positive Staining Pattern

Patient and Tumor Characteristics	NPNT Phenotype Positive Cases						All Cases[d]
	Nuclear Staining[a]	Diffuse Cytoplasmic Staining[b]	Single Cells Positive	Granular Cytoplasmic Staining[c]	Granular Cytoplasmic Staining <10%	Granular Cytoplasmic Staining ≥10%	
Number of cases (%)	385 (45.7)	424 (50.4)	129 (15.3)	116 (13.8)	60 (7.1)	56 (6.7)	842
Mean age at diagnosis (SD)	73.0 (9.7)	72.6 (9.8)	71.3 (10.4)	72.8 (9.3)	72.3 (9.2)	73.3 (9.4)	72.0 (10.4)
Stage at diagnosis (%, 95% CI)							
I	180 (44, 39-49)	200 (49, 44-54)	74 (18, 14-22)	62 (15, 12-19)	29 (7, 5-10)	33 (8, 5-11)	411 (49)
II	158 (47,42-53)	178 (53, 48-59)	42 (13, 9-16)	41 (12, 9-16)	23 (7, 4-10)	18 (5, 3-8)	333 (40)
III	26 (51, 37-65)	21 (41, 28-55)	6 (12, 3-21)	7 (14, 4-23)	5 (10, 2-18)	2 (4, 0-9)	51 (6)
IV	20 (49, 33-64)	24 (59, 43-74)	7 (17, 5-29)	6 (15, 4-26)	3 (7, 0-15)	3 (7, 0-15)	41 (5)
Lymph node status at diagnosis (%, 95% CI)							
Positive	141 (47, 42-53)	152 (51, 45-57)	39 (13, 9-17)	35 (12, 8-15)	22 (7, 4-10)	13 (4, 2-7)	297 (35)
Negative	129 (49, 43-55)	139 (53, 47-59)	48 (18, 14-23)	37 (14, 10-18)	13 (5, 2-8)	24 (9, 6-13)	264 (31)
Negative, <5 nodes[e]	30 (45, 33-58)	31 (47, 35-59)	13 (20, 10-29)	11 (17, 8-26)	7 (11, 3-18)	4 (6, 0-12)	66 (8)
Unknown	85 (40, 33-46)	102 (47, 41-54)	29 (13, 9-18)	33 (15, 11-20)	18 (8, 5-12)	15 (7, 4-10)	215 (26)
Molecular subtype (%, 95% CI)							
Luminal A	202 (50, 45-55)	191 (47, 42-52)	43 (11, 8-14)	45 (11, 8-14)	22 (5, 3-8)	23 (6, 3-8)	404 (48)
Luminal B HER2-	93 (41, 35-47)	127 (56, 49-62)	61 (27, 21-33)	36 (16, 11-21)	22 (10, 6-14)	14 (6, 3-9)	227 (27)
Luminal B HER2+	24 (38, 26-49)	44 (69, 57-80)	13 (20, 10-30)	10 (16, 7-25)	4 (6, 3-12)	6 (9, 2-17)	64 (8)
HER2 type	28 (49, 36-62)	29 (51, 38-64)	4 (7, 0-14)	11 (19, 9-30)	6 (11, 2-19)	5 (9, 1-16)	57 (7)
Five negative	12 (40, 22-58)	14 (47, 28-65)	2 (7, 0-16)	3 (10, 0-21)	2 (7, 0-16)	1 (3, 0-10)	30 (4)
Basal	26 (43, 31-56)	19 (32, 20-44)	6 (10, 2-18)	11 (18, 8-28)	4 (7, 0-13)	7 (12, 3-20)	60 (7)
Number of breast cancer deaths	154	164	50	48	29	19	331
Age-adjusted HR (95% CI)[f]	1.12 (0.90-1.39)	1.04 (0.84-1.30)	0.98 (0.72-1.32)	1.24 (0.91-1.70)	1.61 (1.10-2.37)	0.92 (0.57-1.47)	-

Abbreviations: SD: standard deviation, CI: confidence interval, HR: hazard ratio.

[a] Negative: <1% positive tumor cells, positive: ≥1% positive tumor cells.

[b] Negative: staining index 0-2, positive: staining index ≥3.

[c] <10% and ≥10% granular cytoplasmic staining combined.

[d] Regardless of NPNT expression.

[e] Negative, but less than 5 nodes examined.

[f] Adjusted for age at diagnosis in 5-year categories; reference group is patients with negative staining pattern for the respective phenotype.

xCELLigence Adhesion and Migration Assay

The xCELLigence system (ACEA Biosciences Inc, San Diego, CA) was used for RTCA of adhesion and migration according to previous reports [22–25]. For adhesion assays E-plates (Cat.: 05469830001) were coated with recombinant mouse NPNT (Cat.: 4298-NP-050, R&D Systems, Minneapolis, NE) at 0.4, 2, or 10 μg/ml for 4 hours at 37°C prior to seeding. 66cl4- and 4T1-cell variants were detached from tissue culture vessels using 0.03% EDTA, spun and washed with serum-free medium, and seeded at either 20,000 or 40,000 cells/well, respectively, in serum-free medium. Adhesion was recorded by electrical impedance every 5 minutes for 24 hours. The arbitrary unit "cell index" is a measure of impedance, and the value is dependent on the number of cells, the size and shape of the cells, and the cell attachment quality. For the RGD peptide blocking experiments, E-plates were coated with 2 μg/ml recombinant mouse NPNT and blocked with 3% BSA for 1 hour at 37°C. The 66cl4-EV cells were detached with EDTA and seeded in serum-free medium containing a scrambled control peptide (Cat.: H-3166, H-Gly-Arg-Gly-Glu-Ser-OH Trifluoroacetate) or an RGD-blocking peptide (Cat.: H-1346, H-Gly-Arg-Gly-Asp-OH) at 0.5 mg/ml (Bachem, Bubendorf, Switzerland). Adhesion was analyzed at 9 hours after seeding. Migration was performed using xCELLigence CIM plates (Cat.: 05665825001) containing 160 μl medium with 10% serum in the lower chamber and 60,000 cells (66cl4 cell variants) in serum-free medium in the upper chamber. Wells containing serum-free medium in the lower chamber were included as controls. Cell index was recorded every 5 minutes.

Western Blot Analysis

Cells were lysed in 10 mM Tris-HCl buffer, and 30 μg of sample was run on a 10% Bis-Tris gel (Thermo Fisher Scientific, Waltham, MA). Proteins were transferred to PVDF membranes and incubated with anti-V5 (CST, Danvers, MA) (1:1000), anti-ALIX (CST, Cat.: 13202S, Lot No.: 2, dilution 1:1000), anti-CHMP4B (Atlas Antibodies/Sigma, Cat.: HPA051751, Lot No.: R67106, dilution1:500), and anti-GM130 (BD Biosciences, Cat.: 610822, Lot No.: 7069938, dilution 1:500). Equal loading was confirmed using anti-GAPDH (Abcam, Cat.: ab9484, Lot No.: GR165366-3, dilution 1:5000), and antibody binding was detected using HRP-linked secondary antibodies according to manufacturer's instructions (Dako). Full length blots are shown in Supplementary Figure S3.

Soft Agar Colony Assay

A bottom layer of 0.75% agarose in α-MEM and a top layer of 0.36% agarose/α-MEM mixed with 2000 cells/well were added to each well in 12-well plates. The cells were fed with normal growth medium and left for about 2 weeks with 2-3 medium replacements. Plates were stained with 0.005% crystal violet in 2% ethanol/PBS and colonies counted from triplicate wells per cell line.

Minimal Seeding Colony Assay

Cells were seeded onto plastic (10 cells/well in 12-well plates) and left for 10 days. Medium was replaced twice during the experiment, and the cells were fixed with 6% glutaraldehyde for 30 minutes and stained with 0.1% crystal violet for 30 minutes before rigorous washing with water. Colonies were counted from triplicate wells/cell line.

Proliferation Assay

A total of 1.3×10^6 cells were seeded in 25-cm^2 flasks and counted after 24, 48, and 72 hours with triplicate measurements per condition.

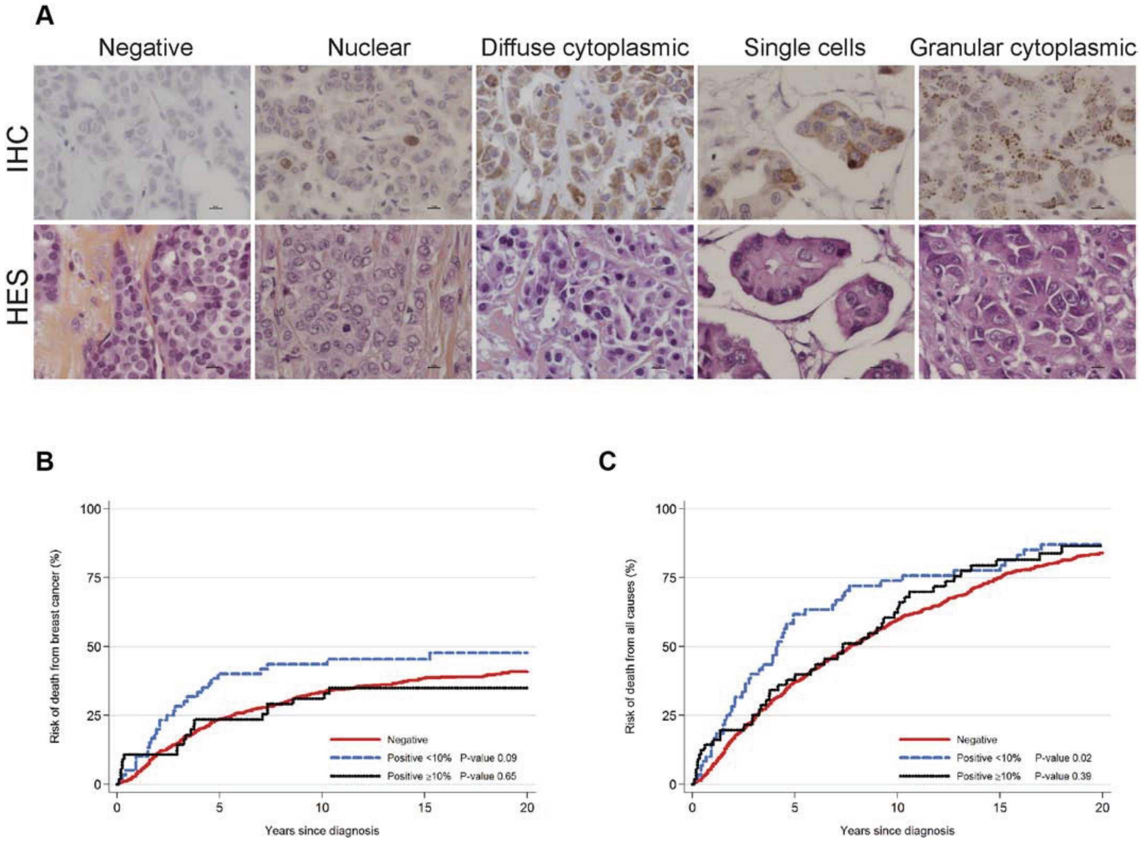

Figure 1. Granular NPNT staining patterns are associated with poor outcome in breast cancer patients. Representative images of IHC- and HES-stained TMA samples showing (A) different staining patterns: no staining, nuclear staining, diffuse cytoplasmic staining, and single cells positive or granular cytoplasmic staining using antibodies towards human NPNT (Atlas Antibodies/Sigma) imaged at 600× magnification. The images show representative cases of each staining phenotype, and the cases shown are Luminal A, Luminal A, Luminal B (HER2−), Luminal A and Luminal B (HER2−), respectively. Scale bars: 50 μm. Survival analysis showing association between no granular cytoplasmic staining (red line), 1-10% granular positive cells (thick dotted blue line), or >10% granular positive cells (solid black line) on (B) cumulative risk of death from breast cancer and (C) overall survival for all 842 patients represented in the TMAs.

RNA Scope ISH

ISH for NPNT mRNA was performed on the same mouse mammary biopsies from the transgenic MMTV-PyMT mice as the IHC staining. Custom-made probes (Mm-AF397008) and RNAscope®2.0 kit (Advanced Cell Diagnostics, Hayward, CA) were used according to the manufacturer's protocol.

Purification and Characterization of Microvesicles and Exosomes

Microvesicles and exosomes were purified using a standardized sequential ultracentrifugation protocol as described by Peinado et al. [26]. Cells were grown in 10% exosome-depleted FCS for 3 days and the cell culture supernatant harvested by centrifugation at 500*g* for 10 minutes. The microvesicle fraction (pellet) was collected by spinning at 12,000*g* for 20 minutes. Finally, the exosome fraction was collected by spinning at 100,000*g* for 70 minutes. Exosomes were washed in 20 ml PBS and pelleted again by ultracentrifugation (Beckman 70Ti rotor). Particle number of isolated microvesicles and exosomes was analyzed using the LM10-HS nanoparticle characterization system (NanoSight, Malvern Instruments Ltd, UK).

Statistical Analyses

We estimated risk of death from breast cancer according to NPNT expression, calculating cumulative incidence and with death from other causes as competing events. Risk of death from any cause was estimated using the Kaplan-Meier method. Equality between curves was assessed using Gray's test and the log-rank test, respectively. We used Cox proportional hazards models to estimate risk of death from breast cancer (censoring at death from other causes) calculating hazard ratios (HRs) with 95% confidence intervals (CIs) and adjusting for age, stage, grade, and subtype. *In vitro* experiments were evaluated in linear regression models. Indicators for each experiment were included to adjust for variation across experiments. In the animal experiments, groups were compared using two-tailed *t* tests.

Results

We showed previously that NPNT can function as a prometastatic protein in mouse breast cancer models [15]. With a well-characterized set of formalin-fixed and paraffin-embedded (FFPE) tumor samples from 842 Norwegian women diagnosed

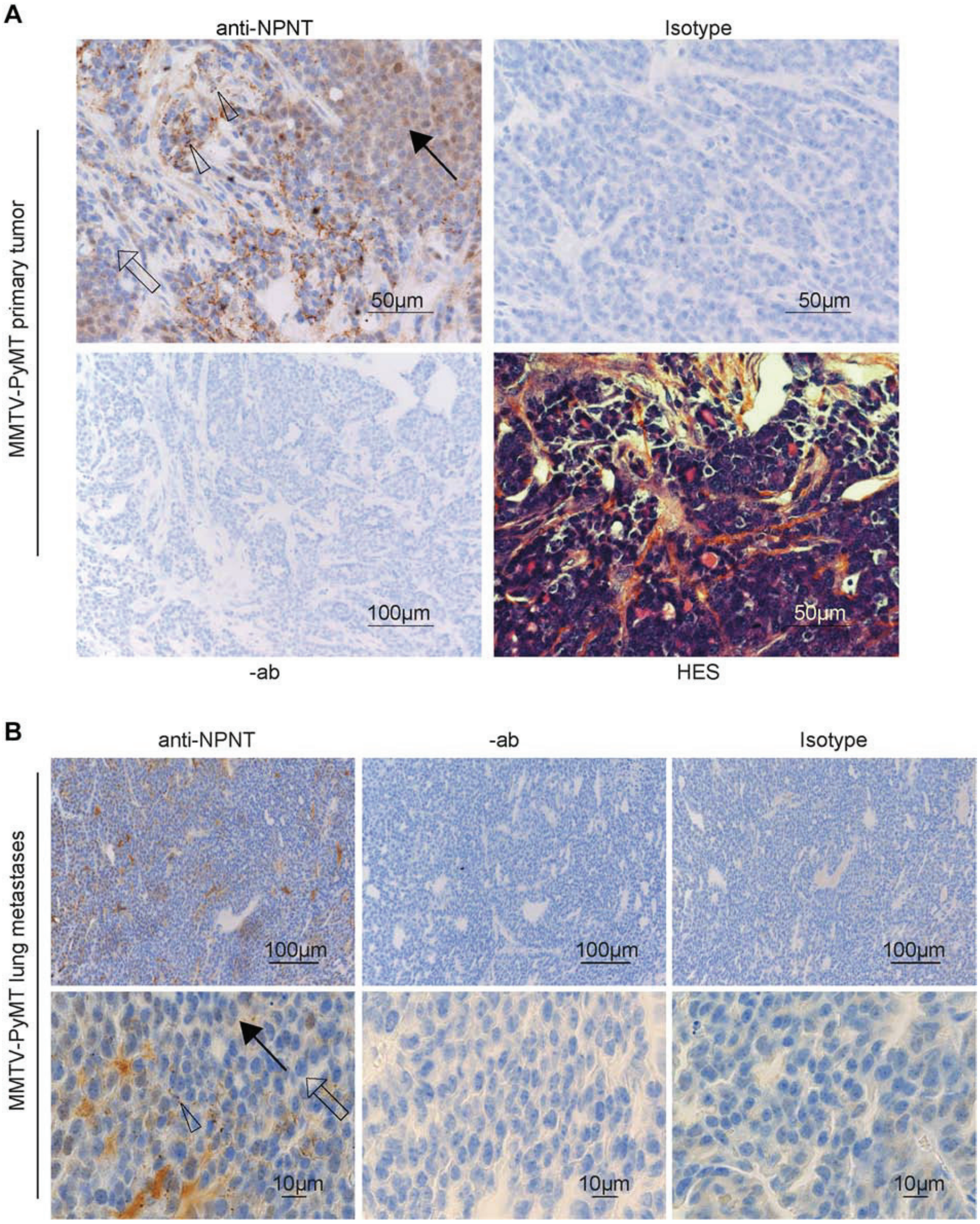

Figure 2. Phenotypically different patterns of NPNT staining in MMTV-PyMT transgenic mouse tumors. (A) Representative images of IHC- and HES-stained MMTV-PyMT primary tumors. NPNT was detected using antibodies towards mouse NPNT (Atlas Antibodies/Sigma). Figure shows antibody-stained sections, IgG Isotype control, control without antibodies (-ab), and HES-stained section from the same region. (B) Representative images of IHC-stained MMTV-PyMT lung metastases. Arrows indicate no staining (open arrow), diffuse cytoplasmic staining (filled arrow), and granular staining (triangle). Images are representative of a series of samples from nine mice.

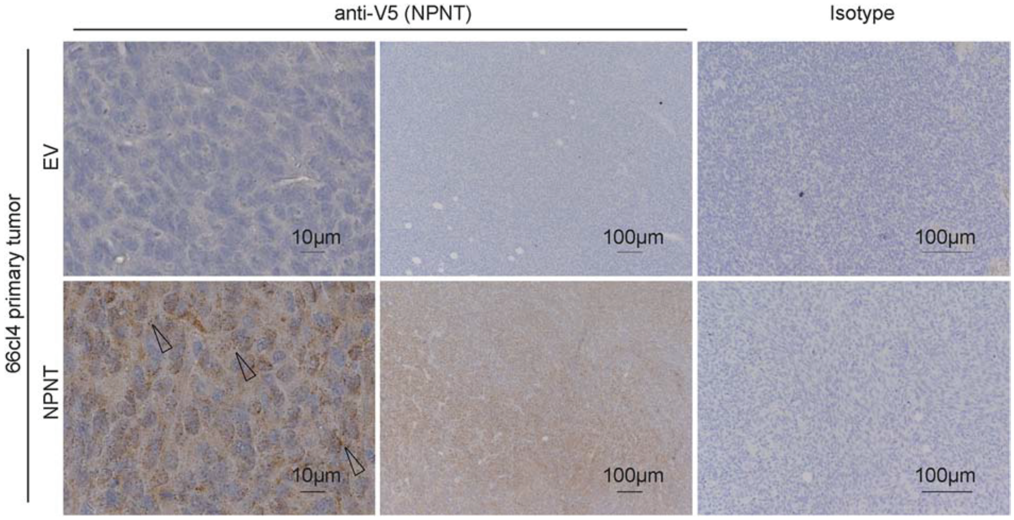

Figure 3. NPNT is located in granules in 66cl4-NPNT primary tumors. Representative images of IHC-stained 66cl4-EV and 66cl4-NPNT primary tumors using V5-specific antibodies (Cell Signaling Technology). The left and middle panels show antibody-stained sections, whereas the right panels show rabbit IgG Isotype staining controls. Granular staining is indicated with open triangles. Images are representative of a series of samples from five mice.

with invasive breast cancer between 1961 and 2008, [17] we assessed NPNT protein expression using IHC on TMAs. Using a standardized protocol developed for this study, we found positive NPNT staining in 596 out of 842 cases (70.8%). Interestingly, although NPNT has been shown previously to be an extracellular matrix protein, [8–10] in this study, we identified intracellular staining that we grouped into four different patterns: nuclear staining; diffuse positive cytoplasmic staining; scattered single cells with strong cytoplasmic staining and granular cytoplasmic staining (Table 1 and Figure 1*A*). Patients with 1-10% granular staining had a poorer prognosis than those with no granular staining, evaluating both risk of death from breast cancer (age-adjusted hazard ratio (HR) 1.61, 95% confidence interval (CI) 1.10-2.37, Table 1) and overall survival (Figure 1, *B* and *C*). In contrast, reduced survival was not found among patients with high (≥10%) granular NPNT staining (HR 0.92, 95% CI 0.57-1.47). In separate analyses of the different molecular subtypes, the association between the presence of any NPNT granular staining and prognosis was strongest for the Luminal A subtype (HR 1.70, 95% CI 0.99-2.90, *P*=.054) (Supplementary Table S1). The remaining staining patterns showed no significant association with prognosis. Adjustment for tumor stage and grade at diagnosis had little influence on the estimates. Taken together, this comprehensive analysis demonstrates for the first time that NPNT is localized intracellularly in a large number of human breast tumors and that low levels of intracellular granular staining may be associated with poor prognosis.

To investigate the presence and appearance of NPNT distribution in mouse breast tumors, we utilized a well-established transgenic mouse model of breast cancer, the MMTV-PyMT model [21,27]. NPNT was expressed at higher levels in isolated primary tumor cells compared to normal primary mammary epithelial cells from wild-type animals (Supplementary Figure S4*A*), and ISH analyses also confirmed that NPNT is exclusively expressed by the tumor cells (Supplementary Figure S4*B*). NPNT protein was present in the tumor cells, with phenotypically different patterns including diffuse cytoplasmic or granular cytoplasmic distribution (Figure 2*A*). Protein localization was tumor-cell-specific with limited staining in the extratumoral stromal tissue. Approximately 10% of the tumor cells had a granular staining pattern of NPNT similar to that found in the human tumors. The granular NPNT staining pattern has also been shown to be present in mouse tibias [28]. Direct comparison between NPNT and the ECM-proteins Collagen V and Fibronectin in ECM-rich areas of MMTV-PyMT tumors showed some signs of extracellular presence of NPNT; however, this was not the major site of localization (Supplementary Figure S2*B*). We investigated NPNT expression patterns in metastases in lung tissue from the MMTV-PyMT animals and found that the tumor cells were diffusely positive in the cytoplasm in the tumor periphery with a few granular-positive tumor cells similar to that of the primary tumors (Figure 2*B*). Taken together, these findings identify MMTV-PyMT–driven tumors as a potential model for further studies on the role of granular NPNT in breast cancer progression and metastasis.

To investigate the *in vivo* function of NPNT, we expressed a V5-tagged NPNT construct in weakly metastatic mouse 66cl4 breast cancer cells that express low endogenous levels of NPNT. End-stage orthotopic tumors were then stained by IHC using an anti-V5 antibody. The 66cl4-NPNT primary tumors revealed both diffuse and granular cytoplasmic NPNT staining similar to the human and MMTV-PyMT tumors (Figure 3). Consistent with our previous finding that reducing the initially high levels of NPNT in the highly metastatic cell line 4T1.2 does not affect primary tumor growth [15], there were no significant differences in tumor volume or weight at endpoint between the 66cl4-NPNT and 66cl4-EV tumors (Supplementary Figure S5, *A* and *B*). Measurement of RTB in spine and lung [15] showed that increased NPNT expression was not sufficient to promote spontaneous metastasis of 66cl4 mammary tumors (Supplementary Figure S5, *C* and *D*). Taken together, these findings demonstrated that the NPNT staining patterns in the human samples could also be observed in the mouse tumors. We suggest that NPNT may be more important for metastatic dissemination than primary tumor growth.

Transcript levels of NPNT are correlated with the metastatic propensity of cells in the 4T1 model, with negligible levels in the low and weakly metastatic 67NR, 168FARN, and 66cl4 cells and higher levels in the more metastatic 4TO7 and 4T1 cells (Supplementary Figure S6*A*). Similarly, IHC staining of orthotopic primary tumors showed some weak cytoplasmic NPNT staining in 67NR tumors and slightly stronger NPNT staining in patches in 4T1 tumors

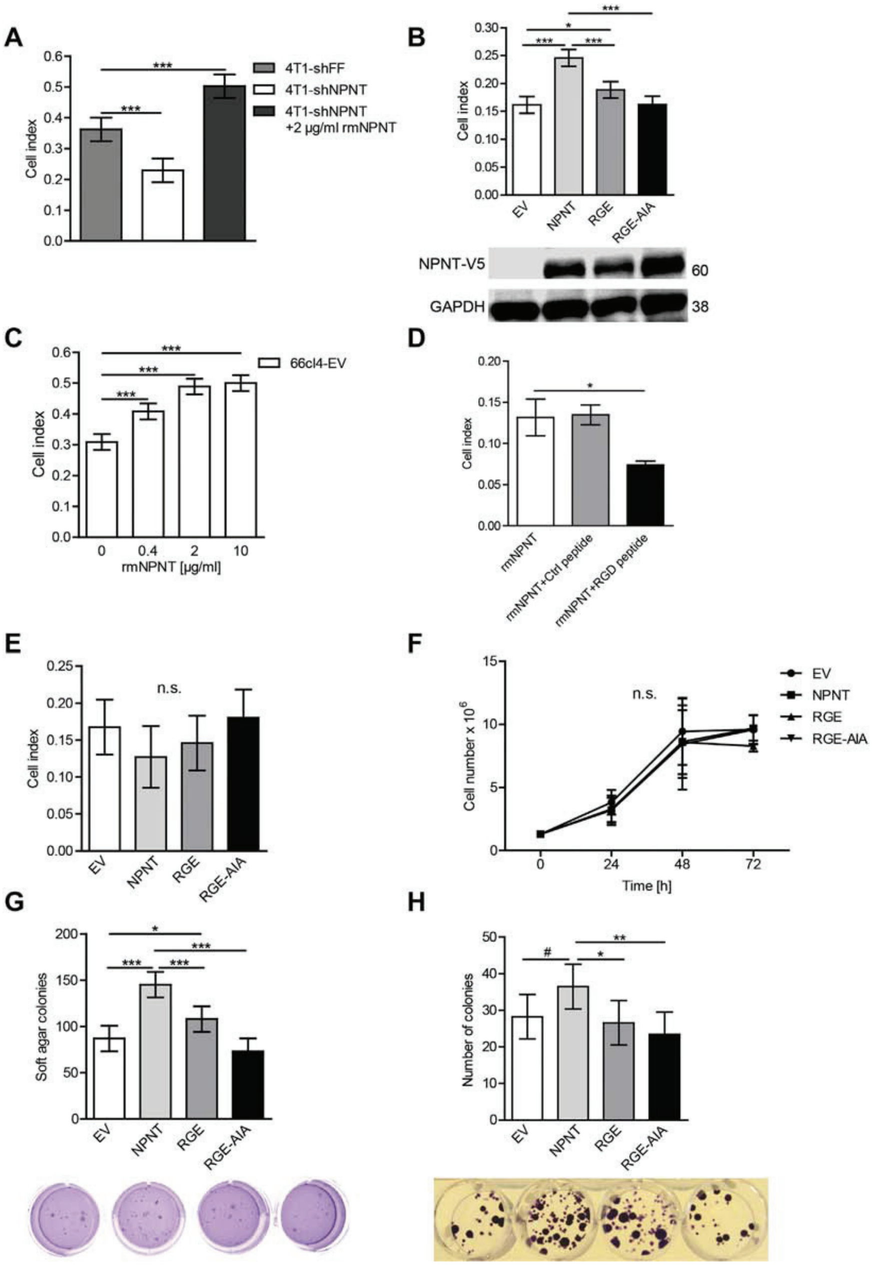

(Supplementary Figure S6*B*). Granular NPNT staining was not observed in these tissue samples. Using 4T1 cells with high endogenous NPNT levels, we created clones with stable knockdown of NPNT using shRNAs (Supplementary Figure S6*C*). The 4T1-shNPNT cell line displayed a significantly reduced ability to attach to uncoated wells compared to the 4T1-shFF (control) cells, but adhesion could be rescued by addition of 2 μg/ml recombinant mouse NPNT (rmNPNT) (Figure 4*A*). The 4T1-shFF and 4T1-shNPNT lines both showed a dose-dependent increase in adhesion to rmNPNT-coated plates 1 hour after seeding (Supplementary Figure S6*D*).

Previous research has demonstrated that binding of NPNT to its receptor integrin α8β1 is mediated through both the high-affinity RGD sequence and an additional downstream enhancer site (EIE) [29,30]. An adhesion assay of 66cl4 cells with enhanced expression of either native NPNT or NPNT mutants (RGE or RGE-AIA) showed that while exogenous NPNT enhanced adhesion, disruption of the RGD-site alone or of both the RGD and the EIE sites significantly reduced adhesion (Figure 4*B*). Increased NPNT protein expression was confirmed by Western blot. The 66cl4-EV cells showed a dose-dependent increase in adhesion to plates coated with rmNPNT (Figure 4*C*), and this adhesion was reduced in the presence of a RGD-blocking peptide, demonstrating the involvement of RGD-binding integrins (Figure 4*D*). There was no impact on either migration or proliferation upon NPNT overexpression (Figure 4, *E* and *F*). A soft agar colony forming assay showed that the 66cl4-NPNT cells exhibited a significantly increased capacity to grow in an anchorage-independent manner (Figure 4*G*). This increase was abolished when both RGD and EIE were mutated. Furthermore, using a minimal density seeding assay with 10 cells per well, we observed that cells expressing NPNT had a tendency towards increased ability to grow colonies from single cells (P=.064) (Figure 4*H*). Again, this increase was reduced when both RGD and EIE were mutated. Taken together, these *in vitro* assays indicate that NPNT is involved in adhesion and anchorage-independent growth, implying a role for NPNT in colony formation at the secondary site.

The 66cl4 tumor has low spontaneous metastatic capacity, and we have found that expression of NPNT is not sufficient to increase spontaneous metastasis. However, it is possible that NPNT can influence the ability of tumor cells to lodge in the lung and grow into metastatic lesions. To address this, we inoculated mice with tumor cells via the tail vein and measured subsequent colonization of the lung. We found that NPNT does promote lung colonization and that this is mediated via the RGD and EIE sites as shown by both the increased lung weight and lung tumor burden in mice injected with cells expressing wild-type NPNT compared to the empty vector (EV) cells (Figure 5*A* and *B*). There was no significant difference between cells expressing wild-type NPNT and the RGE mutant, but the increased colonization capability was completely abolished in the double mutant, demonstrating the importance of the enhancer EIE site in the ability to colonize the lung. Images of representative lungs from each group show that the increased lung weight (Figure 5*A*) and relative tumor burden (RTB, Figure 5*B*) were caused by an increased number of metastatic lesions and not just an increase in size of the colonies (Figure 5*C*). In summary, this experimental metastasis assay showed that NPNT promotes lung colonization via the enhancer (EIE) sites, possibly aided by the RGD motif, and confirms an *in vivo* effect of the two motifs responsible for integrin interaction. IHC staining of lung metastases from the lung colonization assay showed that also the tumor cells in the metastatic lesions displayed a granular pattern of NPNT staining (Figure 5*D*).

Cancer cell extracellular vesicles and their role in angiogenesis, tumor progression, and metastasis is of increasing interest in cancer research [31–33], and NPNT has been detected previously in proteomic characterizations of isolated exosomes from human ductal saliva and colorectal cancer cells [34,35]. The granular staining patterns observed in the human samples, MMTV-PyMT tissues, 66cl4-NPNT primary tumors, and metastases prompted us to speculate that these granular structures could be multivesicular bodies containing exosomes. To address this, we isolated both exosomes and microvesicles from 66cl4-NPNT cells using well-established protocols [26]. ALIX and CHMP4B are commonly used markers for exosome-containing multivesicular bodies [35–37]. By Western blot, we show that NPNT co-purified with ALIX and CHMP4B in extracellular vesicles released from cells expressing both wild-type and mutant NPNT (Figure 6*A*), hinting that the localization of NPNT to microvesicles and exosomes is not integrin-dependent. In accordance with the recommended guidelines for extracellular vesicle characterization [38], we

Figure 4. NPNT increases adhesion and anchorage-independent growth. (A) Adhesion of 4T1-shFF and 4T1-shNPNT cells in an xCELLigence adhesion assay. The figure shows rescue of adhesion in 4T1-shNPNT cells in plates coated with 2 μg/ml recombinant mouse NPNT (rmNPNT). 4T1-shFF cells express a nontargeting control shRNA. Data are presented as mean cell index ± 95% CI from two experiments (n=4), 1 hour after seeding. (B) xCELLigence adhesion assay of 66cl4-cells expressing either EV or NPNT wild-type, NPNT RGE, or NPNT RGE-AIA mutants in uncoated plates. Data are presented as mean cell index ± 95%CI from four experiments (n=3-12), 1 hour after seeding. Lower panel shows Western blot of cell lysates confirming NPNT overexpression detected with the anti-V5 antibody. The image is cropped to display only relevant bands, but the full blot is shown in Supplementary Figure S3*A*. (C) Adhesion assay of 66cl4-EV cells in plates coated with rmNPNT at 0.4 μg/ml, 2 μg/ml, or 10 μg/ml prior to seeding. Data are presented as mean cell index ± 95% CI from two experiments (n=4), 1 hour after seeding. (D) Adhesion assay of 66cl4-EV cells in rmNPNT-coated wells in presence of either scrambled peptide or RGD-blocking peptide. Data are presented as mean cell index±SEM from three experiments with n=2 in each experiment. (E) Migration assay in xCELLigence CIM-plates using 66cl4-cells expressing either EV or NPNT wild-type, NPNT RGE, or NPNT RGE-AIA mutants. Migration towards 10% FCS was recorded every 5 minutes, and data are presented as mean cell index ± 95%CI at 12 hours from 5 individual experiments with n=2-4 technical replicates in each experiment. (F) Cell proliferation assay with 1.3×10^6 cells per 25-cm^2 flask. Cells were harvested and counted after 24, 48, and 72 hours, and data are shown as mean ± SD from three individual experiments. (G) Soft agar assay for anchorage-independent growth of 66cl4-cells expressing EV, NPNT, NPNT RGE, or NPNT RGE-AIA. Two thousand cells/well in 12-well plates were seeded in 0.36% agarose/α-MEM medium containing 10% FCS and grown for 10 days. Data presented as mean ± 95% CI from 3 individual experiments (n=3-9). (H) Clonogenic cell survival assay with minimal seeding density of 66cl4-cells expressing EV, NPNT, NPNT RGE, or NPNT RGE-AIA. A total of 10 cells/well were seeded in 12-well plates and grown as single colonies for 10 days. Graph shows number of colonies as mean ±95% CI from five individual experiments with n=3-9 replicates per experiment. # indicates P=.064 when comparing EV-cells with NPNT-expressing cells. All *in vitro* data except the qRT-PCR and the proliferation assay were analyzed with linear regression models. ***P<.0001, **P<.005, *P<.05.

show that the isolated vesicles were negative for the Golgi marker GM130. Immunofluorescence staining of 66cl4-NPNT lung metastases and MMTV-PyMT tumor tissues confirmed colocalization of NPNT with CHMP4B, leading us to propose that the cytoplasmic granular structures could be NPNT-containing multivesicular bodies (Figure 6, *B* and *C*). In conclusion, we have demonstrated that NPNT is present in extracellular vesicles and that NPNT facilitates colonization at the metastatic site via its integrin-binding sites.

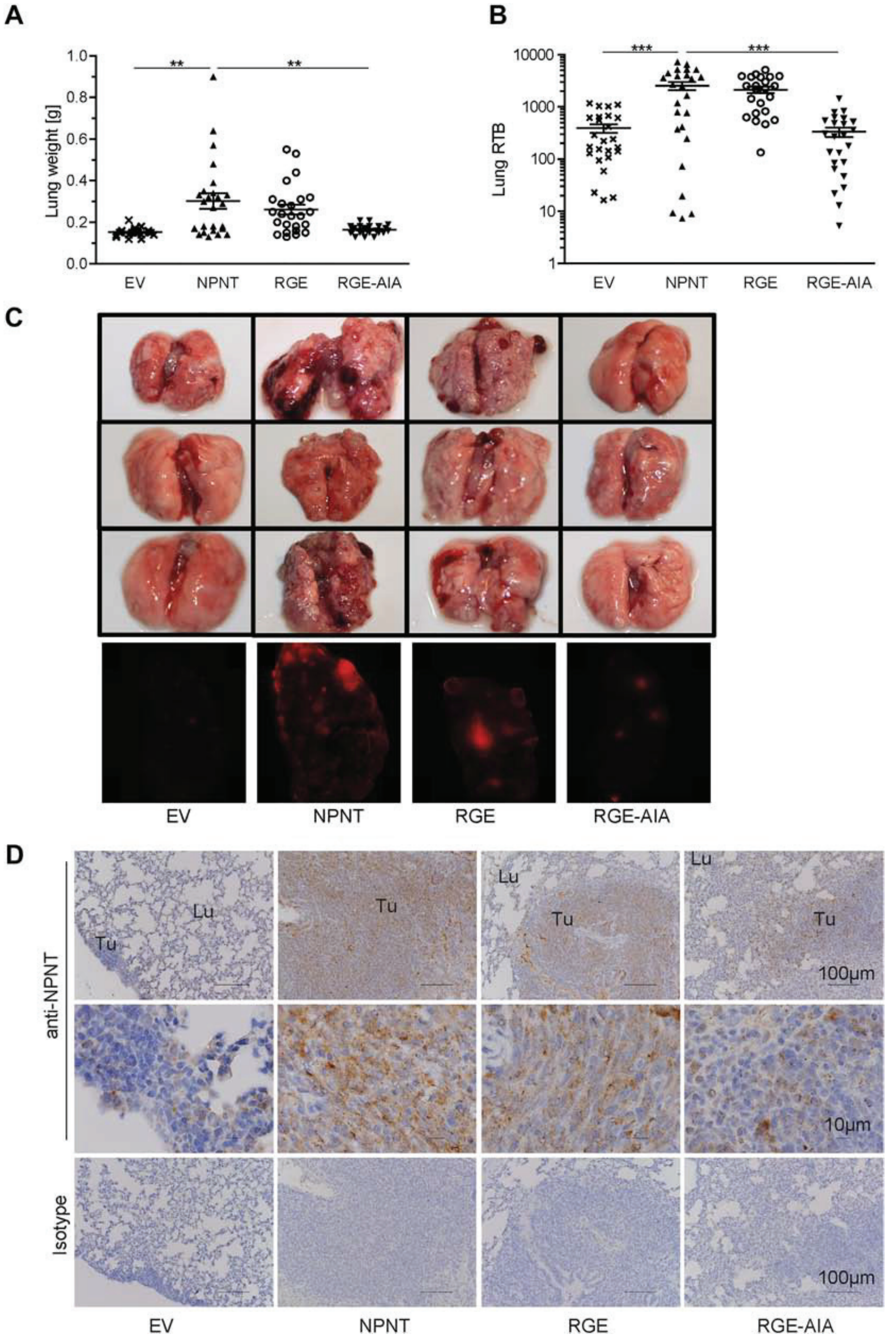

Discussion

We found positive NPNT staining in the majority of patient samples (70.8%), demonstrating that NPNT is present in human breast tumors. Although NPNT has been shown by others to be an extracellular matrix protein, we found that it is also localized intracellularly in tumor cells. Interestingly, in our patients' tumors, granular intracellular staining in less than 10% of the cells was associated with decreased survival. In addition, we showed the presence of several phenotypically different intracellular staining patterns, including diffuse cytoplasmic and nuclear NPNT staining; however, neither of these was correlated with survival. This may reflect a preference of the antibody to recognize the core protein and not the highly glycosylated secreted forms of the protein when analyzed by IHC.

We did not observe any association between granular NPNT staining and lymph node metastasis in our patient samples. The total number of cases with known metastases was 297. However, lymph node status was not reported in 215 (25.5%) cases, and the granular staining pattern was observed in only 116 (13.8%) cases. Our analyses showed an association between granular staining patterns (<10% positive tumor cells) and poor outcome in patients with luminal A subtype (P=.054), but since numbers were lower for the other subtypes, statistical power was limited in these subgroups.

The nonlinear U-shaped correlation between granular cytoplasmic staining of NPNT and survival is similar to that shown for various tumor markers in glioma [39], prostate [40,41], colorectal [42,43], and pancreatic cancer [44,45]. In addition, a recent study reported a U-shaped correlation between HER2 protein expression and overall survival of breast cancer patients treated with the tyrosine kinase inhibitor lapatinib [46]. The explanation for this phenomenon is unclear in most cases. Similarly, we identified nuclear staining of NPNT in a proportion of the patient samples. This has also been reported in human MCF-7 breast cancer cells on the Human Protein Atlas website available from www.proteinatlas.org [47]. The possible function of NPNT in the nucleus is unknown and should be followed up in future studies. Taken together, this is the first extensive characterization of NPNT expression in a large cohort of breast cancer patients, and although the results need to be verified by similar studies of other cohorts, they warrant further investigation into the role of NPNT in breast cancer.

We have shown previously that reduced NPNT expression in the highly metastatic 4T1.2 cells caused a significant reduction in metastatic tumor burden in lung, spine, and kidneys, [15], and in the present study, we show that enhanced expression of NPNT in low-metastatic 66cl4 cells increased the colonization capacity in the lungs. Our lung colonization data clearly demonstrated that 66cl4 cells expressing NPNT have a significantly increased capability to seed and grow in the lungs in an integrin-dependent manner. Our results are supported by findings from Sánches-Cortés et al. showing that the RGD and the FEI or EIE sites function synergistically and are both important for the interaction between NPNT and its integrin receptor [29]. Previous reports showed that the main receptor for NPNT is integrin α8β1 [8,10]. However, we cannot exclude the possibility that NPNT might also interact with other receptors, for example, integrin αVβ3, on the lung endothelium during the metastatic process [19]. Our findings will prompt further studies on the role of NPNT in breast cancer using experimental models. The IHC of the MMTV-PyMT tissues revealed staining patterns similar to those in human cancers, suggesting that this might be a suitable model for further studies.

NPNT has been shown previously to be involved in breast cancer metastasis in mice [15,16]. Although we were unable to show a link between NPNT expression and metastasis in our patient material, the results from the experimental models showed that tumor cells expressing NPNT were more prone to establish colonies in lungs and to display increased adhesion and anchorage-independent growth *in vitro* in an integrin-dependent manner.

The role of extracellular vesicles in tumor progression and metastasis is an emerging topic in cancer research, and exosomes have been shown to facilitate increased proliferation, evasion of apoptosis, stimulation of migration, invasion, and metastasis in addition to resistance to therapy (reviewed in [48–51]). Furthermore, the packaging of exosomal content is likely to be specific since the exosomal content influences organotropic dissemination [52]. The data presented here suggest for the first time that NPNT may be localized in mouse breast cancer cell–derived exosomes, and our *in vivo* data revealed that there might be a link between NPNT-containing exosomes and increased metastatic capacity.

In conclusion, NPNT was originally described as an extracellular matrix protein [8,10], but the findings from mouse tumor tissues presented here show intracellular NPNT staining in primary tumors both diffusely in the cytoplasm and in exosome-containing multivesicular bodies. We found that granular intracellular staining in less than 10 % of tumor cells was associated with decreased survival in a large cohort of breast cancer patients and that the integrin-binding site was important for lung colonization of 66cl4 cells in our animal model. There are clearly several mechanisms of action for NPNT in promoting breast cancer, warranting further investigation into NPNT as a potential prognostic marker and a possible future target for therapy in a subgroup of breast cancer patients.

Supplementary data to this article can be found online at https://doi.org/10.1016/j.neo.2018.02.008.

Acknowledgements and Funding

The mouse cell lines 67NR, 168FARN, 66cl4, 4TO7, and 4T1 were kindly provided by Dr. Fred Miller. We thank Dr. Naoko Morimura

Figure 5. NPNT promotes colonization of the lung via its integrin-binding motifs. 66cl4-cells expressing EV, NPNT wild-type, NPNT RGE, or NPNT RGE-AIA mutants were injected into the lateral tail vein to assess tumor cell colonization of the lung using 24-25 mice per group. (A) Lungs were collected after 3 weeks and weighed (mean±SD). $^{**}P<.0005$ when analyzed by two-tailed t test. The data have been merged from two separate experiments using 14-15 and 9-10 mice per group. (B) RTB assay using genomic DNA from whole lung lysates as template (n=24-25). Graphs show mean RTB ± SD, $^{***}P<.0001$ when analyzed by two-tailed t-test. (C) Images of three representative lungs from each group of mice. Macroscopic view of representative lung lobes imaged to detect mCherry positive tumor cells (bottom row). The tissues were imaged using the EVOS FL Auto Cell Imaging System with an inverted microscope and a Sony ICX445 monochrome CCD camera and visualized using 4× objectives. Each image was created using a stitch of several images to cover the entire lung lobe. (D) Representative images of IHC-stained lungs from mice using NPNT antibodies (Atlas Antibodies/Sigma). The top and middle rows show antibody-stained sections at two different magnifications, whereas the lower row shows rabbit IgG isotype staining controls. Scale bars: top and lower row: 100 μm, middle row: 10 μm. Tu: indicates tumor area, Lu: indicates normal lung tissue. Images are representative of a series of samples from five mice.

for the pcDNA3-POEM-Fc vector. We thank Knut Sverre Grøn, Shalini Vasudev Rao, and Ulrike Neckmann for skillful technical assistance with animal experiments; Borgny Ytterhus, Bjørn Munkvold, and Negar Shahini for valuable help with histology; and Hector Peinado, Lucia Robado de Lope, and Marta Hergueta-Redondo for collaboration regarding exosome isolation protocols. The study received funding from the Research Council of Norway [grant number 197282], The Liaison Committee between

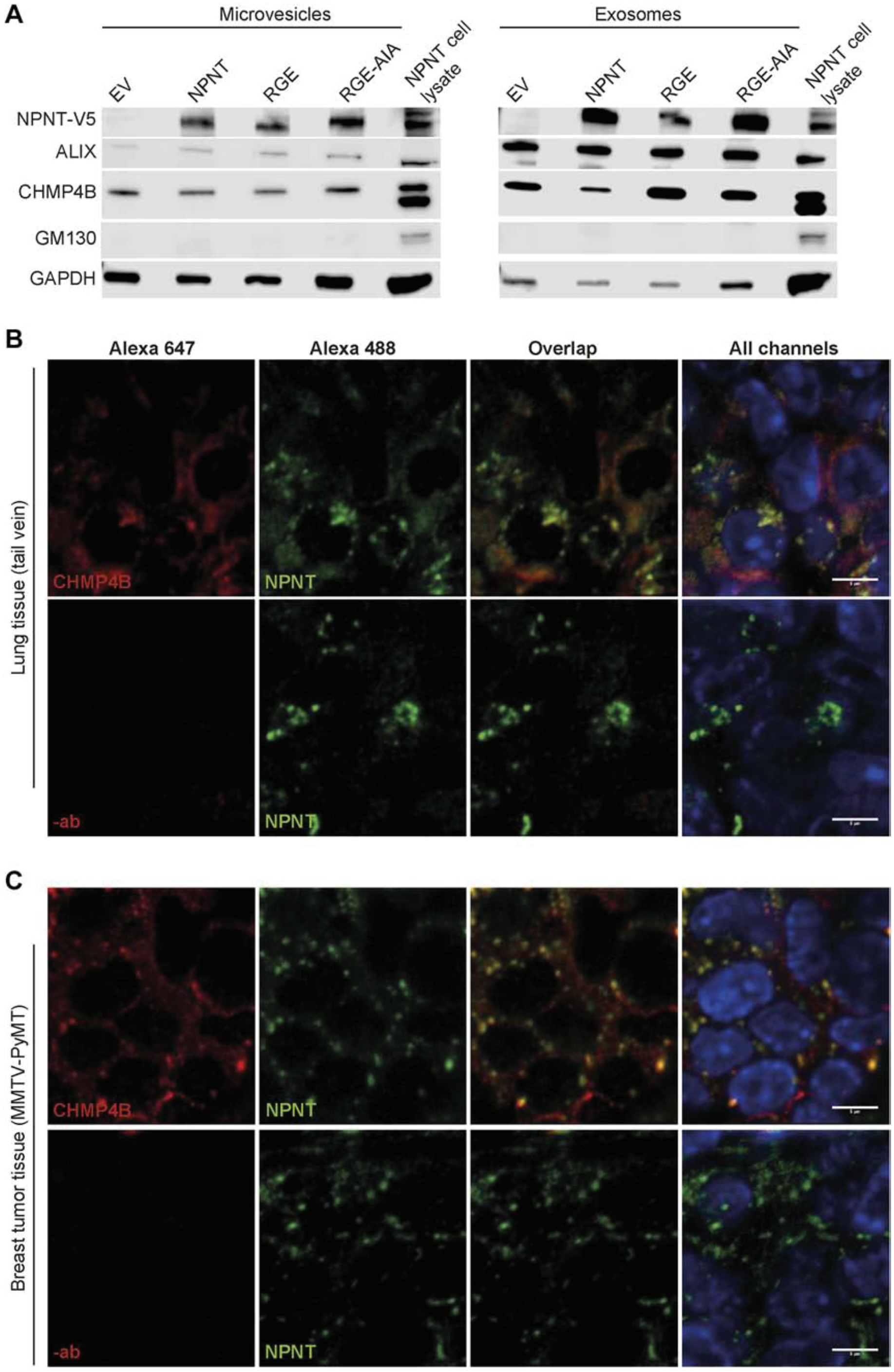

the Central Norway Regional Health Authority and the Norwegian University of Science and Technology (NTNU) [grant numbers 46056732, 46055600, and 46077600], the Cancer Fund at St. Olav's Hospital in Trondheim, The Northern Norway Regional Health Authority (Helse Nord RHF), UiT-The Arctic University of Norway [grant number SFP1232-15], and The National Cancer Institute at NIH. We acknowledge fellowships from the National Breast Cancer Foundation of Australia to Richard Redvers and Robin Anderson. The Research Council of Norway is acknowledged for the support to the Norwegian Micro- and Nano-Fabrication Facility, NorFab [grant number 245963/F50].

Author contributions

T.S.S., R.O.H., R.L.A., and G.S. conceived the project. T.S.S., J.T., R.P.R., A.M.B., R.L.A., and G.S. designed the experiments. T.S.S., J.T., R.P.R., S.N.M., B.L.E., J.M.L., J.D., and G.S. conducted experiments. T.S.S., J.T., M.V., A.M.B., S.O., S.L., and G.S. performed data analysis. T.S.S., M.V., S.N.M., A.M.B., R.O.H, R.L.A., and G.S. wrote and critically appraised the manuscript. All authors have read and revised the manuscript.

Conflicts of Interest

The authors declare that they have no competing interests.

References

[1] Jemal A, Bray F, Center MM, Ferlay J, Ward E, and Forman D (2011). Global cancer statistics. *CA Cancer J Clin* **61**, 69–90.

[2] Kast K, Link T, Friedrich K, Petzold A, Niedostatek A, Schoffer O, Werner C, Klug SJ, Werner A, and Gatzweiler A, et al (2015). Impact of breast cancer subtypes and patterns of metastasis on outcome. *Breast Cancer Res Treat* **150**, 621–629.

[3] Chambers AF, Groom AC, and MacDonald IC (2002). Dissemination and growth of cancer cells in metastatic sites. *Nat Rev* **2**, 563–572.

[4] Toss A and Cristofanilli M (2015). Molecular characterization and targeted therapeutic approaches in breast cancer. *Breast Cancer Res* **17**, 60.

[5] Perou CM, Sorlie T, Eisen MB, van de Rijn M, Jeffrey SS, Rees CA, Pollack JR, Ross DT, Johnsen H, and Akslen LA, et al (2000). Molecular portraits of human breast tumours. *Nature* **406**, 747–752.

[6] Sorlie T, Perou CM, Tibshirani R, Aas T, Geisler S, Johnsen H, Hastie T, Eisen MB, van de Rijn M, and Jeffrey SS, et al (2001). Gene expression patterns of breast carcinomas distinguish tumor subclasses with clinical implications. *Proc Natl Acad Sci U S A* **98**, 10869–10874.

[7] Esposito A, Criscitiello C, and Curigliano G (2015). Highlights from the 14(th) St Gallen International Breast Cancer Conference 2015 in Vienna: dealing with classification, prognostication, and prediction refinement to personalize the treatment of patients with early breast cancer. *Ecancermedicalscience* **9**, 518.

[8] Brandenberger R, Schmidt A, Linton J, Wang D, Backus C, Denda S, Muller U, and Reichardt LF (2001). Identification and characterization of a novel extracellular matrix protein nephronectin that is associated with integrin alpha8beta1 in the embryonic kidney. *J Cell Biol* **154**, 447–458.

[9] Linton JM, Martin GR, and Reichardt LF (2007). The ECM protein nephronectin promotes kidney development via integrin alpha8beta1-mediated stimulation of Gdnf expression. *Development* **134**, 2501–2509.

[10] Morimura N, Tezuka Y, Watanabe N, Yasuda M, Miyatani S, Hozumi N, and Tezuka Ki K (2001). Molecular cloning of POEM: a novel adhesion molecule that interacts with alpha8beta1 integrin. *J Biol Chem* **276**, 42172–42181.

[11] Fujiwara H, Ferreira M, Donati G, Marciano DK, Linton JM, Sato Y, Hartner A, Sekiguchi K, Reichardt LF, and Watt FM (2011). The basement membrane of hair follicle stem cells is a muscle cell niche. *Cell* **144**, 577–589.

[12] Toyoshima KE, Asakawa K, Ishibashi N, Toki H, Ogawa M, Hasegawa T, Irie T, Tachikawa T, Sato A, and Takeda A, et al (2012). Fully functional hair follicle regeneration through the rearrangement of stem cells and their niches. *Nat Commun* **3**, 784.

[13] Patra C, Diehl F, Ferrazzi F, van Amerongen MJ, Novoyatleva T, Schaefer L, Muhlfeld C, Jungblut B, and Engel FB (2011). Nephronectin regulates atrioventricular canal differentiation via Bmp4-Has2 signaling in zebrafish. *Development* **138**, 4499–4509.

[14] Patra C, Ricciardi F, and Engel FB (2012). The functional properties of nephronectin: an adhesion molecule for cardiac tissue engineering. *Biomaterials* **33**, 4327–4335.

[15] Eckhardt BL, Parker BS, van Laar RK, Restall CM, Natoli AL, Tavaria MD, Stanley KL, Sloan EK, Moseley JM, and Anderson RL (2005). Genomic analysis of a spontaneous model of breast cancer metastasis to bone reveals a role for the extracellular matrix. *Mol Cancer Res* **3**, 1–13.

[16] Borowsky AD, Namba R, Young LJ, Hunter KW, Hodgson JG, Tepper CG, McGoldrick ET, Muller WJ, Cardiff RD, and Gregg JP (2005). Syngeneic mouse mammary carcinoma cell lines: two closely related cell lines with divergent metastatic behavior. *Clin Exp Metastasis* **22**, 47–59.

[17] Engstrom MJ, Opdahl S, Hagen AI, Romundstad PR, Akslen LA, Haugen OA, Vatten LJ, and Bofin AM (2013). Molecular subtypes, histopathological grade and survival in a historic cohort of breast cancer patients. *Breast Cancer Res Treat* **140**, 463–473.

[18] Aslakson CJ and Miller FR (1992). Selective events in the metastatic process defined by analysis of the sequential dissemination of subpopulations of a mouse mammary tumor. *Cancer Res* **52**, 1399–1405.

[19] Sloan EK, Pouliot N, Stanley KL, Chia J, Moseley JM, Hards DK, and Anderson RL (2006). Tumor-specific expression of alphavbeta3 integrin promotes spontaneous metastasis of breast cancer to bone. *Breast Cancer Res* **8**, R20.

[20] Carter RZ, Micocci KC, Natoli A, Redvers RP, Paquet-Fifield S, Martin AC, Denoyer D, Ling X, Kim SH, and Tomasin R, et al (2015). Tumour but not stromal expression of beta3 integrin is essential, and is required early, for spontaneous dissemination of bone-metastatic breast cancer. *J Pathol* **235**, 760–772.

[21] Guy CT, Cardiff RD, and Muller WJ (1992). Induction of mammary tumors by expression of polyomavirus middle T oncogene: a transgenic mouse model for metastatic disease. *Mol Cell Biol* **12**, 954–961.

[22] Selvik LK, Rao S, Steigedal TS, Haltbakk I, Misund K, Bruland T, Prestvik WS, Laegreid A, and Thommesen L (2014). Salt-inducible kinase 1 (SIK1) is induced by gastrin and inhibits migration of gastric adenocarcinoma cells. *PLoS One* **9**e112485.

[23] Steigedal TS, Prestvik WS, Selvik LK, Fjeldbo CS, Bruland T, Laegreid A, and Thommesen L (2013). Gastrin-induced proliferation involves MEK partner 1 (MP1). *In Vitro Cell Dev Biol Anim* **49**, 162–169.

[24] Scrace S, O'Neill E, Hammond EM, and Pires IM (2013). Use of the xCELLigence system for real-time analysis of changes in cellular motility and adhesion in physiological conditions. *Methods Mol Biol* **1046**, 295–306.

[25] Hamidi H, Lilja J, and Ivaska J (2017). Using xCELLigence RTCA Instrument to Measure Cell Adhesion. *Bio Protoc* 7.

[26] Peinado H, Aleckovic M, Lavotshkin S, Matei I, Costa-Silva B, Moreno-Bueno G, Hergueta-Redondo M, Williams C, Garcia-Santos G, and Ghajar C, et al (2012). Melanoma exosomes educate bone marrow progenitor cells toward a pro-metastatic phenotype through MET. *Nat Med* **18**, 883–891.

Figure 6. NPNT is localized in extracellular vesicles. (A) Western blot of isolated microvesicles and exosomes from 66cl4-cells expressing EV, NPNT wild-type, NPNT RGE, or NPNT RGE-AIA detected with anti-V5 antibodies (CST). ALIX and CHMP4B were used as markers for microvesicles and exosomes, GM130 as a negative control and GAPDH for normalization control. Whole-cell lysates of 66cl4-NPNT cells were included as control. The images are cropped to display only relevant bands. Full-length blots are shown in Supplementary Figure S3. IF showing colocalization between the exosomal marker CHMP4B and NPNT detected with anti-CHMP4B and NPNT antibodies (Abnova) and visualized with Alexa Fluor 647 and Alexa Fluor 488 secondary antibodies, respectively, of (B) lung samples from *in vivo* lung colonization assay and (C) MMTV-PyMT mammary tumor samples. Images are representative of a series from five mice. Nuclei were stained with Hoechst. -ab reflects a control with no primary antibody. Scale bar; 5 μm

[27] Lin EY, Jones JG, Li P, Zhu L, Whitney KD, Muller WJ, and Pollard JW (2003). Progression to malignancy in the polyoma middle T oncoprotein mouse breast cancer model provides a reliable model for human diseases. *Am J Pathol* **163**, 2113–2126.

[28] Kuek V, Yang Z, Chim SM, Zhu S, Xu H, Chow ST, Tickner J, Rosen V, Erber W, and Li X, et al (2016). NPNT is expressed by osteoblasts and mediates angiogenesis via the activation of extracellular signal-regulated kinase. *Sci Rep* **6**, 36210.

[29] Sanchez-Cortes J and Mrksich M (2011). Using self-assembled monolayers to understand alpha8beta1-mediated cell adhesion to RGD and FEI motifs in nephronectin. *ACS Chem Biol* **6**, 1078–1086.

[30] Sato Y, Uemura T, Morimitsu K, Sato-Nishiuchi R, Manabe R, Takagi J, Yamada M, and Sekiguchi K (2009). Molecular basis of the recognition of nephronectin by integrin alpha8beta1. *J Biol Chem* **284**, 14524–14536.

[31] Azmi AS, Bao B, and Sarkar FH (2013). Exosomes in cancer development, metastasis, and drug resistance: a comprehensive review. *Cancer Metastasis Rev* **32**, 623–642.

[32] van der Pol E, Boing AN, Harrison P, Sturk A, and Nieuwland R (2012). Classification, functions, and clinical relevance of extracellular vesicles. *Pharmacol Rev* **64**, 676–705.

[33] Zomer A, Maynard C, Verweij FJ, Kamermans A, Schafer R, Beerling E, Schiffelers RM, de Wit E, Berenguer J, and Ellenbroek SI, et al (2015). In vivo imaging reveals extracellular vesicle-mediated phenocopying of metastatic behavior. *Cell* **161**, 1046–1057.

[34] Gonzalez-Begne M, Lu B, Han X, Hagen FK, Hand AR, Melvin JE, and Yates JR (2009). Proteomic analysis of human parotid gland exosomes by multidimensional protein identification technology (MudPIT). *J Proteome Res* **8**, 1304–1314.

[35] Demory Beckler M, Higginbotham JN, Franklin JL, Ham AJ, Halvey PJ, Imasuen IE, Whitwell C, Li M, Liebler DC, and Coffey RJ (2013). Proteomic analysis of exosomes from mutant KRAS colon cancer cells identifies intercellular transfer of mutant KRAS. *Mol Cell Proteomics* **12**, 343–355.

[36] Mathivanan S, Lim JW, Tauro BJ, Ji H, Moritz RL, and Simpson RJ (2010). Proteomics analysis of A33 immunoaffinity-purified exosomes released from the human colon tumor cell line LIM1215 reveals a tissue-specific protein signature. *Mol Cell Proteomics* **9**, 197–208.

[37] Willms E, Johansson HJ, Mager I, Lee Y, Blomberg KE, Sadik M, Alaarg A, Smith CI, Lehtio J, and El Andaloussi S, et al (2016). Cells release subpopulations of exosomes with distinct molecular and biological properties. *Sci Rep* **6**, 22519.

[38] Lotvall J, Hill AF, Hochberg F, Buzas EI, Di Vizio D, Gardiner C, Gho YS, Kurochkin IV, Mathivanan S, and Quesenberry P, et al (2014). Minimal experimental requirements for definition of extracellular vesicles and their functions: a position statement from the International Society for Extracellular Vesicles. *J Extracell Vesicles* **3**, 26913.

[39] Wang S, Chen Y, Qu F, He S, Huang X, Jiang H, Jin T, Wan S, and Xing J (2014). Association between leukocyte telomere length and glioma risk: a case-control study. *Neuro-Oncology* **16**, 505–512.

[40] Salonia A, Abdollah F, Capitanio U, Suardi N, Briganti A, Gallina A, Colombo R, Ferrari M, Castagna G, and Rigatti P, et al (2012). Serum sex steroids depict a nonlinear u-shaped association with high-risk prostate cancer at radical prostatectomy. *Clin Cancer Res* **18**, 3648–3657.

[41] Sandblom G, Ladjevardi S, Garmo H, and Varenhorst E (2008). The impact of prostate-specific antigen level at diagnosis on the relative survival of 28,531 men with localized carcinoma of the prostate. *Cancer* **112**, 813–819.

[42] Aleksandrova K, Chuang SC, Boeing H, Zuo H, Tell GS, Pischon T, Jenab M, Bueno-de-Mesquita B, Vollset SE, and Midttun O, et al (2015). A prospective study of the immune system activation biomarker neopterin and colorectal cancer risk. *J Natl Cancer Inst* **107**.

[43] Cui Y, Cai Q, Qu S, Chow WH, Wen W, Xiang YB, Wu J, Rothman N, Yang G, and Shu XO, et al (2012). Association of leukocyte telomere length with colorectal cancer risk: nested case-control findings from the Shanghai Women's Health Study. *Cancer Epidemiol Biomark Prev* **21**, 1807–1813.

[44] Chuang SC, Stolzenberg-Solomon R, Ueland PM, Vollset SE, Midttun O, Olsen A, Tjonneland A, Overvad K, Boutron-Ruault MC, and Morois S, et al (2011). A U-shaped relationship between plasma folate and pancreatic cancer risk in the European Prospective Investigation into Cancer and Nutrition. *Eur J Cancer* **47**, 1808–1816.

[45] Skinner HG, Gangnon RE, Litzelman K, Johnson RA, Chari ST, Petersen GM, and Boardman LA (2012). Telomere length and pancreatic cancer: a case-control study. *Cancer Epidemiol Biomark Prev* **21**, 2095–2100.

[46] Duchnowska R, Sperinde J, Czartoryska-Arlukowicz B, Mysliwiec P, Winslow J, Radecka B, Petropoulos C, Demlova R, Orlikowska M, and Kowalczyk A, et al (2017). Predictive value of quantitative HER2, HER3 and p95HER2 levels in HER2-positive advanced breast cancer patients treated with lapatinib following progression on trastuzumab. *Oncotarget* **8**, 104149–104159.

[47] Thul PJ, Akesson L, Wiking M, Mahdessian D, Geladaki A, Ait Blal H, Alm T, Asplund A, Bjork L, and Breckels LM, et al (2017). A subcellular map of the human proteome. *Science* 356.

[48] Wu CY, Du SL, Zhang J, Liang AL, and Liu YJ (2017). Exosomes and breast cancer: a comprehensive review of novel therapeutic strategies from diagnosis to treatment. *Cancer Gene Ther* **24**, 6–12.

[49] Lowry MC, Gallagher WM, and O'Driscoll L (2015). The role of exosomes in breast cancer. *Clin Chem* **61**, 1457–1465.

[50] Yu S, Cao H, Shen B, and Feng J (2015). Tumor-derived exosomes in cancer progression and treatment failure. *Oncotarget* **6**, 37151–37168.

[51] Villagrasa A, Alvarez PJ, Osuna A, Garrido JM, Aranega A, and Rodriguez-Serrano F (2014). Exosomes derived from breast cancer cells, small trojan horses? *J Mammary Gland Biol Neoplasia* **19**, 303–313.

[52] Hoshino A, Costa-Silva B, Shen TL, Rodrigues G, Hashimoto A, Tesic Mark M, Molina H, Kohsaka S, Di Giannatale A, and Ceder S, et al (2015). Tumour exosome integrins determine organotropic metastasis. *Nature* **527**, 329–335.

Supplementary legends

Figure S1. Optimization of the of anti-human NPNT (Atlas Antibodies/Sigma) antibody using normal human kidney and breast cancer tissues. The tissues were stained at 1:50, 1:100 and 1:200 dilution and the results show that the optimal dilution is 1:100 for the human tissues. Rabbit IgG isotype control and control without antibody (-ab) shown in lower panels. Scale bar: 50µm.

Figure S2. Controls for anti-human NPNT (Atlas Antibodies/Sigma) and anti-mouse NPNT (Abnova) antibodies on mouse tissues. (A) Side-by-side comparison of NPNT antibodies (Atlas Antibodies/Sigma and Abnova) showing overlapping patterns between the two antibodies in MMTV-PyMT mammary tumors and kidney tissues. Scale bar: 100µm for mammary tumor and 50µm for kidney. (B) Side-by-side comparison of NPNT staining (Atlas Antibodies/Sigma) in mMTV-PyMT tumors with the extracellular matrix proteins Collagen V and Fibronectin. Scale bar: 50µm.

Figure S3. Uncropped images of immunoblots displayed in main figures. (A) Uncropped version of immunoblot displayed in main Figure 4B. Membranes were incubated with anti-V5 (CST) and GAPDH (Abcam) antibodies prior to development. Inset shows cropped area shown in main figure. (B-E) Uncropped versions of immunoblots displayed in main Figure 6A. The membranes were cut horizontally prior to incubation with antibodies for ALIX (CST), V5 (CST), GAPDH (Abcam), GM130 (BD Biosciences) and CHMP4B (Atlas Antibodies/Sigma).

Figure S4. NPNT is expressed by mammary epithelial cells in MMTV-PyMT transgenic animals. (A) Quantitative real time PCR (qRT-PCR) analysis of NPNT expression levels in primary cells isolated from a normal mammary gland (FVB mouse) or from mammary tumor tissue from three different MMTV-PyMT transgenic animals (#1177, #1178 and #1179). Data are presented as mean ±SD of triplicate measurements. (B) ISH (left panel) and IHC (right panel) of serial sectioned mouse normal mammary gland (MG) and MMTV-PyMT tumor tissue at both non-invasive and invasive stages. The second and fourth rows show different images of non-invasive tumors, with higher magnification of the images in the fourth row. The sections for IHC were stained using the anti-NPNT antibody (Atlas Antibodies/Sigma). “-ab” reflects a control with no primary antibody.

Figure S5. NPNT overexpression does not affect primary tumor growth and spontaneous metastasis. (A) 66cl4-cells expressing either empty vector (EV) or NPNT were injected into the mammary fat pad of mice (n=15 per group) and the tumor volume was measured using electronic calipers. (B) Average weights of the tumors at the end of the experiment did not show any significant difference between the two groups of 66cl4-EV and 66cl4-NPNT tumors. The mice were sacrificed on day 35 after inoculation. Relative Tumor Burden (RTB) assay using genomic DNA from whole (C) spine or (D) lung lysates as template (n=13-14).

Figure S6. NPNT increases attachment in a dose-dependent manner. (A) qRT-PCR analysis of NPNT levels in mouse cell lines. Data are presented as mean ±SD of triplicate measurements from a representative experiment. (B) IHC staining of 67NR and 4T1 primary orthotopic tumors using anti-NPNT antibodies (Abnova). Staining “hot-spots” are shown. -ab reflects a control with no primary antibody. The images are representative of 3 animals per cell line. (C) Quantitative real time PCR verification of NPNT knockdown in 4T1-shNPNT cells compared to 4T1-shFF control cells. Data is presented as mean ±SD of three biological replicates. *, $p<0.05$. (D) xCELLigence attachment assay of 4T1-shFF control cells and 4T1-shNPNT in xCELLigence E-plates plates coated with recombinant mouse NPNT at 0.4 µg/ml, 2 µg/ml or 10 µg/ml prior to seeding. Data is presented as mean cell index ±SD (n=4) from a representative experiment 1 hour after seeding.

Construction of 66cl4-NPNT and 4T1-shNPNT cells

The expression construct for full length and mutated mouse NPNT in 66cl4 cells was generated by subcloning transcript variant 2 of NPNT from pcDNA3-POEM-Fc[1] into pcDNA3.1-v5-His (Invitrogen). For generation of retroviruses, the DNA fragment encoding the NPNT-V5-His fusion protein was amplified using Platinum Fx® taq polymerase (Invitrogen), and subcloned into the EcoRI site of pBABE-puro[2]. Retroviruses were produced using the Phoenix-Eco and PT67 cells and used to transduce mCherry-positive 66cl4 cells.

The 4T1 cell line used for stable NPNT knockdown was created in an earlier variant of the 4T1 cells than the 4T1.2 cell line described previously.[3]Six 97-mer shRNA oligonucleotides targeting mouse NPNT were cloned into MSCV-Neo-miR30FF retroviral transfer vector (Addgene) to generate 4T1-cells with stable NPNT knockdown.[4,5] Retroviral packaging and transduction of 4T1 cells was done as described previously.[5]

Primers

Primers for cDNA cloning of full length mouse NPNT transcript variant 2:

mNPNTFwd 5’- GGAATTCGCTTATCGAA-3’

mNPNTRev 5’-CGATAATTCCAATGCGATGCAA-3’

Mutagenesis primers for mutating NPNT RGD→ RGE

Mut-RGD-RGE-Fwd: 5’ CTCAGAAACCCAGAGGAGAGGTGTTCATTCCACGGCAGC 3’

Mut-RGD-RGE-Rev: 5’ GCTGCCGTGGAATGAACACCTCTCCTCTGGGTTTCTGAG 3’

Mutagenesis primers for mutating NPNT EIE→ AIA

Mut-EIE-AIA-Fwd: 5’ GACCTGTTTGAGATATTTGCAATCGCAAGAGGGGTCAGCGC 3’

Mut-EIE-AIA-Rev: 5’ GCGCTGACCCCTCTTGCGATTGCAAATATCTCAAACAGGTC 3’

Cells were verified by sequencing both before and after all experiments.

Hairpin sequences for cloning of shRNAs into 4T1 cells:

Hairpin sequence shNPNT: 5’ TGCTGTTGACAGTGAGCGAAGTGACACTCTCGAAGTACAGTAGTGAAGCCACAGATGTACTGTACTTCGAGAGTGTCACTGTGCCTACTGCCTCGGA 3’

Hairpin sequence: shFF: 5’

TGCTGTTGACAGTGAGCGAGCTCCCGTGAATTGGAATCCTAGTGAAGCCACAGATGTAGGATTCCAATTCAGCGGGAGCCTGCCTACTGCCTCGGA 3’

The following primers were used to detect mouse NPNT with qRT-PCR analyses:

mNPNTFwd 5’-TGCCCTATCGTGTTCCATG-3’

mNPNTRev 5’-ACTCTTCCAGTCGCACATTC-3’

Primers for RTB Assay

mCherryFwd 5’ GACCACCTACAAGGCCAAGAAG 3’

mCherryRev 5’ AGGTGATGTCCAACTTGATGTTGA 3’

mCherry probe 5’ 6FAM-CAGCTGCCCGGCGCCTACA –TAMRA 3’

mVimFwd 5’ AGCTGCTAACTACCAGGACACTATTG 3’

mVimRev 5’ CGA AGG TGA CGA GCC ATC TC 3’

mVimentin probe 5’ VIC- CCT TCA TGT TTT GGA TCT CAT CCT GCA GG –TAMRA 3’

Information regarding peptides used in xCELLigence adhesion assay:

RGD peptide sequence: H-Gly-Arg-Gly-Asp-Ser-H (Cat: H1345, Bachem).

Control peptide: H-Gly-Arg-Gly-Glu-Ser-OH trifluoroacetate (Cat: H3166, Bachem).

REFERENCES

1 Morimura, N. *et al.* Molecular cloning of POEM: a novel adhesion molecule that interacts with alpha8beta1 integrin. *J. Biol. Chem.* **276**, 42172-42181, doi:10.1074/jbc.M103216200 (2001).

2 Morgenstern, J. P. & Land, H. A series of mammalian expression vectors and characterisation of their expression of a reporter gene in stably and transiently transfected cells. *Nucleic Acids Res* **18**, 1068 (1990).

3 Eckhardt, B. L. *et al.* Genomic analysis of a spontaneous model of breast cancer metastasis to bone reveals a role for the extracellular matrix. *Molecular cancer research : MCR* **3**, 1-13 (2005).

4 Lamar, J. M. *et al.* The Hippo pathway target, YAP, promotes metastasis through its TEAD-interaction domain. *Proc. Natl. Acad. Sci. U. S. A.* **109**, E2441-2450, doi:10.1073/pnas.1212021109 (2012).

5 Stern, P. *et al.* A system for Cre-regulated RNA interference in vivo. *Proc. Natl. Acad. Sci. U. S. A.* **105**, 13895-13900, doi:10.1073/pnas.0806907105 (2008).

Supplementary Table S1

Table S1: Risk of death from breast cancer according to NPNT granular cytoplasmic staining pattern and molecular subtype.

Granular cytoplasmic staining	Molecular subtype											
	Luminal A			**Luminal B[2]**			**HER2 type**			**Triple negative phenotype[3]**		
	Cases (deaths)	**HR[1] (95% CI)**	**P-value**	**Cases (deaths)**	**HR[1] (95% CI)**	**P-value**	**Cases (deaths)**	**HR[1] (95% CI)**	**P-value**	**Cases (deaths)**	**HR[1] (95% CI)**	**P-value**
No	359 (114)	1		245 (106)	1		46 (28)	1		76 (35)	1	
Yes	45 (16)	1.70 (0.99-2.90)	0.054	46 (17)	0.69 (0.40-1.17)	0.17	11 (6)	0.69 (0.23-2.10)	0.52	14 (9)	1.48 (0.68-3.22)	0.32

[1] Adjusted for age at diagnosis in 5-year categories, [2] Luminal B includes both Luminal B HER2- and Luminal B HER2+ subtypes, [3] Triple negative includes both Five negative and Basal subtypes

Figure S1

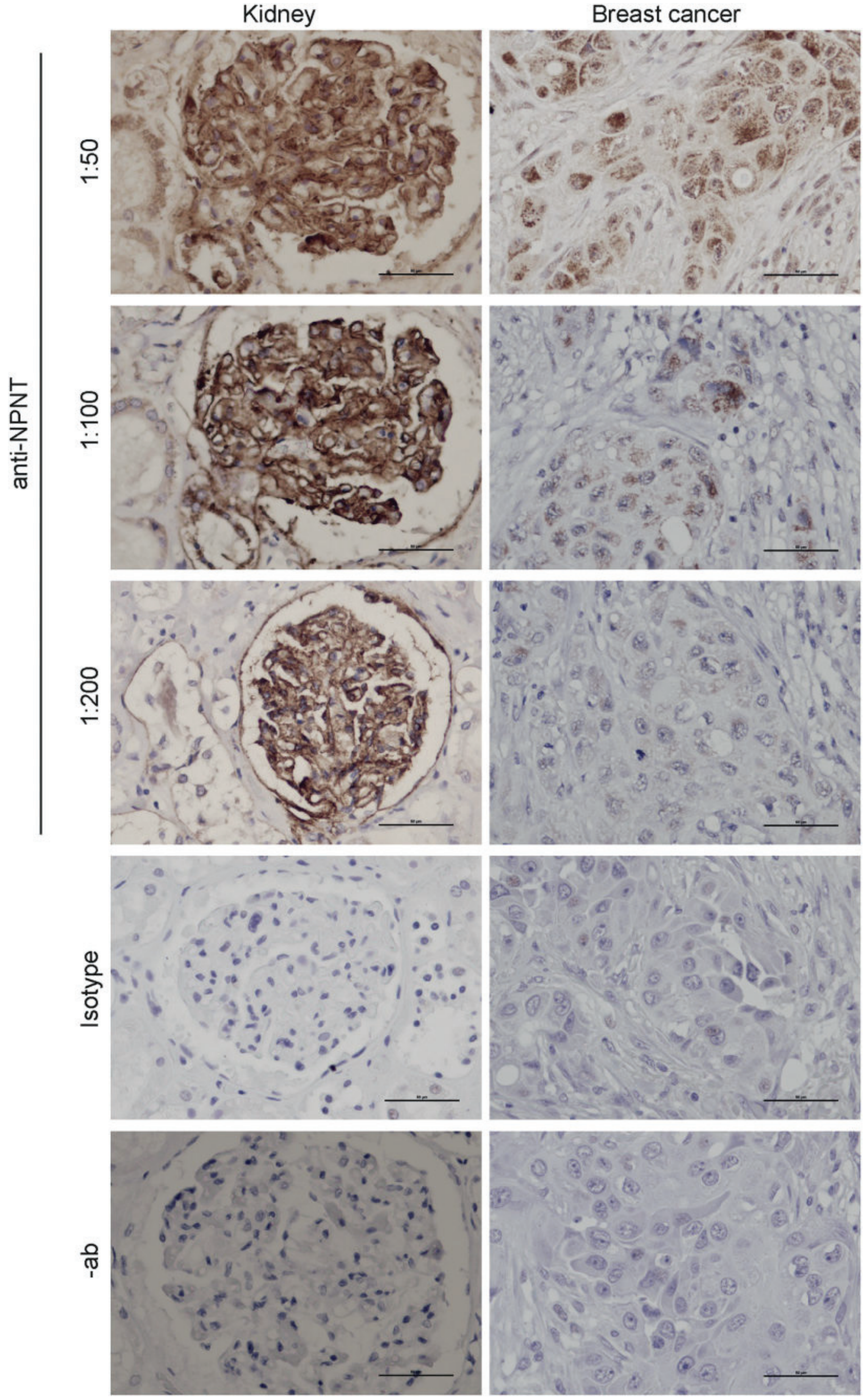

Figure S2

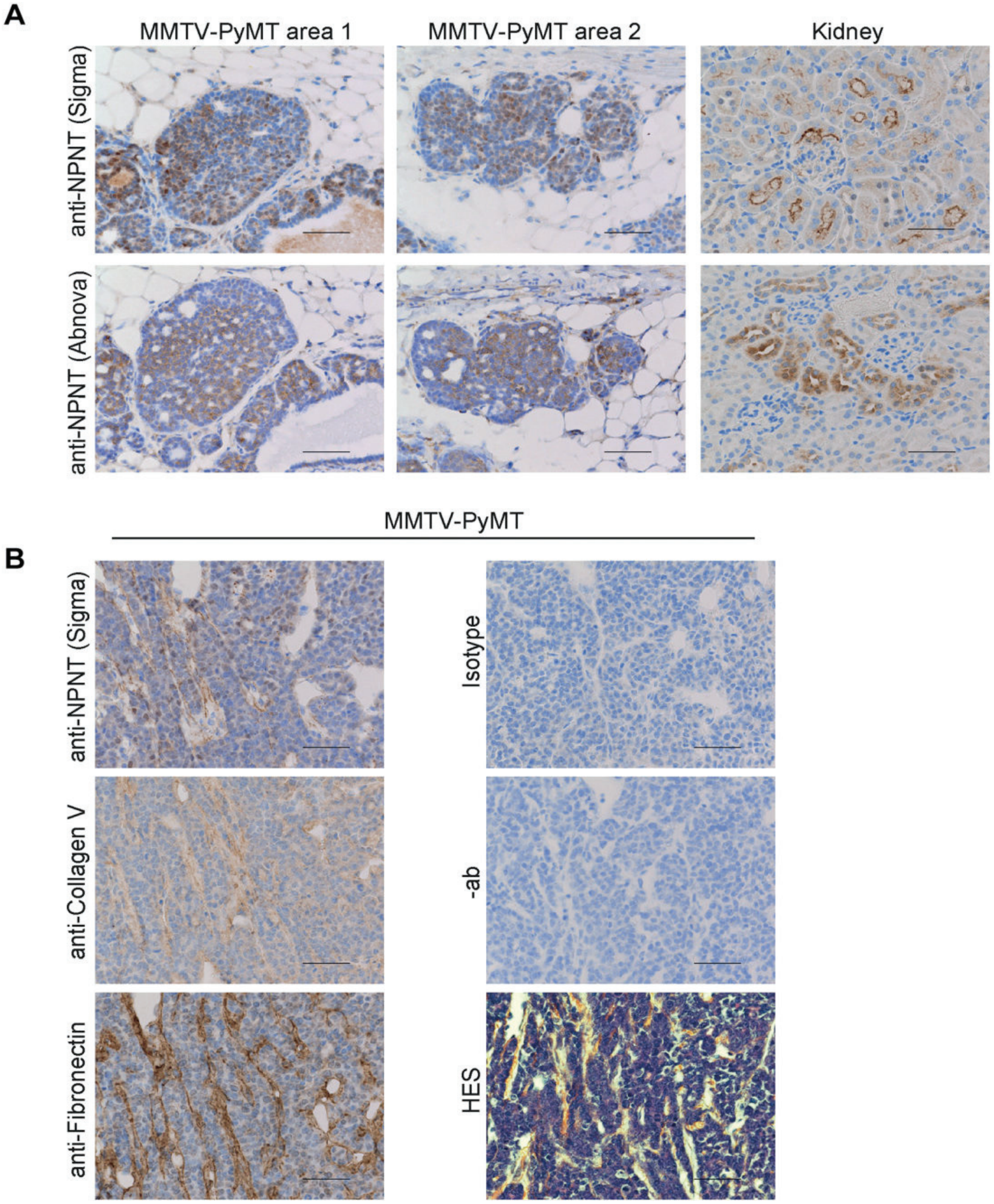
A
MMTV-PyMT area 1
MMTV-PyMT area 2
Kidney
anti-NPNT (Sigma)
anti-NPNT (Abnova)
MMTV-PyMT
B
anti-NPNT (Sigma)
anti-Collagen V
anti-Fibronectin
Isotype
-ab
HES

Figure S3

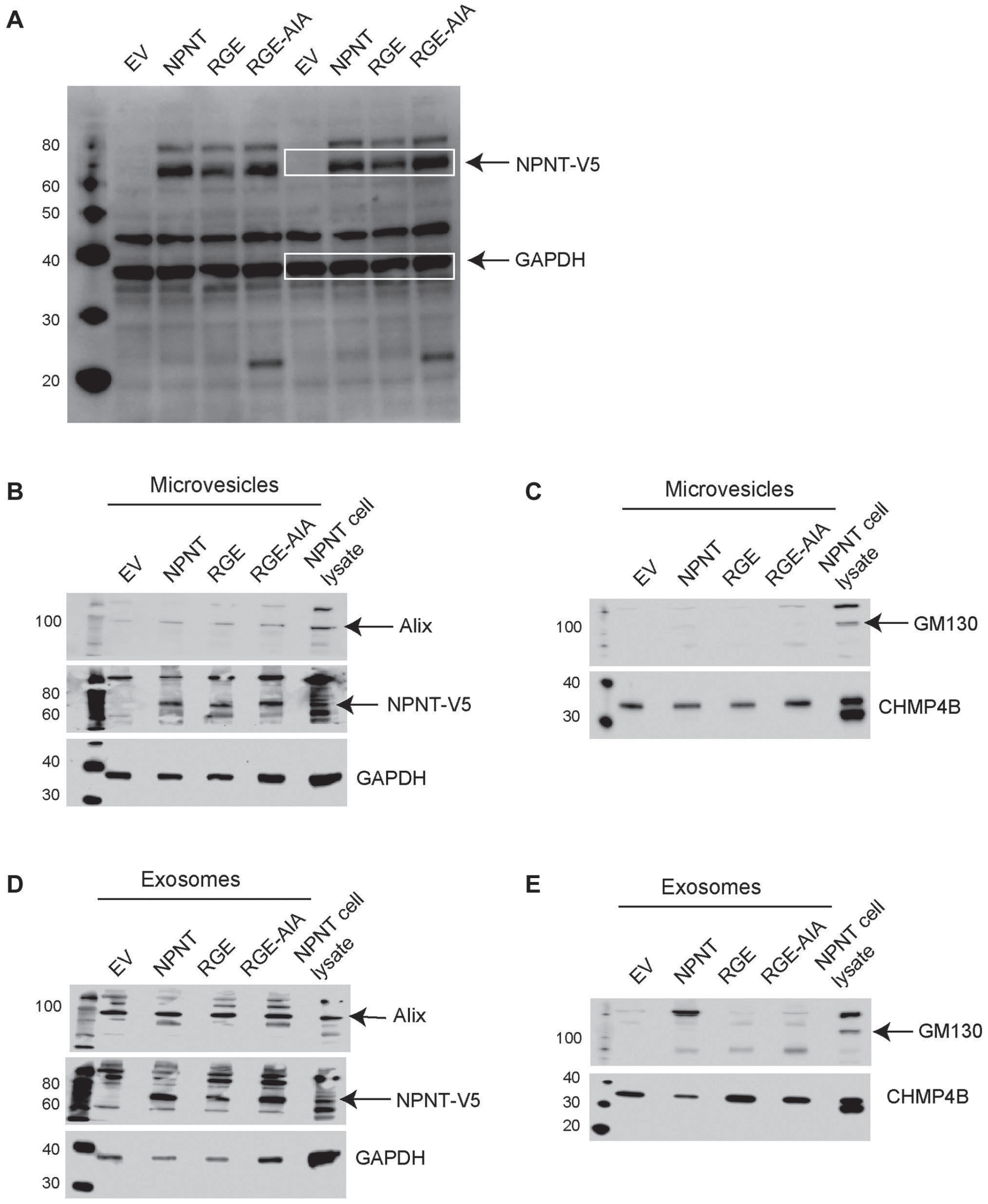
A
EV
NPNT
RGE
RGE-AIA
EV
NPNT
RGE
RGE-AIA
80
60
50
40
30
20
NPNT-V5
GAPDH
B
Microvesicles
EV
NPNT
RGE
RGE-AIA
NPNT cell lysate
100
Alix
80
60
NPNT-V5
40
30
GAPDH
C
Microvesicles
EV
NPNT
RGE
RGE-AIA
NPNT cell lysate
100
GM130
40
30
CHMP4B
D
Exosomes
EV
NPNT
RGE
RGE-AIA
NPNT cell lysate
100
Alix
80
60
NPNT-V5
40
30
GAPDH
E
Exosomes
EV
NPNT
RGE
RGE-AIA
NPNT cell lysate
100
GM130
40
30
20
CHMP4B

Figure S4

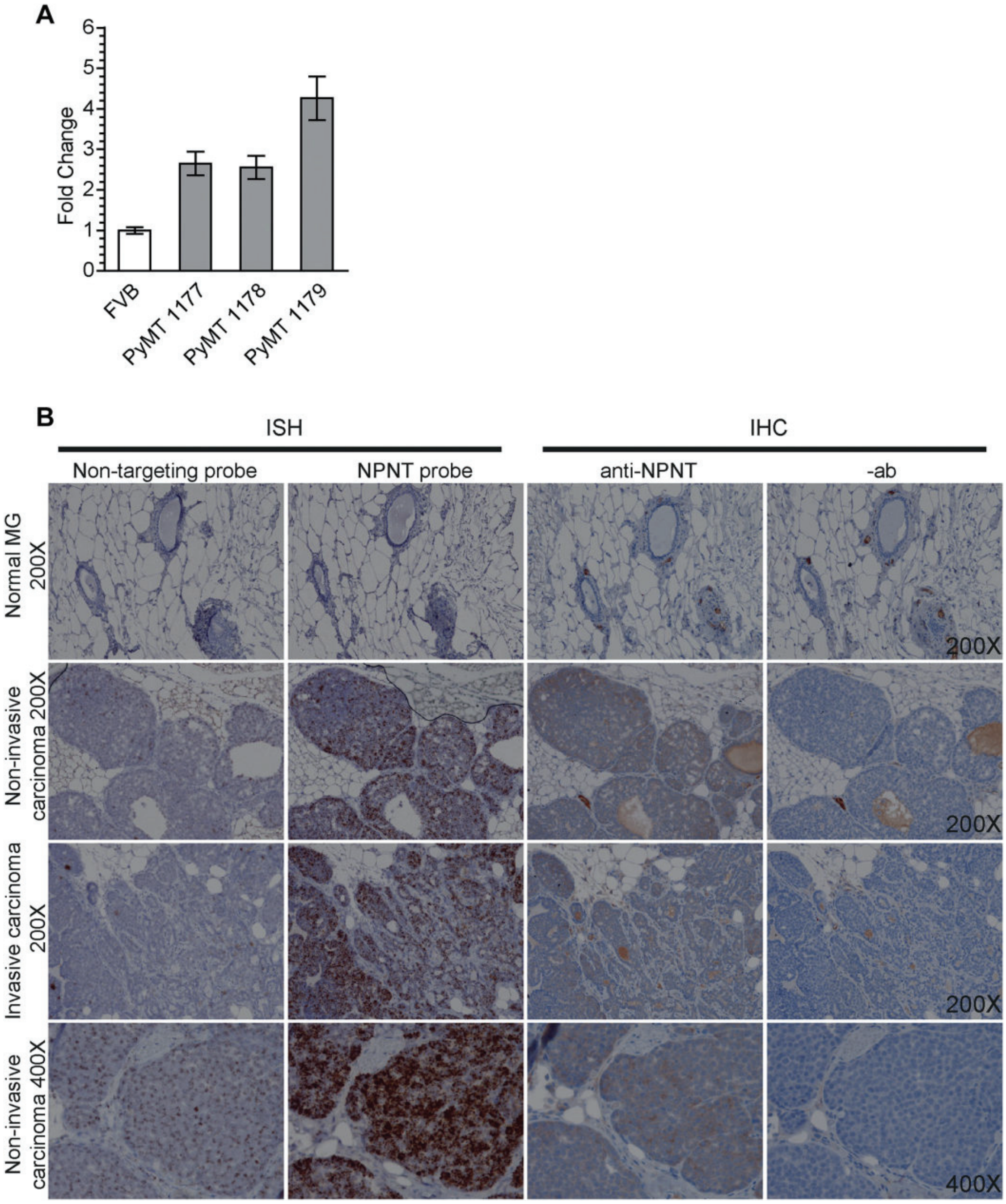
A
Fold Change
0
1
2
3
4
5
6
FVB
PyMT 1177
PyMT 1178
PyMT 1179
B
ISH
IHC
Non-targeting probe
NPNT probe
anti-NPNT
-ab
Normal MG 200X
Non-invasive carcinoma 200X
Invasive carcinoma 200X
Non-invasive carcinoma 400X
200X
200X
200X
400X

Figure S5

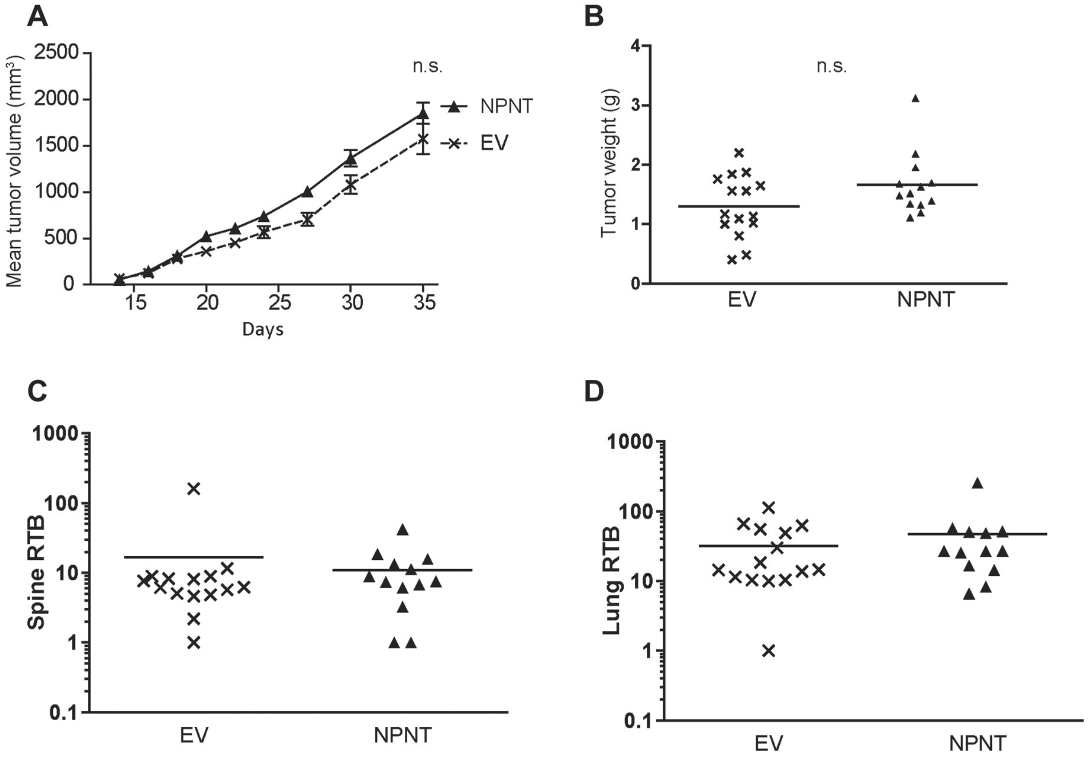
A
Mean tumor volume (mm^3)
2500
2000
1500
1000
500
0
15
20
25
30
35
Days
n.s.
NPNT
EV
B
Tumor weight (g)
4
3
2
1
0
n.s.
EV
NPNT
C
Spine RTB
1000
100
10
1
0.1
EV
NPNT
D
Lung RTB
1000
100
10
1
0.1
EV
NPNT

Figure S6

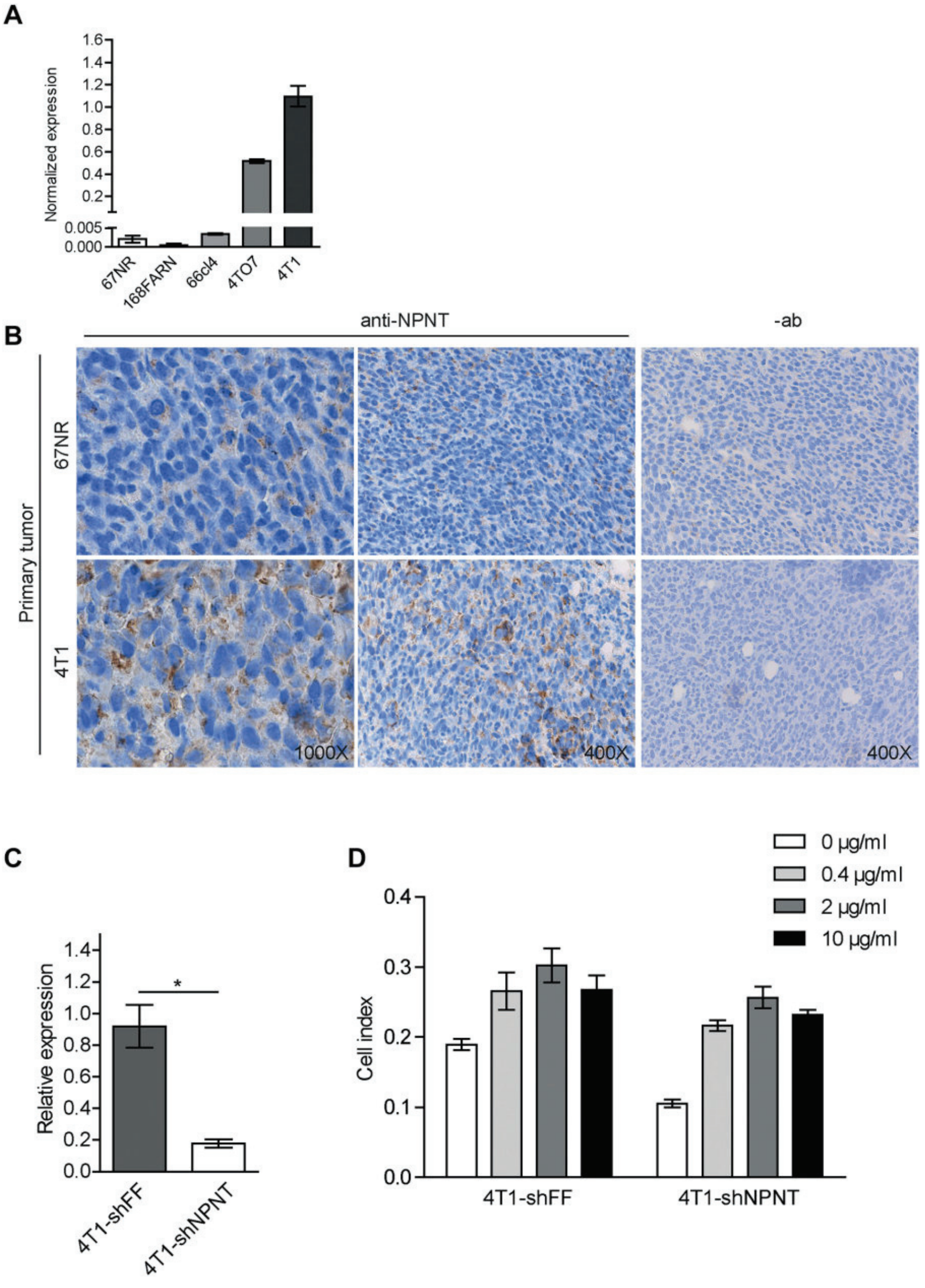
A
Normalized expression
1.6
1.4
1.2
1.0
0.8
0.6
0.4
0.2
0.005
0.000
67NR
168FARN
66cl4
4TO7
4T1
B
anti-NPNT
-ab
Primary tumor
67NR
4T1
1000X
400X
400X
C
Relative expression
1.4
1.2
1.0
0.8
0.6
0.4
0.2
0.0
*
4T1-shFF
4T1-shNPNT
D
0 µg/ml
0.4 µg/ml
2 µg/ml
10 µg/ml
Cell index
0.4
0.3
0.2
0.1
0.0
4T1-shFF
4T1-shNPNT

Paper II

Nephronectin mediates p38 MAPK-induced cell viability via its integrin binding enhancer motif

Jimita Toraskar[1, 2], Synnøve N. Magnussen[3], Konika Chawla[1, 4] , Gunbjørg Svineng[3] and Tonje S. Steigedal[1, 2]

[1]Department of Clinical and Molecular Medicine, Faculty of Medicine and Health Sciences, Norwegian University of Science and Technology (NTNU), Trondheim, Norway
[2]Central Norway Regional Health Authority, Stjørdal, Norway
[3] Department of Medical Biology, Faculty of Health Sciences, UiT-The Arctic University of Norway, Tromsø, Norway
[4]Bioinformatics Core Facility-BioCore, NTNU, Trondheim, Norway

Correspondence: Jimita Toraskar, Department of Clinical and Molecular Medicine, Faculty of Medicine and Health Sciences, NTNU, Postbox 8905, N-7491 Trondheim, Norway.
E-mail: jimita.toraskar@ntnu.no Mobile: +47-99673377

ABSTRACT:

Nephronectin (NPNT) is an extracellular matrix (ECM) protein involved in kidney development. We recently reported intracellular NPNT as a potential prognostic marker in breast cancer and that NPNT promotes metastasis in an integrin-dependent manner. Here we used Reverse Phase Protein Array (RPPA) to analyze NPNT-triggered intracellular signaling in the 66cl4 mouse breast cancer cell line. The results showed that the integrin binding enhancer motif is important for the cellular effects upon NPNT interaction with its receptors, including phosphorylation of p38 mitogen activated protein kinase (MAPK). Furthermore, analysis using prediction tools suggests involvement of NPNT in promoting cell viability. In conclusion, our results indicate that NPNT, via its integrin binding motifs, promote cell viability through phosphorylation of p38 MAPK.

Keywords: Breast Cancer, Extracellular matrix, Nephronectin, Integrin, Cell viability

Abbreviations: NPNT, nephronectin; ECM, extracellular matrix; RPPA, reverse phase protein array; MAPK, mitogen activated protein kinase; EV, empty vector; RGE, mutated RGD motif of Nephronectin; AIA, mutated EIE motif of Nephronectin; rmNPNT, recombinant Nephronectin; IPA, ingenuity pathway analysis

1. Introduction

The cell-extracellular matrix (ECM) interaction plays a vital role in tissue homeostasis, as well as in determining the fate of cancer cells [1]. The composition of the ECM and competitive binding among integrins determines whether cells survive, differentiate, proliferate, migrate or influence shape and cell polarity (reviewed in [2-4]). Integrins are transmembrane receptors well known for their ability to link ECM ligands to the cytoskeleton and transduce signals, which effects cellular responses. Several integrins (α8β1, αVβ3, αVβ5, αVβ6, and α4β7) are shown to bind to NPNT [5, 6], where some are known to bind the common RGD (Arg-Gly-Asp) integrin binding motif [2]. NPNT contains an additional integrin-binding motif, known as the EIE (Glu-Ile-Glu) enhancer motif, located downstream of the RGD motif and known to interact mainly with integrin α8β1 [7, 8]. ECM-integrin interactions are known to influence breast cancer progression and altered expression of integrins may predict poor survival in breast cancer [9, 10]. Also, in breast cancer tissues the expression of ECM components is often elevated compared to normal tissues [11]. High expression levels of NPNT has been linked to the metastatic propensity of mouse breast cancer cells in a model of spontaneous metastasis [12]. In a different syngeneic mouse model of breast cancer, higher levels of NPNT were reported in metastatic mammary tumor cells compared to non-metastatic cells [13]. Our recent results show that NPNT overexpressing 66cl4 cells (66cl4-NPNT) have an increased ability to form lung metastases compared to 66cl4-empty vector cells (66cl4-EV) in an experimental metastasis assay. A single point mutation of the RGD motif alone (66cl4-RGE) was not sufficient to reduce the number of NPNT induced metastatic lesions. However, tumor burden was significantly reduced in mice injected with cells overexpressing NPNT mutated in both the RGD and enhancer EIE motif (66cl4-RGE-AIA). This highlights the importance of NPNT-integrin interaction in the formation of lung metastasis [14]. The current study aimed to investigate the biological function of NPNT in the 66cl4 cell line. We performed a comprehensive analysis using reverse phase protein array (RPPA) to further identify molecular signals triggered by the NPNT-integrin interaction. Using *in vitro* assays, we confirm the involvement of NPNT in promoting cell viability.

2. Material and methods

2.1. Cell culture

As described previously, 66cl4 cells were stably transduced to overexpress NPNT or NPNT mutants (RGE or RGE-AIA), while 66cl4 empty vector cells (EV) were used as a control [14]. Furthermore, shRNA was used to knock-down NPNT protein levels in 4T1 cells (sh-NPNT), while a non-targeting shRNA in 4T1 cells was used as a control (sh-ctr) [14]. All cell lines were cultured in (1X) Minimum Essential Medium α (Thermo Fisher Scientific, Cat: 22561021), supplemented with 10% fetal bovine serum, 1% (v/v) penicillin-streptomycin and 1M hepes buffer (Thermo Fisher Scientific, Cat: 15630080). Cell lines were routinely tested for mycoplasma infection.

2.2. Immunofluorescence

66cl4-EV and 66cl4-NPNT were cultured for 24 hours in serum-free medium to evaluate the cell surface localization of NPNT. 66cl4-EV cells were used as negative control. The effect of incubating 66cl4-EV cells with 2 µg/ml recombinant mouse NPNT (rmNPNT) (R&D systems, Cat: 4298-NP-050) in PBS for 1 hour prior fixing was also investigated. Cells were fixed with 4 % Paraformaldehyde (PFA). Permeabilization of cells was avoided to visualize extracellular NPNT. Anti-collagen V (Abcam, Cat: ab7046) was used as a positive control. NPNT was identified with anti-NPNT (Abnova, Cat: PAB8467) (1:150) and Alexa Fluor®488 as secondary antibody (Abcam, Cat: ab150077) (1:1000). Images were captured using confocal laser scanning microscope (Zeiss LSM 510 Meta). Hoechst was used to stain the nucleus.

2.3. Reverse Phase Protein Array (RPPA)

66cl4-EV, 66cl4-NPNT, 66cl4-RGE and 66cl4-RGE-AIA cells were grown in serum free medium for 24 hours and then collected at 80 % confluency using a cell scraper and snap frozen in liquid nitrogen. To investigate the effect of rmNPNT, 66cl4-EV cells were seeded on plates pre-coated with 2 µg/µl rmNPNT in serum free medium for 24 hours. Control plates were pre-incubated with PBS alone. Frozen cell pellets (more than 1 million cells) were analyzed at the

MD Anderson Cancer Center, RPPA core facility, USA. RPPA is high throughput functional proteomics analysis designed to analyze cellular protein activity in signaling networks by measuring protein levels (both total and phosphorylated forms) using high quality validated antibodies [15, 16]. Considering values from all four biological replicates, the average signal intensity of proteins was calculated. Significant log fold changes in protein expression values in three different groups (‘NPNT vs EV’, ‘EV_{rmNPNT} vs EV’ and, ‘RGE vs RGE-AIA’) were analyzed further.

2.4. Immunoblotting

The protein concentration of the whole cell lysates were measured by BioRad protein assay (BioRad, Cat: 500-0006). A total of 50 µg protein was loaded in NuPAGE Novex 10% (Invitrogen, Cat: NP0301BOX). Protein transferred to a PVDF membrane was further incubated with primary antibodies: p38 MAPK (1:1000) (CST, Cat: 9212), and phospho-p38 MAPK (1:1000) (CST, Cat: 9211). Bound primary antibodies were detected using an appropriate HRP linked secondary antibody (Dako, Cat: P0447 or P0399) and imaged using Supersignal West Femto substrate (Pierce, Cat: 34096) with the Odyssey Fc system (Li-Cor biosciences). Western blots were quantified using Image studio 3.1 software. Statistical analyses were performed using two tailed Student’s t-tests assuming equal variance.

2.5. Ingenuity Pathway Analysis (IPA)

IPA (Qiagen) is a web-based program which uses algorithms to connect protein expression values to its corresponding biological response. The RPPA analysis resulted in a list of differentially expressed proteins (log-fold change) between the RGE and RGE-AIA group, which was further analyzed by IPA to identify the cellular function most likely to be affected by the alteration in the NPNT enhancer motif. IPA bases its analysis on already published information about protein networks. A stronger prediction (lower p-value) is made when several proteins are present within the same pathway.

2.6. Cell viability assay

A total of 2500 cells per well were seeded in a 384 well plate in serum free medium for 24 hours. Cells were lysed using the Cell Titer-Glo luminescent cell viability assay kit (Promega, Cat: G7570). The endpoint of this assay reports luminescence, which is proportional to ATP generated from cells surviving in serum free medium. The p38 MAPK inhibitor BIRB 796 (Axon, Cat: 1358) was used at 4 µM, which was found to be the optimal concentration for 66cl4 and 4T1 cell lines. The cells were grown in serum free medium and simultaneously exposed to BIRB 796 for 24 hours. Cell viability was also measured in 66cl4-EV cells when incubated with serum free medium supplemented with rmNPNT (2 µg/ml).

3. Results and Discussion

3. 1. Cell surface distribution of NPNT in 66cl4 cells

Although NPNT is mostly documented to be an extracellular protein [6, 17, 18], we have recently shown that NPNT is localized intracellularly in the cytoplasm and packed in vesicles/granules in breast cancer tissues and in exosomes isolated from cell lines [14]. Our previous findings showing an integrin-dependent metastasis-promoting effect also suggest extracellular localization and function of NPNT in breast cancer. To visualize the cell surface distribution of NPNT in 66cl4 cells overexpressing NPNT (66cl4-NPNT) we imaged the cells using immunofluorescence microscopy (Fig. 1a). In this experimental setup, without permeabilization of the cells, the results showed an extracellular focal distribution of NPNT. 66cl4-EV cells cultured in serum free medium for 24 hours were used as a negative control. Recombinant NPNT (2 µg/ml) added to the 66cl4-EV cells for 1 hour prior to fixing could be detected in a similar location as wild type-NPNT in 66cl4-NPNT cells. Collagens are major constituents of ECM, and staining for collagen V showed a similar pattern as staining for NPNT, further demonstrating extracellular localization of NPNT in the 66cl4 cells. Using Z-stack images of the 66cl4-NPNT cells, we plotted a Z profile showing the signal intensity in the green (NPNT-Alexa 488) and blue (nucleus-Hoechst) channels as a function of distance from the surface of the culture dish (Fig. 1b). The graph shows that the signal derived from NPNT is located below the nucleus, close to the surface of the plate (Video S1). This points to an extracellular localization of NPNT, as has already been shown by others [6, 17, 18]. Seeding equal numbers of 66cl4-EV cells on rmNPNT coated plates and uncoated plates showed that presence of rmNPNT increased the proportion of cells that attached and spread out compared to the uncoated plates where a large number of cells still remained rounded at 24 hours (Fig. 1c). This is in line with our previous finding showing involvement of NPNT in promoting cell adhesion [14].

3. 2. RPPA analysis of NPNT-mediated signaling

Various ECM proteins contribute in establishing the phenotype of mammary epithelial cells and can regulate tissue-specific function in an autocrine or paracrine manner [19]. To elucidate the downstream intracellular signaling effects of extracellular NPNT, we used high-throughput RPPA functional proteomics that allow the measurement of protein levels and relative amounts of phosphorylated proteins in several samples using 300 different antibodies simultaneously [20, 21]. The signal intensity from protein-antibody binding was quantified and used for data analysis. The three circles in the Venn diagram represent: 1) the proteins regulated by seeding control cells (66cl4-EV) on plates coated with rmNPNT (EV_{rmNPNT} vs EV), 2) the proteins regulated by the NPNT overexpression (NPNT vs EV), and 3) the proteins regulated by the integrin binding enhancer motif alone (RGE vs RGE-AIA) (Fig. 2a/ Table S1). The four proteins in the overlap between these three comparisons were identified as p38 MAPK, Src, Mnk1, and Rad51 (Fig. 2b) and may represent possible common players of NPNT induced signaling. Dual phosphorylation of p38 MAPK at T180 and Y182 activates downstream intracellular signals to regulate growth, differentiation, survival and respond to stress [22, 23]. Src is a downstream effector in integrin signaling and phosphorylation of Src at Y527 is usually transient and renders the enzyme less active [24, 25]. Rad51 is known for its role in DNA repair [26]. Mnk1 acts downstream in p38 MAPK signaling pathway [27]. The presence of either wild type NPNT or NPNT-RGE increased phosphorylation of p38 MAPK (T180 and Y182) and phosphorylation of Src (Y527), while the double mutant of NPNT did not (Fig. 2b). Rad51 protein levels increased when cells were seeded onto rmNPNT or expressing either wild type NPNT or NPNT-RGE, while cells expressing NPNT with the double mutation did not show any increase in Rad51 protein levels. For Mnk1 the effect was opposite. Compared to 66cl4-EV control cells, Mnk1 protein levels were reduced in cells seeded onto rmNPNT or expressing either wild type NPNT or NPNT carrying the RGD-mutation, while cells expressing NPNT mutated in both the RGD and the enhancer motif EIE did not display altered protein levels of Mnk1 (Fig. 2b). Suppression of Mnk1 expression has been reported to increase the eukaryotic transcription initiation factor 4F activity (eIF4F)[28], a factor known to promote survival of breast cancer cells [29]. Interestingly, in the presence of NPNT, total Mnk1 levels were reduced (Fig. 2b). Further studies are required to identify the involvement of transcription factors such as eIF4F, and apoptosis-regulating proteins influenced by NPNT induced signaling. The RPPA analysis suggests that NPNT influences on the total protein levels of Mnk1 and Rad51 and the phosphorylation status of p38 MAPK and Src. These results also point to the importance of the integrin enhancer motif in these regulatory processes.

3. 3. NPNT promotes cell viability via its enhancer motif

Ingenuity Pathway Analysis (IPA) can recognize the RPPA protein signal intensities and correlate them to their corresponding genes and then predict potential downstream cellular functions. We have utilized the dataset from the 'RGE vs RGE-AIA' group to specifically identify the molecular and cellular functions supported by the integrin-binding enhancer motif of NPNT. Cell death and survival, cellular growth and proliferation, and cellular development are some of the top categories which were predicted to be influenced by the NPNT enhancer motif (Table 1). In each of the categories we could investigate further the specific cellular functions using the up-and downregulated proteins expression values from the RGE vs RGE-AIA group. There were 69 proteins pointing towards a role of the NPNT enhancer motif in cell viability (Fig. 3 and Table 1). Rad51, p38 MAPK (shown as MAPK14), Mnk1 (shown as MKNK1) and Src are among those 69 proteins known to influence cell viability (Fig. 3). In line with our results, NPNT has also previously been reported involved in survival of osteoblasts [30]. NPNT is known to interact with integrin α8β1 [8, 31], and integrins activate survival pathways via PI3K-kinase or MAPKs [3, 32]. Phosphorylated p38 MAPK can have a pleiotropic role; mediating either cell survival or cell death depending on the cell type, disease stage and type of stimulus [33-35]. Activated p38 MAPK can phosphorylate various transcription factors as well as anti-apoptotic (Bcl-2) and pro-apoptotic (Bad) proteins [36]. In breast cancer, phosphorylated p38 MAPK has been linked to poor outcomes [37]. Interestingly, interference with p38 MAPK signaling in cancer cells has been shown to reduce the tumor promoting capacities of the microenvironment [38], potentiate the effect of conventional chemotherapies (reviewed in [39]), and was therefore chosen for further analysis in this study.

3. 4. NPNT mediates cell viability via p38 signaling pathways

Results from the RPPA and IPA analyses indicated that NPNT and its integrin binding motifs could be involved in determining cell viability via p38 MAPK phosphorylation in our study model. An *in vitro* cell viability assay was used to analyze the different 66cl4 cells. An increase in viability was seen when EV cells were incubated with serum free medium containing rmNPNT, or when 66cl4 cells were overexpressing wild-type NPNT. In cells where both integrin-binding motifs were mutated (RGE-AIA), there was a reduction in viability compared to cells overexpressing wild-type NPNT (Fig. 4a). Exposure of 66cl4-EV cells to rmNPNT (EV $_{\text{rmNPNT}}$) coating for 24 hours in serum free media stimulated p38 MAPK phosphorylation compared to control cells (Fig. S1a), thus confirming the results obtained from RPPA. To further explore the involvement of p38 MAPK in NPNT-induced viability, we utilized the p38 MAPK inhibitor, BIRB 796, known to inhibit all p38 MAPK isoforms *in vitro* [40]. The viability of control cells (EV) was unaffected by p38 MAPK inhibition, thereby excluding any off-target effects that may interfere with viability in this particular assay. On the other hand, a significant decrease in viability was seen in both 66cl4-NPNT and 66cl4-NPNT-RGE cells when phosphorylation of p38 MAPK was inhibited using BIRB 796, while addition of BIRB 796 to cells carrying the double mutation (RGE-AIA) had no statistically significant effect on cell viability. This indicates that p38 MAPK functions downstream of NPNT and regulates viability of the 66cl4 cells. These observations were further validated by comparing the parental 66cl4 cells, with low endogenous NPNT, to the parental 4T1 cells, with high endogenous NPNT levels [12, 14]. The 66cl4 cell line generally showed lower p38 MAPK phosphorylation compared to the 4T1 cells (Fig.S1b). When 4T1 cells were treated with the p38 MAPK inhibitor, viability was markedly reduced (Fig. 4b). Next, we analyzed 4T1 cells with stable shRNA knock-down of NPNT, 4T1 (sh-NPNT)[14]. The knock-down generally decreased the cell viability of the 4T1 (sh-NPNT) cells compared to the parental 4T1 cells. Furthermore, treatment with the p38 MAPK inhibitor did not further decrease the viability (Fig. 4b). 4T1 cells, expressing a non-targeting shRNA (sh-ctr), responded similarly as the 4T1 parental cells.

Taken together, these results demonstrate a role for NPNT and its integrin binding motifs, in particular the EIE-enhancer motif, in the induction of p38 MAPK signaling and cell viability. There are four members of the p38 family (p38α, p38β, p38γ, p38δ), of which p38α (MAPK14) is best studied and expressed in most cell types [41]. However, further investigation is needed to elaborate on the role specific role of the different p38 isoforms. Results from the current study are summarized in Fig. 4c and show that NPNT can activate p38 MAPK and by that promote viability in 66cl4 breast cancer cells. The requirement of the NPNT EIE-enhancer motif in the activation of p38 MAPK is a novel finding, making this a potential drug target in tumors with high NPNT expression. Interestingly, though the RGD motif has shown great promise as a therapeutic target [2], drugs such as Cilengitide have failed in clinical trials due to lack of efficiency [42]. Based on the current findings, we therefore suggest that dual targeting of the RGD and EIE-enhancer motif could prove to be more efficient for cancers with high NPNT levels.

Acknowledgements

The study received funding from the Central Norway Regional Health Authority (Project number: 46077600), North Norwegian Regional Health Authorities (Project number SFP1232-15) The Erna and Olav Aakre Foundation for Cancer Research, The Blix Family Fund for Medical Research, and UiT – The Arctic University of Norway. We also acknowledge services carried out at MD Anderson Cancer Center, USA funded by NCI # CA16672. Dr. Fred Miller kindly provided 66cl4 and 4T1, mouse cell lines. We express our gratitude to Dr. Naoko Morimura for the pcDNA3-POEM-Fc vector and Dr. Peter McCourt for linguistic revision. We appreciate the technical supervision received from Bjørnar Sporsheim and Kjartan Wøllo Egeberg with handling of confocal microscope.

References

[1] D.S. Dolberg, R. Hollingsworth, M. Hertle, M.J. Bissell, Wounding and its role in RSV-mediated tumor formation, Science (New York, N.Y.), 230 (1985) 676-678.

[2] M. Nieberler, U. Reuning, F. Reichart, J. Notni, H.J. Wester, M. Schwaiger, M. Weinmuller, A. Rader, K. Steiger, H. Kessler, Exploring the Role of RGD-Recognizing Integrins in Cancer, Cancers (Basel), 9 (2017).

[3] D.G. Stupack, Get a ligand, get a life: integrins, signaling and cell survival, Journal of Cell Science, 115 (2002) 3729-3738.

[4] P.H. Vachon, Integrin signaling, cell survival, and anoikis: distinctions, differences, and differentiation, Journal of signal transduction, 2011 (2011) 738137.

[5] N. Morimura, Y. Tezuka, N. Watanabe, M. Yasuda, S. Miyatani, N. Hozumi, K. Tezuka Ki, Molecular cloning of POEM: a novel adhesion molecule that interacts with alpha8beta1 integrin, J Biol Chem, 276 (2001) 42172-42181.

[6] R. Brandenberger, A. Schmidt, J. Linton, D. Wang, C. Backus, S. Denda, U. Müller, L.F. Reichardt, Identification and characterization of a novel extracellular matrix protein nephronectin that is associated with integrin α8β1 in the embryonic kidney, The Journal of Cell Biology, 154 (2001) 447-458.

[7] J. Sanchez-Cortes, M. Mrksich, Using self-assembled monolayers to understand alpha8beta1-mediated cell adhesion to RGD and FEI motifs in nephronectin, ACS Chem Biol, 6 (2011) 1078-1086.

[8] Y. Sato, T. Uemura, K. Morimitsu, R. Sato-Nishiuchi, R. Manabe, J. Takagi, M. Yamada, K. Sekiguchi, Molecular basis of the recognition of nephronectin by integrin alpha8beta1, J Biol Chem, 284 (2009) 14524-14536.

[9] P.B. dos Santos, J.S. Zanetti, A. Ribeiro-Silva, E.I. Beltrao, Beta 1 integrin predicts survival in breast cancer: a clinicopathological and immunohistochemical study, Diagnostic pathology, 7 (2012) 104.

[10] K.M. Moore, G.J. Thomas, S.W. Duffy, J. Warwick, R. Gabe, P. Chou, I.O. Ellis, A.R. Green, S. Haider, K. Brouilette, A. Saha, S. Vallath, R. Bowen, C. Chelala, D. Eccles, W.J. Tapper, A.M. Thompson, P. Quinlan, L. Jordan, C. Gillett, A. Brentnall, S. Violette, P.H. Weinreb, J. Kendrew, S.T. Barry, I.R. Hart, J.L. Jones, J.F. Marshall, Therapeutic targeting of integrin alphavbeta6 in breast cancer, J Natl Cancer Inst, 106 (2014).

[11] J. Insua-Rodriguez, T. Oskarsson, The extracellular matrix in breast cancer, Adv Drug Deliv Rev, 97 (2016) 41-55.

[12] B.L. Eckhardt, B.S. Parker, R.K. van Laar, C.M. Restall, A.L. Natoli, M.D. Tavaria, K.L. Stanley, E.K. Sloan, J.M. Moseley, R.L. Anderson, Genomic analysis of a spontaneous model of breast cancer metastasis to bone reveals a role for the extracellular matrix, Molecular cancer research : MCR, 3 (2005) 1-13.

[13] A.D. Borowsky, R. Namba, L.J. Young, K.W. Hunter, J.G. Hodgson, C.G. Tepper, E.T. McGoldrick, W.J. Muller, R.D. Cardiff, J.P. Gregg, Syngeneic mouse mammary carcinoma cell lines: two closely related cell lines with divergent metastatic behavior, Clinical & experimental metastasis, 22 (2005) 47-59.

[14] T.S. Steigedal, J. Toraskar, R.P. Redvers, M. Valla, S.N. Magnussen, A.M. Bofin, S. Opdahl, S. Lundgren, B.L. Eckhardt, J.M. Lamar, J. Doherty, R.O. Hynes, R.L. Anderson, G. Svineng, Nephronectin is Correlated with Poor Prognosis in Breast Cancer and Promotes Metastasis via its Integrin-Binding Motifs, Neoplasia (New York, N.Y.), 20 (2018) 387-400.

[15] B.T. Hennessy, Y. Lu, A.M. Gonzalez-Angulo, M.S. Carey, S. Myhre, Z. Ju, M.A. Davies, W. Liu, K. Coombes, F. Meric-Bernstam, I. Bedrosian, M. McGahren, R. Agarwal, F. Zhang, J. Overgaard, J. Alsner, R.M. Neve, W.L. Kuo, J.W. Gray, A.L. Borresen-Dale, G.B. Mills, A Technical Assessment of the Utility of Reverse Phase Protein Arrays for the Study of the Functional Proteome in Non-microdissected Human Breast Cancers, Clinical proteomics, 6 (2010) 129-151.

[16] Z. Ju, W. Liu, P.L. Roebuck, D.R. Siwak, N. Zhang, Y. Lu, M.A. Davies, R. Akbani, J.N. Weinstein, G.B. Mills, K.R. Coombes, Development of a robust classifier for quality control of reverse-phase protein arrays, Bioinformatics (Oxford, England), 31 (2015) 912-918.

[17] Y. Sun, V. Kuek, H. Qiu, J. Tickner, L. Chen, H. Wang, W. He, J. Xu, The emerging role of NPNT in tissue injury repair and bone homeostasis, Journal of cellular physiology, 233 (2018) 1887-1894.

[18] S. Kahai, S.C. Lee, D.Y. Lee, J. Yang, M. Li, C.H. Wang, Z. Jiang, Y. Zhang, C. Peng, B.B. Yang, MicroRNA miR-378 regulates nephronectin expression modulating osteoblast differentiation by targeting GalNT-7, PloS one, 4 (2009) e7535.

[19] M.H. Barcellos-Hoff, M.J. Bissell, A Role for the Extracellular Matrix in Autocrine and Paracrine Regulation of Tissue-Specific Functions, in: L.C. Krey, B.J. Gulyas, J.A. McCracken (Eds.) Autocrine and Paracrine Mechanisms in Reproductive Endocrinology, Springer US, Boston, MA, 1989, pp. 137-155.

[20] R. Akbani, K.F. Becker, N. Carragher, T. Goldstein, L. de Koning, U. Korf, L. Liotta, G.B. Mills, S.S. Nishizuka, M. Pawlak, E.F. Petricoin, 3rd, H.B. Pollard, B. Serrels, J. Zhu, Realizing the promise of reverse phase protein arrays for clinical, translational, and basic research: a workshop report: the RPPA (Reverse Phase Protein Array) society, Molecular & cellular proteomics : MCP, 13 (2014) 1625-1643.

[21]https://www.mdanderson.org/research/research-resources/core-facilities/functional-proteomics-rppa-core/antibody-information-and-protocols.html.

[22] K.P. Wilson, M.J. Fitzgibbon, P.R. Caron, J.P. Griffith, W. Chen, P.G. McCaffrey, S.P. Chambers, M.S. Su, Crystal structure of p38 mitogen-activated protein kinase, J Biol Chem, 271 (1996) 27696-27700.

[23] A. Cuadrado, A.R. Nebreda, Mechanisms and functions of p38 MAPK signalling, The Biochemical journal, 429 (2010) 403-417.

[24] M.P. Playford, M.D. Schaller, The interplay between Src and integrins in normal and tumor biology, Oncogene, 23 (2004) 7928-7946.

[25] S. Zhang, D. Yu, Targeting Src family kinases in anti-cancer therapies: turning promise into triumph, Trends in Pharmacological Sciences, 33 (2012) 122-128.

[26] P. Sung, L. Krejci, S. Van Komen, M.G. Sehorn, Rad51 recombinase and recombination mediators, J Biol Chem, 278 (2003) 42729-42732.

[27] R. Fukunaga, T. Hunter, MNK1, a new MAP kinase-activated protein kinase, isolated by a novel expression screening method for identifying protein kinase substrates, The EMBO journal, 16 (1997) 1921-1933.

[28] A. O'Loghlen, V.M. Gonzalez, M. Salinas, M.E. Martin, Suppression of human Mnk1 by small interfering RNA increases the eukaryotic initiation factor 4F activity in HEK293T cells, FEBS letters, 578 (2004) 31-35.

[29] H.G. Wendel, E. De Stanchina, J.S. Fridman, A. Malina, S. Ray, S. Kogan, C. Cordon-Cardo, J. Pelletier, S.W. Lowe, Survival signalling by Akt and eIF4E in oncogenesis and cancer therapy, Nature, 428 (2004) 332-337.

[30] M. Ikehata, A. Yamada, N. Morimura, M. Itose, T. Suzawa, T. Shirota, D. Chikazu, R. Kamijo, Wnt/beta-catenin signaling activates nephronectin expression in osteoblasts, Biochem Biophys Res Commun, 484 (2017) 231-234.
[31] L.M. Schnapp, N. Hatch, D.M. Ramos, I.V. Klimanskaya, D. Sheppard, R. Pytela, The human integrin alpha 8 beta 1 functions as a receptor for tenascin, fibronectin, and vitronectin, J Biol Chem, 270 (1995) 23196-23202.
[32] E. Farias, M. Lu, X. Li, L.M. Schnapp, Integrin alpha8beta1-fibronectin interactions promote cell survival via PI3 kinase pathway, Biochem Biophys Res Commun, 329 (2005) 305-311.
[33] H.K. Koul, M. Pal, S. Koul, Role of p38 MAP Kinase Signal Transduction in Solid Tumors, Genes Cancer, 4 (2013) 342-359.
[34] J.S. Park, S. Carter, D.B. Reardon, R. Schmidt-Ullrich, P. Dent, P.B. Fisher, Roles for basal and stimulated p21(Cip-1/WAF1/MDA6) expression and mitogen-activated protein kinase signaling in radiation-induced cell cycle checkpoint control in carcinoma cells, Molecular biology of the cell, 10 (1999) 4231-4246.
[35] H.C. Reinhardt, A.S. Aslanian, J.A. Lees, M.B. Yaffe, p53-deficient cells rely on ATM- and ATR-mediated checkpoint signaling through the p38MAPK/MK2 pathway for survival after DNA damage, Cancer Cell, 11 (2007) 175-189.
[36] K. Takeda, I. Naguro, H. Nishitoh, A. Matsuzawa, H. Ichijo, Apoptosis signaling kinases: from stress response to health outcomes, Antioxidants & redox signaling, 15 (2011) 719-761.
[37] F.J. Esteva, A.A. Sahin, T.L. Smith, Y. Yang, L. Pusztai, R. Nahta, T.A. Buchholz, A.U. Buzdar, G.N. Hortobagyi, S.S. Bacus, Prognostic significance of phosphorylated P38 mitogen-activated protein kinase and HER-2 expression in lymph node-positive breast carcinoma, Cancer, 100 (2004) 499-506.
[38] C. Suarez-Cuervo, M.A. Merrell, L. Watson, K.W. Harris, E.L. Rosenthal, H.K. Vaananen, K.S. Selander, Breast cancer cells with inhibition of p38alpha have decreased MMP-9 activity and exhibit decreased bone metastasis in mice, Clinical & experimental metastasis, 21 (2004) 525-533.
[39] A. Igea, A.R. Nebreda, The Stress Kinase p38alpha as a Target for Cancer Therapy, Cancer Res, 75 (2015) 3997-4002.
[40] Y. Kuma, G. Sabio, J. Bain, N. Shpiro, R. Marquez, A. Cuenda, BIRB796 inhibits all p38 MAPK isoforms in vitro and in vivo, J Biol Chem, 280 (2005) 19472-19479.
[41] A. Cuenda, S. Rousseau, p38 MAP-kinases pathway regulation, function and role in human diseases, Biochim Biophys Acta, 1773 (2007) 1358-1375.
[42] R. Stupp, M.E. Hegi, T. Gorlia, S.C. Erridge, J. Perry, Y.K. Hong, K.D. Aldape, B. Lhermitte, T. Pietsch, D. Grujicic, J.P. Steinbach, W. Wick, R. Tarnawski, D.H. Nam, P. Hau, A. Weyerbrock, M.J. Taphoorn, C.C. Shen, N. Rao, L. Thurzo, U. Herrlinger, T. Gupta, R.D. Kortmann, K. Adamska, C. McBain, A.A. Brandes, J.C. Tonn, O. Schnell, T. Wiegel, C.Y. Kim, L.B. Nabors, D.A. Reardon, M.J. van den Bent, C. Hicking, A. Markivskyy, M. Picard, M. Weller, Cilengitide combined with standard treatment for patients with newly diagnosed glioblastoma with methylated MGMT promoter (CENTRIC EORTC 26071-22072 study): a multicentre, randomised, open-label, phase 3 trial, The Lancet. Oncology, 15 (2014) 1100-1108.

Figure legends

Fig. 1: *Cell surface distribution of NPNT in 66cl4 cells* **(a)** Immunofluorescence microscopy showing extracellular NPNT detected on 66cl4 cells expressing wild type NPNT and 66cl4-EV cells when pre-incubated with rmNPNT for 1 hour prior fixing. 66cl4-EV was used as a negative control. Detection of collagen V on 66cl4-NPNT cells was used as a positive control. Primary antibodies were visualized with Alexa Fluor 488. Nucleus is stained blue with Hoechst. Scale bar 10 µm. **(b)** Z profile comparing the green and blue channels was calculated by normalizing mean intensity per slice in the stack for each channel using the image of 66cl4 cells overexpressing NPNT shown above. **(c)** Brightfield microscopy images of 66cl4-EV cells growing on uncoated plates (EV) in contrast to rmNPNT coated plates (EV_{rmNPNT}) at 24 hours.

Fig. 2: *RPPA analysis of NPNT-mediated signaling.* The Venn diagram includes number of proteins significantly regulated and/or modified (p<0. 05) in all four biological replicates. **(a)** The pink circle in the Venn diagram, 'NPNT vs EV' denotes the log fold change values triggered in 66cl4-NPNT cells in comparison to 66cl4-EV cells. The blue circle, 'EV_{rmNPNT} vs EV' represents 66cl4-EV cells cultured on rmNPNT (EV_{rmNPNT}) in comparison to 66cl4-EV cells seeded in non-coated wells. The purple circle represents proteins regulated by the integrin binding motifs of NPNT; the effect of a single mutation in the RGD motif (RGD -> RGE) versus mutations in both RGD and EIE motifs (RGD-EIE -> RGE-AIA). **(b)** Box plot showing log2 protein abundance of the four overlapping proteins from the Venn diagram.

Fig. 3: *NPNT promotes cell viability via its enhancer motif.* Representation of the 69 upregulated (red) or downregulated (green) proteins (shown as gene symbols) identified by IPA to have a direct relationship with cell viability. The asterisk indicates that multiple proteins in the dataset file map to a single gene.

Fig. 4: *NPNT mediates cell viability via p38 signaling pathways* **(a)** Indicated variants of 66cl4 cells were treated with (+/-) 4 µM p38 MAPK inhibitor (BIRB 796) for 24 hours, in addition to serum deprivation. Where indicated, 66cl4-EV cells were stimulated by adding 2 µg/ml rmNPNT to the cell culture medium. Cell viability was determined using CellTiter-Glo. **(b)** Viability of NPNT expressing, 4T1 cells with a NPNT-targeted short hairpin (sh-NPNT) and a non-targeting shRNA (sh-ctr) was tested using CellTiter-Glo. Significance is tested using a two tailed Student's t-test. **P*<0. 05, ***P*<0. 005, *** *P*<0. 0001. N = number of independent

experiments, n = total number of replicates in each test group. **(c)** Illustration summarizing the cellular effects of integrin binding to wild-type or mutated NPNT via p38 MAPK.

Table 1: *Top predicted molecular and cellular functions.* RPPA results from RGE vs RGE-AIA group were analyzed using the web-based software application Ingenuity Pathway Analysis (IPA) tool to identify the most significant NPNT-responsive functions.

Categories	Sub-categories	p-Value	Predicted Activation State	No. of Molecules
Cell Death and Survival				
	Cell viability	2.18E-44	Increased	69
Cellular Growth and Proliferation				
	Colony formation	6.2E-35	Increased	44
Cellular Development				
	Maturation of cells	1.03E-24	Increased	32

Figure 1

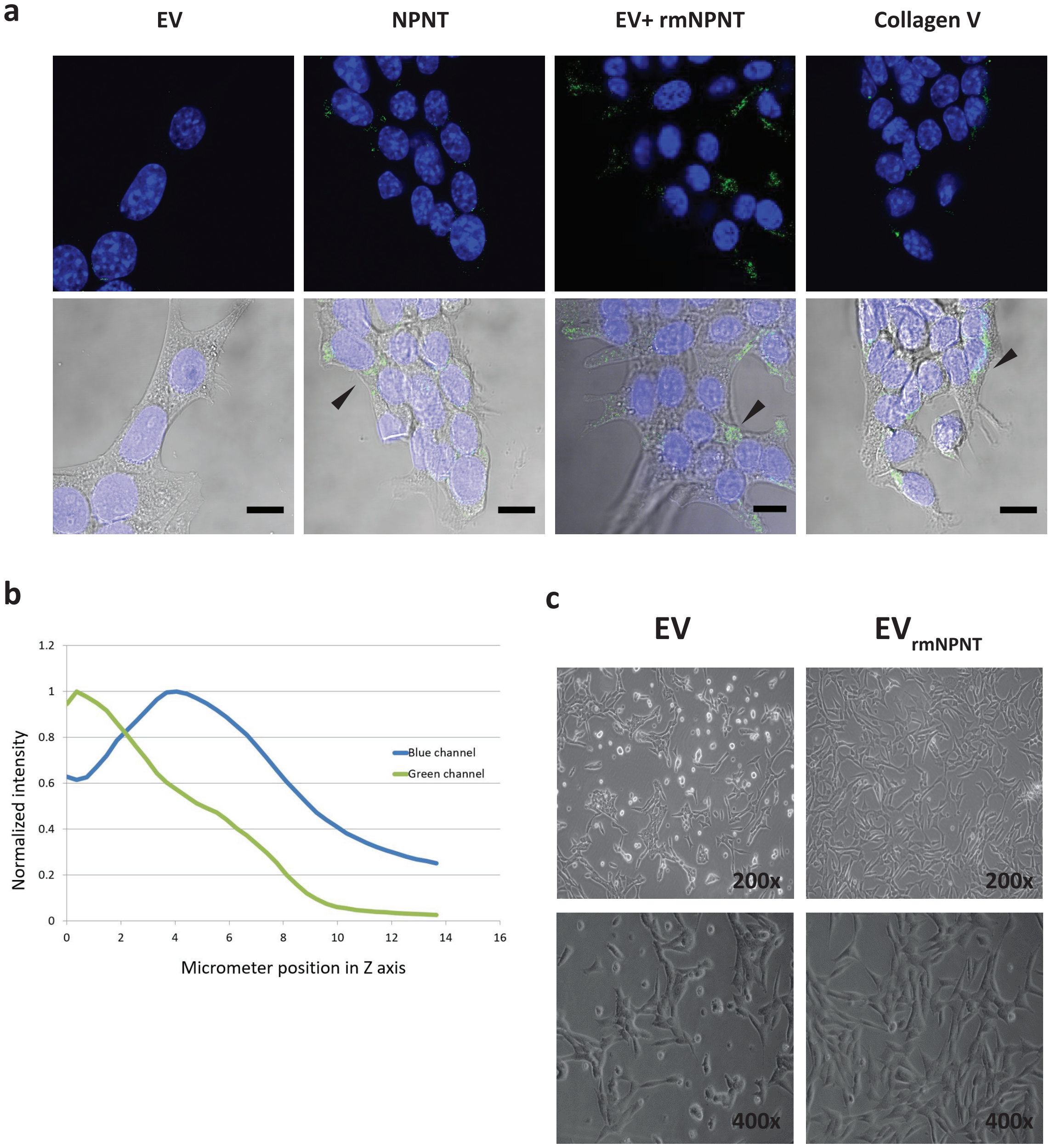
a
EV
NPNT
EV+ rmNPNT
Collagen V
b
1.2
1
0.8
0.6
0.4
0.2
0
Normalized intensity
0
2
4
6
8
10
12
14
16
Micrometer position in Z axis
Blue channel
Green channel
c
EV
EV$_{rmNPNT}$
200x
200x
400x
400x

Figure 2

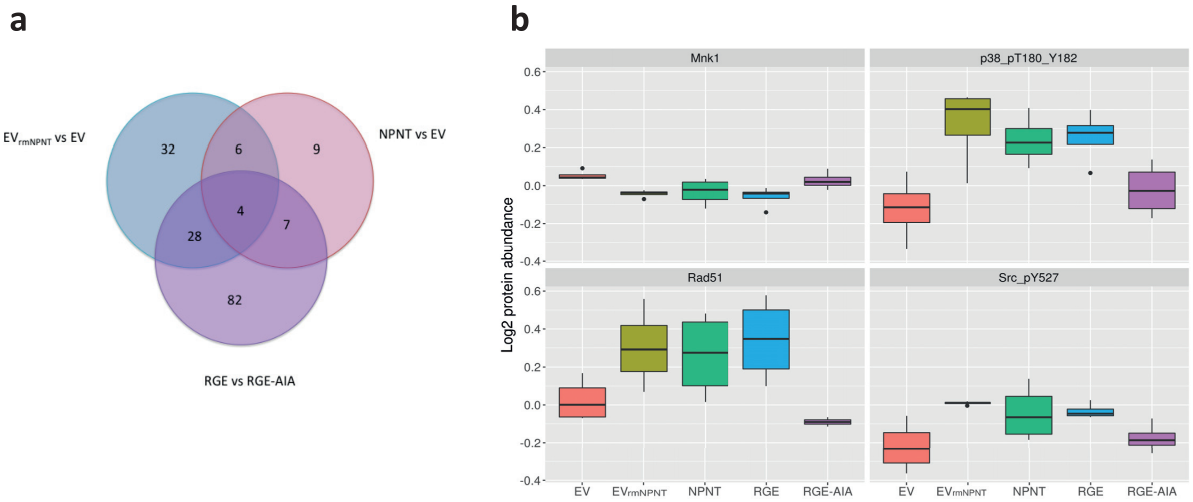
a
EV$_{rmNPNT}$ vs EV
NPNT vs EV
RGE vs RGE-AIA
32
6
9
4
28
7
82
b
Mnk1
p38_pT180_Y182
Rad51
Src_pY527
Log2 protein abundance
0.6
0.4
0.2
0.0
-0.2
-0.4
EV
EV$_{rmNPNT}$
NPNT
RGE
RGE-AIA

Figure 3

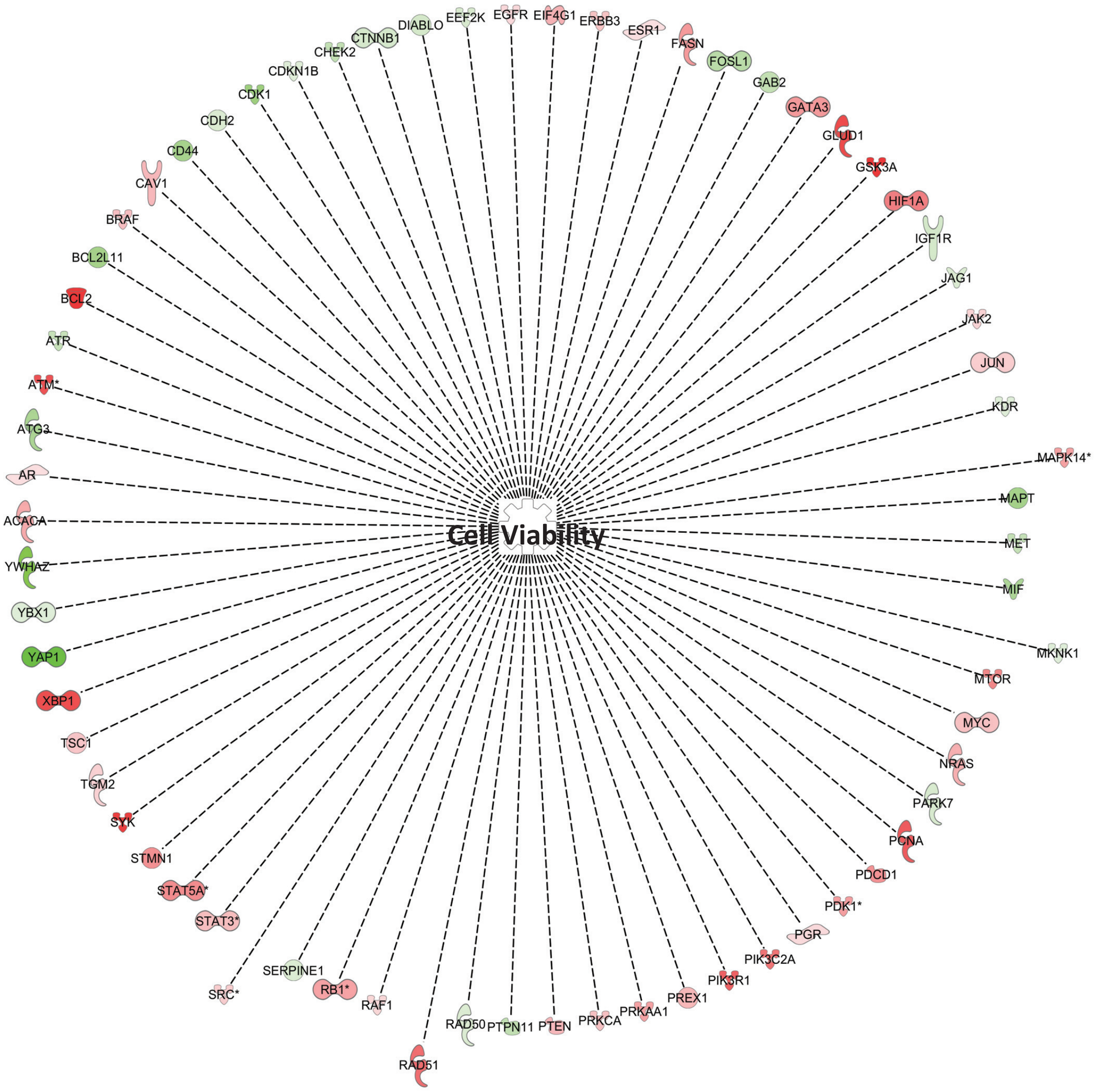
Cell Viability
ACACA
AR
ATG3
ATM*
ATR
BCL2
BCL2L11
BRAF
CAV1
CD44
CDH2
CDK1
CDKN1B
CHEK2
CTNNB1
DIABLO
EEF2K
EGFR
EIF4G1
ERBB3
ESR1
FASN
FOSL1
GAB2
GATA3
GLUD1
GSK3A
HIF1A
IGF1R
JAG1
JAK2
JUN
KDR
MAPK14*
MAPT
MET
MIF
MKNK1
MTOR
MYC
NRAS
PARK7
PCNA
PDCD1
PDK1*
PGR
PIK3C2A
PIK3R1
PREX1
PRKAA1
PRKCA
PTEN
PTPN11
RAD50
RAD51
RAF1
RB1*
SERPINE1
SRC*
STAT3*
STAT5A*
STMN1
SYK
TGM2
TSC1
XBP1
YAP1
YBX1
YWHAZ

Figure 4

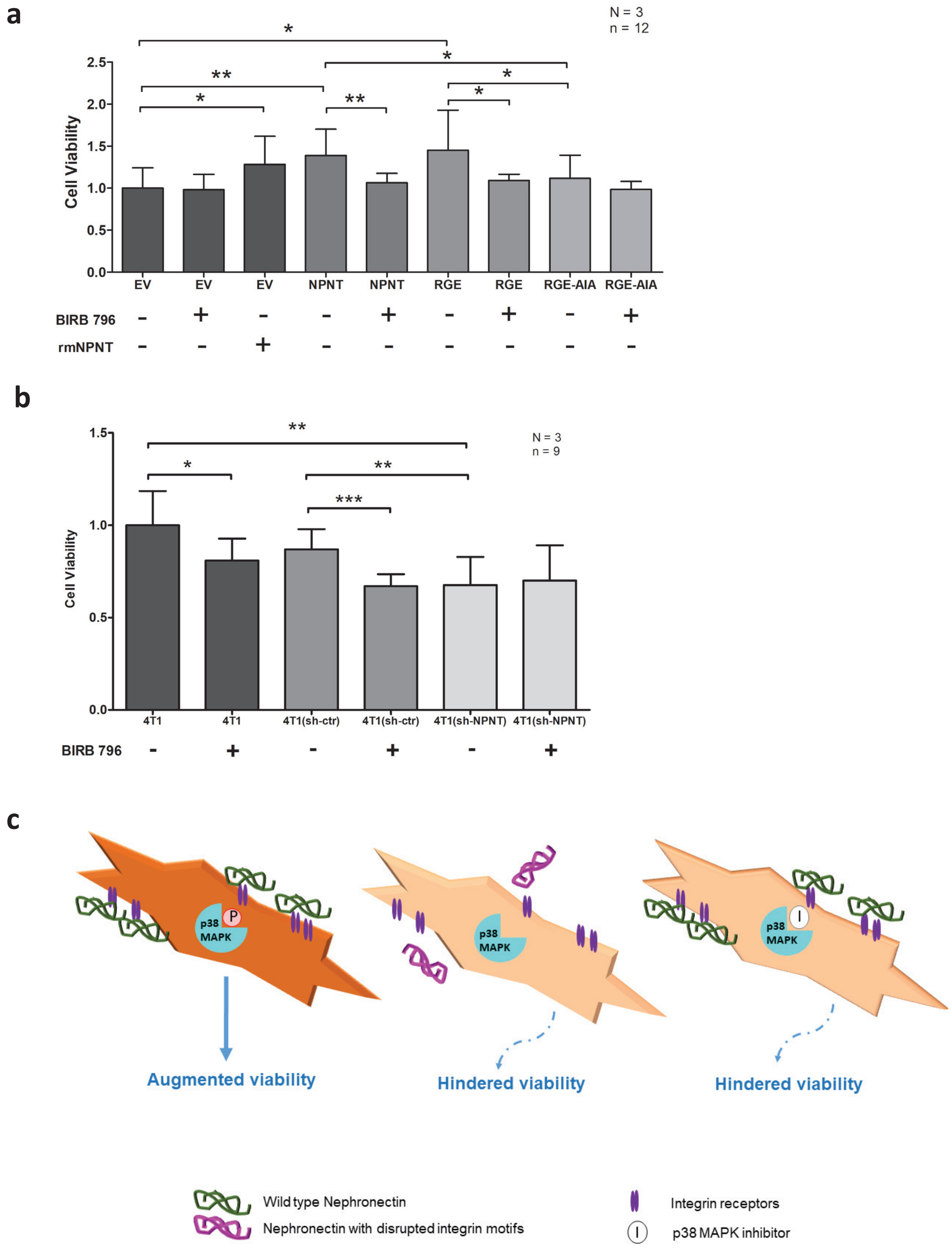
a
N = 3
n = 12
Cell Viability
2.5
2.0
1.5
1.0
0.5
0.0
*
**
*
**
*
*
*
EV
EV
EV
NPNT
NPNT
RGE
RGE
RGE-AIA
RGE-AIA
BIRB 796
-
+
-
-
+
-
+
-
+
rmNPNT
-
-
+
-
-
-
-
-
-
b
N = 3
n = 9
Cell Viability
1.5
1.0
0.5
0.0
**
*
**
***
4T1
4T1
4T1(sh-ctr)
4T1(sh-ctr)
4T1(sh-NPNT)
4T1(sh-NPNT)
BIRB 796
-
+
-
+
-
+
c
p38 MAPK
P
p38 MAPK
p38 MAPK
I
Augmented viability
Hindered viability
Hindered viability
Wild type Nephronectin
Nephronectin with disrupted integrin motifs
Integrin receptors
I
p38 MAPK inhibitor

Supplementary legends

Video S1: Z-stack sections in 66cl4-NPNT cells were compiled to visualize the signal for NPNT (green channel). Each image in the section has a voxel depth of 0.36 µm. Assuming the reflection coming from the culture plate to be zero, we get the highest intensity for NPNT-alexa488 at the 4th section. This means we get the highest intensity signal for NPNT at 1.4 µm (0.36*4).

Table S1: *RPPA details*. List of differentially expressed proteins shown in the Venn diagram, Fig.2a.

Fig. S1: *Phosphorylation of p38 MAPK in the presence of NPNT* **(a)** Immunoblotting for detecting phosphorylation levels of p38 MAPK using whole cell lysates made of 66cl4-EV and 66cl4-$EV_{rmNPNT.}$ cultured under serum-free conditions for 24 hours. **(b)** Immunoblotting for phospho-p38 MAPK and total-p38 MAPK level using lysates from mother cell lines, 66cl4 and 4T1, grown on uncoated plates for 24 hours in serum free conditions. Quantification of optical density represents the mean of three independent experiments. Significance is tested using a two tailed Student's t-test assuming equal variance. *P<0. 05, **P<0. 005, *** P<0. 0001.

Figure S1

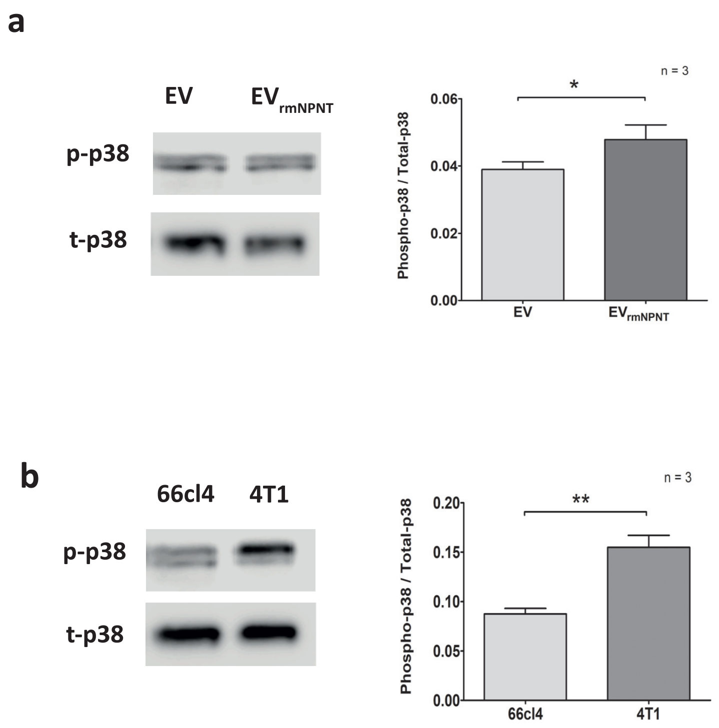
a
EV
EV$_{rmNPNT}$
p-p38
t-p38
n = 3
*
Phospho-p38 / Total-p38
0.06
0.04
0.02
0.00
EV
EV$_{rmNPNT}$
b
66cl4
4T1
p-p38
t-p38
n = 3
**
Phospho-p38 / Total-p38
0.20
0.15
0.10
0.05
0.00
66cl4
4T1

Table S1

Gene	Antibody	logFC_EVR-EV	P.Value_EVR-EV	logFC_NPNT-EV	P.Value_NPNT-EV	logFC_ΔRGD-ΔRGDΔEIE	P.Value_ΔRGD-ΔRGDΔEIE
OCT.4	Src_pY416	0.010841896	0.859928626	-0.199031547	0.003577582	-0.121005703	0.059319053
NDRG1	NDRG1_pT346	0.12985959	0.128585858	0.204107433	0.021390075	-0.123593956	0.147036728
RPS6K	p90RSK_pT573	0.02305851	0.592315755	0.135998935	0.004232499	0.056035382	0.200561927
AXL	Axl	-0.093680316	0.08622482	-0.119237838	0.032392378	-0.051052068	0.337759623
RPS6KA1	RSK	0.026772041	0.488312547	0.101693825	0.014034972	0.030206985	0.4349922
PEA15	PEA.15	-0.018206461	0.743911619	-0.264138063	9.58E-05	0.035186817	0.5292585
PRKCB	PKC.b.II_pS660	0.076711007	0.346638843	0.179993258	0.034649857	0.023803343	0.768078618
PPIF	Cyclophilin.F	0.102598484	0.127809535	0.207899401	0.004179538	-0.017494291	0.789538231
PARP1	PARP1	-0.021901747	0.687525881	0.149009265	0.011356545	0.002638478	0.961279244
EIFGE	eIF4E	-0.286541849	8.72E-07	-0.076171619	0.082225137	0.006917994	0.869923258
EIF4E	eIF4E_pS209	-0.177262142	0.009353489	-0.048551114	0.442004424	-0.119593387	0.067189766
HISTH3	DM.Histone.H3	-0.16586435	0.003043858	-0.072392125	0.158675516	-0.079457394	0.123613483
VTCN	B7.H4	-0.152418251	0.005817337	-0.041814032	0.409222732	-0.057345952	0.261107587
PAK1	PAK1	-0.118556383	0.01778206	-0.048009811	0.309513559	0.044774286	0.342476515
COG3	COG3	-0.113149353	0.001751114	-0.046011593	0.159854093	-0.030897134	0.338955529
IRF1	IRF.1	-0.1089811	0.008086753	-0.004362232	0.907896987	0.026891125	0.478354829
SDHA	SDHA	-0.107478327	0.003070932	-0.030659898	0.350851124	0.038447366	0.244825362
INPP4B	INPP4b	-0.105221053	0.039265664	-0.064828556	0.189969325	0.043837408	0.370103022
BCL2A1	Bcl2A1	-0.09759928	0.02797047	-0.005585186	0.893810474	0.033001802	0.43360579
TUBAIA	D.a.Tubulin	-0.093536589	0.01949652	0.018707464	0.618200662	-0.04663383	0.221109173
COL6A1	Collagen.VI	-0.084837539	0.04511025	-0.039111657	0.337167211	-0.024092646	0.551626931
FOXM1	FoxM1	-0.083951112	0.026349329	-0.068037041	0.0664093	0.01509842	0.671797895
DPP4	CD26	-0.083485563	0.009079862	-0.000123805	0.996639389	0.024442003	0.409556239
RPS6KB1	p70.S6K_pT389	-0.079206902	0.010391297	-0.013761868	0.629924797	0.025827951	0.36919508
RAB11A	Rab11	-0.070061242	0.031784174	0.001940262	0.949808319	0.059461926	0.064365285
PAICS	PAICS	-0.064316894	0.033623982	-0.00404692	0.887619004	0.009274613	0.746290474
PRKAA2	AMPK.a2_pS345	-0.061634967	0.040693031	-0.029870303	0.302511146	0.045301703	0.123851561
XPA	XPA	0.091776164	0.046278508	0.004005798	0.927221526	0.002448143	0.955479891
PDCD4	Pdcd4	0.111694673	0.006121611	0.042539625	0.25882744	-0.021915465	0.556288155
EGFR	EGFR_pY1173	0.142704638	0.003222898	0.015594573	0.720037385	0.016245895	0.708903931

BRAF	B.Raf	0.143136761	0.022107232	0.079508624	0.184321579	-0.05261506	0.373971176
KIT	c.Kit	0.145101499	0.003407721	-0.021682657	0.627007383	0.03996869	0.373618497
XPF	XPF	0.147511205	0.024840166	0.065463163	0.295634318	0.029642067	0.632231381
CHEK2	Chk2_pT68	0.153235863	0.002935154	-0.000662144	0.988538896	-0.027069286	0.558670316
BAK1	Bak	0.163774926	0.000961101	-0.019257299	0.656570781	-0.042127032	0.335009612
RBM15	RBM15	0.163888082	0.043168199	0.077201593	0.322207772	0.14938796	0.063180639
ACACA	ACC1	0.186115032	0.001691448	0.094212787	0.082826259	0.086304025	0.110061567
ADAR1	ADAR1	0.189157306	0.004716095	0.084933023	0.170540121	-0.060041131	0.327182583
BAD	Bad_pS112	0.19077437	0.015144991	0.06493262	0.37819343	0.005663996	0.938151317
PTGS3	Cox.IV	0.26125845	0.04423033	0.121260188	0.331834374	0.084071436	0.498535376
ATRX	ATRX	0.441560179	0.000288392	0.209134569	0.052482465	0.092194559	0.375148045
ETS1	Ets.1	-0.24623588	0.06927583	-0.05257617	0.68683031	-0.279814761	0.041150018
STAT5A	Stat5a	-0.142443749	0.263266187	-0.046969271	0.708461848	0.282508638	0.033172859
CD44	CD44	-0.136896287	0.058748411	-0.097608962	0.168815912	-0.25418844	0.001293425
PAX8	PAX8	-0.12902807	0.052715487	-0.103487803	0.114480333	-0.155227829	0.022159842
MIF	MIF	-0.123585016	0.055686488	-0.042396682	0.494707367	-0.230868007	0.001087222
RIP	RIP	-0.110898943	0.078537106	-0.065946122	0.283905939	-0.14317919	0.026435731
STMN1	Stathmin.1	-0.106873349	0.090907339	0.062580773	0.311252205	0.325501624	2.36E-05
RPS6	S6	-0.100320062	0.272249847	0.122206427	0.184090583	0.618558608	7.25E-07
JAK2	Jak2	-0.093043419	0.137763077	0.005190019	0.932225448	0.130330179	0.042366766
ERBB3	HER3_pY1289	-0.082071698	0.076120017	0.005554968	0.900713455	0.1704616	0.000875902
RB1	Rb_pS807_S811	-0.080211575	0.198773875	0.084367222	0.177389499	0.272440739	0.000193432
CD274	PD.L1	-0.079250708	0.210127632	-0.040090933	0.520215824	-0.13725498	0.036113823
IRS1	Caspase.8	-0.075656862	0.087739806	-0.042266129	0.32846331	-0.255188473	5.40E-06
ATR	ATR_pS428	-0.074118177	0.123213215	0.014939205	0.749366097	-0.15049661	0.0037357
SLC16A4	MCT4	-0.074049974	0.169962279	-0.033335646	0.529247715	-0.215067668	0.000479245
CHEK2	Chk2	-0.072409715	0.137021591	-0.057555577	0.232693581	-0.166564001	0.001866563
ITGA2	CD49b	-0.070477613	0.293657782	-0.040676332	0.540864426	-0.192002743	0.007923994
LRP6	LRP6_pS1490	-0.06717084	0.1774789	-0.07150005	0.152314813	0.133425125	0.011431101
MAPT	Tau	-0.062395444	0.221092273	-0.076753433	0.135763287	-0.257570846	3.69E-05
ERRFI1	MIG6	-0.062153995	0.366262602	0.016436188	0.809445804	-0.233903709	0.002261128
RPS6	S6_pS240_S244	-0.060497054	0.493076291	-0.132538491	0.141355629	0.583551272	1.17E-06
STAT3	Stat3	-0.055701468	0.371308701	0.046839233	0.450905709	0.190003977	0.00522358

ERCC5	ERCC5	-0.052678636	0.434744702	0.005678998	0.932399452	0.139346193	0.04736543
CDK1	CDK1	-0.051803038	0.516303227	-0.043441031	0.585679241	-0.288282797	0.001413071
PRKCA	PKC.a_pS657	-0.04906814	0.267230377	0.029228294	0.504612536	0.181332531	0.000391586
ATM	ATM	-0.047968961	0.162880714	-0.006457284	0.847514389	-0.077417244	0.029609533
JAG1	Jagged1	-0.047881169	0.134252578	-0.003182651	0.918517383	-0.09818323	0.004363219
EGFR	EGFR	-0.046248481	0.165405283	-0.023547714	0.472412576	0.114797481	0.001819312
AR	AR	-0.046088659	0.062539906	0.018635487	0.435320463	0.066564727	0.009789579
STAT3	Stat3_pY705	-0.035477589	0.360028948	-0.028347099	0.462936009	-0.080594107	0.045551124
CTNNB1	b.Catenin_pT41_S45	-0.033505217	0.312614534	-0.05735598	0.091057145	-0.106275338	0.003559074
PDK1	PDK1	-0.027585885	0.47377725	-0.011244258	0.769131392	0.129243811	0.002589121
AIM1	Aurora.B	-0.026175699	0.577663942	-0.014625343	0.755107967	-0.115335763	0.021136161
RAD50	Rad50	-0.025952339	0.52565683	-0.020336173	0.618310478	-0.094663674	0.02837916
MET	c.Met	-0.024489838	0.544944591	0.000158597	0.996858097	-0.159174455	0.000650794
CCND3	Cyclin.D3	-0.022619542	0.623427285	-0.014910144	0.745795844	-0.211129655	0.000137094
KDR	VEGFR.2	-0.01874291	0.623462434	-0.047708124	0.218562681	-0.08109134	0.042849941
ZAP70	ZAP.70	-0.014832379	0.607562841	-0.016651765	0.564566627	-0.137402663	8.97E-05
HSBP1	HSP27	-0.014718348	0.695397134	-0.031443265	0.405971563	-0.109546266	0.007567776
SRSF1	SF2	-0.010048075	0.839989411	-0.091152176	0.077772327	-0.10414897	0.046192953
SERPINE1	PAI.1	-0.001098447	0.976441751	-0.019783529	0.596081521	-0.096219962	0.01608023
PGR	PR	0.013953375	0.662744049	0.000534999	0.986627586	0.108753278	0.002411584
MYO2A	Myosin.IIa_pS1943	0.016925246	0.895313858	-0.186257632	0.15755114	0.555362518	0.000268208
SRC	Src	0.017168638	0.625888536	-0.031389495	0.375929945	-0.077330952	0.036898784
BCL2	Bcl2	0.021526902	0.814637213	0.1118771	0.23088983	0.608702749	1.21E-06
BABAM1	MERIT40_pS29	0.036231852	0.509208042	0.041995301	0.44504925	-0.149575781	0.011418788
ESR1	ER.a_pS118	0.036511998	0.326137609	-0.006988723	0.849240356	0.076483908	0.047400279
DUSP4	DUSP4	0.037748815	0.384226478	0.05167028	0.23730774	-0.138600055	0.003717624
TSC1	TSC1	0.038402189	0.513236891	0.002359229	0.967794137	0.169550236	0.007886624
MAPK14	p38.MAPK	0.038702778	0.519325362	-0.010594048	0.859341671	0.160476538	0.012899053
CLDN7	Claudin.7	0.03919715	0.33003421	-0.029596217	0.459853325	-0.091553367	0.02991888
ATG3	Atg3	0.039864544	0.326379143	-0.055223704	0.178465566	-0.237954801	5.94E-06
INSRB	IR.b	0.043895959	0.240157216	-0.013944201	0.704832151	-0.242655112	1.30E-06
RPS6	S6_pS235_S236	0.044007241	0.580626135	-0.144956589	0.078674408	0.576292853	3.13E-07
PTEN	PTEN	0.046721648	0.537115398	0.049179606	0.516126559	0.204596137	0.012061449

PIK3R1	PI3K.p85	0.04799038	0.558182895	-0.015673205	0.847784646	0.471462799	8.40E-06
CDKN1B	p27.Kip.1	0.050285245	0.097826752	-0.032333911	0.277828096	-0.064462784	0.037473856
GYS1	Gys_pS641	0.056593654	0.141985965	0.014711703	0.695639825	0.120286154	0.003895393
PIK3C2A	PI3K.p110.a	0.060398374	0.185781613	0.027744048	0.536528747	0.414514452	5.79E-09
RAF1	C.Raf_pS338	0.060651417	0.24215569	-0.030148365	0.556065984	0.116150924	0.03148099
CMC2	Cox2	0.062736902	0.247852474	0.045618427	0.397187055	0.173175932	0.003564618
YWHAZ	X14.3.3.zeta	0.06886934	0.053877355	0.060229985	0.088528565	-0.391894011	1.32E-10
TGM2	Transglutaminase	0.071565479	0.11478092	0.067789233	0.134047521	0.131034142	0.006628571
PREX1	PREX1	0.075007558	0.146032106	0.020748224	0.68048169	0.207242103	0.000431732
CAV1	Caveolin.1	0.077197667	0.191843147	0.073823106	0.211208356	0.203233857	0.00189406
BRAF	B.Raf_pS445	0.079218225	0.120565204	0.016779782	0.735199394	0.184977801	0.001102708
PDK1	PDK1_pS241	0.079914047	0.187143368	0.04371726	0.463967924	0.284910973	8.32E-05
AKT1S1	PRAS40	0.089180841	0.15782481	0.089896102	0.154673593	-0.147451553	0.024587132
HIF1A	Hif.1.alpha	0.090887126	0.453496951	0.059749817	0.620812794	0.380133714	0.004359705
PECAM1	CD31	0.095586677	0.259966388	0.086221984	0.308209879	0.25213528	0.006030841
MTOR	mTOR	0.096963435	0.256533156	0.071651694	0.398472072	0.354568269	0.000344771
IGF1R	IGF1R_pY1135_Y1136	0.104384733	0.067000044	-0.066714108	0.230615232	-0.116067304	0.04354526
FASN	FASN	0.129915823	0.215420347	0.116645715	0.264331341	0.299338935	0.007766726
NRAS	N.Ras	0.162977207	0.090284241	0.075807072	0.418127123	0.232094005	0.019527667
PTPN11	SHP.2_pY542	0.164667579	0.052655471	-0.075269965	0.358503838	-0.167158762	0.049474038
H2BFM	Ubq.Histone.H2B	0.175192546	0.077538719	0.070173058	0.465456957	0.225431746	0.026399824
UGT1A	UGT1A	0.191734199	0.133091477	0.117269608	0.350081848	0.282680731	0.031551219
GCLM	GCLM	0.229237306	0.052816698	0.221633358	0.060456045	0.288035863	0.01751469
TUFM	TUFM	0.252053172	0.057169679	0.201571544	0.122453915	0.33866827	0.013290559
BIRC3	c.IAP2	0.254490259	0.06560264	0.166646811	0.217269485	0.367451273	0.010616151
XBP1	XBP.1	0.272913156	0.069291241	0.208365731	0.158644233	0.535795307	0.001156009
GLUD	Glutamate.D1.2	0.299109662	0.053810036	0.257603361	0.093062613	0.547029623	0.0012187
RAD51	Rad51	0.277689076	0.02080928	0.236844685	0.045004947	0.432818593	0.000833905
MKNK1	Mnk1	-0.095639723	0.012035793	-0.085073612	0.023390492	-0.085685561	0.022524168
SRC	Src_pY527	0.231436637	0.001097655	0.17804457	0.008408807	0.142631082	0.029880155
MAPK14	p38_pT180_Y182	0.443183228	0.002851851	0.361230351	0.011944446	0.277404051	0.046704223
ENY2	ENY2	0.149053983	0.00124477	-0.02771387	0.495878983	-0.474792149	8.88E-11
BCL2L11	Bim	0.124716628	0.011516864	-0.085089951	0.072811718	-0.258145766	1.09E-05

CD29	CD29	0.15358763	0.005325362	-0.017401399	0.728250087	-0.283137408	1.10E-05
MYC	c.Myc	-0.129011755	0.010135304	0.055706739	0.23598644	0.179104929	0.000782038
ATM	ATM_pS1981	0.381164231	0.010504675	0.217610246	0.123657941	0.522576053	0.00092565
EIF4G1	eIF4G	-0.212356374	0.001424972	0.062187281	0.294628816	0.221352744	0.000984505
ULK1	ULK1_pS757	-0.199175311	0.002312556	0.026743305	0.646480492	-0.205217527	0.001804423
GSK3A.B	GSK.3a.b	0.372883033	0.041719476	0.286413764	0.110572232	0.607912199	0.001959158
ROCK1	Rock.1	-0.242367023	0.009100975	-0.103112645	0.235109657	-0.293481519	0.00224024
STAT5	Stat5_pY694	0.215838245	0.040461951	0.093388214	0.355454213	0.337919044	0.002580404
ACACA	ACC_pS79	0.205118203	0.018568009	0.127179405	0.128537583	0.248922301	0.005462974
RB1	Rb	-0.130175437	0.007633018	-0.003772481	0.932662909	-0.134948774	0.005960365
KAT2A	GCN5L2	-0.08829456	0.025170812	0.012357989	0.739159042	0.109826962	0.006844985
SYK	Syk	0.541974466	0.011505754	0.280328764	0.166820626	0.585274823	0.00697943
DIABLO	Smac	0.082509975	0.045028366	0.019199089	0.625068235	-0.115445494	0.007104392
JUN	c.Jun_pS73	0.158248062	0.003726413	-0.03844123	0.436988918	0.143889973	0.007372482
MSI2	MSI2	-0.17692707	0.020174509	-0.064035668	0.373263454	-0.199146333	0.01004647
FOSL1	FRA.1	-0.154287126	0.044492168	-0.019863505	0.785872956	-0.191544175	0.014863628
PCNA	PCNA	0.620859146	0.004079343	0.32659972	0.104759754	0.489294325	0.019050376
PDCD1	Pdcd.1L1	0.335537983	0.017022898	0.136346787	0.304237999	0.318604512	0.02260446
NOTCH3	Notch3	0.166052152	0.026493552	-0.054885842	0.439011328	0.169032997	0.024181782
PRKAA1	AMPKa_pT172	0.285954274	0.021916238	0.084663349	0.471738191	0.275306448	0.02668986
VASP	VASP	-0.156321797	0.000400558	-0.048975058	0.202158399	-0.087625105	0.028289666
YBX1	YB1_pS102	0.102756836	0.005042063	0.007615141	0.818721386	-0.076032648	0.030677745
PIK3BC	PI3K.p110.b	0.20484715	0.048820631	0.132525047	0.190418389	0.225736442	0.031487495
CDC25C	cdc25C	-0.11974777	0.019577263	-0.026905188	0.576129218	-0.107985443	0.033212529
PARK7	DJ1	0.115102352	0.019151894	-0.042893082	0.355075001	-0.10269459	0.034278739
ANXA7	Annexin.VII	0.157211084	0.000235721	0.007594313	0.832827213	-0.075894132	0.04463264
YAP1	YAP_pS127	0.153775205	0.06260462	0.338260896	0.000298365	-0.562937031	4.29E-07
GAB2	Gab2	0.031425789	0.19948335	0.132269322	1.56E-05	-0.162008107	9.43E-07
WIPI1	WIPI1	-0.003775698	0.9272142	-0.212272458	3.77E-05	0.205680987	5.50E-05
GATA3	GATA3	0.136128316	0.178527637	0.209234922	0.044310129	0.298104944	0.006111846
CDH2	N.Cadherin	-0.015071168	0.643795266	-0.09467736	0.007695256	-0.096014657	0.006998801
EEF2K	eEF2K	-0.043976851	0.226344369	-0.075114505	0.045263195	-0.101190184	0.009209645
NF2	Merlin	-0.057018217	0.068881569	0.070416159	0.027557477	-0.064941559	0.040454608

GSK3A.B	GSK.3a.b_pS21_S9	0.221664941	0.001317337	0.130855373	0.040258951	0.099491426	0.111313462
BECN1	Beclin	0.333324662	0.00691202	0.310526734	0.01098597	0.152806931	0.184333348
NDUFB4	NDUFB4	0.248244085	0.002260311	0.19237917	0.013612735	0.051945731	0.475115216
GLS	Glutaminase	-0.136492991	0.000865031	-0.096104984	0.012488969	-0.008545856	0.810407438
EIF4EBP1	X4E.BP1	0.2011071	0.000608838	0.112881084	0.034534588	0.004296776	0.932244551
LC3AB	LC3A.B	0.306583529	0.000415637	0.216171181	0.007607768	-0.001510107	0.983740673

Paper III

A novel truncated form of Nephronectin is present in small extracellular vesicles isolated from 66cl4-cells

Jimita Toraskar[1, 2], Synnøve N. Magnussen[3], Lars Hagen[1,4], Animesh Sharma[1,4], Linh Hoang[1,5], Geir Bjørkøy[1,6], Gunbjørg Svineng[3] and Tonje S. Steigedal[1,2]

[1]Department of Clinical and Molecular Medicine, Faculty of Medicine and Health Sciences, Norwegian University of Science and Technology (NTNU), Trondheim, Norway

[2]Central Norway Regional Health authority, Stjørdal, Norway

[3]Department of Medical Biology, Faculty of Health Sciences, UiT-The Arctic University of Norway, Tromsø, Norway

[4]PROMEC, Proteomics and Modomics Experimental Core Facility, NTNU, Trondheim, and the Central Norway Regional Health Authority, Stjørdal, Norway

[5]CMIC, Cellular and Molecular Imaging Core Facility, NTNU, Trondheim, Norway

[6]Centre of Molecular Inflammation Research, Faculty of Medicine and Health Sciences, NTNU, Trondheim, Norway

Correspondence: Jimita Toraskar, Department of Clinical and Molecular Medicine, Faculty of Medicine and Health Sciences, NTNU, Postbox 8905, N-7491 Trondheim, Norway.
E-mail: jimita.toraskar@ntnu.no Mobile:+47-99673377

ABSTRACT:

Extracellular vesicles are emerging as biomarkers in breast cancer. Our recent report suggested that an intracellular granular staining pattern of the extracellular matrix protein Nephronectin (NPNT) in breast tumor sections correlated with poor prognosis. Furthermore, the results showed that NPNT is localized in extracellular vesicles derived from mouse breast cancer cells. In this study we performed proteomic analysis which reveals that several proteins, including tumor promoting molecules are differentially expressed in the cargo of small extracellular vesicles (sEVs) upon NPNT expression in mouse breast cancer cells. We identify three different forms of NPNT at 80, 60 and 20 kDa. We report that the native form of NPNT at 60 kDa gets further glycosylated and is detected as the 80 kDa NPNT, which may be processed by matrix metalloproteinases to a shorter form of around 20 kDa, not previously described. Although both 80 kDa and 20 kDa NPNT are detected in sEVs derived from breast cancer cells, the 20 kDa form of NPNT is concentrated in sEVs. In summary, we here show that a novel truncated form of NPNT is found in sEVs derived from breast cancer cells.

Keywords: Breast Cancer, Nephronectin, Small Extracellular Vesicles

Introduction

Extracellular vesicles can be classified according to the size: exosomes (30-100 nm), microvesicles (100-1000 nm), apoptotic bodies (50 nm to 2 µm) and oncosomes (1-10 µm)[1]. Microvesicles are bi-lipid-membrane vesicles originating from the plasma membrane[2], initially disregarded as cellular debris but now recognized as biologically significant[3-4]. Extracellular proteins may enter into the intraluminal vesicles (ILVs) within multivesicular bodies (MVBs)[2] on inward budding of the plasma membrane. The invaginations of the limiting membrane of the MVBs further allows several intracellular proteins to enter in the ILVs[5-6]. The content of MVBs is either released as exosomes into the extracellular milieu or into the lysosomes for degradation[7-8]. The secreted exosomes may release their contents into a recipient cell by fusion, or interact with the target cells via cell surface proteins[9-10]. Ultra-centrifugation is regarded as the gold standard for exosome isolation [11-12]. However, it has been found that pellet of vesicles obtained after spinning the supernatant of cells at 100,000 x g for 70 minutes (min) contains a heterogeneous population of membrane vesicles, in addition to enriched exosomes[13-16]. Therefore, the preferred terminology for the isolated fraction is small extracellular vesicles (sEVs)[17].

The content of sEVs is not random[18], rather the cargo is cell and disease-type specific; and may deliver discrete molecular messages that inflict a biological response[19]. The sEVs are found to carry proteins[20], lipids[21], transposable genetic elements[22], double stranded DNA[23], mitochondrial DNA[24] and several types of RNAs[25]. Several extracellular matrix (ECM) proteins such as collagen[26], fibronectin[27], vitronectin[28], and NPNT are detected in sEVs[29]. NPNT has previously been reported in isolated sEVs from human ductal saliva[30], colorectal cancer cells[31] and mouse breast cancer cells[32-33].

Breast cancer is a heterogeneous disease and intercellular vesicular communication via sEVs may add to the complexity of the disease[34]. The sEVs released by breast cancer cells can survive in acidic and hypoxic environments and deliver pro-cancerous proteins and transcripts to their target cells[35]. This induces a range of cellular responses within their target cells, to promote breast cancer development, progression, metastasis and resistance towards therapy[33, 36-38]. We have previously reported a correlation between intracellular granular NPNT staining pattern and decreased survival of breast cancer patients[32]. This granular staining pattern could represent NPNT-containing MVBs in tumor cells. Similar NPNT-positive granules have been observed in MMTV-PyMT tumor tissues and lung metastases from NPNT-expressing 66cl4 mouse breast cancer cells[32]. Furthermore, we have showed that NPNT is localized in sEVs isolated from 66cl4 cells overexpressing NPNT and that the localization of NPNT in sEVs is not dependent on the interaction of NPNT with the integrins[32].

Here we examine the sEVs isolated from the supernatant of the 66cl4 cells overexpressing either wild-type NPNT (66cl4-NPNT) or NPNT mutated in the integrin binding sites (66cl4-NPNT-RGE and 66cl4-NPNT-RGEAIA). As a control, 66cl4 cells containing an empty vector (EV) were used (66cl4-EV). We report several proteins that are differentially packed in sEVs derived from 66cl4-NPNT cells compared to sEVs derived from 66cl4-EV cells. We have identified NPNT of 80-, 60- and 20 kDa when analyzing whole cell lysates of 66cl4-NPNT cells. The 80 kDa NPNT is the highly glycosylated form of the less glycosylated 60 kDa NPNT. We show here for the first time that a 20 kDa truncated form of NPNT, is highly concentrated in sEVs.

Material and Methods

2.1. Cell culture

The gene for NPNT was cloned, V5-tagged in the C-terminal and the integrin-binding motifs mutated and expressed in the mouse breast cancer cell line, 66cl4, as previously described[32]. Four different variants of 66cl4 cell lines were created that harbored either an empty vector (66cl4-EV), expressed wild-type NPNT (66cl4-NPNT), NPNT where the RGD integrin-binding motif was mutated (66cl4-RGE), or where both the RGD and EIE-integrin binding motifs were mutated (66cl4-RGE-AIA)[32]. All 66cl4-variants were cultured in (1X) Minimum Essential Medium α (Thermo Fisher Scientific, Cat: 22561021), supplemented with 10% fetal calf serum, 1% (v/v) penicillin-streptomycin and 1M HEPES buffer (Thermo Fisher Scientific, Cat: 15630080).

2.2. Isolation of extracellular vesicles

Fetal calf serum (FCS) was depleted of extracellular vesicles using serial centrifugation and standard protocols[32, 39-40]. 66cl4 cell variants were grown in vesicular-free media for 3 days to reach approximately 80% confluency. The collected supernatant was centrifuged at 500 x g for 10 min to remove cellular debris. The supernatant was carefully transferred and ultracentrifuged at 12000 x g for 20 min using a Beckman 70Ti rotor to isolate microvesicles (pellet fraction 1 / MVs). The supernatant was transferred to clean tubes and re-pelleted by ultra-centrifugation at 100,000 x g for 70 min, to isolate small extracellular vesicles (pellet fraction 2 / sEVs). PBS was used to wash both fractions of MVs and sEVs.

2.3. Preparation for scanning electron microscopy (SEM)

Cultured cells grown on Thermanox coverslip (Chemi-Teknik AS, Cat: 72280) were fixed with a solution of 2.5% glutaraldehyde (GA) with 2% paraformaldehyde (PFA) in 0.1 M HEPES buffer for 2-4 hrs at room temperature. Cells were washed in 0.1 M HEPES buffer, subsequently dehydrated using increasing ethanol concentrations (25, 50, 70, 90, 2 x 100%), for 5 min each, followed by drying using hexamethyldisiloxane (HMDS) (50% and 2 x 100%, diluted in absolute ethanol), for 20 min each and transferred to a desiccator to keep the samples dry. The dried samples were mounted on aluminum pins with double sided carbon tape and sputter coated (Polaron) with 30 nm Gold/Palladium. Samples were examined using a scanning electron microscope (Teneo SEM, Thermo Fisher Scientific) at a voltage of 5 kV.

2.4. Preparation for transmission electron microscopy (TEM)

MVs and sEVs isolated and purified as described above were resuspended and fixed in cold 2% PFA in PBS. A droplet of MVs and sEVs were put on Formvar-carbon coated copper grids (200 mesh) for 5 min, fixed in 2.5% GA in 0.1 M Sorensen's phosphate buffer for 10 min, washed in reverse osmosis (RO) water, stained with 2% uranyl acetate (UA) in Milli-Q water for 4 min, and embedded in a solution of 2% UA and 3% polyvinyl alcohol (diluted 1:10) for 10 min. The excess liquid on the grids was then removed with filter paper (hardened) and air dried. Grids were examined using a transmission electron microscope (JSM-1011 TEM, JEOL), at 100.000x magnification and a voltage of 80 kV. Images were captured with a Morada digital camera with iTEM software (BoRAS).

2.5. Uptake of small extracellular vesicles

The pellet of sEVs was labelled with PKH26 (Sigma, MINI26), a dye taken up by the lipid membrane of sEVs. 66cl4-EV cells supplemented with sEVs from 66cl4-EV and 66cl4-NPNT cells for 4 hrs were fixed with 4% PFA. Images were captured using multi-channel fluorescence imaging system (Thermo Fisher Scientific, EVOS).

2.6. Immunoblotting

Protein lysates were prepared using a mix of RIPA buffer (Thermo Fischer Scientific, Cat: 89901) and HALT phosphatase inhibitor single use cocktail (Thermo Fischer Scientific, Cat: 78428). In certain experiments, cells were pre-treated with a final concentration of 100 nM of BafilomycinA1 (Sigma, Cat: SML1661) or 1X eBiocience^{TM} Protein Transport Inhibitor cocktail (PTI) (Invitrogen, Cat: 00-4980-93) for not more than 6 hrs. To test the effect of GM6001 (Abcam, Cat: ab120845) on NPNT, cells were exposed to 10 µM of GM6001 for 24 hrs. To investigate the post-translational modification of NPNT, whole cell lysates were digested with different de-glycosylation enzymes as per the company protocol (New England Biolabs, Cat: P0704, P0733 and P0720). Samples equivalent to 30 µg each were loaded on a 10% Bis-Tris gel (Invitrogen). PVDF membranes were incubated with anti-V5 (CST, 13202) (1:1000) overnight at 4˚C. Unspecific binding was prevented by pre-incubating membrane in 5% BSA for 1 hr at room temperature. Anti-GAPDH (Abcam, Cat: ab9484) (1:5000) and Anti-Alix (CST, Cat: 2171) were used as markers for whole cell lysate and sEVs respectively. Pelleted fractions were checked for several other vesicular markers as previously reported[32]. HRP linked secondary antibody anti-mouse (Dako, Cat: P0447) (1:5000) or HRP-linked anti-rabbit (Dako, Cat: P0399) (1: 5000) were used. Supersignal west femto substrate (Pierce, Cat: 34096) with Odyssey Fc system (Li-Cor –biosciences) was used for image analysis.

2.7. Immunoprecipitation and gel electrophoresis

V5-tagged NPNT was pulled down from 7 mg of whole cell lysates using 100 µl of anti-V5 (CST, Cat: 13202) (1:50) coated Dynabeads^{TM} Protein G (Thermo Fisher Scientific, Cat: 10003D) for 2 hrs at 4˚C. The beads were washed twice in PBS and proteins were eluted in LDS sample buffer (Invitrogen) for gel electrophoresis. 1D PAGE of eluted proteins was performed in 10% NuPAGE Noves Bis-Tris gels using MOPS buffer. Proteins were visualized using SimplyBlue gel stain and three bands (20, 60 and 80 kDa) were excised from the gel.

2.8. In gel digestion and mass spectrometry

SimplyBlue stained protein bands corresponding to 80, 60 and 20 kDa respectively were manually cut out from the gel and in-gel tryptic digestion was performed as previously described[41]. After desalting[42], peptides were dried down in a SpeedVac centrifuge and resuspended in 0.1% formic acid. The peptides were analyzed on a LC-MS/MS platform consisting of an Easy-nLC 1000 UHPLC system (Thermo Fisher Scientific) interfaced with an LTQ-Orbitrap Elite hybrid mass spectrometer (Thermo Fisher Scientific) via a nanospray ESI ion source (Proxeon, Odense). Peptides were injected into a C-18 trap column (Acclaim PepMap100, 75 µm i. d. x 2 cm, C18, 3 µm, 100 Å, Thermo Fisher Scientific) and further separated on a C-18 analytical column (Acclaim PepMap100, 75 µm i. d. x 50 cm, C18, 2 µm, 100 Å, Thermo Fisher Scientific) using a multistep gradient with buffer A (0.1% formic acid) and buffer B (CH3CN, 0.1% formic acid): From 0-6% B in 5 min, 6-12% B in 39 min, 12-20% B in 80 min, 20-28% B in 31 min, 28-40% B in 4 min, 40-100% B in 1 min, 100% B in 9 min, 100-0% B in 1 min and 10 min with 100% A. The flow rate was 250 nl/min. Peptides eluted were analyzed on the LTQ-Orbitrap Elite hybrid mass spectrometer operating in positive ion- and data dependent acquisition mode using the following parameters: Electrospray voltage 1.9 kV, CID fragmentation with normalized collision energy 35, automatic gain control target value of 1E6 for Orbitrap MS and 1E3 for MS/MS scans. Each MS scan (m/z 300–1600) was acquired at a resolution of 120,000 FWHM, followed by 20 MS/MS scans triggered for intensities above 500, at a maximum ion injection time of 200 ms for MS and 120 ms for MS/MS scans.

Proteins were quantified by processing MS data using in Max Quant v 1.5.8.3[43]. Preview 2.3.5 (Protein Metrics Inc.) was used to inspect the raw data to determine optimal search criteria. Namely, following search parameters were used: enzyme specified as trypsin with maximum two missed cleavages allowed; mass tolerance set to 20 ppm; oxidation of Methionine and deamidation of Asparagine and Glutamine as dynamic post-translational modification and carbamidomethylation of Cysteine as a fixed modification. These were imported in MaxQuant which uses m/z and RT values to align each run against each other sample with one min window match-between-run function and 20 min overall sliding window using a clustering based technique. These are further queried against the UniProtKB/Swiss-Prot database (Release April 2017 Mouse proteome with Isoforms; 59684 sequences and MaxQuant's internal contaminants database) using Andromeda built into MaxQuant. Both protein and peptide identifications FDR was set to 1% thus only peptides with high confidence were used for final protein group identification. Peak abundances were extracted by integrating the area under the peak curve. Each protein group abundance was normalized by the total abundance of all identified peptides for each run and protein by calculated median summing all unique and razor peptide ion abundances for each protein using label free quantification algorithm[44] with minimum peptides ≥ 1. Protein group abundances were imported and analyzed using R software. Given the structure of the data, the statistical analysis was performed using a two-way analysis of variance (ANOVA) in order to consider the levels of variance at batch as well as test groups. Data were log2-transformed before the analysis. Proteins were considered identified if they were quantified in at least 75% of the biological replicates. Noise with standard deviation of 0.01 is added to compensate for the missing values followed by principal component analysis to find and remove the batch effect. Table containing normalized log2 intensity values after the removal of the component, row representing the proteins and column representing the samples, is scaled by row, namely the median of row was subtracted and the result was divided by the standard deviation of the row. Pearson’s correlation coefficients were calculated in both dimensions over the values obtained are further used for hierarchical clustering using average linkage procedure (Fig. 2d). Perseus plugins[45] are employed to carry out these steps. List of protein groups with permutation based FDR<5% and S0 of 0.1[46] are presented in Table S2 while Ingenuity Pathway Analysis (IPA) of the two broad clusters are presented in Table S3.

2.9. Ingenuity Pathway Analysis

In order to characterize the enrichment of functional category for selected protein groups (Table S1, quantified in at least 3 out of 4 biological replicates), they were mapped to canonical pathways database of IPA (Qiagen)[47]. The p-values based on Fisher’s exact test over categorical distribution are corrected using Benjamini Hochberg procedure. They represent the statistical significance of the identified canonical functions, namely lower the p-value higher the proportion of identified proteins, overlapping with the particular canonical function.

3. Results and Discussion

3.1. Overexpression of NPNT in 66cl4 cells does not affect the secretion or uptake of sEVs

To visualize the surface morphology and sEVs of 66cl4 cells, we utilized SEM. Several spherical particles in the nanometers size were observed on/around the cell surface (Fig. 1a), suggesting presence of extracellular vesicles. To confirm the presence of extracellular vesicles we used differential ultra-centrifugation and isolated extracellular vesicles from the supernatant of the 66cl4 cells, where pellet fraction 1 was collected upon spinning at 12,000 x g for 20 min and pellet fraction 2 was collected upon spinning at 100,000 g for 70 min. The isolated extracellular vesicles in the two pellets were characterized by TEM (Fig. 1b), which is considered to be a standard tool for characterizing extracellular vesicles[48]. Double membrane vesicles were identified in both pelleted fractions 1 and 2. Fraction 1 displayed a homogenous population of vesicles within the range 100-1000 nm, characteristic of MVs. Fraction 2 displayed vesicles within the range of 30-100 nm in diameter, characteristic of sEVs (Fig.1b). Overexpression of NPNT in 66cl4 cells did not alter the morphology nor the size of the MVs and sEVs as observed by TEM analyses. The ability of sEVs to exert a functional effect mainly depends on their internalization and subsequent release of its content in recipient cells. We have previously detected NPNT protein in sEVs derived from 66cl4-NPNT cells[32]. To investigate if the presence or absence of NPNT in the sEVs affects its uptake, we treated sEVs derived from 66cl4-EV cells and 66cl4-NPNT cells with PKH26, a lypophilic dye. 66cl4-EV cells were incubated with PKH26-labeled sEVs for 4 hrs prior to fixing and thorough washing of cells with PBS. PKH26-labelled vesicles were observed as red dots on and most likely within 66cl4-EV cells (Fig. 1c), indicating that these vesicles are taken up, or are bound to the surface of 66cl4-EV cells irrespective of their source and content.

3.2. Overexpression of NPNT in 66cl4 cells alters the content of sEVs

To investigate the protein composition of sEVs upon NPNT overexpression, shotgun MS was performed on lysed sEVs derived from 66cl4-EV and 66cl4-NPNT cells. The Venn diagram (Fig. 2a) shows the number of proteins identified in sEVs isolated from 66cl4-EV and 66cl4-NPNT cells. A total of 1750 proteins were identified to be common between the sEVs isolated from both cell lines. As expected, several well-known tumor and vesicular markers were detected in this common fraction between sEVs of both cell lines (Fig. S1c). A 62% similarity to the previously reported sEVs-derived from parental 66cl4 cells was observed[33]. IPA analyses suggest that the majority of proteins in our data came from the cytoplasmic fraction of the cell (Fig. 2b), and were enzymatic in nature (Fig. 2c). NPNT was detected as one of the 275 proteins found only in sEVs derived from 66cl4-NPNT cells (Fig. 2a and Table S1). NPNT is known to bind different types of integrins[49], and IPA analyses showed that several proteins identified in sEVs derived from 66cl4-NPNT cells are involved in integrin signaling pathway (Fig. S1b). Several kinases known for their role in tumor development such as mTOR[50], and JAK[51] were detected only in sEVs from 66cl4-NPNT cells (Table S1). Ceruloplasmin, a known biomarker for breast cancer[52] was only present in sEVs from 66cl4-NPNT cells. Two major clusters were identified when protein IDs passing a false discovery rate of 5% were clustered over z-scores (Fig. 2d / Table S2). IPA analyzes suggest that increase in protein levels of molecules in cluster 0 will increase proliferation, increase cell survival and increase organization of cytoskeleton/cytoplasm. Whereas increased levels of proteins in cluster 1 will decrease cell death, decrease apoptosis, increase lesion/malignancy and increase cell cycle progression (Table S3). Basically, the two clusters in the heat map identify molecules which have functionally complementary roles in cell growth and differentiation. Several other studies have shown that change in a single oncoprotein /oncogene can alter the contents of vesicular cargo and further incorporate tumor promoting proteins in sEVs[31, 53-55]. Taken together, the proteins enriched in sEVs derived from NPNT expressing breast cancer cells might represent markers that are involved in mechanisms affecting breast cancer progression and metastasis.

3.3. Truncated form of NPNT is concentrated in sEVs isolated from 66cl4-NPNT cells

The predicted molecular weight of mouse NPNT (561 aminoacids) is 61 kDa. Our immunoblot analysis of 66cl4 cells overexpressing full length NPNT with a C-terminal V5-tag showed three bands of approximately 20 kDa, 60 kDa and 80 kDa (Fig. 3a). Interestingly, immunoblotting of lysed sEVs revealed only two bands, one at 20 kDa and 80 kDa (Fig. 3b). At the same time there was an increase in the relative amount of the 20 kDa NPNT in sEVs compared to the 80 kDa NPNT (Fig. 3b). This could indicate that there is a selective sorting process involved in the vesicular packaging of NPNT. This phenomenon of the 20 kDa NPNT to be concentrated was seen in both sEVs (Fig. 3b) and MVs (Fig. S1c). Of note, we have observed that the quality of immunoblot gets compromised upon freeze-thaw cycles of sEVs and this might explain the difference in intensities in the 20 kDa bands in Fig. 3b and 3e.

To investigate whether the different apparent sizes of NPNT were due to post-translational modifications, we pulled-down NPNT from the whole cell lysates using V5 antibody and analyzed it by MS. Six unique NPNT peptide sequences were detected in the 80 kDa NPNT (Table 1), covering almost the full span of the protein (Fig. 3c). This verifies that the 80 kDa NPNT is a full-length version of the protein. Four unique peptides matched the 60 kDa NPNT, including the first peptide (amino acids 28-37), indicating that the 60 kDa NPNT is most likely also a full-length version of the protein. One unique NPNT-derived peptide was detected in the 20 kDa NPNT (amino acid 446-459). This indicates that the 20 kDa NPNT is mostly harboring the MAM-domain of the C-terminal part of the protein. Further, to identify whether post-translational modifications such as glycosylation contribute to differences between the three NPNT bands, whole cell lysates and sEVs were treated with PNGase F, O-Glycosidase or α2-3, 6, 8 neuraminidase. These enzymes remove N- and O- linked glycans with or without sialic acid cap, thereby reducing the apparent molecular size of NPNT on immunoblot. Upon PNGase F treatment (-N), a reduction in the molecular size was observed for both the 60 kDa and 80 kDa bands in whole cell lysates (Fig. 3d), and of the 80 kDa NPNT of sEVs (Fig. 3e). There was no shift in any of the bands upon treatment with O-glycosidase (-O) alone. However, co-treatment with O-glycosidase and α2-3, 6, 8 neuraminidase (-S) resulted in a major band shift in the 80 kDa NPNT for both cell- and sEVs lysates. This suggests that the 80 kDa NPNT has O-glycosylation but with a sialic acid cap. A similar glycosylation pattern of NPNT secreted by osteoblasts has previously been reported [56]. A high degree of N- and O-glycosylation is predicted in the region between the EGF repeats and the MAM domains[49]. Aberrant glycosylation patterns of secreted glycoproteins are known to contribute in tumor development and progression[57-58]. It remains to be investigated whether the glycosylation pattern of NPNT would influence breast cancer progression. The glycosylation patterns are also crucial for sorting of proteins into extracellular vesicles[59-61]. Our results indicate that the 60 kDa band is far less glycosylated than the 80 kDa band, while the 20 kDa band is not glycosylated. The heavily glycosylated 80 kDa NPNT, containing both N- and O-glycosylations is recruited into sEVs (Fig. 3e), while the less glycosylated 60 kDa NPNT is not detected in either sEVs or MVs. N-glycosylations are mainly added when proteins transition through the endoplasmic reticulum[62], while O-glycosylations are generally initiated in Golgi[63].

3.4. Intracellular protein trafficking controls the protein levels of the truncated NPNT

The intracellular protein trafficking pathways are often manipulated in cancer cells and a better understanding of this aspect is important for developing therapeutic interventions[64]. To investigate the intracellular NPNT trafficking, we employed a mixture of Brefeldin A and Monensin to block transport from endoplasmic reticulum to the Golgi apparatus, and Bafilomycin A1 (BafA1) that inhibits degradation of endocytosed "cargo" by neutralizing the lysosomes[65] (Fig. 5c). Hence, any endocytosed protein, including NPNT, ends up being accumulated in the cytoplasm. 66cl4-EV and -NPNT cells were exposed to 100 nM BafA1, whole cell lysates harvested and analyzed by immunoblotting for the V5-tag. By inhibiting degradation of endocytosed proteins, there was a significant accumulation of the 20 kDa NPNT (Fig. 4a), and a slight increase in 80 kDa NPNT. 66cl4-EV and -NPNT cells were exposed to 1X PTI, whole cell lysates harvested and analyzed by immunoblotting towards the V5-tag. Inhibiting the secretion resulted in an accumulation of the 60 kDa band of NPNT, with a corresponding reduction of the 80 kDa and 20 kDa bands (Fig. 4a). Cells expressing the mutated forms of NPNT showed similar changes when exposed to PTI or BafA1 (Fig. 4b and 4c). Taken together, these results indicate that the 60 kDa NPNT is not a secreted version of NPNT, but rather the 'native' protein. This could also explain the limited amount of glycosylations present in the 60 kDa NPNT (Fig. 3a), and its absence in the sEVs (Fig. 3b). Both 80 kDa and 20 kDa accumulate in the cytoplasm upon BafA1 treatment, indicating that they are both endocytosed from the extracellular milieu. The 80 kDa NPNT is most likely the secreted full-length version of NPNT, having both N- and sialic acid capped O-glycosylations.

3.5. Matrix metalloproteinases (MMPs) are involved in proteolytic processing of full length NPNT

Having identified the truncated form of NPNT we further analyzed whether proteases such as MMPs are involved in this processing by utilizing GM6001, a broad spectrum MMP inhibitor. 66cl4-NPNT cells were treated with 10 µM GM6001 for 24 hrs and whole cell lysates were analyzed by immunoblotting for the V5-tag. A significant reduction in the relative amounts of 20 kDa NPNT was observed (Fig. 5a). We already know that the extracellularly located 80 kDa

NPNT can be endocytosed by the cells. When MMP-cleavage is inhibited, the amount of endocytosed 20 kDa NPNT is reduced. This indicates that the 20 kDa NPNT is a cleaved form of NPNT and that this cleavage is at least in parts mediated by MMPs. MMPs can cleave proteins intracellularly and extracellularly[66]. Several metalloproteinases are also packed inside extracellular vesicles, capable of further altering the vesicular cargo by proteolytic processing[67-68]. Cleaved proteins packed in tumor- derived extracellular vesicles are reported to be biologically active[55, 69]. Further investigation is needed to identify if the cleaved NPNT packed in sEVs has a biological significance. Our study on NPNT trafficking in 66cl4 cells is the first to report a truncated form of NPNT at 20 kDa, mainly harboring the MAM-domain part of the protein (Fig. 5b). The exact MMP cleavage site and the identity of the MMPs capable of cleaving NPNT remains to be determined.

Though there are several challenges while analyzing the vesicular proteome using MS, the composition of sEVs derived from 66cl4-NPNT cells helps us to picture the molecular fingerprint of exosomes in cells with high NPNT levels. Results from the current study are summarized in Fig. 5c and shows that the native form of NPNT gets glycosylated and modified at ER and Golgi and the secreted full-length NPNT (80 kDa) probably gets cleaved by MMPs. Both the highly glycosylated NPNT (80 kDa) and the truncated form of NPNT (20 kDa) is perhaps endocytosed/pinocytosed and gets incorporated into the ILVs within a MVB. These ILVs packed with NPNT inside a MVB can either be released as exosomes or be degraded by lysosomes.

Acknowledgements

The study received funding from the Central Norway Regional Health Authority (Project number: 46077600), North Norwegian Regional Health Authorities (Project number SFP1232-15), The Erna and Olav Aakre Foundation for Cancer Research, The Blix Family Fund for Medical Research, and UiT – The Arctic University of Norway. Dr. Fred Miller kindly provided 66cl4 and 4T1, mouse cell lines. We express our gratitude to Dr. Naoko Morimura for the pcDNA3-POEM-Fc vector and Dr. Peter McCourt for linguistic revision. We thank Hector Peinado, Lucia Robado de Lope, and Marta Hergueta-Redondo for collaboration regarding exosome isolation protocols.

References

1. The International society for extracellular vesicles www.isev.org.
2. van der Pol, E.; Boing, A. N.; Harrison, P.; Sturk, A.; Nieuwland, R., Classification, functions, and clinical relevance of extracellular vesicles. *Pharmacol Rev* **2012,** *64* (3), 676-705.
3. Pucci, F.; Pittet, M. J., Molecular pathways: tumor-derived microvesicles and their interactions with immune cells in vivo. *Clin Cancer Res* **2013,** *19* (10), 2598-604.
4. Jansen, F.; Yang, X.; Proebsting, S.; Hoelscher, M.; Przybilla, D.; Baumann, K.; Schmitz, T.; Dolf, A.; Endl, E.; Franklin, B. S.; Sinning, J. M.; Vasa-Nicotera, M.; Nickenig, G.; Werner, N., MicroRNA expression in circulating microvesicles predicts cardiovascular events in patients with coronary artery disease. *J Am Heart Assoc* **2014,** *3* (6), e001249.
5. Palmulli, R.; van Niel, G., To be or not to be... secreted as exosomes, a balance finely tuned by the mechanisms of biogenesis. *Essays in biochemistry* **2018,** *62* (2), 177-191.
6. Thery, C., Exosomes: secreted vesicles and intercellular communications. *F1000 biology reports* **2011,** *3*, 15.
7. Pan, B. T.; Teng, K.; Wu, C.; Adam, M.; Johnstone, R. M., Electron microscopic evidence for externalization of the transferrin receptor in vesicular form in sheep reticulocytes. *J Cell Biol* **1985,** *101* (3), 942-8.
8. Harding, C.; Heuser, J.; Stahl, P., Endocytosis and intracellular processing of transferrin and colloidal gold-transferrin in rat reticulocytes: demonstration of a pathway for receptor shedding. *European journal of cell biology* **1984,** *35* (2), 256-63.
9. Montecalvo, A.; Larregina, A. T.; Shufesky, W. J.; Stolz, D. B.; Sullivan, M. L.; Karlsson, J. M.; Baty, C. J.; Gibson, G. A.; Erdos, G.; Wang, Z.; Milosevic, J.; Tkacheva, O. A.; Divito, S. J.; Jordan, R.; Lyons-Weiler, J.; Watkins, S. C.; Morelli, A. E., Mechanism of transfer of functional microRNAs between mouse dendritic cells via exosomes. *Blood* **2012,** *119* (3), 756-66.
10. Costa Verdera, H.; Gitz-Francois, J. J.; Schiffelers, R. M.; Vader, P., Cellular uptake of extracellular vesicles is mediated by clathrin-independent endocytosis and macropinocytosis. *J Control Release* **2017,** *266*, 100-108.
11. Li, P.; Kaslan, M.; Lee, S. H.; Yao, J.; Gao, Z., Progress in Exosome Isolation Techniques. *Theranostics* **2017,** *7* (3), 789-804.
12. Thery, C.; Amigorena, S.; Raposo, G.; Clayton, A., Isolation and characterization of exosomes from cell culture supernatants and biological fluids. *Current protocols in cell biology* **2006,** *Chapter 3*, Unit 3.22.
13. Bobrie, A.; Colombo, M.; Krumeich, S.; Raposo, G.; Thery, C., Diverse subpopulations of vesicles secreted by different intracellular mechanisms are present in exosome preparations obtained by differential ultracentrifugation. *Journal of extracellular vesicles* **2012,** *1*.
14. Willms, E.; Johansson, H. J.; Mager, I.; Lee, Y.; Blomberg, K. E.; Sadik, M.; Alaarg, A.; Smith, C. I.; Lehtio, J.; El Andaloussi, S.; Wood, M. J.; Vader, P., Cells release subpopulations of exosomes with distinct molecular and biological properties. *Scientific reports* **2016,** *6*, 22519.
15. Kowal, J.; Arras, G.; Colombo, M.; Jouve, M.; Morath, J. P.; Primdal-Bengtson, B.; Dingli, F.; Loew, D.; Tkach, M.; Thery, C., Proteomic comparison defines novel markers to characterize heterogeneous populations of extracellular vesicle subtypes. *Proc Natl Acad Sci U S A* **2016,** *113* (8), E968-77.
16. Zhang, H.; Freitas, D.; Kim, H. S.; Fabijanic, K.; Li, Z.; Chen, H.; Mark, M. T.; Molina, H.; Martin, A. B.; Bojmar, L.; Fang, J.; Rampersaud, S.; Hoshino, A.; Matei, I.; Kenific, C. M.; Nakajima, M.; Mutvei, A. P.; Sansone, P.; Buehring, W.; Wang, H.; Jimenez, J. P.; Cohen-Gould, L.; Paknejad, N.; Brendel, M.; Manova-Todorova, K.; Magalhaes, A.; Ferreira, J. A.; Osorio, H.; Silva, A. M.; Massey, A.; Cubillos-Ruiz, J. R.; Galletti, G.; Giannakakou, P.; Cuervo, A. M.; Blenis, J.; Schwartz, R.; Brady, M. S.; Peinado, H.; Bromberg, J.; Matsui, H.; Reis, C. A.; Lyden, D., Identification of distinct nanoparticles and subsets of extracellular vesicles by asymmetric flow field-flow fractionation. *Nat Cell Biol* **2018,** *20* (3), 332-343.

17. Hessvik, N. P.; Llorente, A., Current knowledge on exosome biogenesis and release. *Cellular and molecular life sciences : CMLS* **2018,** *75* (2), 193-208.
18. Edgar, J. R., Q&A: What are exosomes, exactly? *BMC Biol* **2016,** *14*, 46.
19. Gangoda, L.; Boukouris, S.; Liem, M.; Kalra, H.; Mathivanan, S., Extracellular vesicles including exosomes are mediators of signal transduction: are they protective or pathogenic? *Proteomics* **2015,** *15* (2-3), 260-71.
20. Li, A.; Zhang, T.; Zheng, M.; Liu, Y.; Chen, Z., Exosomal proteins as potential markers of tumor diagnosis. *J Hematol Oncol* **2017,** *10* (1), 175.
21. Choi, D. S.; Kim, D. K.; Kim, Y. K.; Gho, Y. S., Proteomics, transcriptomics and lipidomics of exosomes and ectosomes. *Proteomics* **2013,** *13* (10-11), 1554-71.
22. Balaj, L.; Lessard, R.; Dai, L.; Cho, Y. J.; Pomeroy, S. L.; Breakefield, X. O.; Skog, J., Tumour microvesicles contain retrotransposon elements and amplified oncogene sequences. *Nat Commun* **2011,** *2*, 180.
23. Kahlert, C.; Melo, S. A.; Protopopov, A.; Tang, J.; Seth, S.; Koch, M.; Zhang, J.; Weitz, J.; Chin, L.; Futreal, A.; Kalluri, R., Identification of double-stranded genomic DNA spanning all chromosomes with mutated KRAS and p53 DNA in the serum exosomes of patients with pancreatic cancer. *J Biol Chem* **2014,** *289* (7), 3869-75.
24. Guescini, M.; Genedani, S.; Stocchi, V.; Agnati, L. F., Astrocytes and Glioblastoma cells release exosomes carrying mtDNA. *J Neural Transm (Vienna)* **2010,** *117* (1), 1-4.
25. Valadi, H.; Ekstrom, K.; Bossios, A.; Sjostrand, M.; Lee, J. J.; Lotvall, J. O., Exosome-mediated transfer of mRNAs and microRNAs is a novel mechanism of genetic exchange between cells. *Nat Cell Biol* **2007,** *9* (6), 654-9.
26. Zhao, X.; Wu, Y.; Duan, J.; Ma, Y.; Shen, Z.; Wei, L.; Cui, X.; Zhang, J.; Xie, Y.; Liu, J., Quantitative proteomic analysis of exosome protein content changes induced by hepatitis B virus in Huh-7 cells using SILAC labeling and LC-MS/MS. *J Proteome Res* **2014,** *13* (12), 5391-402.
27. Park, J. E.; Tan, H. S.; Datta, A.; Lai, R. C.; Zhang, H.; Meng, W.; Lim, S. K.; Sze, S. K., Hypoxic tumor cell modulates its microenvironment to enhance angiogenic and metastatic potential by secretion of proteins and exosomes. *Mol Cell Proteomics* **2010,** *9* (6), 1085-99.
28. He, M.; Qin, H.; Poon, T. C.; Sze, S. C.; Ding, X.; Co, N. N.; Ngai, S. M.; Chan, T. F.; Wong, N., Hepatocellular carcinoma-derived exosomes promote motility of immortalized hepatocyte through transfer of oncogenic proteins and RNAs. *Carcinogenesis* **2015,** *36* (9), 1008-18.
29. www.exocarta.org.
30. Gonzalez-Begne, M.; Lu, B.; Han, X.; Hagen, F. K.; Hand, A. R.; Melvin, J. E.; Yates, J. R., Proteomic analysis of human parotid gland exosomes by multidimensional protein identification technology (MudPIT). *J Proteome Res* **2009,** *8* (3), 1304-14.
31. Demory Beckler, M.; Higginbotham, J. N.; Franklin, J. L.; Ham, A. J.; Halvey, P. J.; Imasuen, I. E.; Whitwell, C.; Li, M.; Liebler, D. C.; Coffey, R. J., Proteomic analysis of exosomes from mutant KRAS colon cancer cells identifies intercellular transfer of mutant KRAS. *Mol Cell Proteomics* **2013,** *12* (2), 343-55.
32. Steigedal, T. S.; Toraskar, J.; Redvers, R. P.; Valla, M.; Magnussen, S. N.; Bofin, A. M.; Opdahl, S.; Lundgren, S.; Eckhardt, B. L.; Lamar, J. M.; Doherty, J.; Hynes, R. O.; Anderson, R. L.; Svineng, G., Nephronectin is Correlated with Poor Prognosis in Breast Cancer and Promotes Metastasis via its Integrin-Binding Motifs. *Neoplasia* **2018,** *20* (4), 387-400.
33. Gangoda, L.; Liem, M.; Ang, C. S.; Keerthikumar, S.; Adda, C. G.; Parker, B. S.; Mathivanan, S., Proteomic Profiling of Exosomes Secreted by Breast Cancer Cells with Varying Metastatic Potential. *Proteomics* **2017,** *17* (23-24).
34. Maia, J.; Caja, S.; Strano Moraes, M. C.; Couto, N.; Costa-Silva, B., Exosome-Based Cell-Cell Communication in the Tumor Microenvironment. *Front Cell Dev Biol* **2018,** *6*, 18.
35. King, H. W.; Michael, M. Z.; Gleadle, J. M., Hypoxic enhancement of exosome release by breast cancer cells. *BMC cancer* **2012,** *12*, 421.

36. Green, T. M.; Alpaugh, M. L.; Barsky, S. H.; Rappa, G.; Lorico, A., Breast Cancer-Derived Extracellular Vesicles: Characterization and Contribution to the Metastatic Phenotype. *Biomed Res Int* **2015,** *2015*, 634865.
37. Hoshino, A.; Costa-Silva, B.; Shen, T. L.; Rodrigues, G.; Hashimoto, A.; Tesic Mark, M.; Molina, H.; Kohsaka, S.; Di Giannatale, A.; Ceder, S.; Singh, S.; Williams, C.; Soplop, N.; Uryu, K.; Pharmer, L.; King, T.; Bojmar, L.; Davies, A. E.; Ararso, Y.; Zhang, T.; Zhang, H.; Hernandez, J.; Weiss, J. M.; Dumont-Cole, V. D.; Kramer, K.; Wexler, L. H.; Narendran, A.; Schwartz, G. K.; Healey, J. H.; Sandstrom, P.; Labori, K. J.; Kure, E. H.; Grandgenett, P. M.; Hollingsworth, M. A.; de Sousa, M.; Kaur, S.; Jain, M.; Mallya, K.; Batra, S. K.; Jarnagin, W. R.; Brady, M. S.; Fodstad, O.; Muller, V.; Pantel, K.; Minn, A. J.; Bissell, M. J.; Garcia, B. A.; Kang, Y.; Rajasekhar, V. K.; Ghajar, C. M.; Matei, I.; Peinado, H.; Bromberg, J.; Lyden, D., Tumour exosome integrins determine organotropic metastasis. *Nature* **2015,** *527* (7578), 329-35.
38. Lowry, M. C.; Gallagher, W. M.; O'Driscoll, L., The Role of Exosomes in Breast Cancer. *Clin Chem* **2015,** *61* (12), 1457-65.
39. Peinado, H.; Aleckovic, M.; Lavotshkin, S.; Matei, I.; Costa-Silva, B.; Moreno-Bueno, G.; Hergueta-Redondo, M.; Williams, C.; Garcia-Santos, G.; Ghajar, C.; Nitadori-Hoshino, A.; Hoffman, C.; Badal, K.; Garcia, B. A.; Callahan, M. K.; Yuan, J.; Martins, V. R.; Skog, J.; Kaplan, R. N.; Brady, M. S.; Wolchok, J. D.; Chapman, P. B.; Kang, Y.; Bromberg, J.; Lyden, D., Melanoma exosomes educate bone marrow progenitor cells toward a pro-metastatic phenotype through MET. *Nat Med* **2012,** *18* (6), 883-91.
40. Ochieng, J.; Pratap, S.; Khatua, A. K.; Sakwe, A. M., Anchorage-independent growth of breast carcinoma cells is mediated by serum exosomes. *Exp Cell Res* **2009,** *315* (11), 1875-88.
41. Shevchenko, A.; Wilm, M.; Vorm, O.; Mann, M., Mass spectrometric sequencing of proteins silver-stained polyacrylamide gels. *Analytical chemistry* **1996,** *68* (5), 850-8.
42. Rappsilber, J.; Ishihama, Y.; Mann, M., Stop and go extraction tips for matrix-assisted laser desorption/ionization, nanoelectrospray, and LC/MS sample pretreatment in proteomics. *Analytical chemistry* **2003,** *75* (3), 663-70.
43. Cox, J.; Mann, M., MaxQuant enables high peptide identification rates, individualized p.p.b.-range mass accuracies and proteome-wide protein quantification. *Nature biotechnology* **2008,** *26* (12), 1367-72.
44. Cox, J.; Hein, M. Y.; Luber, C. A.; Paron, I.; Nagaraj, N.; Mann, M., Accurate proteome-wide label-free quantification by delayed normalization and maximal peptide ratio extraction, termed MaxLFQ. *Mol Cell Proteomics* **2014,** *13* (9), 2513-26.
45. https://github.com/JurgenCox/perseus-plugins.
46. Tusher, V. G.; Tibshirani, R.; Chu, G., Significance analysis of microarrays applied to the ionizing radiation response. *Proc Natl Acad Sci U S A* **2001,** *98* (9), 5116-21.
47. Ingenuity Pathway Analysis. https://www.qiagenbioinformatics.com/products/ingenuity-pathway-analysis/.
48. Wu, Y.; Deng, W.; Klinke, D. J., 2nd, Exosomes: improved methods to characterize their morphology, RNA content, and surface protein biomarkers. *The Analyst* **2015,** *140* (19), 6631-42.
49. Brandenberger, R.; Schmidt, A.; Linton, J.; Wang, D.; Backus, C.; Denda, S.; Müller, U.; Reichardt, L. F., Identification and characterization of a novel extracellular matrix protein nephronectin that is associated with integrin α8β1 in the embryonic kidney. *The Journal of Cell Biology* **2001,** *154* (2), 447-458.
50. Xu, K.; Liu, P.; Wei, W., mTOR signaling in tumorigenesis. *Biochimica et biophysica acta* **2014,** *1846* (2), 638-54.
51. Yan, J.; Zhang, B.; Hosseinzadeh, Z.; Lang, F., Down-Regulation of Store-Operated Ca2+ Entry and Na+ Ca2+ Exchange in MCF-7 Breast Cancer Cells by Pharmacological JAK3 Inhibition. *Cellular physiology and biochemistry : international journal of experimental cellular physiology, biochemistry, and pharmacology* **2016,** *38* (4), 1643-51.

52. Vaidya, S. M.; Kamalakar, P. L., Copper and ceruloplasmin levels in serum of women with breast cancer. *Indian journal of medical sciences* **1998,** *52* (5), 184-7.
53. Amorim, M.; Fernandes, G.; Oliveira, P.; Martins-de-Souza, D.; Dias-Neto, E.; Nunes, D., The overexpression of a single oncogene (ERBB2/HER2) alters the proteomic landscape of extracellular vesicles. *Proteomics* **2014,** *14* (12), 1472-9.
54. Nazarenko, I.; Rana, S.; Baumann, A.; McAlear, J.; Hellwig, A.; Trendelenburg, M.; Lochnit, G.; Preissner, K. T.; Zoller, M., Cell surface tetraspanin Tspan8 contributes to molecular pathways of exosome-induced endothelial cell activation. *Cancer research* **2010,** *70* (4), 1668-78.
55. Thompson, C. A.; Purushothaman, A.; Ramani, V. C.; Vlodavsky, I.; Sanderson, R. D., Heparanase regulates secretion, composition, and function of tumor cell-derived exosomes. *J Biol Chem* **2013,** *288* (14), 10093-9.
56. Kahai, S.; Lee, S. C.; Lee, D. Y.; Yang, J.; Li, M.; Wang, C. H.; Jiang, Z.; Zhang, Y.; Peng, C.; Yang, B. B., MicroRNA miR-378 regulates nephronectin expression modulating osteoblast differentiation by targeting GalNT-7. *PloS one* **2009,** *4* (10), e7535.
57. Munkley, J.; Elliott, D. J., Hallmarks of glycosylation in cancer. *Oncotarget* **2016,** *7* (23), 35478-89.
58. Pinho, S. S.; Reis, C. A., Glycosylation in cancer: mechanisms and clinical implications. *Nature reviews. Cancer* **2015,** *15* (9), 540-55.
59. Menck, K.; Scharf, C.; Bleckmann, A.; Dyck, L.; Rost, U.; Wenzel, D.; Dhople, V. M.; Siam, L.; Pukrop, T.; Binder, C.; Klemm, F., Tumor-derived microvesicles mediate human breast cancer invasion through differentially glycosylated EMMPRIN. *Journal of molecular cell biology* **2015,** *7* (2), 143-53.
60. Moreno-Gonzalo, O.; Villarroya-Beltri, C.; Sanchez-Madrid, F., Post-translational modifications of exosomal proteins. *Frontiers in immunology* **2014,** *5*, 383.
61. Liang, Y.; Eng, W. S.; Colquhoun, D. R.; Dinglasan, R. R.; Graham, D. R.; Mahal, L. K., Complex N-linked glycans serve as a determinant for exosome/microvesicle cargo recruitment. *J Biol Chem* **2014,** *289* (47), 32526-37.
62. Schwarz, F.; Aebi, M., Mechanisms and principles of N-linked protein glycosylation. *Current opinion in structural biology* **2011,** *21* (5), 576-82.
63. Gill, D. J.; Chia, J.; Senewiratne, J.; Bard, F., Regulation of O-glycosylation through Golgi-to-ER relocation of initiation enzymes. *J Cell Biol* **2010,** *189* (5), 843-58.
64. Goldenring, J. R., A central role for vesicle trafficking in epithelial neoplasia: intracellular highways to carcinogenesis. *Nature reviews. Cancer* **2013,** *13* (11), 813-20.
65. Mauvezin, C.; Neufeld, T. P., Bafilomycin A1 disrupts autophagic flux by inhibiting both V-ATPase-dependent acidification and Ca-P60A/SERCA-dependent autophagosome-lysosome fusion. *Autophagy* **2015,** *11* (8), 1437-8.
66. Cauwe, B.; Opdenakker, G., Intracellular substrate cleavage: a novel dimension in the biochemistry, biology and pathology of matrix metalloproteinases. *Critical reviews in biochemistry and molecular biology* **2010,** *45* (5), 351-423.
67. Shiomi, T.; Lemaitre, V.; D'Armiento, J.; Okada, Y., Matrix metalloproteinases, a disintegrin and metalloproteinases, and a disintegrin and metalloproteinases with thrombospondin motifs in non-neoplastic diseases. *Pathol Int* **2010,** *60* (7), 477-96.
68. Shimoda, M.; Khokha, R., Proteolytic factors in exosomes. *Proteomics* **2013,** *13* (10-11), 1624-36.
69. Roucourt, B.; Meeussen, S.; Bao, J.; Zimmermann, P.; David, G., Heparanase activates the syndecan-syntenin-ALIX exosome pathway. *Cell research* **2015,** *25* (4), 412-28.

Figure legends

Fig. 1: Overexpression of NPNT in 66cl4 cells does not affect the secretion or uptake of sEVs

(a) SEM of 66cl4-EV and 66cl4-NPNT cells cultured in medium free of serum vesicles for 24 hrs, showed extracellular vesicles released by these cells. Red arrows point at potential extracellular vesicles. Scale bar, upper row 5µm and lower row 2µm. **(b)** Fraction of MVs and sEVs isolated from 66cl4-EV and 66cl4-NPNT cell lines were stained with uranyl acetate and viewed by electron microscopy. Scale bar, 100 nm. **(c)** 66cl4-EV cells were incubated with 40 µg of PKH26 stained sEVs derived from 66cl4-EV and 66cl4-NPNT cells and imaged after 4 hrs to check for internalization of exosomes. Scale bar, 100µm.

Fig. 2: Overexpression of NPNT in 66cl4 cells alters the content of sEVs

(a) Venn diagram of proteins identified in sEVs isolated from 66cl4-EV and 66cl4-NPNT cells. A total 1750 proteins were identified to be common between the sEVs isolated from both the cell lines. The numbers indicate that a certain protein was present in at least 3 out of 4 replicates. **(b)** Pie chart shows distribution of 1750 common proteins based on their subcellular localization. **(c)** Pie chart showing distribution of 1750 common proteins based on their molecular nature. **(d)** Heat map of proteins differentially expressed in sEVs derived from 66cl4-EV and 66cl4-NPNT cells, considering proteins from all 4 replicates.

Fig. 3: Truncated form of NPNT is concentrated in sEVs isolated from 66cl4-NPNT cells

(a) Immunoblotting for V5-tagged NPNT using whole cell lysates of 66cl4-EV, 66cl4-NPNT, 66cl4-NPNT-RGE and 66cl4-NPNT-RGEAIA cells **(b)** Immunoblotting for V5-tagged NPNT using lysates made from the sEVs isolated from supernatant of 66cl4-EV, 66cl4-NPNT, 66cl4-NPNT-RGE and 66cl4-NPNT-RGEAIA cells. **(c)** Positional information of mouse NPNT sequences used for characterization of NPNT. Lysates made from whole cell **(d)** and small extracellular vesicles **(e)** of 66cl4 cells over expressing NPNT were treated with different glycosylation enzymes and observed for reduction in molecular size of NPNT. '-N' denotes removal of N-glycosylation by PNGase F treatment. '-O' denotes removal of O-glycosylation by O-glycosidase. '-S' symbolizes removal of sialic acid cap. '-O&S' denotes removal of sialic acid cap and O-glycosylation.

Fig.4: Intracellular protein trafficking controls the protein level of the truncated form of NPNT

(a) Immunoblotting for V5 tagged NPNT was used to detect differential expression of NPNT when 66cl4 overexpressing cells were exposed to 100 nM BafilomycinA1 (BafA1) or 1X Protein Transport Inhibitor cocktail (PTI). **(b)** Immunoblotting was used to detect differential expression of V5 tagged NPNT in 66cl4-RGE cells post exposure to 100 nM BafA1 or 1X PTI for 6 hrs. **(c)** Immunoblotting for V5 tagged NPNT using whole cell lysates of 66cl4-RGE-AIA cells post exposure to 100 nM BafA1 or 1X PTI for 6 hrs. Results here are presented in-terms of a fold change after normalizing with GAPDH. Quantification of optical density represents the mean of at least three independent experiments.

Fig.5: Matrix metalloproteinases are involved in proteolytic processing of full length NPNT

(a) Immunoblotting for V5 tagged NPNT post exposure to 10µM GM6001 for 24 hrs. Results here are presented in-terms of a fold change after normalizing with GAPDH. Quantification of optical density represents the mean of at least three independent experiments. **(b)** Illustration showing the structural differences in NPNT at 80, 60 and 20 kDa. The 80 kDa NPNT, is the full length protein having a putative signal peptide, the EGF repeats, glycosylation sites, integrin binding motifs and the MAM domain. The 60 kDa NPNT is also a full-length protein but with fewer attached glycans, as opposed to the 80 kDa NPNT. The 20 kDa NPNT is the truncated form of NPNT harboring mainly the MAM domain and the C-terminal V5-tag. **(c)** Illustration showing the probable route of NPNT secretion, endocytosis, degradation or selective sorting into extracellular vesicles. Upon glycosylation at endoplasmic reticulum and Golgi, NPNT is secreted via secretory vesicles. The secreted NPNT probably interacts with cell surface receptors such as integrins or is cleaved by matrix metalloproteases (MMPs). The cleaved NPNT adhering to the cell surface could further be takenup. Several factors dictate the fate of multivesicular bodies, depending on which the endocytosed and/or pinocytosed NPNT is then released as exosomes or degraded by lysosomes.

Table 1: ***Characterization of forms of NPNT at 80, 60 and 20 kDa.*** Whole cell lysates from 66cl4-NPNT cells were used for gel electrophoresis post immunoprecipitation with anti-V5 coated beads. In the eluted proteins different NPNT tryptic peptides were detected in the 80kDa, 60kD and 20 kDa NPNT-V5 bands. The table represents results from three biological replicates.

NPNT sequence	Length	Start position	End position	20KDa	60KDa	80KDa
QIVSSIGLCR	10	28	37	-	✓	✓
CQCPSPGLQLAPDGR	15	151	165	-	-	✓
TCVDIDECATGR	12	166	177	-	✓	✓
EKDSDLHWETAR	12	405	416	-	✓	✓
DSDLHWETAR	10	407	416	-	✓	✓
DPAGGQYLTVSAAK	14	417	430	✓	-	✓

Figure 1

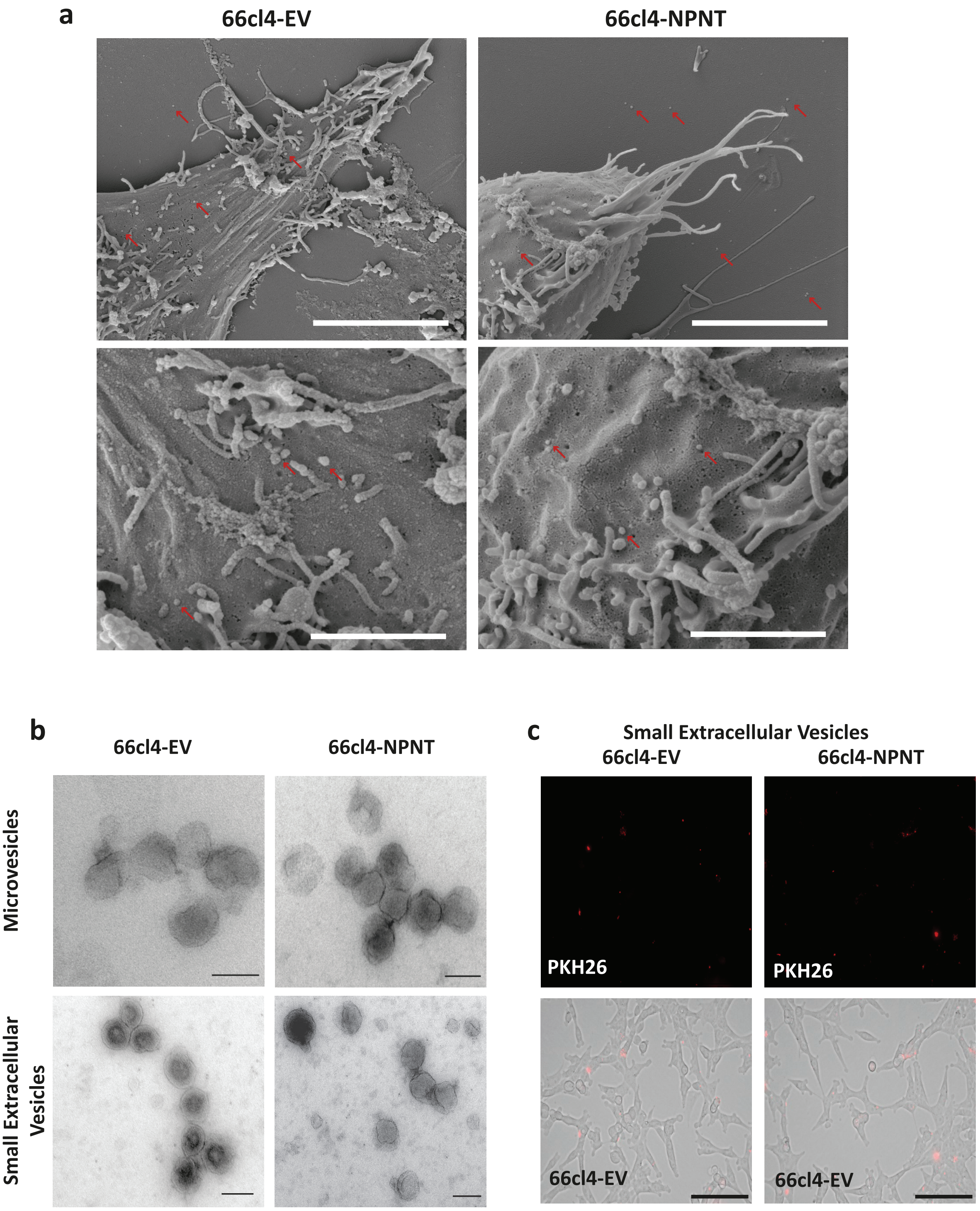
a
66cl4-EV
66cl4-NPNT
b
66cl4-EV
66cl4-NPNT
Microvesicles
Small Extracellular Vesicles
c
Small Extracellular Vesicles
66cl4-EV
66cl4-NPNT
PKH26
PKH26
66cl4-EV
66cl4-EV

Figure 2

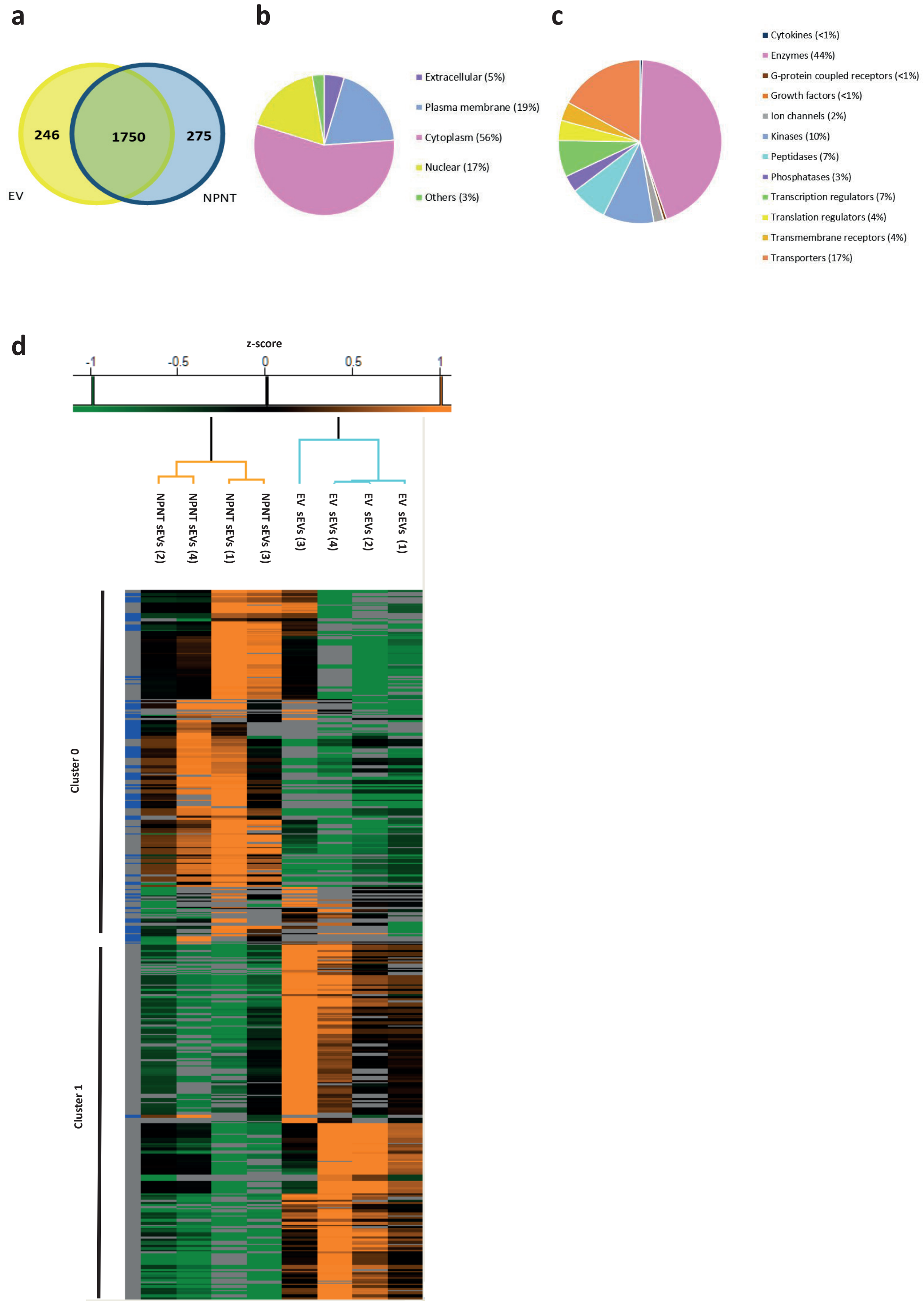
a
246
1750
275
EV
NPNT
b
Extracellular (5%)
Plasma membrane (19%)
Cytoplasm (56%)
Nuclear (17%)
Others (3%)
c
Cytokines (<1%)
Enzymes (44%)
G-protein coupled receptors (<1%)
Growth factors (<1%)
Ion channels (2%)
Kinases (10%)
Peptidases (7%)
Phosphatases (3%)
Transcription regulators (7%)
Translation regulators (4%)
Transmembrane receptors (4%)
Transporters (17%)
d
z-score
-1
-0.5
0
0.5
1
NPNT sEVs (2)
NPNT sEVs (4)
NPNT sEVs (1)
NPNT sEVs (3)
EV sEVs (3)
EV sEVs (4)
EV sEVs (2)
EV sEVs (1)
Cluster 0
Cluster 1

Figure 3

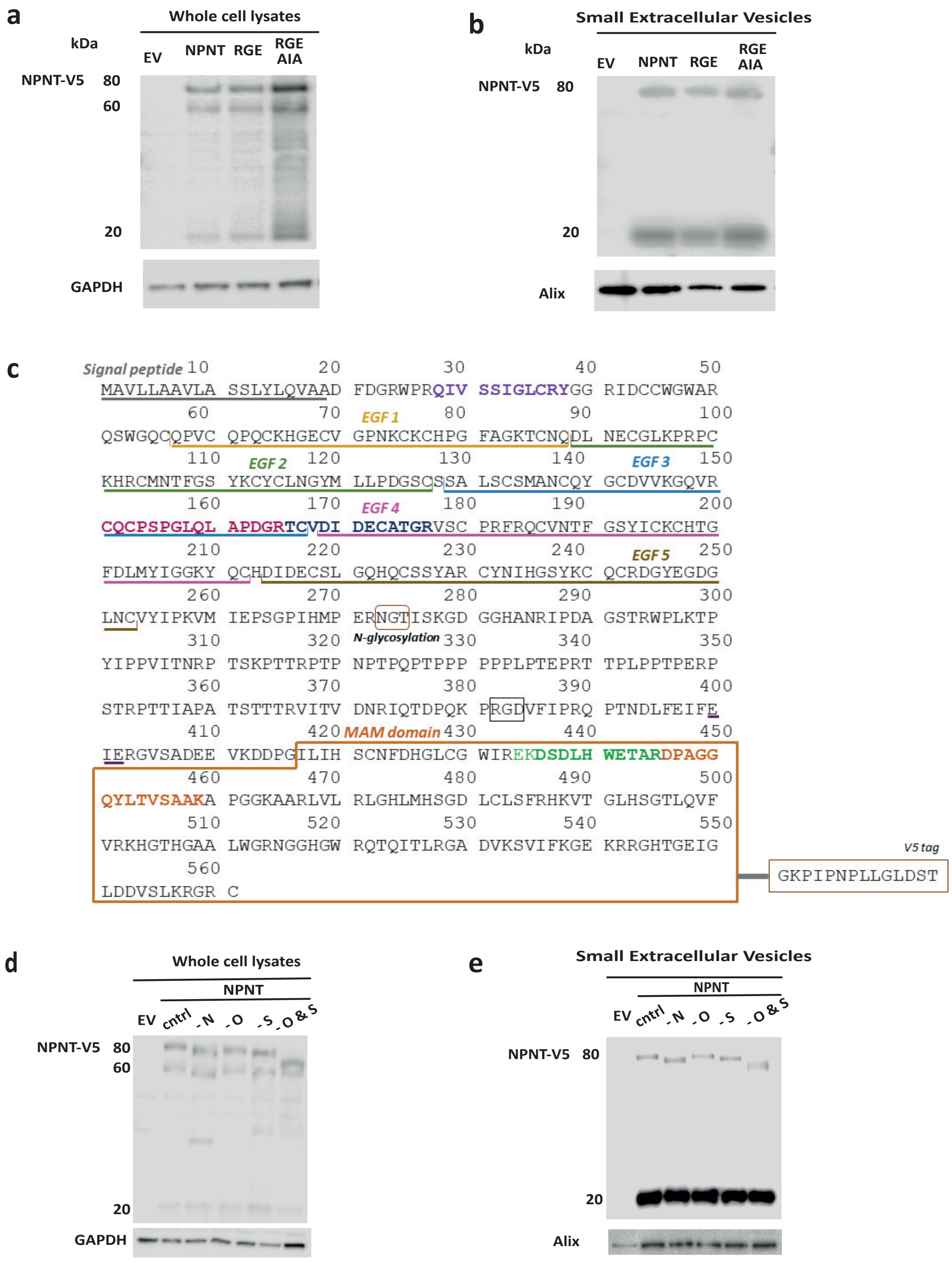
a
Whole cell lysates
kDa
EV
NPNT
RGE
RGE AIA
NPNT-V5
80
60
20
GAPDH
b
Small Extracellular Vesicles
kDa
EV
NPNT
RGE
RGE AIA
NPNT-V5
80
20
Alix
c
Signal peptide
10 20 30 40 50
MAVLLAAVLA SSLYLQVAAD FDGRWPRQIV SSIGLCRYGG RIDCCWGWAR
60 70 EGF 1 80 90 100
QSWGQCQPVC QPQCKHGECV GPNKCKCHPG FAGKTCNQDL NECGLKPRPC
110 EGF 2 120 130 140 EGF 3 150
KHRCMNTFGS YKCYCLNGYM LLPDGSCSSA LSCSMANCQY GCDVVKGQVR
160 170 EGF 4 180 190 200
CQCPSPGLQL APDGRTCVDI DECATGRVSC PRFRQCVNTF GSYICKCHTG
210 220 230 240 EGF 5 250
FDLMYIGGKY QCHDIDECSL GQHQCSSYAR CYNIHGSYKC QCRDGYEGDG
260 270 280 290 300
LNCVYIPKVM IEPSGPIHMP ERNGTISKGD GGHANRIPDA GSTRWPLKTP
310 320 N-glycosylation 330 340 350
YIPPVITNRP TSKPTTRPTP NPTPQPTPPP PPPLPTEPRT TPLPPTPERP
360 370 380 390 400
STRPTTIAPA TSTTTRVITV DNRIQTDPQK PRGDVFIPRQ PTNDLFEIFE
410 420 MAM domain 430 440 450
IERGVSADEE VKDDPGILIH SCNFDHGLCG WIREKDSDLH WETARDPAGG
460 470 480 490 500
QYLTVSAAKA PGGKAARLVL RLGHLMHSGD LCLSFRHKVT GLHSGTLQVF
510 520 530 540 550
VRKHGTHGAA LWGRNGGHGW RQTQITLRGA DVKSVIFKGE KRRGHTGEIG
560
LDDVSLKRGR C
V5 tag
GKPIPNPLLGLDST
d
Whole cell lysates
NPNT
EV
cntrl
-N
-O
-S
-O & S
NPNT-V5
80
60
20
GAPDH
e
Small Extracellular Vesicles
NPNT
EV
cntrl
-N
-O
-S
-O & S
NPNT-V5
80
20
Alix

Figure 4

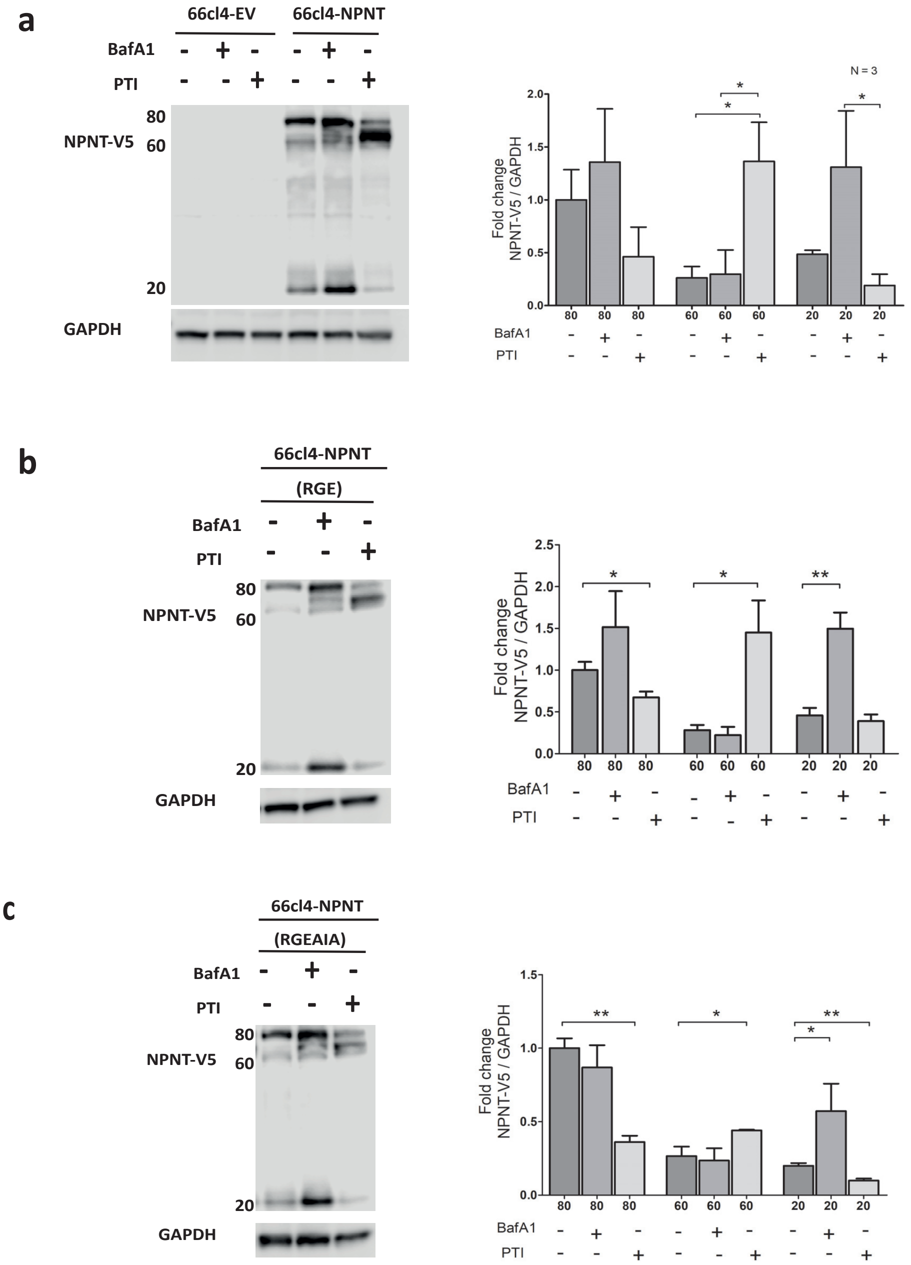
a
66cl4-EV
66cl4-NPNT
BafA1 - + - - + -
PTI - - + - - +
80
60
20
NPNT-V5
GAPDH
N = 3
Fold change NPNT-V5 / GAPDH
0.0
0.5
1.0
1.5
2.0
80 80 80 60 60 60 20 20 20
BafA1 - + - - + - - + -
PTI - - + - - + - - +
*
*
*
b
66cl4-NPNT
(RGE)
BafA1 - + -
PTI - - +
80
60
20
NPNT-V5
GAPDH
Fold change NPNT-V5 / GAPDH
0.0
0.5
1.0
1.5
2.0
2.5
80 80 80 60 60 60 20 20 20
BafA1 - + - - + - - + -
PTI - - + - - + - - +
*
*
**
c
66cl4-NPNT
(RGEAIA)
BafA1 - + -
PTI - - +
80
60
20
NPNT-V5
GAPDH
Fold change NPNT-V5 / GAPDH
0.0
0.5
1.0
1.5
80 80 80 60 60 60 20 20 20
BafA1 - + - - + - - + -
PTI - - + - - + - - +
**
*
*
**

Figure 5

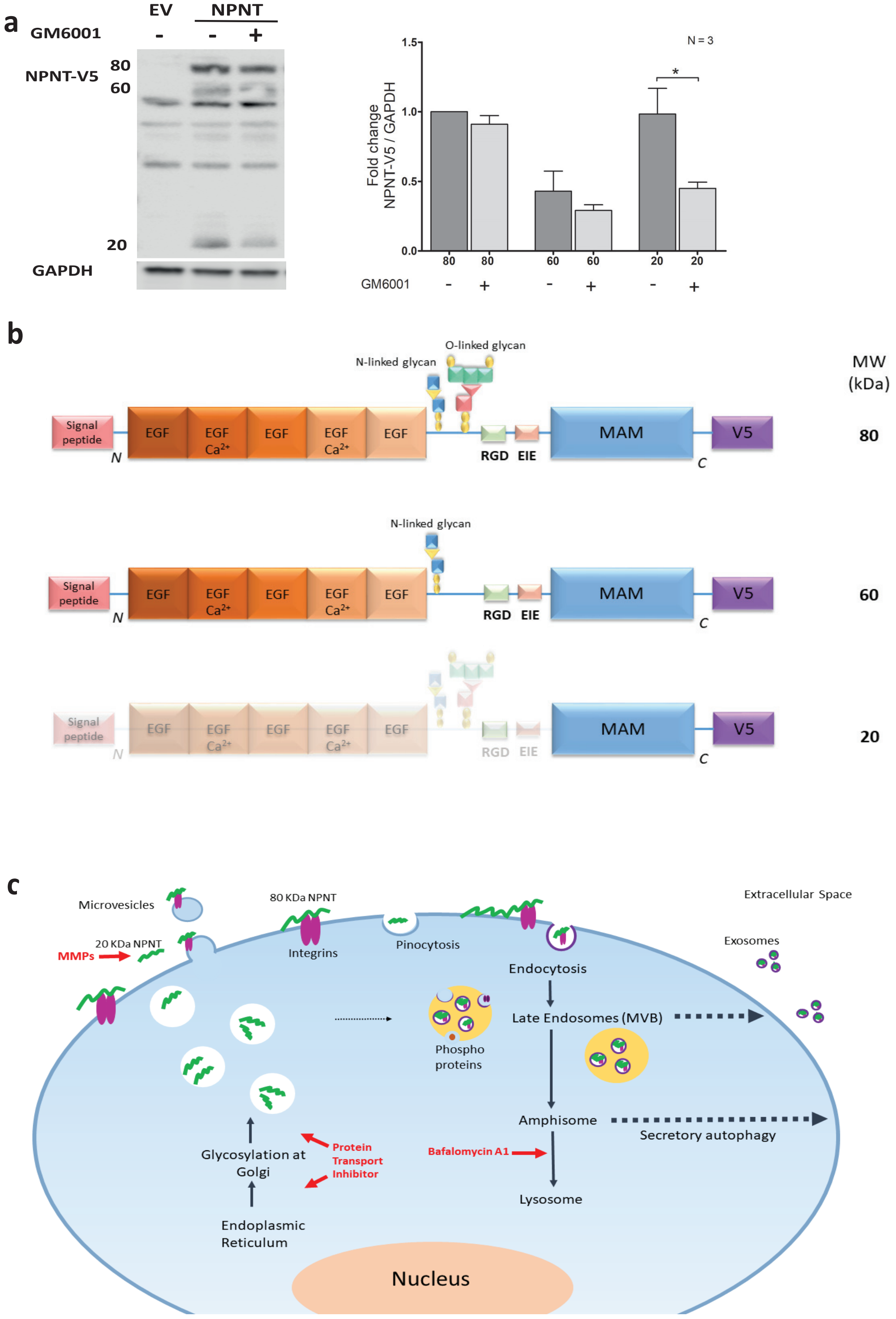
a
EV
NPNT
GM6001
-
-
+
NPNT-V5
80
60
20
GAPDH
N = 3
Fold change NPNT-V5 / GAPDH
1.5
1.0
0.5
0.0
*
80
80
60
60
20
20
GM6001
-
+
-
+
-
+
b
MW (kDa)
N-linked glycan
O-linked glycan
Signal peptide
EGF
EGF Ca2+
EGF
EGF Ca2+
EGF
RGD
EIE
MAM
V5
N
C
80
N-linked glycan
60
20
c
Microvesicles
20 KDa NPNT
MMPs
80 KDa NPNT
Integrins
Pinocytosis
Extracellular Space
Exosomes
Endocytosis
Late Endosomes (MVB)
Phospho proteins
Amphisome
Secretory autophagy
Bafalomycin A1
Lysosome
Glycosylation at Golgi
Protein Transport Inhibitor
Endoplasmic Reticulum
Nucleus

Supplementary legends

Fig. S1: (a) Markers expected to be present sEVs derived from tumor cell lines. **(b)** IPA identifies top signaling pathways based on 2025 Uniprot IDs detected in sEVs isolated from 66cl4-NPNT cells. **(c)** Immunoblotting for V5-tagged NPNT using lysates made from MVs isolated from 66cl4-EV and 66cl4-NPNTcells.

Table S1: List of proteins detected in lysates of sEVs isolated from 66cl4-EV and –NPNT cells; in continuation with the Venn diagram (Fig. 2a). Unmapped protein IDs include (P03975, P68433, P62806, G3UYJ7, and A0A0R4J0T7).

Table S2: List of proteins detected in sEVs derived from 66cl4-EV and 66cl4-NPNT cells, which pass FDR 5%. Proteins are clustered over z-scores using row median (Fig. 2d).

Table S3: Functional roles of proteins identified in cluster 0 and cluster 1 (Fig. 2d) as predicted by IPA analysis.

Figure S1

a

Ag-presentation	HLA-1A
Cytokines and cognate receptors	ILR, TNFR, TNF-α, TfR…
Cytoskeletal proteins	Actin, Ezrin, Radixin, Moesin…
Enzymes	Pyruvate kinase, enolase…
Lysosomal markers	LAMP1, LAMP2…
Membrane adhesion	Integrin, annexins…
Membrane transport and fusion	RAB protein family, flotilin
Molecular chaperones	HSP family…
MVB markers	TSG101, PDCD6IP (ALIX)
Tetraspanins	CD9, CD63, CD82…
Tumor Antigens	TJP1, CD44, GPC1…

b

Top Canonical pathways	p-value
EIF2 Signaling	5.47E-61
Integrin Signaling	1.55E-44
Regulation of eIF4 and p70S6K Signaling	8.81E-41
mTOR Signaling	5.37E-33
Axonal Guidance Signaling	9.41E-33

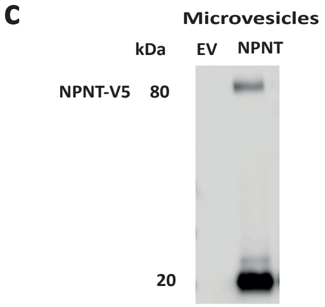

Table S1

NPNT only_275

ID	Symbol	Entrez Gene Name	Location	Type(s)
Q8JZN5	ACAD9	acyl-CoA dehydrogenase family member 9	Cytoplasm	enzyme
A2AL50	AGPS	alkylglycerone phosphate synthase	Cytoplasm	enzyme
Q9CZU0	Akr1c20	aldo-keto reductase family 1, member C20	Other	enzyme
P61208	ARL4C	ADP ribosylation factor like GTPase 4C	Nucleus	enzyme
Q9CPX6	ATG3	autophagy related 3	Cytoplasm	enzyme
B1AXY5	B4GALT1	beta-1,4-galactosyltransferase 1	Cytoplasm	enzyme
Q8BWP8-2	B4GAT1	beta-1,4-glucuronyltransferase 1	Cytoplasm	enzyme
O35855	BCAT2	branched chain amino acid transaminase 2	Cytoplasm	enzyme
P24270	CAT	catalase	Cytoplasm	enzyme
Q8K297	COLGALT1	collagen beta(1-O)galactosyltransferase 1	Cytoplasm	enzyme
P56391	COX6B1	cytochrome c oxidase subunit 6B1	Cytoplasm	enzyme
G3X9T8	CP	ceruloplasmin	Extracellular Space	enzyme
Q9CQX2	CYB5B	cytochrome b5 type B	Cytoplasm	enzyme
Q9D0M3-2	CYC1	cytochrome c1	Cytoplasm	enzyme
O35215	DDT	D-dopachrome tautomerase	Cytoplasm	enzyme
Q61655	DDX19A	DEAD-box helicase 19A	Nucleus	enzyme
Q9CWX9	DDX47	DEAD-box helicase 47	Nucleus	enzyme
Q6Q899	DDX58	DExD/H-box helicase 58	Cytoplasm	enzyme
Q80X98	DHX38	DEAH-box helicase 38	Nucleus	enzyme
Q9ESX5	DKC1	dyskerin pseudouridine synthase 1	Nucleus	enzyme
Q80VJ3	DNPH1	2'-deoxynucleoside 5'-phosphate N-hydrolase 1	Nucleus	enzyme
Q8BH95	ECHS1	enoyl-CoA hydratase, short chain 1	Cytoplasm	enzyme
E9QM61	ERCC5	ERCC excision repair 5, endonuclease	Nucleus	enzyme
Q8BHK9	ERCC6L	ERCC excision repair 6 like, spindle assembly checkpoint helicase	Nucleus	enzyme
Q91W61	FBXL15	F-box and leucine rich repeat protein 15	Cytoplasm	enzyme
Q3UGI9	FBXO7	F-box protein 7	Cytoplasm	enzyme
Q60928	GGT1	gamma-glutamyltransferase 1	Plasma Membrane	enzyme
Q9QUH0	GLRX	glutaredoxin	Cytoplasm	enzyme
Q8K0C9	GMDS	GDP-mannose 4,6-dehydratase	Cytoplasm	enzyme
P29387	GNB4	G protein subunit beta 4	Plasma Membrane	enzyme
Q99LH1	GNL2	G protein nucleolar 2	Nucleus	enzyme
A2AQR0	GPD2	glycerol-3-phosphate dehydrogenase 2	Cytoplasm	enzyme
P11352	GPX1	glutathione peroxidase 1	Cytoplasm	enzyme
Q61425	HADH	hydroxyacyl-CoA dehydrogenase	Cytoplasm	enzyme
Q80XR6	HNRNPAB	heterogeneous nuclear ribonucleoprotein A/B	Nucleus	enzyme
Q8BIJ6	IARS2	isoleucyl-tRNA synthetase 2, mitochondrial	Cytoplasm	enzyme

Q3U0V1	KHSRP	KH-type splicing regulatory protein	Nucleus	enzyme
P17897	LYZ	lysozyme	Extracellular Space	enzyme
D3YTR5	MBD3	methyl-CpG binding domain protein 3	Nucleus	enzyme
Q91YR5	METTL13	methyltransferase like 13	Other	enzyme
Q80UM7	MOGS	mannosyl-oligosaccharide glucosidase	Cytoplasm	enzyme
Q8CC86	NAPRT	nicotinate phosphoribosyltransferase	Cytoplasm	enzyme
Q9JI75	NQO2	N-ribosyldihydronicotinamide:quinone reductase 2	Cytoplasm	enzyme
Q1HFZ0	NSUN2	NOP2/Sun RNA methyltransferase family member 2	Nucleus	enzyme
P29758	OAT	ornithine aminotransferase	Cytoplasm	enzyme
Q921K2	PARP1	poly(ADP-ribose) polymerase 1	Nucleus	enzyme
A0A0G2JF67	PDE5A	phosphodiesterase 5A	Cytoplasm	enzyme
Q9D051	PDHB	pyruvate dehydrogenase E1 beta subunit	Cytoplasm	enzyme
Q9QUR7	PIN1	peptidylprolyl cis/trans isomerase, NIMA-interacting 1	Nucleus	enzyme
O35134	POLR1A	RNA polymerase I subunit A	Nucleus	enzyme
A0A0R4J0V5	POLR2A	RNA polymerase II subunit A	Nucleus	enzyme
O08795-2	PRKCSH	protein kinase C substrate 80K-H	Cytoplasm	enzyme
Q8BW00	PTRH1	peptidyl-tRNA hydrolase 1 homolog	Cytoplasm	enzyme
Q8R2Y8	PTRH2	peptidyl-tRNA hydrolase 2	Cytoplasm	enzyme
Q8BG51	RHOT1	ras homolog family member T1	Cytoplasm	enzyme
Z4YLT8	RNF11	ring finger protein 11	Cytoplasm	enzyme
Q9ET26	RNF114	ring finger protein 114	Extracellular Space	enzyme
Q5DTM8	RNF20	ring finger protein 20	Nucleus	enzyme
E9Q5F9-2	SETD2	SET domain containing 2	Cytoplasm	enzyme
Q9QYY8-2	SPAST	spastin	Nucleus	enzyme
Q9Z2I9	SUCLA2	succinate-CoA ligase ADP-forming beta subunit	Cytoplasm	enzyme
Q9D939	SULT1C2	sulfotransferase family 1C member 2	Cytoplasm	enzyme
P21981	TGM2	transglutaminase 2	Cytoplasm	enzyme
Q8BXZ1	TMX3	thioredoxin related transmembrane protein 3	Cytoplasm	enzyme
A0A087WNZ7	TRIP12	thyroid hormone receptor interactor 12	Cytoplasm	enzyme
Q3UX10	TUBAL3	tubulin alpha like 3	Other	enzyme
E9PXX7	TXNDC5	thioredoxin domain containing 5	Cytoplasm	enzyme
A0A0R4J1F6	UAP1	UDP-N-acetylglucosamine pyrophosphorylase 1	Nucleus	enzyme
Q9Z1F9	UBA2	ubiquitin like modifier activating enzyme 2	Cytoplasm	enzyme
Q9CR09	UFC1	ubiquitin-fold modifier conjugating enzyme 1	Cytoplasm	enzyme
Q91ZJ5-2	UGP2	UDP-glucose pyrophosphorylase 2	Cytoplasm	enzyme
Q8R1I1	UQCR10	ubiquinol-cytochrome c reductase, complex III subunit X	Cytoplasm	enzyme
Q9CR68	UQCRFS1	ubiquinol-cytochrome c reductase, Rieske iron-sulfur polypeptide 1	Cytoplasm	enzyme
P59268	ZDHHC9	zinc finger DHHC-type containing 9	Cytoplasm	enzyme
Q8BMC0	LPAR6	lysophosphatidic acid receptor 6	Plasma Membrane	G-protein coupled receptor
Q9CQI3	GMFB	glia maturation factor beta	Cytoplasm	growth factor

Q62000	OGN	osteoglycin	Extracellular Space	growth factor
P04202	TGFB1	transforming growth factor beta 1	Extracellular Space	growth factor
P37172	ACVR1	activin A receptor type 1	Plasma Membrane	kinase
Q9Z110-2	ALDH18A1	aldehyde dehydrogenase 18 family member A1	Cytoplasm	kinase
P16277	BLK	BLK proto-oncogene, Src family tyrosine kinase	Cytoplasm	kinase
Q91YS8	CAMK1	calcium/calmodulin dependent protein kinase I	Cytoplasm	kinase
P49615	CDK5	cyclin dependent kinase 5	Nucleus	kinase
E9Q605	CHUK	conserved helix-loop-helix ubiquitous kinase	Cytoplasm	kinase
Q9DC28-2	CSNK1D	casein kinase 1 delta	Cytoplasm	kinase
J3QN85	FGFR1	fibroblast growth factor receptor 1	Plasma Membrane	kinase
Q5F258	GIT1	GIT ArfGAP 1	Nucleus	kinase
Q62137-2	JAK3	Janus kinase 3	Cytoplasm	kinase
Q9JLN9	MTOR	mechanistic target of rapamycin kinase	Nucleus	kinase
Q6P9R2	OXSR1	oxidative stress responsive 1	Nucleus	kinase
A0A0R4J0G0	PCK2	phosphoenolpyruvate carboxykinase 2, mitochondrial	Cytoplasm	kinase
Q91XU3	PIP4K2C	phosphatidylinositol-5-phosphate 4-kinase type 2 gamma	Cytoplasm	kinase
P70268	PKN1	protein kinase N1	Cytoplasm	kinase
P68181-2	PRKACB	protein kinase cAMP-activated catalytic subunit beta	Cytoplasm	kinase
Q4VA93	PRKCA	protein kinase C alpha	Cytoplasm	kinase
P70336	ROCK2	Rho associated coiled-coil containing protein kinase 2	Cytoplasm	kinase
Q91VJ4	STK38	serine/threonine kinase 38	Nucleus	kinase
O88393	TGFBR3	transforming growth factor beta receptor 3	Plasma Membrane	kinase
Q0KL02-3	TRIO	trio Rho guanine nucleotide exchange factor	Cytoplasm	kinase
Q9CPN9	2210010C04Rik	RIKEN cDNA 2210010C04 gene	Extracellular Space	other
Q9CQD4	2610002M06Rik	RIKEN cDNA 2610002M06 gene	Cytoplasm	other
Q9QZB7	ACTR10	actin related protein 10 homolog	Cytoplasm	other
F6QH25	ALCAM	activated leukocyte cell adhesion molecule	Plasma Membrane	other
Q505D1	ANKRD28	ankyrin repeat domain 28	Cytoplasm	other
G5E8V9	ARFIP1	ADP ribosylation factor interacting protein 1	Cytoplasm	other
D3Z0V2	ARHGEF7	Rho guanine nucleotide exchange factor 7	Cytoplasm	other
Q9R0Q6	ARPC1A	actin related protein 2/3 complex subunit 1A	Extracellular Space	other
Q9JK81	C12orf10	chromosome 12 open reading frame 10	Nucleus	other
Q3TQQ9-3	C1orf112	chromosome 1 open reading frame 112	Other	other
A0A0A0MQF7	C1orf21	chromosome 1 open reading frame 21	Other	other
Q9CR86	CARHSP1	calcium regulated heat stable protein 1	Cytoplasm	other
Q8K3W3	CASC3	cancer susceptibility 3	Nucleus	other
Q9D8X2	CCDC124	coiled-coil domain containing 124	Other	other
D3Z2Z1	CLIP1	CAP-Gly domain containing linker protein 1	Cytoplasm	other
Q9JKY0	CNOT9	CCR4-NOT transcription complex subunit 9	Cytoplasm	other
A0A140T8W1	COL6A5	collagen type VI alpha 5 chain	Extracellular Space	other

Q8BXC6	COMMD2	COMM domain containing 2	Other	other
Q9CZ04-2	COPS7A	COP9 signalosome subunit 7A	Cytoplasm	other
Q9D2V7	CORO7/CORO7-PAM16	coronin 7	Cytoplasm	other
E9Q8Z5	CTNND1	catenin delta 1	Nucleus	other
E9Q586	DCTN1	dynactin subunit 1	Cytoplasm	other
E9PXV7	DIAPH1	diaphanous related formin 1	Plasma Membrane	other
Q9JMC3	DNAJA4	DnaJ heat shock protein family (Hsp40) member A4	Nucleus	other
Q5SRI3	DOCK2	dedicator of cytokinesis 2	Cytoplasm	other
Q7TMD7	DSG4	desmoglein 4	Plasma Membrane	other
Q91ZU6-5	Dst	dystonin	Plasma Membrane	other
Q8C845	EFHD2	EF-hand domain family member D2	Other	other
Q3THJ3	EIF1AD	eukaryotic translation initiation factor 1A domain containing	Nucleus	other
O70194	EIF3D	eukaryotic translation initiation factor 3 subunit D	Cytoplasm	other
Q7TT37	ELP1	elongator complex protein 1	Cytoplasm	other
Q99KI3	EMC3	ER membrane protein complex subunit 3	Nucleus	other
Q99K41	EMILIN1	elastin microfibril interfacer 1	Extracellular Space	other
Q6PGF7	EXOC8	exocyst complex component 8	Plasma Membrane	other
Q9D6U8	FAM162A	family with sequence similarity 162 member A	Cytoplasm	other
Q642K5	FAU	FAU, ubiquitin like and ribosomal protein S30 fusion	Cytoplasm	other
Q08879-2	FBLN1	fibulin 1	Extracellular Space	other
P02301	Gm7426	embryonic H3 histone	Other	other
P36916	GNL1	G protein nucleolar 1 (putative)	Nucleus	other
A2ATI9	GORASP2	golgi reassembly stacking protein 2	Cytoplasm	other
B2RR03	GP1BB	glycoprotein Ib platelet beta subunit	Plasma Membrane	other
Q8VDU0	GPSM2	G protein signaling modulator 2	Nucleus	other
Q99LP6	GRPEL1	GrpE like 1, mitochondrial	Cytoplasm	other
Q3UGR5	HDHD2	haloacid dehalogenase like hydrolase domain containing 2	Cytoplasm	other
G3X9B1	HEATR1	HEAT repeat containing 1	Nucleus	other
E9PZP8	HERC1	HECT and RLD domain containing E3 ubiquitin protein ligase family member 1	Cytoplasm	other
Q8VDM6	HNRNPUL1	heterogeneous nuclear ribonucleoprotein U like 1	Nucleus	other
Q61635	Ifi47	interferon gamma inducible protein 47	Cytoplasm	other
Q8CAQ8-2	IMMT	inner membrane mitochondrial protein	Cytoplasm	other
A0A1L1SRP4	KIF23	kinesin family member 23	Cytoplasm	other
A6BLY7	KRT28	keratin 28	Cytoplasm	other
Q9D1R2	KTI12	KTI12 chromatin associated homolog	Other	other
Q9JHS3	LAMTOR2	late endosomal/lysosomal adaptor, MAPK and MTOR activator 2	Cytoplasm	other
Q60787	LCP2	lymphocyte cytosolic protein 2	Cytoplasm	other
Q922Q8	LRRC59	leucine rich repeat containing 59	Cytoplasm	other
B1B1E2	LTBP1	latent transforming growth factor beta binding protein 1	Extracellular Space	other

P61327	MAGOH	mago homolog, exon junction complex core component	Nucleus	other
A0A0R4J0J7	MAMDC2	MAM domain containing 2	Extracellular Space	other
A0A0A6YXE3	MBNL1	muscleblind like splicing regulator 1	Nucleus	other
Q9D1H9	MFAP4	microfibril associated protein 4	Extracellular Space	other
E9Q9T8	MYBPC3	myosin binding protein C, cardiac	Cytoplasm	other
D6RFN5	NINJ1	ninjurin 1	Plasma Membrane	other
E9Q5C9	Nolc1	nucleolar and coiled-body phosphoprotein 1	Nucleus	other
E9QN31	NOP2	NOP2 nucleolar protein	Nucleus	other
A2ABY2	NPB	neuropeptide B	Extracellular Space	other
Q91V88	NPNT	nephronectin	Plasma Membrane	other
Q9CQ48	NUDCD2	NudC domain containing 2	Cytoplasm	other
Q9CQF3	NUDT21	nudix hydrolase 21	Nucleus	other
Q8R480	NUP85	nucleoporin 85	Cytoplasm	other
E9Q7L3	PBRM1	polybromo 1	Nucleus	other
Q6PB90	Pcdhb14	protocadherin beta 14	Other	other
O35226-2	PSMD4	proteasome 26S subunit, non-ATPase 4	Cytoplasm	other
Q9EST4-3	PSMG2	proteasome assembly chaperone 2	Nucleus	other
F8VQ28	PXN	paxillin	Cytoplasm	other
Q80UJ7	RAB3GAP1	RAB3 GTPase activating protein catalytic subunit 1	Cytoplasm	other
Q99KG3-2	RBM10	RNA binding motif protein 10	Nucleus	other
Q80WQ6	RHBDF2	rhomboid 5 homolog 2	Cytoplasm	other
Q9JLI8	SART3	squamous cell carcinoma antigen recognized by T cells 3	Nucleus	other
G5E8J9	SCYL2	SCY1 like pseudokinase 2	Cytoplasm	other
P82349	SGCB	sarcoglycan beta	Plasma Membrane	other
O89032-3	SH3PXD2A	SH3 and PX domains 2A	Cytoplasm	other
P62317	SNRPD2	small nuclear ribonucleoprotein D2 polypeptide	Nucleus	other
P62305	Snrpe	small nuclear ribonucleoprotein E	Nucleus	other
Q4VAA7	SNX33	sorting nexin 33	Cytoplasm	other
Q9DBG7	SRPRA	SRP receptor alpha subunit	Cytoplasm	other
P47758	SRPRB	SRP receptor beta subunit	Cytoplasm	other
Q3TFP0	SRSF10	serine and arginine rich splicing factor 10	Nucleus	other
Q9CY50	SSR1	signal sequence receptor subunit 1	Cytoplasm	other
Q3UGN9	STAM	signal transducing adaptor molecule	Cytoplasm	other
Q8C079	STRIP1	striatin interacting protein 1	Nucleus	other
Q64310	SURF4	surfeit 4	Cytoplasm	other
Q6A028	SWAP70	switching B cell complex subunit SWAP70	Cytoplasm	other
Q9Z1A1	TFG	TRK-fused gene	Cytoplasm	other
O08710	TG	thyroglobulin	Extracellular Space	other
Q9CXE7	TMED5	transmembrane p24 trafficking protein 5	Cytoplasm	other
P52875	TMEM165	transmembrane protein 165	Plasma Membrane	other

A0A0R4J1Z3	TMEM33	transmembrane protein 33	Cytoplasm	other
Q61033	TMPO	thymopoietin	Nucleus	other
Q9CYG7	TOMM34	translocase of outer mitochondrial membrane 34	Cytoplasm	other
F8WJG3	TRA2B	transformer 2 beta homolog	Nucleus	other
Q7TT21	TSC2	TSC complex subunit 2	Cytoplasm	other
Q8CD92-2	TTC27	tetratricopeptide repeat domain 27	Other	other
D3Z0R8	TTC7A	tetratricopeptide repeat domain 7A	Plasma Membrane	other
Q9D883	U2af1	U2 small nuclear ribonucleoprotein auxiliary factor (U2AF) 1	Nucleus	other
Q6NV83-3	U2SURP	U2 snRNP associated SURP domain containing	Nucleus	other
P61961	UFM1	ubiquitin fold modifier 1	Cytoplasm	other
Q99KD5	UNC45A	unc-45 myosin chaperone A	Plasma Membrane	other
Q5SSI6	UTP18	UTP18, small subunit processome component	Nucleus	other
Q3UMB9	WASHC4	WASH complex subunit 4	Cytoplasm	other
E9Q4P1	WDFY1	WD repeat and FYVE domain containing 1	Cytoplasm	other
Q8BFQ4	WDR82	WD repeat domain 82	Nucleus	other
A0A1W2P7Q6	XPOT	exportin for tRNA	Nucleus	other
Q9CQU5	ZWINT	ZW10 interacting kinetochore protein	Nucleus	other
Q8CG16	C1R	complement C1r	Extracellular Space	peptidase
Q99KK7	DPP3	dipeptidyl peptidase 3	Cytoplasm	peptidase
Q8BVG4	DPP9	dipeptidyl peptidase 9	Cytoplasm	peptidase
Q91YP2	NLN	neurolysin	Cytoplasm	peptidase
B2RUR8	OTUD7B	OTU deubiquitinase 7B	Cytoplasm	peptidase
P99026	PSMB4	proteasome subunit beta 4	Cytoplasm	peptidase
Q60841-3	RELN	reelin	Extracellular Space	peptidase
E9PV45	USP24	ubiquitin specific peptidase 24	Nucleus	peptidase
A0A1B0GRV0	BPNT1	3'(2'), 5'-bisphosphate nucleotidase 1	Nucleus	phosphatase
G3X9J6	NT5C2	5'-nucleotidase, cytosolic II	Cytoplasm	phosphatase
Q3UFY7	NT5C3B	5'-nucleotidase, cytosolic IIIB	Cytoplasm	phosphatase
Q9JKX6	NUDT5	nudix hydrolase 5	Cytoplasm	phosphatase
Q61469	Plpp1	phospholipid phosphatase 1	Plasma Membrane	phosphatase
P35831	PTPN12	protein tyrosine phosphatase, non-receptor type 12	Cytoplasm	phosphatase
A2BE93	SET	SET nuclear proto-oncogene	Nucleus	phosphatase
Q8K019-2	BCLAF1	BCL2 associated transcription factor 1	Nucleus	transcription regulator
Q64152-2	BTF3	basic transcription factor 3	Nucleus	transcription regulator
O35864	COPS5	COP9 signalosome subunit 5	Nucleus	transcription regulator
Q91YZ2	CTBP2	C-terminal binding protein 2	Nucleus	transcription regulator
Q3TUE1	FUBP1	far upstream element binding protein 1	Nucleus	transcription regulator
G3UYD0	GTF2I	general transcription factor IIi	Nucleus	transcription regulator
Q8BX02	KANK2	KN motif and ankyrin repeat domains 2	Nucleus	transcription regulator
Q9D071-2	MMS19	MMS19 homolog, cytosolic iron-sulfur assembly component	Nucleus	transcription regulator

P25799	NFKB1	nuclear factor kappa B subunit 1	Nucleus	transcription regulator
Q62422	OSTF1	osteoclast stimulating factor 1	Nucleus	transcription regulator
Q9WU28	PFDN5	prefoldin subunit 5	Nucleus	transcription regulator
P67778	PHB	prohibitin	Nucleus	transcription regulator
P42669	PURA	purine rich element binding protein A	Nucleus	transcription regulator
Q8C2Q3	RBM14	RNA binding motif protein 14	Nucleus	transcription regulator
Q60707	TBX2	T-box 2	Nucleus	transcription regulator
Q8R3N6	THOC1	THO complex 1	Nucleus	transcription regulator
Q3UA06	TRIP13	thyroid hormone receptor interactor 13	Cytoplasm	transcription regulator
O88477	IGF2BP1	insulin like growth factor 2 mRNA binding protein 1	Cytoplasm	translation regulator
Z4YJT3	LARP1	La ribonucleoprotein domain family member 1	Cytoplasm	translation regulator
A0A0G2JE26	ANTXR2	anthrax toxin receptor 2	Plasma Membrane	transmembrane receptor
Q7TQH7	LRP10	LDL receptor related protein 10	Plasma Membrane	transmembrane receptor
P32507-2	NECTIN2	nectin cell adhesion molecule 2	Plasma Membrane	transmembrane receptor
Q9JLZ8	SIGIRR	single Ig and TIR domain containing	Plasma Membrane	transmembrane receptor
P25118	TNFRSF1A	TNF receptor superfamily member 1A	Plasma Membrane	transmembrane receptor
Q9JHZ2	ANKH	ANKH inorganic pyrophosphate transport regulator	Plasma Membrane	transporter
Q8BMS7	ATP2C1	ATPase secretory pathway Ca2+ transporting 1	Cytoplasm	transporter
Q9D3D9	ATP5F1D	ATP synthase F1 subunit delta	Cytoplasm	transporter
Q9DB20	ATP5PO	ATP synthase peripheral stalk subunit OSCP	Cytoplasm	transporter
A0A0A6YX18	ATP6V1H	ATPase H+ transporting V1 subunit H	Cytoplasm	transporter
D3Z315	COPE	coatomer protein complex subunit epsilon	Cytoplasm	transporter
P61924	COPZ1	coatomer protein complex subunit zeta 1	Cytoplasm	transporter
B2RXV4	FLVCR1	feline leukemia virus subgroup C cellular receptor 1	Plasma Membrane	transporter
P28231	GJB3	gap junction protein beta 3	Plasma Membrane	transporter
P01942	HBA1/HBA2	hemoglobin subunit alpha 2	Extracellular Space	transporter
Q8K2V6	IPO11	importin 11	Nucleus	transporter
Q60716-2	P4HA2	prolyl 4-hydroxylase subunit alpha 2	Cytoplasm	transporter
J3QQ30	PITPNA	phosphatidylinositol transfer protein alpha	Cytoplasm	transporter
Q80ZX0	SEC24B	SEC24 homolog B, COPII coat complex component	Cytoplasm	transporter
Q99JR1	SFXN1	sideroflexin 1	Cytoplasm	transporter
Q8BRU6	SLC18A2	solute carrier family 18 member A2	Plasma Membrane	transporter
F7BP73	SLC22A23	solute carrier family 22 member 23	Other	transporter
Q9CR62	SLC25A11	solute carrier family 25 member 11	Cytoplasm	transporter
Q8BMD8	SLC25A24	solute carrier family 25 member 24	Cytoplasm	transporter
P14246	SLC2A2	solute carrier family 2 member 2	Plasma Membrane	transporter
Q3U1J0-2	SLC38A5	solute carrier family 38 member 5	Plasma Membrane	transporter
P62075	TIMM13	translocase of inner mitochondrial membrane 13	Cytoplasm	transporter
Q5SRX1-3	TOM1L2	target of myb1 like 2 membrane trafficking protein	Cytoplasm	transporter
G3X8X7	VPS16	VPS16, CORVET/HOPS core subunit	Cytoplasm	transporter

EV only_246

ID	Symbol	Entrez Gene Name	Location	Type(s)
Q8BR63	1700047I17Rik2/Fam177a	family with sequence similarity 177, member A	Other	other
Q8R420	ABCA3	ATP binding cassette subfamily A member 3	Plasma Membrane	transporter
Q8BWT1	ACAA2	acetyl-CoA acyltransferase 2	Cytoplasm	enzyme
P50544	ACADVL	acyl-CoA dehydrogenase very long chain	Cytoplasm	enzyme
P62737	ACTA2	actin, alpha 2, smooth muscle, aorta	Cytoplasm	other
Q8BUE4	AIFM2	apoptosis inducing factor, mitochondria associated 2	Cytoplasm	enzyme
E9QQ10	Akap9	A kinase (PRKA) anchor protein (yotiao) 9	Cytoplasm	other
P45377	AKR1B10	aldo-keto reductase family 1 member B10	Cytoplasm	enzyme
P24549	ALDH1A1	aldehyde dehydrogenase 1 family member A1	Cytoplasm	enzyme
P53995	ANAPC1	anaphase promoting complex subunit 1	Nucleus	other
D3YYE1	Anp32a	acidic (leucine-rich) nuclear phosphoprotein 32 family, member A	Nucleus	other
Q9EST5	Anp32b	acidic (leucine-rich) nuclear phosphoprotein 32 family, member B	Nucleus	other
G3X8P9	AOX1	aldehyde oxidase 1	Cytoplasm	enzyme
P35585	AP1M1	adaptor related protein complex 1 mu 1 subunit	Cytoplasm	transporter
Q8BSL7	Arf2	ADP-ribosylation factor 2	Cytoplasm	other
S4R203	ARHGAP12	Rho GTPase activating protein 12	Cytoplasm	other
O88848	ARL6	ADP ribosylation factor like GTPase 6	Cytoplasm	transporter
F6QKK2	ARL8A	ADP ribosylation factor like GTPase 8A	Cytoplasm	enzyme
Q78IK2	ATP5MD	ATP synthase membrane subunit DAPIT	Cytoplasm	other
Q9CR51	ATP6V1G1	ATPase H+ transporting V1 subunit G1	Cytoplasm	transporter
Q8C4G3	ATP9A	ATPase phospholipid transporting 9A (putative)	Cytoplasm	transporter
Q7TQH0-2	ATXN2L	ataxin 2 like	Nucleus	other
Q61335	BCAP31	B cell receptor associated protein 31	Cytoplasm	transporter
Q9CY64	BLVRA	biliverdin reductase A	Cytoplasm	enzyme
Q91Z96	BMP2K	BMP2 inducible kinase	Nucleus	kinase
Q9D172	C21orf33/LOC102724023	chromosome 21 open reading frame 33	Cytoplasm	other
P0DP28	Calm1 (includes others)	calmodulin 1	Nucleus	other
P25322	CCND1	cyclin D1	Nucleus	transcription regulator
Q8BGU5-2	CCNY	cyclin Y	Nucleus	other
Q64314-2	CD34	CD34 molecule	Plasma Membrane	other
Q8CII2	CDC123	cell division cycle 123	Cytoplasm	other
Q6A068	CDC5L	cell division cycle 5 like	Nucleus	transcription regulator
Q924Z4	CERS2	ceramide synthase 2	Nucleus	transcription regulator
Q8BJF9	CHMP2B	charged multivesicular body protein 2B	Cytoplasm	other
F8WIK0	CIAPIN1	cytokine induced apoptosis inhibitor 1	Cytoplasm	other
Z4YL78	CKAP5	cytoskeleton associated protein 5	Nucleus	transcription regulator
B1ATV0	CLCN5	chloride voltage-gated channel 5	Plasma Membrane	ion channel
Q63870	COL7A1	collagen type VII alpha 1 chain	Extracellular Space	other

Q62426	CSTB	cystatin B	Cytoplasm	peptidase
F2Z3X3	CUEDC1	CUE domain containing 1	Other	other
Q9D4H8	CUL2	cullin 2	Nucleus	enzyme
Q8VDF3-2	DAPK2	death associated protein kinase 2	Cytoplasm	kinase
Q8BHC4	DCAKD	dephospho-CoA kinase domain containing	Cytoplasm	other
D3Z0M9	DDX23	DEAD-box helicase 23	Nucleus	enzyme
F8WIG5	DIAPH3	diaphanous related formin 3	Cytoplasm	enzyme
E9Q9H2	DNAJC2	DnaJ heat shock protein family (Hsp40) member C2	Nucleus	other
P13864	DNMT1	DNA methyltransferase 1	Nucleus	enzyme
Q8CHR6	DPYD	dihydropyrimidine dehydrogenase	Cytoplasm	enzyme
Q7TSF0	Dsg1c	desmoglein 1 gamma	Plasma Membrane	other
O70251	EEF1B2	eukaryotic translation elongation factor 1 beta 2	Cytoplasm	translation regulator
P48024	Eif1	eukaryotic translation initiation factor 1	Other	other
Q8BMJ3	EIF1AY	eukaryotic translation initiation factor 1A, Y-linked	Other	translation regulator
Q8BTJ4-2	ENPP4	ectonucleotide pyrophosphatase/phosphodiesterase 4	Cytoplasm	enzyme
Q99K30	EPS8L2	EPS8 like 2	Cytoplasm	other
Q9DC16	ERGIC1	endoplasmic reticulum-golgi intermediate compartment 1	Cytoplasm	other
P14234	FGR	FGR proto-oncogene, Src family tyrosine kinase	Nucleus	kinase
P97807-2	FH	fumarate hydratase	Cytoplasm	enzyme
Q9JJ28	FLII	FLII, actin remodeling protein	Nucleus	other
A2AKG8	FOCAD	focadhesin	Plasma Membrane	other
A2AJ72	FUBP3	far upstream element binding protein 3	Nucleus	transcription regulator
Q9DCD6	GABARAP	GABA type A receptor-associated protein	Cytoplasm	transporter
Q8BUU7	GALK2	galactokinase 2	Cytoplasm	kinase
Q8K0D5	GFM1	G elongation factor mitochondrial 1	Cytoplasm	translation regulator
E9PVA6	GIT2	GIT ArfGAP 2	Nucleus	other
D3Z7P3-2	GLS	glutaminase	Cytoplasm	enzyme
P18872-2	GNAO1	G protein subunit alpha o1	Plasma Membrane	enzyme
Q61011	GNB3	G protein subunit beta 3	Plasma Membrane	enzyme
D3YVW2	GOLIM4	golgi integral membrane protein 4	Cytoplasm	other
Q99MK8	GRK2	G protein-coupled receptor kinase 2	Cytoplasm	kinase
Q810D6	GRWD1	glutamate rich WD repeat containing 1	Nucleus	other
P13020-2	GSN	gelsolin	Extracellular Space	other
P10649	GSTM5	glutathione S-transferase mu 5	Cytoplasm	enzyme
Q99JY0	HADHB	hydroxyacyl-CoA dehydrogenase trifunctional multienzyme complex subunit beta	Cytoplasm	enzyme
Q61191	HCFC1	host cell factor C1	Nucleus	transcription regulator
Q3UDW8	HGSNAT	heparan-alpha-glucosaminide N-acetyltransferase	Cytoplasm	enzyme
P43275	Hist1h1a	histone cluster 1, H1a	Nucleus	other
P01899	HLA-A	major histocompatibility complex, class I, A	Plasma Membrane	other
Q8R3H7	HS2ST1	heparan sulfate 2-O-sulfotransferase 1	Cytoplasm	enzyme

Q99N15	HSD17B10	hydroxysteroid 17-beta dehydrogenase 10	Cytoplasm	enzyme
P51660	HSD17B4	hydroxysteroid 17-beta dehydrogenase 4	Cytoplasm	enzyme
P17156	HSPA2	heat shock protein family A (Hsp70) member 2	Cytoplasm	other
O35632	HYAL2	hyaluronoglucosaminidase 2	Cytoplasm	enzyme
D3Z376	ICA1	islet cell autoantigen 1	Cytoplasm	other
P70404	IDH3G	isocitrate dehydrogenase 3 (NAD(+)) gamma	Cytoplasm	enzyme
P15208	INSR	insulin receptor	Plasma Membrane	kinase
Q9Z1M2	IRGM	immunity related GTPase M	Cytoplasm	enzyme
D3Z4D1	JTB	jumping translocation breakpoint	Plasma Membrane	other
Q9Z2X8	KEAP1	kelch like ECH associated protein 1	Cytoplasm	transcription regulator
P97329	KIF20A	kinesin family member 20A	Cytoplasm	transporter
E9Q1Z0	Krt90	keratin 90	Cytoplasm	other
A0A087WQQ5	Ktn1	kinectin 1	Cytoplasm	other
Q05CL8	LARP7	La ribonucleoprotein domain family member 7	Nucleus	other
Q3U9G9	LBR	lamin B receptor	Nucleus	enzyme
Q8C142	LDLRAP1	low density lipoprotein receptor adaptor protein 1	Cytoplasm	transporter
D3YWS8	LENG8	leukocyte receptor cluster member 8	Other	other
P37913	LIG1	DNA ligase 1	Nucleus	enzyme
Q8CGK3	LONP1	lon peptidase 1, mitochondrial	Cytoplasm	peptidase
H3BLL3	LRCH4	leucine rich repeats and calponin homology domain containing 4	Cytoplasm	transcription regulator
A2ARV4	LRP2	LDL receptor related protein 2	Plasma Membrane	transporter
B9EHV0	LRRC7	leucine rich repeat containing 7	Plasma Membrane	other
F7ACR9	Macf1	microtubule-actin crosslinking factor 1	Cytoplasm	enzyme
Q9Z1B5	MAD2L1	mitotic arrest deficient 2 like 1	Nucleus	other
Q9ESL4-2	MAP3K20	mitogen-activated protein kinase kinase kinase 20	Cytoplasm	kinase
P47811	MAPK14	mitogen-activated protein kinase 14	Cytoplasm	kinase
P28667	MARCKSL1	MARCKS like 1	Cytoplasm	other
E9Q9N6	MARK2	microtubule affinity regulating kinase 2	Cytoplasm	kinase
Q99KE1	ME2	malic enzyme 2	Cytoplasm	enzyme
Q8BP48	METAP1	methionyl aminopeptidase 1	Cytoplasm	peptidase
Q9DC37	MFSD1	major facilitator superfamily domain containing 1	Other	transporter
Q9EQQ9	MGEA5	meningioma expressed antigen 5 (hyaluronidase)	Cytoplasm	enzyme
E9PVX6	MKI67	marker of proliferation Ki-67	Nucleus	other
Q6ZQI3	MLEC	malectin	Plasma Membrane	other
P53690	MMP14	matrix metallopeptidase 14	Extracellular Space	peptidase
Q8K396	MND1	meiotic nuclear divisions 1	Nucleus	other
A0A0J9YU83	MORC3	MORC family CW-type zinc finger 3	Nucleus	other
Q9CXW2	MRPS22	mitochondrial ribosomal protein S22	Cytoplasm	other
Q8VE22	MRPS23	mitochondrial ribosomal protein S23	Cytoplasm	other
Q9CY16	MRPS28	mitochondrial ribosomal protein S28	Cytoplasm	other
A2AMV1	MRTO4	MRT4 homolog, ribosome maturation factor	Cytoplasm	other

Q9CZU3	MTREX	Mtr4 exosome RNA helicase	Nucleus	other
K3W4L0	MYO18A	myosin XVIIIA	Cytoplasm	other
Q8BWZ3-2	NAA25	N(alpha)-acetyltransferase 25, NatB auxiliary subunit	Cytoplasm	other
Q9CQ75	NDUFA2	NADH:ubiquinone oxidoreductase subunit A2	Cytoplasm	enzyme
Q9DCT2	NDUFS3	NADH:ubiquinone oxidoreductase core subunit S3	Cytoplasm	enzyme
Q9ES74	NEK7	NIMA related kinase 7	Nucleus	kinase
Q99L48	NMD3	NMD3 ribosome export adaptor	Nucleus	other
D3YU12	NMRAL1	NmrA like redox sensor 1	Nucleus	other
O70310	NMT1	N-myristoyltransferase 1	Cytoplasm	enzyme
Q5RJG1	NOL10	nucleolar protein 10	Nucleus	other
Q6GQT9	NOMO1 (includes others)	NODAL modulator 1	Plasma Membrane	other
Q6DFW4	NOP58	NOP58 ribonucleoprotein	Nucleus	enzyme
P60670	NPLOC4	NPL4 homolog, ubiquitin recognition factor	Nucleus	other
D3YUV1	NRBP1	nuclear receptor binding protein 1	Nucleus	kinase
Q8R2U4	NTMT1	N-terminal Xaa-Pro-Lys N-methyltransferase 1	Nucleus	enzyme
Q99P88	NUP155	nucleoporin 155	Nucleus	transporter
Q63850	NUP62	nucleoporin 62	Nucleus	transporter
Q99JX7	NXF1	nuclear RNA export factor 1	Nucleus	other
Q60597	OGDH	oxoglutarate dehydrogenase	Cytoplasm	enzyme
Q8R4V5-2	OIT3	oncoprotein induced transcript 3	Nucleus	other
Q8K212	PACS1	phosphofurin acidic cluster sorting protein 1	Cytoplasm	other
Q99JB8	PACSIN3	protein kinase C and casein kinase substrate in neurons 3	Cytoplasm	other
Q61205	PAFAH1B3	platelet activating factor acetylhydrolase 1b catalytic subunit 3	Cytoplasm	enzyme
E9PYJ2	PARD3	par-3 family cell polarity regulator	Plasma Membrane	other
F7D432	Pcmt1	protein-L-isoaspartate (D-aspartate) O-methyltransferase 1	Cytoplasm	enzyme
Q6NS46	PDCD11	programmed cell death 11	Nucleus	other
Q99K01	PDXDC1	pyridoxal dependent decarboxylase domain containing 1	Cytoplasm	other
Q9CQF7	PFDN1	prefoldin subunit 1	Cytoplasm	transcription regulator
O70591	PFDN2	prefoldin subunit 2	Cytoplasm	other
Q501J7-2	PHACTR4	phosphatase and actin regulator 4	Plasma Membrane	other
P52431	POLD1	DNA polymerase delta 1, catalytic subunit	Nucleus	enzyme
B2RXW8	PPFIA1	PTPRF interacting protein alpha 1	Plasma Membrane	phosphatase
Q8C8U0	PPFIBP1	PPFIA binding protein 1	Plasma Membrane	other
Q9QZH3	PPIE	peptidylprolyl isomerase E	Nucleus	enzyme
D3Z3A0	PPP1R2	protein phosphatase 1 regulatory inhibitor subunit 2	Cytoplasm	phosphatase
G5E8R4	PPP6R3	protein phosphatase 6 regulatory subunit 3	Cytoplasm	other
G3UW86	PRC1	protein regulator of cytokinesis 1	Nucleus	other
Q8BZ03	PRKD2	protein kinase D2	Cytoplasm	kinase
Q9R1C7	PRPF40A	pre-mRNA processing factor 40 homolog A	Nucleus	other
Q99JF8	PSIP1	PC4 and SFRS1 interacting protein 1	Nucleus	transcription regulator
O35955	PSMB10	proteasome subunit beta 10	Cytoplasm	peptidase

P22437	PTGS1	prostaglandin-endoperoxide synthase 1	Cytoplasm	enzyme
P58389	PTPA	protein phosphatase 2 phosphatase activator	Cytoplasm	phosphatase
P29351	PTPN6	protein tyrosine phosphatase, non-receptor type 6	Cytoplasm	phosphatase
Q80U78-2	PUM1	pumilio RNA binding family member 1	Cytoplasm	other
A2CG35	RAB12	RAB12, member RAS oncogene family	Cytoplasm	enzyme
Q91ZR1	RAB4B	RAB4B, member RAS oncogene family	Plasma Membrane	enzyme
E9PYG6	RASA1	RAS p21 protein activator 1	Cytoplasm	transporter
Q8R3C6	RBM19	RNA binding motif protein 19	Nucleus	other
Q05186	RCN1	reticulocalbin 1	Cytoplasm	other
Q9WUK4	RFC2	replication factor C subunit 2	Nucleus	other
Q60855	RIPK1	receptor interacting serine/threonine kinase 1	Plasma Membrane	kinase
Q05CH9	RNF123	ring finger protein 123	Cytoplasm	other
D6RIK9	RPGRIP1L	RPGRIP1 like	Cytoplasm	other
Q9CQR2	RPS21	ribosomal protein S21	Cytoplasm	other
Q6ZWY3	RPS27L	ribosomal protein S27 like	Cytoplasm	translation regulator
Q9Z2B9	RPS6KA4	ribosomal protein S6 kinase A4	Cytoplasm	kinase
Q8BVY0	RSL1D1	ribosomal L1 domain containing 1	Nucleus	other
Q8BVR6-3	RSPRY1	ring finger and SPRY domain containing 1	Other	other
F7CVW0	SBNO1	strawberry notch homolog 1	Other	enzyme
Q9JKV5	SCAMP4	secretory carrier membrane protein 4	Cytoplasm	other
A8Y5H7	SEC14L1	SEC14 like lipid binding 1	Cytoplasm	transporter
G3X972	SEC24C	SEC24 homolog C, COPII coat complex component	Cytoplasm	transporter
Q01102	SELP	selectin P	Plasma Membrane	transmembrane receptor
Q8K4Z5	SF3A1	splicing factor 3a subunit 1	Nucleus	other
G5E866	SF3B1	splicing factor 3b subunit 1	Nucleus	other
Q91V61	SFXN3	sideroflexin 3	Cytoplasm	transporter
Q91VW3	SH3BGRL3	SH3 domain binding glutamate rich protein like 3	Nucleus	other
Q9Z179	SHCBP1	SHC binding and spindle associated 1	Other	other
Q6NZR5	SKIV2L	Ski2 like RNA helicase	Nucleus	enzyme
A0A087WQH8	SLC35A4	solute carrier family 35 member A4	Cytoplasm	transporter
Q9D8M3	SLC48A1	solute carrier family 48 member 1	Cytoplasm	transporter
Q9EPT5	SLCO2A1	solute carrier organic anion transporter family member 2A1	Plasma Membrane	transporter
Q8C3Y6	SMAD1	SMAD family member 1	Nucleus	transcription regulator
Q8BUN5	SMAD3	SMAD family member 3	Nucleus	transcription regulator
Q3UNN4	SMARCC1	SWI/SNF related, matrix associated, actin dependent regulator of chromatin subfamily c member 1	Nucleus	transcription regulator
Q9CW03	SMC3	structural maintenance of chromosomes 3	Nucleus	other
Q8CG47	SMC4	structural maintenance of chromosomes 4	Nucleus	transporter
D3YTR6	SPNS1	sphingolipid transporter 1 (putative)	Cytoplasm	transporter
O88811-2	STAM2	signal transducing adaptor molecule 2	Cytoplasm	other
Q9CQ26	STAMBP	STAM binding protein	Nucleus	enzyme

P42232	STAT5B	signal transducer and activator of transcription 5B	Nucleus	transcription regulator
Q9JI10-2	STK3	serine/threonine kinase 3	Cytoplasm	kinase
P54227	STMN1	stathmin 1	Cytoplasm	other
B2RQS1	STRN3	striatin 3	Nucleus	transcription regulator
P58404-2	STRN4	striatin 4	Cytoplasm	other
B7ZCB8	STX16	syntaxin 16	Cytoplasm	transporter
Q8VDS8-3	STX18	syntaxin 18	Cytoplasm	transporter
O88983	STX8	syntaxin 8	Plasma Membrane	other
Q9CX34	SUGT1	SGT1 homolog, MIS12 kinetochore complex assembly cochaperone	Nucleus	other
Q8C0M5	SUSD6	sushi domain containing 6	Other	other
E9QP46	SYNE2	spectrin repeat containing nuclear envelope protein 2	Nucleus	other
Q3UKC1	TAX1BP1	Tax1 binding protein 1	Cytoplasm	other
Q9QXE7	TBL1X	transducin beta like 1 X-linked	Nucleus	transcription regulator
P10711	TCEA1	transcription elongation factor A1	Nucleus	transcription regulator
Q9Z1T2	THBS4	thrombospondin 4	Extracellular Space	other
Q9D880	TIMM50	translocase of inner mitochondrial membrane 50	Cytoplasm	phosphatase
D3Z4L9	TNFAIP2	TNF alpha induced protein 2	Extracellular Space	other
P58871	TNKS1BP1	tankyrase 1 binding protein 1	Nucleus	other
Q8CGB6-2	TNS2	tensin 2	Plasma Membrane	other
Q04750	TOP1	DNA topoisomerase I	Nucleus	enzyme
Q9ER41	TOR1B	torsin family 1 member B	Cytoplasm	enzyme
Q99MS8	TPGS1	tubulin polyglutamylase complex subunit 1	Cytoplasm	enzyme
E9QMQ3	TRIOBP	TRIO and F-actin binding protein	Nucleus	other
Q62348	TSN	translin	Nucleus	other
F8VPK0	TTC37	tetratricopeptide repeat domain 37	Nucleus	other
Q91YR1	TWF1	twinfilin actin binding protein 1	Cytoplasm	kinase
Q9Z0P5	TWF2	twinfilin actin binding protein 2	Cytoplasm	kinase
Q80X50	Ubap2l	ubiquitin-associated protein 2-like	Nucleus	other
P62838	UBE2D2	ubiquitin conjugating enzyme E2 D2	Cytoplasm	enzyme
Q9ES00	UBE4B	ubiquitination factor E4B	Cytoplasm	enzyme
A2AWT5	UBTF	upstream binding transcription factor, RNA polymerase I	Nucleus	transcription regulator
Q9JKB1	UCHL3	ubiquitin C-terminal hydrolase L3	Cytoplasm	peptidase
A0A0A6YXG9	UCK2	uridine-cytidine kinase 2	Cytoplasm	kinase
Q9CQB4	UQCRB	ubiquinol-cytochrome c reductase binding protein	Cytoplasm	enzyme
A0A1L1SV73	USP47	ubiquitin specific peptidase 47	Cytoplasm	peptidase
A2ALR9	USP48	ubiquitin specific peptidase 48	Plasma Membrane	peptidase
B0QZN5	VAMP2	vesicle associated membrane protein 2	Plasma Membrane	other
Q9WV55	VAPA	VAMP associated protein A	Plasma Membrane	other
Q8BX70-3	VPS13C	vacuolar protein sorting 13 homolog C	Cytoplasm	other
Q8R307	VPS18	VPS18, CORVET/HOPS core subunit	Cytoplasm	transporter
Q8CCB4-2	VPS53	VPS53, GARP complex subunit	Cytoplasm	other

Q91XH6	VTI1B	vesicle transport through interaction with t-SNAREs 1B	Plasma Membrane	transporter
Q8C2E7	WASHC5	WASH complex subunit 5	Cytoplasm	other
Q8BH57-3	WDR48	WD repeat domain 48	Cytoplasm	peptidase
Q8BJ05-2	ZC3H14	zinc finger CCCH-type containing 14	Nucleus	other
Q62384	ZPR1	ZPR1 zinc finger	Nucleus	other

Common_1750

ID	Symbol	Entrez Gene Name	Location	Type(s)
Q9D2R0	AACS	acetoacetyl-CoA synthetase	Cytoplasm	enzyme
Q8BGQ7	AARS	alanyl-tRNA synthetase	Cytoplasm	enzyme
J3QNY6	ABCB11	ATP binding cassette subfamily B member 11	Plasma Membrane	transporter
P06795	Abcb1b	ATP-binding cassette, sub-family B (MDR/TAP), member 1B	Plasma Membrane	transporter
O35379	ABCC1	ATP binding cassette subfamily C member 1	Plasma Membrane	transporter
E9Q467	ABCC4	ATP binding cassette subfamily C member 4	Plasma Membrane	transporter
P61222	ABCE1	ATP binding cassette subfamily E member 1	Cytoplasm	transporter
Q6P542	ABCF1	ATP binding cassette subfamily F member 1	Cytoplasm	transporter
Q99LE6	ABCF2	ATP binding cassette subfamily F member 2	Cytoplasm	transporter
Q7M759	ABHD17B	abhydrolase domain containing 17B	Plasma Membrane	peptidase
B7ZCU4	ABI1	abl interactor 1	Cytoplasm	other
Q5SWU9	ACACA	acetyl-CoA carboxylase alpha	Cytoplasm	enzyme
A0A0R4J083	ACADL	acyl-CoA dehydrogenase long chain	Cytoplasm	enzyme
P45952	ACADM	acyl-CoA dehydrogenase medium chain	Cytoplasm	enzyme
Q8QZT1	ACAT1	acetyl-CoA acetyltransferase 1	Cytoplasm	enzyme
Q8CAY6	ACAT2	acetyl-CoA acetyltransferase 2	Cytoplasm	enzyme
Q3V117	ACLY	ATP citrate lyase	Cytoplasm	enzyme
P28271	ACO1	aconitase 1	Cytoplasm	enzyme
Q99KI0	ACO2	aconitase 2	Cytoplasm	enzyme
Q91V12-2	ACOT7	acyl-CoA thioesterase 7	Cytoplasm	enzyme
Q9D358	ACP1	acid phosphatase 1	Cytoplasm	phosphatase
P24638	ACP2	acid phosphatase 2, lysosomal	Cytoplasm	phosphatase
Q9QUJ7-2	ACSL4	acyl-CoA synthetase long chain family member 4	Cytoplasm	enzyme
P60710	ACTB	actin beta	Cytoplasm	other
P68033	ACTC1	actin, alpha, cardiac muscle 1	Cytoplasm	enzyme
P63260	ACTG1	actin gamma 1	Cytoplasm	other
Q7TPR4	ACTN1	actinin alpha 1	Cytoplasm	transcription regulator
P57780	ACTN4	actinin alpha 4	Cytoplasm	transcription regulator
P61164	ACTR1A	ARP1 actin related protein 1 homolog A	Cytoplasm	other
P61161	ACTR2	ARP2 actin related protein 2 homolog	Plasma Membrane	other
Q99JY9	ACTR3	ARP3 actin related protein 3 homolog	Plasma Membrane	other
O35598	ADAM10	ADAM metallopeptidase domain 10	Plasma Membrane	peptidase
O88839-3	ADAM15	ADAM metallopeptidase domain 15	Plasma Membrane	peptidase
E9PXU2	ADAM17	ADAM metallopeptidase domain 17	Plasma Membrane	peptidase
E9Q638	ADAM9	ADAM metallopeptidase domain 9	Plasma Membrane	peptidase
A0A0G2JDE3	ADGRL2	adhesion G protein-coupled receptor L2	Plasma Membrane	G-protein coupled receptor

P00329	ADH1C	alcohol dehydrogenase 1C (class I), gamma polypeptide	Cytoplasm	enzyme
P28474	ADH5	alcohol dehydrogenase 5 (class III), chi polypeptide	Cytoplasm	enzyme
P55264	ADK	adenosine kinase	Nucleus	kinase
P54822	ADSL	adenylosuccinate lyase	Cytoplasm	enzyme
P46664	ADSS	adenylosuccinate synthase	Cytoplasm	enzyme
Q9QZQ1-2	AFDN	afadin, adherens junction formation factor	Nucleus	other
F8VPN4	AGL	amylo-alpha-1, 6-glucosidase, 4-alpha-glucanotransferase	Cytoplasm	enzyme
Q8CJG0	AGO2	argonaute 2, RISC catalytic component	Cytoplasm	translation regulator
Z4YK85	AGRN	agrin	Plasma Membrane	other
P50247	AHCY	adenosylhomocysteinase	Cytoplasm	enzyme
Q80SW1	AHCYL1	adenosylhomocysteinase like 1	Cytoplasm	enzyme
E9Q616	AHNAK	AHNAK nucleoprotein	Nucleus	other
F7DBB3	AHNAK2	AHNAK nucleoprotein 2	Cytoplasm	other
Q8BK64	AHSA1	activator of HSP90 ATPase activity 1	Cytoplasm	other
Q8C4Q6	AIDA	axin interactor, dorsalization associated	Cytoplasm	other
P31230	AIMP1	aminoacyl tRNA synthetase complex interacting multifunctional protein 1	Extracellular Space	cytokine
Q8R010	AIMP2	aminoacyl tRNA synthetase complex interacting multifunctional protein 2	Plasma Membrane	other
Q9R0Y5	AK1	adenylate kinase 1	Cytoplasm	kinase
Q9WTP7	AK3	adenylate kinase 3	Cytoplasm	kinase
Q9JII6	AKR1A1	aldo-keto reductase family 1 member A1	Cytoplasm	enzyme
P45376	AKR1B1	aldo-keto reductase family 1 member B	Cytoplasm	enzyme
P45377	AKR1B10	aldo-keto reductase family 1 member B10	Cytoplasm	enzyme
Q9JLI0	Akr1c12/Akr1c13	aldo-keto reductase family 1, member C13	Other	enzyme
Q8K023-2	AKR1C3	aldo-keto reductase family 1 member C3	Cytoplasm	enzyme
P10518	ALAD	aminolevulinate dehydratase	Cytoplasm	enzyme
A0A1B0GSU0	ALDH16A1	aldehyde dehydrogenase 16 family member A1	Cytoplasm	enzyme
P24549	ALDH1A1	aldehyde dehydrogenase 1 family member A1	Cytoplasm	enzyme
P47738	ALDH2	aldehyde dehydrogenase 2 family (mitochondrial)	Cytoplasm	enzyme
P47739	ALDH3A1	aldehyde dehydrogenase 3 family member A1	Cytoplasm	enzyme
Q8BH00	ALDH8A1	aldehyde dehydrogenase 8 family member A1	Cytoplasm	enzyme
Q9JLJ2	ALDH9A1	aldehyde dehydrogenase 9 family member A1	Cytoplasm	enzyme
P05064	ALDOA	aldolase, fructose-bisphosphate A	Cytoplasm	enzyme
P09242	ALPL	alkaline phosphatase, liver/bone/kidney	Plasma Membrane	phosphatase
A2AE27	AMPD2	adenosine monophosphate deaminase 2	Cytoplasm	enzyme
Q9R045	ANGPTL2	angiopoietin like 2	Extracellular Space	other
G5E8J2	ANK1	ankyrin 1	Plasma Membrane	other
Q810B6	ANKFY1	ankyrin repeat and FYVE domain containing 1	Cytoplasm	transcription regulator

Q8K298	ANLN	anillin actin binding protein	Cytoplasm	other
Q6P9J9	ANO6	anoctamin 6	Plasma Membrane	ion channel
Q9EST5	Anp32b	acidic (leucine-rich) nuclear phosphoprotein 32 family, member B	Nucleus	other
P10107	ANXA1	annexin A1	Plasma Membrane	enzyme
P97384	ANXA11	annexin A11	Nucleus	other
P07356	ANXA2	annexin A2	Plasma Membrane	other
O35639	ANXA3	annexin A3	Cytoplasm	enzyme
P97429	ANXA4	annexin A4	Plasma Membrane	other
P48036	ANXA5	annexin A5	Plasma Membrane	transporter
F8WIT2	ANXA6	annexin A6	Plasma Membrane	ion channel
Q07076	ANXA7	annexin A7	Plasma Membrane	ion channel
Q921D0	ANXA8/ANXA8L1	annexin A8 like 1	Plasma Membrane	other
G3X8P9	AOX1	aldehyde oxidase 1	Cytoplasm	enzyme
Q5SVG5	AP1B1	adaptor related protein complex 1 beta 1 subunit	Cytoplasm	transporter
Q8CBB7	AP1G1	adaptor related protein complex 1 gamma 1 subunit	Cytoplasm	transporter
P17426-2	AP2A1	adaptor related protein complex 2 alpha 1 subunit	Cytoplasm	transporter
P17427	AP2A2	adaptor related protein complex 2 alpha 2 subunit	Cytoplasm	transporter
Q9DBG3	Ap2b1	adaptor-related protein complex 2, beta 1 subunit	Plasma Membrane	other
Q3TWV4	AP2M1	adaptor related protein complex 2 mu 1 subunit	Cytoplasm	transporter
P62743	AP2S1	adaptor related protein complex 2 sigma 1 subunit	Cytoplasm	transporter
Q9Z1T1	AP3B1	adaptor related protein complex 3 beta 1 subunit	Plasma Membrane	transporter
O54774	AP3D1	adaptor related protein complex 3 delta 1 subunit	Cytoplasm	transporter
H7BWY2	AP3M1	adaptor related protein complex 3 mu 1 subunit	Cytoplasm	transporter
Q9DCR2	AP3S1	adaptor related protein complex 3 sigma 1 subunit	Cytoplasm	transporter
Q8BVF7-2	APH1A	aph-1 homolog A, gamma-secretase subunit	Cytoplasm	peptidase
O35841	API5	apoptosis inhibitor 5	Cytoplasm	other
E9Q1Y3	APOB	apolipoprotein B	Extracellular Space	transporter
Q3UZ24	Apol7e (includes others)	apolipoprotein L 7e	Other	other
Q8VDU3	Apol9a/Apol9b	apolipoprotein L 9b	Other	other
Q9Z1R3	APOM	apolipoprotein M	Plasma Membrane	transporter
P08030	APRT	adenine phosphoribosyltransferase	Cytoplasm	enzyme
Q02013	AQP1	aquaporin 1 (Colton blood group)	Plasma Membrane	transporter
Q5XJY5	ARCN1	archain 1	Cytoplasm	other
P84078	ARF1	ADP ribosylation factor 1	Cytoplasm	enzyme
P61750	ARF4	ADP ribosylation factor 4	Cytoplasm	enzyme
P84084	ARF5	ADP ribosylation factor 5	Cytoplasm	enzyme
P62331	ARF6	ADP ribosylation factor 6	Plasma Membrane	transporter
A2A5R2	ARFGEF2	ADP ribosylation factor guanine nucleotide exchange factor 2	Cytoplasm	other

Q5FWK3	ARHGAP1	Rho GTPase activating protein 1	Cytoplasm	other
Q99PT1	ARHGDIA	Rho GDP dissociation inhibitor alpha	Cytoplasm	other
Q61599	ARHGDIB	Rho GDP dissociation inhibitor beta	Cytoplasm	enzyme
E9PUF7	ARHGEF1	Rho guanine nucleotide exchange factor 1	Cytoplasm	other
E9Q0A3	ARHGEF11	Rho guanine nucleotide exchange factor 11	Cytoplasm	other
F8VQN6	ARHGEF12	Rho guanine nucleotide exchange factor 12	Cytoplasm	other
H3BJU7	ARHGEF2	Rho/Rac guanine nucleotide exchange factor 2	Cytoplasm	other
Q66JY6	ARHGEF39	Rho guanine nucleotide exchange factor 39	Plasma Membrane	other
S4R189	ARHGEF40	Rho guanine nucleotide exchange factor 40	Other	other
P61211	ARL1	ADP ribosylation factor like GTPase 1	Cytoplasm	enzyme
Q9D0J4	ARL2	ADP ribosylation factor like GTPase 2	Cytoplasm	enzyme
Q9WUL7	ARL3	ADP ribosylation factor like GTPase 3	Cytoplasm	enzyme
O88848	ARL6	ADP ribosylation factor like GTPase 6	Cytoplasm	transporter
A0A0U1RPY6	ARL6IP1	ADP ribosylation factor like GTPase 6 interacting protein 1	Cytoplasm	other
Q8R5J9	ARL6IP5	ADP ribosylation factor like GTPase 6 interacting protein 5	Cytoplasm	other
F6QKK2	ARL8A	ADP ribosylation factor like GTPase 8A	Cytoplasm	enzyme
Q9CQW2	ARL8B	ADP ribosylation factor like GTPase 8B	Plasma Membrane	enzyme
Q91Z25	ARPC1B	actin related protein 2/3 complex subunit 1B	Cytoplasm	other
Q9CVB6	ARPC2	actin related protein 2/3 complex subunit 2	Cytoplasm	other
Q9JM76	ARPC3	actin related protein 2/3 complex subunit 3	Cytoplasm	other
P59999	ARPC4	actin related protein 2/3 complex subunit 4	Cytoplasm	other
Q9CPW4	ARPC5	actin related protein 2/3 complex subunit 5	Cytoplasm	other
Q99KN1	ARRDC1	arrestin domain containing 1	Cytoplasm	other
Q9WV54	ASAH1	N-acylsphingosine amidohydrolase 1	Cytoplasm	enzyme
Q91YI0	ASL	argininosuccinate lyase	Cytoplasm	enzyme
O54984	ASNA1	arsA arsenite transporter, ATP-binding, homolog 1 (bacterial)	Nucleus	transporter
Q61024	ASNS	asparagine synthetase (glutamine-hydrolyzing)	Cytoplasm	enzyme
Q99MQ4	ASPN	asporin	Extracellular Space	other
P16460	ASS1	argininosuccinate synthase 1	Cytoplasm	enzyme
Q9CWJ9	ATIC	5-aminoimidazole-4-carboxamide ribonucleotide formyltransferase/IMP cyclohydrolase	Cytoplasm	enzyme
Q6PA06	ATL2	atlastin GTPase 2	Cytoplasm	other
Q91YH5	ATL3	atlastin GTPase 3	Cytoplasm	other
E9QKK8	ATP11C	ATPase phospholipid transporting 11C	Plasma Membrane	transporter
Q8VDN2	ATP1A1	ATPase Na+/K+ transporting subunit alpha 1	Plasma Membrane	transporter
D3YYN7	ATP1A2	ATPase Na+/K+ transporting subunit alpha 2	Plasma Membrane	transporter
P97370	ATP1B3	ATPase Na+/K+ transporting subunit beta 3	Plasma Membrane	transporter
O55143	ATP2A2	ATPase sarcoplasmic/endoplasmic reticulum Ca2+ transporting 2	Cytoplasm	transporter

G5E829	ATP2B1	ATPase plasma membrane Ca2+ transporting 1	Plasma Membrane	transporter
Q03265	ATP5F1A	ATP synthase F1 subunit alpha	Cytoplasm	transporter
P56480	ATP5F1B	ATP synthase F1 subunit beta	Cytoplasm	transporter
Q8C2Q8	ATP5F1C	ATP synthase F1 subunit gamma	Cytoplasm	transporter
Q06185	Atp5k	ATP synthase, H+ transporting, mitochondrial F1F0 complex, subunit E	Cytoplasm	enzyme
P56135	ATP5MF	ATP synthase membrane subunit f	Cytoplasm	transporter
Q9CQQ7	ATP5PB	ATP synthase peripheral stalk-membrane subunit b	Cytoplasm	transporter
Q9CYN9	ATP6AP2	ATPase H+ transporting accessory protein 2	Cytoplasm	transporter
K3W4T3	ATP6V0A1	ATPase H+ transporting V0 subunit a1	Cytoplasm	transporter
P50516	ATP6V1A	ATPase H+ transporting V1 subunit A	Plasma Membrane	transporter
P62814	ATP6V1B2	ATPase H+ transporting V1 subunit B2	Cytoplasm	transporter
P50518	ATP6V1E1	ATPase H+ transporting V1 subunit E1	Cytoplasm	transporter
A2AG68	ATP7A	ATPase copper transporting alpha	Plasma Membrane	transporter
Q9WU60	ATRN	attractin	Extracellular Space	other
P28658	ATXN10	ataxin 10	Cytoplasm	other
Q6PE80	AXL	AXL receptor tyrosine kinase	Plasma Membrane	kinase
L7N467	B230307C23Rik	RIKEN cDNA B230307C23 gene	Other	other
Q9JMK0	B4GALT5	beta-1,4-galactosyltransferase 5	Cytoplasm	enzyme
Q91YN9	BAG2	BCL2 associated athanogene 2	Cytoplasm	other
Q9JLV1	BAG3	BCL2 associated athanogene 3	Cytoplasm	other
Q8CI32	BAG5	BCL2 associated athanogene 5	Cytoplasm	other
Q3UF95	BAG6	BCL2 associated athanogene 6	Nucleus	enzyme
Q8BKX1	BAIAP2	BAI1 associated protein 2	Plasma Membrane	kinase
O54962	BANF1	barrier to autointegration factor 1	Nucleus	other
Q91XV3	BASP1	brain abundant membrane attached signal protein 1	Nucleus	transcription regulator
A0A1B0GT81	BAX	BCL2 associated X, apoptosis regulator	Cytoplasm	transporter
Q61140	BCAR1	BCAR1, Cas family scaffolding protein	Plasma Membrane	enzyme
Q9CWI3	BCCIP	BRCA2 and CDKN1A interacting protein	Nucleus	other
O35490	BHMT	betaine--homocysteine S-methyltransferase	Cytoplasm	enzyme
Q6P1B9	BIN1	bridging integrator 1	Nucleus	other
S4R1L5	BIRC6	baculoviral IAP repeat containing 6	Cytoplasm	enzyme
Q8R016	BLMH	bleomycin hydrolase	Cytoplasm	peptidase
Q923D2	BLVRB	biliverdin reductase B	Cytoplasm	enzyme
P98063	BMP1	bone morphogenetic protein 1	Extracellular Space	peptidase
Q60607	BMPR1A	bone morphogenetic protein receptor type 1A	Plasma Membrane	kinase
O35607	BMPR2	bone morphogenetic protein receptor type 2	Plasma Membrane	kinase
D3Z223	BPGM	bisphosphoglycerate mutase	Extracellular Space	phosphatase
Q91VR8	BRK1	BRICK1, SCAR/WAVE actin nucleating complex subunit	Cytoplasm	other

Q8K2Q7	BROX	BRO1 domain and CAAX motif containing	Cytoplasm	other
K3W4Q8	BSG	basigin (Ok blood group)	Plasma Membrane	transporter
Q8R2Q8	Bst2	bone marrow stromal cell antigen 2	Plasma Membrane	other
A0A140LHA2	BUB3	BUB3, mitotic checkpoint protein	Nucleus	other
A0A087WQS2	BZW1	basic leucine zipper and W2 domains 1	Cytoplasm	translation regulator
Q91VK1	BZW2	basic leucine zipper and W2 domains 2	Cytoplasm	translation regulator
Q8C708	C16orf54	chromosome 16 open reading frame 54	Extracellular Space	other
Q8BWQ6	C16orf62	chromosome 16 open reading frame 62	Other	other
D3YZT8	C1orf106	chromosome 1 open reading frame 106	Other	other
Q8R5L1	C1QBP	complement C1q binding protein	Cytoplasm	transcription regulator
D3YZ61	C1QTNF3	C1q and TNF related 3	Extracellular Space	other
Q8K201	C5orf15	chromosome 5 open reading frame 15	Other	other
Q8BH35-2	C8B	complement C8 beta chain	Extracellular Space	other
Q06138	CAB39	calcium binding protein 39	Cytoplasm	enzyme
Q9CXW3	CACYBP	calcyclin binding protein	Nucleus	other
B2RQC6	CAD	carbamoyl-phosphate synthetase 2, aspartate transcarbamylase, and dihydroorotase	Cytoplasm	enzyme
E9PYN1	CADM1	cell adhesion molecule 1	Plasma Membrane	other
Q8VCQ8	Cald1	caldesmon 1	Plasma Membrane	other
P0DP28	Calm1 (includes others)	calmodulin 1	Nucleus	other
P14211	CALR	calreticulin	Cytoplasm	transcription regulator
E9Q1W0	CAMK2D	calcium/calmodulin dependent protein kinase II delta	Cytoplasm	kinase
Q923T9-3	CAMK2G	calcium/calmodulin dependent protein kinase II gamma	Cytoplasm	kinase
Q6ZQ38	CAND1	cullin associated and neddylation dissociated 1	Cytoplasm	transcription regulator
P35564	CANX	calnexin	Cytoplasm	other
P40124	CAP1	cyclase associated actin cytoskeleton regulatory protein 1	Plasma Membrane	other
Q99LB4	CAPG	capping actin protein, gelsolin like	Nucleus	other
O35350	CAPN1	calpain 1	Cytoplasm	peptidase
O08529	CAPN2	calpain 2	Cytoplasm	peptidase
O08688	CAPN5	calpain 5	Cytoplasm	peptidase
Q9R1S8	CAPN7	calpain 7	Cytoplasm	peptidase
O88456	CAPNS1	calpain small subunit 1	Cytoplasm	peptidase
Q5RKN9	CAPZA1	capping actin protein of muscle Z-line alpha subunit 1	Cytoplasm	other
P47754	CAPZA2	capping actin protein of muscle Z-line alpha subunit 2	Cytoplasm	other
P47757-2	CAPZB	capping actin protein of muscle Z-line beta subunit	Cytoplasm	other
D3YUP1	CARM1	coactivator associated arginine methyltransferase 1	Nucleus	transcription regulator
D3Z030	CARMIL1	capping protein regulator and myosin 1 linker 1	Cytoplasm	enzyme
Q9ER72	CARS	cysteinyl-tRNA synthetase	Cytoplasm	enzyme
A0A067XG53	CASK	calcium/calmodulin dependent serine protein kinase	Plasma Membrane	kinase

P49817	CAV1	caveolin 1	Plasma Membrane	transmembrane receptor
O54724	CAVIN1	caveolae associated protein 1	Nucleus	transcription regulator
Q63918	CAVIN2	caveolae associated protein 2	Plasma Membrane	other
P48758	CBR1	carbonyl reductase 1	Cytoplasm	enzyme
Q9DCC5	CBX3	chromobox 3	Nucleus	transcription regulator
Q8K1A6	CC2D1A	coiled-coil and C2 domain containing 1A	Cytoplasm	transcription regulator
F6XC25	CC2D1B	coiled-coil and C2 domain containing 1B	Nucleus	transcription regulator
Q8BGU5-2	CCNY	cyclin Y	Nucleus	other
P80314	CCT2	chaperonin containing TCP1 subunit 2	Cytoplasm	kinase
P80318	CCT3	chaperonin containing TCP1 subunit 3	Cytoplasm	other
P80315	CCT4	chaperonin containing TCP1 subunit 4	Cytoplasm	other
P80316	CCT5	chaperonin containing TCP1 subunit 5	Cytoplasm	other
P80317	CCT6A	chaperonin containing TCP1 subunit 6A	Cytoplasm	other
P80313	CCT7	chaperonin containing TCP1 subunit 7	Cytoplasm	other
P42932	CCT8	chaperonin containing TCP1 subunit 8	Cytoplasm	enzyme
Q8R422	CD109	CD109 molecule	Plasma Membrane	other
O35566	CD151	CD151 molecule (Raph blood group)	Plasma Membrane	other
Q9JLQ0	CD2AP	CD2 associated protein	Cytoplasm	other
Q3U429	CD37	CD37 molecule	Plasma Membrane	other
Q3U8S1	CD44	CD44 molecule (Indian blood group)	Plasma Membrane	other
Q61735-2	CD47	CD47 molecule	Plasma Membrane	transmembrane receptor
P41731	CD63	CD63 molecule	Plasma Membrane	other
P40237	CD82	CD82 molecule	Plasma Membrane	other
P40240	CD9	CD9 molecule	Plasma Membrane	other
G3X8W7	CDC23	cell division cycle 23	Nucleus	enzyme
P60766	Cdc42	cell division cycle 42	Plasma Membrane	enzyme
H7BX44	CDC42BPA	CDC42 binding protein kinase alpha	Cytoplasm	kinase
Q7TT50	CDC42BPB	CDC42 binding protein kinase beta	Cytoplasm	kinase
Q8BHL7	CDC42SE1	CDC42 small effector 1	Plasma Membrane	other
Q9WTR5	CDH13	cadherin 13	Plasma Membrane	other
D3YYT0	CDH2	cadherin 2	Plasma Membrane	other
P11440	CDK1	cyclin dependent kinase 1	Nucleus	kinase
A0A0R4J0T5	Celf1	CUGBP, Elav-like family member 1	Nucleus	other
H7BX26	CEP170	centrosomal protein 170	Nucleus	other
Q8BT07	CEP55	centrosomal protein 55	Cytoplasm	other
P18760	CFL1	cofilin 1	Nucleus	other
P45591	CFL2	cofilin 2	Extracellular Space	other
E9QAS4	CHD4	chromodomain helicase DNA binding protein 4	Nucleus	enzyme
Q921W0	CHMP1A	charged multivesicular body protein 1A	Extracellular Space	peptidase

Q99LU0	CHMP1B	charged multivesicular body protein 1B	Plasma Membrane	enzyme
Q9DB34	CHMP2A	charged multivesicular body protein 2A	Cytoplasm	other
Q9CQ10	CHMP3	charged multivesicular body protein 3	Cytoplasm	other
Q9D8B3	CHMP4B	charged multivesicular body protein 4B	Cytoplasm	other
Q9D7F7	CHMP4C	charged multivesicular body protein 4C	Cytoplasm	other
Q9D7S9	CHMP5	charged multivesicular body protein 5	Cytoplasm	other
B1AZ42	CHMP6	charged multivesicular body protein 6	Cytoplasm	other
Q9D1P4	CHORDC1	cysteine and histidine rich domain containing 1	Other	other
B0R091	CHP1	calcineurin like EF-hand protein 1	Cytoplasm	transporter
A0A0R4J0I4	CHTF18	chromosome transmission fidelity factor 18	Nucleus	other
E9QL53	CIT	citron rho-interacting serine/threonine kinase	Cytoplasm	kinase
Z4YL78	CKAP5	cytoskeleton associated protein 5	Nucleus	transcription regulator
E9Q6L0	CLASP1	cytoplasmic linker associated protein 1	Cytoplasm	other
Q9Z0S7	CLDN9	claudin 9	Plasma Membrane	other
Q9CQX5	CLDND1	claudin domain containing 1	Plasma Membrane	other
O88200	CLEC11A	C-type lectin domain containing 11A	Extracellular Space	growth factor
Q9Z1Q5	CLIC1	chloride intracellular channel 1	Nucleus	ion channel
Q9QYB1	CLIC4	chloride intracellular channel 4	Plasma Membrane	ion channel
Q5SXR6	CLTC	clathrin heavy chain	Plasma Membrane	other
Q06890	CLU	clusterin	Cytoplasm	other
A0A0R4J140	CLUH	clustered mitochondria homolog	Cytoplasm	translation regulator
Q8R1G2	CMBL	carboxymethylenebutenolidase homolog	Cytoplasm	enzyme
Q9D486	CMIP	c-Maf inducing protein	Cytoplasm	other
Q9DBP5	CMPK1	cytidine/uridine monophosphate kinase 1	Nucleus	kinase
P53996-2	CNBP	CCHC-type zinc finger nucleic acid binding protein	Nucleus	transcription regulator
Q9D1A2	CNDP2	carnosine dipeptidase 2	Cytoplasm	peptidase
Q8BMA3	CNKSR3	CNKSR family member 3	Plasma Membrane	kinase
Q08093	CNN2	calponin 2	Cytoplasm	other
Q9DAW9	CNN3	calponin 3	Cytoplasm	other
Q32NY4-2	CNNM3	cyclin and CBS domain divalent metal cation transport mediator 3	Other	other
B7ZWL1	CNOT1	CCR4-NOT transcription complex subunit 1	Cytoplasm	other
P16330-2	CNP	2',3'-cyclic nucleotide 3' phosphodiesterase	Cytoplasm	enzyme
B1AZ15	COBLL1	cordon-bleu WH2 repeat protein like 1	Extracellular Space	other
Q8C0L8	COG5	component of oligomeric golgi complex 5	Cytoplasm	transporter
E9Q0X4	COL16A1	collagen type XVI alpha 1 chain	Extracellular Space	other
E9QPX1	COL18A1	collagen type XVIII alpha 1 chain	Extracellular Space	other
P02463	COL4A1	collagen type IV alpha 1 chain	Extracellular Space	other
P08122	COL4A2	collagen type IV alpha 2 chain	Extracellular Space	other

Q04857	COL6A1	collagen type VI alpha 1 chain	Extracellular Space	other
Q02788	COL6A2	collagen type VI alpha 2 chain	Extracellular Space	other
E9PWQ3	COL6A3	collagen type VI alpha 3 chain	Extracellular Space	other
E9Q6A6	COL6A6	collagen type VI alpha 6 chain	Extracellular Space	other
Q8CF98	COLEC10	collectin subfamily member 10	Cytoplasm	peptidase
Q8K4Q8	COLEC12	collectin subfamily member 12	Plasma Membrane	transmembrane receptor
Q8CIE6	COPA	coatomer protein complex subunit alpha	Cytoplasm	transporter
Q9JIF7	COPB1	coatomer protein complex subunit beta 1	Cytoplasm	transporter
O55029	COPB2	coatomer protein complex subunit beta 2	Cytoplasm	transporter
Q9QZE5	COPG1	coatomer protein complex subunit gamma 1	Cytoplasm	transporter
P61202	Cops2	COP9 signalosome subunit 2	Nucleus	transcription regulator
O88543	COPS3	COP9 signalosome subunit 3	Cytoplasm	other
O88544	COPS4	COP9 signalosome subunit 4	Cytoplasm	peptidase
D3Z0F5	COPS6	COP9 signalosome subunit 6	Nucleus	other
O89053	CORO1A	coronin 1A	Cytoplasm	other
Q9WUM3	CORO1B	coronin 1B	Cytoplasm	other
Q9WUM4	CORO1C	coronin 1C	Cytoplasm	other
Q9CQI6	COTL1	coactosin like F-actin binding protein 1	Cytoplasm	other
P19783	COX4I1	cytochrome c oxidase subunit 4I1	Cytoplasm	enzyme
Q9CPQ1	Cox6c	cytochrome c oxidase subunit VIc	Cytoplasm	enzyme
Q8C166	CPNE1	copine 1	Nucleus	transporter
A0A0R4J1D0	CPNE2	copine 2	Cytoplasm	other
Q8BT60	CPNE3	copine 3	Cytoplasm	kinase
Q9DC53	CPNE8	copine 8	Cytoplasm	other
Q9EPU4	CPSF1	cleavage and polyadenylation specific factor 1	Nucleus	other
Q64735-2	CR1L	complement C3b/C4b receptor 1 like	Plasma Membrane	other
Q9DCT8	Crip2	cysteine rich protein 2	Plasma Membrane	other
Q64010	CRK	CRK proto-oncogene, adaptor protein	Cytoplasm	other
Q8CJ40-3	CROCC	ciliary rootlet coiled-coil, rootletin	Plasma Membrane	other
P47199	CRYZ	crystallin zeta	Cytoplasm	enzyme
Q9CZU6	CS	citrate synthase	Cytoplasm	enzyme
Q91W50	CSDE1	cold shock domain containing E1	Cytoplasm	enzyme
Q9ERK4	CSE1L	chromosome segregation 1 like	Nucleus	transporter
P41241	CSK	C-terminal Src kinase	Cytoplasm	kinase
E9Q4G7	CSNK1A1	casein kinase 1 alpha 1	Cytoplasm	kinase
A0A0U1RPD7	CSNK1G1	casein kinase 1 gamma 1	Cytoplasm	kinase
Q60737	CSNK2A1	casein kinase 2 alpha 1	Nucleus	kinase
O54833	CSNK2A2	casein kinase 2 alpha 2	Cytoplasm	kinase
P67871	CSNK2B	casein kinase 2 beta	Cytoplasm	kinase

P97315	CSRP1	cysteine and glycine rich protein 1	Nucleus	other
Q62426	CSTB	cystatin B	Cytoplasm	peptidase
P58466	CTDSP1	CTD small phosphatase 1	Nucleus	phosphatase
Q8BX07	CTDSP2	CTD small phosphatase 2	Nucleus	phosphatase
P26231	CTNNA1	catenin alpha 1	Plasma Membrane	other
E0CXB9	CTNNA2	catenin alpha 2	Plasma Membrane	other
Q02248	CTNNB1	catenin beta 1	Nucleus	transcription regulator
G3X9V2	CTNND1	catenin delta 1	Nucleus	other
P70698	CTPS1	CTP synthase 1	Nucleus	enzyme
F8WIR1	CTSD	cathepsin D	Cytoplasm	peptidase
Q60598	CTTN	cortactin	Plasma Membrane	other
Q9WTX6	CUL1	cullin 1	Nucleus	enzyme
Q9JLV5	CUL3	cullin 3	Nucleus	enzyme
Q3TCH7	CUL4A	cullin 4A	Nucleus	other
P97792	CXADR	CXADR, Ig-like cell adhesion molecule	Plasma Membrane	transmembrane receptor
H7BX38	CXCL12	C-X-C motif chemokine ligand 12	Extracellular Space	cytokine
Q9DCN2-2	Cyb5r3	cytochrome b5 reductase 3	Cytoplasm	enzyme
Q7TMB8	CYFIP1	cytoplasmic FMR1 interacting protein 1	Cytoplasm	other
P18406	CYR61	cysteine rich angiogenic inducer 61	Extracellular Space	other
D3YVS7	Cystm1	cysteine-rich transmembrane module containing 1	Cytoplasm	other
A0A1B0GRX7	CYTH2	cytohesin 2	Cytoplasm	other
Q8BPM0-3	DAAM1	dishevelled associated activator of morphogenesis 1	Cytoplasm	other
Q62165	DAG1	dystroglycan 1	Plasma Membrane	transmembrane receptor
Q8VDF3-2	DAPK2	death associated protein kinase 2	Cytoplasm	kinase
Q922B2	DARS	aspartyl-tRNA synthetase	Cytoplasm	enzyme
P31786	DBI	diazepam binding inhibitor, acyl-CoA binding protein	Cytoplasm	other
P53395	DBT	dihydrolipoamide branched chain transacylase E2	Cytoplasm	enzyme
Q80TR8-4	DCAF1	DDB1 and CUL4 associated factor 1	Nucleus	kinase
Q99KJ8	DCTN2	dynactin subunit 2	Cytoplasm	other
A2AC16	DCXR	dicarbonyl and L-xylulose reductase	Cytoplasm	enzyme
Q9CWS0	DDAH1	dimethylarginine dimethylaminohydrolase 1	Cytoplasm	enzyme
Q99LD8	DDAH2	dimethylarginine dimethylaminohydrolase 2	Cytoplasm	enzyme
Q3U1J4	DDB1	damage specific DNA binding protein 1	Nucleus	other
O54734	DDOST	dolichyl-diphosphooligosaccharide--protein glycosyltransferase non-catalytic subunit	Cytoplasm	enzyme
Q62371	DDR2	discoidin domain receptor tyrosine kinase 2	Plasma Membrane	kinase
Q91VR5	DDX1	DEAD-box helicase 1	Nucleus	enzyme
Q9JJY4	DDX20	DEAD-box helicase 20	Nucleus	transcription regulator
Q9JIK5	DDX21	DExD-box helicase 21	Nucleus	enzyme

Q8VDW0	DDX39A	DExD-box helicase 39A	Nucleus	enzyme
Q62167	DDX3X	DEAD-box helicase 3, X-linked	Cytoplasm	enzyme
Q8BTS0	DDX5	DEAD-box helicase 5	Nucleus	enzyme
P54823	DDX6	DEAD-box helicase 6	Nucleus	enzyme
Q91YP3	DERA	deoxyribose-phosphate aldolase	Cytoplasm	enzyme
P00375	DHFR	dihydrofolate reductase	Nucleus	enzyme
O35286	DHX15	DEAH-box helicase 15	Nucleus	enzyme
E9QNN1	DHX9	DExH-box helicase 9	Nucleus	enzyme
F8WI56	DIP2A	disco interacting protein 2 homolog A	Nucleus	transcription regulator
Q3UH60	DIP2B	disco interacting protein 2 homolog B	Cytoplasm	other
B2RQC7	DIP2B	disco interacting protein 2 homolog B	Cytoplasm	other
B2RQ71	DIP2C	disco interacting protein 2 homolog C	Other	other
Q8BMF4	DLAT	dihydrolipoamide S-acetyltransferase	Cytoplasm	enzyme
Q811D0-2	DLG1	discs large MAGUK scaffold protein 1	Plasma Membrane	kinase
Q9D2G2	DLST	dihydrolipoamide S-succinyltransferase	Cytoplasm	enzyme
Q91XQ0-2	DNAH8	dynein axonemal heavy chain 8	Cytoplasm	enzyme
P63037	DNAJA1	DnaJ heat shock protein family (Hsp40) member A1	Nucleus	other
Q9QYJ0	DNAJA2	DnaJ heat shock protein family (Hsp40) member A2	Nucleus	enzyme
Q9QYJ3	DNAJB1	DnaJ heat shock protein family (Hsp40) member B1	Nucleus	transcription regulator
Q9D832	DNAJB4	DnaJ heat shock protein family (Hsp40) member B4	Nucleus	other
G3X922	DNAJC13	DnaJ heat shock protein family (Hsp40) member C13	Cytoplasm	other
G5E8T0	DNAJC5	DnaJ heat shock protein family (Hsp40) member C5	Plasma Membrane	other
Q9QYI3	DNAJC7	DnaJ heat shock protein family (Hsp40) member C7	Cytoplasm	other
Q8K1M6-3	DNM1L	dynamin 1 like	Cytoplasm	enzyme
Q3T9X3	DNM2	dynamin 2	Plasma Membrane	enzyme
Q3TVK3	DNPEP	aspartyl aminopeptidase	Cytoplasm	peptidase
B2RY04	DOCK5	dedicator of cytokinesis 5	Cytoplasm	other
A0A0U1RNK7	DOCK7	dedicator of cytokinesis 7	Plasma Membrane	other
E9QMR2	DOCK9	dedicator of cytokinesis 9	Cytoplasm	other
O08553	DPYSL2	dihydropyrimidinase like 2	Cytoplasm	enzyme
Q9QXB9	DRG2	developmentally regulated GTP binding protein 2	Cytoplasm	other
E9Q557	DSP	desmoplakin	Plasma Membrane	other
Q9R0P5	DSTN	destrin, actin depolymerizing factor	Cytoplasm	other
Q8R3P2	DTX2	deltex E3 ubiquitin ligase 2	Nucleus	other
Q6PDK8	DTX4	deltex E3 ubiquitin ligase 4	Cytoplasm	enzyme
Q9JHU4	DYNC1H1	dynein cytoplasmic 1 heavy chain 1	Cytoplasm	peptidase
O88487	Dync1i2	dynein cytoplasmic 1 intermediate chain 2	Cytoplasm	other
Q8R1Q8	DYNC1LI1	dynein cytoplasmic 1 light intermediate chain 1	Cytoplasm	other
P63168	DYNLL1	dynein light chain LC8-type 1	Cytoplasm	other

E9QL12	DYSF	dysferlin	Plasma Membrane	other
Q9CS74	ECD	ecdysoneless cell cycle regulator	Nucleus	transcription regulator
Q4PZA2-3	ECE1	endothelin converting enzyme 1	Plasma Membrane	peptidase
F8WI14	ECM1	extracellular matrix protein 1	Extracellular Space	transporter
G5E896	EDC4	enhancer of mRNA decapping 4	Cytoplasm	other
P10126	EEF1A1	eukaryotic translation elongation factor 1 alpha 1	Cytoplasm	translation regulator
O70251	EEF1B2	eukaryotic translation elongation factor 1 beta 2	Cytoplasm	translation regulator
E9QN08	EEF1D	eukaryotic translation elongation factor 1 delta	Cytoplasm	translation regulator
Q9D8N0	EEF1G	eukaryotic translation elongation factor 1 gamma	Cytoplasm	translation regulator
P58252	EEF2	eukaryotic translation elongation factor 2	Cytoplasm	translation regulator
Q8BPB5	EFEMP1	EGF containing fibulin extracellular matrix protein 1	Extracellular Space	enzyme
P52795	EFNB1	ephrin B1	Plasma Membrane	other
P52800	EFNB2	ephrin B2	Plasma Membrane	kinase
A0A1D5RLL3	EFR3A	EFR3 homolog A	Plasma Membrane	other
A2AH85	EFTUD2	elongation factor Tu GTP binding domain containing 2	Nucleus	enzyme
Q9WVK4	EHD1	EH domain containing 1	Cytoplasm	other
Q8BH64	EHD2	EH domain containing 2	Nucleus	other
Q9QXY6	EHD3	EH domain containing 3	Cytoplasm	other
Q9EQP2	EHD4	EH domain containing 4	Plasma Membrane	enzyme
P48024	Eif1	eukaryotic translation initiation factor 1	Other	other
Q8BJW6	EIF2A	eukaryotic translation initiation factor 2A	Cytoplasm	translation regulator
Q99LD9	EIF2B2	eukaryotic translation initiation factor 2B subunit beta	Cytoplasm	other
Q6ZWX6	EIF2S1	eukaryotic translation initiation factor 2 subunit alpha	Cytoplasm	translation regulator
Q99L45	EIF2S2	eukaryotic translation initiation factor 2 subunit beta	Cytoplasm	translation regulator
Q9Z0N1	EIF2S3	eukaryotic translation initiation factor 2 subunit gamma	Cytoplasm	translation regulator
P23116	EIF3A	eukaryotic translation initiation factor 3 subunit A	Cytoplasm	other
Q8JZQ9	EIF3B	eukaryotic translation initiation factor 3 subunit B	Cytoplasm	translation regulator
Q8R1B4	EIF3C	eukaryotic translation initiation factor 3 subunit C	Cytoplasm	translation regulator
P60229	EIF3E	eukaryotic translation initiation factor 3 subunit E	Cytoplasm	other
Q9DCH4	EIF3F	eukaryotic translation initiation factor 3 subunit F	Cytoplasm	translation regulator
Q91WK2	EIF3H	eukaryotic translation initiation factor 3 subunit H	Cytoplasm	other
Q9QZD9	EIF3I	eukaryotic translation initiation factor 3 subunit I	Cytoplasm	translation regulator
Q9DBZ5	EIF3K	eukaryotic translation initiation factor 3 subunit K	Cytoplasm	translation regulator
Q8QZY1	EIF3L	eukaryotic translation initiation factor 3 subunit L	Cytoplasm	other
Q99JX4	EIF3M	eukaryotic translation initiation factor 3 subunit M	Cytoplasm	other
P60843	EIF4A1	eukaryotic translation initiation factor 4A1	Cytoplasm	translation regulator
P10630	EIF4A2	eukaryotic translation initiation factor 4A2	Cytoplasm	translation regulator
Q91VC3	EIF4A3	eukaryotic translation initiation factor 4A3	Nucleus	enzyme
Q8BGD9	EIF4B	eukaryotic translation initiation factor 4B	Cytoplasm	translation regulator

P63073	EIF4E	eukaryotic translation initiation factor 4E	Cytoplasm	translation regulator
E9Q9E1	EIF4G1	eukaryotic translation initiation factor 4 gamma 1	Cytoplasm	translation regulator
G3XA17	EIF4G2	eukaryotic translation initiation factor 4 gamma 2	Cytoplasm	translation regulator
Q9WUK2	EIF4H	eukaryotic translation initiation factor 4H	Cytoplasm	translation regulator
P59325	EIF5	eukaryotic translation initiation factor 5	Cytoplasm	translation regulator
P63242	EIF5A	eukaryotic translation initiation factor 5A	Cytoplasm	translation regulator
Q05D44	EIF5B	eukaryotic translation initiation factor 5B	Cytoplasm	translation regulator
O55135	EIF6	eukaryotic translation initiation factor 6	Cytoplasm	translation regulator
P70372	ELAVL1	ELAV like RNA binding protein 1	Cytoplasm	other
Q8BPU7	ELMO1	engulfment and cell motility 1	Cytoplasm	other
P62869	Elob	elongin B	Nucleus	transcription regulator
A0A087WNT1	ELOC	elongin C	Nucleus	transcription regulator
Q9CZX0-2	ELP3	elongator acetyltransferase complex subunit 3	Nucleus	enzyme
E9QK48	EML2	echinoderm microtubule associated protein like 2	Cytoplasm	other
A0A0A6YXC8	ENAH	ENAH, actin regulator	Plasma Membrane	other
P17182	ENO1	enolase 1	Cytoplasm	enzyme
P21550	ENO3	enolase 3	Cytoplasm	enzyme
A2A841	EPB41	erythrocyte membrane protein band 4.1	Plasma Membrane	other
O70318	EPB41L2	erythrocyte membrane protein band 4.1 like 2	Plasma Membrane	other
Q03145	EPHA2	EPH receptor A2	Plasma Membrane	kinase
Q03137	EPHA4	EPH receptor A4	Plasma Membrane	kinase
P54763	EPHB2	EPH receptor B2	Plasma Membrane	kinase
P54754	EPHB3	EPH receptor B3	Plasma Membrane	kinase
E9PWK7	EPHB4	EPH receptor B4	Plasma Membrane	kinase
Q9D379	EPHX1	epoxide hydrolase 1	Cytoplasm	peptidase
Q8CGC7	EPRS	glutamyl-prolyl-tRNA synthetase	Cytoplasm	enzyme
Q08509	EPS8	epidermal growth factor receptor pathway substrate 8	Plasma Membrane	peptidase
Q80TH2-1	ERBIN	erbb2 interacting protein	Cytoplasm	other
Q9DC16	ERGIC1	endoplasmic reticulum-golgi intermediate compartment 1	Cytoplasm	other
A0A0R4J1G5	ERLIN1	ER lipid raft associated 1	Plasma Membrane	other
Q9D1Q6	ERP44	endoplasmic reticulum protein 44	Cytoplasm	enzyme
H3BKH6	ESD	esterase D	Cytoplasm	enzyme
Q3U7R1	ESYT1	extended synaptotagmin 1	Cytoplasm	other
Q3TZZ7	ESYT2	extended synaptotagmin 2	Plasma Membrane	other
Q8BWY3	ETF1	eukaryotic translation termination factor 1	Cytoplasm	translation regulator
Q99LC5	ETFA	electron transfer flavoprotein alpha subunit	Cytoplasm	transporter
Q9DCW4	ETFB	electron transfer flavoprotein beta subunit	Cytoplasm	transporter
P20934	EVI2A	ecotropic viral integration site 2A	Plasma Membrane	transmembrane receptor
Q6KAR6	EXOC3	exocyst complex component 3	Plasma Membrane	transporter

O35382	EXOC4	exocyst complex component 4	Cytoplasm	transporter
P97464	EXT1	exostosin glycosyltransferase 1	Cytoplasm	enzyme
E9Q1M5	EXT2	exostosin glycosyltransferase 2	Cytoplasm	enzyme
P26040	EZR	ezrin	Plasma Membrane	other
O88792	F11R	F11 receptor	Plasma Membrane	other
Q8BH61	F13A1	coagulation factor XIII A chain	Extracellular Space	enzyme
O88634	F2RL3	F2R like thrombin or trypsin receptor 3	Plasma Membrane	G-protein coupled receptor
A0A0G2JGS5	F3	coagulation factor III, tissue factor	Plasma Membrane	transmembrane receptor
B2RRC9	F8	coagulation factor VIII	Extracellular Space	other
Q05816	FABP5	fatty acid binding protein 5	Cytoplasm	transporter
P54731	FAF1	Fas associated factor 1	Nucleus	other
Q6A0A9	FAM120A	family with sequence similarity 120A	Cytoplasm	other
Q3UW53	FAM129A	family with sequence similarity 129 member A	Cytoplasm	other
Q8R1F1	FAM129B	family with sequence similarity 129 member B	Cytoplasm	transcription regulator
A2ATL0	FAM171A1	family with sequence similarity 171 member A1	Cytoplasm	other
Q8C0Z1	FAM234A	family with sequence similarity 234 member A	Plasma Membrane	other
Q921M7	FAM49B	family with sequence similarity 49 member B	Extracellular Space	other
A0A0N4SV29	FANCD2	Fanconi anemia complementation group D2	Nucleus	other
F8VPU2	FARP1	FERM, ARH/RhoGEF and pleckstrin domain protein 1	Plasma Membrane	other
D3Z4C0	FARP2	FERM, ARH/RhoGEF and pleckstrin domain protein 2	Cytoplasm	other
E9PWY9	FARSA	phenylalanyl-tRNA synthetase alpha subunit	Cytoplasm	enzyme
Q9WUA2	FARSB	phenylalanyl-tRNA synthetase beta subunit	Cytoplasm	enzyme
P19096	FASN	fatty acid synthase	Cytoplasm	enzyme
F2Z4A3	FAT1	FAT atypical cadherin 1	Plasma Membrane	other
P35550	FBL	fibrillarin	Nucleus	enzyme
P37889-2	FBLN2	fibulin 2	Extracellular Space	other
Q61554	FBN1	fibrillin 1	Extracellular Space	other
F6T356	FBXO11	F-box protein 11	Cytoplasm	enzyme
Q920E5	FDPS	farnesyl diphosphate synthase	Cytoplasm	enzyme
Q8CIB5	FERMT2	fermitin family member 2	Cytoplasm	other
Q8K1B8	FERMT3	fermitin family member 3	Cytoplasm	enzyme
E9PV24	FGA	fibrinogen alpha chain	Extracellular Space	other
E9PX60	FGFR2	fibroblast growth factor receptor 2	Plasma Membrane	kinase
Q3UER8	FGG	fibrinogen gamma chain	Extracellular Space	other
P97807-2	FH	fumarate hydratase	Cytoplasm	enzyme
A2AEX8	FHL1	four and a half LIM domains 1	Cytoplasm	other
Q6P9Q4	Fhod1	formin homology 2 domain containing 1	Cytoplasm	other
P26883	FKBP1A	FK506 binding protein 1A	Cytoplasm	enzyme
P30416	FKBP4	FK506 binding protein 4	Nucleus	enzyme

B7FAU9	FLNA	filamin A	Cytoplasm	other
Q80X90	FLNB	filamin B	Cytoplasm	other
Q8VHX6	FLNC	filamin C	Cytoplasm	other
O08917	FLOT1	flotillin 1	Plasma Membrane	other
Q60634	FLOT2	flotillin 2	Plasma Membrane	other
Q8BLU0	FLRT2	fibronectin leucine rich transmembrane protein 2	Plasma Membrane	other
A0A1W2P6X3	Fmnl1	formin-like 1	Cytoplasm	other
F8VPR2	FMNL2	formin like 2	Cytoplasm	other
Q6ZPF4	FMNL3	formin like 3	Cytoplasm	other
A0A087WR50	FN1	fibronectin 1	Extracellular Space	enzyme
A0A087WSN6	FN1	fibronectin 1	Extracellular Space	enzyme
P11276	FN1	fibronectin 1	Extracellular Space	enzyme
Q8K274	FN3KRP	fructosamine 3 kinase related protein	Cytoplasm	kinase
E9Q8I9	FRY	FRY microtubule binding protein	Extracellular Space	other
F8VQ05	FRYL	FRY like transcription coactivator	Other	other
Q61553	FSCN1	fascin actin-bundling protein 1	Cytoplasm	other
P09528	FTH1	ferritin heavy chain 1	Cytoplasm	enzyme
P29391	FTL	ferritin light chain	Cytoplasm	enzyme
Q99LJ1	FUCA1	alpha-L-fucosidase 1	Cytoplasm	enzyme
Q7TMC8	FUK	fucokinase	Cytoplasm	kinase
Q9WTS2	FUT8	fucosyltransferase 8	Cytoplasm	enzyme
Q61584-4	FXR1	FMR1 autosomal homolog 1	Cytoplasm	other
F6TWM7	FXYD5	FXYD domain containing ion transport regulator 5	Plasma Membrane	ion channel
P39688	FYN	FYN proto-oncogene, Src family tyrosine kinase	Plasma Membrane	kinase
Q61090	FZD7	frizzled class receptor 7	Plasma Membrane	G-protein coupled receptor
P97855	G3BP1	G3BP stress granule assembly factor 1	Nucleus	enzyme
Q00612	G6PD	glucose-6-phosphate dehydrogenase	Cytoplasm	enzyme
P60521	GABARAPL2	GABA type A receptor associated protein like 2	Cytoplasm	other
P54818	GALC	galactosylceramidase	Cytoplasm	enzyme
Q9R0N0	GALK1	galactokinase 1	Cytoplasm	kinase
Q8BHN3	GANAB	glucosidase II alpha subunit	Cytoplasm	enzyme
P16858	GAPDH	glyceraldehyde-3-phosphate dehydrogenase	Cytoplasm	enzyme
Q6PAR5-2	GAPVD1	GTPase activating protein and VPS9 domains 1	Cytoplasm	other
Q9CZD3	GARS	glycyl-tRNA synthetase	Cytoplasm	enzyme
Q64737	GART	phosphoribosylglycinamide formyltransferase, phosphoribosylglycinamide synthetase, phosphoribosylaminoimidazole synthetase	Cytoplasm	enzyme
O09172	GCLM	glutamate-cysteine ligase modifier subunit	Cytoplasm	enzyme
E9PVA8	GCN1	GCN1, eIF2 alpha kinase activator homolog	Cytoplasm	translation regulator

P50396	GDI1	GDP dissociation inhibitor 1	Cytoplasm	other
Q61598	GDI2	GDP dissociation inhibitor 2	Cytoplasm	other
Q6P6L6	GEMIN4	gem nuclear organelle associated protein 4	Nucleus	other
A2AFQ9	GEMIN5	gem nuclear organelle associated protein 5	Nucleus	other
P47856-2	GFPT1	glutamine--fructose-6-phosphate transaminase 1	Cytoplasm	enzyme
G3UYG6	GIGYF2	GRB10 interacting GYF protein 2	Cytoplasm	other
Q9Z0G0	GIPC1	GIPC PDZ domain containing family member 1	Cytoplasm	other
P23242	GJA1	gap junction protein alpha 1	Plasma Membrane	transporter
P28229	GJC1	gap junction protein gamma 1	Plasma Membrane	ion channel
F8WHM5	GLG1	golgi glycoprotein 1	Cytoplasm	other
Q9CYL5	GLIPR2	GLI pathogenesis related 2	Cytoplasm	other
H9H9R4	GLMP	glycosylated lysosomal membrane protein	Cytoplasm	transcription regulator
Q9CPU0	GLO1	glyoxalase I	Cytoplasm	enzyme
Q9CPV4-3	GLOD4	glyoxalase domain containing 4	Cytoplasm	enzyme
Q9CQM9	GLRX3	glutaredoxin 3	Cytoplasm	enzyme
P26443	GLUD1	glutamate dehydrogenase 1	Cytoplasm	enzyme
E9QAZ2	Gm10020	ribosomal protein L15 pseudogene	Other	other
G3X9L6	Gm10250	ATP synthase, H+ transporting, mitochondrial F0 complex, subunit d pseudogene	Other	other
F6YVP7	Gm10260	ribosomal protein S18 pseudogene	Other	other
F6QL70	Gm17669	predicted gene, 17669	Other	other
A0A0J9YUZ4	Gm21596/Hmgb1	high mobility group box 1	Nucleus	transcription regulator
Q922H4	GMPPA	GDP-mannose pyrophosphorylase A	Cytoplasm	enzyme
Q8BTZ7	GMPPB	GDP-mannose pyrophosphorylase B	Cytoplasm	enzyme
Q3THK7	GMPS	guanine monophosphate synthase	Nucleus	enzyme
P21278	GNA11	G protein subunit alpha 11	Plasma Membrane	enzyme
P27600	GNA12	G protein subunit alpha 12	Plasma Membrane	enzyme
P27601	GNA13	G protein subunit alpha 13	Plasma Membrane	enzyme
P08752	GNAI2	G protein subunit alpha i2	Plasma Membrane	enzyme
Q9DC51	GNAI3	G protein subunit alpha i3	Cytoplasm	enzyme
P21279	GNAQ	G protein subunit alpha q	Plasma Membrane	enzyme
P63094	GNAS	GNAS complex locus	Plasma Membrane	enzyme
P62874	GNB1	G protein subunit beta 1	Plasma Membrane	enzyme
P62880	GNB2	G protein subunit beta 2	Plasma Membrane	enzyme
Q3UW64	GNE	glucosamine (UDP-N-acetyl)-2-epimerase/N-acetylmannosamine kinase	Cytoplasm	kinase
Q9CXP8	GNG10	G protein subunit gamma 10	Plasma Membrane	enzyme
A0A0N4SVT3	GNG12	G protein subunit gamma 12	Plasma Membrane	enzyme
P63213	GNG2	G protein subunit gamma 2	Plasma Membrane	enzyme

Q80SZ7	GNG5	G protein subunit gamma 5	Plasma Membrane	other
Q9JK38	GNPNAT1	glucosamine-phosphate N-acetyltransferase 1	Cytoplasm	enzyme
Q91VW5	GOLGA4	golgin A4	Cytoplasm	other
Q91W53	GOLGA7	golgin A7	Cytoplasm	other
D3YVW2	GOLIM4	golgi integral membrane protein 4	Cytoplasm	other
P05201	GOT1	glutamic-oxaloacetic transaminase 1	Cytoplasm	enzyme
P05202	GOT2	glutamic-oxaloacetic transaminase 2	Cytoplasm	enzyme
O35930	GP1BA	glycoprotein Ib platelet alpha subunit	Plasma Membrane	transmembrane receptor
Q9QZF2	GPC1	glypican 1	Plasma Membrane	transmembrane receptor
P51655	GPC4	glypican 4	Plasma Membrane	transmembrane receptor
A0JNY3	GPHN	gephyrin	Plasma Membrane	enzyme
P06745	GPI	glucose-6-phosphate isomerase	Extracellular Space	enzyme
P35802	GPM6A	glycoprotein M6A	Plasma Membrane	ion channel
Q99P91	GPNMB	glycoprotein nmb	Plasma Membrane	enzyme
G5E8C3	GPRC5A	G protein-coupled receptor class C group 5 member A	Plasma Membrane	G-protein coupled receptor
G3UXW9	GPS1	G protein pathway suppressor 1	Nucleus	other
S4R1E5	GPX4	glutathione peroxidase 4	Cytoplasm	enzyme
Q60631	GRB2	growth factor receptor bound protein 2	Cytoplasm	kinase
O70293-2	GRK6	G protein-coupled receptor kinase 6	Plasma Membrane	kinase
E9QAQ5	GSK3B	glycogen synthase kinase 3 beta	Nucleus	kinase
Q8R050-2	GSPT1	G1 to S phase transition 1	Cytoplasm	translation regulator
P47791-2	GSR	glutathione-disulfide reductase	Cytoplasm	enzyme
P24472	Gsta4	glutathione S-transferase, alpha 4	Other	enzyme
P13745	GSTA5	glutathione S-transferase alpha 5	Cytoplasm	enzyme
P15626	GSTM1	glutathione S-transferase mu 1	Cytoplasm	enzyme
P48774	GSTM3	glutathione S-transferase mu 3	Cytoplasm	enzyme
P10649	GSTM5	glutathione S-transferase mu 5	Cytoplasm	enzyme
O09131	GSTO1	glutathione S-transferase omega 1	Cytoplasm	enzyme
P19157	GSTP1	glutathione S-transferase pi 1	Cytoplasm	enzyme
Q80YP4	GUCY1B1	guanylate cyclase 1 soluble subunit beta 1	Cytoplasm	enzyme
P12265	GUSB	glucuronidase beta	Cytoplasm	enzyme
A0A1B0GT92	GYS1	glycogen synthase 1	Cytoplasm	enzyme
A0A0N4SV66	H2AFJ	H2A histone family member J	Cytoplasm	other
Q3THW5	H2AFV	H2A histone family member V	Nucleus	other
Q9QZQ8-2	H2AFY	H2A histone family member Y	Nucleus	other
Q8BMS1	HADHA	hydroxyacyl-CoA dehydrogenase trifunctional multienzyme complex subunit alpha	Cytoplasm	enzyme
Q99JY0	HADHB	hydroxyacyl-CoA dehydrogenase trifunctional multienzyme complex subunit beta	Cytoplasm	enzyme

E9PYA3	HAGH	hydroxyacylglutathione hydrolase	Cytoplasm	enzyme
P35492	HAL	histidine ammonia-lyase	Cytoplasm	enzyme
Q61035	HARS	histidyl-tRNA synthetase	Cytoplasm	enzyme
B2RY58	HCN4	hyperpolarization activated cyclic nucleotide gated potassium channel 4	Plasma Membrane	ion channel
Q8VDJ3	HDLBP	high density lipoprotein binding protein	Nucleus	transporter
Q3U487	HECTD3	HECT domain E3 ubiquitin protein ligase 3	Cytoplasm	enzyme
E9Q2E4	HECTD4	HECT domain E3 ubiquitin protein ligase 4	Nucleus	other
A2AS05	HELZ2	helicase with zinc finger 2	Nucleus	transcription regulator
P29416	HEXA	hexosaminidase subunit alpha	Cytoplasm	enzyme
O09173	HGD	homogentisate 1,2-dioxygenase	Cytoplasm	enzyme
B1ATZ0	HGS	hepatocyte growth factor-regulated tyrosine kinase substrate	Cytoplasm	other
Q9JLZ6-2	HIC2	HIC ZBTB transcriptional repressor 2	Nucleus	other
P70349	HINT1	histidine triad nucleotide binding protein 1	Nucleus	enzyme
P43275	Hist1h1a	histone cluster 1, H1a	Nucleus	other
P43276	Hist1h1b	histone cluster 1, H1b	Nucleus	other
P15864	HIST1H1C	histone cluster 1 H1 family member c	Nucleus	other
P43277	HIST1H1D	histone cluster 1 H1 family member d	Nucleus	other
P43274	Hist1h1e	histone cluster 1, H1e	Nucleus	other
Q8CGP2	HIST1H2BO	histone cluster 1 H2B family member o	Nucleus	other
A0A1W2P768	HIST1H3C	histone cluster 1 H3 family member c	Nucleus	other
Q64522	HIST2H2AB	histone cluster 2 H2A family member b	Nucleus	other
Q64523	HIST2H2AC	histone cluster 2 H2A family member c	Nucleus	other
P17710-3	HK1	hexokinase 1	Cytoplasm	kinase
P01902	HLA-A	major histocompatibility complex, class I, A	Plasma Membrane	other
P01900	HLA-A	major histocompatibility complex, class I, A	Plasma Membrane	other
Q8HWB2	HLA-A	major histocompatibility complex, class I, A	Plasma Membrane	other
P01897	HLA-A	major histocompatibility complex, class I, A	Plasma Membrane	other
P04223	HLA-A	major histocompatibility complex, class I, A	Plasma Membrane	other
Q8JZK9	HMGCS1	3-hydroxy-3-methylglutaryl-CoA synthase 1	Cytoplasm	enzyme
Q5EBP8	Hnrnpa1	heterogeneous nuclear ribonucleoprotein A1	Nucleus	other
O88569	HNRNPA2B1	heterogeneous nuclear ribonucleoprotein A2/B1	Nucleus	other
A2AL12	Hnrnpa3	heterogeneous nuclear ribonucleoprotein A3	Nucleus	transporter
Q9Z204-2	HNRNPC	heterogeneous nuclear ribonucleoprotein C (C1/C2)	Nucleus	other
Q60668-3	HNRNPD	heterogeneous nuclear ribonucleoprotein D	Nucleus	transcription regulator
Q9Z2X1	HNRNPF	heterogeneous nuclear ribonucleoprotein F	Nucleus	other
Q8C2Q7	HNRNPH1	heterogeneous nuclear ribonucleoprotein H1	Nucleus	other
P61979-2	HNRNPK	heterogeneous nuclear ribonucleoprotein K	Nucleus	transcription regulator
G5E924	HNRNPL	heterogeneous nuclear ribonucleoprotein L	Nucleus	other

Q9D0E1	HNRNPM	heterogeneous nuclear ribonucleoprotein M	Nucleus	other
Q8VHM5	HNRNPR	heterogeneous nuclear ribonucleoprotein R	Nucleus	other
Q8VEK3	HNRNPU	heterogeneous nuclear ribonucleoprotein U	Nucleus	transporter
Q61646	HP	haptoglobin	Extracellular Space	peptidase
Z4YKB8	HP1BP3	heterochromatin protein 1 binding protein 3	Nucleus	other
P62748	HPCAL1	hippocalcin like 1	Cytoplasm	other
Q61411	HRAS	HRas proto-oncogene, GTPase	Plasma Membrane	enzyme
O70503	HSD17B12	hydroxysteroid 17-beta dehydrogenase 12	Cytoplasm	enzyme
P07901	HSP90AA1	heat shock protein 90 alpha family class A member 1	Cytoplasm	enzyme
P11499	HSP90AB1	heat shock protein 90 alpha family class B member 1	Cytoplasm	enzyme
P08113	HSP90B1	heat shock protein 90 beta family member 1	Cytoplasm	other
P17879	Hspa1b	heat shock protein 1B	Cytoplasm	other
P16627	HSPA1L	heat shock protein family A (Hsp70) member 1 like	Cytoplasm	other
Q3U2G2	HSPA4	heat shock protein family A (Hsp70) member 4	Cytoplasm	other
P20029	HSPA5	heat shock protein family A (Hsp70) member 5	Cytoplasm	enzyme
P63017	HSPA8	heat shock protein family A (Hsp70) member 8	Cytoplasm	enzyme
P38647	HSPA9	heat shock protein family A (Hsp70) member 9	Cytoplasm	other
P14602-3	HSPB1	heat shock protein family B (small) member 1	Cytoplasm	other
P63038	HSPD1	heat shock protein family D (Hsp60) member 1	Cytoplasm	enzyme
Q64433	HSPE1	heat shock protein family E (Hsp10) member 1	Cytoplasm	enzyme
Q05793	HSPG2	heparan sulfate proteoglycan 2	Extracellular Space	enzyme
E9PZ16	HSPG2	heparan sulfate proteoglycan 2	Extracellular Space	enzyme
B1B0C7	HSPG2	heparan sulfate proteoglycan 2	Extracellular Space	enzyme
Q61699-2	HSPH1	heat shock protein family H (Hsp110) member 1	Cytoplasm	other
Q9R118	HTRA1	HtrA serine peptidase 1	Extracellular Space	peptidase
A2AFQ0	HUWE1	HECT, UBA and WWE domain containing 1, E3 ubiquitin protein ligase	Nucleus	transcription regulator
Q9JKR6	HYOU1	hypoxia up-regulated 1	Cytoplasm	other
Q8BU30	IARS	isoleucyl-tRNA synthetase	Cytoplasm	enzyme
F6RPJ9	IDE	insulin degrading enzyme	Extracellular Space	peptidase
O88844	IDH1	isocitrate dehydrogenase (NADP(+)) 1, cytosolic	Cytoplasm	enzyme
P54071	IDH2	isocitrate dehydrogenase (NADP(+)) 2, mitochondrial	Cytoplasm	enzyme
P70404	IDH3G	isocitrate dehydrogenase 3 (NAD(+)) gamma	Cytoplasm	enzyme
Q64282	IFIT1B	interferon induced protein with tetratricopeptide repeats 1B	Cytoplasm	other
Q99J93	IFITM2	interferon induced transmembrane protein 2	Cytoplasm	other
Q9CQW9	IFITM3	interferon induced transmembrane protein 3	Plasma Membrane	other
E9QNX9	IGF1R	insulin like growth factor 1 receptor	Plasma Membrane	transmembrane receptor
Q07113	IGF2R	insulin like growth factor 2 receptor	Plasma Membrane	transmembrane receptor
P47877	IGFBP2	insulin like growth factor binding protein 2	Extracellular Space	other

Q6ZQA6	IGSF3	immunoglobulin superfamily member 3	Plasma Membrane	other
Q8R366	IGSF8	immunoglobulin superfamily member 8	Plasma Membrane	other
A0A0R4J0T4	IKBKB	inhibitor of nuclear factor kappa B kinase subunit beta	Cytoplasm	kinase
P14719	IL1RL1	interleukin 1 receptor like 1	Plasma Membrane	transmembrane receptor
V9GX00	IL6ST	interleukin 6 signal transducer	Plasma Membrane	transmembrane receptor
Q9CXY6	ILF2	interleukin enhancer binding factor 2	Nucleus	transcription regulator
Q9Z1X4	ILF3	interleukin enhancer binding factor 3	Nucleus	transcription regulator
O55222	ILK	integrin linked kinase	Plasma Membrane	kinase
Q924B0	IMPA1	inositol monophosphatase 1	Cytoplasm	phosphatase
P24547	IMPDH2	inosine monophosphate dehydrogenase 2	Cytoplasm	enzyme
E9QLA5	INF2	inverted formin, FH2 and WH2 domain containing	Cytoplasm	other
P15208	INSR	insulin receptor	Plasma Membrane	kinase
Q8VI75	IPO4	importin 4	Nucleus	transporter
Q8BKC5	IPO5	importin 5	Nucleus	transporter
Q9EPL8	IPO7	importin 7	Nucleus	transporter
E9QKZ2	IPO9	importin 9	Nucleus	transporter
Q9JKF1	IQGAP1	IQ motif containing GTPase activating protein 1	Cytoplasm	other
F8VQ29	IQGAP3	IQ motif containing GTPase activating protein 3	Plasma Membrane	other
J7NUP1	Irgm1	immunity-related GTPase family M member 1	Cytoplasm	other
Q64339	ISG15	ISG15 ubiquitin-like modifier	Extracellular Space	other
Q9CX00	IST1	IST1, ESCRT-III associated factor	Cytoplasm	other
Q8C863	ITCH	itchy E3 ubiquitin protein ligase	Nucleus	enzyme
Q99KW9	ITFG1	integrin alpha FG-GAP repeat containing 1	Plasma Membrane	other
Q3V3R4	ITGA1	integrin subunit alpha 1	Plasma Membrane	other
Q62469	ITGA2	integrin subunit alpha 2	Plasma Membrane	transmembrane receptor
Q9QUM0	ITGA2B	integrin subunit alpha 2b	Plasma Membrane	transmembrane receptor
Q62470	ITGA3	integrin subunit alpha 3	Plasma Membrane	other
Q792F9	ITGA4	integrin subunit alpha 4	Plasma Membrane	transmembrane receptor
P11688	ITGA5	integrin subunit alpha 5	Plasma Membrane	transmembrane receptor
Q61739-2	ITGA6	integrin subunit alpha 6	Plasma Membrane	transmembrane receptor
Q3TZS3	ITGA7	integrin subunit alpha 7	Plasma Membrane	other
P43406	ITGAV	integrin subunit alpha V	Plasma Membrane	transmembrane receptor
P09055	ITGB1	integrin subunit beta 1	Plasma Membrane	transmembrane receptor
Q542I8	ITGB2	integrin subunit beta 2	Plasma Membrane	transmembrane receptor
O54890	ITGB3	integrin subunit beta 3	Plasma Membrane	transmembrane receptor
A2A863-2	ITGB4	integrin subunit beta 4	Plasma Membrane	transmembrane receptor
Q6PE70	ITGB5	integrin subunit beta 5	Plasma Membrane	other
B1AYG7	ITGB6	integrin subunit beta 6	Plasma Membrane	other
O89051	ITM2B	integral membrane protein 2B	Plasma Membrane	other

A0A087WRM2	ITM2C	integral membrane protein 2C	Cytoplasm	other
P70227	ITPR3	inositol 1,4,5-trisphosphate receptor type 3	Cytoplasm	ion channel
B1ASP2	JAK1	Janus kinase 1	Cytoplasm	kinase
Q02257	JUP	junction plakoglobin	Plasma Membrane	other
Q99MN1	KARS	lysyl-tRNA synthetase	Cytoplasm	enzyme
Q5SVQ0-5	KAT7	lysine acetyltransferase 7	Nucleus	enzyme
Q80UY2	KCMF1	potassium channel modulatory factor 1	Extracellular Space	enzyme
Q922M3	KCTD10	potassium channel tetramerization domain containing 10	Nucleus	ion channel
Q8BGV7	KCTD13	potassium channel tetramerization domain containing 13	Nucleus	ion channel
Q6PDI5-2	KIAA0368	KIAA0368	Cytoplasm	other
E9Q9B7	KIDINS220	kinase D interacting substrate 220	Nucleus	transcription regulator
Q6P9P6	KIF11	kinesin family member 11	Nucleus	other
L0N7N1	KIF14	kinesin family member 14	Cytoplasm	enzyme
E9Q5G3	KIF23	kinesin family member 23	Cytoplasm	other
P28740-2	KIF2A	kinesin family member 2A	Cytoplasm	other
P33174	KIF4A	kinesin family member 4A	Nucleus	other
Q61768	KIF5B	kinesin family member 5B	Cytoplasm	other
Q80W68	KIRREL1	kirre like nephrin family adhesion molecule 1	Plasma Membrane	other
Q5UE59	KLC1	kinesin light chain 1	Cytoplasm	other
A3KGI3	KNL1	kinetochore scaffold 1	Nucleus	other
P52293	KPNA2	karyopherin subunit alpha 2	Nucleus	transporter
O35344	KPNA3	karyopherin subunit alpha 3	Nucleus	transporter
O35343	KPNA4	karyopherin subunit alpha 4	Nucleus	transporter
Q4FJZ2	KPNA6	karyopherin subunit alpha 6	Nucleus	transporter
P70168	KPNB1	karyopherin subunit beta 1	Nucleus	transporter
P32883-2	KRAS	KRAS proto-oncogene, GTPase	Cytoplasm	enzyme
Q3UV17	KRT76	keratin 76	Cytoplasm	other
E9Q1Z0	Krt90	keratin 90	Cytoplasm	other
A2ARD6	KYNU	kynureninase	Cytoplasm	enzyme
Q61001	LAMA5	laminin subunit alpha 5	Extracellular Space	other
E9QN70	LAMB1	laminin subunit beta 1	Extracellular Space	other
F8VQJ3	LAMC1	laminin subunit gamma 1	Extracellular Space	other
P11438	LAMP1	lysosomal associated membrane protein 1	Plasma Membrane	other
P17047-3	LAMP2	lysosomal associated membrane protein 2	Plasma Membrane	enzyme
Q9CQ22	LAMTOR1	late endosomal/lysosomal adaptor, MAPK and MTOR activator 1	Plasma Membrane	other
Q9CPY7-2	LAP3	leucine aminopeptidase 3	Cytoplasm	peptidase
E9QLR3	LAPTM4A	lysosomal protein transmembrane 4 alpha	Cytoplasm	other
Q8BMJ2	LARS	leucyl-tRNA synthetase	Cytoplasm	enzyme

A2BE28-2	LAS1L	LAS1 like, ribosome biogenesis factor	Nucleus	other
Q61792	LASP1	LIM and SH3 protein 1	Cytoplasm	transporter
P16301	LCAT	lecithin-cholesterol acyltransferase	Extracellular Space	enzyme
Q564E2	LDHA	lactate dehydrogenase A	Cytoplasm	enzyme
P16125	LDHB	lactate dehydrogenase B	Cytoplasm	enzyme
P35951	LDLR	low density lipoprotein receptor	Plasma Membrane	transporter
Q8C142	LDLRAP1	low density lipoprotein receptor adaptor protein 1	Cytoplasm	transporter
D3YWS8	LENG8	leukocyte receptor cluster member 8	Other	other
O89013	LEPROT	leptin receptor overlapping transcript	Plasma Membrane	other
P16045	LGALS1	galectin 1	Extracellular Space	other
Q8C253	LGALS3	galectin 3	Extracellular Space	other
Q07797	LGALS3BP	galectin 3 binding protein	Plasma Membrane	transmembrane receptor
B1AQR8	LGALS9B	galectin 9B	Cytoplasm	other
Q8VED9	LGALSL	galectin like	Other	other
D3Z698	LHFPL2	LHFPL tetraspan subfamily member 2	Other	enzyme
Q8BM86	LHFPL6	LHFPL tetraspan subfamily member 6	Other	other
A0A0R4J005	LIMS1	LIM zinc finger domain containing 1	Plasma Membrane	other
O88952	LIN7C	lin-7 homolog C, crumbs cell polarity complex component	Cytoplasm	other
A0A0R4J0S4	LLGL1	LLGL1, scribble cell polarity complex component	Cytoplasm	other
J3QJU5	LLGL2	LLGL2, scribble cell polarity complex component	Cytoplasm	other
Q9D0F3	LMAN1	lectin, mannose binding 1	Cytoplasm	other
Q9DBH5	LMAN2	lectin, mannose binding 2	Cytoplasm	transporter
Q8K0B2-3	LMBRD1	LMBR1 domain containing 1	Cytoplasm	other
P48678	LMNA	lamin A/C	Nucleus	other
P14733	LMNB1	lamin B1	Nucleus	other
Q8C129	LNPEP	leucyl and cystinyl aminopeptidase	Cytoplasm	peptidase
Q8CGK3	LONP1	lon peptidase 1, mitochondrial	Cytoplasm	peptidase
E9Q600	LOXL4	lysyl oxidase like 4	Extracellular Space	enzyme
P11152	LPL	lipoprotein lipase	Cytoplasm	enzyme
A0A0R4J0I9	LRP1	LDL receptor related protein 1	Plasma Membrane	transmembrane receptor
A2ARV4	LRP2	LDL receptor related protein 2	Plasma Membrane	transporter
O88572	LRP6	LDL receptor related protein 6	Plasma Membrane	transmembrane receptor
Q6PB66	LRPPRC	leucine rich pentatricopeptide repeat containing	Cytoplasm	other
A0A0R4J0W6	LRRC40	leucine rich repeat containing 40	Nucleus	other
A2AKH7	LRRC57	leucine rich repeat containing 57	Cytoplasm	other
Q8BGR2	LRRC8D	leucine rich repeat containing 8 VRAC subunit D	Plasma Membrane	G-protein coupled receptor
Q3TYX2	LRRN4CL	LRRN4 C-terminal like	Other	other
P24527	LTA4H	leukotriene A4 hydrolase	Cytoplasm	enzyme
P50284	LTBR	lymphotoxin beta receptor	Plasma Membrane	transmembrane receptor

A0A087WQ65	LY6E	lymphocyte antigen 6 family member E	Plasma Membrane	other
Q60767	LY75	lymphocyte antigen 75	Plasma Membrane	transmembrane receptor
P25911	LYN	LYN proto-oncogene, Src family tyrosine kinase	Cytoplasm	kinase
J3QP56	LYPLA1	lysophospholipase I	Cytoplasm	enzyme
Q9WTL7	LYPLA2	lysophospholipase II	Cytoplasm	enzyme
P24668	M6PR	mannose-6-phosphate receptor, cation dependent	Cytoplasm	transporter
F7ACR9	Macf1	microtubule-actin crosslinking factor 1	Cytoplasm	enzyme
Q9ER67	MAGED2	MAGE family member D2	Plasma Membrane	other
A0A1W2P788	MAN1A1	mannosidase alpha class 1A member 1	Cytoplasm	enzyme
P27046	MAN2A1	mannosidase alpha class 2A member 1	Cytoplasm	enzyme
Q9CQV6	MAP1LC3B	microtubule associated protein 1 light chain 3 beta	Cytoplasm	other
P31938	MAP2K1	mitogen-activated protein kinase kinase 1	Cytoplasm	kinase
Q91YS7	MAP2K2	mitogen-activated protein kinase kinase 2	Cytoplasm	kinase
O09110	MAP2K3	mitogen-activated protein kinase kinase 3	Cytoplasm	kinase
A0A087WS76	MAP3K19	mitogen-activated protein kinase kinase kinase 19	Other	kinase
E9PWG9	MAP3K5	mitogen-activated protein kinase kinase kinase 5	Cytoplasm	kinase
B2RUE8	MAP4K4	mitogen-activated protein kinase kinase kinase kinase 4	Cytoplasm	kinase
P63085	MAPK1	mitogen-activated protein kinase 1	Cytoplasm	kinase
P47811	MAPK14	mitogen-activated protein kinase 14	Cytoplasm	kinase
Q80Y86	MAPK15	mitogen-activated protein kinase 15	Cytoplasm	kinase
Q63844	MAPK3	mitogen-activated protein kinase 3	Cytoplasm	kinase
Q61166	MAPRE1	microtubule associated protein RP/EB family member 1	Cytoplasm	other
D3YYK8	Mapre2	microtubule-associated protein, RP/EB family, member 2	Cytoplasm	other
P26645	Marcks	myristoylated alanine rich protein kinase C substrate	Plasma Membrane	other
E9QB02	MARS	methionyl-tRNA synthetase	Cytoplasm	enzyme
P98064-2	Masp1	mannan-binding lectin serine peptidase 1	Extracellular Space	peptidase
Q91X83	MAT1A	methionine adenosyltransferase 1A	Cytoplasm	enzyme
Q3THS6	MAT2A	methionine adenosyltransferase 2A	Cytoplasm	enzyme
Q99LB6-2	MAT2B	methionine adenosyltransferase 2B	Cytoplasm	enzyme
Q8K310	MATR3	matrin 3	Nucleus	other
G3UYM8	MCF2L	MCF.2 cell line derived transforming sequence like	Cytoplasm	other
P97310	MCM2	minichromosome maintenance complex component 2	Nucleus	enzyme
P25206	MCM3	minichromosome maintenance complex component 3	Nucleus	enzyme
P49717	MCM4	minichromosome maintenance complex component 4	Nucleus	enzyme
Q52KC3	MCM5	minichromosome maintenance complex component 5	Nucleus	enzyme
P97311	MCM6	minichromosome maintenance complex component 6	Nucleus	enzyme
Q61881	MCM7	minichromosome maintenance complex component 7	Nucleus	enzyme
P14152	MDH1	malate dehydrogenase 1	Cytoplasm	enzyme
P08249	MDH2	malate dehydrogenase 2	Cytoplasm	enzyme

P06801	ME1	malic enzyme 1	Cytoplasm	enzyme
Q99KE1	ME2	malic enzyme 2	Cytoplasm	enzyme
Q91VH6	MEMO1	mediator of cell motility 1	Cytoplasm	other
F8VQL0	MET	MET proto-oncogene, receptor tyrosine kinase	Plasma Membrane	kinase
Q8BP48	METAP1	methionyl aminopeptidase 1	Cytoplasm	peptidase
P21956	MFGE8	milk fat globule-EGF factor 8 protein	Extracellular Space	other
Q9EQQ9	MGEA5	meningioma expressed antigen 5 (hyaluronidase)	Cytoplasm	enzyme
Q9D074	MGRN1	mahogunin ring finger 1	Cytoplasm	enzyme
F6ZBL2	MIB1	mindbomb E3 ubiquitin protein ligase 1	Cytoplasm	enzyme
P34884	MIF	macrophage migration inhibitory factor	Extracellular Space	cytokine
Q76LS9-2	MINDY1	MINDY lysine 48 deubiquitinase 1	Cytoplasm	peptidase
Q8VDV8	MITD1	microtubule interacting and trafficking domain containing 1	Cytoplasm	other
E9PVX6	MKI67	marker of proliferation Ki-67	Nucleus	other
Q6ZQI3	MLEC	malectin	Plasma Membrane	other
Q9D2Y4-2	MLKL	mixed lineage kinase domain like pseudokinase	Cytoplasm	kinase
Q3UDM0	MOB1B	MOB kinase activator 1B	Cytoplasm	other
B9EKJ3	MON2	MON2 homolog, regulator of endosome-to-Golgi trafficking	Cytoplasm	other
D3Z3E8	MOV10	Mov10 RISC complex RNA helicase	Nucleus	enzyme
P70290	MPP1	membrane palmitoylated protein 1	Plasma Membrane	kinase
Q9JLB0-2	MPP6	membrane palmitoylated protein 6	Plasma Membrane	kinase
Q3TEW6	MPZL1	myelin protein zero like 1	Plasma Membrane	other
Q64449	MRC2	mannose receptor C type 2	Plasma Membrane	transmembrane receptor
Q8VCJ6	MRGPRF	MAS related GPR family member F	Plasma Membrane	G-protein coupled receptor
Q9CQT1	MRI1	methylthioribose-1-phosphate isomerase 1	Cytoplasm	translation regulator
Q9CXW2	MRPS22	mitochondrial ribosomal protein S22	Cytoplasm	other
P43247	MSH2	mutS homolog 2	Nucleus	enzyme
P54276	MSH6	mutS homolog 6	Nucleus	enzyme
Q61468	MSLN	mesothelin	Extracellular Space	other
P26041	MSN	moesin	Plasma Membrane	other
P00405	MT-CO2	cytochrome c oxidase subunit II	Cytoplasm	enzyme
Q9CQ65	MTAP	methylthioadenosine phosphorylase	Nucleus	enzyme
Q791V5	MTCH2	mitochondrial carrier 2	Cytoplasm	other
Q922D8	MTHFD1	methylenetetrahydrofolate dehydrogenase, cyclohydrolase and formyltetrahydrofolate synthetase 1	Cytoplasm	enzyme
Q3V3R1	MTHFD1L	methylenetetrahydrofolate dehydrogenase (NADP+ dependent) 1 like	Cytoplasm	enzyme
Q6P572	MTMR2	myotubularin related protein 2	Cytoplasm	phosphatase
P62774	MTPN	myotrophin	Nucleus	transcription regulator
Q78HU3	MVB12A	multivesicular body subunit 12A	Cytoplasm	other

Q6KAU4	MVB12B	multivesicular body subunit 12B	Cytoplasm	other
Q9EQK5	MVP	major vault protein	Nucleus	other
Q9DBV4	MXRA8	matrix remodeling associated 8	Cytoplasm	other
O35682	MYADM	myeloid associated differentiation marker	Nucleus	other
Q7TPV4	MYBBP1A	MYB binding protein 1a	Nucleus	transcription regulator
F6SMY7	MYCBP2	MYC binding protein 2, E3 ubiquitin protein ligase	Nucleus	enzyme
Q5SV64	MYH10	myosin heavy chain 10	Cytoplasm	enzyme
K3W4R2	MYH14	myosin heavy chain 14	Extracellular Space	enzyme
Q8VDD5	MYH9	myosin heavy chain 9	Cytoplasm	enzyme
A0A087WRZ7	MYL1	myosin light chain 1	Cytoplasm	other
Q3THE2	MYL12A	myosin light chain 12A	Cytoplasm	other
Q6ZWQ9	MYL12B	myosin light chain 12B	Cytoplasm	other
Q60605-2	MYL6	myosin light chain 6	Cytoplasm	enzyme
F8VQB6	MYO10	myosin X	Cytoplasm	enzyme
K3W4L0	MYO18A	myosin XVIIIA	Cytoplasm	other
Q9WTI7-3	MYO1C	myosin IC	Cytoplasm	enzyme
Q9WTI7-2	MYO1C	myosin IC	Cytoplasm	enzyme
E9Q634	MYO1E	myosin IE	Cytoplasm	enzyme
D3YZ62	MYO5A	myosin VA	Cytoplasm	enzyme
Q9QY06	MYO9B	myosin IXB	Cytoplasm	enzyme
Q69ZN7	MYOF	myoferlin	Nucleus	other
G3X8Y3	NAA15	N(alpha)-acetyltransferase 15, NatA auxiliary subunit	Nucleus	transcription regulator
Q8BWZ3-2	NAA25	N(alpha)-acetyltransferase 25, NatB auxiliary subunit	Cytoplasm	other
Q6PGB6-2	NAA50	N(alpha)-acetyltransferase 50, NatE catalytic subunit	Cytoplasm	enzyme
G3UWC2	NAALAD2	N-acetylated alpha-linked acidic dipeptidase 2	Plasma Membrane	peptidase
Q60817	NACA	nascent polypeptide-associated complex alpha subunit	Cytoplasm	transcription regulator
Q99J77	NANS	N-acetylneuraminate synthase	Cytoplasm	enzyme
Q3TF41	NAP1L1	nucleosome assembly protein 1 like 1	Nucleus	other
B7ZNL2	NAP1L4	nucleosome assembly protein 1 like 4	Cytoplasm	other
Q9DB05	NAPA	NSF attachment protein alpha	Cytoplasm	transporter
Q8BP47	NARS	asparaginyl-tRNA synthetase	Cytoplasm	enzyme
Q99MD9	NASP	nuclear autoantigenic sperm protein	Nucleus	other
Q8K224	NAT10	N-acetyltransferase 10	Nucleus	enzyme
Q8CH77-2	NAV1	neuron navigator 1	Other	enzyme
E9Q9L6	NBEAL2	neurobeachin like 2	Cytoplasm	other
Q8K2Z4	NCAPD2	non-SMC condensin I complex subunit D2	Nucleus	other
Q99M51	NCK1	NCK adaptor protein 1	Cytoplasm	kinase
A2AS98	NCKAP1	NCK associated protein 1	Plasma Membrane	other
P09405	NCL	nucleolin	Nucleus	other

Q8BNY6	NCS1	neuronal calcium sensor 1	Plasma Membrane	other
P57716	NCSTN	nicastrin	Plasma Membrane	peptidase
Q8R0W6	NDFIP1	Nedd4 family interacting protein 1	Cytoplasm	other
F6RT43	NDFIP2	Nedd4 family interacting protein 2	Cytoplasm	other
Q91WD5	NDUFS2	NADH:ubiquinone oxidoreductase core subunit S2	Cytoplasm	enzyme
P46935	Nedd4	neural precursor cell expressed, developmentally down-regulated 4	Cytoplasm	enzyme
E9PXB7	NEDD4L	neural precursor cell expressed, developmentally down-regulated 4-like, E3 ubiquitin protein ligase	Cytoplasm	enzyme
Q8CFI0-3	NEDD4L	neural precursor cell expressed, developmentally down-regulated 4-like, E3 ubiquitin protein ligase	Cytoplasm	enzyme
P29595	NEDD8	neural precursor cell expressed, developmentally down-regulated 8	Nucleus	enzyme
Q8K1R7	NEK9	NIMA related kinase 9	Nucleus	kinase
Q7TQG5	NEO1	neogenin 1	Plasma Membrane	transcription regulator
Q6P5H2-2	Nes	nestin	Cytoplasm	other
Q9WTK5	NFKB2	nuclear factor kappa B subunit 2	Nucleus	transcription regulator
Q9Z1J3-2	NFS1	NFS1, cysteine desulfurase	Cytoplasm	enzyme
P10493	NID1	nidogen 1	Extracellular Space	other
P15532	NME1	NME/NM23 nucleoside diphosphate kinase 1	Cytoplasm	kinase
Q01768	NME2	NME/NM23 nucleoside diphosphate kinase 2	Nucleus	kinase
Q5RJG1	NOL10	nucleolar protein 10	Nucleus	other
Q99K48	NONO	non-POU domain containing octamer binding	Nucleus	other
Q9D6Z1	NOP56	NOP56 ribonucleoprotein	Nucleus	other
Q6DFW4	NOP58	NOP58 ribonucleoprotein	Nucleus	enzyme
Q01705-4	NOTCH1	notch 1	Plasma Membrane	transcription regulator
G5E8J0	NOTCH2	notch 2	Plasma Membrane	transcription regulator
Q61982	NOTCH3	notch 3	Plasma Membrane	transcription regulator
O35604	NPC1	NPC intracellular cholesterol transporter 1	Cytoplasm	transporter
Q11011	NPEPPS	aminopeptidase puromycin sensitive	Cytoplasm	peptidase
Q61937	NPM1	nucleophosmin 1	Nucleus	transcription regulator
P97300-1	Nptn	neuroplastin	Plasma Membrane	other
Q8CJ26	Nradd	neurotrophin receptor associated death domain	Extracellular Space	cytokine
A0A0G2JGP4	NRAS	NRAS proto-oncogene, GTPase	Plasma Membrane	enzyme
D3YUV1	NRBP1	nuclear receptor binding protein 1	Nucleus	kinase
O35375-2	NRP2	neuropilin 2	Plasma Membrane	kinase
P46460	NSF	N-ethylmaleimide sensitive factor, vesicle fusing ATPase	Cytoplasm	transporter
Q9CZ44	NSFL1C	NSFL1 cofactor	Cytoplasm	other
Q9JM14	NT5C	5', 3'-nucleotidase, cytosolic	Cytoplasm	phosphatase

O09118	NTN1	netrin 1	Extracellular Space	other
A0A0G2JGQ4	NUB1	negative regulator of ubiquitin like proteins 1	Nucleus	other
O35685	NUDC	nuclear distribution C, dynein complex regulator	Cytoplasm	other
E9Q7G0	NUMA1	nuclear mitotic apparatus protein 1	Nucleus	other
Q99P88	NUP155	nucleoporin 155	Nucleus	transporter
B9EJ54	NUP205	nucleoporin 205	Nucleus	other
Q8BJ71	NUP93	nucleoporin 93	Nucleus	other
P61971	NUTF2	nuclear transport factor 2	Nucleus	transporter
P11928	OAS1	2'-5'-oligoadenylate synthetase 1	Cytoplasm	enzyme
Q8VI94	OASL	2'-5'-oligoadenylate synthetase like	Cytoplasm	enzyme
Q60597	OGDH	oxoglutarate dehydrogenase	Cytoplasm	enzyme
Q8CGY8	OGT	O-linked N-acetylglucosamine (GlcNAc) transferase	Cytoplasm	enzyme
Q9CZ30	OLA1	Obg like ATPase 1	Cytoplasm	enzyme
Q5FWX7	OSBPL9	oxysterol binding protein like 9	Cytoplasm	transporter
Q7TQI3	Otub1	OTU domain, ubiquitin aldehyde binding 1	Cytoplasm	enzyme
A0A0R4J260	OTUD4	OTU deubiquitinase 4	Other	peptidase
Q9Z1M0	P2RX7	purinergic receptor P2X 7	Plasma Membrane	ion channel
Q60715	P4HA1	prolyl 4-hydroxylase subunit alpha 1	Cytoplasm	enzyme
P09103	P4HB	prolyl 4-hydroxylase subunit beta	Cytoplasm	enzyme
Q3TGU7	PA2G4	proliferation-associated 2G4	Nucleus	transcription regulator
P29341	PABPC1	poly(A) binding protein cytoplasmic 1	Cytoplasm	translation regulator
A3KFU5	PABPC4	poly(A) binding protein cytoplasmic 4	Cytoplasm	translation regulator
Q8K212	PACS1	phosphofurin acidic cluster sorting protein 1	Cytoplasm	other
Q9WVE8	PACSIN2	protein kinase C and casein kinase substrate in neurons 2	Cytoplasm	transporter
Q99JB8	PACSIN3	protein kinase C and casein kinase substrate in neurons 3	Cytoplasm	other
P63005	PAFAH1B1	platelet activating factor acetylhydrolase 1b regulatory subunit 1	Cytoplasm	enzyme
Q61206	PAFAH1B2	platelet activating factor acetylhydrolase 1b catalytic subunit 2	Cytoplasm	enzyme
Q61205	PAFAH1B3	platelet activating factor acetylhydrolase 1b catalytic subunit 3	Cytoplasm	enzyme
P16331	PAH	phenylalanine hydroxylase	Cytoplasm	enzyme
Q9DCL9	PAICS	phosphoribosylaminoimidazole carboxylase and phosphoribosylaminoimidazolesuccinocarboxamide synthase	Cytoplasm	enzyme
Q8CIN4	PAK2	p21 (RAC1) activated kinase 2	Cytoplasm	kinase
Q9Z0P4	PALM	paralemmin	Plasma Membrane	other
Q60967	PAPSS1	3'-phosphoadenosine 5'-phosphosulfate synthase 1	Cytoplasm	enzyme
Q99LX0	PARK7	Parkinsonism associated deglycase	Nucleus	enzyme
Q8BZ20	PARP12	poly(ADP-ribose) polymerase family member 12	Nucleus	other

E9PYK3	PARP4	poly(ADP-ribose) polymerase family member 4	Cytoplasm	enzyme
Q9EPC1	PARVA	parvin alpha	Cytoplasm	other
Q9ES46	PARVB	parvin beta	Cytoplasm	other
P60335	PCBP1	poly(rC) binding protein 1	Nucleus	translation regulator
Q61990	PCBP2	poly(rC) binding protein 2	Nucleus	other
E9PXF0	PCDH17	protocadherin 17	Plasma Membrane	other
Q8VHR0	PCDH18	protocadherin 18	Extracellular Space	other
Q91XX1	PCDHGC3	protocadherin gamma subfamily C, 3	Plasma Membrane	other
Q9R0L6	PCM1	pericentriolar material 1	Cytoplasm	other
P17918	PCNA	proliferating cell nuclear antigen	Nucleus	enzyme
Q61398	PCOLCE	procollagen C-endopeptidase enhancer	Extracellular Space	other
Q8C7K6	PCYOX1L	prenylcysteine oxidase 1 like	Other	other
Q8VE70	PDCD10	programmed cell death 10	Cytoplasm	other
Q6NS46	PDCD11	programmed cell death 11	Nucleus	other
P56812	PDCD5	programmed cell death 5	Nucleus	other
P12815	PDCD6	programmed cell death 6	Cytoplasm	other
Q9WU78	PDCD6IP	programmed cell death 6 interacting protein	Cytoplasm	other
P26618	PDGFRA	platelet derived growth factor receptor alpha	Plasma Membrane	kinase
E9QPE2	PDGFRB	platelet derived growth factor receptor beta	Plasma Membrane	kinase
P27773	PDIA3	protein disulfide isomerase family A member 3	Cytoplasm	peptidase
A0A0R4J0Z1	PDIA4	protein disulfide isomerase family A member 4	Cytoplasm	enzyme
Q922R8	PDIA6	protein disulfide isomerase family A member 6	Cytoplasm	enzyme
Q8CI51	PDLIM5	PDZ and LIM domain 5	Cytoplasm	other
Q3TJD7	PDLIM7	PDZ and LIM domain 7	Cytoplasm	other
E9QPI5	PDS5A	PDS5 cohesin associated factor A	Nucleus	other
F8WHU5	PDS5B	PDS5 cohesin associated factor B	Nucleus	other
Q99K01	PDXDC1	pyridoxal dependent decarboxylase domain containing 1	Cytoplasm	other
P70296	PEBP1	phosphatidylethanolamine binding protein 1	Cytoplasm	other
Q8BFY6	PEF1	penta-EF-hand domain containing 1	Cytoplasm	other
Q9DBD5	PELP1	proline, glutamate and leucine rich protein 1	Nucleus	other
Q11136	PEPD	peptidase D	Cytoplasm	peptidase
Q5SQ20	PES1	pescadillo ribosomal biogenesis factor 1	Nucleus	other
Q5SUR0	PFAS	phosphoribosylformylglycinamidine synthase	Cytoplasm	enzyme
G3UYF9	PFDN6	prefoldin subunit 6	Cytoplasm	other
P12382	PFKL	phosphofructokinase, liver type	Cytoplasm	kinase
Q8C605	PFKP	phosphofructokinase, platelet	Cytoplasm	kinase
P62962	PFN1	profilin 1	Cytoplasm	other
Q9DBJ1	PGAM1	phosphoglycerate mutase 1	Cytoplasm	phosphatase
Q9DCD0	PGD	phosphogluconate dehydrogenase	Cytoplasm	enzyme

P09411	PGK1	phosphoglycerate kinase 1	Cytoplasm	kinase
Q9CQ60	PGLS	6-phosphogluconolactonase	Cytoplasm	enzyme
Q9D0F9	PGM1	phosphoglucomutase 1	Cytoplasm	enzyme
O55022	PGRMC1	progesterone receptor membrane component 1	Plasma Membrane	transmembrane receptor
Q8BHF7	PGS1	phosphatidylglycerophosphate synthase 1	Cytoplasm	enzyme
O35129	PHB2	prohibitin 2	Cytoplasm	transcription regulator
Q9QWH1	PHC2	polyhomeotic homolog 2	Nucleus	other
Q61753	PHGDH	phosphoglycerate dehydrogenase	Cytoplasm	enzyme
Q6PE66	PHKA2	phosphorylase kinase regulatory subunit alpha 2	Cytoplasm	kinase
Q9WV95	PHLDA3	pleckstrin homology like domain family A member 3	Plasma Membrane	other
E9PWB1	PHLDB1	pleckstrin homology like domain family B member 1	Cytoplasm	other
Q9DAK9	PHPT1	phosphohistidine phosphatase 1	Cytoplasm	phosphatase
Q2TBE6	PI4K2A	phosphatidylinositol 4-kinase type 2 alpha	Cytoplasm	kinase
E9Q3L2	PI4KA	phosphatidylinositol 4-kinase alpha	Cytoplasm	kinase
Q7M6Y3-2	PICALM	phosphatidylinositol binding clathrin assembly protein	Cytoplasm	other
E2JF22	PIEZO1	piezo type mechanosensitive ion channel component 1	Cytoplasm	ion channel
Q9JHG7	PIK3CG	phosphatidylinositol-4,5-bisphosphate 3-kinase catalytic subunit gamma	Cytoplasm	kinase
O70172	PIP4K2A	phosphatidylinositol-5-phosphate 4-kinase type 2 alpha	Cytoplasm	kinase
Q80XI4	PIP4K2B	phosphatidylinositol-5-phosphate 4-kinase type 2 beta	Cytoplasm	kinase
F8WHW3	PIP4P1	phosphatidylinositol-4,5-bisphosphate 4-phosphatase 1	Cytoplasm	phosphatase
Q9CZX7	PIP4P2	phosphatidylinositol-4,5-bisphosphate 4-phosphatase 2	Cytoplasm	phosphatase
D3YUY3	PIP5K1A	phosphatidylinositol-4-phosphate 5-kinase type 1 alpha	Cytoplasm	kinase
Q8JZZ5	PITPNB	phosphatidylinositol transfer protein beta	Cytoplasm	transporter
P52480-2	PKM	pyruvate kinase M1/2	Cytoplasm	kinase
P52480	PKM	pyruvate kinase M1/2	Cytoplasm	kinase
Q9ESG9	PKMYT1	protein kinase, membrane associated tyrosine/threonine 1	Cytoplasm	kinase
G3UZM9	PKN2	protein kinase N2	Cytoplasm	kinase
A2AS45	PKP4	plakophilin 4	Plasma Membrane	other
P47713	PLA2G4A	phospholipase A2 group IVA	Cytoplasm	enzyme
P51432	PLCB3	phospholipase C beta 3	Cytoplasm	enzyme
Q8K2J0	PLCD3	phospholipase C delta 3	Cytoplasm	enzyme
Q8CIH5	PLCG2	phospholipase C gamma 2	Cytoplasm	enzyme
Q9QXS1-2	PLEC	plectin	Cytoplasm	other
Q8CAG6	PLEK	pleckstrin	Cytoplasm	other
Q9QZC7-2	PLEKHB2	pleckstrin homology domain containing B2	Other	other
Q9DBG5	PLIN3	perilipin 3	Cytoplasm	other
Q07832	PLK1	polo like kinase 1	Nucleus	kinase
Q9R0E1	PLOD3	procollagen-lysine,2-oxoglutarate 5-dioxygenase 3	Cytoplasm	enzyme

Q9R1Q7	PLP2	proteolipid protein 2	Cytoplasm	transporter
G3XA61	PLPP2	phospholipid phosphatase 2	Plasma Membrane	phosphatase
A0A1C7CYV0	PLS3	plastin 3	Cytoplasm	other
Q9JJ00	PLSCR1	phospholipid scramblase 1	Plasma Membrane	enzyme
Q9DCW2	Plscr2	phospholipid scramblase 2	Cytoplasm	other
Q9JIZ9	PLSCR3	phospholipid scramblase 3	Plasma Membrane	enzyme
A2A5K2	PLTP	phospholipid transfer protein	Extracellular Space	enzyme
P70206	PLXNA1	plexin A1	Plasma Membrane	transmembrane receptor
P70207	PLXNA2	plexin A2	Plasma Membrane	transmembrane receptor
B2RXS4	PLXNB2	plexin B2	Plasma Membrane	transmembrane receptor
Q60953	PML	promyelocytic leukemia	Nucleus	transcription regulator
A2AJT5	PNISR	PNN interacting serine and arginine rich protein	Nucleus	other
Q543K9	PNP	purine nucleoside phosphorylase	Nucleus	enzyme
Q923G2	POLR2H	RNA polymerase II subunit H	Nucleus	enzyme
P37040	POR	cytochrome p450 oxidoreductase	Cytoplasm	enzyme
Q9D819	PPA1	pyrophosphatase (inorganic) 1	Cytoplasm	enzyme
B2RXW8	PPFIA1	PTPRF interacting protein alpha 1	Plasma Membrane	phosphatase
P17742	PPIA	peptidylprolyl isomerase A	Cytoplasm	enzyme
P24369	PPIB	peptidylprolyl isomerase B	Cytoplasm	enzyme
P30412	PPIC	peptidylprolyl isomerase C	Cytoplasm	enzyme
Q9CR16	PPID	peptidylprolyl isomerase D	Cytoplasm	enzyme
Q9CXG3	PPIL4	peptidylprolyl isomerase like 4	Nucleus	enzyme
P62137	PPP1CA	protein phosphatase 1 catalytic subunit alpha	Cytoplasm	phosphatase
P62141	PPP1CB	protein phosphatase 1 catalytic subunit beta	Cytoplasm	phosphatase
P63087	Ppp1cc	protein phosphatase 1, catalytic subunit, gamma isoform	Cytoplasm	phosphatase
P63330	PPP2CA	protein phosphatase 2 catalytic subunit alpha	Cytoplasm	phosphatase
Q76MZ3	PPP2R1A	protein phosphatase 2 scaffold subunit Aalpha	Cytoplasm	phosphatase
Q6P1F6	PPP2R2A	protein phosphatase 2 regulatory subunit Balpha	Cytoplasm	phosphatase
Q91V89	PPP2R5D	protein phosphatase 2 regulatory subunit B'delta	Nucleus	phosphatase
P63328-2	PPP3CA	protein phosphatase 3 catalytic subunit alpha	Cytoplasm	phosphatase
E9Q481	PPP4R3A	protein phosphatase 4 regulatory subunit 3A	Plasma Membrane	other
Q60676	PPP5C	protein phosphatase 5 catalytic subunit	Nucleus	phosphatase
Q9CQR6	PPP6C	protein phosphatase 6 catalytic subunit	Nucleus	phosphatase
G5E8R4	PPP6R3	protein phosphatase 6 regulatory subunit 3	Cytoplasm	other
G3UW86	PRC1	protein regulator of cytokinesis 1	Nucleus	other
P35700	PRDX1	peroxiredoxin 1	Cytoplasm	enzyme
Q61171	PRDX2	peroxiredoxin 2	Cytoplasm	enzyme
O08807	PRDX4	peroxiredoxin 4	Cytoplasm	enzyme
P99029-2	PRDX5	peroxiredoxin 5	Cytoplasm	enzyme

O08709	PRDX6	peroxiredoxin 6	Cytoplasm	enzyme
Q9QUR6	PREP	prolyl endopeptidase	Cytoplasm	peptidase
Q5EG47	PRKAA1	protein kinase AMP-activated catalytic subunit alpha 1	Cytoplasm	kinase
P05132	PRKACA	protein kinase cAMP-activated catalytic subunit alpha	Cytoplasm	kinase
O54950	PRKAG1	protein kinase AMP-activated non-catalytic subunit gamma 1	Nucleus	kinase
Q9DBC7	PRKAR1A	protein kinase cAMP-dependent type I regulatory subunit alpha	Cytoplasm	kinase
P31324	PRKAR2B	protein kinase cAMP-dependent type II regulatory subunit beta	Cytoplasm	kinase
P68404-2	PRKCB	protein kinase C beta	Cytoplasm	kinase
Q8BZ03	PRKD2	protein kinase D2	Cytoplasm	kinase
Q9JIF0-2	PRMT1	protein arginine methyltransferase 1	Nucleus	enzyme
Q8CIG8	PRMT5	protein arginine methyltransferase 5	Cytoplasm	enzyme
Q99KP6	PRPF19	pre-mRNA processing factor 19	Nucleus	enzyme
Q9R1C7	PRPF40A	pre-mRNA processing factor 40 homolog A	Nucleus	other
Q91YR7	PRPF6	pre-mRNA processing factor 6	Nucleus	transcription regulator
Q99PV0	PRPF8	pre-mRNA processing factor 8	Nucleus	other
Q8C5R8	PRPS1L1	phosphoribosyl pyrophosphate synthetase 1-like 1	Other	kinase
G3UXL2	Prps1l3	phosphoribosyl pyrophosphate synthetase 1-like 3	Other	kinase
B1AT82	PRPSAP1	phosphoribosyl pyrophosphate synthetase associated protein 1	Extracellular Space	other
Q7TSC1	PRRC2A	proline rich coiled-coil 2A	Cytoplasm	other
S4R2J9	PRRC2C	proline rich coiled-coil 2C	Cytoplasm	other
Q792Z1	PRSS1	protease, serine 1	Cytoplasm	peptidase
Q9D6X6	PRSS23	protease, serine 23	Extracellular Space	peptidase
E9PZ00	PSAP	prosaposin	Extracellular Space	enzyme
Q99K85	PSAT1	phosphoserine aminotransferase 1	Cytoplasm	enzyme
P49769	PSEN1	presenilin 1	Plasma Membrane	peptidase
Q9R1P4	PSMA1	proteasome subunit alpha 1	Cytoplasm	peptidase
P49722	PSMA2	proteasome subunit alpha 2	Cytoplasm	peptidase
O70435	PSMA3	proteasome subunit alpha 3	Cytoplasm	peptidase
Q9R1P0	PSMA4	proteasome subunit alpha 4	Cytoplasm	peptidase
Q9Z2U1	PSMA5	proteasome subunit alpha 5	Cytoplasm	peptidase
Q9QUM9	PSMA6	proteasome subunit alpha 6	Cytoplasm	peptidase
Q9Z2U0	PSMA7	proteasome subunit alpha 7	Cytoplasm	peptidase
O09061	PSMB1	proteasome subunit beta 1	Cytoplasm	peptidase
O35955	PSMB10	proteasome subunit beta 10	Cytoplasm	peptidase
Q9R1P3	PSMB2	proteasome subunit beta 2	Cytoplasm	peptidase
Q9R1P1	PSMB3	proteasome subunit beta 3	Cytoplasm	peptidase

O55234	PSMB5	proteasome subunit beta 5	Cytoplasm	peptidase
Q60692	PSMB6	proteasome subunit beta 6	Nucleus	peptidase
P70195	PSMB7	proteasome subunit beta 7	Cytoplasm	peptidase
P62192	PSMC1	proteasome 26S subunit, ATPase 1	Nucleus	peptidase
P46471	PSMC2	proteasome 26S subunit, ATPase 2	Nucleus	peptidase
O88685	PSMC3	proteasome 26S subunit, ATPase 3	Nucleus	enzyme
P54775	PSMC4	proteasome 26S subunit, ATPase 4	Nucleus	peptidase
P62196	PSMC5	proteasome 26S subunit, ATPase 5	Nucleus	transcription regulator
P62334	PSMC6	proteasome 26S subunit, ATPase 6	Nucleus	peptidase
Q3TXS7	PSMD1	proteasome 26S subunit, non-ATPase 1	Cytoplasm	other
Q8BG32	PSMD11	proteasome 26S subunit, non-ATPase 11	Cytoplasm	other
Q9D8W5	PSMD12	proteasome 26S subunit, non-ATPase 12	Cytoplasm	other
Q9WVJ2	PSMD13	proteasome 26S subunit, non-ATPase 13	Cytoplasm	peptidase
O35593	PSMD14	proteasome 26S subunit, non-ATPase 14	Cytoplasm	peptidase
Q8VDM4	PSMD2	proteasome 26S subunit, non-ATPase 2	Cytoplasm	other
P14685	PSMD3	proteasome 26S subunit, non-ATPase 3	Cytoplasm	other
Q8BJY1	PSMD5	proteasome 26S subunit, non-ATPase 5	Other	other
Q99JI4	PSMD6	proteasome 26S subunit, non-ATPase 6	Cytoplasm	enzyme
P26516	PSMD7	proteasome 26S subunit, non-ATPase 7	Cytoplasm	other
Q9CPS5	PSMD8	proteasome 26S subunit, non-ATPase 8	Cytoplasm	other
G3UXZ5	PSME1	proteasome activator subunit 1	Cytoplasm	other
G3X9V0	PSME2	proteasome activator subunit 2	Cytoplasm	peptidase
Q8BGJ5	PTBP1	polypyrimidine tract binding protein 1	Nucleus	enzyme
Q9R0Q7	PTGES3	prostaglandin E synthase 3	Cytoplasm	enzyme
Q9WV91	PTGFRN	prostaglandin F2 receptor inhibitor	Plasma Membrane	other
P26350	Ptma (includes others)	prothymosin alpha	Nucleus	other
O70274	PTP4A2	protein tyrosine phosphatase type IVA, member 2	Cytoplasm	phosphatase
P58389	PTPA	protein phosphatase 2 phosphatase activator	Cytoplasm	phosphatase
P35235	PTPN11	protein tyrosine phosphatase, non-receptor type 11	Cytoplasm	phosphatase
Q6PB44-2	PTPN23	protein tyrosine phosphatase, non-receptor type 23	Cytoplasm	phosphatase
P29351	PTPN6	protein tyrosine phosphatase, non-receptor type 6	Cytoplasm	phosphatase
Q91V35	PTPRA	protein tyrosine phosphatase, receptor type A	Plasma Membrane	phosphatase
F8VQD7	PTPRG	protein tyrosine phosphatase, receptor type G	Plasma Membrane	phosphatase
A2AWF8	PTPRJ	protein tyrosine phosphatase, receptor type J	Plasma Membrane	phosphatase
B2RRF0	PTPRK	protein tyrosine phosphatase, receptor type K	Plasma Membrane	phosphatase
B0V2N1-4	PTPRS	protein tyrosine phosphatase, receptor type S	Plasma Membrane	phosphatase
Q8R143	PTTG1IP	PTTG1 interacting protein	Nucleus	other
Q80U78-2	PUM1	pumilio RNA binding family member 1	Cytoplasm	other
Q8K094	Pvr	poliovirus receptor	Plasma Membrane	other

Q3UQ28	PXDN	peroxidasin	Extracellular Space	enzyme
Q9DCC4	PYCR3	pyrroline-5-carboxylate reductase 3	Cytoplasm	enzyme
Q8CI94	PYGB	glycogen phosphorylase B	Cytoplasm	enzyme
Q9ET01	PYGL	glycogen phosphorylase L	Cytoplasm	enzyme
Q9WUB3	PYGM	glycogen phosphorylase, muscle associated	Cytoplasm	enzyme
Q61838	Pzp	PZP, alpha-2-macroglobulin like	Extracellular Space	other
Q8BML9	Qars	glutaminyl-tRNA synthetase	Cytoplasm	enzyme
P61027	RAB10	RAB10, member RAS oncogene family	Cytoplasm	enzyme
P46638	RAB11B	RAB11B, member RAS oncogene family	Cytoplasm	enzyme
A2CG35	RAB12	RAB12, member RAS oncogene family	Cytoplasm	enzyme
Q9DD03	RAB13	RAB13, member RAS oncogene family	Plasma Membrane	enzyme
Q91V41	RAB14	RAB14, member RAS oncogene family	Cytoplasm	enzyme
P35293	RAB18	RAB18, member RAS oncogene family	Cytoplasm	enzyme
P62821	RAB1A	RAB1A, member RAS oncogene family	Cytoplasm	enzyme
Q9D1G1	RAB1B	RAB1B, member RAS oncogene family	Cytoplasm	other
P35282	RAB21	RAB21, member RAS oncogene family	Cytoplasm	enzyme
P35285	RAB22A	RAB22A, member RAS oncogene family	Cytoplasm	enzyme
Q9D4I9	RAB23	RAB23, member RAS oncogene family	Cytoplasm	enzyme
Q99P58	RAB27B	RAB27B, member RAS oncogene family	Cytoplasm	enzyme
P53994	RAB2A	RAB2A, member RAS oncogene family	Cytoplasm	enzyme
Q3TXV4	RAB31	RAB31, member RAS oncogene family	Cytoplasm	enzyme
Q9CZE3	RAB32	RAB32, member RAS oncogene family	Cytoplasm	enzyme
A0A140LIX7	RAB34	RAB34, member RAS oncogene family	Cytoplasm	enzyme
Q0PD20	RAB34	RAB34, member RAS oncogene family	Cytoplasm	enzyme
Q6PHN9	RAB35	RAB35, member RAS oncogene family	Cytoplasm	enzyme
P56371	RAB4A	RAB4A, member RAS oncogene family	Cytoplasm	enzyme
Q9CQD1	RAB5A	RAB5A, member RAS oncogene family	Cytoplasm	enzyme
P61021	RAB5B	RAB5B, member RAS oncogene family	Cytoplasm	enzyme
P35278	RAB5C	RAB5C, member RAS oncogene family	Cytoplasm	enzyme
P35279	RAB6A	RAB6A, member RAS oncogene family	Cytoplasm	enzyme
P51150	RAB7A	RAB7A, member RAS oncogene family	Cytoplasm	enzyme
P55258	RAB8A	RAB8A, member RAS oncogene family	Plasma Membrane	enzyme
P61028	RAB8B	RAB8B, member RAS oncogene family	Cytoplasm	enzyme
Q9R0M6	RAB9A	RAB9A, member RAS oncogene family	Cytoplasm	enzyme
P63001	RAC1	Rac family small GTPase 1	Plasma Membrane	enzyme
Q05144	RAC2	Rac family small GTPase 2	Cytoplasm	enzyme
Q9WVM1	RACGAP1	Rac GTPase activating protein 1	Cytoplasm	transporter
P68040	RACK1	receptor for activated C kinase 1	Cytoplasm	enzyme
P54728	RAD23B	RAD23 homolog B, nucleotide excision repair protein	Nucleus	other

O08602	Raet1a	retinoic acid early transcript 1, alpha	Plasma Membrane	other
P63321	RALA	RAS like proto-oncogene A	Cytoplasm	enzyme
Q9JIW9	RALB	RAS like proto-oncogene B	Cytoplasm	enzyme
P62827	RAN	RAN, member RAS oncogene family	Nucleus	enzyme
P34022	RANBP1	RAN binding protein 1	Nucleus	other
P46061	RANGAP1	Ran GTPase activating protein 1	Nucleus	other
P62835	RAP1A	RAP1A, member of RAS oncogene family	Cytoplasm	enzyme
Q99JI6	RAP1B	RAP1B, member of RAS oncogene family	Cytoplasm	enzyme
E9Q912	RAP1GDS1	Rap1 GTPase-GDP dissociation stimulator 1	Cytoplasm	other
Q80ZJ1	RAP2A	RAP2A, member of RAS oncogene family	Plasma Membrane	enzyme
P61226	RAP2B	RAP2B, member of RAS oncogene family	Plasma Membrane	enzyme
Q8BU31	RAP2C	RAP2C, member of RAS oncogene family	Cytoplasm	enzyme
Q9D0I9	RARS	arginyl-tRNA synthetase	Cytoplasm	enzyme
E9PYG6	RASA1	RAS p21 protein activator 1	Cytoplasm	transporter
Q60790	RASA3	RAS p21 protein activator 3	Plasma Membrane	ion channel
Q9QUG9	RASGRP2	RAS guanyl releasing protein 2	Cytoplasm	other
Q60973	RBBP7	RB binding protein 7, chromatin remodeling factor	Nucleus	transcription regulator
O89086	RBM3	RNA binding motif protein 3	Cytoplasm	other
Q8VH51-2	RBM39	RNA binding motif protein 39	Nucleus	transcription regulator
Q8BK67	RCC2	regulator of chromosome condensation 2	Nucleus	other
P26043	RDX	radixin	Cytoplasm	other
Q9CQU3	RER1	retention in endoplasmic reticulum sorting receptor 1	Cytoplasm	other
A2ALB1	REXO4	REX4 homolog, 3'-5' exonuclease	Nucleus	transcription regulator
Q9WUK4	RFC2	replication factor C subunit 2	Nucleus	other
Q6A0D4	RFTN1	raftlin, lipid raft linker 1	Plasma Membrane	other
Q64374	RGN	regucalcin	Nucleus	enzyme
Q6PIX5	RHBDF1	rhomboid 5 homolog 1	Cytoplasm	other
Q921J2	RHEB	Ras homolog, mTORC1 binding	Cytoplasm	enzyme
Q9QUI0	RHOA	ras homolog family member A	Cytoplasm	enzyme
P62746	RHOB	ras homolog family member B	Cytoplasm	enzyme
Q62159	RHOC	ras homolog family member C	Plasma Membrane	enzyme
P97348	RHOD	ras homolog family member D	Cytoplasm	enzyme
P84096	RHOG	ras homolog family member G	Cytoplasm	enzyme
P61588	RND3	Rho family GTPase 3	Cytoplasm	enzyme
O54965	RNF13	ring finger protein 13	Cytoplasm	enzyme
Q3U2C5	RNF149	ring finger protein 149	Cytoplasm	enzyme
A0A171EBL2	RNF213	ring finger protein 213	Cytoplasm	enzyme
Q91VI7	RNH1	ribonuclease/angiogenin inhibitor 1	Cytoplasm	other
Q8VCT3	RNPEP	arginyl aminopeptidase	Cytoplasm	peptidase

Q9EPK2-3	RP2	RP2, ARL3 GTPase activating protein	Cytoplasm	enzyme
Q5SWN2	RPA1	replication protein A1	Nucleus	other
Q6ZWV3	RPL10	ribosomal protein L10	Cytoplasm	translation regulator
Q5XJF6	RPL10A	ribosomal protein L10a	Nucleus	other
Q9CXW4	RPL11	ribosomal protein L11	Cytoplasm	other
P35979	RPL12	ribosomal protein L12	Nucleus	other
P47963	RPL13	ribosomal protein L13	Nucleus	other
P19253	RPL13A	ribosomal protein L13a	Cytoplasm	other
Q9CR57	RPL14	ribosomal protein L14	Cytoplasm	other
Q6ZWZ7	RPL17	ribosomal protein L17	Cytoplasm	other
P35980	RPL18	ribosomal protein L18	Cytoplasm	other
P62717	RPL18A	ribosomal protein L18a	Cytoplasm	other
A2A547	RPL19	ribosomal protein L19	Cytoplasm	other
Q9CQM8	RPL21	ribosomal protein L21	Cytoplasm	other
P67984	RPL22	ribosomal protein L22	Nucleus	other
P62830	RPL23	ribosomal protein L23	Cytoplasm	other
A0A140T8M7	Rpl23a-ps3	ribosomal protein L23A, pseudogene 3	Other	other
Q8BP67	RPL24	ribosomal protein L24	Cytoplasm	other
B1ARA3	RPL26	ribosomal protein L26	Cytoplasm	other
P61358	RPL27	ribosomal protein L27	Cytoplasm	other
P14115	RPL27A	ribosomal protein L27a	Cytoplasm	other
P41105	RPL28	ribosomal protein L28	Cytoplasm	other
P27659	RPL3	ribosomal protein L3	Nucleus	other
P62889	RPL30	ribosomal protein L30	Cytoplasm	other
P62900	RPL31	ribosomal protein L31	Cytoplasm	other
P62911	Rpl32	ribosomal protein L32	Cytoplasm	other
Q9D1R9	Rpl34 (includes others)	ribosomal protein L34	Cytoplasm	other
Q6ZWV7	RPL35	ribosomal protein L35	Cytoplasm	other
O55142	RPL35A	ribosomal protein L35a	Cytoplasm	other
Q6ZWZ4	Rpl36	ribosomal protein L36	Nucleus	other
P61514	RPL37A	ribosomal protein L37a	Cytoplasm	other
Q9JJI8	RPL38	ribosomal protein L38	Cytoplasm	other
Q9D8E6	RPL4	ribosomal protein L4	Cytoplasm	enzyme
P47962	RPL5	ribosomal protein L5	Cytoplasm	other
P47911	RPL6	ribosomal protein L6	Nucleus	other
P14148	RPL7	ribosomal protein L7	Nucleus	transcription regulator
P12970	RPL7A	ribosomal protein L7a	Cytoplasm	other
P62918	RPL8	ribosomal protein L8	Cytoplasm	other
P51410	RPL9	ribosomal protein L9	Nucleus	other

P14869	RPLP0	ribosomal protein lateral stalk subunit P0	Cytoplasm	other
P47955	Rplp1 (includes others)	ribosomal protein, large, P1	Nucleus	other
P99027	RPLP2	ribosomal protein lateral stalk subunit P2	Cytoplasm	other
Q91YQ5	RPN1	ribophorin I	Cytoplasm	enzyme
Q9DBG6	RPN2	ribophorin II	Cytoplasm	enzyme
P63325	RPS10	ribosomal protein S10	Cytoplasm	other
P62281	RPS11	ribosomal protein S11	Cytoplasm	other
Q6ZWZ6	RPS12	ribosomal protein S12	Cytoplasm	other
P62301	RPS13	ribosomal protein S13	Cytoplasm	other
P62264	RPS14	ribosomal protein S14	Cytoplasm	translation regulator
P62843	RPS15	ribosomal protein S15	Cytoplasm	other
P62245	RPS15A	ribosomal protein S15a	Cytoplasm	other
P14131	RPS16	ribosomal protein S16	Cytoplasm	other
P63276	RPS17	ribosomal protein S17	Cytoplasm	other
D3YUT3	RPS19	ribosomal protein S19	Cytoplasm	other
P25444	RPS2	ribosomal protein S2	Cytoplasm	other
P60867	RPS20	ribosomal protein S20	Cytoplasm	other
P62267	RPS23	ribosomal protein S23	Cytoplasm	translation regulator
P62849-2	RPS24	ribosomal protein S24	Cytoplasm	other
A0A1L1SQA8	RPS25	ribosomal protein S25	Cytoplasm	other
P62855	RPS26	ribosomal protein S26	Cytoplasm	other
A0A0G2JDW7	Rps27/Rps27rt	ribosomal protein S27	Other	other
P62983	RPS27A	ribosomal protein S27a	Cytoplasm	other
G3UYV7	RPS28	ribosomal protein S28	Cytoplasm	other
P62274	RPS29	ribosomal protein S29	Cytoplasm	other
P62908	RPS3	ribosomal protein S3	Cytoplasm	enzyme
P97351	Rps3a1	ribosomal protein S3A1	Cytoplasm	other
P62702	RPS4Y1	ribosomal protein S4, Y-linked 1	Cytoplasm	other
D3YYM6	RPS5	ribosomal protein S5	Cytoplasm	other
P62754	RPS6	ribosomal protein S6	Cytoplasm	other
P18654	RPS6KA3	ribosomal protein S6 kinase A3	Cytoplasm	kinase
P62082	RPS7	ribosomal protein S7	Cytoplasm	other
P62242	RPS8	ribosomal protein S8	Cytoplasm	other
Q6ZWN5	RPS9	ribosomal protein S9	Cytoplasm	translation regulator
P14206	RPSA	ribosomal protein SA	Cytoplasm	translation regulator
Q80X95	RRAGA	Ras related GTP binding A	Cytoplasm	enzyme
Q99K70	RRAGC	Ras related GTP binding C	Cytoplasm	enzyme
P10833	RRAS	RAS related	Cytoplasm	enzyme
P62071	RRAS2	RAS related 2	Plasma Membrane	enzyme

P07742	RRM1	ribonucleotide reductase catalytic subunit M1	Nucleus	enzyme
P11157	RRM2	ribonucleotide reductase regulatory subunit M2	Nucleus	enzyme
Q9D031	RSU1	Ras suppressor protein 1	Cytoplasm	other
Q99LF4	RTCB	RNA 2',3'-cyclic phosphate and 5'-OH ligase	Cytoplasm	enzyme
Q9ES97-3	RTN3	reticulon 3	Cytoplasm	other
Q99P72	RTN4	reticulon 4	Cytoplasm	other
Q9CQE8	RTRAF	RNA transcription, translation and transport factor	Nucleus	other
P60122	RUVBL1	RuvB like AAA ATPase 1	Nucleus	transcription regulator
Q9WTM5	RUVBL2	RuvB like AAA ATPase 2	Nucleus	transcription regulator
P08207	S100A10	S100 calcium binding protein A10	Cytoplasm	other
P50543	S100a11	S100 calcium binding protein A11	Cytoplasm	other
A0A0G2JGD2	S100A4	S100 calcium binding protein A4	Cytoplasm	other
P14069	S100A6	S100 calcium binding protein A6	Cytoplasm	transporter
Q99JZ4	SAR1A	secretion associated Ras related GTPase 1A	Cytoplasm	enzyme
Q9CQC9	SAR1B	secretion associated Ras related GTPase 1B	Cytoplasm	enzyme
Q6PDS3-2	SARM1	sterile alpha and TIR motif containing 1	Plasma Membrane	transmembrane receptor
P26638	SARS	seryl-tRNA synthetase	Cytoplasm	enzyme
P70122	SBDS	SBDS, ribosome maturation factor	Nucleus	other
Q9ERN0	SCAMP2	secretory carrier membrane protein 2	Cytoplasm	transporter
E9Q855	SCAMP3	secretory carrier membrane protein 3	Cytoplasm	transporter
Q61009	SCARB1	scavenger receptor class B member 1	Plasma Membrane	transporter
O35114	SCARB2	scavenger receptor class B member 2	Plasma Membrane	other
Q80U72	SCRIB	scribbled planar cell polarity protein	Cytoplasm	other
P18828-2	SDC1	syndecan 1	Plasma Membrane	enzyme
O35988	SDC4	syndecan 4	Plasma Membrane	other
O08992	SDCBP	syndecan binding protein	Plasma Membrane	enzyme
Q8K2B3	SDHA	succinate dehydrogenase complex flavoprotein subunit A	Cytoplasm	enzyme
Q9CQA3	SDHB	succinate dehydrogenase complex iron sulfur subunit B	Cytoplasm	enzyme
Q9D1M0	SEC13	SEC13 homolog, nuclear pore and COPII coat complex component	Cytoplasm	transporter
O08547	SEC22B	SEC22 homolog B, vesicle trafficking protein (gene/pseudogene)	Cytoplasm	other
Q9D662	SEC23B	Sec23 homolog B, coat complex II component	Extracellular Space	transporter
G3X972	SEC24C	SEC24 homolog C, COPII coat complex component	Cytoplasm	transporter
Q6NXL1	SEC24D	SEC24 homolog D, COPII coat complex component	Cytoplasm	transporter
Q3UPL0	SEC31A	SEC31 homolog A, COPII coat complex component	Cytoplasm	other
P61620	SEC61A1	Sec61 translocon alpha 1 subunit	Cytoplasm	transporter
O08665	SEMA3A	semaphorin 3A	Extracellular Space	other
A0A0J9YTY0	SEPT11	septin 11	Nucleus	other

P42208	SEPT2	septin 2	Cytoplasm	enzyme
E9Q1G8	SEPT7	septin 7	Cytoplasm	other
Q80UG5-3	SEPT9	septin 9	Cytoplasm	enzyme
Q9QZI8	SERINC1	serine incorporator 1	Plasma Membrane	transporter
Q9QZI9	SERINC3	serine incorporator 3	Cytoplasm	transporter
Q8BHJ6	SERINC5	serine incorporator 5	Plasma Membrane	transporter
Q60854	SERPINB6	serpin family B member 6	Cytoplasm	other
Q9DAV6	Serpinb9b	serine (or cysteine) peptidase inhibitor, clade B, member 9b	Cytoplasm	other
P32261	SERPINC1	serpin family C member 1	Extracellular Space	enzyme
P19324	SERPINH1	serpin family H member 1	Extracellular Space	other
D3YZC9	Sf1	splicing factor 1	Nucleus	other
Q921M3	SF3B3	splicing factor 3b subunit 3	Nucleus	other
Q8VIJ6	SFPQ	splicing factor proline and glutamine rich	Nucleus	other
A2ACH6	SGCD	sarcoglycan delta	Cytoplasm	other
Q9D4B1	SGMS2	sphingomyelin synthase 2	Plasma Membrane	enzyme
Q91VW3	SH3BGRL3	SH3 domain binding glutamate rich protein like 3	Nucleus	other
Q921I6	SH3BP4	SH3 domain binding protein 4	Cytoplasm	other
Q62419	SH3GL1	SH3 domain containing GRB2 like 1, endophilin A2	Cytoplasm	other
A0A0G2JEC4	SH3GLB1	SH3 domain containing GRB2 like, endophilin B1	Cytoplasm	enzyme
P98083-2	SHC1	SHC adaptor protein 1	Cytoplasm	other
Q9Z179	SHCBP1	SHC binding and spindle associated 1	Other	other
Q8CA71	SHISA4	shisa family member 4	Other	other
P50431	SHMT1	serine hydroxymethyltransferase 1	Cytoplasm	enzyme
Q3TFD0	SHMT2	serine hydroxymethyltransferase 2	Cytoplasm	enzyme
Q6NZR5	SKIV2L	Ski2 like RNA helicase	Nucleus	enzyme
Q9WTX5	SKP1	S-phase kinase associated protein 1	Nucleus	transcription regulator
E9QM38	SLC12A2	solute carrier family 12 member 2	Plasma Membrane	transporter
F8WIJ0	SLC12A4	solute carrier family 12 member 4	Plasma Membrane	transporter
Q9WVL3	SLC12A7	solute carrier family 12 member 7	Plasma Membrane	transporter
P53986	SLC16A1	solute carrier family 16 member 1	Plasma Membrane	transporter
Q9EQN9	SLC19A2	solute carrier family 19 member 2	Plasma Membrane	transporter
O35874	SLC1A4	solute carrier family 1 member 4	Plasma Membrane	transporter
Q9ESU7	SLC1A5	solute carrier family 1 member 5	Plasma Membrane	transporter
Q61609	SLC20A1	solute carrier family 20 member 1	Plasma Membrane	transporter
Q80UP8	SLC20A2	solute carrier family 20 member 2	Plasma Membrane	transporter
Q9EPR4	SLC23A2	solute carrier family 23 member 2	Plasma Membrane	transporter
Q8BH59	SLC25A12	solute carrier family 25 member 12	Cytoplasm	transporter
Q8VEM8	SLC25A3	solute carrier family 25 member 3	Cytoplasm	transporter
P48962	SLC25A4	solute carrier family 25 member 4	Cytoplasm	transporter

P51881	SLC25A5	solute carrier family 25 member 5	Cytoplasm	transporter
Q9JIM1-2	SLC29A1	solute carrier family 29 member 1 (Augustine blood group)	Plasma Membrane	transporter
P17809	SLC2A1	solute carrier family 2 member 1	Plasma Membrane	transporter
P32037	SLC2A3	solute carrier family 2 member 3	Plasma Membrane	transporter
Q8K211	SLC31A1	solute carrier family 31 member 1	Plasma Membrane	transporter
J3QNE8	SLC38A10	solute carrier family 38 member 10	Cytoplasm	other
Q8CFE6	SLC38A2	solute carrier family 38 member 2	Plasma Membrane	transporter
Q6P5F6	SLC39A10	solute carrier family 39 member 10	Extracellular Space	transporter
D3Z6P5	SLC39A14	solute carrier family 39 member 14	Plasma Membrane	transporter
Q8C145	SLC39A6	solute carrier family 39 member 6	Plasma Membrane	transporter
P10852	SLC3A2	solute carrier family 3 member 2	Plasma Membrane	transporter
A2AMH5	SLC44A1	solute carrier family 44 member 1	Plasma Membrane	transporter
Q8BY89-2	SLC44A2	solute carrier family 44 member 2	Extracellular Space	transporter
Q9D8M3	SLC48A1	solute carrier family 48 member 1	Cytoplasm	transporter
F8VQC9	SLC4A7	solute carrier family 4 member 7	Plasma Membrane	transporter
Q9JKZ2	SLC5A3	solute carrier family 5 member 3	Plasma Membrane	transporter
Q5U4D8	SLC5A6	solute carrier family 5 member 6	Plasma Membrane	transporter
O35316	SLC6A6	solute carrier family 6 member 6	Plasma Membrane	transporter
E9Q151	SLC6A8	solute carrier family 6 member 8	Cytoplasm	transporter
Q09143	SLC7A1	solute carrier family 7 member 1	Plasma Membrane	transporter
Q9Z127	SLC7A5	solute carrier family 7 member 5	Plasma Membrane	transporter
Q8BGK6	SLC7A6	solute carrier family 7 member 6	Plasma Membrane	transporter
P70441	SLC9A3R1	SLC9A3 regulator 1	Plasma Membrane	other
O54988-2	SLK	STE20 like kinase	Nucleus	kinase
Q62432-2	SMAD2	SMAD family member 2	Nucleus	transcription regulator
Q91ZW3	SMARCA5	SWI/SNF related, matrix associated, actin dependent regulator of chromatin, subfamily a, member 5	Nucleus	transcription regulator
Q9CU62	SMC1A	structural maintenance of chromosomes 1A	Nucleus	transporter
Q8CG47	SMC4	structural maintenance of chromosomes 4	Nucleus	transporter
Q6P5D8	SMCHD1	structural maintenance of chromosomes flexible hinge domain containing 1	Nucleus	enzyme
P58242	SMPDL3B	sphingomyelin phosphodiesterase acid like 3B	Extracellular Space	enzyme
A2A5Z6-2	SMURF2	SMAD specific E3 ubiquitin protein ligase 2	Cytoplasm	enzyme
Q9D3L3	SNAP23	synaptosome associated protein 23	Plasma Membrane	transporter
Q78PY7	SND1	staphylococcal nuclease and tudor domain containing 1	Nucleus	enzyme
Q9CZ28	SNF8	SNF8, ESCRT-II complex subunit	Cytoplasm	enzyme
Q6P4T2	SNRNP200	small nuclear ribonucleoprotein U5 subunit 200	Nucleus	enzyme
Q62376	SNRNP70	small nuclear ribonucleoprotein U1 subunit 70	Nucleus	other
P27048	SNRPB	small nuclear ribonucleoprotein polypeptides B and B1	Nucleus	other

P62315	SNRPD1	small nuclear ribonucleoprotein D1 polypeptide	Nucleus	other
P62320	SNRPD3	small nuclear ribonucleoprotein D3 polypeptide	Nucleus	other
Q61235	SNTB2	syntrophin beta 2	Plasma Membrane	other
Q6ZWQ5	SNX12	sorting nexin 12	Cytoplasm	transporter
Q8BVL3	SNX17	sorting nexin 17	Cytoplasm	transporter
Q8C788	SNX18	sorting nexin 18	Cytoplasm	transporter
Q9CWK8	SNX2	sorting nexin 2	Cytoplasm	transporter
Q3UHD6-2	SNX27	sorting nexin family member 27	Cytoplasm	other
Q78ZM0	SNX3	sorting nexin 3	Cytoplasm	transporter
Q9D8U8	SNX5	sorting nexin 5	Cytoplasm	transporter
Q6P8X1	SNX6	sorting nexin 6	Cytoplasm	transporter
Q91VH2	SNX9	sorting nexin 9	Cytoplasm	transporter
A0A0A0MQ80	SPATA5	spermatogenesis associated 5	Cytoplasm	other
A0A0J9YUR2	SPECC1	sperm antigen with calponin homology and coiled-coil domains 1	Nucleus	other
Q8R1X6	Spg20	spastic paraplegia 20, spartin (Troyer syndrome) homolog (human)	Plasma Membrane	other
Q8K1I3	SPP2	secreted phosphoprotein 2	Extracellular Space	other
Q9JJF9	SPPL2A	signal peptide peptidase like 2A	Plasma Membrane	peptidase
Q91XH5	SPR	sepiapterin reductase	Cytoplasm	enzyme
P16546	SPTAN1	spectrin alpha, non-erythrocytic 1	Plasma Membrane	other
Q62261	SPTBN1	spectrin beta, non-erythrocytic 1	Plasma Membrane	other
Q64337-2	SQSTM1	sequestosome 1	Cytoplasm	transcription regulator
F8WI90	SRC	SRC proto-oncogene, non-receptor tyrosine kinase	Cytoplasm	kinase
Q91Z67	SRGAP2	SLIT-ROBO Rho GTPase activating protein 2	Cytoplasm	other
Q6P069-2	SRI	sorcin	Cytoplasm	transporter
Q64674	SRM	spermidine synthase	Cytoplasm	enzyme
Q8BMA6	SRP68	signal recognition particle 68	Nucleus	other
F8VQC1	SRP72	signal recognition particle 72	Nucleus	kinase
H7BX95	SRSF1	serine and arginine rich splicing factor 1	Nucleus	other
Q62093	SRSF2	serine and arginine rich splicing factor 2	Nucleus	transcription regulator
P84104-2	SRSF3	serine and arginine rich splicing factor 3	Nucleus	other
Q9D8S5	Srsf5	serine/arginine-rich splicing factor 5	Nucleus	other
Q3TWW8	SRSF6	serine and arginine rich splicing factor 6	Nucleus	other
Q8BL97-3	SRSF7	serine and arginine rich splicing factor 7	Nucleus	other
P32067	SSB	Sjogren syndrome antigen B	Nucleus	enzyme
A2AW05	SSRP1	structure specific recognition protein 1	Nucleus	other
P56873	SSSCA1	Sjogren syndrome/scleroderma autoantigen 1	Other	other
F8WJK8	ST13	ST13, Hsp70 interacting protein	Cytoplasm	other

O88811-2	STAM2	signal transducing adaptor molecule 2	Cytoplasm	other
Q9CQ26	STAMBP	STAM binding protein	Nucleus	enzyme
Q8C3V4	STAT1	signal transducer and activator of transcription 1	Nucleus	transcription regulator
P42227-2	STAT3	signal transducer and activator of transcription 3	Nucleus	transcription regulator
P52633	STAT6	signal transducer and activator of transcription 6	Nucleus	transcription regulator
Q9CWR7	STEAP1	STEAP family member 1	Plasma Membrane	transporter
Q8BWB6	STEAP2	STEAP2 metalloreductase	Plasma Membrane	transporter
Q8CI59	STEAP3	STEAP3 metalloreductase	Cytoplasm	transporter
Q60864	STIP1	stress induced phosphoprotein 1	Cytoplasm	other
O55098	STK10	serine/threonine kinase 10	Cytoplasm	kinase
Q99KH8	STK24	serine/threonine kinase 24	Cytoplasm	kinase
P54116	STOM	stomatin	Plasma Membrane	other
Q8CDJ8	STON1	stonin 1	Plasma Membrane	other
Q9Z1Z2	STRAP	serine/threonine kinase receptor associated protein	Plasma Membrane	other
P46978	STT3A	STT3A, catalytic subunit of the oligosaccharyltransferase complex	Plasma Membrane	enzyme
Q9WUD1	STUB1	STIP1 homology and U-box containing protein 1	Cytoplasm	enzyme
Q9ER00	STX12	syntaxin 12	Cytoplasm	other
Q8VDS8-3	STX18	syntaxin 18	Cytoplasm	transporter
Q3TJ55	STX2	syntaxin 2	Cytoplasm	transporter
P70452	STX4	syntaxin 4	Plasma Membrane	transporter
Q8BH40	STX7	syntaxin 7	Plasma Membrane	transporter
O08599	STXBP1	syntaxin binding protein 1	Cytoplasm	transporter
F8WGM5	STXBP2	syntaxin binding protein 2	Plasma Membrane	transporter
Q60770	STXBP3	syntaxin binding protein 3	Plasma Membrane	transporter
Q9WUM5	SUCLG1	succinate-CoA ligase alpha subunit	Cytoplasm	enzyme
H7BWX9	SUMO2	small ubiquitin-like modifier 2	Nucleus	enzyme
G3X956	SUPT16H	SPT16 homolog, facilitates chromatin remodeling subunit	Nucleus	transcription regulator
Q8C0M5	SUSD6	sushi domain containing 6	Other	other
F8WJD4	SYMPK	symplekin	Cytoplasm	other
Q7TMK9	SYNCRIP	synaptotagmin binding cytoplasmic RNA interacting protein	Nucleus	other
E9QP46	SYNE2	spectrin repeat containing nuclear envelope protein 2	Nucleus	other
H3BJY1	SYNGR2	synaptogyrin 2	Cytoplasm	other
D6RFU9	SYPL1	synaptophysin like 1	Plasma Membrane	transporter
Q9WVA4	TAGLN2	transgelin 2	Cytoplasm	other
A0A1B0GR11	TALDO1	transaldolase 1	Cytoplasm	enzyme
Q5F2E8	TAOK1	TAO kinase 1	Cytoplasm	kinase
Q921F2	TARDBP	TAR DNA binding protein	Nucleus	transcription regulator
Q9D0R2	TARS	threonyl-tRNA synthetase	Nucleus	enzyme

Q3UKC1	TAX1BP1	Tax1 binding protein 1	Cytoplasm	other
Q9DBG9	TAX1BP3	Tax1 binding protein 3	Cytoplasm	transcription regulator
Q9CXF4	TBC1D15	TBC1 domain family member 15	Cytoplasm	other
P11983	TCP1	t-complex 1	Cytoplasm	other
Q8K1H7	TCP11L2	t-complex 11 like 2	Other	other
Q3ULB1	TES	testin LIM domain protein	Plasma Membrane	other
Q3URQ0	TEX10	testis expressed 10	Nucleus	other
Q62351	TFRC	transferrin receptor	Plasma Membrane	transporter
E9Q1D5	TGFB1I1	transforming growth factor beta 1 induced transcript 1	Nucleus	transcription regulator
P82198	TGFBI	transforming growth factor beta induced	Extracellular Space	other
Q9D5H8	TGFBR1	transforming growth factor beta receptor 1	Plasma Membrane	kinase
Q62312-2	TGFBR2	transforming growth factor beta receptor 2	Plasma Membrane	kinase
P35441	THBS1	thrombospondin 1	Extracellular Space	other
Q9Z1T2	THBS4	thrombospondin 4	Extracellular Space	other
A0A0B4J1G6	TIGIT	T cell immunoreceptor with Ig and ITIM domains	Plasma Membrane	other
Q99JR5	TINAGL1	tubulointerstitial nephritis antigen like 1	Extracellular Space	transporter
Q9DCD5	TJAP1	tight junction associated protein 1	Plasma Membrane	other
B9EHJ3	TJP1	tight junction protein 1	Plasma Membrane	other
P04184	TK1	thymidine kinase 1	Cytoplasm	kinase
P40142	TKT	transketolase	Cytoplasm	enzyme
P26039	TLN1	talin 1	Plasma Membrane	other
P58021	TM9SF2	transmembrane 9 superfamily member 2	Plasma Membrane	transporter
Q9ET30	TM9SF3	transmembrane 9 superfamily member 3	Cytoplasm	transporter
Q8BH24	TM9SF4	transmembrane 9 superfamily member 4	Cytoplasm	transporter
Q9D1D4	TMED10	transmembrane p24 trafficking protein 10	Cytoplasm	transporter
E9Q7G1	TMED7	transmembrane p24 trafficking protein 7	Cytoplasm	transporter
Q99KF1	TMED9	transmembrane p24 trafficking protein 9	Cytoplasm	transporter
Q8VC04	TMEM106A	transmembrane protein 106A	Cytoplasm	other
Q80X71	TMEM106B	transmembrane protein 106B	Cytoplasm	other
Q8CFU0	Tmem198b	transmembrane protein 198b	Other	other
Q8VEK0	TMEM30A	transmembrane protein 30A	Cytoplasm	transporter
D3YVM2	TMEM59	transmembrane protein 59	Plasma Membrane	peptidase
Q91YT8	TMEM63A	transmembrane protein 63A	Cytoplasm	other
A2AQJ7	TMEM87A	transmembrane protein 87A	Cytoplasm	other
F6V084	TMX1	thioredoxin related transmembrane protein 1	Cytoplasm	enzyme
O70479	TNFAIP1	TNF alpha induced protein 1	Plasma Membrane	ion channel
Q9QZM4	TNFRSF10A	TNF receptor superfamily member 10a	Plasma Membrane	transmembrane receptor
Q9CR75	TNFRSF12A	TNF receptor superfamily member 12A	Plasma Membrane	transmembrane receptor
Q8BFY9-2	TNPO1	transportin 1	Nucleus	transporter

Q6P2B1	TNPO3	transportin 3	Cytoplasm	other
Q9QZ06	TOLLIP	toll interacting protein	Cytoplasm	other
Q3UDC3	TOM1	target of myb1 membrane trafficking protein	Cytoplasm	transporter
Q923U0	TOM1L1	target of myb1 like 1 membrane trafficking protein	Cytoplasm	other
Q04750	TOP1	DNA topoisomerase I	Nucleus	enzyme
Q01320	TOP2A	DNA topoisomerase II alpha	Nucleus	enzyme
Q9Z0L0	TPBG	trophoblast glycoprotein	Plasma Membrane	other
Q99MS8	TPGS1	tubulin polyglutamylase complex subunit 1	Cytoplasm	enzyme
P17751	TPI1	triosephosphate isomerase 1	Cytoplasm	enzyme
P21107-2	TPM3	tropomyosin 3	Cytoplasm	other
Q6IRU2	Tpm4	tropomyosin 4	Cytoplasm	other
Q64514-2	TPP2	tripeptidyl peptidase 2	Cytoplasm	peptidase
P63028	TPT1	tumor protein, translationally-controlled 1	Cytoplasm	other
Q61382	TRAF4	TNF receptor associated factor 4	Cytoplasm	other
Q9CQN1	TRAP1	TNF receptor associated protein 1	Cytoplasm	enzyme
O55013	TRAPPC3	trafficking protein particle complex 3	Cytoplasm	other
Q8BGX0-3	TRIM23	tripartite motif containing 23	Nucleus	enzyme
Q62318	TRIM28	tripartite motif containing 28	Nucleus	transcription regulator
Q8CH72	TRIM32	tripartite motif containing 32	Nucleus	transcription regulator
Q8C0E3-2	TRIM47	tripartite motif containing 47	Cytoplasm	other
Q8C0E3	TRIM47	tripartite motif containing 47	Cytoplasm	other
Q8CJ53-4	TRIP10	thyroid hormone receptor interactor 10	Cytoplasm	other
E9Q512	TRIP11	thyroid hormone receptor interactor 11	Cytoplasm	transcription regulator
Q9Z1Y4	TRIP6	thyroid hormone receptor interactor 6	Extracellular Space	cytokine
E9QKG3	TRMT11	tRNA methyltransferase 11 homolog	Other	enzyme
Q61187	TSG101	tumor susceptibility 101	Cytoplasm	transcription regulator
Q62348	TSN	translin	Nucleus	other
Q8QZY6	TSPAN14	tetraspanin 14	Plasma Membrane	other
F7BWT7	TSPAN15	tetraspanin 15	Plasma Membrane	other
A0A1L1SRJ4	TSPAN3	tetraspanin 3	Plasma Membrane	other
Q9CQ88	TSPAN31	tetraspanin 31	Plasma Membrane	other
Q9DCK3	TSPAN4	tetraspanin 4	Plasma Membrane	other
D3Z641	TSPAN5	tetraspanin 5	Plasma Membrane	other
Q99L96	TSPAN6	tetraspanin 6	Plasma Membrane	other
Q3UHG5	TSPAN7	tetraspanin 7	Plasma Membrane	other
D3YXN7	TSPAN9	tetraspanin 9	Plasma Membrane	other
P23591	TSTA3	tissue specific transplantation antigen P35B	Plasma Membrane	enzyme
Q3UDE2	TTLL12	tubulin tyrosine ligase like 12	Other	other
Q3TH73	TTYH2	tweety family member 2	Other	ion channel

Q6P5F7	TTYH3	tweety family member 3	Plasma Membrane	ion channel
P68369	TUBA1A	tubulin alpha 1a	Cytoplasm	other
P05213	TUBA1B	tubulin alpha 1b	Cytoplasm	other
P68368	TUBA4A	tubulin alpha 4a	Cytoplasm	other
P99024	TUBB	tubulin beta class I	Cytoplasm	other
Q9CWF2	TUBB2B	tubulin beta 2B class IIb	Cytoplasm	other
Q9D6F9	TUBB4A	tubulin beta 4A class IVa	Cytoplasm	other
P68372	TUBB4B	tubulin beta 4B class IVb	Cytoplasm	other
Q922F4	TUBB6	tubulin beta 6 class V	Cytoplasm	other
P83887	TUBG1	tubulin gamma 1	Cytoplasm	other
A0A1B0GR08	TUBGCP2	tubulin gamma complex associated protein 2	Cytoplasm	peptidase
Q8BFR5	TUFM	Tu translation elongation factor, mitochondrial	Cytoplasm	translation regulator
Q91YR1	TWF1	twinfilin actin binding protein 1	Cytoplasm	kinase
P10639	TXN	thioredoxin	Cytoplasm	enzyme
Q9CQM5	TXNDC17	thioredoxin domain containing 17	Cytoplasm	enzyme
Q8CDN6	TXNL1	thioredoxin like 1	Cytoplasm	enzyme
Q9JMH6-2	TXNRD1	thioredoxin reductase 1	Cytoplasm	enzyme
Q3TW96	UAP1L1	UDP-N-acetylglucosamine pyrophosphorylase 1 like 1	Other	other
Q02053	UBA1	ubiquitin like modifier activating enzyme 1	Cytoplasm	enzyme
D3Z061	UBA6	ubiquitin like modifier activating enzyme 6	Cytoplasm	enzyme
Q80X50	Ubap2l	ubiquitin-associated protein 2-like	Nucleus	other
P62838	UBE2D2	ubiquitin conjugating enzyme E2 D2	Cytoplasm	enzyme
A0A0G2JE32	UBE2D3	ubiquitin conjugating enzyme E2 D3	Cytoplasm	enzyme
P61087	UBE2K	ubiquitin conjugating enzyme E2 K	Cytoplasm	transcription regulator
P68037	UBE2L3	ubiquitin conjugating enzyme E2 L3	Nucleus	enzyme
P61082	UBE2M	ubiquitin conjugating enzyme E2 M	Cytoplasm	enzyme
P61089	UBE2N	ubiquitin conjugating enzyme E2 N	Cytoplasm	enzyme
Q6ZPJ3	UBE2O	ubiquitin conjugating enzyme E2 O	Nucleus	enzyme
Q9D2M8	UBE2V2	ubiquitin conjugating enzyme E2 V2	Cytoplasm	enzyme
Q9Z2M6	UBL3	ubiquitin like 3	Cytoplasm	other
A2AN08-3	UBR4	ubiquitin protein ligase E3 component n-recognin 4	Nucleus	enzyme
Q91WB7	UBTD1	ubiquitin domain containing 1	Other	other
A2AWT5	UBTF	upstream binding transcription factor, RNA polymerase I	Nucleus	transcription regulator
Q3U1V6	UEVLD	UEV and lactate/malate dehyrogenase domains	Cytoplasm	enzyme
O88693	UGCG	UDP-glucose ceramide glucosyltransferase	Cytoplasm	enzyme
O70475	UGDH	UDP-glucose 6-dehydrogenase	Nucleus	enzyme
Q6P5E4	UGGT1	UDP-glucose glycoprotein glucosyltransferase 1	Cytoplasm	enzyme
P13439	UMPS	uridine monophosphate synthetase	Cytoplasm	enzyme
B2RUP2-2	UNC13D	unc-13 homolog D	Cytoplasm	other

Q8K1S3-2	UNC5B	unc-5 netrin receptor B	Plasma Membrane	transmembrane receptor
Q9EPU0-2	UPF1	UPF1, RNA helicase and ATPase	Nucleus	enzyme
Q9CZ13	UQCRC1	ubiquinol-cytochrome c reductase core protein 1	Cytoplasm	enzyme
Q9DB77	UQCRC2	ubiquinol-cytochrome c reductase core protein 2	Cytoplasm	enzyme
Q3UEL5	UROC1	urocanate hydratase 1	Cytoplasm	enzyme
P70697	UROD	uroporphyrinogen decarboxylase	Cytoplasm	enzyme
Q9Z1Z0	USO1	USO1 vesicle transport factor	Cytoplasm	transporter
E9PYI8	USP14	ubiquitin specific peptidase 14	Cytoplasm	peptidase
Q8R5H1-5	USP15	ubiquitin specific peptidase 15	Cytoplasm	peptidase
A2ALR9	USP48	ubiquitin specific peptidase 48	Plasma Membrane	peptidase
Q3U4W8	USP5	ubiquitin specific peptidase 5	Cytoplasm	peptidase
A2AI52	USP8	ubiquitin specific peptidase 8	Cytoplasm	peptidase
Q4FE56	USP9X	ubiquitin specific peptidase 9, X-linked	Plasma Membrane	peptidase
E9Q6R7	UTRN	utrophin	Plasma Membrane	transmembrane receptor
A0A1D5RLY2	VAC14	Vac14, PIKFYVE complex component	Cytoplasm	other
P63024	VAMP3	vesicle associated membrane protein 3	Plasma Membrane	other
P70280	VAMP7	vesicle associated membrane protein 7	Cytoplasm	transporter
A0A0R4J0R1	VAMP8	vesicle associated membrane protein 8	Plasma Membrane	transporter
Q80Z96	VANGL1	VANGL planar cell polarity protein 1	Cytoplasm	other
Q9WV55	VAPA	VAMP associated protein A	Plasma Membrane	other
Q9Z1Q9	VARS	valyl-tRNA synthetase	Cytoplasm	enzyme
Q9CZT5	VASN	vasorin	Plasma Membrane	other
P70460	VASP	vasodilator stimulated phosphoprotein	Plasma Membrane	other
Q62465	VAT1	vesicle amine transport 1	Plasma Membrane	transporter
Q64727	VCL	vinculin	Plasma Membrane	enzyme
Q01853	VCP	valosin containing protein	Cytoplasm	enzyme
A0A0R4J0M9	VCPIP1	valosin containing protein interacting protein 1	Cytoplasm	peptidase
Q60932-2	VDAC1	voltage dependent anion channel 1	Cytoplasm	ion channel
Q60930	VDAC2	voltage dependent anion channel 2	Cytoplasm	ion channel
Q60931	VDAC3	voltage dependent anion channel 3	Cytoplasm	ion channel
P20152	VIM	vimentin	Cytoplasm	other
Q8BX70-3	VPS13C	vacuolar protein sorting 13 homolog C	Cytoplasm	other
Q9CQ80	VPS25	vacuolar protein sorting 25 homolog	Cytoplasm	other
Q9D1C8	VPS28	VPS28, ESCRT-I subunit	Cytoplasm	transporter
D3Z645	VPS29	VPS29, retromer complex component	Cytoplasm	transporter
Q9EQH3	VPS35	VPS35, retromer complex component	Cytoplasm	transporter
Q91XD6	VPS36	vacuolar protein sorting 36 homolog	Cytoplasm	other
Q8R0J7	VPS37B	VPS37B, ESCRT-I subunit	Cytoplasm	other
Q8R105	VPS37C	VPS37C, ESCRT-I subunit	Cytoplasm	other

Q8VEJ9	VPS4A	vacuolar protein sorting 4 homolog A	Cytoplasm	enzyme
P46467	VPS4B	vacuolar protein sorting 4 homolog B	Cytoplasm	transporter
Q8C754	VPS52	VPS52, GARP complex subunit	Cytoplasm	other
Q9CR26	VTA1	vesicle trafficking 1	Cytoplasm	other
Q99KC8	VWA5A	von Willebrand factor A domain containing 5A	Nucleus	other
P32921-2	WARS	tryptophanyl-tRNA synthetase	Cytoplasm	enzyme
Q8BH43	WASF2	WAS protein family member 2	Plasma Membrane	other
Q8VHI6	WASF3	WAS protein family member 3	Cytoplasm	other
Q6PGL7-2	WASHC2A/WASHC2C	WASH complex subunit 2A	Cytoplasm	other
Q91YD9	Wasl	Wiskott-Aldrich syndrome-like (human)	Cytoplasm	other
P97765	WBP2	WW domain binding protein 2	Cytoplasm	transcription regulator
O88342	WDR1	WD repeat domain 1	Extracellular Space	other
Q4VBE8	WDR18	WD repeat domain 18	Nucleus	other
E0CYH4	WDR26	WD repeat domain 26	Cytoplasm	other
Q99J09	WDR77	WD repeat domain 77	Nucleus	transcription regulator
S4R1X1	WDR91	WD repeat domain 91	Cytoplasm	other
A0A1D5RM92	WWP2	WW domain containing E3 ubiquitin protein ligase 2	Cytoplasm	enzyme
Q3UE92	XPNPEP1	X-prolyl aminopeptidase 1	Cytoplasm	peptidase
Q6P5F9	XPO1	exportin 1	Nucleus	transporter
E9PUW7	XPO7	exportin 7	Nucleus	transporter
A2A7S7	YARS	tyrosyl-tRNA synthetase	Cytoplasm	enzyme
P62960	YBX1	Y-box binding protein 1	Nucleus	transcription regulator
Q04736	YES1	YES proto-oncogene 1, Src family tyrosine kinase	Cytoplasm	kinase
Q9CQW1	YKT6	YKT6 v-SNARE homolog	Cytoplasm	enzyme
Q9CQV8	YWHAB	tyrosine 3-monooxygenase/tryptophan 5-monooxygenase activation protein beta	Cytoplasm	transcription regulator
P62259	YWHAE	tyrosine 3-monooxygenase/tryptophan 5-monooxygenase activation protein epsilon	Cytoplasm	other
P61982	YWHAG	tyrosine 3-monooxygenase/tryptophan 5-monooxygenase activation protein gamma	Cytoplasm	other
P68510	YWHAH	tyrosine 3-monooxygenase/tryptophan 5-monooxygenase activation protein eta	Cytoplasm	transcription regulator
F6VW30	YWHAQ	tyrosine 3-monooxygenase/tryptophan 5-monooxygenase activation protein theta	Cytoplasm	other
P63101	YWHAZ	tyrosine 3-monooxygenase/tryptophan 5-monooxygenase activation protein zeta	Cytoplasm	enzyme
D3Z5I1	ZC3HAV1	zinc finger CCCH-type containing, antiviral 1	Plasma Membrane	other
Q5Y5T1-2	ZDHHC20	zinc finger DHHC-type containing 20	Plasma Membrane	enzyme
Q8VDZ4	ZDHHC5	zinc finger DHHC-type containing 5	Nucleus	enzyme

Q7TSH3	ZNF516	zinc finger protein 516	Nucleus	other
Q0GGX2	ZNF541	zinc finger protein 541	Nucleus	other
Q62523	ZYX	zyxin	Plasma Membrane	other
E9Q5W5	ZZEF1	zinc finger ZZ-type and EF-hand domain containing 1	Other	other

Table S2

T: Majority protein IDs	T: Protein names	T: Gene names	C: Cluster	**NPNT_sEVs (2)**	**NPNT_sEVs (4)**	**NPNT_sEVs (1)**	**NPNT_sEVs (3)**	**EV_sEVs (3)**	**EV_sEVs (4)**	**EV_sEVs (2)**	**EV_sEVs (1)**
Q91VK1	Basic leucine zipper and W2 domain-containing protein 2	Bzw2	Cluster -0	-0.0395729	0.0395729	1.12104	0.923976	0.525842	-1.59211	-1.26278	-0.693159
Q60854;F8WIV2;K7E6F1;E9Q108;E9Q0P9	Serpin B6	Serpinb6;Serpinb6a	Cluster -0	-0.040683	0.040683	1.11998	0.920076	0.51154	-1.59642	-1.26498	-0.696688
E9PYK3		Parp4	Cluster -0	-0.0611554	0	1.04677	0.877103	0.564682	-1.52281	-1.22205	NaN
Q5SQ20;Q9EQ61	Pescadillo homolog	Pes1	Cluster -0	-0.0568402	0	1.04984	0.885809	0.593686	-1.51084	-1.21443	NaN
Q9JKY0	Cell differentiation protein RCD1 homolog	Rqcd1	Cluster -0	-0.347259	-0.275625	0.827368	0.638779	0.275625	-1.90654	NaN	NaN
A2AQR0;Q64521	Glycerol-3-phosphate dehydrogenase;Glycerol-3-phosphate dehydrogenase, mitochondrial	Gpd2	Cluster -0	-0.347143	-0.275459	0.827507	0.63885	0.275459	-1.90653	NaN	NaN
Q9CQF3;A0A1D5RM23;A0A1D5RLS2	Cleavage and polyadenylation specificity factor subunit 5	Nudt21	Cluster -0	-0.349128	-0.278312	0.825122	0.637612	0.278312	-1.90678	NaN	NaN
A0A0G2JDW7;Q6ZWU9;A0A0G2JG29	40S ribosomal protein S27	Rps27	Cluster -0	-0.0315469	0.0315469	1.12742	0.951065	0.628376	-1.5593	-1.24551	-0.666961
Q61699-2;Q61699;E9Q0U7	Heat shock protein 105 kDa	Hsph1	Cluster -0	-0.0308712	0.0308712	1.12786	0.953257	0.63693	-1.55641	-1.24395	-0.664704
Q9JKX6;A2ATT5;A0A0A6YVU1	ADP-sugar pyrophosphatase	Nudt5	Cluster -0	-0.386564	-0.332381	0.77883	0.613362	0.332381	-1.90967	NaN	NaN
Q9D0M3-2;Q9D0M3	Cytochrome c1, heme protein, mitochondrial	Cyc1	Cluster -0	-0.391355	-0.339333	0.772723	0.610132	0.339333	-1.90976	NaN	NaN
Q9DB20	ATP synthase subunit O, mitochondrial	Atp5o	Cluster -0	-0.395796	-0.345784	0.767023	0.607113	0.345784	-1.90979	NaN	NaN
Q9D3D9	ATP synthase subunit delta, mitochondrial	Atp5d	Cluster -0	-0.411034	-0.367972	0.747182	0.596555	0.367972	-1.90947	NaN	NaN
D3Z2Z1;F8WIA1;Q922J3;Q922J3-2;D3Z3M7;F6RCU2	CAP-Gly domain-containing linker protein 1	Clip1	Cluster -0	-0.422413	-0.384593	0.732075	0.588472	0.384593	-1.9088	NaN	NaN
P99026	Proteasome subunit beta type-4	Psmb4	Cluster -0	-0.418767	-0.379262	0.736943	0.591081	0.379262	-1.90906	NaN	NaN
Q9DB77	Cytochrome b-c1 complex subunit 2, mitochondrial	Uqcrc2	Cluster -0	-0.0144845	0	1.1665	1.05061	0.955736	-1.50069	NaN	-0.608099
Q922H4	Mannose-1-phosphate guanyltransferase alpha	Gmppa	Cluster -0	-0.0192353	0	1.06797	0.953732	0.838674	-1.3958	-1.13923	NaN
Q8K310;A0A087WSU2	Matrin-3	Matr3	Cluster -0	-0.0256234	0	1.16616	1.03512	0.887678	-1.54102	NaN	-0.636573
Q80UP8	Sodium-dependent phosphate transporter 2	Slc20a2	Cluster -0	-0.0237059	0.0237059	1.3078	NaN	0.884371	NaN	-1.40659	-0.726594
Q80U78-2;Q80U78-3;Q80U78;E9Q6M7;Q3TTW5	Pumilio homolog 1	Pum1	Cluster -0	-0.0271841	0	1.166	1.03284	0.878037	-1.54653	NaN	-0.640506
Q64374	Regucalcin	Rgn	Cluster -0	-0.013001	0	1.16643	1.05258	0.964706	-1.49518	NaN	-0.604253
Q64282	Interferon-induced protein with tetratricopeptide repeats 1	Ifit1	Cluster -0	-0.0294392	0	1.16572	1.0295	0.864064	-1.55442	NaN	-0.646164
Q05144	Ras-related C3 botulinum toxin substrate 2	Rac2	Cluster -0	-0.0193024	0	1.16653	1.04407	0.926459	-1.51835	NaN	-0.620501
P70372	ELAV-like protein 1	Elavl1	Cluster -0	-0.0416093	0	1.16315	1.01055	0.787729	-1.59575	NaN	-0.676194
P54818	Galactocerebrosidase	Galc	Cluster -0	-0.0212181	0	1.16647	1.0414	0.914748	-1.52529	NaN	-0.625397
P48962	ADP/ATP translocase 1	Slc25a4	Cluster -0	-0.0192832	0.0192832	1.13295	0.988578	0.781244	-1.50393	-1.21482	-0.624875
K3W4R2;Q6URW6-2;Q6URW6;Q6URW6-3;A0A140LI60	Myosin-14	Myh14	Cluster -0	-0.0266779	0	1.16606	1.03358	0.881168	-1.54474	NaN	-0.639232
A0A0R4J0W6;Q9CRC8	Leucine-rich repeat-containing protein 40	Lrrc40	Cluster -0	-0.0328733	0	1.16517	1.02431	0.842681	-1.5663	NaN	-0.654725

H3BJU7;H3BJX8;H3BJ45;H3BJ40;H3BKH9;Q60875-5;Q60875-4;Q60875;Q60875-2;Q60875-3	Rho guanine nucleotide exchange factor 2	Arhgef2	Cluster -0	-0.0207112	0	1.16649	1.04211	0.917852	-1.52346	NaN	-0.624103
Q9Z1F9	SUMO-activating enzyme subunit 2	Uba2	Cluster -0	-0.443844	-0.416021	0.702925	0.572769	0.416021	-1.90649	NaN	NaN
Q61425	Hydroxyacyl-coenzyme A dehydrogenase, mitochondrial	Hadh	Cluster -0	-0.462461	-0.443459	0.676837	0.558601	0.443459	-1.90333	NaN	NaN
P67778;Q5SQG5	Prohibitin	Phb	Cluster -0	-0.456127	-0.434111	0.685794	0.563477	0.434111	-1.90453	NaN	NaN
A2ATI9;Q99JX3;A2ATI8;A2ATI6;Q99JX3-2	Golgi reassembly-stacking protein 2	Gorasp2	Cluster -0	-0.45272	-0.429087	0.690578	0.566076	0.429087	-1.90512	NaN	NaN
O89032-3;O89032-2;O89032	SH3 and PX domain-containing protein 2A	Sh3pxd2a	Cluster -0	-0.459856	-0.439612	0.680532	0.560614	0.439612	-1.90384	NaN	NaN
E9PXX7;Q91W90;A0A0R4J1Y7	Thioredoxin domain-containing protein 5	Txndc5	Cluster -0	-0.474445	-0.461194	0.659652	0.549212	0.461194	-1.90072	NaN	NaN
Q8CAQ8-2;Q8CAQ8;Q8CAQ8-3;Q8CAQ8-5;A0A0U1RP81	MICOS complex subunit Mic60	Immt	Cluster -0	-0.484432	-0.476014	0.645092	0.541223	0.476014	-1.89818	NaN	NaN
Q921K2;P11103	Poly [ADP-ribose] polymerase 1	Parp1	Cluster -0	NaN	-0.777429	0.208573	0.103799	0	NaN	-1.82793	NaN
Q9CWX9;A0A0N4SVT1;F6QKD2	Probable ATP-dependent RNA helicase DDX47	Ddx47	Cluster -0	NaN	-1.01614	0.264038	0.129521	0	NaN	NaN	-1.69734
G3X9B1		Heatr1	Cluster -0	NaN	-1.69404	0.325979	0.109498	-0.109498	NaN	NaN	NaN
Q7TSC1;G3UX48	Protein PRRC2A	Prrc2a	Cluster -0	-0.108443	0	0.998931	0.768717	0.234206	-1.63641	-1.29104	NaN
A0A0R4J0Z1;P08003	Protein disulfide-isomerase A4	Pdia4	Cluster -0	-0.104506	0	1.00395	0.77869	0.262647	-1.62823	-1.28635	NaN
G3UYF9;Q03958	Prefoldin subunit 6	Pfdn6	Cluster -0	-0.112639	0	0.993367	0.75789	0.203703	-1.64485	-1.29581	NaN
Q99L45	Eukaryotic translation initiation factor 2 subunit 2	Eif2s2	Cluster -0	-0.132308	0	1.23874	0.956221	0.303627	NaN	-1.59557	-0.946369
Q9JM14;A2A9X5	5(3)-deoxyribonucleotidase, cytosolic type	Nt5c	Cluster -0	-0.134585	0	1.23699	0.951502	0.288201	NaN	-1.59945	-0.951364
Q9Z2I9	Succinyl-CoA ligase [ADP-forming] subunit beta, mitochondrial	Sucla2	Cluster -0	-0.349156	-0.179588	1.37453	1.0152	0.179588	NaN	NaN	-1.37609
Q91YP2	Neurolysin, mitochondrial	Nln	Cluster -0	-0.379443	-0.221784	1.34568	1.0015	0.221784	NaN	NaN	-1.3942
Q80VJ3	2-deoxynucleoside 5-phosphate N-hydrolase 1	Dnph1	Cluster -0	-0.398859	-0.249025	1.32613	0.991978	0.249025	NaN	NaN	-1.40508
E9PXV7;E9PV41;O08808;F6XC54;D3Z074	Protein diaphanous homolog 1	Diap1;Diaph1	Cluster -0	-0.367199	-0.204682	1.35758	1.0072	0.204682	NaN	NaN	-1.38704
P70268;P70268-2;D6RH37	Serine/threonine-protein kinase N1	Pkn1	Cluster -0	-0.396933	-0.246317	1.3281	0.992948	0.246317	NaN	NaN	-1.40403
Q8JZN5	Acyl-CoA dehydrogenase family member 9, mitochondrial	Acad9	Cluster -0	-0.294561	-0.167035	1.07322	0.79709	0.167035	NaN	-1.75222	NaN
G3UYD0;Q3UHU8;Q9ESZ8-5;Q9ESZ8-4;Q9ESZ8-3;Q9ESZ8-6;Q9ESZ8-2;Q9ESZ8;G3UYJ6	General transcription factor II-I	Gtf2i	Cluster -0	-0.687617	-0.476754	1.48948	1.03987	0	NaN	NaN	NaN
Q61033	Lamina-associated polypeptide 2, isoforms alpha/zeta	Tmpo	Cluster -0	-0.800558	-0.60155	1.42355	0.985263	0	NaN	NaN	NaN
Q02013	Aquaporin-1	Aqp1	Cluster -0	-0.0903584	0	1.02038	0.81306	0.36341	-1.59688	-1.26788	NaN
P63325;Q3UW83	40S ribosomal protein S10	Rps10	Cluster -0	-0.0471696	0.0471696	1.11293	0.89644	0.426971	-1.62059	-1.277	-0.716933
P70404	Isocitrate dehydrogenase [NAD] subunit gamma 1, mitochondrial	Idh3g	Cluster -0	-0.0512452	0.0512452	1.10773	0.880887	0.373162	-1.63481	-1.28376	-0.72927
Q9R1C7;A0A1B0GRU8;Q9R1C7-2	Pre-mRNA-processing factor 40 homolog A	Prpf40a	Cluster -0	-0.12032	0	1.24688	0.980034	0.383833	NaN	-1.574	-0.919531
Q64522	Histone H2A type 2-B	Hist2h2ab	Cluster -0	-0.10836	0	1.25318	1.00213	0.462233	NaN	-1.55063	-0.891866
Q9JLV1	BAG family molecular chaperone regulator 3	Bag3	Cluster -0	-0.103237	0	1.12226	0.888984	0.376239	-1.77043	NaN	-0.814627
Q99LJ1	Tissue alpha-L-fucosidase	Fuca1	Cluster -0	0	0.254262	1.35755	0.919873	-0.305208	NaN	-1.50689	-0.939352
Q792F9;Q00651	Integrin alpha-4	Itga4	Cluster -0	0	0.264744	1.34985	0.899371	-0.374771	NaN	-1.50395	-0.946917
P21550	Beta-enolase	Eno3	Cluster -0	0	0.254003	1.35772	0.920363	-0.303509	NaN	-1.50694	-0.939156

P49717	DNA replication licensing factor MCM4	Mcm4	Cluster -0	0	0.250083	1.36024	0.927692	-0.277825	NaN	-1.50766	-0.936146
Q5SWN2;Q8VEE4	Replication protein A 70 kDa DNA-binding subunit;Replication protein A 70 kDa DNA-binding subunit, N-terminally processed	Rpa1	Cluster -0	0.153943	0.378056	1.30709	0.924889	-0.153943	-1.59469	-1.12988	-0.652768
Q8K298	Actin-binding protein anillin	Anln	Cluster -0	0.0799568	0.279682	1.23555	0.884393	-0.0799568	-1.63716	-1.19488	-0.701578
F6XC25;Q8BRN9	Coiled-coil and C2 domain-containing protein 1B	Cc2d1b	Cluster -0	0.0980588	0.303836	1.2536	0.894696	-0.0980588	-1.62757	-1.17958	-0.689993
Q8CJ26;A0A0G2JH13	Death domain-containing membrane protein NRADD	Nradd	Cluster -0	0.106955	0.315683	1.26234	0.89967	-0.106955	-1.62266	-1.17191	-0.684215
P40237;A2AIJ1	CD82 antigen;Tetraspanin	Cd82	Cluster -0	0.0521589	0.242494	1.20714	0.868071	-0.0521589	-1.65091	-1.21765	-0.718927
Q9D8W5;B1AT36;Q3TRH2	26S proteasome non-ATPase regulatory subunit 12	Psmd12	Cluster -0	0.0539454	0.244888	1.209	0.869138	-0.0539454	-1.65006	-1.21621	-0.717825
P61089	Ubiquitin-conjugating enzyme E2 N	Ube2n	Cluster -0	0.0431443	0.23041	1.19776	0.862649	-0.0431443	-1.65511	-1.22483	-0.724434
Q09143;E9Q3N1	High affinity cationic amino acid transporter 1	Slc7a1	Cluster -0	0.0474583	0.236193	1.20226	0.865254	-0.0474583	-1.65311	-1.22141	-0.721803
Q9D2R0	Acetoacetyl-CoA synthetase	Aacs	Cluster -0	0	0.232404	1.36931	0.958674	-0.164014	NaN	-1.50861	-0.921468
Q9D1R9;A0A0G2JGY8;A0A0G2JEY6;D3YWC0	60S ribosomal protein L34	Rpl34;Gm2178	Cluster -0	0	0.230462	1.37009	0.961879	-0.151706	NaN	-1.5085	-0.91975
Q9CPU0	Lactoylglutathione lyase	Glo1	Cluster -0	0	0.219805	1.37366	0.978808	-0.0848062	NaN	-1.50713	-0.909971
Q8BVF7-2;Q8BVF7	Gamma-secretase subunit APH-1A	Aph1a	Cluster -0	0	0.222915	1.37275	0.973983	-0.104213	NaN	-1.50765	-0.912884
Q64449;A2AAA9	C-type mannose receptor 2	Mrc2	Cluster -0	0	0.241636	1.36502	0.942908	-0.223044	NaN	-1.50858	-0.929353
Q62165	Dystroglycan;Alpha-dystroglycan;Beta-dystroglycan	Dag1	Cluster -0	0	0.221135	1.37328	0.976756	-0.0930943	NaN	-1.50736	-0.911224
Q60953;Q60953-2;D3Z3A6;D3YXR5;F7BTZ2	Protein PML	Pml	Cluster -0	0	0.232224	1.36939	0.958972	-0.162871	NaN	-1.5086	-0.921309
Q11136	Xaa-Pro dipeptidase	Pepd	Cluster -0	0	0.231729	1.36959	0.959792	-0.159731	NaN	-1.50858	-0.920873
Q03137;Q03137-2	Ephrin type-A receptor 4	Epha4	Cluster -0	0	0.223768	1.37248	0.972642	-0.109557	NaN	-1.50778	-0.913676
Q02257	Junction plakoglobin	Jup	Cluster -0	0	0.227853	1.37108	0.966125	-0.135231	NaN	-1.50828	-0.917411
O70251;A0A087WS46	Elongation factor 1-beta	Eef1b;Eef1b2	Cluster -0	0.131875	0.380903	1.50079	NaN	-0.131875	NaN	-1.38416	-0.807378
J3QNE8;Q5I012-4;Q5I012-3;Q5I012-2;Q5I012	Putative sodium-coupled neutral amino acid transporter 10	Slc38a10	Cluster -0	0	0.226229	1.37166	0.968736	-0.125005	NaN	-1.5081	-0.915936
S4R2J9;A0A0A0MQ79;Q3TLH4-5;Q3TLH4;S4R294	Protein PRRC2C	Prrc2c	Cluster -0	0	0.233309	1.36893	0.957167	-0.169763	NaN	-1.50865	-0.922261
D3Z0F5;O88545	COP9 signalosome complex subunit 6	Cops6	Cluster -0	0	0.225716	1.37183	0.969554	-0.12178	NaN	-1.50804	-0.915468
Q9CYN9	Renin receptor	Atp6ap2	Cluster -0	0	0.214124	1.37508	0.987392	-0.0495697	NaN	-1.5059	-0.904521
Q99LC5	Electron transfer flavoprotein subunit alpha, mitochondrial	Etfa	Cluster -0	-0.0212324	0.181431	1.3564	0.983188	0	NaN	-1.52435	-0.914607
Q91YD9	Neural Wiskott-Aldrich syndrome protein	Wasl	Cluster -0	-0.00830912	0.196426	1.36873	0.992908	0	NaN	-1.51179	-0.903633
Q8K1R7	Serine/threonine-protein kinase Nek9	Nek9	Cluster -0	0	0.206342	1.3765	0.998665	-0.001778	NaN	-1.50369	-0.896799
Q61609	Sodium-dependent phosphate transporter 1	Slc20a1	Cluster -0	-0.0148394	0.188853	1.36253	0.988015	0	NaN	-1.51816	-0.909195
Q3TEW6;A0A0A6YWA2	Myelin protein zero-like protein 1	Mpzl1	Cluster -0	-0.0217324	0.18085	1.35592	0.982809	0	NaN	-1.52483	-0.915029
P62320;A0A1W2P7K5	Small nuclear ribonucleoprotein Sm D3	Snrpd3	Cluster -0	0	0.212845	1.37536	0.989282	-0.0416768	NaN	-1.50558	-0.903272
P26350;A0A087WP98;A0A087WPN6	Prothymosin alpha;Prothymosin alpha, N-terminally processed;Thymosin alpha	Ptma	Cluster -0	0	0.206232	1.37652	0.998821	-0.00110701	NaN	-1.50365	-0.896688
B2RY58;O70507	Potassium/sodium hyperpolarization-activated cyclic nucleotide-gated channel 4	Hcn4	Cluster -0	0	0.212375	1.37545	0.989973	-0.0387825	NaN	-1.50546	-0.902811
O35930	Platelet glycoprotein Ib alpha chain	Gp1ba	Cluster -0	0	0.209859	1.37593	0.993638	-0.0233119	NaN	-1.50476	-0.900326
Q9WV54	Acid ceramidase;Acid ceramidase subunit alpha;Acid ceramidase subunit beta	Asah1	Cluster -0	0	0.186944	1.10189	0.771544	-0.131544	-1.63237	-1.21395	NaN
Q8R5L1;O35658	Complement component 1 Q subcomponent-binding protein, mitochondrial	C1qbp	Cluster -0	-0.0168332	0.146561	1.09355	0.792678	0	-1.62638	-1.22838	NaN

Q4VBE8	WD repeat-containing protein 18	Wdr18	Cluster -0	0.0148096	0.192335	1.16769	0.845203	-0.0148096	-1.66749	-1.24681	-0.741386
P00405	Cytochrome c oxidase subunit 2	Mtco2	Cluster -0	-0.0122407	0.155871	1.13818	0.827968	0.0122407	-1.67816	-1.26691	-0.75705
A0A140LIX7			Cluster -0	-0.010959	0.1576	1.1396	0.828798	0.010959	-1.67768	-1.26598	-0.75632
A2A7S7;Q91WQ3	Tyrosine--tRNA ligase;Tyrosine--tRNA ligase, cytoplasmic;Tyrosine--tRNA ligase, cytoplasmic, N-terminally processed	Yars	Cluster -0	-0.00716208	0.157979	1.10408	0.800896	0	-1.62024	-1.2204	NaN
Q99K70;B1AWT2;B1AWT3;Q7TT45	Ras-related GTP-binding protein C;Ras-related GTP-binding protein D	Rragc;Rragd	Cluster -0	-0.0848077	0.107201	1.2927	0.933146	0	NaN	-1.58277	-0.966597
Q8R5J9	PRA1 family protein 3	Arl6ip5	Cluster -0	-0.109236	0.078475	1.26686	0.912927	0	NaN	-1.60374	-0.985686
Q8K023-2;Q8K023;D3Z3P8;Q91WT7;Q91WR5	Aldo-keto reductase family 1 member C18;Aldo-keto reductase family 1 member C21	Akr1c18;Akr1c6;Akr1c14;Akr1c21	Cluster -0	-0.0883572	0.103035	1.28899	0.930242	0	NaN	-1.58587	-0.969401
Q80X71;D3Z0M2;D3Z191;D3Z6E0	Transmembrane protein 106B	Tmem106b	Cluster -0	-0.0900166	0.101086	1.28725	0.928881	0	NaN	-1.58731	-0.970709
A2ALR9;Q3V0C5;Q3V0C5-5;Q3V0C5-2;A2ALR8	Ubiquitin carboxyl-terminal hydrolase 48	Usp48	Cluster -0	-0.0931623	0.0973893	1.28395	0.926293	0	NaN	-1.59004	-0.973181
Q61140;Q61140-2	Breast cancer anti-estrogen resistance protein 1	Bcar1	Cluster -0	-0.104703	0.0838143	1.27171	0.916721	0	NaN	-1.59991	-0.982181
Q8BHF7;F8WI04	CDP-diacylglycerol--glycerol-3-phosphate 3-phosphatidyltransferase, mitochondrial	Pgs1	Cluster -0	-0.0427478	0.156395	1.33542	0.966668	0	NaN	-1.54474	-0.932574
E9PX60;E9Q5C3;E9PX88;E9PXV8;E9PX67;E9Q7E6;E9Q700;E9PX90;D3Z5M8;E9Q5C2;E9Q7C7;E9Q708;E9Q7T0;E9PVU6;E9Q7E8;E9QK53;P21803-2;P21803	Receptor protein-tyrosine kinase;Fibroblast growth factor receptor;Fibroblast growth factor receptor 2	Fgfr2	Cluster -0	-0.0451306	0.153617	1.33306	0.964812	0	NaN	-1.54696	-0.93454
O09110;O09110-2	Dual specificity mitogen-activated protein kinase kinase 3	Map2k3	Cluster -0	-0.0676343	0.127328	1.31041	0.947029	0	NaN	-1.56754	-0.952881
Q9Z110-2;Q9Z110	Delta-1-pyrroline-5-carboxylate synthase;Glutamate 5-kinase;Gamma-glutamyl phosphate reductase	Aldh18a1	Cluster -0	-0.103165	0.103165	1.26817	0.89077	-0.1095	NaN	-1.60156	NaN
Q9CYG7;Q9CYG7-2	Mitochondrial import receptor subunit TOM34	Tomm34	Cluster -0	-0.120365	0.0604663	1.2222	NaN	0	NaN	-1.57736	NaN
Q91VJ4	Serine/threonine-protein kinase 38	Stk38	Cluster -0	-0.1185	0.0808187	1.25517	0.88657	-0.0808187	NaN	-1.61599	NaN
Q3UV17	Keratin, type II cytoskeletal 2 oral	Krt76	Cluster -0	-0.120375	0.0653387	1.25482	0.903525	0	NaN	-1.61302	-0.994225
Q6P9R2	Serine/threonine-protein kinase OSR1	Oxsr1	Cluster -0	-0.135456	0.0574028	1.24018	0.879694	-0.0574028	NaN	-1.63191	NaN
P49769	Presenilin-1;Presenilin-1 NTF subunit;Presenilin-1 CTF subunit;Presenilin-1 CTF12	Psen1	Cluster -0	-0.159712	0.0187559	1.21104	0.869391	0	NaN	-1.6444	-1.02355
Q9WUB3;E9PUM3	Glycogen phosphorylase, muscle form;Alpha-1,4 glucan phosphorylase	Pygm	Cluster -0	-0.136308	0.0465074	1.23733	0.889875	0	NaN	-1.62599	-1.00626
Q9CWR7;F7AFI0	Metalloreductase STEAP1	Steap1	Cluster -0	-0.173202	0	1.19604	0.861265	0.0166395	NaN	-1.65387	-1.03061
A0A140T8M7;P62751	60S ribosomal protein L23a	Rpl23a	Cluster -0	-0.17205	0.00408327	1.19689	0.858384	0	NaN	-1.65379	-1.03248
P70336;P70336-2;F8VPK5	Rho-associated protein kinase 2;Rho-associated protein kinase	Rock2	Cluster -0	-0.176265	0.00066277	1.20196	0.861667	-0.00066277	NaN	-1.66786	NaN
Q9CZ44;Q9CZ44-3;A2AT02;Q9CZ44-2	NSFL1 cofactor p47	Nsfl1c	Cluster -0	-0.153009	0	1.22016	0.910937	0.161068	NaN	-1.62818	-0.990494
D3YYN7;Q6PIE5;A0A0G2JGX4;Q8VCE0;Q6PIC6	Sodium/potassium-transporting ATPase subunit alpha-2;Sodium/potassium-transporting ATPase subunit alpha-3	Atp1a2;Atp1a3	Cluster -0	-0.158391	0	1.21433	0.898251	0.123111	NaN	-1.63564	-1.00148
P16330-2;P16330	2,3-cyclic-nucleotide 3-phosphodiesterase	Cnp	Cluster -0	-0.154674	0	1.2184	0.907053	0.149364	NaN	-1.63054	-0.993916
Q8K212	Phosphofurin acidic cluster sorting protein 1	Pacs1	Cluster -0	-0.135417	0	0.959068	0.695354	0.0344446	-1.6856	-1.31754	NaN
Q6PB66	Leucine-rich PPR motif-containing protein, mitochondrial	Lrpprc	Cluster -0	-0.135189	0	0.959448	0.696012	0.036172	-1.68523	-1.31736	NaN

Q8BH59	Calcium-binding mitochondrial carrier protein Aralar1	Slc25a12	Cluster -0	-0.134126	0	0.961203	0.699073	0.0442065	-1.68352	-1.31651	NaN
Q8BGK6;A0A1D5RMA4;A0A1D5RMI7;A0A1D5RM43;Q8BGK6-2	Y+L amino acid transporter 2	Slc7a6	Cluster -0	-0.165241	0	1.20629	0.881532	0.074245	NaN	-1.6445	-1.01516
Q8BH40;O70439	Syntaxin-7	Stx7	Cluster -0	-0.165767	0	1.20565	0.880222	0.0704715	NaN	-1.64515	-1.01619
B2RXW8;B2RXQ2		Ppfia1	Cluster -0	-0.163863	0	1.20797	0.884949	0.0841307	NaN	-1.64278	-1.01243
D6RFU9;O09117-2;O09117	Synaptophysin-like protein 1	Sypl;Sypl1	Cluster -0	-0.169066	0	1.20149	0.871908	0.0466779	NaN	-1.64913	-1.02264
Q9Z0S7;Q9Z262	Claudin-9;Claudin-6	Cldn9;Cldn6	Cluster -0	-0.127474	0	0.971835	0.717901	0.0941924	-1.67239	-1.31079	NaN
P98064-2;P98064	Mannan-binding lectin serine protease 1;Mannan-binding lectin serine protease 1 heavy chain;Mannan-binding lectin serine protease 1 light chain	Masp1	Cluster -0	-0.131433	0	0.965582	0.706763	0.0645054	-1.67911	-1.31427	NaN
P16301	Phosphatidylcholine-sterol acyltransferase	Lcat	Cluster -0	-0.130488	0	0.967095	0.709441	0.0716141	-1.67753	-1.31346	NaN
P56812;D3Z7Q5	Programmed cell death protein 5	Pdcd5	Cluster -0	-0.130737	0	0.966697	0.708735	0.0697375	-1.67795	-1.31367	NaN
Q9WTL7	Acyl-protein thioesterase 2	Lypla2	Cluster -0	-0.129386	0	1.08965	0.823398	0.18798	-1.8256	NaN	-0.865896
P54071	Isocitrate dehydrogenase [NADP], mitochondrial	Idh2	Cluster -0	-0.0707522	0.0707522	1.07415	0.798478	0.107831	-1.69213	-1.30726	-0.784086
P24472	Glutathione S-transferase A4	Gsta4	Cluster -0	-0.0515834	0.102621	1.09388	0.801895	0.0515834	-1.69165	-1.29465	-0.778932
A0A1B0GT81;Q07813;A0A1B0GTA4;A0A1B0GS13	Apoptosis regulator BAX	Bax	Cluster -0	-0.0703295	0.0703295	1.07504	0.800417	0.113752	-1.69108	-1.30691	-0.78297
O54724	Polymerase I and transcript release factor	Ptrf	Cluster -0	-0.0652667	0.0652667	1.08509	0.823029	0.183785	-1.67787	-1.30218	-0.769402
Q9ES74;Q3TN15	Serine/threonine-protein kinase Nek7	Nek7	Cluster -0	NaN	NaN	NaN	NaN	0.350135	0	-1.37018	NaN
Q9JMC3	DnaJ homolog subfamily A member 4	Dnaja4	Cluster -0	-0.169616	0	1.55315	NaN	0.358023	NaN	NaN	-1.19615
Q5DTM8;A2AIR2;Q5DTM8-2	E3 ubiquitin-protein ligase BRE1A	Rnf20	Cluster -0	0.157162	1.03169	1.03584	-0.157162	NaN	NaN	-1.15243	-1.21867
Q7TT37	Elongator complex protein 1	Ikbkap	Cluster -0	0.1594	1.03593	1.036	-0.1594	NaN	NaN	-1.14901	-1.21759
P58871;Z4YJL4	182 kDa tankyrase-1-binding protein	Tnks1bp1	Cluster -0	NaN	NaN	NaN	NaN	0.865104	0	NaN	-1.11875
Z4YLT8;Q9QYK7	RING finger protein 11	Rnf11	Cluster -0	0.337438	NaN	1.25715	0	NaN	NaN	-1.03641	-1.10977
Q9JHZ2	Progressive ankylosis protein	Ankh	Cluster -0	0.168211	1.05257	1.03654	-0.168211	NaN	NaN	-1.13544	-1.2132
Q8BMD8	Calcium-binding mitochondrial carrier protein SCaMC-1	Slc25a24	Cluster -0	0.165159	1.04682	1.03637	-0.165159	NaN	NaN	-1.14016	-1.21474
Q3UX10	Tubulin alpha chain-like 3	Tubal3	Cluster -0	0.167537	1.0513	1.03651	-0.167537	NaN	NaN	-1.13648	-1.21354
B2RR03;P56400	Platelet glycoprotein Ib beta chain	Gp1bb	Cluster -0	0.169359	1.05473	1.0366	-0.169359	NaN	NaN	-1.13366	-1.21262
Q91YZ2;P56546;P56546-2;E9PWQ9;E9Q0T4	C-terminal-binding protein 2	Ctbp2	Cluster -0	0.165346	1.04717	1.03638	-0.165346	NaN	NaN	-1.13987	-1.21465
P68181-2;P68181-3;P68181;P68181-4	cAMP-dependent protein kinase catalytic subunit beta	Prkacb	Cluster -0	0.177378	1.06979	1.03697	-0.177378	NaN	NaN	-1.12113	-1.20846
P32507-2;P32507	Nectin-2	Pvrl2	Cluster -0	NaN	0.97024	1.03721	0	NaN	NaN	-0.983849	-1.00741
Q9CY64;A2ASB8;A2ASB7;A2ASB1	Biliverdin reductase A	Blvra	Cluster -0	NaN	NaN	NaN	NaN	0.957707	0	NaN	-1.04058
Q9D880	Mitochondrial import inner membrane translocase subunit TIM50	Timm50	Cluster -0	NaN	NaN	NaN	NaN	1.04938	0	NaN	-0.948046
Q9CQ75	NADH dehydrogenase [ubiquinone] 1 alpha subcomplex subunit 2	Ndufa2	Cluster -0	NaN	NaN	NaN	NaN	1.00523	0	NaN	-0.994744
Q8BRU6	Synaptic vesicular amine transporter	Slc18a2	Cluster -0	NaN	0.99686	1.04702	0	NaN	NaN	-0.960528	-0.99368
A0A0R4J0T7;Q01721	Growth arrest-specific protein 1	Gas1	Cluster -0	NaN	NaN	NaN	NaN	1.00272	0	NaN	-0.997273
Q8BH57-3;Q8BH57-2;Q8BH57;A0A1L1SS76	WD repeat-containing protein 48	Wdr48	Cluster -0	NaN	NaN	NaN	NaN	1.03831	0	NaN	-0.960163
Q642K5;P62862	40S ribosomal protein S30	Fau	Cluster -0	NaN	0.816827	0.975946	0	NaN	NaN	-1.10557	-1.07612
Q9QZB7	Actin-related protein 10	Actr10	Cluster -0	-1.19747	0.752366	NaN	0	NaN	NaN	NaN	NaN
Q9EST4-3;Q9EST4	Proteasome assembly chaperone 2	Psmg2	Cluster -0	-0.0111209	0.540667	0.771543	0	NaN	-1.76416	NaN	NaN
Q9CZ04-2;Q9CZ04;D3Z440;D3YVI6	COP9 signalosome complex subunit 7a	Cops7a	Cluster -0	0	0.598673	0.733955	-0.0936518	NaN	-1.75901	NaN	NaN

Q8CD92-2;Q8CD92	Tetratricopeptide repeat protein 27	Ttc27	Cluster -0	-0.000921153	0.556081	0.77791	0	NaN	-1.7566	NaN	NaN
Q8BHC4;B0QZX9	Dephospho-CoA kinase domain-containing protein	Dcakd	Cluster -0	NaN	NaN	NaN	-0.0170149	1.72369	NaN	-0.168222	0.0170149
E9Q035;P47758	Signal recognition particle receptor subunit beta	Gm20425;Srprb	Cluster -0	0	0.575295	0.759746	-0.0400301	NaN	-1.7579	NaN	NaN
P24288;E9Q4K3;Q8CBC8;B2KFA8	Branched-chain-amino-acid aminotransferase, cytosolic;Branched-chain-amino-acid aminotransferase	Bcat1	Cluster -0	NaN	NaN	NaN	-0.0478516	1.72672	NaN	-0.117788	0.0478516
Q9CZU0;Q8VC77		Akr1c20	Cluster -0	0.0392211	0.917076	NaN	-0.0392211	NaN	NaN	NaN	-1.4683
Q80X98		Dhx38	Cluster -0	0.0324532	0.906338	NaN	-0.0324532	NaN	NaN	NaN	-1.47528
P25799;P25799-3;P25799-2;P25799-4	Nuclear factor NF-kappa-B p105 subunit;Nuclear factor NF-kappa-B p50 subunit	Nfkb1	Cluster -0	0.0441122	0.924791	NaN	-0.0441122	NaN	NaN	NaN	-1.46317
P56391;A0A140LIU3	Cytochrome c oxidase subunit 6B1	Cox6b1	Cluster -0	-0.084554	0.791744	0.084554	NaN	NaN	-1.53585	NaN	NaN
Q9JLN9	Serine/threonine-protein kinase mTOR	Mtor	Cluster -0	-0.110708	0.722754	0.110708	NaN	NaN	-1.56624	NaN	NaN
Q9JI75	Ribosyldihydronicotinamide dehydrogenase [quinone]	Nqo2	Cluster -0	-0.336852	0.697381	0.336852	NaN	NaN	NaN	-1.51219	NaN
Q9DBG7	Signal recognition particle receptor subunit alpha	Srpr	Cluster -0	-0.319609	0.768384	0.319609	NaN	NaN	NaN	-1.48502	NaN
Q9D2V7	Coronin-7	Coro7	Cluster -0	-0.327026	0.738384	0.327026	NaN	NaN	NaN	-1.49696	NaN
Q91ZJ5-2;Q91ZJ5	UTP--glucose-1-phosphate uridylyltransferase	Ugp2	Cluster -0	-0.32667	0.739842	0.32667	NaN	NaN	NaN	-1.4964	NaN
Q8BX02;Q8BX02-2	KN motif and ankyrin repeat domain-containing protein 2	Kank2	Cluster -0	-0.126377	0.68027	0.126377	NaN	NaN	-1.58281	NaN	NaN
Q8BW00	Probable peptidyl-tRNA hydrolase	Ptrh1	Cluster -0	-0.313437	0.792761	0.313437	NaN	NaN	NaN	-1.4748	NaN
Z4YJT3;Q6ZQ58	La-related protein 1	Larp1	Cluster -0	-0.177815	0.534455	0.177815	NaN	NaN	-1.62823	NaN	NaN
Q5SRX1-3;Q5SRX1-4;Q5SRX1-2;Q5SRX1;Q5SXA5;Q5SXA4;Q5SRX1-5	TOM1-like protein 2	Tom1l2	Cluster -0	-0.107404	0.731604	0.107404	NaN	NaN	-1.56259	NaN	NaN
Q3UA06;Q3UA06-2	Pachytene checkpoint protein 2 homolog	Trip13	Cluster -0	-0.309301	0.808802	0.309301	NaN	NaN	NaN	-1.46782	NaN
F6QH25;E9Q4G8;E9Q3Q6;Q61490	CD166 antigen	Alcam	Cluster -0	-0.133655	0.660233	0.133655	NaN	NaN	-1.59008	NaN	NaN
P61961;H7BWZ1;D3YW97	Ubiquitin-fold modifier 1	Ufm1	Cluster -0	-0.101873	0.746328	0.101873	NaN	NaN	-1.55635	NaN	NaN
Q9D1H9;Q9D1H9-2	Microfibril-associated glycoprotein 4	Mfap4	Cluster -0	0	1.20507	0.18457	NaN	NaN	NaN	-0.755964	-1.39365
Q9CQU5;A0A1W2P7M1	ZW10 interactor	Zwint	Cluster -0	0	1.23661	0.123371	NaN	NaN	NaN	-0.708282	-1.39782
P42669	Transcriptional activator protein Pur-alpha	Pura	Cluster -0	0	1.22936	0.137837	NaN	NaN	NaN	-0.719649	-1.39706
Q3UGN9;P70297	Signal transducing adapter molecule 1	Stam	Cluster -0	0	1.23121	0.134177	NaN	NaN	NaN	-0.716779	-1.39726
Q99KD5;D6RIN1	Protein unc-45 homolog A	Unc45a	Cluster -0	0.333416	1.38575	0.501131	-0.861122	NaN	-1.36554	-0.333416	NaN
O08710	Thyroglobulin	Tg	Cluster -0	0.306049	1.37776	0.411273	-0.97066	NaN	-1.3428	-0.306049	NaN
B1AXY5;P15535-2;P15535	Beta-1,4-galactosyltransferase 1;Lactose synthase A protein;N-acetyllactosamine synthase;Beta-N-acetylglucosaminylglycopeptide beta-1,4-galactosyltransferase;Beta-N-acetylglucosaminyl-glycolipid beta-1,4-galactosyltransferase;Processed beta-1,4-galactosyltransferase 1	B4galt1	Cluster -0	0.337905	1.3865	0.516133	-0.842188	NaN	-1.36879	-0.337905	NaN
F8VQ28;Q8VI36-2;Q8VI36;A0A0J9YV30;A0A1D5RMM8	Paxillin	Pxn	Cluster -0	0.334703	1.38598	0.505426	-0.85572	NaN	-1.36649	-0.334703	NaN
Q9CZE3;A0A140LHK2;Q8QZZ8	Ras-related protein Rab-32;Ras-related protein Rab-38	Rab32;Rab38	Cluster -0	0.440302	0.928782	0.677247	0.0317964	-2.26789	-0.545775	-0.0317964	-0.203961
Q8C708	Transmembrane protein C16orf54 homolog		Cluster -0	0.439913	0.928216	0.672386	0.0275321	-2.27123	-0.540365	-0.0275321	-0.201971

Q921F2;A0A087WRZ5;Q8R0B4;Q8BLD4;Q6VYI5;Q6VYI4;A0A087WR97;A0A087WQA5;A0A087WSH7;A0A087WRP4;H3BJV1	TAR DNA-binding protein 43	Tardbp	Cluster -0	0.438245	0.925741	0.652219	0.0099209	-2.28464	-0.517936	-0.0099209	-0.193718
Q8K211	High affinity copper uptake protein 1	Slc31a1	Cluster -0	0.441647	0.930704	0.694739	0.047223	-2.25554	-0.56529	-0.047223	-0.211142
A2AFQ0;Q7TMY8;Q7TMY8-3;Q7TMY8-4;Q7TMY8-2	E3 ubiquitin-protein ligase HUWE1	Huwe1	Cluster -0	0.443379	0.933079	0.71888	0.0686897	-2.23761	-0.592276	-0.0686897	-0.221072
Q3THE2	Myosin regulatory light chain 12B	Myl12b	Cluster -0	0.44295	0.932502	0.712679	0.0631554	-2.24232	-0.585335	-0.0631554	-0.218519
Q99J93;A0A1B0GT68	Interferon-induced transmembrane protein 2	Ifitm2	Cluster -0	0.433362	0.918175	0.59882	-0.0360362	-2.31687	-0.458799	0.0360362	-0.17195
Q62426	Cystatin-B	Cstb	Cluster -0	0.436635	0.923296	0.633808	-0.00603279	-2.29628	-0.497506	0.00603279	-0.186198
P43276	Histone H1.5	Hist1h1b	Cluster -0	0.437055	0.923941	0.638531	-0.00195176	-2.29335	-0.502745	0.00195176	-0.188127
P62849-2;P62849-3;P62849	40S ribosomal protein S24	Rps24	Cluster -0	0.435575	0.921654	0.622129	-0.0160949	-2.30338	-0.484568	0.0160949	-0.181435
G3X9J6;E9Q9M1;Q3V1L4	Cytosolic purine 5-nucleotidase	Nt5c2	Cluster -0	0.415673	1.36628	0.79126	-0.457777	NaN	-1.39716	-0.415673	NaN
P29758	Ornithine aminotransferase, mitochondrial	Oat	Cluster -0	0.413684	1.36779	0.783767	-0.469294	NaN	-1.39727	-0.413684	NaN
Q9JHS3;D3YTS4	Ragulator complex protein LAMTOR2	Lamtor2	Cluster -0	0.164932	0.879011	0.802619	-0.164932	NaN	-1.6381	NaN	-0.919442
Q6PGF7	Exocyst complex component 8	Exoc8	Cluster -0	0.176909	0.901445	0.803093	-0.176909	NaN	-1.62666	NaN	-0.913144
Q5SSI6	U3 small nucleolar RNA-associated protein 18 homolog	Utp18	Cluster -0	0.166819	0.882553	0.802704	-0.166819	NaN	-1.63632	NaN	-0.918462
F8WJG3;P62996	Transformer-2 protein homolog beta	Tra2b	Cluster -0	0.176137	0.900001	0.803067	-0.176137	NaN	-1.62741	NaN	-0.913556
O70194	Eukaryotic translation initiation factor 3 subunit D	Eif3d	Cluster -0	0.169384	0.887363	0.802813	-0.169384	NaN	-1.63389	NaN	-0.917123
Q8BMS7;H3BL44;H3BIX7;Q3UZR5;Q80XR2;H3BLI6	Calcium-transporting ATPase;Calcium-transporting ATPase type 2C member 1	Atp2c1	Cluster -0	0.225727	1.15888	1.03683	-0.225727	NaN	NaN	-1.04241	-1.18045
P25118	Tumor necrosis factor receptor superfamily member 1A	Tnfrsf1a	Cluster -0	0.237871	1.18079	1.03614	-0.237871	NaN	NaN	-1.02176	-1.17259
Q60841-3;Q60841-2;Q60841	Reelin	Reln	Cluster -0	0.189976	0.925795	0.803434	-0.189976	NaN	-1.61378	NaN	-0.906052
Q62000	Mimecan	Ogn	Cluster -0	0.188306	0.92269	0.803401	-0.188306	NaN	-1.61545	NaN	-0.906971
P61924	Coatomer subunit zeta-1	Copz1	Cluster -0	0.154116	0.858659	0.802061	-0.154116	NaN	-1.64813	NaN	-0.924963
E9Q586;D3YX34;E9Q3M3;O08788-2;O08788	Dynactin subunit 1	Dctn1	Cluster -0	0.157503	0.865041	0.802249	-0.157503	NaN	-1.64502	NaN	-0.923251
O35864	COP9 signalosome complex subunit 5	Cops5	Cluster -0	0.15476	0.859873	0.802097	-0.15476	NaN	-1.64754	NaN	-0.924639
Q8BU31	Ras-related protein Rap-2c	Rap2c	Cluster -0	0.450936	0.939566	0.889438	0.227186	-2.07779	-0.7855	-0.227186	-0.292124
Q76MZ3	Serine/threonine-protein phosphatase 2A 65 kDa regulatory subunit A alpha isoform	Ppp2r1a	Cluster -0	0.450977	0.939509	0.891944	0.229616	-2.07495	-0.788379	-0.229616	-0.293185
P62082;F6SVV1	40S ribosomal protein S7	Rps7;Gm9493	Cluster -0	0.45117	0.939128	0.905376	0.24269	-2.0595	-0.803815	-0.24269	-0.298858
Q5UE59;E9Q7C9;Q7TNF4;Q8CD76;O88447	Kinesin light chain 1	Klc1	Cluster -0	0.451133	0.939216	0.902588	0.23997	-2.06275	-0.800612	-0.23997	-0.29768
A0A0N4SV66;C0HKE9;C0HKE8;C0HKE7;C0HKE6;C0HKE5;C0HKE4;C0HKE3;C0HKE2;C0HKE1;Q8CGP6;Q8R1M2;Q8CGP7;Q8CGP5;Q8BFU2	Histone H2A type 1-H;Histone H2A.J;Histone H2A type 1-K;Histone H2A type 1-F;Histone H2A type 3	Hist1h2ah;H2afj;Hist1h2ak;Hist1h2af;Hist3h2a	Cluster -0	0.450906	0.939598	0.887864	0.225662	-2.07956	-0.783691	-0.225662	-0.291459
Q6PE66;A2AHQ7;Q8BWJ3	Phosphorylase b kinase regulatory subunit alpha, liver isoform	Phka2	Cluster -0	0.451043	0.939409	0.895967	0.233522	-2.07037	-0.792995	-0.233522	-0.294881
Q9Z2U1	Proteasome subunit alpha type-5	Psma5	Cluster -0	0.445991	0.936366	0.760239	0.105991	-2.20436	-0.638712	-0.105991	-0.238154
A0A0G2JE32;A0A0G2JGL0;P61079	Ubiquitin-conjugating enzyme E2 D3	Ube2d3	Cluster -0	0.44692	0.937408	0.777073	0.121367	-2.18988	-0.657683	-0.121367	-0.245131
A0A0R4J1G5;Q91X78	Erlin-1	Erlin1	Cluster -0	0.447098	0.9376	0.780487	0.1245	-2.18688	-0.661538	-0.1245	-0.24655
Q9R0Q6;A0A0G2JF52;D3YVI5	Actin-related protein 2/3 complex subunit 1A	Arpc1a	Cluster -0	0.225728	0.991735	0.803419	-0.225728	NaN	-1.57641	NaN	-0.885447
Q9QYY8-2;Q9QYY8	Spastin	Spast	Cluster -0	0.241058	1.0197	0.802978	-0.241058	NaN	-1.5594	NaN	-0.876063

Q8BXC6	COMM domain-containing protein 2	Commd2	Cluster -0	0.221137	0.983324	0.803499	-0.221137	NaN	-1.58138	NaN	-0.888192
A0A0R4J0V5;P08775	DNA-directed RNA polymerase II subunit RPB1	Polr2a	Cluster -0	0.22718	0.994392	0.803388	-0.22718	NaN	-1.57482	NaN	-0.884572
Q61635		Ifi47	Cluster -0	0.233181	1.00535	0.803237	-0.233181	NaN	-1.56821	NaN	-0.880926
Q8JZK9	Hydroxymethylglutaryl-CoA synthase, cytoplasmic	Hmgcs1	Cluster -0	0.449227	0.939463	0.827956	0.168574	-2.14259	-0.715299	-0.168574	-0.26632
P57716	Nicastrin	Ncstn	Cluster -0	0.4497	0.939709	0.841173	0.181022	-2.12939	-0.730336	-0.181022	-0.271848
P15864	Histone H1.2	Hist1h1c	Cluster -0	0.448884	0.93923	0.819129	0.160304	-2.15118	-0.705274	-0.160304	-0.262633
D3YZ62;D3Z4J3;Q99104	Unconventional myosin-Va	Myo5a	Cluster -0	0.44806	0.938548	0.8001	0.142591	-2.16915	-0.683706	-0.142591	-0.254702
Q8CBB6;Q8CGP2;Q8CGP1;Q6ZWY9;Q64525;Q64478;Q64475;P10854;P10853;Q8CGP2-2;Q9D2U9;Q8CGP0;Q64524;P70696	Histone H2B;Histone H2B type 1-P;Histone H2B type 1-K;Histone H2B type 1-C/E/G;Histone H2B type 2-B;Histone H2B type 1-H;Histone H2B type 1-B;Histone H2B type 1-M;Histone H2B type 1-F/J/L;Histone H2B type 3-A;Histone H2B type 3-B;Histone H2B type 2-E;Histone H2B type 1-A	Hist1h2br;Hist1h2bp;Hist1h2bk;Hist1h2bc;Hist2h2bb;Hist1h2bh;Hist1h2bb;Hist1h2bm;Hist1h2bf;Hist3h2ba;Hist3h2bb;Hist2h2be;Hist1h2ba	Cluster -0	0.448722	0.939111	0.815267	0.156696	-2.15489	-0.700895	-0.156696	-0.261025
Q3UFY7;Q3UFY7-4;A0A0R4J146;Q3UFY7-2	7-methylguanosine phosphate-specific 5-nucleotidase	Nt5c3b	Cluster -0	0.21012	0.963071	0.803598	-0.21012	NaN	-1.59311	NaN	-0.89466
Q60707;P70324-2;P70324	T-box transcription factor TBX2;T-box transcription factor TBX3	Tbx2;Tbx3	Cluster -0	NaN	1.18499	0.961992	0	NaN	-1.16767	NaN	-0.554014
Q9D939	Sulfotransferase 1C2	Sult1c2	Cluster -0	NaN	1.15094	0.963849	0	NaN	-1.24333	-0.447742	NaN
A0A0A6YX18;Q8BVE3	V-type proton ATPase subunit H	Atp6v1h	Cluster -0	0.537708	NaN	1.13511	0	NaN	-1.40425	NaN	-0.671182
P61208	ADP-ribosylation factor-like protein 4C	Arl4c	Cluster -0	0.186748	NaN	0.876926	0	NaN	-1.57645	NaN	-0.84317
Q8BMC0	Lysophosphatidic acid receptor 6	Lpar6	Cluster -0	0.128162	0.976175	1.03303	-0.128162	NaN	NaN	-1.19571	-1.23182
Q6Q899;A2AP29;Q6Q899-2	Probable ATP-dependent RNA helicase DDX58	Ddx58	Cluster -0	0.120187	0.960735	1.03201	-0.120187	NaN	NaN	-1.20728	-1.23513
A0A0G2JF67;Q8CG03	cGMP-specific 3,5-cyclic phosphodiesterase	Pde5a	Cluster -0	0.126974	0.97388	1.03288	-0.126974	NaN	NaN	-1.19744	-1.23232
E9PZP8		Herc1	Cluster -0	0.132879	0.985272	1.03358	-0.132879	NaN	NaN	-1.18879	-1.2298
Q61166	Microtubule-associated protein RP/EB family member 1	Mapre1	Cluster -0	0.451121	0.935139	0.970636	0.307616	-1.97755	-0.879333	-0.307616	-0.326606
Q9QUM9;E0CXB1	Proteasome subunit alpha type-6	Psma6	Cluster -0	0.451176	0.935514	0.966412	0.303338	-1.98322	-0.874417	-0.303338	-0.324799
Q9WVE8	Protein kinase C and casein kinase substrate in neurons protein 2	Pacsin2	Cluster -0	0.451355	0.937544	0.938911	0.275742	-2.01887	-0.842496	-0.275742	-0.313074
Q9QZQ8-2;Q9QZQ8	Core histone macro-H2A.1	H2afy	Cluster -0	0.451317	0.936738	0.950937	0.287754	-2.00355	-0.856434	-0.287754	-0.318193
Q9CQM8;O09167	60S ribosomal protein L21	Rpl21	Cluster -0	0.451338	0.937093	0.945846	0.282663	-2.01009	-0.850535	-0.282663	-0.316027
Q8C7K6	Prenylcysteine oxidase-like	Pcyox1l	Cluster -0	0.451355	0.937609	0.93779	0.274631	-2.02028	-0.841207	-0.274631	-0.312598
D3Z0V2;A0A0R4J0X8;Q9ES28-8;Q9ES28-4;Q9ES28-3;Q9ES28-2;Q9ES28-7;Q9ES28;Q9ES28-6;Q9ES28-5	Rho guanine nucleotide exchange factor 7	Arhgef7	Cluster -0	0.147466	1.01324	1.03505	-0.147466	NaN	NaN	-1.16711	-1.22326
Q62422	Osteoclast-stimulating factor 1	Ostf1	Cluster -0	0.151086	1.02014	1.03537	-0.151086	NaN	NaN	-1.16165	-1.22157
P61027	Ras-related protein Rab-10	Rab10	Cluster -0	0.417908	0.887526	1.0574	0.402949	-1.8173	-1.04103	-0.456636	-0.402949
Q9JM76;H7BWZ3;A0A0G2JFK7;D3Z2F7;D3Z2F8	Actin-related protein 2/3 complex subunit 3	Arpc3	Cluster -0	0.419312	0.889486	1.05531	0.400439	-1.82233	-1.03609	-0.451932	-0.400439
Q61469;Q61469-2	Lipid phosphate phosphohydrolase 1	Ppap2a	Cluster -0	0.0351939	0.791631	1.01481	-0.0351939	NaN	NaN	-1.32194	-1.26233
Q9QUR7	Peptidyl-prolyl cis-trans isomerase NIMA-interacting 1	Pin1	Cluster -0	0	NaN	0.955938	0.0206919	NaN	NaN	-1.29149	-1.19072
P47856-2;P47856	Glutamine--fructose-6-phosphate aminotransferase [isomerizing] 1	Gfpt1	Cluster -0	0.443149	0.922074	1.01612	0.355222	-1.90723	-0.946423	-0.367804	-0.355222
Q8VDU0	G-protein-signaling modulator 2	Gpsm2	Cluster -0	-0.363617	0.363617	0.504684	NaN	NaN	NaN	NaN	-1.57507
Q99PV0	Pre-mRNA-processing-splicing factor 8	Prpf8	Cluster -0	0.446993	0.927194	1.00908	0.347439	-1.92077	-0.930885	-0.353447	-0.347439
P10518	Delta-aminolevulinic acid dehydratase	Alad	Cluster -0	0.446913	0.927091	1.00922	0.3476	-1.92049	-0.93121	-0.353743	-0.3476
P35564	Calnexin	Canx	Cluster -0	0.448596	0.929322	1.00607	0.34414	-1.92642	-0.924296	-0.347374	-0.34414
O88393;A0A0R4J097	Transforming growth factor beta receptor type 3	Tgfbr3	Cluster -0	0.166163	NaN	1.10903	0	NaN	NaN	-1.17622	-1.16574

Q9CXE7	Transmembrane emp24 domain-containing protein 5	Tmed5	Cluster -0	0.0836854	0.889126	1.02604	-0.0836854	NaN	NaN	-1.25845	-1.2486
Q64152-2;Q64152	Transcription factor BTF3	Btf3	Cluster -0	0.163933	NaN	1.10698	0	NaN	NaN	-1.17788	-1.16633
Q99KK7	Dipeptidyl peptidase 3	Dpp3	Cluster -0	0.162242	NaN	1.10543	0	NaN	NaN	-1.17914	-1.16676
Q78PY7;Q3TJ56	Staphylococcal nuclease domain-containing protein 1	Snd1	Cluster -0	0.450751	0.933117	0.990934	0.328329	-1.94954	-0.903008	-0.328329	-0.335301
Q60928;F6WUX1;D3Z4Q6;D3YVY4;D3Z266	Gamma-glutamyltranspeptidase 1;Gamma-glutamyltranspeptidase 1 heavy chain;Gamma-glutamyltranspeptidase 1 light chain	Ggt1	Cluster -0	0.203709	NaN	1.14302	0	NaN	NaN	-1.14764	-1.1554
E9Q5F9-2;E9Q5F9	Histone-lysine N-methyltransferase SETD2	Setd2	Cluster -0	0.199774	NaN	1.1395	0	NaN	NaN	-1.15069	-1.15653
P29387	Guanine nucleotide-binding protein subunit beta-4	Gnb4	Cluster -0	0.199204	NaN	1.13898	0	NaN	NaN	-1.15113	-1.15669
J3QN85;P16092-4;P16092-5;P16092-2;P16092-6;P16092;P16092-3	Fibroblast growth factor receptor;Fibroblast growth factor receptor 1	Fgfr1	Cluster -0	0.193653	NaN	1.134	0	NaN	NaN	-1.1554	-1.15827
P53395	Lipoamide acyltransferase component of branched-chain alpha-keto acid dehydrogenase complex, mitochondrial	Dbt	Cluster -0	0.431544	0.906373	1.03613	0.377871	-1.86607	-0.991463	-0.409789	-0.377871
P82349	Beta-sarcoglycan	Sgcb	Cluster -0	0.0940077	NaN	1.04138	0	NaN	NaN	-1.22798	-1.18269
E9QM61;P35689	DNA repair protein complementing XP-G cells homolog	Ercc5	Cluster -0	0.0930263	NaN	1.04044	0	NaN	NaN	-1.22866	-1.18289
F7BP73;Q3UHH2-2;Q3UHH2	Solute carrier family 22 member 23	Slc22a23	Cluster -0	0.0712866	NaN	1.01945	0	NaN	NaN	-1.24343	-1.18723
Q64310;E0CXD9;F7CH13	Surfeit locus protein 4	Surf4	Cluster -0	0.113415	NaN	1.05987	0	NaN	NaN	-1.21447	-1.17851
D6RFN5;D3YW25;O70131	Ninjurin-1	Ninj1	Cluster -0	0.124509	NaN	1.07034	0	NaN	NaN	-1.2066	-1.176
Q3U1J0-2;Q3U1J0	Sodium-coupled neutral amino acid transporter 5	Slc38a5	Cluster -0	0.118082	NaN	1.06429	0	NaN	NaN	-1.21117	-1.17746
Q3UGR5	Haloacid dehalogenase-like hydrolase domain-containing protein 2	Hdhd2	Cluster -0	0.056183	0.943666	NaN	-0.056183	NaN	NaN	NaN	-1.45024
A0A0G2JE26;Q6DFX2	Anthrax toxin receptor 2	Antxr2	Cluster -0	0.0794635	0.979412	NaN	-0.0794635	NaN	NaN	NaN	-1.42412
E9PV45;B1AY13	Ubiquitin carboxyl-terminal hydrolase;Ubiquitin carboxyl-terminal hydrolase 24	Usp24	Cluster -0	0.072905	0.969429	NaN	-0.072905	NaN	NaN	NaN	-1.43163
A0A087WQ65;A0A087WRZ2;A0A087WNT2;A0A087WPY4;Q99JA5;Q64253	Lymphocyte antigen 6E	Ly6e	Cluster -0	0.419168	0.881201	1.11112	0.462057	-1.72377	-1.09415	-0.505418	-0.419168
P14069	Protein S100-A6	S100a6	Cluster -0	0.419965	0.881248	1.11681	0.468305	-1.71414	-1.09838	-0.509275	-0.419965
P11688	Integrin alpha-5;Integrin alpha-5 heavy chain;Integrin alpha-5 light chain	Itga5	Cluster -0	0.41844	0.881134	1.10596	0.456421	-1.7324	-1.09031	-0.501933	-0.41844
Q6PDK8	E3 ubiquitin-protein ligase DTX4	Dtx4	Cluster -0	0.424804	0.880995	1.15272	0.508191	-1.65097	-1.12485	-0.533773	-0.424804
Q06890;E9PUU2;E9PXG5;E9Q8Y5;E9Q9B8	Clusterin;Clusterin beta chain;Clusterin alpha chain	Clu	Cluster -0	0.428008	0.880144	1.17795	0.53679	-1.60387	-1.14326	-0.551178	-0.428008
Q8C2Q7;O35737	Heterogeneous nuclear ribonucleoprotein H;Heterogeneous nuclear ribonucleoprotein H, N-terminally processed	Hnrnph1	Cluster -0	0.424496	0.881038	1.15036	0.505545	-1.65525	-1.12313	-0.532159	-0.424496
P62315	Small nuclear ribonucleoprotein Sm D1	Snrpd1	Cluster -0	0.423306	0.881186	1.14136	0.495475	-1.67143	-1.11651	-0.525992	-0.423306
P56135;F8WHP8	ATP synthase subunit f, mitochondrial	Atp5j2	Cluster -0	0.43221	0.877931	1.21353	0.578002	-1.53323	-1.1689	-0.576003	-0.43221
Q80ZJ1;Q80ZJ1-2	Ras-related protein Rap-2a	Rap2a	Cluster -0	0.430828	0.87882	1.20148	0.563926	-1.55774	-1.16026	-0.567562	-0.430828
Q8K0C9	GDP-mannose 4,6 dehydratase	Gmds	Cluster -0	NaN	0.211057	0.595758	-0.211057	NaN	NaN	-1.59874	NaN
A2ABY2;A2ABY0;Q8K4P1	Neuropeptide B;Neuropeptide B-29	Npb	Cluster -0	NaN	0.228341	0.594454	-0.228341	NaN	NaN	-1.59447	NaN
E9QN31;Q922K7	Probable 28S rRNA (cytosine-C(5))-methyltransferase	Nop2	Cluster -0	NaN	0.187071	0.597361	-0.187071	NaN	NaN	-1.60411	NaN
Q5F258;Q68FF6	ARF GTPase-activating protein GIT1	Git1	Cluster -0	NaN	0.878801	0.857532	0	NaN	-1.39946	NaN	-0.730663

A0A0A0MQF7;Q8K207	Uncharacterized protein C1orf21 homolog	1700025G04Rik	Cluster -0	-0.124155	NaN	0.922549	0.124155	NaN	NaN	-1.45536	NaN
A0A1B0GRV0;Q9Z0S1	3(2),5-bisphosphate nucleotidase 1	Bpnt1	Cluster -0	NaN	0.948597	0.883592	0	NaN	-1.35494	NaN	-0.695384
P06801;Q3TQP6	NADP-dependent malic enzyme;Malic enzyme	Me1	Cluster -0	0.23598	0.486076	1.37937	0.964677	-0.23598	-1.53736	-1.05011	-0.59406
Q61001	Laminin subunit alpha-5	Lama5	Cluster -0	0.234167	0.483702	1.37786	0.963857	-0.234167	-1.53874	-1.05196	-0.595408
Q9CZD3	Glycine--tRNA ligase	Gars	Cluster -0	0.208457	0.449961	1.35596	0.951939	-0.208457	-1.55782	-1.07779	-0.61431
O88456;A0A0R4IZW8;A0A0R4J1C2	Calpain small subunit 1	Capns1	Cluster -0	0.216259	0.460213	1.36268	0.955615	-0.216259	-1.55215	-1.07004	-0.608622
P62960;A2BGG7	Nuclease-sensitive element-binding protein 1	Ybx1	Cluster -0	0.212187	0.454866	1.35918	0.953705	-0.212187	-1.55512	-1.0741	-0.6116
Q9JK38	Glucosamine 6-phosphate N-acetyltransferase	Gnpnat1	Cluster -0	0	0.276547	1.33941	0.874671	-0.454666	NaN	-1.49884	-0.954575
Q8BHK9	DNA excision repair protein ERCC-6-like	Ercc6l	Cluster -0	0	0.299422	1.22222	NaN	-0.696294	NaN	-1.38986	NaN
Q6P9P6	Kinesin-like protein KIF11	Kif11	Cluster -0	0	0.295289	1.3186	0.831563	-0.585334	NaN	-1.4864	-0.964665
Q3TUE1;A0A0G2JGW9;A0A0G2JFY5;Q3UUU2;Q91WJ8;Q91WJ8-2;A0A0G2JG00;A0A0G2JFK2	Far upstream element-binding protein 1	Fubp1	Cluster -0	0	0.293312	1.23698	NaN	-0.646553	NaN	-1.40207	NaN
Q06185	ATP synthase subunit e, mitochondrial	Atp5i	Cluster -0	0	0.28056	1.33541	0.865857	-0.482241	NaN	-1.49664	-0.956958
Q9ET30	Transmembrane 9 superfamily member 3	Tm9sf3	Cluster -0	0.272651	0.533985	1.40919	0.980661	-0.272651	-1.50813	-1.01175	-0.566206
O70503	Very-long-chain 3-oxoacyl-CoA reductase	Hsd17b12	Cluster -0	0.331219	0.610025	1.45352	1.00378	-0.331219	-1.45661	-0.946836	-0.519549
Q7TPV4	Myb-binding protein 1A	Mybbp1a	Cluster -0	0.273205	0.534715	1.40964	0.980895	-0.273205	-1.50766	-1.01115	-0.565775
Q9WTX5	S-phase kinase-associated protein 1	Skp1	Cluster -0	0.331042	0.6366	1.63248	NaN	-0.331042	NaN	-1.14266	-0.636327
Q9D2Y4-2;Q9D2Y4	Mixed lineage kinase domain-like protein	Mlkl	Cluster -0	0.345297	0.654475	1.63907	NaN	-0.345297	NaN	-1.12227	-0.622236
Q6A0D4	Raftlin	Rftn1	Cluster -0	0.297389	0.59416	1.61534	NaN	-0.297389	NaN	-1.18904	-0.668556
Q923T9-3;Q923T9-2;Q923T9;Q5SVI9;Q5SVJ1;Q5SVI3;Q5SVI0;Q5SVI2;Q68EG2;Q5SVI1;Q5SVJ0;P28652	Calcium/calmodulin-dependent protein kinase type II subunit gamma;Calcium/calmodulin-dependent protein kinase type II subunit beta	Camk2g;Camk2b	Cluster -0	0.388551	0.708334	1.65648	NaN	-0.388551	NaN	-1.0576	-0.577804
B2RUR8	OTU domain-containing protein 7B	Otud7b	Cluster -0	-1.10974	NaN	0.876631	0	NaN	NaN	NaN	NaN
Q99KI3	ER membrane protein complex subunit 3	Emc3	Cluster -0	-1.11119	NaN	0.874795	0	NaN	NaN	NaN	NaN
Q9CQE8	UPF0568 protein C14orf166 homolog		Cluster -0	0.399282	0.697569	1.49963	1.02673	-0.399282	-1.38891	-0.865518	-0.461817
Q01320	DNA topoisomerase 2-alpha	Top2a	Cluster -0	0.383075	0.676805	1.4892	1.02167	-0.383075	-1.40583	-0.88548	-0.475919
P70195	Proteasome subunit beta type-7	Psmb7	Cluster -0	0.426902	0.732836	1.51659	1.03478	-0.426902	-1.35889	-0.830606	-0.437244
A2AS05;A2AS03;E9QAM5	Helicase with zinc finger domain 2	Helz2	Cluster -0	0.433092	0.743169	1.51778	1.03107	-0.449969	-1.35236	-0.821253	-0.433092
F6RPJ9;Q9JHR7	Insulin-degrading enzyme	Ide	Cluster -0	0.418912	0.72265	1.51179	1.03253	-0.418912	-1.36773	-0.840819	-0.444425
Q61735-2;Q61735	Leukocyte surface antigen CD47	Cd47	Cluster -0	0.437791	0.766101	1.50138	0.993044	-0.573142	-1.34731	-0.803582	-0.437791
Q60767;A2AW86	Lymphocyte antigen 75	Ly75	Cluster -0	0.437489	0.764518	1.50269	0.995858	-0.564349	-1.34779	-0.804921	-0.437489
A2AS45;Q68FH0-2;Q68FH0;A2AS47;A2AS44	Plakophilin-4	Pkp4	Cluster -0	0.43644	0.759138	1.50692	1.0052	-0.534793	-1.34926	-0.809328	-0.43644
Q5F2E8	Serine/threonine-protein kinase TAO1	Taok1	Cluster -0	0.435164	0.752851	1.51148	1.01571	-0.500895	-1.35069	-0.814226	-0.435164
P54731	FAS-associated factor 1	Faf1	Cluster -0	0.477966	0.824504	1.66547	NaN	-0.531059	NaN	-0.898602	-0.477966
E9Q7G0;A0A1B0GSW3		Numa1	Cluster -0	0.477985	0.825512	1.66338	NaN	-0.538842	NaN	-0.896894	-0.477985
O88811-2;O88811	Signal transducing adapter molecule 2	Stam2	Cluster -0	0.477857	0.821084	1.67223	NaN	-0.505236	NaN	-0.904171	-0.477857
P61971	Nuclear transport factor 2	Nutf2	Cluster -0	0.442552	0.795349	1.47149	0.93463	-0.745786	-1.33423	-0.774941	-0.442552
P13745;Q6P8Q0;P10648;D3Z6A6;D3YZV3;E9Q6L7	Glutathione S-transferase A1;Glutathione S-transferase A1, N-terminally processed;Glutathione S-transferase;Glutathione S-transferase A2	Gsta1;Gsta2;Gm10639	Cluster -0	0.441928	0.790837	1.4769	0.944521	-0.717785	-1.33685	-0.779903	-0.441928

P18654;B1AXN9	Ribosomal protein S6 kinase alpha-3	Rps6ka3	Cluster -0	0.442672	0.796259	1.47036	0.932588	-0.751507	-1.33367	-0.773911	-0.442672
P50396	Rab GDP dissociation inhibitor alpha	Gdi1	Cluster -0	0	0.280113	0.998475	0.557262	-0.781077	-1.63601	-1.15214	NaN
Q791V5;A2AFW6;Q9D050	Mitochondrial carrier homolog 2	Mtch2	Cluster -0	0	0.320756	0.909332	0.423387	-1.10382	-1.58295	-1.08019	NaN
Q3TH73;Q3TH73-2	Protein tweety homolog 2	Ttyh2	Cluster -0	0.439325	0.774543	1.49392	0.977468	-0.620987	-1.3444	-0.796113	-0.439325
O54962	Barrier-to-autointegration factor;Barrier-to-autointegration factor, N-terminally processed	Banf1	Cluster -0	0.438767	0.7714	1.4968	0.983378	-0.602996	-1.34556	-0.798962	-0.438767
P63213	Guanine nucleotide-binding protein G(I)/G(S)/G(O) subunit gamma-2	Gng2	Cluster -0	0.438754	0.771323	1.49687	0.983522	-0.602551	-1.34559	-0.79903	-0.438754
Q8VEK3;G3XA10	Heterogeneous nuclear ribonucleoprotein U	Hnrnpu;Gm28062	Cluster -0	0.440544	0.781815	1.48678	0.963275	-0.663369	-1.34138	-0.789197	-0.440544
A0A1L1SQA8;P62852	40S ribosomal protein S25	Rps25	Cluster -0	0.440519	0.781633	1.48698	0.963644	-0.66229	-1.34145	-0.789371	-0.440519
P23591	GDP-L-fucose synthase	Tsta3	Cluster -0	0.440877	0.783867	1.48464	0.959132	-0.675558	-1.34042	-0.787152	-0.440877
P35980;A0A1B0GSS8;A0A1B0GQU8;A0A1B0GSA8;A0A1B0GSF7	60S ribosomal protein L18	Rpl18	Cluster -0	0.444674	0.848633	1.3692	0.775391	-1.14295	-1.27502	-0.690224	-0.444674
Q3U429;Q61470;A0A1B0GS72;Q3U1W9;A0A1B0GSZ7	Tetraspanin;Leukocyte antigen CD37	Cd37	Cluster -0	0.444125	0.852811	1.35598	0.757151	-1.18311	-1.26652	-0.680038	-0.444125
Q08879-2	Fibulin-1	Fbln1	Cluster -0	-0.411656	0.207781	0.901985	0	NaN	NaN	NaN	-1.72447
Q9D071-2;Q9D071;Q9D071-3;E9PW47;F7C9N6	MMS19 nucleotide excision repair protein homolog	Mms19	Cluster -0	-0.416013	0.200585	0.898412	0	NaN	NaN	NaN	-1.72614
P62900;A0A0A6YX26;A0A0A6YXL3	60S ribosomal protein L31	Rpl31	Cluster -0	0.443243	0.857606	1.33894	0.734174	-1.23238	-1.2554	-0.66709	-0.443243
Q9CQW1	Synaptobrevin homolog YKT6	Ykt6	Cluster -0	0.442868	0.859244	1.33261	0.725759	-1.25008	-1.2512	-0.662304	-0.442868
Q922Q8	Leucine-rich repeat-containing protein 59	Lrrc59	Cluster -0	-0.40076	0.225693	0.910803	0	NaN	NaN	NaN	-1.72014
O35343;A0A0B4J1E7	Importin subunit alpha-3	Kpna4	Cluster -0	0.441495	0.86399	1.31207	0.698952	-1.30523	-1.23749	-0.646998	-0.441495
Q9QXS1-2;Q9QXS1;Q9QXS1-10;Q9QXS1-9;Q9QXS1-12;Q9QXS1-11;Q9QXS1-13;Q9QXS1-5;Q9QXS1-16;Q9QXS1-4;Q9QXS1-14;Q9QXS1-6;Q9QXS1-7;Q9QXS1-8;Q9QXS1-15;E9Q3W4	Plectin	Plec	Cluster -0	0.441543	0.863848	1.31274	0.699812	-1.30349	-1.23794	-0.647494	-0.441543
Q923D2;E9PZC3;E9PZC4	Flavin reductase (NADPH)	Blvrb	Cluster -0	0.44163	0.863586	1.31395	0.701382	-1.30031	-1.23876	-0.648392	-0.44163
P62301;Q921R2	40S ribosomal protein S13	Rps13	Cluster -0	0.440992	0.865394	1.30529	0.690247	-1.32276	-1.23292	-0.641992	-0.440992
Q9QZD9	Eukaryotic translation initiation factor 3 subunit I	Eif3i	Cluster -0	0.440573	0.86646	1.29989	0.68336	-1.33649	-1.22925	-0.638015	-0.440573
Q8R2Y8	Peptidyl-tRNA hydrolase 2, mitochondrial	Ptrh2	Cluster -0	-0.324176	0.348357	0.968274	0	NaN	NaN	NaN	-1.68404
Q9WU28;E9PZ62	Prefoldin subunit 5	Pfdn5	Cluster -0	-0.371582	0.273083	0.933615	0	NaN	NaN	NaN	-1.70755
D3YUT3;D3Z722;Q9CZX8;D3YUG3;D3Z5R8;S4R223	40S ribosomal protein S19	Rps19	Cluster -0	0.437627	0.87216	1.2658	0.640761	-1.41899	-1.20579	-0.613204	-0.437627
Q8R105	Vacuolar protein sorting-associated protein 37C	Vps37c	Cluster -0	0.437426	0.872464	1.26368	0.638146	-1.42392	-1.2043	-0.61167	-0.437426
P16331	Phenylalanine-4-hydroxylase	Pah	Cluster -0	0.437054	0.873	1.25976	0.633353	-1.43291	-1.20157	-0.608853	-0.437054
Q8VHX6;Q8VHX6-2	Filamin-C	Flnc	Cluster -0	0.437256	0.872709	1.26187	0.635928	-1.42808	-1.20305	-0.610371	-0.437256
H3BKH6;Q9R0P3;H3BLJ9;H3BJL6;H3BJP2;H3BK43	S-formylglutathione hydrolase	Esd	Cluster -0	0.438085	0.871437	1.27072	0.6468	-1.40753	-1.2092	-0.616754	-0.438085
P55258	Ras-related protein Rab-8A	Rab8a	Cluster -0	0.436026	0.874336	1.24931	0.620651	-1.45651	-1.19426	-0.60137	-0.436026
Q9DAV6		Serpinb9b	Cluster -0	0.435169	0.875318	1.24088	0.61049	-1.47513	-1.18833	-0.595357	-0.435169
Q63918	Serum deprivation-response protein	Sdpr	Cluster -0	0.444466	0.812602	1.44732	0.892958	-0.858909	-1.32168	-0.753599	-0.444466
Q8BGU5-2;Q8BGU5	Cyclin-Y	Ccny	Cluster -0	0.467964	0.864047	1.5051	NaN	-0.971804	NaN	-0.778281	-0.467964

E9QKK8;F6Q8D3;Q9QZW0-2;Q9QZW0	Phospholipid-transporting ATPase;Phospholipid-transporting ATPase 11C	Atp11c	Cluster -0	0.470303	0.8615	1.52779	NaN	-0.922052	NaN	-0.794439	-0.470303
P29595	NEDD8	Nedd8	Cluster -0	0.470581	0.861132	1.53063	NaN	-0.915622	NaN	-0.796476	-0.470581
Q8VCQ8;E9QA16;E9Q0M9;D3Z6I7;E9QA15;S4R1T7		Cald1	Cluster -0	0.445431	0.833179	1.4089	0.832651	-1.01043	-1.29961	-0.721615	-0.445431
P51432	1-phosphatidylinositol 4,5-bisphosphate phosphodiesterase beta-3	Plcb3	Cluster -0	0.445429	0.834426	1.40612	0.828503	-1.02038	-1.29794	-0.719372	-0.445429
P58242	Acid sphingomyelinase-like phosphodiesterase 3b	Smpdl3b	Cluster -0	0.445432	0.833164	1.40893	0.832691	-1.01033	-1.29963	-0.721633	-0.445432
Q3TQQ9-3;Q3TQQ9;Q3TQQ9-2	Uncharacterized protein C1orf112 homolog		Cluster -0	NaN	0.00544642	0.710455	-0.00544642	NaN	NaN	NaN	-1.57962
Q9DC28-2;Q9DC28;Q3TYE1;F7A4U8	Casein kinase I isoform delta	Csnk1d;Csnk1e	Cluster -0	NaN	0.00147261	0.711282	-0.00147261	NaN	NaN	NaN	-1.57926
Q3TCH7	Cullin-4A	Cul4a	Cluster -0	0.44543	0.832462	1.41047	0.835009	-1.00476	-1.30055	-0.722887	-0.44543
P62814	V-type proton ATPase subunit B, brain isoform	Atp6v1b2	Cluster -0	0.445431	0.832199	1.41104	0.835861	-1.0027	-1.30089	-0.723345	-0.445431
Q60817;P70670	Nascent polypeptide-associated complex subunit alpha;Nascent polypeptide-associated complex subunit alpha, muscle-specific form	Naca	Cluster -0	0.445426	0.831647	1.41223	0.837662	-0.998336	-1.3016	-0.724318	-0.445426
Q9JKR6	Hypoxia up-regulated protein 1	Hyou1	Cluster -0	0.445193	0.8234	1.42875	0.863075	-0.93566	-1.31128	-0.737898	-0.445193
Q9DCN2-2;Q9DCN2;F2Z456;A0A0A0MQM3	NADH-cytochrome b5 reductase 3;NADH-cytochrome b5 reductase 3 membrane-bound form;NADH-cytochrome b5 reductase 3 soluble form;NADH-cytochrome b5 reductase	Cyb5r3	Cluster -0	0.445383	0.828952	1.41788	0.846245	-0.977419	-1.30495	-0.728929	-0.445383
P97311;Q3ULG5	DNA replication licensing factor MCM6;DNA helicase	Mcm6	Cluster -0	0.445357	0.827889	1.42004	0.84955	-0.969297	-1.30622	-0.730697	-0.445357
Q9DAK9	14 kDa phosphohistidine phosphatase	Phpt1	Cluster -0	0.445331	0.826985	1.42184	0.85233	-0.962446	-1.30727	-0.732179	-0.445331
Q80UJ7;A0A1D5RLG3	Rab3 GTPase-activating protein catalytic subunit	Rab3gap1	Cluster -0	NaN	0.0139259	0.708664	-0.0139259	NaN	NaN	NaN	-1.58032
Q9JLI8	Squamous cell carcinoma antigen recognized by T-cells 3	Sart3	Cluster -0	-0.962347	0.0299327	1.43948	-0.0299327	NaN	NaN	NaN	NaN
A0A087WNZ7;G5E870;A0A0B4J1N9	E3 ubiquitin-protein ligase TRIP12	Trip12	Cluster -0	-0.960661	0.0401546	1.44011	-0.0401546	NaN	NaN	NaN	NaN
Q8BWP8-2;Q8BWP8	Beta-1,4-glucuronyltransferase 1	B4gat1	Cluster -0	-0.962105	0.0314246	1.43958	-0.0314246	NaN	NaN	NaN	NaN
D3YUV1		Nrbp1	Cluster -0	0.445261	0.840935	1.3905	0.805594	-1.07432	-1.2884	-0.706899	-0.445261
Q9QZM4	Tumor necrosis factor receptor superfamily member 10B	Tnfrsf10b	Cluster -0	0.445181	0.842422	1.38665	0.800055	-1.08712	-1.286	-0.703854	-0.445181
Q6NV83-3;Q6NV83-2;Q6NV83	U2 snRNP-associated SURP motif-containing protein	U2surp	Cluster -0	NaN	1.53299	0.69319	-0.545843	NaN	-0.933526	0	NaN
Q91Z96;Q91Z96-2	BMP-2-inducible protein kinase	Bmp2k	Cluster -0	-1.37364	NaN	NaN	NaN	1.03483	NaN	0.145335	-0.145335
Q8R2U4;A0A0A6YXY1;A2APZ3;A0A0A6YX97	N-terminal Xaa-Pro-Lys N-methyltransferase 1;N-terminal Xaa-Pro-Lys N-methyltransferase 1, N-terminally processed	Ntmt1	Cluster -1	-1.09288	NaN	NaN	NaN	1.33984	NaN	0.0722834	-0.0722834
Q8BIJ6;E9PWN2	Isoleucine--tRNA ligase, mitochondrial	Iars2	Cluster -1	-1.09106	NaN	0.899767	0	NaN	NaN	NaN	NaN
P14234	Tyrosine-protein kinase Fgr	Fgr	Cluster -1	-1.06603	NaN	NaN	NaN	1.36194	NaN	0.0658912	-0.0658912
F8WIG5;Q9Z207	Protein diaphanous homolog 3	Diap3;Diaph3	Cluster -1	-1.09916	NaN	NaN	NaN	1.33453	NaN	0.0737901	-0.0737901
D3Z4D1;O88824	Protein JTB	Jtb	Cluster -1	-1.10761	NaN	NaN	NaN	1.32729	NaN	0.0758273	-0.0758273
E9Q9N6;E9PYX3;A0A0R4J227;A0A0R4J0B1;Q3T9A3;F6ZS70;E9QMP6;Q05512-3;Q05512-4;Q05512;Q05512-2	Serine/threonine-protein kinase MARK2	Mark2	Cluster -1	-1.10177	NaN	NaN	NaN	1.3323	NaN	0.0744196	-0.0744196
S4R203;B2RUJ8		Arhgap12	Cluster -1	-1.06979	NaN	NaN	NaN	1.35891	NaN	0.0667804	-0.0667804

A0A1W2P7Q6;Q9CRT8	Exportin-T	Xpot	Cluster -1	-1.12581	0	0.855891	NaN	NaN	NaN	NaN	NaN
Q8K3W3	Protein CASC3	Casc3	Cluster -1	-1.1234	NaN	0.859052	0	NaN	NaN	NaN	NaN
Q9EPT5;Q9EPT5-2	Solute carrier organic anion transporter family member 2A1	Slco2a1	Cluster -1	-0.438456	NaN	NaN	0	1.94534	NaN	-0.141626	0.0578505
Q9CY16	28S ribosomal protein S28, mitochondrial	Mrps28	Cluster -1	-0.431812	NaN	NaN	0	1.94749	NaN	-0.126784	0.0687807
Q9CQX2	Cytochrome b5 type B	Cyb5b	Cluster -1	NaN	-0.340526	1.3726	0	NaN	NaN	NaN	NaN
Q6PB90	Protocadherin beta-14	Pcdhb14	Cluster -1	NaN	-0.327539	1.37576	0	NaN	NaN	NaN	NaN
O08528;E9Q5B5	Hexokinase-2;Hexokinase	Hk2	Cluster -1	-0.440318	NaN	NaN	0	1.9447	NaN	-0.145801	0.0547729
S4R1M0;S4R2V1;S4R1S4;P06800-3;P06800-2;P06800	Protein-tyrosine-phosphatase;Receptor-type tyrosine-protein phosphatase C	Ptprc	Cluster -1	-0.426498	NaN	NaN	0	1.94907	NaN	-0.114972	0.0774685
Q9Z1D1	Eukaryotic translation initiation factor 3 subunit G	Eif3g	Cluster -1	NaN	NaN	NaN	-1.25232	1.3782	0.718227	0	-0.128046
Q9CR68	Cytochrome b-c1 complex subunit Rieske, mitochondrial;Cytochrome b-c1 complex subunit 11	Uqcrfs1	Cluster -1	-1.16854	0	0.796561	NaN	NaN	NaN	NaN	NaN
P17156	Heat shock-related 70 kDa protein 2	Hspa2	Cluster -1	-1.14841	NaN	NaN	NaN	1.29091	NaN	0.0857752	-0.0857752
B0QZN5;P63044	Vesicle-associated membrane protein 2	Vamp2	Cluster -1	-1.18806	NaN	NaN	NaN	1.25308	NaN	0.0956523	-0.0956523
D3Z4L9;Q61333	Tumor necrosis factor alpha-induced protein 2	Tnfaip2	Cluster -1	-1.17959	NaN	NaN	NaN	1.26138	NaN	0.0935234	-0.0935234
Q7TSH2	Phosphorylase b kinase regulatory subunit beta	Phkb	Cluster -1	-1.1654	NaN	NaN	-1.48147	0.863456	0.818855	0.12452	-0.12452
Q61165	Sodium/hydrogen exchanger 1	Slc9a1	Cluster -1	-1.15765	NaN	NaN	-1.44633	0.936099	0.815018	0.117113	-0.117113
Q60738	Zinc transporter 1	Slc30a1	Cluster -1	-1.15757	NaN	NaN	-1.446	0.936772	0.814977	0.117043	-0.117043
P47941	Crk-like protein	Crkl	Cluster -1	-1.16114	NaN	NaN	-1.46152	0.905347	0.816784	0.120283	-0.120283
Q3TFP0;Q9R0U0-3;Q9R0U0-2;Q9R0U0	Serine/arginine-rich splicing factor 10	Srsf10	Cluster -1	-1.19209	0	0.760873	NaN	NaN	NaN	NaN	NaN
Q9CR62;Q5SX46	Mitochondrial 2-oxoglutarate/malate carrier protein	Slc25a11	Cluster -1	NaN	-1.71591	0.22531	0.0494863	-0.0494863	NaN	NaN	NaN
Q99K30;Q99K30-2	Epidermal growth factor receptor kinase substrate 8-like protein 2	Eps8l2	Cluster -1	-1.60548	NaN	NaN	NaN	0	1.12731	0.289171	-0.260748
Q61191;B1AUX2	Host cell factor 1;HCF N-terminal chain 1;HCF N-terminal chain 2;HCF N-terminal chain 3;HCF N-terminal chain 4;HCF N-terminal chain 5;HCF N-terminal chain 6;HCF C-terminal chain 1;HCF C-terminal chain 2;HCF C-terminal chain 3;HCF C-terminal chain 4;HCF C-terminal chain 5;HCF C-terminal chain 6	Hcfc1	Cluster -1	-1.62092	NaN	NaN	NaN	0	1.10624	0.267968	-0.277555
A2A4I8;A2A4I9;O70423-2;Q812C9;O70423	Amine oxidase;Membrane primary amine oxidase;Retina-specific copper amine oxidase	Aoc3;Aoc2	Cluster -1	-1.63956	NaN	NaN	NaN	0	1.07915	0.241122	-0.29859
Q8C4G3;Q8C288;A2AQC3;O70228	Phospholipid-transporting ATPase;Probable phospholipid-transporting ATPase IIA	Atp9a	Cluster -1	-1.67327	NaN	NaN	NaN	0	1.02453	0.188344	-0.339155
Q7TMD7	Desmoglein-4	Dsg4	Cluster -1	-0.833507	-0.796181	NaN	1.01856	0.796181	NaN	NaN	NaN
Q8BH95	Enoyl-CoA hydratase, mitochondrial	Echs1	Cluster -1	-0.809311	-0.80482	1.02447	NaN	0.80482	NaN	NaN	NaN
Q9JI10-2;Q9JI10	Serine/threonine-protein kinase 3;Serine/threonine-protein kinase 3 36kDa subunit;Serine/threonine-protein kinase 3 20kDa subunit	Stk3	Cluster -1	-1.63317	NaN	NaN	NaN	0.27625	0.424426	-0.27625	NaN
Q6DFZ1;Q6A099		Gbf1	Cluster -1	NaN	-1.66663	NaN	NaN	0.13871	0.428804	-0.13871	NaN
Q8CGB6-2;Q8CGB6-4;Q8CGB6;Q8CGB6-3	Tensin-2	Tns2	Cluster -1	-1.62602	NaN	NaN	NaN	0.174024	0.543601	-0.174024	NaN
Q8R420	ATP-binding cassette sub-family A member 3	Abca3	Cluster -1	-1.75968	NaN	NaN	NaN	0.0875547	0.825507	0	-0.463038

O35632;A0A0A6YXZ3;A0A0A6YXJ6;A0A0A6YX37;Q8C309	Hyaluronidase-2;Hyaluronidase	Hyal2	Cluster -1	NaN	-1.59631	NaN	NaN	-0.0767725	0.663337	0.0767725	NaN
Q148V8	Protein FAM83H	Fam83h	Cluster -1	NaN	-1.64078	NaN	NaN	0.0275874	0.553474	-0.0275874	NaN
Q9QXE7	F-box-like/WD repeat-containing protein TBL1X	Tbl1x	Cluster -1	NaN	NaN	NaN	NaN	0.240954	1.33019	-0.240954	-1.05569
Q9JK81;F8WGG3;F7A3N3	UPF0160 protein MYG1, mitochondrial	Myg1	Cluster -1	-0.489481	-0.310079	1.60253	NaN	0.310079	NaN	NaN	NaN
Q91W61	F-box/LRR-repeat protein 15	Fbxl15	Cluster -1	-0.421307	-0.217967	1.65151	NaN	0.217967	NaN	NaN	NaN
D3Z315;O89079;F6YFR7	Coatomer subunit epsilon	Cope	Cluster -1	-0.431344	-0.231355	1.64526	NaN	0.231355	NaN	NaN	NaN
G5E8J9;Q8CFE4	SCY1-like protein 2	Scyl2	Cluster -1	-0.472186	-0.286442	1.61646	NaN	0.286442	NaN	NaN	NaN
Q9Z1A1;B8JJG9;B8JJG7;B8JJG8;B8JJG6		Tfg	Cluster -1	-0.15133	0	1.55789	NaN	0.473505	NaN	NaN	-1.15146
Q9CQJ4;A0A087WRE9	E3 ubiquitin-protein ligase RING2	Rnf2	Cluster -1	NaN	NaN	NaN	NaN	NaN	0.76155	0	-1.19165
Q8CII2;Q8CII2-2	Cell division cycle protein 123 homolog	Cdc123	Cluster -1	NaN	NaN	NaN	NaN	NaN	0.761845	0	-1.19147
E9QMV2;Q4KML4;A0A1W2P7X0	Costars family protein ABRACL	Abracl	Cluster -1	NaN	NaN	NaN	NaN	NaN	0.760728	0	-1.19218
Q63850	Nuclear pore glycoprotein p62	Nup62	Cluster -1	NaN	NaN	NaN	NaN	NaN	0.761011	0	-1.192
Q9QUH0	Glutaredoxin-1	Glrx	Cluster -1	-0.438634	-0.30532	1.28334	0.970612	0.30532	NaN	NaN	-1.42552
Q9D051	Pyruvate dehydrogenase E1 component subunit beta, mitochondrial	Pdhb	Cluster -1	-0.485343	-0.372321	1.22814	0.942114	0.372321	NaN	NaN	-1.44613
E9Q9T8;Q3UIK0;O70468;Q3TF37	Myosin-binding protein C, cardiac-type	Mybpc3	Cluster -1	-0.423702	-0.284108	1.29984	0.978935	0.284108	NaN	NaN	-1.41815
Q3U0V1	Far upstream element-binding protein 2	Khsrp	Cluster -1	-0.487458	-0.37538	1.22551	0.940731	0.37538	NaN	NaN	-1.44697
Q99LH1	Nucleolar GTP-binding protein 2	Gnl2	Cluster -1	-0.300957	NaN	0.955306	0.300957	NaN	NaN	NaN	-1.38067
Q8C2Q3;E9QL13;Q8C2Q3-2	RNA-binding protein 14	Rbm14	Cluster -1	-0.291086	NaN	0.960372	0.291086	NaN	NaN	NaN	-1.38138
P60670;P60670-2	Nuclear protein localization protein 4 homolog	Nploc4	Cluster -1	-0.297719	-0.532723	NaN	NaN	0	1.57074	1.07719	NaN
P59268	Palmitoyltransferase ZDHHC9	Zdhhc9	Cluster -1	-0.302393	NaN	0.954563	0.302393	NaN	NaN	NaN	-1.38055
P52875;D3YV67	Transmembrane protein 165	Tmem165	Cluster -1	-0.30166	NaN	0.954943	0.30166	NaN	NaN	NaN	-1.38061
P25322	G1/S-specific cyclin-D1	Ccnd1	Cluster -1	-0.236765	-0.458075	NaN	NaN	0	1.5833	1.10782	NaN
J3QQ30;J3QPW1;P53810	Phosphatidylinositol transfer protein alpha isoform	Pitpna	Cluster -1	-0.307966	NaN	0.95166	0.307966	NaN	NaN	NaN	-1.38009
E9Q4P1		Wdfy1	Cluster -1	-0.296293	NaN	0.95771	0.296293	NaN	NaN	NaN	-1.38102
E9Q8Z5;P30999-2;P30999-3;E9Q903;E9Q906	Catenin delta-1	Ctnnd1	Cluster -1	-0.298985	NaN	0.956325	0.298985	NaN	NaN	NaN	-1.38082
Q9ESX5;B7ZCL7	H/ACA ribonucleoprotein complex subunit 4	Dkc1	Cluster -1	-0.849271	1.13081	NaN	0	NaN	NaN	NaN	NaN
A2AJ72;Q3TIX6;A0A0A6YVV5		Fubp3	Cluster -1	-0.852018	NaN	-1.50857	NaN	0.860445	0.507848	0	NaN
Q3UGI9;Q3UD93;Q3U7U3	F-box only protein 7	Fbxo7	Cluster -1	-0.909831	1.08268	NaN	0	NaN	NaN	NaN	NaN
Q60716-2;Q5SX75;Q60716	Prolyl 4-hydroxylase subunit alpha-2	P4ha2	Cluster -1	-0.950698	1.04698	NaN	0	NaN	NaN	NaN	NaN
G3X9T8;G3X8Q5;E9PZD8;Q61147	Ceruloplasmin	Cp	Cluster -1	-0.939261	1.05726	NaN	0	NaN	NaN	NaN	NaN
E9PXY1;A2A432-2;A2A432;J3QJX0	Cullin-4B	Cul4b	Cluster -1	-0.959417	NaN	-1.86579	NaN	0.344231	0.666586	0.133277	-0.133277
D3Z0R8;Q8BGB2	Tetratricopeptide repeat protein 7A	Ttc7;Ttc7a	Cluster -1	-0.943868	1.05314	NaN	0	NaN	NaN	NaN	NaN
Q8C8U0;Q8C8U0-3;Q8C8U0-2	Liprin-beta-1	Ppfibp1	Cluster -1	-0.95854	NaN	-1.85611	NaN	0.397419	0.667076	0.128665	-0.128665
Q8BVG4;Q8BVG4-2	Dipeptidyl peptidase 9	Dpp9	Cluster -1	-0.980873	1.01877	NaN	0	NaN	NaN	NaN	NaN
P10711;E9PYD5;P10711-2	Transcription elongation factor A protein 1	Tcea1	Cluster -1	-0.958836	NaN	-1.85886	NaN	0.382927	0.666982	0.129931	-0.129931
Q8BMJ3	Eukaryotic translation initiation factor 1A, X-chromosomal	Eif1ax	Cluster -1	-0.958436	NaN	-1.85521	NaN	0.402069	0.6671	0.128257	-0.128257

F6V084;Q8VBT0	Thioredoxin-related transmembrane protein 1	Tmx1	Cluster -1	-0.422635	-0.881241	-1.13633	-0.48987	1.68034	1.11281	0.522553	0.422635
Q8BK64	Activator of 90 kDa heat shock protein ATPase homolog 1	Ahsa1	Cluster -1	-0.423846	-0.881125	-1.14543	-0.500023	1.66414	1.11951	0.528782	0.423846
A0A0G2JDE3;A0A0G2JFV3;A0A0G2JG66;A0A0G2JDF4;A0A0G2JFF5;A0A0G2JDK6;A0A0G2JGM8;Q8JZZ7;Q8JZZ7-2;A0A0G2JEQ8;A0A0G2JH16	Latrophilin-2	Lphn2	Cluster -1	-0.421305	-0.881283	-1.12653	-0.479003	1.69748	1.10557	0.515874	0.421305
Q91VI7;A0A1B0GSG5	Ribonuclease inhibitor	Rnh1	Cluster -1	-0.421615	-0.881281	-1.12881	-0.481526	1.69352	1.10725	0.517426	0.421615
Q8C788;Q91ZR2	Sorting nexin;Sorting nexin-18	Snx18	Cluster -1	-0.419712	-0.881242	-1.115	-0.466309	1.71723	1.09703	0.508041	0.419712
Q8CJG0	Protein argonaute-2	Ago2	Cluster -1	-0.418519	-0.881138	-1.10651	-0.457019	1.73149	1.09072	0.502301	0.418519
Q9R1S8;F2Z3X0	Calpain-7	Capn7	Cluster -1	-0.419005	-0.881191	-1.10997	-0.460803	1.7257	1.09329	0.504641	0.419005
A0A1L1SRJ4;Q9QY33	Tetraspanin-3	Tspan3	Cluster -1	-0.838429	NaN	-1.52603	-0.87469	1.3207	0.672396	0.082676	0
Q8CI59;Q8CI59-2;A0A0R4J1G9;E9QN92;D3YTP0	Metalloreductase STEAP3	Steap3	Cluster -1	-0.837166	NaN	-1.5177	-0.864347	1.34041	0.667766	0.0776764	0
Q9EQP2	EH domain-containing protein 4	Ehd4	Cluster -1	-0.423497	-0.895296	-1.04895	-0.392862	1.83733	1.02114	0.437748	0.392862
Q9DBH5	Vesicular integral-membrane protein VIP36	Lman2	Cluster -1	-0.428355	-0.902001	-1.04131	-0.383883	1.85469	1.00337	0.420982	0.383883
Q3ULB1;Q921W7;P47226-2;P47226	Testin	Tes	Cluster -1	-0.436059	-0.912521	-1.02857	-0.369213	1.88212	0.974274	0.393703	0.369213
E9Q855;Q3UXS0;O35609	Secretory carrier-associated membrane protein 3	Scamp3	Cluster -1	-0.433603	-0.909181	-1.03271	-0.373945	1.87339	0.983678	0.40249	0.373945
O08529	Calpain-2 catalytic subunit	Capn2	Cluster -1	-0.426655	-0.899661	-1.04402	-0.387042	1.84863	1.00963	0.426874	0.387042
Q920E5	Farnesyl pyrophosphate synthase	Fdps	Cluster -1	-0.826642	NaN	-1.45864	-0.793614	1.46749	0.635381	0.0443641	0
P97855	Ras GTPase-activating protein-binding protein 1	G3bp1	Cluster -1	-0.817563	NaN	-1.41562	-0.744459	1.54859	0.612197	0.0220343	0
Q8R3H7	Heparan sulfate 2-O-sulfotransferase 1	Hs2st1	Cluster -1	-0.863016	NaN	NaN	-0.806496	1.4993	0.597392	0	NaN
P35285;A2ARZ7	Ras-related protein Rab-22A	Rab22a	Cluster -1	-0.414444	-0.880442	-1.07834	-0.426506	1.7773	1.06966	0.483338	0.414444
Q8BMA6;A2AAN2	Signal recognition particle subunit SRP68	Srp68	Cluster -1	-0.413423	-0.880189	-1.07144	-0.419119	1.78815	1.06448	0.478716	0.413423
Q9D0K2;Q3UJQ9	Succinyl-CoA:3-ketoacid coenzyme A transferase 1, mitochondrial;Succinyl-CoA:3-ketoacid-coenzyme A transferase	Oxct1	Cluster -1	NaN	NaN	NaN	NaN	1.41293	NaN	0	-0.06016
Q9JJ28	Protein flightless-1 homolog	Flii	Cluster -1	-0.92024	NaN	NaN	-0.914404	1.3946	0.610019	0	NaN
Q6ZWX6	Eukaryotic translation initiation factor 2 subunit 1	Eif2s1	Cluster -1	-0.415829	-0.884613	-1.06046	-0.406646	1.80981	1.04831	0.463575	0.406646
A0A1D5RLL3;Q8BG67;Q8BG67-2	Protein EFR3 homolog A	Efr3a	Cluster -1	-0.412701	-0.879993	-1.06662	-0.413964	1.79567	1.06084	0.475487	0.412701
Q6ZWQ5;Q3TGS7;Q3V2H3;O70493	Sorting nexin-12	Snx12	Cluster -1	-0.413278	-0.881032	-1.06413	-0.411126	1.80063	1.05713	0.472001	0.411126
Q9CZW5	Mitochondrial import receptor subunit TOM70	Tomm70a	Cluster -1	NaN	NaN	NaN	-1.22247	1.14531	0.311309	-0.311309	NaN
E9PUK3;E9PUI5;Q8K012-2;Q8K012	Formin-binding protein 1-like	Fnbp1l	Cluster -1	-0.894638	NaN	NaN	-0.865461	1.44393	0.604699	0	NaN
Q99JF8;A2BI12;Q99JF8-2;F6RB63	PC4 and SFRS1-interacting protein	Psip1	Cluster -1	-1.32546	NaN	NaN	NaN	1.09928	NaN	0.131783	-0.131783
Q63870	Collagen alpha-1(VII) chain	Col7a1	Cluster -1	NaN	-1.2826	NaN	-0.898416	1.11889	0.543949	0	NaN
A2AQN5;A2AQN4;Q9QXG4	Acetyl-coenzyme A synthetase, cytoplasmic	Acss2	Cluster -1	NaN	-1.30466	NaN	-0.955593	1.04239	0.546006	0	NaN
Q3U9G9	Lamin-B receptor	Lbr	Cluster -1	-1.28732	NaN	NaN	NaN	1.146	NaN	0.121416	-0.121416
Q05186	Reticulocalbin-1	Rcn1	Cluster -1	-1.36079	NaN	NaN	NaN	0.908824	0.401433	NaN	-0.401433
Q9JL60	Glucocorticoid modulatory element-binding protein 1	Gmeb1	Cluster -1	NaN	NaN	-1.38898	NaN	0.979464	0.23599	-0.23599	NaN

Q8BTI9	Phosphatidylinositol 4,5-bisphosphate 3-kinase catalytic subunit beta isoform	Pik3cb	Cluster -1	NaN	-1.46665	NaN	-1.29431	0.793489	0.721952	0.106918	-0.106918
Q9CZU3	Superkiller viralicidic activity 2-like 2	Skiv2l2	Cluster -1	-1.52195	NaN	NaN	NaN	0.781137	NaN	0.191693	-0.191693
Q9D172;A0A1W2P870;A0A1W2P7B6	ES1 protein homolog, mitochondrial	D10Jhu81e	Cluster -1	NaN	-1.32059	NaN	-1.00129	0.977017	0.546717	0	NaN
Q921M3-2	Splicing factor 3B subunit 3	Sf3b3	Cluster -1	NaN	-1.34104	NaN	-1.06915	0.871998	0.546023	0	NaN
A0A0J9YU83;F7BJB9		Morc3	Cluster -1	-0.831193	NaN	-1.46357	NaN	0.952173	0.510342	0	NaN
Q8K396	Meiotic nuclear division protein 1 homolog	Mnd1	Cluster -1	NaN	-1.31385	NaN	-0.98139	1.00598	0.546516	0	NaN
Q8QZT1	Acetyl-CoA acetyltransferase, mitochondrial	Acat1	Cluster -1	-0.488436	-0.927573	NaN	-0.617302	1.46238	1.06904	0.488436	NaN
Q9WVA4;A0A0A6YXG6	Transgelin-2	Tagln2	Cluster -1	-0.42952	-0.879511	-1.1904	-0.551093	1.57974	1.15228	0.559829	0.42952
Q9DBD5	Proline-, glutamic acid- and leucine-rich protein 1	Pelp1	Cluster -1	-0.431239	-0.878578	-1.205	-0.568031	1.55064	1.16279	0.570023	0.431239
Q8BZ20	Poly [ADP-ribose] polymerase 12	Parp12	Cluster -1	-0.43225	-0.877903	-1.21387	-0.578406	1.53253	1.16914	0.576245	0.43225
Q922D8;A0A1W2P733	C-1-tetrahydrofolate synthase, cytoplasmic;Methylenetetrahydrofolate dehydrogenase;Methenyltetrahydrofolate cyclohydrolase;Formyltetrahydrofolate synthetase;C-1-tetrahydrofolate synthase, cytoplasmic, N-terminally processed	Mthfd1	Cluster -1	-0.43151	-0.878407	-1.20734	-0.570757	1.54589	1.16446	0.571665	0.43151
Q9WU60	Attractin	Atrn	Cluster -1	-0.434818	-0.875687	-1.23751	-0.606442	1.48249	1.18594	0.592956	0.434818
Q9D662	Protein transport protein Sec23B	Sec23b	Cluster -1	-0.435602	-0.874837	-1.2451	-0.61557	1.46585	1.1913	0.598367	0.435602
Q3UHG5;Q62283	Tetraspanin;Tetraspanin-7	Tspan7	Cluster -1	-0.433477	-0.876943	-1.22495	-0.591482	1.50939	1.17704	0.584056	0.433477
O88792	Junctional adhesion molecule A	F11r	Cluster -1	-0.433211	-0.877166	-1.22252	-0.5886	1.51452	1.17531	0.582343	0.433211
F8VQD7;Q05909;E9Q6E7	Protein-tyrosine-phosphatase;Receptor-type tyrosine-protein phosphatase gamma	Ptprg	Cluster -1	-0.433498	-0.876924	-1.22515	-0.59172	1.50897	1.17718	0.584204	0.433498
B2RRF0;A0A1W2P7Y1;P35822	Protein-tyrosine-phosphatase;Receptor-type tyrosine-protein phosphatase kappa	Ptprk	Cluster -1	-0.434513	-0.875997	-1.23462	-0.602984	1.48876	1.18389	0.590899	0.434513
A2ACH6;P82347	Delta-sarcoglycan	Sgcd	Cluster -1	-0.4349	-0.875605	-1.2383	-0.607384	1.48078	1.1865	0.59351	0.4349
Q3TBT3-3;Q3TBT3;Q3TBT3-2	Stimulator of interferon genes protein	Tmem173	Cluster -1	NaN	NaN	NaN	-1.39684	1.219	0.730953	0	-0.169072
Q9CR51	V-type proton ATPase subunit G 1	Atp6v1g1	Cluster -1	NaN	NaN	NaN	-1.49267	1.09221	0.734714	0	-0.198028
Q62312-2;Q62312	TGF-beta receptor type-2	Tgfbr2	Cluster -1	-0.4404	-0.866877	-1.2977	-0.680576	1.34202	1.22776	0.636405	0.4404
P63005;P63005-2	Platelet-activating factor acetylhydrolase IB subunit alpha	Pafah1b1	Cluster -1	-0.441293	-0.864574	-1.3093	-0.695378	1.31245	1.23562	0.64494	0.441293
Q3U8S1;A2APM5;A2APM3;A2APM4;E9QKM8;Q80X37;A2APM1;A2APM2;P15379-2;P15379-3;P15379-6;P15379-11;P15379-5;P15379-10;P15379-9;P15379-4;P15379-8;P15379-7;P15379	CD44 antigen	Cd44	Cluster -1	-0.440656	-0.866258	-1.30094	-0.684692	1.33384	1.22996	0.638784	0.440656
Q9D3L3;O09044;B0R030;E9Q8A1;B0R029	Synaptosomal-associated protein;Synaptosomal-associated protein 23	Snap23	Cluster -1	-0.441119	-0.865066	-1.30695	-0.69237	1.31849	1.23404	0.64321	0.441119
A0A0U1RQ57			Cluster -1	-1.15352	NaN	NaN	-1.42935	0.969421	0.812864	0.113618	-0.113618
P51863	V-type proton ATPase subunit d 1	Atp6v0d1	Cluster -1	-1.14932	NaN	NaN	-1.41296	1.00059	0.810618	0.110293	-0.110293
P70460	Vasodilator-stimulated phosphoprotein	Vasp	Cluster -1	-0.439548	-0.868757	-1.28737	-0.667527	1.36763	1.22069	0.62884	0.439548
Q9EPK2-3;Q9EPK2;Q9EPK2-2;Q9EPK2-4	Protein XRP2	Rp2	Cluster -1	-0.438922	-0.869982	-1.28007	-0.658404	1.38532	1.21567	0.623527	0.438922

A2AKH7;Q8JZX5;Q9D1G5	Leucine-rich repeat-containing protein 57	Lrrc57	Cluster -1	-0.438989	-0.869856	-1.28082	-0.659346	1.38351	1.21619	0.624076	0.438989
Q04736	Tyrosine-protein kinase Yes	Yes1	Cluster -1	-0.438804	-0.870195	-1.27872	-0.656722	1.38856	1.21474	0.622547	0.438804
P01899	H-2 class I histocompatibility antigen, D-B alpha chain	H2-D1	Cluster -1	NaN	-1.56248	NaN	NaN	0.555092	0.353929	NaN	-0.353929
A0A087WQQ5;F8VQC7;Q61595-5;Q61595;A0A087WNW3;A0A087WQI3;A0A087WQ25;A0A087WRS1;Q61595-6;Q61595-9;Q61595-15	Kinectin	Ktn1	Cluster -1	NaN	-1.56021	NaN	NaN	0.563052	0.352651	NaN	-0.352651
D3YU12;Q8K2T1;G5E8S7;Q8K2T1-2	NmrA-like family domain-containing protein 1	Nmral1	Cluster -1	NaN	-1.5566	NaN	NaN	0.575413	0.350646	NaN	-0.350646
P70202	Latexin	Lxn	Cluster -1	-1.13771	NaN	NaN	-1.37104	1.07626	0.804195	0.101981	-0.101981
D3YVU0;Q9D9M2-2;P62069;Q9D9M2	Ubiquitin carboxyl-terminal hydrolase 12;Ubiquitin carboxyl-terminal hydrolase 46	Usp46;Usp12	Cluster -1	-1.1406	NaN	NaN	-1.38108	1.05862	0.805818	0.103949	-0.103949
Q9JKV5	Secretory carrier-associated membrane protein 4	Scamp4	Cluster -1	-1.14203	NaN	NaN	-1.38615	1.04962	0.806617	0.104947	-0.104947
O54984	ATPase Asna1	Asna1	Cluster -1	-0.437533	-0.872307	-1.26477	-0.639488	1.42138	1.20507	0.612465	0.437533
P29416	Beta-hexosaminidase subunit alpha	Hexa	Cluster -1	-0.43802	-0.871551	-1.27	-0.645925	1.4092	1.2087	0.616235	0.43802
P46978	Dolichyl-diphosphooligosaccharide--protein glycosyltransferase subunit STT3A	Stt3a	Cluster -1	-0.562777	-0.984824	NaN	-0.854283	1.14862	1.16085	0.562777	NaN
Q9DCR2	AP-3 complex subunit sigma-1	Ap3s1	Cluster -1	-0.559873	-0.983006	NaN	-0.844313	1.16355	1.15761	0.559873	NaN
Q6PGB6-2;Q6PGB6;Q6PGB6-4;Q6PGB6-3;Q6PGB6-5	N-alpha-acetyltransferase 50	Naa50	Cluster -1	-0.556407	-0.98078	NaN	-0.832509	1.18101	1.15371	0.556407	NaN
Q8C0E3-2	Tripartite motif-containing protein 47	Trim47	Cluster -1	-0.444439	-0.850586	-1.36318	-0.767047	1.16144	1.27117	0.685575	0.444439
Q8BH64	EH domain-containing protein 2	Ehd2	Cluster -1	-0.443428	-0.856738	-1.3422	-0.738532	1.22315	1.25755	0.669552	0.443428
Q64737	Trifunctional purine biosynthetic protein adenosine-3;Phosphoribosylamine--glycine ligase;Phosphoribosylformylglycinamidine cyclo-ligase;Phosphoribosylglycinamide formyltransferase	Gart	Cluster -1	-0.44437	-0.851107	-1.36152	-0.764749	1.16649	1.2701	0.684292	0.44437
E9PUF7;Q61210;Q61210-4;Q61210-3;F6ZN61	Rho guanine nucleotide exchange factor 1	Arhgef1	Cluster -1	-0.444158	-0.85262	-1.35662	-0.758026	1.18121	1.26693	0.680525	0.444158
O35375-2;O35375-3;O35375-4;O35375	Neuropilin-2	Nrp2	Cluster -1	-0.444127	-0.852805	-1.356	-0.757183	1.18304	1.26654	0.680059	0.444127
Q80X95;Q6NTA4	Ras-related GTP-binding protein A;Ras-related GTP-binding protein B	Rraga;Rragb	Cluster -1	-0.677808	NaN	-1.10901	-0.427914	1.94817	0.571065	0	0.0780945
Q60607;P36895	Receptor protein serine/threonine kinase;Bone morphogenetic protein receptor type-1A	Bmpr1a	Cluster -1	-0.688177	NaN	-1.1296	-0.447863	1.92771	0.573157	0	0.0725564
Q60676;F7BX26	Serine/threonine-protein phosphatase 5;Serine/threonine-protein phosphatase	Ppp5c	Cluster -1	-0.683267	NaN	-1.11984	-0.438392	1.93749	0.572179	0	0.0751914
Q91YS7;Q63932	Dual specificity mitogen-activated protein kinase kinase 2	Map2k2	Cluster -1	-0.450773	-0.939722	-0.880748	-0.218788	2.08749	0.775533	0.218788	0.288462
Q8BHL7	CDC42 small effector protein 1	Cdc42se1	Cluster -1	-0.451307	-0.936665	-0.951923	-0.288744	2.00228	0.857582	0.288744	0.318616
Q62432-2;Q62432;E9Q3M0	Mothers against decapentaplegic homolog 2;Mothers against decapentaplegic homolog	Smad2	Cluster -1	-0.451353	-0.937791	-0.934709	-0.271573	2.02413	0.837646	0.271573	0.311288
F8VQ29		Iqgap3	Cluster -1	-0.45128	-0.936393	-0.955601	-0.292445	1.99749	0.861861	0.292445	0.320188
P98063	Bone morphogenetic protein 1	Bmp1	Cluster -1	-0.451306	-0.936653	-0.952076	-0.288896	2.00208	0.857759	0.288896	0.31868
Q61035	Histidine--tRNA ligase, cytoplasmic	Hars	Cluster -1	-0.746902	NaN	-1.24735	-0.56507	1.79601	0.582909	0	0.0390695
Q9D832	DnaJ homolog subfamily B member 4	Dnajb4	Cluster -1	-0.743284	NaN	-1.24003	-0.557616	1.80499	0.582423	0	0.0412498

Q3TZZ7	Extended synaptotagmin-2	Esyt2	Cluster -1	-0.739909	NaN	-1.23321	-0.550696	1.81326	0.581955	0	0.0432678
B1B0C7		Hspg2	Cluster -1	-0.451041	-0.939416	-0.895792	-0.233351	2.07057	0.792793	0.233351	0.294807
P25911;P25911-2	Tyrosine-protein kinase Lyn	Lyn	Cluster -1	-0.451226	-0.93893	-0.910964	-0.248154	2.05294	0.810244	0.248154	0.301223
Q6DFW4;A0A0A0MQ76	Nucleolar protein 58	Nop58	Cluster -1	-0.442567	-0.885845	NaN	-0.222329	1.86829	0.655777	NaN	0.222329
O88200	C-type lectin domain family 11 member A	Clec11a	Cluster -1	-0.424631	-0.86891	NaN	-0.285051	1.8123	0.785962	NaN	0.285051
P47811;P47811-4;P47811-3;B2KF35;P47811-2;B2KF34	Mitogen-activated protein kinase 14	Mapk14	Cluster -1	-0.432988	-0.877132	NaN	-0.257077	1.83873	0.728037	NaN	0.257077
A0A0X1KG62;Q8C4Y3	Negative elongation factor B	Nelfb	Cluster -1	NaN	NaN	-1.17633	-0.521783	1.74971	0.5303	-0.0252866	0.0252866
Q99KE1	NAD-dependent malic enzyme, mitochondrial	Me2	Cluster -1	-0.711958	NaN	-1.17703	-0.494412	1.87781	0.577559	0	0.0594548
P24638;B7ZCF4;B7ZCF5	Lysosomal acid phosphatase	Acp2	Cluster -1	-0.720378	NaN	-1.19391	-0.511179	1.85907	0.578977	0	0.0546735
P50431;G3UZ26;G3UYY1	Serine hydroxymethyltransferase, cytosolic;Serine hydroxymethyltransferase	Shmt1	Cluster -1	-0.729668	NaN	-1.21257	-0.529862	1.8377	0.580449	0	0.0493047
Q8C0E3	Tripartite motif-containing protein 47	Trim47	Cluster -1	-0.447697	-0.928141	-1.00777	-0.345999	1.92324	0.928	0.350793	0.345999
P57780;A0A1L1SV25;E9Q2W9	Alpha-actinin-4	Actn4	Cluster -1	-0.450193	-0.931433	-1.00304	-0.340832	1.93203	0.917679	0.341286	0.340832
P59325	Eukaryotic translation initiation factor 5	Eif5	Cluster -1	-0.450456	-0.931783	-1.00246	-0.340209	1.93306	0.916504	0.340209	0.340256
Q99KP6;Q99KP6-2;Q99KP6-3	Pre-mRNA-processing factor 19	Prpf19	Cluster -1	NaN	-1.20252	-1.29536	-0.673916	1.45232	0.558931	0.0142003	0
Q6P572;Q9Z2D1	Myotubularin-related protein 2	Mtmr2	Cluster -1	NaN	-1.20092	-1.28086	-0.657978	1.47661	0.551226	0.00719007	0
A0A1L1STE6;Q9D6R2;Q9D6R2-2	Isocitrate dehydrogenase [NAD] subunit alpha, mitochondrial	Idh3a	Cluster -1	NaN	-1.13937	NaN	-0.604376	1.43846	0.517098	0	NaN
F6W4D3;D3YY36;Q9DBD0	Inhibitor of carbonic anhydrase	1300017J02Rik;Ica	Cluster -1	-0.770966	NaN	-1.31118	NaN	1.53981	0.561622	0.00109148	-0.00109148
Q8C0M5;Q8BGE4	Sushi domain-containing protein 6	Susd6	Cluster -1	NaN	-1.18183	-1.22066	-0.592554	1.5709	0.542381	0	0.0151969
Q8VI94	2-5-oligoadenylate synthase-like protein 1	Oasl1	Cluster -1	-0.793343	NaN	-1.34217	-0.66406	1.66822	0.587497	0	0.00942246
Q9R0L6;Q9R0L6-2	Pericentriolar material 1 protein	Pcm1	Cluster -1	-0.451231	-0.935921	-0.961551	-0.298427	1.98969	0.868762	0.298427	0.322721
Q8K274	Ketosamine-3-kinase	Fn3krp	Cluster -1	-0.451034	-0.934612	-0.976345	-0.313418	1.9698	0.885984	0.313418	0.329046
P52800;F6RSU6	Ephrin-B2	Efnb2	Cluster -1	-0.451205	-0.93572	-0.963989	-0.300886	1.98646	0.871594	0.300886	0.323762
P18406	Protein CYR61	Cyr61	Cluster -1	-0.451126	-0.935166	-0.970377	-0.30735	1.9779	0.879027	0.30735	0.32649
E9QNX9;Q60751	Tyrosine-protein kinase receptor;Insulin-like growth factor 1 receptor;Insulin-like growth factor 1 receptor alpha chain;Insulin-like growth factor 1 receptor beta chain	Igf1r	Cluster -1	-0.450868	-0.9337	-0.985447	-0.322704	1.95724	0.896601	0.322704	0.332949
O88839-3;O88839-2;O88839;O88839-4	Disintegrin and metalloproteinase domain-containing protein 15	Adam15	Cluster -1	-0.451015	-0.934506	-0.977432	-0.314523	1.96832	0.88725	0.314523	0.329517
A0A0R4J0T5;P28659-2;P28659-3;P28659;P28659-4	CUGBP Elav-like family member 1	Celf1	Cluster -1	NaN	-1.04929	-0.930685	-0.30006	1.91344	0.521101	0	0.0999082
A2AJT5;A2AJT4;A2AJT3	Arginine/serine-rich protein PNISR	Pnisr	Cluster -1	NaN	-1.05604	-0.944004	-0.312818	1.9009	0.522559	0	0.0964121
P17918;A0A140T8V5	Proliferating cell nuclear antigen	Pcna	Cluster -1	-0.614505	NaN	-0.984392	-0.310125	2.05806	0.556312	0	0.109895
E9PXU2;Q9Z0F8;Q9Z0F8-2	Disintegrin and metalloproteinase domain-containing protein 17	Adam17	Cluster -1	-0.622452	NaN	-0.999942	-0.324566	2.04556	0.558337	0	0.106077
A0A1D5RLY2;Q80WQ2	Protein VAC14 homolog	Vac14	Cluster -1	-0.631137	NaN	-1.01697	-0.340455	2.0315	0.560495	0	0.10185
A2BE28-2;A2BE28	Ribosomal biogenesis protein LAS1L	Las1l	Cluster -1	-0.612693	NaN	-0.980851	-0.306846	2.06086	0.555845	0	0.110759
Q9JLV5;E9Q4T8	Cullin-3	Cul3	Cluster -1	-0.448047	-0.938534	-0.799811	-0.142325	2.16942	0.683377	0.142325	0.254581
A0A067XG53;O70589-3;O70589-4;O70589-5;O70589;O70589-2	Peripheral plasma membrane protein CASK	Cask	Cluster -1	-0.448408	-0.938854	-0.807826	-0.149765	2.16195	0.692454	0.149765	0.257916
Q6IRU2	Tropomyosin alpha-4 chain	Tpm4	Cluster -1	-0.448382	-0.938833	-0.807253	-0.149231	2.16249	0.691809	0.149231	0.257682
Q9ERN0;A0A1L1SUU4	Secretory carrier-associated membrane protein 2	Scamp2	Cluster -1	-0.599999	NaN	-0.956069	-0.283998	2.08	0.552502	0	0.116747

A0A140LHA2;Q9WVA3;A0A140LJ21	Mitotic checkpoint protein BUB3	Bub3	Cluster -1	-0.608956	NaN	-0.973549	-0.300096	2.06658	0.554873	0	0.112533
P62869	Transcription elongation factor B polypeptide 2	Tceb2	Cluster -1	-0.601934	NaN	-0.959842	-0.287466	2.07714	0.553019	0	0.115841
A2AC16;Q91X52	L-xylulose reductase	Dcxr	Cluster -1	-0.595265	NaN	-0.946845	-0.275537	2.08692	0.551228	0	0.118951
Q99MK8;Q7TS64	Beta-adrenergic receptor kinase 1	Adrbk1	Cluster -1	NaN	-1.01151	NaN	-0.316214	1.65874	0.354146	NaN	0
Q925I1;Q925I1-2	ATPase family AAA domain-containing protein 3	Atad3	Cluster -1	NaN	-1.01457	NaN	-0.322187	1.655	0.357537	NaN	0
Q61011	Guanine nucleotide-binding protein G(I)/G(S)/G(T) subunit beta-3	Gnb3	Cluster -1	NaN	-1.0041	NaN	-0.301829	1.66763	0.345965	NaN	0
Q8CG48	Structural maintenance of chromosomes protein 2	Smc2	Cluster -1	NaN	-1.04342	NaN	-0.380175	1.61691	0.390301	NaN	0
Q99JB8;B1AW92;B1AW94;B1AW93;B1AW91;A6PWR1	Protein kinase C and casein kinase II substrate protein 3	Pacsin3	Cluster -1	-0.657876	NaN	-1.06958	-0.390115	1.98544	0.566772	0	0.088464
A2AW05;Q08943;Q08943-2	FACT complex subunit SSRP1	Ssrp1	Cluster -1	-0.647502	NaN	-1.04913	-0.370712	2.00382	0.564404	0	0.0937261
P35235;P35235-2	Tyrosine-protein phosphatase non-receptor type 11	Ptpn11	Cluster -1	-0.653043	NaN	-1.06004	-0.381053	1.99409	0.565681	0	0.0909274
B9EHJ3;P39447;A0A0U1RPW2	Tight junction protein ZO-1	Tjp1	Cluster -1	-0.449613	-0.939674	-0.838573	-0.178567	2.13202	0.727375	0.178567	0.27076
Q5Y5T1-2;Q5Y5T1	Probable palmitoyltransferase ZDHHC20	Zdhhc20	Cluster -1	-0.449164	-0.939424	-0.826254	-0.166976	2.14426	0.713363	0.166976	0.265607
A0A0A6YXC8;E9QKR1;A0A0A6YW06;Q03173-6;Q03173-3;Q03173-4;J3QNM3;E9QKQ9;E9QLZ9;Q03173-5;Q03173	Protein enabled homolog	Enah	Cluster -1	-0.499087	NaN	-0.761053	-0.109671	2.20478	0.522323	0	0.160688
P43275	Histone H1.1	Hist1h1a	Cluster -1	-0.497316	NaN	-0.757659	-0.106716	2.20658	0.521741	0	0.161407
Q9Z1J3-2;Q9Z1J3	Cysteine desulfurase, mitochondrial	Nfs1	Cluster -1	-0.465542	-0.902172	NaN	-0.121694	1.93443	0.444673	NaN	0.121694
Q9DCC4	Pyrroline-5-carboxylate reductase 3	Pycrl	Cluster -1	-0.466371	-0.902585	NaN	-0.117398	1.93663	0.435602	NaN	0.117398
Q8BX70-3;Q8BX70;Q8BX70-2	Vacuolar protein sorting-associated protein 13C	Vps13c	Cluster -1	-0.463671	-0.901181	NaN	-0.131174	1.92939	0.464671	NaN	0.131174
O88848;D3Z067;O88848-2	ADP-ribosylation factor-like protein 6	Arl6	Cluster -1	-0.465899	-0.902352	NaN	-0.119853	1.93538	0.440785	NaN	0.119853
Q61205;D3Z7E6;D3Z2X5;Q8CA83	Platelet-activating factor acetylhydrolase IB subunit gamma	Pafah1b3	Cluster -1	-0.466547	-0.90267	NaN	-0.116478	1.93709	0.433658	NaN	0.116478
P63024	Vesicle-associated membrane protein 3	Vamp3	Cluster -1	-0.442895	-0.932428	-0.711913	-0.0624708	2.24289	0.584478	0.0624708	0.218202
Q60598;Q921L6	Src substrate cortactin	Cttn	Cluster -1	-0.442031	-0.931239	-0.699878	-0.0517737	2.25181	0.571025	0.0517737	0.213252
Q8R016;E9PY26	Bleomycin hydrolase	Blmh	Cluster -1	-0.5078	NaN	-0.777763	-0.124257	2.19575	0.525158	0	0.157128
Q62418-3;Q62418-2;Q62418	Drebrin-like protein	Dbnl	Cluster -1	NaN	NaN	-0.800862	-0.17836	2.034	0.421541	-0.077323	0.077323
P13864;J3QNW0;P13864-2	DNA (cytosine-5)-methyltransferase 1;DNA (cytosine-5)-methyltransferase	Dnmt1	Cluster -1	NaN	NaN	-0.810534	-0.186744	2.02888	0.424501	-0.0761398	0.0761398
P97807-2;P97807	Fumarate hydratase, mitochondrial	Fh	Cluster -1	NaN	-0.970252	-0.781463	-0.160628	2.03741	0.50229	0	0.137047
Q6ZWZ4;A0A140T8K6;P47964	60S ribosomal protein L36	Rpl36	Cluster -1	-0.522971	NaN	-0.806919	-0.149854	2.17928	0.53	0	0.150829
Q9QWH1;Q9QWH1-2	Polyhomeotic-like protein 2	Phc2	Cluster -1	-0.530429	NaN	-0.821274	-0.162529	2.17084	0.532333	0	0.147686
O70172;F6RJE8	Phosphatidylinositol 5-phosphate 4-kinase type-2 alpha	Pip4k2a	Cluster -1	-0.553206	NaN	-0.865229	-0.201641	2.14356	0.539263	0	0.137887
A2ALB1;A2ALB2;Q6PAQ4	RNA exonuclease 4	Rexo4	Cluster -1	-0.544304	NaN	-0.84803	-0.186282	2.1545	0.53659	0	0.141753
J3QJU5;Q3TJ91	Lethal(2) giant larvae protein homolog 2	Llgl2	Cluster -1	-0.542247	NaN	-0.844059	-0.182746	2.15697	0.535966	0	0.14264
B1AZ15;B1AZ14;Q3UMF0-3;Q3UMF0-4;Q3UMF0-2;Q3UMF0	Cordon-bleu protein-like 1	Cobll1	Cluster -1	-0.445012	-0.935187	-0.743885	-0.0911602	2.2179	0.62032	0.0911602	0.231389
P53996-2;P53996-3	Cellular nucleic acid-binding protein	Cnbp	Cluster -1	-0.444443	-0.934468	-0.734859	-0.0830221	2.22515	0.610188	0.0830221	0.227662
F8WI56;D3Z7D3;Q8BWT5	Disco-interacting protein 2 homolog A	Dip2a	Cluster -1	-0.56549	NaN	-0.889002	-0.22299	2.12789	0.542872	0	0.132473

P11928;Q8K469;Q05BJ7	2-5-oligoadenylate synthase 1A	Oas1a;Oas1g	Cluster -1	-0.567364	NaN	-0.892634	-0.226264	2.12544	0.543414	0	0.131638
Q9JJ78;D3YVF2	Lymphokine-activated killer T-cell-originated protein kinase	Pbk	Cluster -1	-0.632374	NaN	NaN	-0.310617	1.83542	0.367247	NaN	0
Q9CX34	Suppressor of G2 allele of SKP1 homolog	Sugt1	Cluster -1	-0.663037	NaN	NaN	-0.37568	1.8042	0.405093	NaN	0
Q8K0D5	Elongation factor G, mitochondrial	Gfm1	Cluster -1	-0.64783	NaN	NaN	-0.343168	1.82027	0.386225	NaN	0
Q8BYC6;A0A0R4J1T3	Serine/threonine-protein kinase TAO3	Taok3	Cluster -1	-0.653876	NaN	NaN	-0.356035	1.81402	0.393703	NaN	0
Q61335	B-cell receptor-associated protein 31	Bcap31	Cluster -1	-0.624075	NaN	NaN	-0.293334	1.84308	0.357136	NaN	0
Q8C3Y6;P70340	Mothers against decapentaplegic homolog;Mothers against decapentaplegic homolog 1	Smad1	Cluster -1	-0.629592	NaN	NaN	-0.304809	1.83802	0.363853	NaN	0
Q05CH9;Q5XPI3;Q5XPI3-2	E3 ubiquitin-protein ligase RNF123	Rnf123	Cluster -1	-0.639821	NaN	NaN	-0.326241	1.82826	0.376368	NaN	0
Q91XH5;G3UXX3;Q64105	Sepiapterin reductase	Spr	Cluster -1	-0.580314	NaN	-0.917761	-0.249008	2.10803	0.547103	0	0.125813
H3BJY1;H3BJ78;H3BKF4;H3BIZ8;B0QZP8;O55101	Synaptogyrin-2	Syngr2;Gm20708	Cluster -1	-0.575211	NaN	-0.907853	-0.24002	2.11499	0.545663	0	0.128121
P34022;H7BX22	Ran-specific GTPase-activating protein	Ranbp1	Cluster -1	-0.573294	NaN	-0.904133	-0.236652	2.11757	0.545117	0	0.128984
Q9DBZ5;Q9DBZ5-2;Q3TY56	Eukaryotic translation initiation factor 3 subunit K	Eif3k	Cluster -1	-0.457171	-0.897184	NaN	-0.161992	1.91133	0.529526	NaN	0.161992
Q8BPB5	EGF-containing fibulin-like extracellular matrix protein 1	Efemp1	Cluster -1	-0.45112	-0.892825	NaN	-0.188273	1.89385	0.584636	NaN	0.188273
P58389;A2AWE9	Serine/threonine-protein phosphatase 2A activator	Ppp2r4	Cluster -1	-0.458243	-0.897897	NaN	-0.157113	1.91436	0.519274	NaN	0.157113
A0A1B0GRX7;Q99KH2;A0A1B0GRB2;P63034-3;P63034-2;P63034;A0A1B0GRB8;G5E8Q4;O08967	Cytohesin-2;Cytohesin-3	Cyth2;Cyth3	Cluster -1	-0.460386	-0.899261	NaN	-0.147128	1.92037	0.498275	NaN	0.147128
P25206	DNA replication licensing factor MCM3	Mcm3	Cluster -1	-0.454506	-0.895331	NaN	-0.173821	1.9037	0.554352	NaN	0.173821
Q91VH2	Sorting nexin-9	Snx9	Cluster -1	-0.44764	-0.93815	-0.791194	-0.134356	2.1773	0.673628	0.134356	0.250995
H7BX95;Q6PDM2;Q6PDM2-3;Q6PDM2-2	Serine/arginine-rich splicing factor 1	Srsf1	Cluster -1	-0.446972	-0.937465	-0.778087	-0.122294	2.189	0.658824	0.122294	0.24555
Q60864	Stress-induced-phosphoprotein 1	Stip1	Cluster -1	-0.446517	-0.936964	-0.769547	-0.114477	2.19643	0.649196	0.114477	0.242009
P58404-2;P58404;V9GXE7	Striatin-4	Strn4	Cluster -1	-0.452599	NaN	-0.500983	NaN	1.87497	0.169278	NaN	0
E9QQ10;Q70FJ1-3;Q70FJ1-2;Q70FJ1	A-kinase anchor protein 9	Akap9	Cluster -1	-0.471347	NaN	NaN	0	1.93159	NaN	-0.216339	0.00258646
E9PYJ2;F6TSJ9;E0CXR8;E0CZE2;E0CZ83;B7ZNY3;F6S7Z1;G3XA13;A5D6P2;Q99NH2-3;Q99NH2-2;Q99NH2;A0A0R4J1Y4;Q99NH2-5;Q99NH2-4;F6UGU7;E0CX45;E0CY24;E0CXL4	Partitioning defective 3 homolog	Pard3	Cluster -1	-0.487302	NaN	-0.590318	NaN	1.83542	0.212813	NaN	0
E9PV44;O35143	ATPase inhibitor, mitochondrial	Atpif1	Cluster -1	-0.462565	NaN	NaN	0	1.93578	NaN	-0.19618	0.0175373
Q9CQ88	Tetraspanin-31	Tspan31	Cluster -1	-0.550281	NaN	-0.627418	0	2.27824	0.232087	-0.243265	0.0116715
P61514;A0A1D5RL86	60S ribosomal protein L37a	Rpl37a	Cluster -1	-0.486172	NaN	-0.632893	0	2.27887	0.38227	-0.108147	0.109616
A0A0R4J260;B2RRE7	OTU domain-containing protein 4	Otud4	Cluster -1	NaN	-0.960272	-0.593303	0	2.14953	0.256678	-0.19557	0.0356097
P18828-2;P18828	Syndecan-1	Sdc1	Cluster -1	-0.484944	NaN	-0.63294	0	2.27868	0.385017	-0.105637	0.111419
Q9CQM9;A0A1B0GS58	Glutaredoxin-3	Glrx3	Cluster -1	-0.467065	NaN	-0.699814	-0.0567387	2.23542	0.511563	0	0.173433
Q9CQM5	Thioredoxin domain-containing protein 17	Txndc17	Cluster -1	-0.484335	NaN	-0.732805	-0.0851552	2.21938	0.51743	0	0.166625
Q99MD9;B1AU75;B1AU76;Q99MD9-2	Nuclear autoantigenic sperm protein	Nasp	Cluster -1	-0.472511	NaN	-0.710207	-0.0656659	2.23049	0.513428	0	0.171302
P54728	UV excision repair protein RAD23 homolog B	Rad23b	Cluster -1	-0.47421	NaN	-0.713452	-0.0684579	2.22892	0.514007	0	0.170634
D3Z698;Q8BGA2	Lipoma HMGIC fusion partner-like 2 protein	Lhfpl2	Cluster -1	-0.477308	NaN	-0.719371	-0.0735559	2.22605	0.51506	0	0.169413

Q6P1B9;O08539-2;O08539	Myc box-dependent-interacting protein 1	Bin1	Cluster -1	-0.470493	NaN	-0.706354	-0.0623534	2.23233	0.512738	0	0.172094
Q9Z1X4;Q9Z1X4-3;A0A1L1STE4;Q45VK5;Q9Z1X4-2	Interleukin enhancer-binding factor 3	Ilf3	Cluster -1	-0.264485	-0.66799	-0.453628	NaN	1.9785	0.54189	NaN	0.264485
Q9ES00;G3UZD6	Ubiquitin conjugation factor E4 B	Ube4b	Cluster -1	NaN	-0.935752	NaN	-0.176214	1.73734	0.273788	NaN	0
Q99N15;A2AFQ2;O08756	3-hydroxyacyl-CoA dehydrogenase type-2	Hsd17b10	Cluster -1	NaN	-0.866571	-0.628442	NaN	1.67276	0.236597	NaN	0
Q8R0G9	Nuclear pore complex protein Nup133	Nup133	Cluster -1	NaN	-0.946065	NaN	-0.19444	1.72809	0.284342	NaN	0
A2A4Z1;Q9D1C1	Ubiquitin-conjugating enzyme E2 C	Ube2c	Cluster -1	-0.547663	NaN	-0.751278	NaN	1.74655	0.291881	NaN	0
B1AUN3;Q3UKV0;B1AUN2		Eif2b3	Cluster -1	NaN	-0.948459	NaN	-0.198705	1.72589	0.286807	NaN	0
Q8CIN4	Serine/threonine-protein kinase PAK 2;PAK-2p27;PAK-2p34	Pak2	Cluster -1	-0.438545	-0.926194	-0.655771	-0.0130116	2.28233	0.521882	0.0130116	0.19517
B1ATZ0;B1ATZ1;Q3UMA3;Q99LI8	Hepatocyte growth factor-regulated tyrosine kinase substrate	Hgs	Cluster -1	-0.443294	NaN	-0.654531	-0.0181038	2.2557	0.503247	0	0.182562
G3UZM9;Q8BWW9-2;Q8BWW9;G3UXH4;Q8BWW9-3	Serine/threonine-protein kinase N2	Pkn2	Cluster -1	-0.457032	NaN	-0.680684	-0.0403655	2.24423	0.508086	0	0.177319
A0A087WS76;A0A140LHL6;E9Q3S4	Mitogen-activated protein kinase kinase kinase 19	Map3k19	Cluster -1	-0.472668	-0.905099	NaN	-0.0824024	1.95271	0.361541	NaN	0.0824024
E9QAQ5;Q9WV60	Glycogen synthase kinase-3 beta	Gsk3b	Cluster -1	-0.470084	-0.904212	NaN	-0.0973105	1.94626	0.393129	NaN	0.0973105
P52795	Ephrin-B1	Efnb1	Cluster -1	NaN	-0.871357	-0.607872	-0.00554012	2.14807	0.475364	0	0.17611
Q9DAW9;A0A0G2JDV8	Calponin-3	Cnn3	Cluster -1	NaN	-0.880996	-0.624284	-0.0199071	2.139	0.478119	0	0.172588
Q99J09	Methylosome protein 50	Wdr77	Cluster -1	-0.474449	-0.905573	NaN	-0.0716031	1.95702	0.338624	NaN	0.0716031
Q8CG47;E9Q2X6	Structural maintenance of chromosomes protein 4;Structural maintenance of chromosomes protein	Smc4	Cluster -1	-0.476412	-0.905944	NaN	-0.0591342	1.9616	0.312128	NaN	0.0591342
Q8BP48	Methionine aminopeptidase 1	Metap1	Cluster -1	-0.473749	-0.905401	NaN	-0.0759003	1.95534	0.347747	NaN	0.0759003
A0JNY3;Q8BUV3	Gephyrin;Molybdopterin adenylyltransferase;Molybdopterin molybdenumtransferase	Gphn	Cluster -1	-0.474239	-0.905523	NaN	-0.0729065	1.95651	0.341391	NaN	0.0729065
F6ZBL2;Q80SY4	E3 ubiquitin-protein ligase MIB1	Mib1	Cluster -1	-0.474704	-0.90563	NaN	-0.0700202	1.95762	0.335263	NaN	0.0700202
Q6PIX5	Inactive rhomboid protein 1	Rhbdf1	Cluster -1	-0.443424	NaN	-0.633388	0	2.26861	0.475293	-0.0223408	0.170936
P37889-2;P37889	Fibulin-2	Fbln2	Cluster -1	-0.435963	-0.922259	-0.626369	0.0124468	2.30083	0.489264	-0.0124468	0.183165
P28658	Ataxin-10	Atxn10	Cluster -1	-0.434645	-0.920205	-0.612195	0.0246155	2.30924	0.473578	-0.0246155	0.177391
O54734	Dolichyl-diphosphooligosaccharide--protein glycosyltransferase 48 kDa subunit	Ddost	Cluster -1	-0.435123	-0.920949	-0.617246	0.0202884	2.30628	0.479164	-0.0202884	0.179447
A0A087WSN6;B9EHT6;B7ZNJ1		Fn1	Cluster -1	-0.427518	-0.908662	-0.542466	0.0835303	2.34599	0.396762	-0.0835303	0.149111
E9PWB1;D3Z4N0;D3Z0X5;Q6PDH0;Q6PDH0-2;F6RUK9;F6RYD0;E9Q307;E9PWW4	Pleckstrin homology-like domain family B member 1	Phldb1	Cluster -1	-0.439906	NaN	-0.633328	0	2.26742	0.482722	-0.0154157	0.175855
Q91ZR1	Ras-related protein Rab-4B	Rab4b	Cluster -1	-0.408906	NaN	NaN	0	1.9534	NaN	-0.0762296	0.105894
P35585	AP-1 complex subunit mu-1	Ap1m1	Cluster -1	-0.395952	NaN	NaN	0	1.95574	NaN	-0.0480389	0.126511
Q8BSL7	ADP-ribosylation factor 2	Arf2	Cluster -1	-0.381223	NaN	NaN	0	1.95755	NaN	-0.0163267	0.149636
Q9D1R2	Protein KTI12 homolog	Kti12	Cluster -1	0.438088	1.50084	NaN	-0.438088	NaN	NaN	-0.60303	NaN
Q99L48;Q99L48-2	60S ribosomal export protein NMD3	Nmd3	Cluster -1	NaN	NaN	NaN	-0.507682	1.63488	0.186322	NaN	-0.186322
Q91YR5	Methyltransferase-like protein 13	Mettl13	Cluster -1	0.44854	1.50926	NaN	-0.44854	NaN	NaN	-0.565461	NaN
Q91V88;Q91V88-2;D3YTX1;Q91V88-3;Q91V88-4;D3Z4D3	Nephronectin	Npnt	Cluster -1	0.440002	1.50243	NaN	-0.440002	NaN	NaN	-0.596242	NaN
Q8BWT1	3-ketoacyl-CoA thiolase, mitochondrial	Acaa2	Cluster -1	NaN	NaN	NaN	-0.474025	1.6467	0.178432	NaN	-0.178432
Q8BR63	Protein FAM177A1	Fam177a1	Cluster -1	NaN	NaN	NaN	-0.401597	1.66933	0.161349	NaN	-0.161349
P97329	Kinesin-like protein KIF20A	Kif20a	Cluster -1	NaN	NaN	NaN	-0.501958	1.63695	0.184983	NaN	-0.184983
Q05CL8	La-related protein 7	Larp7	Cluster -1	NaN	NaN	NaN	-0.490954	1.64086	0.182405	NaN	-0.182405

Q9JKB1	Ubiquitin carboxyl-terminal hydrolase isozyme L3	Uchl3	Cluster -1	NaN	NaN	-0.81483	NaN	1.51704	0.131637	NaN	-0.131637
Q5SSZ5	Tensin-3	Tns3	Cluster -1	NaN	NaN	-0.880656	NaN	1.47738	0.144581	NaN	-0.144581
Q91V61;Q91V61-2;Q3U4F0	Sideroflexin-3	Sfxn3	Cluster -1	NaN	NaN	NaN	-0.580324	1.60643	0.203242	NaN	-0.203242
Q8K1S3-2;Q8K1S3	Netrin receptor UNC5B	Unc5b	Cluster -1	-0.0508001	-0.240672	-1.20574	-0.867259	0.0508001	1.65155	1.21873	0.719756
Q80Y86	Mitogen-activated protein kinase 15	Mapk15	Cluster -1	-0.0420862	-0.22899	-1.19665	-0.862012	0.0420862	1.65559	1.22567	0.725077
P27600;A0A0G2JG40	Guanine nucleotide-binding protein subunit alpha-12	Gna12	Cluster -1	-0.0316622	-0.214998	-1.18568	-0.855659	0.0316622	1.66028	1.23385	0.731367
D3YVM2;Q9QY73	Transmembrane protein 59	Tmem59	Cluster -1	-0.0338124	-0.217886	-1.18795	-0.856973	0.0338124	1.65932	1.23217	0.730076
E9PWK7;Q8C8K1;P54761	Receptor protein-tyrosine kinase;Ephrin type-B receptor 4	Ephb4	Cluster -1	-0.0494239	-0.238836	-1.20431	-0.866433	0.0494239	1.6522	1.21983	0.720602
H7BWY2;Q9JKC8	AP-3 complex subunit mu-1	Ap3m1	Cluster -1	-0.06896	-0.264988	-1.22441	-0.878008	0.06896	1.64274	1.204	0.7085
O08688	Calpain-5	Capn5	Cluster -1	-0.0702161	-0.266669	-1.22569	-0.87874	0.0702161	1.64212	1.20296	0.707718
P46460	Vesicle-fusing ATPase	Nsf	Cluster -1	-0.0738945	-0.271584	-1.22943	-0.880886	0.0738945	1.64026	1.19992	0.705407
Q91YP3;A0A0N4SV34;A0A0N4SUV7	Deoxyribose-phosphate aldolase	Dera	Cluster -1	-0.0198224	-0.199084	-1.17307	-0.848337	0.0198224	1.66539	1.24298	0.738426
P00375	Dihydrofolate reductase	Dhfr	Cluster -1	-0.000184851	-0.172634	-1.15183	-0.835957	0.000184851	1.6734	1.25778	0.749917
A0A1C7CYV0;Q99K51;B1AX58	Plastin-3	Pls3	Cluster -1	-0.00697529	-0.181785	-1.15922	-0.84027	0.00697529	1.6707	1.25272	0.745979
O88952	Protein lin-7 homolog C	Lin7c	Cluster -1	-0.00459007	-0.178572	-1.15663	-0.838757	0.00459007	1.67165	1.2545	0.747364
Q9Z2M6	Ubiquitin-like protein 3	Ubl3	Cluster -1	0.0270932	-0.135796	-1.12165	-0.818262	-0.0270932	1.68353	1.2776	0.765439
Q8BPM0-3;Q8BPM0-2;Q8BPM0	Disheveled-associated activator of morphogenesis 1	Daam1	Cluster -1	0	-0.177216	NaN	-0.859636	-0.00036382	1.72088	1.29359	0.771245
Q91V35;P18052-2;P18052	Receptor-type tyrosine-protein phosphatase;Receptor-type tyrosine-protein phosphatase alpha	Ptpra	Cluster -1	0.0268173	-0.136168	-1.12196	-0.818446	-0.0268173	1.68344	1.2774	0.765284
Q9CPW4;Q3UA72	Actin-related protein 2/3 complex subunit 5	Arpc5	Cluster -1	0	-0.165287	-1.12608	NaN	-0.0195578	1.6317	1.22847	0.729843
Q8BGX0-3;Q8BGX0-2;Q8BGX0	E3 ubiquitin-protein ligase TRIM23	Trim23	Cluster -1	-0.00257674	-0.171339	-1.12713	NaN	0	1.63215	1.22597	0.730277
A0A087WNT1;P83940;A0A087WQE6;A0A087WPE4	Transcription elongation factor B polypeptide 1	Tceb1	Cluster -1	-0.00448886	-0.173659	-1.12963	NaN	0	1.63155	1.22485	0.729093
P31786;Q4VWZ5;M0QWU8	Acyl-CoA-binding protein	Dbi	Cluster -1	0	-0.159022	-1.13077	NaN	-0.0612097	1.62865	1.23031	0.725364
Q80SW1	Putative adenosylhomocysteinase 2	Ahcyl1	Cluster -1	-0.220242	-0.465443	-1.36609	-0.957471	0.220242	1.54921	1.06605	0.605706
P97765;A2A860	WW domain-binding protein 2	Wbp2	Cluster -1	-0.20533	-0.445849	-1.35325	-0.950451	0.20533	1.56006	1.08088	0.616571
P70207	Plexin-A2	Plxna2	Cluster -1	-0.206703	-0.447659	-1.35444	-0.951107	0.206703	1.55908	1.07952	0.615577
P35550	rRNA 2-O-methyltransferase fibrillarin	Fbl	Cluster -1	-0.206954	-0.447987	-1.35466	-0.951226	0.206954	1.5589	1.07928	0.615396
B7FAU9;Q8BTM8;B7FAV1	Filamin-A	Flna	Cluster -1	-0.187295	-0.4221	-1.33738	-0.94172	0.187295	1.57271	1.09845	0.629491
Q8CBB7;P22892	AP-1 complex subunit gamma-1	Ap1g1	Cluster -1	-0.172709	-0.402866	-1.32429	-0.93447	0.172709	1.58254	1.11236	0.639771
Q9D8F3;Q9D8F3-2	Solute carrier family 52, riboflavin transporter, member 2	Slc52a2	Cluster -1	-0.473129	-0.744984	NaN	NaN	0	1.5098	0.97039	NaN
P12265	Beta-glucuronidase	Gusb	Cluster -1	-0.485017	-0.76034	NaN	-1.32264	0	1.5151	0.970242	0.447639
Q6PDI5-2;Q6PDI5;A2ALV7	Proteasome-associated protein ECM29 homolog	Ecm29;AI314180	Cluster -1	-0.445023	-0.713521	NaN	-1.29056	0	1.5443	1.0061	0.479807
E9PV24	Fibrinogen alpha chain;Fibrinopeptide A;Fibrinogen alpha chain	Fga	Cluster -1	-0.309094	-0.552576	NaN	-1.17271	0	1.62589	1.11469	0.581228
Q91XQ0-2;Q91XQ0;Q91XQ0-3	Dynein heavy chain 8, axonemal	Dnah8	Cluster -1	-0.390951	-0.649823	NaN	-1.24526	0	1.57992	1.05167	0.521572
Q9ER00	Syntaxin-12	Stx12	Cluster -1	-0.131669	-0.348536	-1.28618	-0.913151	0.131669	1.60838	1.15013	0.66787
V9GX00;Q00560	Interleukin-6 receptor subunit beta	Il6st	Cluster -1	-0.1417	-0.361841	-1.29566	-0.918487	0.1417	1.60231	1.14108	0.661113
D3Z641;P62080	Tetraspanin;Tetraspanin-5	Tspan5	Cluster -1	-0.125936	-0.340923	-1.28071	-0.910065	0.125936	1.61178	1.15525	0.671697
G5E8J0;O35516;O35516-2	Neurogenic locus notch homolog protein 2;Notch 2 extracellular truncation;Notch 2 intracellular domain	Notch2	Cluster -1	-0.150356	-0.373299	-1.30375	-0.923017	0.150356	1.59695	1.13319	0.655227

H3BLL3;Q921G6;H3BIX9	Leucine-rich repeat and calponin homology domain-containing protein 4	Lrch4	Cluster -1	-0.715934	-1.00435	NaN	NaN	-0.325317	1.54222	0.942666	0.325317
E9PUB7;Q2YDW2;D3YX87;Q2YDW2-2	Protein misato homolog 1	Msto1	Cluster -1	-0.589157	-0.840708	NaN	NaN	-0.404119	1.59622	1.03517	0.404119
D3Z376;S4R217;D3Z118;P97411-2;P97411	Islet cell autoantigen 1	Ica1	Cluster -1	-0.706302	-0.991957	NaN	NaN	-0.331678	1.54721	0.950404	0.331678
A0A0A6YXL6;E9Q3Y4;Q9ESE1-2;Q9ESE1;A0A0A6YXX3;Q9ESE1-3;A0A1D5RM41	Lipopolysaccharide-responsive and beige-like anchor protein	Lrba	Cluster -1	-0.758068	-1.05848	NaN	NaN	-0.296699	1.51845	0.907305	0.296699
A0A0R4IZY0;Q8C1A5	Thimet oligopeptidase	Thop1	Cluster -1	-0.53301	-0.76791	NaN	NaN	-0.435915	1.61269	1.07023	0.435915
Q8K1A6;E9PX94	Coiled-coil and C2 domain-containing protein 1A	Cc2d1a	Cluster -1	-0.114046	-0.325117	-1.26925	-0.903586	0.114046	1.61866	1.16574	0.679569
Q9CQ22;A0A0A6YX02	Ragulator complex protein LAMTOR1	Lamtor1	Cluster -1	0.0701385	-0.0774226	-1.07242	-0.789182	-0.0701385	1.69718	1.3071	0.788878
Q8BVL3;D3Z7S9	Sorting nexin-17	Snx17	Cluster -1	0.0683505	-0.0683505	-1.07909	-0.80937	-0.141239	1.68606	1.30519	0.777728
Q78ZM0;O70492;D3Z789;D3Z6Z0	Sorting nexin-3	Snx3	Cluster -1	0.0642516	-0.0642516	-1.08698	-0.827441	-0.197701	1.67507	1.30111	0.766626
P35492	Histidine ammonia-lyase	Hal	Cluster -1	0.0621481	-0.0882802	-1.08171	-0.794689	-0.0621481	1.69487	1.30179	0.784623
P17710-3;G3UVV4;P17710-4;P17710;P17710-2	Hexokinase-1;Hexokinase	Hk1	Cluster -1	0.0685852	-0.0685852	-1.07862	-0.808307	-0.137957	1.68667	1.3054	0.778358
P34884	Macrophage migration inhibitory factor	Mif	Cluster -1	0.0649056	-0.0649056	-1.08577	-0.824611	-0.188763	1.67687	1.3018	0.768415
O88487;A2BFF8;Q3TPJ8;A2BFF9;A2BFF5	Cytoplasmic dynein 1 intermediate chain 2	Dync1i2	Cluster -1	0	-0.13667	-1.1445	NaN	-0.207128	1.61403	1.23382	0.707909
Q8CJ53-4;Q8CJ53-3;Q8CJ53-2;Q8CJ53	Cdc42-interacting protein 4	Trip10	Cluster -1	0	-0.143763	-1.14064	NaN	-0.16127	1.61928	1.23322	0.713691
D3Z7P3-2	Glutaminase kidney isoform, mitochondrial	Gls	Cluster -1	0	-0.170255	NaN	NaN	-0.400576	NaN	1.69979	0.959825
Q9DCW2;D3Z7J3	Phospholipid scramblase 2	Plscr2	Cluster -1	0	-0.127421	-1.14886	NaN	-0.266324	1.60634	1.23392	0.700041
Q99P91;Q8BVA0	Transmembrane glycoprotein NMB	Gpnmb	Cluster -1	0	-0.110799	-1.15485	NaN	-0.37105	1.59022	1.23222	0.684993
P0DP28;P0DP27;P0DP26;Q3UKW2		Calm1	Cluster -1	0	-0.121772	-1.15116	NaN	-0.302147	1.60119	1.23361	0.695056
P54823	Probable ATP-dependent RNA helicase DDX6	Ddx6	Cluster -1	0	-0.121867	-1.15112	NaN	-0.301551	1.60128	1.23362	0.695141
Q99JI4	26S proteasome non-ATPase regulatory subunit 6	Psmd6	Cluster -1	0.0561217	-0.0561217	-1.1007	-0.861539	-0.30805	1.65083	1.29103	0.743642
Q91XX1		Pcdhgc3	Cluster -1	0.0604509	-0.0604509	-1.09371	-0.843676	-0.249586	1.66413	1.29672	0.756034
A0A1D5RM92;Q9DBH0	NEDD4-like E3 ubiquitin-protein ligase WWP2	Wwp2	Cluster -1	0.0596595	-0.0596595	-1.09504	-0.846989	-0.260313	1.66177	1.29574	0.753797
A2AWF8;A2AWF9;E9Q4S7;Q64455	Protein-tyrosine-phosphatase;Receptor-type tyrosine-protein phosphatase eta	Ptprj	Cluster -1	0.0567211	-0.0567211	-1.09977	-0.859105	-0.300001	1.65273	1.29186	0.745378
Q9CWI3	BRCA2 and CDKN1A-interacting protein	Bccip	Cluster -1	0	-0.0729673	-1.16003	NaN	-0.601851	1.54305	1.2197	0.646612
Q3U487	E3 ubiquitin-protein ligase HECTD3	Hectd3	Cluster -1	0.0352119	-0.0352119	-1.12478	-0.938952	-0.581824	1.57462	1.25367	0.679053
P50518;A0A0N4SW07	V-type proton ATPase subunit E 1	Atp6v1e1	Cluster -1	0	-0.0650668	-1.15969	NaN	-0.648778	1.53144	1.21563	0.6379
A0A0U1RNK7;E9PX48;A2A9M5;A2A9M4;Q8R1A4-2;Q8R1A4	Dedicator of cytokinesis protein 7	Dock7	Cluster -1	0.0339007	-0.0339007	-1.12578	-0.943334	-0.598521	1.5692	1.25081	0.674756
A0A1B0GR11;Q93092	Transaldolase	Taldo1	Cluster -1	0	-0.0654378	-1.15972	NaN	-0.646583	1.532	1.21583	0.638315
Q6P1F6	Serine/threonine-protein phosphatase 2A 55 kDa regulatory subunit B alpha isoform	Ppp2r2a	Cluster -1	0	-0.0503083	-1.15778	NaN	-0.735296	1.50816	1.20673	0.621002
Q60692	Proteasome subunit beta type-6	Psmb6	Cluster -1	0	-0.0359633	-1.15434	NaN	-0.81798	1.48357	1.19646	0.603809
A0A0B4J1G6;P86176	T-cell immunoreceptor with Ig and ITIM domains	Tigit	Cluster -1	0	-0.0246279	-1.15055	NaN	-0.882351	1.4628	1.18725	0.58969
Q3UE92;Q6P1B1;S4R1I3	Xaa-Pro aminopeptidase 1	Xpnpep1	Cluster -1	0	-0.0522664	-1.15813	NaN	-0.723901	1.51136	1.208	0.623291

O08582	GTP-binding protein 1	Gtpbp1	Cluster -1	-1.34974	NaN	NaN	NaN	NaN	0.871661	0.457387	-0.457387
P27038	Activin receptor type-2A	Acvr2a	Cluster -1	-1.34979	NaN	NaN	NaN	NaN	0.871727	0.457256	-0.457256
Q8JZW4;A0A0R4J0J1;Q1RLL3	Copine-5;Copine-9	Cpne5;Cpne9	Cluster -1	-1.3503	NaN	NaN	NaN	NaN	0.872462	0.455791	-0.455791
D3YTR6;Q8R0G7;D3YWA9;D3YWU4;A0A0U1RPY3	Protein spinster homolog 1	Spns1	Cluster -1	-1.34875	NaN	NaN	NaN	NaN	0.870249	0.460189	-0.460189
A0A1L1SV73;Q8BY87-2;Q8BY87	Ubiquitin carboxyl-terminal hydrolase 47	Usp47	Cluster -1	-1.348	NaN	NaN	NaN	NaN	0.869187	0.462289	-0.462289
B1ATV0;Q9WVD4	Chloride channel protein;H(+)/Cl(-) exchange transporter 5	Clcn5	Cluster -1	-1.34766	NaN	NaN	NaN	NaN	0.868711	0.463229	-0.463229
Q9DCD6;B1AR50;Q8R3R8	Gamma-aminobutyric acid receptor-associated protein;Gamma-aminobutyric acid receptor-associated protein-like 1	Gabarap;Gabarapl1	Cluster -1	-1.34733	NaN	NaN	NaN	NaN	0.868245	0.464145	-0.464145
Q3THS6;A0A0U1RNT6;A0A0U1RNK6	S-adenosylmethionine synthase isoform type-2	Mat2a	Cluster -1	0.0474578	-0.0474578	-1.11258	-0.895363	-0.423193	1.62162	1.2775	0.717811
Q9WTX6;Q3TPM3	Cullin-1	Cul1	Cluster -1	0.0481898	-0.0481898	-1.11168	-0.892599	-0.413552	1.62422	1.27875	0.720048
Q8R050-2;Q8R050	Eukaryotic peptide chain release factor GTP-binding subunit ERF3A	Gspt1	Cluster -1	0	-0.098114	-1.15787	NaN	-0.449582	1.57599	1.22933	0.672751
Q6PDS3-2;Q6PDS3;Q6PDS3-3	Sterile alpha and TIR motif-containing protein 1	Sarm1	Cluster -1	0	-0.0982701	-1.15784	NaN	-0.448623	1.57618	1.22937	0.672905
P47199;A0A0A6YXR4;V9GXY8;D3YUG9;D3Z2X0	Quinone oxidoreductase	Cryz	Cluster -1	0	-0.0930368	-1.15871	NaN	-0.480688	1.56984	1.2278	0.667671
P45591	Cofilin-2	Cfl2	Cluster -1	0	-0.0989451	-1.15771	NaN	-0.444474	1.57698	1.22956	0.673572
D3YWS8;Q8CBY3	Leukocyte receptor cluster member 8 homolog	Leng8	Cluster -1	0	-0.0952607	-1.15836	NaN	-0.467087	1.57257	1.22849	0.669909
P15532;Q5NC80	Nucleoside diphosphate kinase A;Nucleoside diphosphate kinase	Nme1	Cluster -1	0	-0.0953795	-1.15835	NaN	-0.466358	1.57271	1.22853	0.670028
Q78HU3	Multivesicular body subunit 12A	Mvb12a	Cluster -1	0.0528705	-0.0528705	-1.10548	-0.87453	-0.351543	1.64027	1.28628	0.73411
A0A087WRZ7;A0A0G2JDM3;E9PWG4;A0A0G2JDW2;P05977-2;P05977;P09542	Myosin light chain 1/3, skeletal muscle isoform;Myosin light chain 3	Myl1;Myl3	Cluster -1	0.0540421	-0.0540421	-1.1038	-0.869884	-0.335898	1.64414	1.28804	0.73757
E9PWQ3;J3QQ16;A0A087WS16		Col6a3	Cluster -1	0.0516337	-0.0516337	-1.1072	-0.879377	-0.368008	1.63613	1.28437	0.730429
P83887;Q8VCK3	Tubulin gamma-1 chain;Tubulin gamma-2 chain	Tubg1;Tubg2	Cluster -1	0	-0.0827207	-1.15978	NaN	-0.543322	1.55657	1.22404	0.65704
P62274	40S ribosomal protein S29	Rps29	Cluster -1	0	-0.0862644	-1.15951	NaN	-0.521895	1.56124	1.22542	0.660738
P61087;A0A0J9YUI1;A0A0J9YU07;D3Z4U3	Ubiquitin-conjugating enzyme E2 K	Ube2k	Cluster -1	0	-0.0786393	-1.15998	NaN	-0.567898	1.55102	1.22231	0.65272
F8VPN4;A0A0G2JGI9;F6XXE6		Agl	Cluster -1	0	-0.0828872	-1.15977	NaN	-0.542318	1.55679	1.2241	0.657215
P52633	Signal transducer and transcription activator 6	Stat6	Cluster -1	0	-0.0842439	-1.15968	NaN	-0.534122	1.55859	1.22465	0.658636
Q9CQR6;A0A0N4SVL9	Serine/threonine-protein phosphatase 6 catalytic subunit;Serine/threonine-protein phosphatase 6 catalytic subunit, N-terminally processed	Ppp6c	Cluster -1	0.0433379	-0.0433379	-1.11728	-0.910569	-0.477087	1.60654	1.27009	0.705061
G5E8T0;P60904;A2AUE1	DnaJ homolog subfamily C member 5	Dnajc5	Cluster -1	-0.958057	-1.3797	NaN	-1.35909	0.644619	0.912436	0.288701	0
P49817;D3Z148;H3BKG0	Caveolin-1;Caveolin	Cav1	Cluster -1	-0.445427	-0.831897	-1.41168	-0.836841	1.00033	1.30128	0.723878	0.445427
Q5XJY5	Coatomer subunit delta	Arcn1	Cluster -1	-0.445426	-0.831958	-1.41156	-0.836658	1.00077	1.30121	0.723777	0.445426
Q9CXG3	Peptidyl-prolyl cis-trans isomerase-like 4	Ppil4	Cluster -1	-0.612535	-1.00649	NaN	-1.04128	0.832172	1.20822	0.612535	NaN
P47877;D3YU40	Insulin-like growth factor-binding protein 2	Igfbp2	Cluster -1	-0.599585	-1.00306	NaN	-0.988845	0.928667	1.19776	0.599585	NaN
P00329	Alcohol dehydrogenase 1	Adh1	Cluster -1	-0.607221	-1.00534	NaN	-1.01933	0.873415	1.20415	0.607221	NaN
A0A0R4J0T4;Q5D0E0;O88351;Q3U141	Inhibitor of nuclear factor kappa-B kinase subunit beta	Ikbkb	Cluster -1	-0.595473	-1.00157	NaN	-0.972884	0.95672	1.1941	0.595473	NaN
F8VQJ3;P02468	Laminin subunit gamma-1	Lamc1	Cluster -1	-0.596354	-1.0019	NaN	-0.976281	0.950798	1.19489	0.596354	NaN

O70310	Glycylpeptide N-tetradecanoyltransferase 1	Nmt1	Cluster -1	NaN	-1.60141	NaN	NaN	0.367099	0.407385	NaN	-0.367099
Q9CQR2	40S ribosomal protein S21	Rps21	Cluster -1	NaN	-1.57014	NaN	NaN	0.259224	0.632675	NaN	-0.259224
Q9CZX7	Type 2 phosphatidylinositol 4,5-bisphosphate 4-phosphatase	Tmem55a	Cluster -1	-0.444764	-0.847725	-1.3719	-0.779167	1.13452	1.27674	0.692324	0.444764
P15208	Insulin receptor;Insulin receptor subunit alpha;Insulin receptor subunit beta	Insr	Cluster -1	-0.445207	-0.841932	-1.38794	-0.801908	1.08285	1.28682	0.704877	0.445207
P27046	Alpha-mannosidase 2	Man2a1	Cluster -1	-0.445026	-0.844788	-1.38027	-0.790961	1.10792	1.28202	0.698852	0.445026
Q9JLL0	Cysteine-rich motor neuron 1 protein	Crim1	Cluster -1	-0.950711	NaN	-1.81235	NaN	0.586249	0.665577	0.111495	-0.111495
Q8R349	Cell division cycle protein 16 homolog	Cdc16	Cluster -1	-0.955653	NaN	-1.83663	NaN	0.489536	0.666986	0.120446	-0.120446
Q8C180	Fibroblast growth factor receptor substrate 2	Frs2	Cluster -1	NaN	-1.45764	NaN	-1.43872	0.476846	0.734704	0.138227	-0.138227
Q6NZD2;Q9WV80	Sorting nexin-1	Snx1	Cluster -1	NaN	-1.45581	NaN	-1.44688	0.455848	0.734906	0.140144	-0.140144
Q3UNN4;P97496-2;P97496	SWI/SNF complex subunit SMARCC1	Smarcc1	Cluster -1	NaN	-1.61053	NaN	NaN	0.603495	NaN	0.144869	-0.144869
P54227;D3Z1Z8;D3Z5N2	Stathmin	Stmn1	Cluster -1	-0.950784	NaN	-1.81267	NaN	0.585066	0.665602	0.111607	-0.111607
P97333	Neuropilin-1	Nrp1	Cluster -1	-0.95069	NaN	-1.81226	NaN	0.586589	0.665569	0.111463	-0.111463
Q99LU0	Charged multivesicular body protein 1b-1	Chmp1b1	Cluster -1	-0.946971	-1.31859	NaN	-1.49276	0.278002	0.961745	0.366052	0
P11157	Ribonucleoside-diphosphate reductase subunit M2	Rrm2	Cluster -1	-0.947092	-1.31899	NaN	-1.49219	0.279866	0.961563	0.365688	0
Q61982	Neurogenic locus notch homolog protein 3;Notch 3 extracellular truncation;Notch 3 intracellular domain	Notch3	Cluster -1	-0.947962	-1.3219	NaN	-1.48795	0.293594	0.960201	0.362997	0
Q8VDW0	ATP-dependent RNA helicase DDX39A	Ddx39a	Cluster -1	-0.441461	-0.787664	-1.48052	-0.951277	0.698395	1.33854	0.783266	0.441461
Q80Z96;Q3UXU7;A0A0H2UH25	Vang-like protein 1	Vangl1	Cluster -1	-0.44229	-0.793428	-1.47384	-0.93891	0.733738	1.33537	0.77709	0.44229
B1ASP2;P52332	Tyrosine-protein kinase;Tyrosine-protein kinase JAK1	Jak1	Cluster -1	-0.441691	-0.789238	-1.47875	-0.94796	0.707948	1.33772	0.781621	0.441691
F8WIJ0;Q9JIS8	Solute carrier family 12 member 4	Slc12a4	Cluster -1	-0.441151	-0.785621	-1.48276	-0.955531	0.686071	1.33957	0.785374	0.441151
P10493	Nidogen-1	Nid1	Cluster -1	-0.950782	-1.33188	NaN	-1.47237	0.342588	0.955036	0.353266	0
P11152	Lipoprotein lipase	Lpl	Cluster -1	-0.633321	-1.00593	NaN	-1.13577	0.638584	1.2199	0.633321	NaN
Q9R0N0	Galactokinase	Galk1	Cluster -1	-0.443541	-0.803382	-1.46097	-0.916028	0.797208	1.32893	0.765499	0.443541
Q8R366;G3UYZ1;A0A0R4J117	Immunoglobulin superfamily member 8	Igsf8	Cluster -1	-0.443079	-0.799447	-1.46627	-0.925312	0.771733	1.33164	0.770231	0.443079
Q9DBV4;A2AD97	Matrix-remodeling-associated protein 8	Mxra8	Cluster -1	-0.44283	-0.797484	-1.46881	-0.929817	0.759246	1.33291	0.772508	0.44283
Q61081;A0A1L1STC0	Hsp90 co-chaperone Cdc37;Hsp90 co-chaperone Cdc37, N-terminally processed	Cdc37	Cluster -1	-0.959711	NaN	-1.87645	NaN	0.276606	0.665397	0.139001	-0.139001
E9Q368		Gm17296	Cluster -1	-0.952448	NaN	-1.8911	NaN	0.142957	0.671116	0.159106	-0.142957
A0A140LJL0;P35762	CD81 antigen	Cd81	Cluster -1	-0.959135	NaN	-1.885	NaN	0.211455	0.663662	0.144371	-0.144371
A8Y5H7;A8Y5H7-2;A8Y5H7-3		Sec14l1	Cluster -1	NaN	-1.4399	NaN	-1.49708	0.315803	0.734322	0.152461	-0.152461
Q8BP67	60S ribosomal protein L24	Rpl24	Cluster -1	-0.444366	-0.81149	-1.44907	-0.89585	0.851292	1.32263	0.755102	0.444366
F8WJK8;Q99L47	Hsc70-interacting protein	St13	Cluster -1	-0.444608	-0.814321	-1.44456	-0.888412	0.870804	1.32017	0.751232	0.444608
P41241	Tyrosine-protein kinase CSK	Csk	Cluster -1	-0.444663	-0.815028	-1.44341	-0.886527	0.875716	1.31954	0.750246	0.444663
Q61730;E9Q6I2;Q61730-3	Interleukin-1 receptor accessory protein	Il1rap	Cluster -1	NaN	-1.12898	-1.59988	NaN	0.0306112	0.406041	0	NaN
Q9ESL4-2;Q9ESL4;Q9ESL4-3	Mitogen-activated protein kinase kinase kinase MLT	Zak	Cluster -1	NaN	-1.13778	-1.58719	NaN	0.116128	0.415709	0	NaN
P42232	Signal transducer and activator of transcription 5B	Stat5b	Cluster -1	-0.972758	-1.38005	NaN	NaN	0.48887	0.954047	NaN	0
Q7TQH0-2;A0A0U1RPL0;Q7TQH0-3;Q7TQH0;Q3TGG2;E9Q5Q0	Ataxin-2-like protein	Atxn2l	Cluster -1	-0.969185	-1.37855	NaN	NaN	0.515476	0.945809	NaN	0

P40124	Adenylyl cyclase-associated protein 1	Cap1	Cluster -1	-0.445237	-0.824502	-1.42667	-0.859808	0.943841	1.31007	0.736168	0.445237
Q60790	Ras GTPase-activating protein 3	Rasa3	Cluster -1	-0.445251	-0.824725	-1.42623	-0.859135	0.945507	1.30983	0.735823	0.445251
Q80TR8-4;Q80TR8;Q80TR8-2	Protein VPRBP	Vprbp	Cluster -1	-0.622808	-0.91954	NaN	-1.42294	0	1.39404	0.831332	0.327639
Q9D0J4	ADP-ribosylation factor-like protein 2	Arl2	Cluster -1	-0.624689	-0.921689	NaN	-1.42419	0	1.39214	0.829256	0.325894
Z4YL78;A0A0R4J0K2;K3W4R5;A2AGT5-2;A2AGT5-3;A2AGT5	Cytoskeleton-associated protein 5	Ckap5	Cluster -1	-0.601146	-0.894745	NaN	-1.4083	0	1.41533	0.854872	0.347519
A2CG35;P35283	Ras-related protein Rab-12	Rab12	Cluster -1	-0.580184	-0.870665	NaN	-1.39372	0	1.43509	0.877015	0.366377
Q9Z1Z2	Serine-threonine kinase receptor-associated protein	Strap	Cluster -1	-0.271548	-0.532554	-1.40832	-0.980198	0.271548	1.50903	1.01292	0.567055
Q9R0Q7;D3Z7C6	Prostaglandin E synthase 3	Ptges3	Cluster -1	-0.263148	-0.521599	-1.40162	-0.976628	0.263148	1.51592	1.02185	0.573519
P84084	ADP-ribosylation factor 5	Arf5	Cluster -1	-0.265048	-0.524079	-1.40314	-0.977441	0.265048	1.51437	1.01983	0.572061
G3UXL2;Q9D7G0	Ribose-phosphate pyrophosphokinase 1	Prps1l3;Prps1	Cluster -1	-0.234156	-0.483683	-1.37784	-0.963845	0.234156	1.53875	1.05198	0.59542
P35282	Ras-related protein Rab-21	Rab21	Cluster -1	-0.24562	-0.498697	-1.38736	-0.968992	0.24562	1.52989	1.04019	0.586836
Q8VHK9	ATP-dependent RNA helicase DHX36	Dhx36	Cluster -1	NaN	-0.965128	-1.72787	NaN	-0.0734394	0.928035	0.459298	0.0734394
G5E866;Q99NB9	Splicing factor 3B subunit 1	Sf3b1	Cluster -1	NaN	-0.915531	-1.70791	NaN	-0.111644	0.977571	0.514071	0.111644
Q6GQT9	Nodal modulator 1	Nomo1	Cluster -1	NaN	-0.816143	-1.65969	NaN	-0.183182	1.06521	0.614461	0.183182
Q8VEJ9	Vacuolar protein sorting-associated protein 4A	Vps4a	Cluster -1	-0.304353	-0.575224	-1.43371	-0.993551	0.304353	1.48099	0.977174	0.541286
O54988-2;O54988	STE20-like serine/threonine-protein kinase	Slk	Cluster -1	-0.297508	-0.566338	-1.42852	-0.990844	0.297508	1.487	0.984748	0.54673
P31230;Q3UZG4	Aminoacyl tRNA synthase complex-interacting multifunctional protein 1;Endothelial monocyte-activating polypeptide 2	Aimp1	Cluster -1	-0.289416	-0.555819	-1.42231	-0.987587	0.289416	1.49399	0.993621	0.553122
Q9CWF2;Q7TMM9	Tubulin beta-2B chain;Tubulin beta-2A chain	Tubb2b;Tubb2a	Cluster -1	-0.659461	-0.961275	NaN	-1.44665	0	1.35589	0.789911	0.293053
Q8BH00	Aldehyde dehydrogenase family 8 member A1	Aldh8a1	Cluster -1	-0.66831	-0.971308	NaN	-1.45217	0	1.34626	0.779598	0.284517
Q6NXL1		Sec24d	Cluster -1	-0.711458	-1.01998	NaN	-1.47783	0	1.29685	0.727458	0.241787
E9Q6L0;A0A087WQF1;E9QKH0;J3QP81;A0A087WS18;A0A087WQ95;A0A087WNW8;A0A087WRK0;A0A087WP42;E9QNY9;A0A087WRE8;A0A087WQ31;Q80TV8;Q80TV8-2;A0A0A6YXZ1	CLIP-associating protein 1	Clasp1	Cluster -1	-0.692496	-0.998641	NaN	-1.46681	0	1.31908	0.750759	0.260796
P28867-2;Q1MX40;Q1MX42;P28867;Q1MX41;Q1MX43	Protein kinase C delta type;Protein kinase C delta type regulatory subunit;Protein kinase C delta type catalytic subunit;Protein kinase C	Prkcd	Cluster -1	-0.723851	-1.04058	NaN	NaN	0	1.34698	0.760832	NaN
A0A087WRM2;Q91VK4	Integral membrane protein 2C;CT-BRI3	Itm2c	Cluster -1	-0.313023	-0.586468	-1.4402	-0.996922	0.313023	1.47327	0.967491	0.534334
Q61584-4;Q61584-3;Q61584;A0A0G2JEP0;Q61584-5;Q61584-6;Q61584-7;Q61584-2;A0A0H2UH27	Fragile X mental retardation syndrome-related protein 1	Fxr1	Cluster -1	-0.316954	-0.591564	-1.44311	-0.998431	0.316954	1.46972	0.963066	0.531163
Q91YR7	Pre-mRNA-processing factor 6	Prpf6	Cluster -1	-0.757235	-1.07111	NaN	-1.50266	0	1.23962	0.668521	0.194296
Q8BPU7;Q8BPU7-3	Engulfment and cell motility protein 1	Elmo1	Cluster -1	-0.726689	-1.03705	NaN	-1.48638	0	1.27839	0.708281	0.226244
P24549	Retinal dehydrogenase 1	Aldh1a1	Cluster -1	-0.771079	-1.08647	NaN	-1.50964	0	1.22125	0.649899	0.179457
E9PYA3;A0A0R4J052;G5E8T9;Q99KB8-2;Q99KB8;E9Q2H8	Hydroxyacylglutathione hydrolase, mitochondrial	Hagh	Cluster -1	-0.721314	-1.03103	NaN	-1.4834	0	1.28497	0.715096	0.231758
E9QLR3;Q60961-2;Q60961	Lysosomal-associated transmembrane protein 4A	Laptm4a	Cluster -1	-0.729371	-1.04005	NaN	-1.48786	0	1.27508	0.704861	0.223481

E9PYI8;Q9JMA1	Ubiquitin carboxyl-terminal hydrolase;Ubiquitin carboxyl-terminal hydrolase 14	Usp14	Cluster -1	-0.32657	-0.604009	-1.45016	-1.00206	0.32657	1.46093	0.952157	0.523352
Q99JX7;V9GXF3	Nuclear RNA export factor 1	Nxf1	Cluster -1	NaN	-1.08456	-1.76168	NaN	0.0272526	0.788614	0.311167	-0.0272526
P51660	Peroxisomal multifunctional enzyme type 2;(3R)-hydroxyacyl-CoA dehydrogenase;Enoyl-CoA hydratase 2	Hsd17b4	Cluster -1	NaN	-1.12763	-1.7676	NaN	0.067383	0.729489	0.250618	-0.067383
P53690	Matrix metalloproteinase-14	Mmp14	Cluster -1	NaN	-1.06449	-1.75764	NaN	0.00932474	0.814372	0.337939	-0.00932474
Q9D8U8	Sorting nexin-5	Snx5	Cluster -1	-0.932836	-1.27748	NaN	-1.54138	0.103378	0.975804	0.398888	0
Q8BH35-2;Q8BH35	Complement component C8 beta chain	C8b	Cluster -1	-0.932322	-1.27612	NaN	-1.54271	0.0980987	0.976137	0.399841	0
Q61206;A0A1L1SVK0;A0A1L1SQ76;A0A1L1SRD0	Platelet-activating factor acetylhydrolase IB subunit beta	Pafah1b2	Cluster -1	-0.93126	-1.27333	NaN	-1.54538	0.0873479	0.9768	0.401777	0
A2A5R2	Brefeldin A-inhibited guanine nucleotide-exchange protein 2	Arfgef2	Cluster -1	-0.931153	-1.27305	NaN	-1.54564	0.0862752	0.976865	0.401969	0
Q3URQ0	Testis-expressed sequence 10 protein	Tex10	Cluster -1	-0.92883	-1.26704	NaN	-1.55117	0.0634932	0.978189	0.406036	0
Q9JMK0	Beta-1,4-galactosyltransferase 5	B4galt5	Cluster -1	-0.93659	-1.28764	NaN	-1.531	0.143673	0.973085	0.391534	0
Q9CZT5	Vasorin	Vasn	Cluster -1	-0.934782	-1.2827	NaN	-1.53617	0.123871	0.97446	0.395164	0
Q9CS74	Protein SGT1 homolog	Ecd	Cluster -1	-0.934748	-1.28261	NaN	-1.53626	0.123513	0.974484	0.39523	0
Q91YR1	Twinfilin-1	Twf1	Cluster -1	-0.935935	-1.28584	NaN	-1.53291	0.136416	0.973598	0.392868	0
Q80XI4	Phosphatidylinositol 5-phosphate 4-kinase type-2 beta	Pip4k2b	Cluster -1	-0.935623	-1.28498	NaN	-1.5338	0.132988	0.973836	0.393497	0
Q61382	TNF receptor-associated factor 4	Traf4	Cluster -1	-0.934231	-1.28121	NaN	-1.53768	0.117993	0.974854	0.396236	0
Q60597;Q60597-3;Z4YJV4;Q60597-2;Q60597-4	2-oxoglutarate dehydrogenase, mitochondrial	Ogdh	Cluster -1	-0.935684	-1.28515	NaN	-1.53363	0.133662	0.97379	0.393373	0
G3X8W7;A0A0R4J1W7;Q8BGZ4;Q8BGZ4-2	Cell division cycle protein 23 homolog	Cdc23	Cluster -1	-0.937616	-1.29049	NaN	-1.52792	0.155279	0.972243	0.389391	0
P58021;E9PZ69	Transmembrane 9 superfamily member 2	Tm9sf2	Cluster -1	-0.935502	-1.28465	NaN	-1.53415	0.131664	0.973928	0.39374	0
Q9QXY6	EH domain-containing protein 3	Ehd3	Cluster -1	-0.438112	-0.767823	-1.49993	-0.989942	0.58279	1.34677	0.802104	0.438112
Q8K2Z4;Q8K2Z4-2;A0A0R4J0H7	Condensin complex subunit 1	Ncapd2	Cluster -1	-0.438064	-0.76757	-1.50014	-0.990397	0.581374	1.34685	0.802322	0.438064
P68404-2;P68404	Protein kinase C beta type	Prkcb	Cluster -1	-0.438091	-0.767707	-1.50003	-0.990154	0.58213	1.34681	0.802206	0.438091
O35607	Bone morphogenetic protein receptor type-2	Bmpr2	Cluster -1	-0.438429	-0.769533	-1.49844	-0.986822	0.592432	1.3462	0.800616	0.438429
H7BX44;D3YYN8;E9PVY0;A0A1D5RLQ9;Q3UU96;Q3UU96-2;F6Q5A5;F6YZJ7;F6S5Z6	Non-specific serine/threonine protein kinase;Serine/threonine-protein kinase MRCK alpha	Cdc42bpa	Cluster -1	-0.437324	-0.763654	-1.50339	-0.997383	0.559564	1.34804	0.805642	0.437324
O09172;H3BJA3;A0A0G2JDI4	Glutamate--cysteine ligase regulatory subunit	Gclm	Cluster -1	-0.438207	-0.768346	-1.49948	-0.988993	0.585724	1.3466	0.801651	0.438207
Q8CHR6	Dihydropyrimidine dehydrogenase [NADP(+)]	Dpyd	Cluster -1	-0.998984	-1.3788	NaN	NaN	0.196093	1.03077	NaN	0
Q8R4V5-2;Q8R4V5	Oncoprotein-induced transcript 3 protein	Oit3	Cluster -1	-0.996123	-1.38128	NaN	NaN	0.246661	1.01929	NaN	0
Q3UW64;Q91WG8;G3UYD5;G3UX23;G3UZ98	Bifunctional UDP-N-acetylglucosamine 2-epimerase/N-acetylmannosamine kinase;UDP-N-acetylglucosamine 2-epimerase (hydrolyzing);N-acetylmannosamine kinase	Gne	Cluster -1	-0.440161	-0.779442	-1.48919	-0.967997	0.649396	1.34242	0.791504	0.440161
Q7TMK9;G3V018	Heterogeneous nuclear ribonucleoprotein Q	Syncrip	Cluster -1	-0.4396	-0.776124	-1.49243	-0.974457	0.630077	1.34379	0.79465	0.4396
E9PYG6		Rasa1	Cluster -1	-0.942248	-1.30384	NaN	-1.51237	0.211558	0.967792	0.378842	0
O55022	Membrane-associated progesterone receptor component 1	Pgrmc1	Cluster -1	-0.940959	-1.30003	NaN	-1.517	0.195167	0.969152	0.381942	0
Q9QUG9;Q9QUG9-2	RAS guanyl-releasing protein 2	Rasgrp2	Cluster -1	-0.823598	-1.14421	NaN	-1.53362	0	1.14658	0.575511	0.120935
Q8CFI0-3	E3 ubiquitin-protein ligase NEDD4-like	Nedd4l	Cluster -1	-0.799326	-1.11763	NaN	-1.52305	0	1.18211	0.610656	0.148438
D3Z061;Q8C7R4	Ubiquitin-like modifier-activating enzyme 6	Uba6	Cluster -1	-0.782469	-1.09906	NaN	-1.51518	0	1.20574	0.634282	0.167073

L7N467;Q8BLB2		B230307C23Rik	Cluster -1	-0.794516	-1.11234	NaN	-1.52084	0	1.18894	0.617461	0.153793
F8VQC1;E9Q740	Signal recognition particle subunit SRP72	Srp72	Cluster -1	-0.379912	-0.672745	-1.48712	-1.02065	0.379912	1.40907	0.889333	0.478644
P26618;P26618-2	Platelet-derived growth factor receptor alpha	Pdgfra	Cluster -1	-0.374119	-0.665308	-1.48329	-1.01876	0.374119	1.41496	0.896346	0.483616
B2RUP2-2;B2RUP2;A0A0R4J257	Protein unc-13 homolog D	Unc13d	Cluster -1	-0.857978	-1.18152	NaN	-1.54695	0	1.09296	0.523251	0.0804992
Q3TYX2	LRRN4 C-terminal-like protein	Lrrn4cl	Cluster -1	-0.843511	-1.16587	NaN	-1.54159	0	1.11602	0.545615	0.0977364
Q68FE6	Protein FAM65A	Fam65a	Cluster -1	-1.14555	-1.55771	NaN	NaN	0.0387462	NaN	0.509665	0
D3Z0M9		Ddx23	Cluster -1	-1.11597	-1.53077	NaN	NaN	0	NaN	0.636559	0.0784505
Q9Z1M2;A0A140LIF8		Irgm2	Cluster -1	NaN	-1.58004	NaN	NaN	0	1.14003	0.44877	-0.0491621
B2RQS1;Q9ERG2	Striatin-3	Strn3	Cluster -1	-1.14333	-1.55196	NaN	NaN	0	NaN	0.533027	0.00933956
Q62093	Serine/arginine-rich splicing factor 2	Srsf2	Cluster -1	-0.434943	-0.751788	-1.51222	-1.01744	0.495243	1.35091	0.81502	0.434943
Q8BK67	Protein RCC2	Rcc2	Cluster -1	-0.433888	-0.74683	-1.5155	-1.02538	0.469038	1.35181	0.818662	0.433888
Q9D6Z1;E0CXZ0	Nucleolar protein 56	Nop56	Cluster -1	-0.924085	-1.25508	NaN	-1.56139	0.0195475	0.980463	0.413762	0
Q9CU62	Structural maintenance of chromosomes protein 1A	Smc1a	Cluster -1	-0.925525	-1.25867	NaN	-1.55843	0.032546	0.979829	0.411493	0
Q91YT8;E0CX44;E0CXM3	CSC1-like protein 1	Tmem63a	Cluster -1	-0.922242	-1.25054	NaN	-1.56502	0.00329432	0.98121	0.41658	0
Q99KW9	T-cell immunomodulatory protein	Itfg1	Cluster -1	-0.923613	-1.25392	NaN	-1.56234	0.0153453	0.980661	0.414493	0
Q91W53;Q91W53-2	Golgin subfamily A member 7	Golga7	Cluster -1	-0.432676	-0.741295	-1.5189	-1.03393	0.44028	1.35261	0.822544	0.432676
Q8R1X6;D3Z3F8;Q8R1X6-2	Spartin	Spg20	Cluster -1	-0.432598	-0.740948	-1.5191	-1.03446	0.438477	1.35266	0.822787	0.432598
Q6PGL7-2;Q6PGL7;A0A0N4SV74;A0A0N4SUJ0	WASH complex subunit FAM21	Fam21	Cluster -1	-0.467442	-0.794834	NaN	-1.09623	0.467442	1.41423	0.854081	NaN
F8VQN6;Q8R4H2	Rho guanine nucleotide exchange factor 12	Arhgef12	Cluster -1	-0.433234	-0.743808	-1.51739	-1.03008	0.453297	1.35227	0.820808	0.433234
Q8C253;P16110	Galectin;Galectin-3	Lgals3	Cluster -1	-0.43329	-0.744065	-1.51723	-1.02968	0.454632	1.35224	0.820625	0.43329
P47757-2;A2AMW0;P47757-4	F-actin-capping protein subunit beta	Capzb	Cluster -1	-0.417716	-0.721125	-1.51106	-1.03219	0.417716	1.36904	0.84234	0.445494
D3YYT0;P15116	Cadherin-2	Cdh2	Cluster -1	-0.418358	-0.721943	-1.51146	-1.03237	0.418358	1.36833	0.841525	0.444919
Q99LB6-2;Q99LB6	Methionine adenosyltransferase 2 subunit beta	Mat2b	Cluster -1	-0.886683	-1.21233	NaN	-1.55644	0	1.0449	0.477147	0.0452653
Q61554;Q61555	Fibrillin-1;Fibrillin-2	Fbn1;Fbn2	Cluster -1	-0.89715	-1.22348	NaN	-1.55949	0	1.02656	0.459721	0.0320514
Q05D44	Eukaryotic translation initiation factor 5B	Eif5b	Cluster -1	-0.89699	-1.22331	NaN	-1.55945	0	1.02684	0.45999	0.0322549
O08807;B1AZS9	Peroxiredoxin-4	Prdx4	Cluster -1	-0.892533	-1.21857	NaN	-1.55817	0	1.03471	0.467451	0.0379059
P62835;A0A0G2JE52;A0A0G2JED9	Ras-related protein Rap-1A	Rap1a	Cluster -1	-0.890927	-1.21686	NaN	-1.55771	0	1.03752	0.470123	0.0399324
Q9Z0N1;Q9Z0N2;A2AAW9	Eukaryotic translation initiation factor 2 subunit 3, X-linked;Eukaryotic translation initiation factor 2 subunit 3, Y-linked	Eif2s3x;Eif2s3y	Cluster -1	-0.414991	-0.717654	-1.5094	-1.03141	0.414991	1.37201	0.845795	0.447925
Q9D4B1	Phosphatidylcholine:ceramide cholinephosphotransferase 2	Sgms2	Cluster -1	-0.422827	-0.727642	-1.51415	-1.03364	0.422827	1.36341	0.835823	0.440914
A2ARD6;Q9CXF0;Q6NSV5	Kynureninase	Kynu	Cluster -1	-0.908327	-1.23534	NaN	-1.56249	0	1.00646	0.440723	0.0177077

Table S3

	Cellular functions	p-Value	Predicted Activation State	Molecules	# Molecules
Cluster 0	Cell movement	0.000179	Increased	ALCAM,AQP1,ARHGEF7,ARL4C,ARPC3,B4GALT1,B4GAT1,BAG3,BAX,BCAR1,BCAT1,C1QBP,Cald1,CAPNS1,CD37,CD47,CD82,CLIP1,CLU,CNP,CTBP2,CUL4A,DAG1,DDX58,DIAPH1,ELAVL1,ELP1,EPHA4,FAF1,FGFR1,FGFR2,FLNC,GDI1,GIT1,GP1BA,HUWE1,HYOU1,ITGA4,ITGA5,JUP,LAMA5,LAMTOR2,LCAT,MAP2K3,MAPRE1,MRC2,MTCH2,MTOR,MYH14,MYL12A,MYO5A,NACA,NFKB1,NINJ1,NQO2,PACSIN2,PARP1,PHB,PIN1,PKN1,PLCB3,PLEC,PML,PPFIA1,PSEN1,PXN,RAC2,RAP2A,RAP2C,RELN,RNF20,ROCK2,RPS19,RPS6KA3,S100A6,SH3PXD2A,SND1,TG,TGFBR3,TMPO,TNFRSF10A,TNFRSF1A,Wasl,YARS,YBX1	85
	Cell proliferation of tumor cell lines	0.000000149	Increased	AKR1C3,ALCAM,AQP1,ARHGEF2,ARL4C,ASAH1,BAX,BCAR1,C1QBP,CLIP1,CLU,COPS5,COPS6,COPZ1,CSNK1D,CTBP2,CUL4A,DDX58,EEF1B2,ELAVL1,EPHA4,EXOC8,FGFR1,FGFR2,GGT1,GIT1,GTF2I,H2AFY,HUWE1,IDE,IDH2,IMMT,ITGA5,JUP,LAMA5,LARP1,MAP2K3,MAPRE1,MTOR,MYBBP1A,MYH14,NACA,NCSTN,NFKB1,NUMA1,PACSIN2,PARP1,PHB,PIN1,PML,PPP2R1A,PRKACB,PRPF8,PRRC2C,PSEN1,PSMA5,PSMB7,PURA,PXN,PYGM,RAB8A,RNF20,RPS10,RPS25,RPS6KA3,S100A6,SND1,SPAST,STK38,TARDBP,TBX2,TGFBR3,TMPO,TNFRSF10A,TNFRSF1A,UBA2,UBE2D3,WDR48,YBX1	79
	Migration of cells	0.000198	Increased	ALCAM,AQP1,ARHGEF7,ARL4C,B4GALT1,B4GAT1,BAG3,BAX,BCAR1,BCAT1,C1QBP,CAPNS1,CD37,CD47,CD82,CLU,CNP,CTBP2,CUL4A,DAG1,DDX58,DIAPH1,ELAVL1,ELP1,EPHA4,FAF1,FGFR1,FGFR2,FLNC,GIT1,GP1BA,HUWE1,HYOU1,ITGA4,ITGA5,JUP,LAMA5,LAMTOR2,LCAT,MAP2K3,MAPRE1,MRC2,MTOR,MYL12A,NACA,NFKB1,NINJ1,NQO2,PACSIN2,PARP1,PHB,PIN1,PKN1,PLCB3,PLEC,PML,PPFIA1,PSEN1,PXN,RAC2,RAP2A,RAP2C,RELN,RNF20,ROCK2,RPS19,RPS6KA3,S100A6,SND1,TG,TGFBR3,TMPO,TNFRSF10A,TNFRSF1A,Wasl,YARS,YBX1	77
	Organization of cytoplasm	2.95E-08	Increased	AQP1,ARHGEF2,ARHGEF7,ARPC1A,ARPC3,ATP2C1,B4GAT1,BAG3,BAX,BCAR1,BMP2K,C1QBP,CANX,CAPNS1,CD47,CD82,CLIP1,CLU,CNP,CORO7/CORO7-PAM16,CSNK1D,DAG1,DCTN1,DIAPH1,EPHA4,EXOC8,FGFR1,FGFR2,FLNC,GDI1,GIT1,GORASP2,GPSM2,HERC1,IDE,ITGA4,JUP,KIF11,KLC1,LAMA5,MAPRE1,MTOR,MYO5A,NECTIN2,NEK7,NFKB1,NINJ1,NSFL1C,NUMA1,PACSIN2,PARP1,PFDN5,PHB,PIN1,PKP4,PLEC,PRKACB,PRPF40A,PSEN1,PXN,RAB10,RAB32,RAB8A,RAC2,RAP2A,RELN,ROCK2,RPS6KA3,SPAST,SURF4,TAOK1,TIMM50,TMEM106B,TNFRSF1A,Wasl,YBX1	76
	Cell survival	0.000000137	Increased	ALCAM,ANLN,ANTXR2,ASAH1,ATP1A2,ATP2C1,BAG3,BANF1,BAX,BCAR1,CAMK2G,CD47,CD82,CLU,DHX38,DPP3,ELAVL1,EPHA4,ERCC5,FGFR1,FGFR2,GIT1,H2AFY,HEATR1,HNRNPU,HYOU1,IDE,ITGA5,JUP,KIF11,LAMA5,MAP2K3,MTOR,NCSTN,NEK7,NFKB1,NOP2,NRBP1,OTUD7B,PARP1,PES1,PFDN5,PFDN6,PHB,PHKA2,PIN1,PKN1,PML,PPP2R1A,PRKACB,PRPF8,PSEN1,PSMA6,PSMB4,RAC2,RPA1,RPS6KA3,S100A6,SH3PXD2A,SLC31A1,SLC7A1,SND1,SNRPD1,STAM,STAM2,TARDBP,TBX2,TNFRSF10A,TNFRSF1A,TOP2A,TXNDC5,YBX1	72
	Organization of cytoskeleton	0.000000388	Increased	AQP1,ARHGEF2,ARHGEF7,ARPC1A,ARPC3,ATP2C1,B4GAT1,BAG3,BAX,BCAR1,BMP2K,C1QBP,CANX,CAPNS1,CD47,CD82,CLIP1,CLU,CNP,CORO7/CORO7-PAM16,CSNK1D,DAG1,DCTN1,DIAPH1,EPHA4,FGFR1,FGFR2,FLNC,GDI1,GIT1,GPSM2,HERC1,IDE,ITGA4,JUP,KIF11,KLC1,LAMA5,MAPRE1,MTOR,MYO5A,NECTIN2,NEK7,NFKB1,NINJ1,NUMA1,PACSIN2,PFDN5,PIN1,PKP4,PLEC,PRKACB,PRPF40A,PSEN1,PXN,RAB10,RAB8A,RAC2,RAP2A,RELN,ROCK2,RPS6KA3,SPAST,TAOK1,TMEM106B,TNFRSF1A,Wasl,YBX1	68

	Cell viability	0.00000289	Increased	ANLN,ANTXR2,ASAH1,ATP1A2,ATP2C1,BAG3,BAX,BCAR1,CAMK2G,CD47,CD82,CLU,DHX38,DPP3,ELAVL1,EPHA4,FGFR1,FGFR2,GIT1,H2AFY,HEATR1,HNRNPU,HYOU1,IDE,KIF11,LAMA5,MAP2K3,MTOR,NCSTN,NEK7,NFKB1,NOP2,NRBP1,OTUD7B,PARP1,PES1,PFDN5,PFDN6,PHB,PHKA2,PIN1,PKN1,PML,PPP2R1A,PRKACB,PRPF8,PSEN1,PSMA6,PSMB4,RAC2,RPA1,RPS6KA3,S100A6,SLC31A1,SLC7A1,SND1,SNRPD1,STAM,STAM2,TARDBP,TBX2,TNFRSF10A,TNFRSF1A,TXNDC5,YBX1	65
	Cell death	2.63E-18	Decreased	ABCA3,ACAT1,ACP2,ACTN4,ADAM15,ADAM17,ADGRL2,AGO2,AHSA1,AIMP1,ALDH1A1,AP1G1,ARCN1,ARHGEF1,ASNA1,ATAD3A,B4GALT5,BCAP31,BIN1,BMP1,BMPR1A,BMPR2,BUB3,C8B,CAPN2,CAV1,CC2D1A,CCND1,CD44,CD81,CDC37,CDH2,CKAP5,CLASP1,CLEC11A,CP,CSK,CTNND1,CTTN,CUL1,CUL3,CUL4B,CYR61,DCAF1,DHFR,DIP2A,DNAJC5,DNMT1,DPP9,DPYD,EFEMP1,EFNB1,EFNB2,EHD3,EHD4,EIF2S1,EIF3G,EIF5B,ELMO1,ELOC,EPHB4,FBL,FBN1,FDPS,FGA,FGR,FH,FLNA,FN1,FRS2,FXR1,GABARAP,GCLM,GLRX,GLS,GMEB1,GNA12,GNE,GPHN,GRK2,GSK3B,HK1,HK2,HLA-A,HSD17B10,HSD17B4,HSPA2,HSPG2,HYAL2,IGF1R,IGFBP2,IKBKB,IL6ST,ILF3,INSR,IRGM,JAK1,LGALS3,LIN7C,LYN,MAN2A1,MAP2K2,MAP3K20,MAPK14,MARK2,MAT2A,MIB1,MIF,MMP14,MTMR2,MYBPC3,NASP,NELFB,NME1,NOTCH2,NOTCH3,NRP1,NRP2,NSF,NUP62,NXF1,OAS1,OGDH,PAFAH1B1,PAFAH1B2,PAFAH1B3,PAK2,PARD3,PBK,PCDHGC3,PCNA,PDGFRA,PELP1,PGRMC1,PIK3CB,PITPNA,PKN2,PPP2R2A,PPP5C,PRDX4,PRKCB,PRKCD,PRPF19,PSIP1,PSMD6,PTGES3,PTPA,PTPN11,PTPRA,PTPRC,RAB22A,RAD23B,RANBP1,RAP1A,RASA1,RASGRP2,RNF2,RPL37A,RPS21,RPS29,RRAGA,RRM2,SARM1,SDC1,SEC23B,SF3B1,SF3B3,SGCD,SGMS2,SLC9A1,SLK,SMAD2,SMARCC1,SMC1A,SNX1,SPNS1,SRSF1,SRSF2,SSRP1,STAT5B,STAT6,STEAP3,STIP1,STK3,STMN1,STRAP,SUSD6,SYNGR2,TAGLN2,TAOK3,TEX10,TGFBR2,TMEM173,TMX1,TNFAIP2,TNS2,TRAF4,TRIP10,UBE2C,UBE2K,UBE4B,UNC5B,UQCRFS1,USP47,VAC14,VAMP2,VAMP3,VASN,VASP,WWP2,YES1	211
	Apoptosis	1.31E-12	Decreased	ACTN4,ADAM15,ADAM17,ADGRL2,AGO2,AHSA1,AIMP1,ALDH1A1,ATAD3A,B4GALT5,BCAP31,BIN1,BMP1,BMPR1A,BMPR2,BUB3,CAPN2,CAV1,CCND1,CD44,CDC37,CDH2,CKAP5,CLASP1,CLEC11A,CSK,CTNND1,CTTN,CUL1,CUL3,CUL4B,CYR61,DCAF1,DHFR,DIP2A,DNAJC5,DNMT1,DPP9,EFEMP1,EFNB1,EFNB2,EHD3,EHD4,EIF2S1,ELMO1,ELOC,EPHB4,FBL,FBN1,FGR,FH,FLNA,FN1,FRS2,FXR1,GABARAP,GCLM,GLRX,GLS,GMEB1,GNA12,GNE,GRK2,GSK3B,HK1,HK2,HSD17B10,HSPA2,HSPG2,HYAL2,IGF1R,IKBKB,IL6ST,ILF3,INSR,JAK1,LGALS3,LIN7C,LYN,MAN2A1,MAP2K2,MAP3K20,MAPK14,MAT2A,MIB1,MIF,MMP14,NASP,NELFB,NME1,NOTCH2,NOTCH3,NRP1,NUP62,OAS1,PAFAH1B1,PAFAH1B2,PAFAH1B3,PAK2,PARD3,PBK,PCDHGC3,PCNA,PDGFRA,PELP1,PIK3CB,PITPNA,PKN2,PPP2R2A,PPP5C,PRDX4,PRKCB,PRKCD,PRPF19,PSIP1,PSMD6,PTPA,PTPN11,PTPRC,RAD23B,RANBP1,RAP1A,RASA1,RNF2,RPS29,RRM2,SARM1,SDC1,SEC23B,SF3B1,SGMS2,SLC9A1,SLK,SMAD2,SMARCC1,SNX1,SRSF1,SRSF2,SSRP1,STAT5B,STAT6,STEAP3,STIP1,STK3,STMN1,STRAP,TAGLN2,TAOK3,TGFBR2,TMX1,TNFAIP2,TNS2,TRAF4,UBE4B,UNC5B,USP47,VASN,VASP,WWP2,YES1	160

Cluster 1	Organization of cytoplasm	4.39E-12	Increased	ACP2,ACTN4,ACVR2A,Akap9,AP1G1,ARFGEF2,ARHGAP12,ARHGEF1,ARL2,ARL6,ARPC5,ATRN,ATXN10,BCCIP,BIN1,CAP1,CAPN2,CAPZB,CAV1,CC2D1A,CD44,CD81,CDC42BPA,CDH2,CFL2,CHMP1B,CKAP5,CLASP1,CRKL,CSK,CTNND1,CTTN,CUL4B,CYR61,CYTH2,DAAM1,DBNL,DIAPH3,DOCK7,EFNB1,EFNB2,EHD2,ELMO1,ENAH,EPS8L2,FAM83H,FGR,FLII,FLNA,FN1,Fnbp1l,GABARAP,GBF1,GNA12,GRK2,GSK3B,HEXA,HSD17B10,IGF1R,IKBKB,IL1RAP,INSR,LAMC1,LAMTOR1,LYN,MAN2A1,MAP2K2,MAP3K20,MAPK14,MAPK15,MARK2,MSTO1,NME1,NPLOC4,NRP1,NRP2,NTMT1,NUP62,PAFAH1B1,PAK2,PARD3,PCM1,PDGFRA,PHLDB1,PITPNA,PLS3,PRKCB,PRKCD,PTPN11,PTPRJ,PTPRK,RAB21,RANBP1,RAP1A,SARM1,SLC9A1,SLK,SNX1,SSRP1,STIP1,STMN1,TRIP10,TUBG1,UBA6,UBE4B,UNC5B,VASP,VPS13C	108
	Cell death of tumor cell lines	4.11E-11	Decreased	ABCA3,ADAM17,ADGRL2,AHSA1,AIMP1,BCAP31,BUB3,CAPN2,CAV1,CCND1,CD44,CDC37,CKAP5,CLASP1,CTNND1,CTTN,CUL1,CYR61,DCAF1,DHFR,DNMT1,DPP9,DPYD,EFEMP1,EIF2S1,EIF3G,ELOC,EPHB4,FGR,FN1,GLRX,GLS,GNE,GRK2,GSK3B,HK1,HK2,IGF1R,IGFBP2,IKBKB,IL6ST,INSR,IRGM,JAK1,LGALS3,LYN,MAP2K2,MAPK14,MAT2A,MIB1,MIF,MMP14,NASP,NME1,NOTCH2,NOTCH3,NRP1,NRP2,PAK2,PBK,PCNA,PDGFRA,PELP1,PGRMC1,PIK3CB,PPP2R2A,PPP5C,PRKCB,PRKCD,PRPF19,PSIP1,PTPN11,PTPRC,RAB22A,RAD23B,RASA1,RNF2,RRM2,SDC1,SF3B3,SGMS2,SLC9A1,SMAD2,SMARCC1,SMC1A,SNX1,SRSF1,SRSF2,SSRP1,STAT5B,STAT6,STK3,STMN1,SYNGR2,TAGLN2,TAOK3,TEX10,TGFBR2,TMEM173,TNS2,TRAF4,UBE2C,UBE2K,UNC5B,UQCRFS1,USP47,WWP2	107
	Invasion of cells	4.23E-17	Increased	ACAT1,ACTN4,ADAM15,ADAM17,AGO2,ATAD3A,B4GALT5,BMPR2,CAP1,CAPN2,CAV1,CCND1,CD44,CD81,CDC42BPA,CDH2,COL7A1,CRKL,CSK,CTNND1,CTTN,CUL4B,CYR61,DBNL,DIAPH3,DNAJB4,EFEMP1,ELMO1,ENAH,EPHB4,F11R,FBLN2,FH,FLNA,FN1,GNA12,GSK3B,IGF1R,IGFBP2,IKBKB,ILF3,LAMC1,LGALS3,LYN,MAP2K2,MAP3K20,MAPK14,MIF,MMP14,NME1,NOTCH2,NOTCH3,NRP1,NRP2,PAFAH1B1,PAK2,PARD3,PDGFRA,PIK3CB,PPP2R2A,PRKCB,PRKCD,PTGES3,PTPRA,PTPRJ,PTPRK,RAP1A,RASA1,RNH1,RRM2,SDC1,SEC24D,SLC12A4,SLC9A1,SMAD2,SNAP23,STAT5B,STMN1,TAGLN2,TGFBR2,TJP1,TRIP10,UNC5B,VANGL1,VASP,WBP2,YES1,ZDHHC20	88
	Apoptosis of tumor cell lines	3.03E-08	Decreased	ADAM17,ADGRL2,AHSA1,AIMP1,BCAP31,BUB3,CAPN2,CAV1,CCND1,CD44,CKAP5,CLASP1,CTNND1,CTTN,CYR61,DCAF1,DNMT1,EFEMP1,ELOC,EPHB4,FGR,FN1,GLRX,GLS,GNE,GRK2,GSK3B,HK2,IGF1R,IKBKB,IL6ST,INSR,JAK1,LGALS3,LYN,MAPK14,MAT2A,MIB1,MIF,MMP14,NASP,NME1,NOTCH2,NOTCH3,NRP1,PAK2,PBK,PCNA,PDGFRA,PELP1,PIK3CB,PPP2R2A,PPP5C,PRKCB,PRKCD,PRPF19,PSIP1,PTPN11,PTPRC,RAD23B,RASA1,RNF2,RRM2,SDC1,SGMS2,SLC9A1,SMAD2,SMARCC1,SNX1,SRSF1,SSRP1,STAT5B,STAT6,STK3,STMN1,TAGLN2,TAOK3,TGFBR2,TNS2,TRAF4,UNC5B,WWP2	82
	Cell cycle progression	1.9E-11	Increased	ADGRL2,ARPC5,BCCIP,BMPR1A,BMPR2,BUB3,CAPN2,CAV1,CC2D1A,CCND1,CD44,CDC123,CDC16,CDC23,CDC37,CKAP5,CLASP1,CUL1,CUL3,CYR61,DBI,DHFR,DIAPH3,DNAJB4,DNMT1,ELOC,FLNA,FRS2,GBF1,GNA12,GRK2,GSK3B,HCFC1,IGF1R,IGFBP2,IKBKB,INSR,JTB,LGALS3,LYN,MAP2K2,MAP3K20,MAPK14,MIF,MYBPC3,NASP,NELFB,NME1,NOTCH2,NOTCH3,NUP62,PAFAH1B1,PAK2,PCM1,PCNA,PDGFRA,PELP1,PITPNA,PKN2,PPP2R2A,PPP5C,PRKCB,PRKCD,PTPN11,PTPRC,PTPRK,RNF2,RPL24,SMAD2,SMARCC1,Spg20,SRSF2,SSRP1,STAT5B,STAT6,STMN1,SUGT1,TGFBR2,TUBG1,UBE2C	80

	Advanced stage tumor	8.71E-11	Increased	ACTN4,ADAM15,ADAM17,AOC3,ATAD3A,BMP1,BMPR1A,BMPR2,CAPN2,CAV1,CCND1,CD44,CD81,CDH2,COL6A3,CRYZ,CSK,CTNND1,CTTN,CYR61,DHFR,DNMT1,DPYD,EFEMP1,ENAH,EPHB4,FDPS,FGR,FLII,FLNA,FN1,Fnbp1l,GART,GLRX,GNA12,GPNMB,IGF1R,IGFBP2,IKBKB,INSR,JAK1,KIF20A,LGALS3,LYN,MAP2K2,MCM3,MIF,MMP14,NME1,NRP1,NRP2,PAFAH1B1,PARD3,PBK,PCNA,PDGFRA,PIK3CB,PLS3,PSIP1,PTPN11,PTPRA,PTPRC,PTPRJ,RNH1,RRM2,SDC1,SF3B1,SMAD2,SMC4,SRSF2,STAT6,STEAP3,STMN1,TCEA1,TGFBR2,TRAF4,TUBG1,YES1	78